Unité de Physiologie, Département de Médecine, Université de Fribourg (Suisse)

Lesion of motor cortex in adult non-human primates: post-lesional plasticity and mechanisms of behavioral recovery

Thèse

présentée à la Faculté des Sciences de l'Université de Fribourg pour l'obtention du grade de Doctor rerum naturalium

Spécialité: Neurosciences

par

Alexander Felix Wyss (Suisse)

Thèse numéro 1580

UniPrint

2007

Acknowledgements

General content

Content of Introduction

1. Introduction

Chapter 1 Introduction

1.1 Clinical Context

In industrialized countries brain disorders are one of the major causes for mental or physical impairment. As a consequence of these handicaps the concerned persons are often excluded from work. Such an exclusion from daily work generates an enormous amount of collateral costs for the society and its social institutions (Andlin-Sobocki et al., 2005). Especially health insurances are more and more confronted to these diseases. The reasons for this negative evolution are on one hand that our society consists of more and more elderly people having a potential higher risk to suffer from a brain disorder and on the other hand that our way of life particularly favors some very severe and frequent types of brain disorders as for example stroke. In the following remarks I will mainly concentrate on stroke which is the third most frequent cause for death in industrialized countries and the most frequent one causing permanent acquired intellectual and physical impairments in elderly adults. At the age of 55 to 64 about 300 per 100,000 people suffer from stroke whereas the incidence in the group of the 65 to 74 year olds goes up to 800 cases per 100,000. Men, especially more elderly, are more frequently concerned by stroke than women of the same age. About 15 – 20% of the patients suffering from a stroke die within the first 4 weeks. One third of the survivors recovers completely. Another third becomes independent in the sense that they can do by themselves simple things of daily life but they keep permanent intellectual and physical impairments and are no longer able to work. The last third stays in need of care for the rest of their life.

As already mentioned above the prospective risk of suffering an ischemic stroke is partially a function of social and behavioral (nutrition, tobacco use, stress) factors and longstanding disorders like hypertension, diabetes, disorders of cholesterol and lipid metabolism and obesity (Neuroprotection Models, Mechanisms and Therapies ISBN 3-527-30816-4). Clinical experience shows, that atherosclerosis is the main underlying condition in ischemic stroke.

In addition today the scientific community is more and more interested in the genetic background of individuals suffering from stroke as familial stroke conditions might be expected (Neuroprotection Models, Mechanisms and Therapies ISBN 3-527-30816-4).

1.2 Basic organisation of the motor system in primates

Taking into account the zoological classifications of primates, these creatures can be allocated to four major subgroups: Prosimians, simians, apes and finally humans (for details see

appendix). Obviously, there must be considerable differences amongst these four primate species which make them part of either subgroup. In spite of these particularities, the motor systems of all primates have a lot in common. This makes nonhuman primates an ideal model to investigate the motor system of humans. On the other hand, some special or lacking features in specific subgroups provide insight in the anatomical or physiological basis of human motor neural diseases. The first and second parts of this chapter will focus on the Anatomy and Physiology of the motor system in order to highlight the basic functioning of this complex machinery. The third part will describe more in detail the motor cortical subsystems which are implicated in voluntary execution of skilled hand and finger movements. The fourth part will concentrate on differences especially meaningful in conjunction with the understanding of damage to the corticospinal system in humans after lesion (e.g. stroke) of the motor cortex.

1.2.1 Classical classification of the motor system in different levels

The classical idea about the motor system was that it can be divided into several hierarchical levels, the lowest level controlling the simplest most automatic acts and the highest level controlling the most skilled (least automatic) movements especially the ones of the hand. Because this concept influences the understanding of the motor system until today it is briefly represented in the Figure 1.1 and the Table 1.1 below.

**Figure 1.1
Simplified representation of the motor system.**

CST = corticospinal tract
          (pyramidal tract)
RST = rubrospinal tract*
RetST = reticulospinal tract*
VST = vestibulospinal tract*
          (*= extrapyramidal tracts)

RN = red nucleus
RetN = reticular formation
VN = vestibular nucleus

4
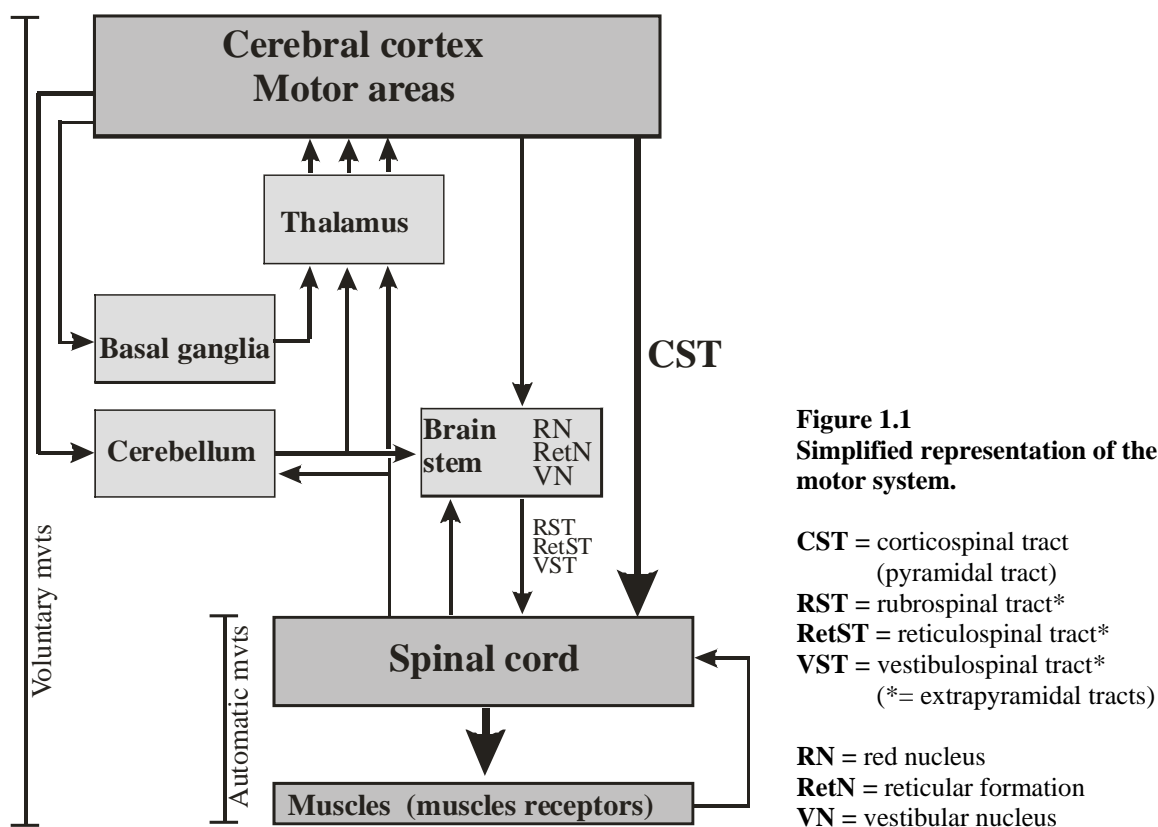
System		Receptors	Control level	Motor function	Level of consciousness
C o r t i c o	*Pyramidal motor system*	lemniscal channels as well as indirectly all sense organs	primary motor cortex and non-primary motor cortical areas	teleokinetic motility, newly acquired locomotion forms	aware, voluntary
S p i n a l	*Para or extra pyramidal system*	lemniscal channels as well as indirectly all sense organs	(*) different cortex areas, brainstem (subcortical centres)	automated, constitutive work movement, habit	aware, involuntary
S y s t e m	*Vestibule cerebellar system*	equilibrium organ, proprioception, exteroception	cerebellum	maintenance of equilibrium, regulation of tonus	unaware
Local motor apparatus		exteroception proprioception	Neuronal network of spinal cord (propriospinal apparatus) many segments	Goal oriented situation conform, locomotory pattern *exteroceptive reflexes* in particular flexion reflexes (swing phase)	unaware, suppressed by higher level centres (*)
Spinal elementary system		proprioception (muscular spindle, golgi tendon receptor)	Spinal cord: one up to few segments	Control of muscle length and muscle tension: myostatic *propriocepiv (= monosynaptic) reflexes* in particular extensor reflex (support phase)	unaware

Table 1.1   Main compartments of the motor system.

1.2.2   More recent concept of the motor system

More recent investigations revealed a more complex arrangement of the motor system, which no longer fits with the original hierarchical concept. It came out that the motor system has

to be seen as a complex network with a multitude of elements influencing each other with respect to a specific motor task executed. So, today the approach is to step by step fit the newly discovered pieces of the enormous "puzzle" into a functional concept towards a better understanding of the motor system.   In 1981, Wiesendanger (Handbook) summarized the knowledge about the connections of the pyramidal tract (today often named corticospinal tract) the most important pathway for skilled finger movements in primates in his widely used scheme as represented in Figure 1.2.

Figure 1.2
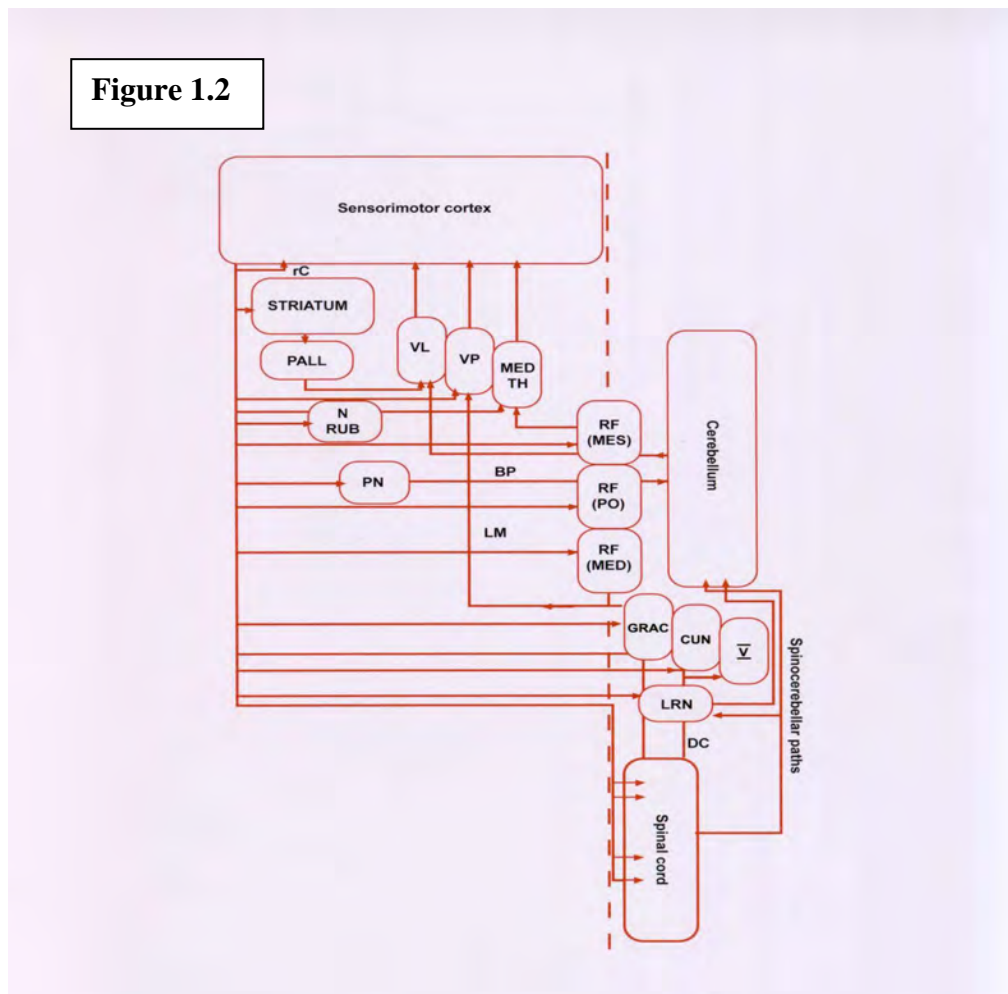
Schematic representation of the connections of the pyramidal tract. Collaterals of pyramidal neurons occur within the cerebral cortex (rC is recurrent collaterals). Other targets of pyramidal axon collaterals include the basal ganglia (striatum), the specific (VP) and unspecific (MED) thalamic nuclei, the red nucleus (N RUB), the pontine nuclei (PN), the mesencephalic (MES), pontine (PO), and the medullary (MED) reticular formation (RF), the dorsal column and trigeminal nuclei (GRAC, CUN, V), and the LRN. Collaterals also distribute at various spinal levels. Pyramidal tract collaterals may function as parts of internal feedback loops. The main internal feedback loops to the cerebral cortex are the lemniscal system (LM) and specific thalamic nuclei (VP), the cerebellum-ventrolateral nucleus of the thalamus (VL), and the pallidum (PALL)–VL system. Dotted line indicates midline. From Wiesendanger (1981) as reproduced in Porter and Lemon (1993).

From a functional point of view the descending output of the sensorimotor cortex (frontal and parietal areas of cerebral cortex) to the thalamus, striatum, the brain stem nuclei (corticobulbar or corticofugal) and the spinal cord can be divided into four subtypes of output A – D see below). Each output type consists of *corticospinal* as well as of *corticobulbar* (= *corticofugal*) neurons.

6

Output A: Movement execution related neurons:

1. Common function:

   - Excitation and inhibition of motoneurons through brainstem descending systems, propriospinal neurons and spinal cord interneurons.

2. Direct pathway:

   - So called *corticomotoneuronal cells* representing corticobulbar (upper motoneurons terminating in motor brain stem nuclei supplying muscles of the head, face, jaw and tongue) and corticospinal neurons terminating monosynaptically on motoneurons.

3. Indirect pathway:

   - Neurons of this category mainly act through polysynaptic brainstem descending systems (e.g. rubrospinal neurons, reticulospinal neurons, vestibulospinal neurons).

Output B: Reflex modulation-related neurons:

This type of corticospinal neurons influences motoneurons via a polysynaptic route in the propriospinal system. The corresponding propriospinal neurons are located in the upper cervical segments. Their axons traverse several spinal segments making synapses with motoneurons. Whether the propriospinal neurons are involved in the descending corticospinal control of motoneurons in primates is still a matter of debate (e.g. Olivier et al., 2001; Sasaki et al., 2004 and corresponding comment of Lemon, 2004).

Output C: Sensory modulation related neurons:

1. Common features:

   - Such cortical efferent neurons are mainly of primary somatosensory (S1) cortex origin.
   - They synapse with neurons of ascending sensory systems at various levels of the neuraxis.
   - Modulate the flow of somatosensory information from the periphery to the cortex most often by inhibition (Widener and Cheney, 1997). As a consequence, the cortex controls many spinal reflexes (Jankowska et al., 1976) and interneural pathways (Mazzocchio et al., 1994).

2. Two main targets of cortical modulation (Fetz, 1968):

   - Dorsal column nuclei.
   - Dorsal horn of the spinal cord (predominant target, Ralston and Ralston, 1985).

Output D: Internal motor program-related neurons:

1. Common features:

   - No direct influence on motoneurons and sensory inputs.

   - Internal signal processing in support of motor program formation and updating in order to produce an adequate movement.

   - Underlying mechanisms not well understood yet

2. Targets:

   - Thalamus, striatum, pons and lateral reticular nucleus (LRN)

1.2.3 Motorcortical subsystems implicated in voluntary execution of skilled hand and finger movements

As we know today, the corticospinal system of all primates consists of a multitude of corticofugal projections originating from different areas (for details see 1.3) and laminas (Table 1.2) of the motor cortex. Figure 1.3 below represents the typical histological appearance of the six motor cortical laminas of the cerebral cortex as revealed by Nissl staining. Note however that the motor cortex (areas 4 and 6) are deprived of layer IV.

Lamina of origin in motor cortex	Corticofugal projection
I	
II	
III	Cortico-cortical
	Corticocallosal
	Corticostriatal
V-a (upper)	Corticostriatal
	Corticorubral
	Corticoreticular
	Corticopontine
	Corticobulbar
	Corticonuclear
V-b (lower)	**Corticospinal (Pyramidal) projections (Betz Cells)**
VI	Corticothalamic

Pial surface

I	Molecular layer
II	External granule cell layer
III	External pyramidal cell layer
IV	Internal granule cell layer
V	Internal pyramidal cell layer
VI	Multiform layer

White matter

Modified from Kandel et al 2000

Figure 1.3

Nissl stain of the six typical laminas of the cerebral cortex.

Table 1.2

Overview of laminar origin of corticofugal projections in primate motor cortex (Modified from Kuypers, 1981 and from Jones and Wise, 1977).

Of these corticofugal projections some are of great clinical importance as they are the anatomic correlate of the capacity to perform voluntary relatively independent finger movements. In healthy primates (some nonhuman primates, great apes, humans) the *direct* <u>mono</u>synaptic *corticospinal projections* (pyramidal projections) are of crucial importance to perform such movements. If these projections are damaged, *indirect* extrapyramidal <u>oligo</u>synaptic projections (e.g. *corticorubral projections, corticoreticular projections*) may partially take over the function of direct corticospinal projections leading to an incomplete recovery of the hand dexterity. In Figure 1.4 below the different parts (lateral /ventral), the most important collaterals in the context of this thesis and the pathways of the pyramidal and selected alternative projections in primates are briefly represented.

The corticospinal tract (pyramidal tract) in primates

A Lateral corticospinal tract

B Ventral corticospinal tract

6
4
3,1,2

Corticorubral projections

Corticoreticular projections

Red nucleus
(magnocellular part)

Medial
brain stem
pathways

Reticular formation

Dorsal
column
nuclei

Rubrospinal tract

Reticulospinal tract

Pyramidal
decussation

Lateral
corticospinal
tract

Ventral
corticospinal
tract
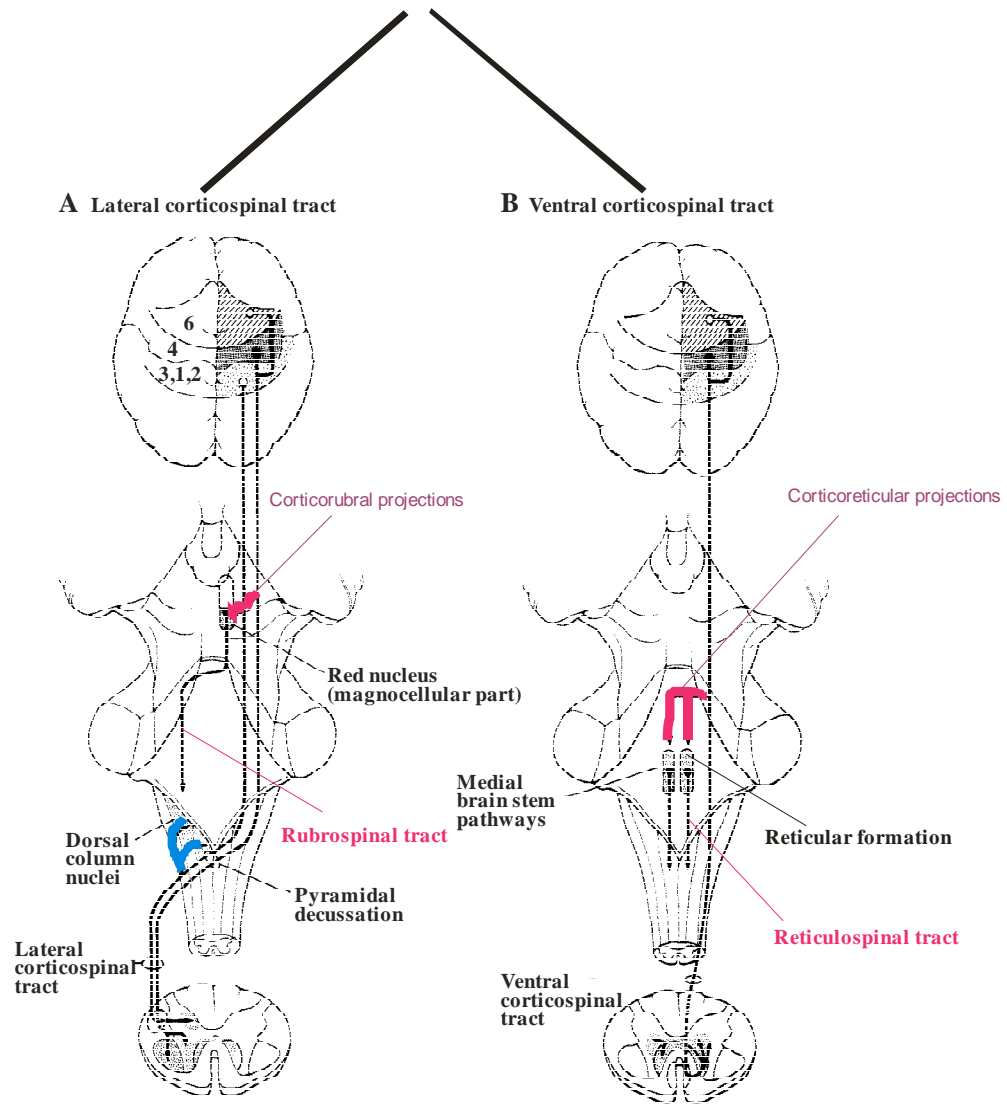
collaterals implicated in sensory modulation

collaterals implicated in post- lesion motor recovery

Medial brain stem pathways:
reticulospinal tract
lateral and medial vestibulospinal tract
tectospinal tracts

Dorsal column nuclei
cuneate nuclei
gracile nuclei

C Distribution of descending
tracts in the cervical cord

Lateral corticospinal tract

rubrospinal tract

lateral vestibulospinal tract
and lateral reticulospinal tract

medial reticulospinal tract
and tectospinal tract

medial vestibulospinal tract

ventral corticospinal tract
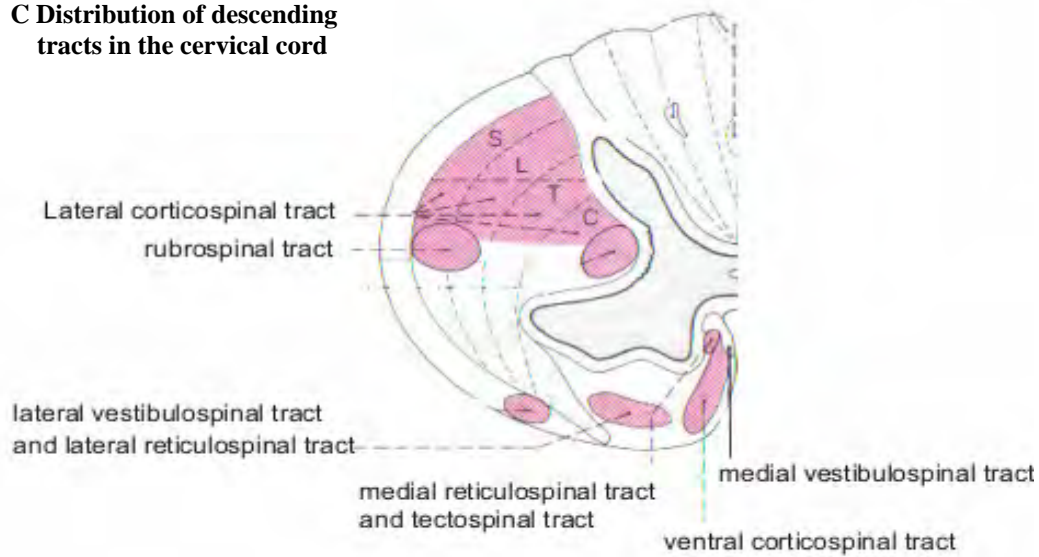
Figure 1.4
The corticospinal tract in primates:
  A) Lateral part
  B) Ventral part
  C) Distribution of descending tracts in the spinal cord at cervical
       level (transversal section)
       (modified from Kandel et al., 2000; Benninghoff, 1994).

Note that about 90 % of the corticospinal projections from the motor cortex cross at the pyramidal decussation whereas only about 10 % of the fibers in the corticospinal tract do not cross at the pyramidal decussation (for details about this subject in the macaque monkey see Rouiller et al., 1996; Lacroix et al., 2004.

1.2.4   Anatomical variations of the corticospinal system in different mammals; a tool to understand post-stroke recovery in humans

In contrast to primates most non primate species have only a limited capacity to perform relatively independent finger movements. In accordance to that, direct corticospinal projections to the motoneuron pool lying in the most ventral part of the spinal cord are best developed in dexterous primates. This was illustrated by linear regression analysis in the work of Heffner and

Masterton (1975). They found a positive correlation between the index of dexterity and the presence and density of direct corticospinal projections into the ventral horn of the cervical segments innervating forelimb muscles. In 1981, Kuypers illustrated this by a representation of the contrasting patterns of corticospinal terminations in four mammals (see Figure 1.5 below).
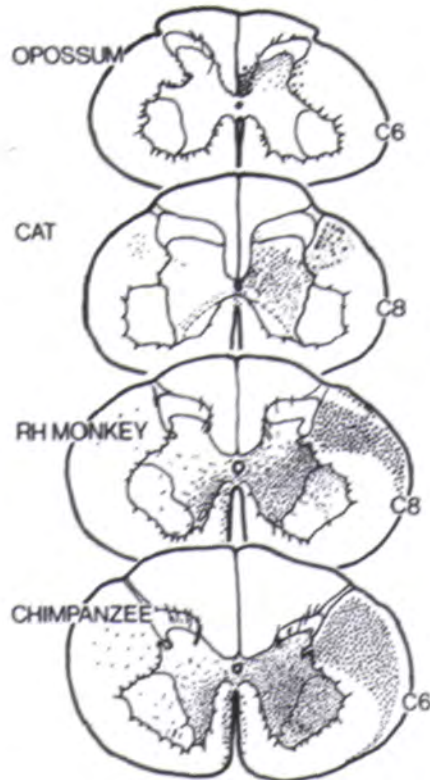
Figure 1.5   Distribution of corticospinal terminations from the left hemisphere to the lower cervical spinal cord in four different species: opossum, cat, rhesus monkey (macaque) and chimpanzee. Projections were revealed by staining of degenerating fibers resulting from large motor cortex lesions. Corticospinal terminations in the opossum are restricted to the dorsal horn, while in the cat there are terminations in both dorsal horn and intermediate zone. A further ventral shift in the extent of terminations occurs in the macaque monkey, in which direct projections to the motoneuron pool are present. These projections are much more pronounced in the chimpanzee. (From Kuypers, 1981.)

Nowadays it becomes more and more clear that cortical control of arm and hand muscles via oligosynaptic pathways are of high importance in terms of recovery after damage to the direct monosynaptic corticospinal system in humans independent whether the lesion is located at a cortical or spinal level. Although these pathways seem to be less developed in humans than in lower mammals, they may be stimulated after damage and therefore become functionally more important. Plasticity of projections to and inside the spinal cord together with post - lesion cortical plasticity is now accepted as an important factor for post - lesion recovery. On the way to come to this conclusion, investigations in mammals with differently developed corticospinal systems were very helpful. In the next paragraph I will briefly illustrate a summary of these findings.

As the significance of indirect pathways is of particular importance in species in which the direct corticospinal system physiologically is present to only a limited extend most studies were done in cat and squirrel monkey. In the cat the indirect corticospinal projections via the C3 – C4 propriospinal neurons (PN) are extremely well developed (Alstermark et al., 1990) additionally lacking direct corticospinal projections. The development of this system was compared to more

dexterous animals (squirrel monkey, data from Nakajima et al., 2000; macaque monkey, data from Maier et al., 1998) and extrapolated to humans with the help of information from clinical TMS studies (data from de Noordhout et al., 1999) as represented in the panel C of Fig 1.6 below (Lemon and Griffiths, 2005). Technically after lesion of the dorsolateral funiculus at the C5 (C5 DLF) level (in human studies, patients with comparable lesion were included) to interrupt the fibres of the lateral corticospinal tract but leaving intact the more ventrally locate PN axons, the corticospinal system was activated via stimulating electrodes implanted in the medullary pyramidal tract. This type of approach permits to electrophysiologically determine the amount of direct corticospinal projections and indirect projections via the alternative C3 – C4 propriospinal neurons pathway. Stimulation effects on motoneurons can be assessed by recording single motor units from a variety of upper limb muscles or from intracellular recordings from alpha – motoneurons. Responses of oligosynaptic pathways are characterized by large, late EPSPs. So consequently a higher proportion of late EPSPs indicate that the information from the motor cortex upper limb muscles travels through indirect pathways (panel A in Fig. 1.6). The more direct corticspinal projections exist in a creature the higher is the amplitude of the monosynaptic EPSPs to supramaximal stimulation of the corticospinal tract (panel B in Fig. 1.6; for reference see Nakajima et al., 2000). Finally the comparison by Lemon and Griffiths (2005) is in accordance with the findings of Heffner and Masterton (1975) (panel D in Fig 1.6) where they claimed that manual dexterity, especially individuated finger movements and precision grip, strongly depends on direct corticospinal projections. The summary of findings presented here shows that we can learn a lot from such experiments about how the motor system controls manual dexterity and which alternative pathways are potential targets for clinical treatment. This knowledge helps clinicians to better estimate what the maximal possible post - lesion recovery in a specific patient would be. As a consequence more effective and more adapted rehabilitative training can be applied.
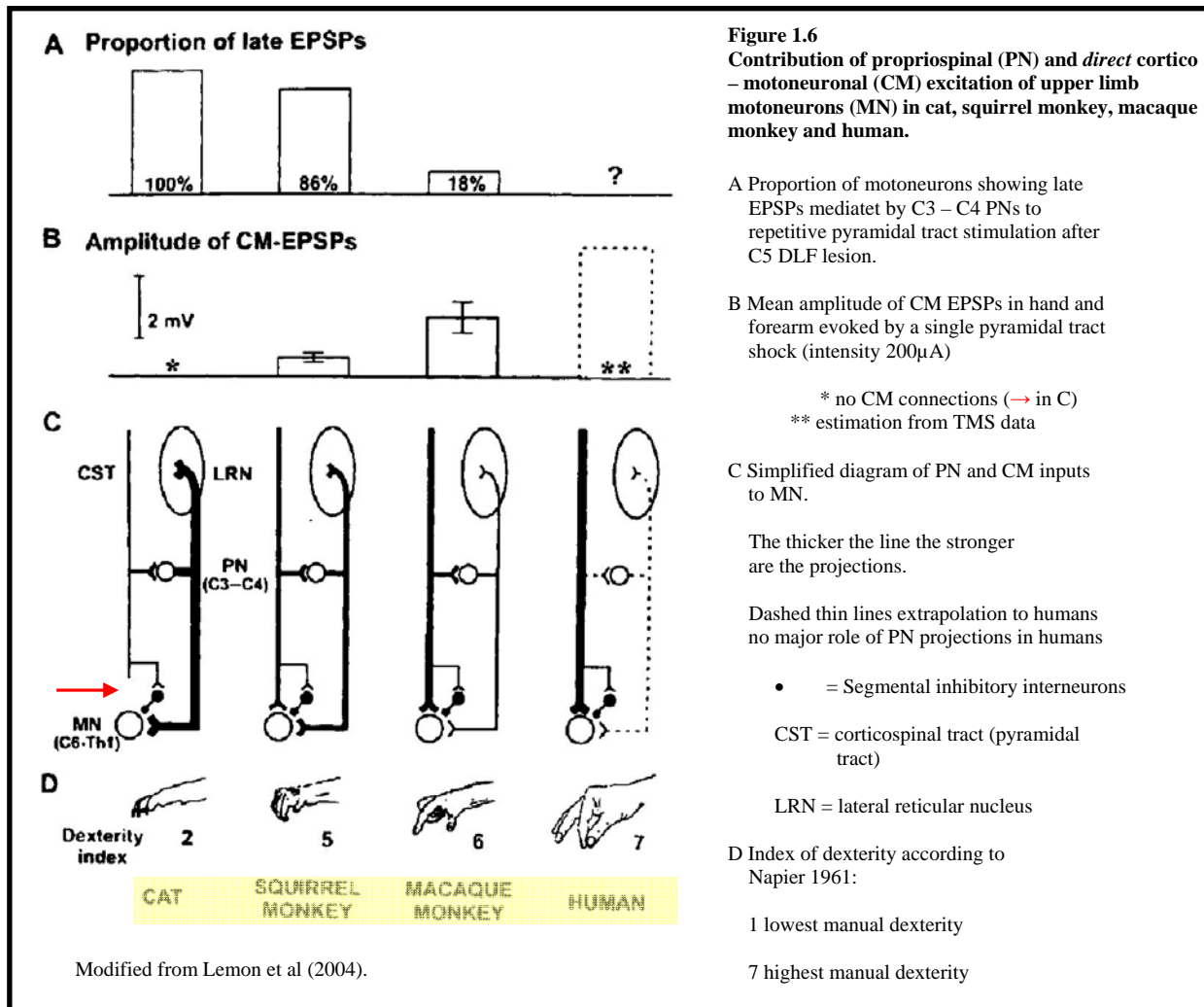
Figure 1.6
Contribution of propriospinal (PN) and *direct* cortico – motoneuronal (CM) excitation of upper limb motoneurons (MN) in cat, squirrel monkey, macaque monkey and human.

A Proportion of motoneurons showing late EPSPs mediatet by C3 – C4 PNs to repetitive pyramidal tract stimulation after C5 DLF lesion.

B Mean amplitude of CM EPSPs in hand and forearm evoked by a single pyramidal tract shock (intensity 200µA)

* no CM connections (→ in C)
** estimation from TMS data

C Simplified diagram of PN and CM inputs to MN.

The thicker the line the stronger are the projections.

Dashed thin lines extrapolation to humans no major role of PN projections in humans

- = Segmental inhibitory interneurons

CST = corticospinal tract (pyramidal tract)

LRN = lateral reticular nucleus

D Index of dexterity according to Napier 1961:

1 lowest manual dexterity

7 highest manual dexterity

Modified from Lemon et al (2004).

1.3 Distribution of corticospinal neurons over cortex

Today Sherrington's simple concept of the "final common pathway" in the motor system is no longer valuable because retrograde tracing studies in the spinal cord of macaque monkeys revealed that corticospinal neurons are not only present in M1 but also in 7 additional motor cortical areas (Dum and Strick, 1991, 1996; Galea and Smith, 1994; Picard and Strick, 1996) . In total there are seven distinct motor representations within the primate frontal lobe namely M1, SMA, CMAd, CMAv, CMAr, PMd and PMv. Six of them, because of their projections to both the spinal cord and the primary motor cortex (M1), are considered as "premotor". Figure 1.7 below represents the motor cortical areas of the frontal lobe and those from which corticospinal projections originate. There are also corticospinal neurons in the primary somatosensory cortex (S1) and in the posterior parietal cortex. They terminate in the spinal cord dorsal horn (Fetz, 1968) and in the dorsal column nuclei (Bentivoglio and Rustioni, 1986). In contrast to them, corticospinal neurons from the frontal lobe target the ventral horn and the intermediate zone of the spinal cord. It is worth to mention that the total number of corticospinal neurons in the arm

14

representation of the premotor areas equals or even exceeds the total number in the arm representation of M1. Additionally the individual premotor areas differ in the number of projections to distal and proximal forelimb muscles. Table 1.3 summarizes the characteristics of corticospinal neurons as described in the studies of Dum and Strick (1991), He et al. (1993, 1995).

Origins of corticospinal projections in the frontal lobe of primates

Figure 1.7
Figure representing the different origins of corticospinal projections in the primate motor cortex. Synonym terms for every subdivision are as well indicated.
M1: Primary motor cortex; PM: Premotor cortex with its dorsal part (PMd) and its ventral part (PMv); SMA: Supplementary motor area; pre-SMA: rostral part of the SMA; SMA-proper: caudal part of the SMA; CMA: Cingulate motor area; CMA-d dorsal part of the cingulate motor area; CMA-r rostral part of the cingulate motor area; CMA-v ventral part of the cingulate motor area; AIP: anterior intraparietal area; AR: arcuate sulcus; CC: corpus callosum; CE: central sulcus; CinS: cingulate sulcus; CS: corticospinal neurons; IP: intraparietal sulcus; L: lateral sulcus; P : sulcus principalis; F1 – F6: classification of motor cortical areas as proposed by Matelli et al., (1985 and 1991); Area 4,6,7,23,24 classification of motor cortical areas as proposed by Brodmann (1909).

Table 1.3   Properties of cortical premotor areas in relation to primary motor cortex (M1)

* injection sites of horseradish peroxidase to identify corresponding muscle groups

Numbers of corticospinal neurons based on data from Dum and Strick (1991), He et.al (1993) and He et al. (1995)

Modified from Cheney et al. (2000)

Cortical area	MI (F1)	SMA (F3,6aβ)	CMAd (6c,24d)	CMAv = CMAc (23c,24d)	CMAr (24c)	PMd = SPcS (F2,6aα)	PMv = APA (F4-F5)
Total number of CS neurons Forelimb *distal* *(C7 – T1)	10,000	2,400	800	1,200	1,200	3,400	1,000
Forelimb *prox.* *(C2 – C4)	10,000	2,800	2,600	1,000	800	3,200	160
Hindlimb *(L6-S1)	10,800	2,800	2,200	1,400	200	2,600	0
% high density bins (cervical, upper 10%)	53	19	15	7	<1	5	<1
Cortical area occupied by forelimb CS neurons (mm²)	84	44	22	14	24	20	18
% of total *frontal* lobe CS projection (note: *frontal* lobe harbors 70% of total CS projections)	51	13	9	6	4	15	2
Density of CS neurons (median, cells/mm²)	300	300	300	300	200	300	200
Electrical excitability (estimated average ICMS threshold, μA)	10	20	30	30	35	60	40
Functional Activity Move execution	+++++	+++	not tested	++++	++	+++	+++
Set related	++	+++	not tested	++	++++	++++	++
Signal related	+	++	not tested	not tested	not tested	+	+++
Special functional role	move execution	♦self-initiated movement ♦sequence ♦bilat. move	movement sequence from memory	not tested	reward based motor selection	sensory guided movement	♦visual grasp ♦imitation (F5)
Directional tuning	YES	YES	not tested	not tested	not tested	YES	not tested

From a functional point of view it is crucial to know that the cortical territories of the motor cortex representing individual muscles and influencing movements about individual joints broadly overlap. This is in sharp contrast to the exact somatotopic representation of sensory inputs in anatomically separated sub-areas within area 3b of S1 as demonstrated in macaques (Nelson et al., 1980). In spite of the overlap in the motor cortex the basic organization in M1 and S1 are the same. Although in M1 we should rather speak about a somatotopic organization of hot spots for producing movements in a particular muscle or at a particular joint. This type of organization was confirmed by ICMS studies where restricted cortical output zones were activated (Schieber, 2001) and elicited contractions in different muscles as well as by an elegant study from Schieber and Hibbard (1993) where they recorded the activity of M1 neurons in monkeys trained to move

individual digits in isolation (Fig. 1.8). Activation patterns in M1 during individuated finger movement are represented in Figure 1.8 below.
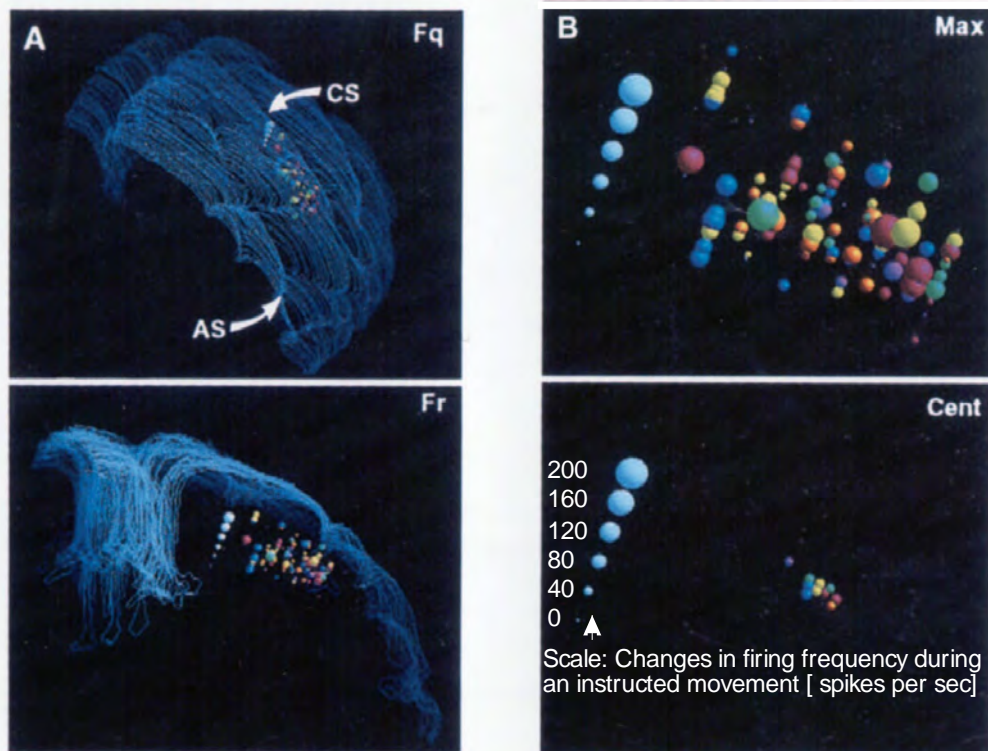
Figure 1.8

Distribution of neuronal activity in M1 during individuated finger movements.

A)   Orienting views reconstructed block left hemisphere:
- Fq = forquarter view
  - CS = central sulcus
  - AS = arcuate sulcus
- Fr = view from frontal pole; interhemispheric fissure on the left
  - Coloured spheres represent the population of M1 neurons recorded
  - Colourcode for instructed flexion / extension movements: red, orange, yellow, green, blue, and violet for digits 1,2,3,4, and 5 and wrist respectively

B) **Max:** Each sphere is sized to represent the maximal change in discharge frequency for that neuron during any of the 12 instructed movements and coloured to represent the instructed digit for that particular movement.

Cent: Centroids for each instructed movement (calculated from data not shown here) Probably the correlates of the somatotopic organized hotspots described above.

Modified from Schieber et al. (1993).

There is good evidence that the observed electrophysiological hotspots in M1 could correspond to the clusters observed by Murray and Coulter (1981). After injections of retrograde tracers in the spinal cord, labeled corticospinal neurons in S1 and M1 were not distributed uniformly over the sensory motor cortex but rather showed spots of aggregation. At these places cell density was higher than in other regions. So far the exact function of such clusters is not known. But Cheney and Fetz (1985) hypothesized that these clusters might represent basic cortical input-output processing units. For example cells of the same cluster in lamina V of M1 could share the same (or similar) muscle field, meaning the set of muscles facilitated or suppressed by the cell's activity. Using spike-triggered averaging of EMG activity and stimulus-triggered averaging of EMG activity they found some characteristics which strongly support their hypothesis. Usually post spike facilitation (PS*p*F) reflects the output organization of a *single* cell and post stimulus facilitation (PS*t*F) the output effects of a cell *population* and other neuronal elements excited by the stimulus. In fact, the PStF involved many CM cells but had the *same* basic profile across synergist muscles as PSpF from the single CM cell at the same site (representative EMG recordings are presented in Fig. 1.9 below). Cheney and Fetz concluded that neighboring cells activated by the stimulus (see PStF EMG pattern in Fig 1.10 below) should have similar patterns of synaptic connections with motoneurons. This was confirmed by the same authors (Cheney and Fetz, 1985) by computing spike-triggered averages from adjacent cells simultaneously recorded through the same electrode. An additional electrophysiological finding was that the relative magnitude of PSpF across different target muscles was similar for different cells in a cluster. This means that cells of a cluster do not only have the same target muscles but also the relative strength of synaptic input to target motor nuclei seems to be similar.
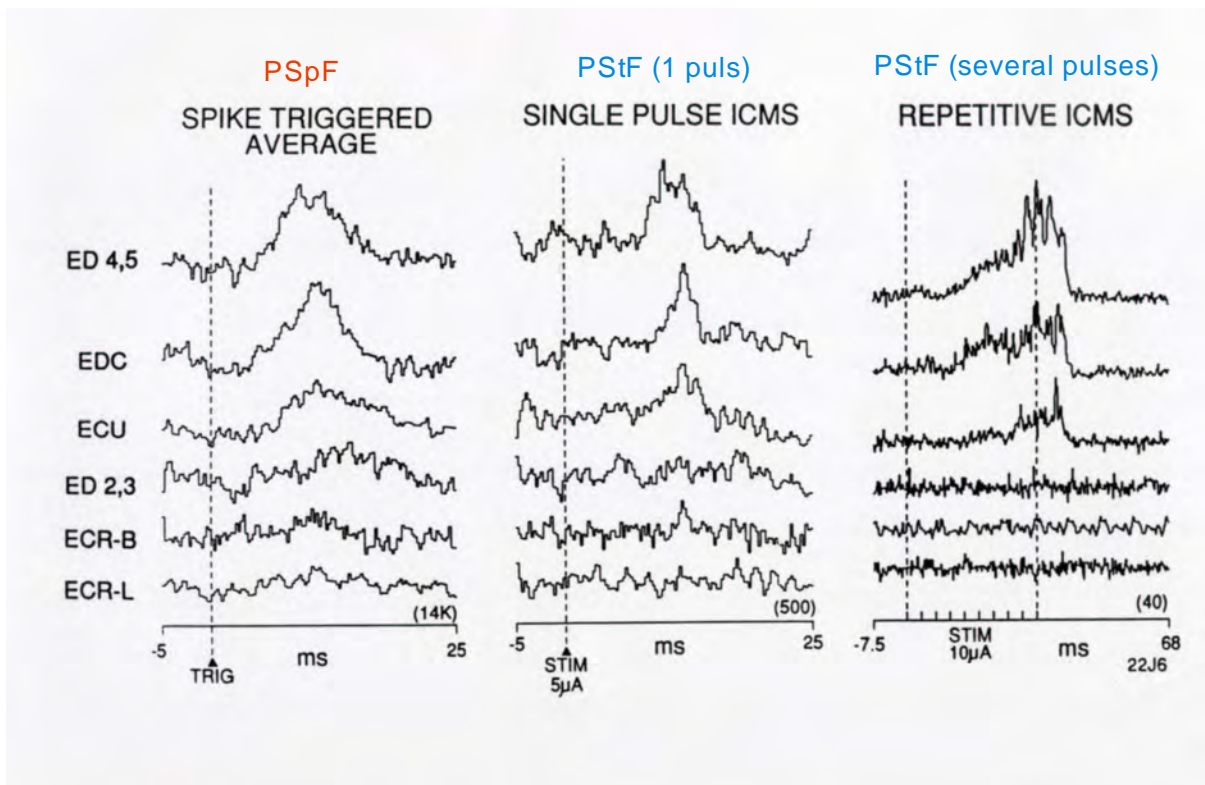
Figure 1.9

PSpF and PStF EMG pattern of representative forearm muscles in monkey following stimulation at a CM cell site in M1:

Clear effects visible in the EMG pattern of ED 4, 5 and EDC, weaker effect in ECU and no clear effect in the other forearm muscles tested.

PStF patterns and PSpF do match for muscles, in which EMG effects were recorded. This confirms the similar pattern of synaptic connections of a single CM and CM clusters terminating on motoneurons of the same muscle.

(PS*t*F) = post stimulus facilitation
(PS*p*F) = post spike facilitation

Modified from Cheney (2002).
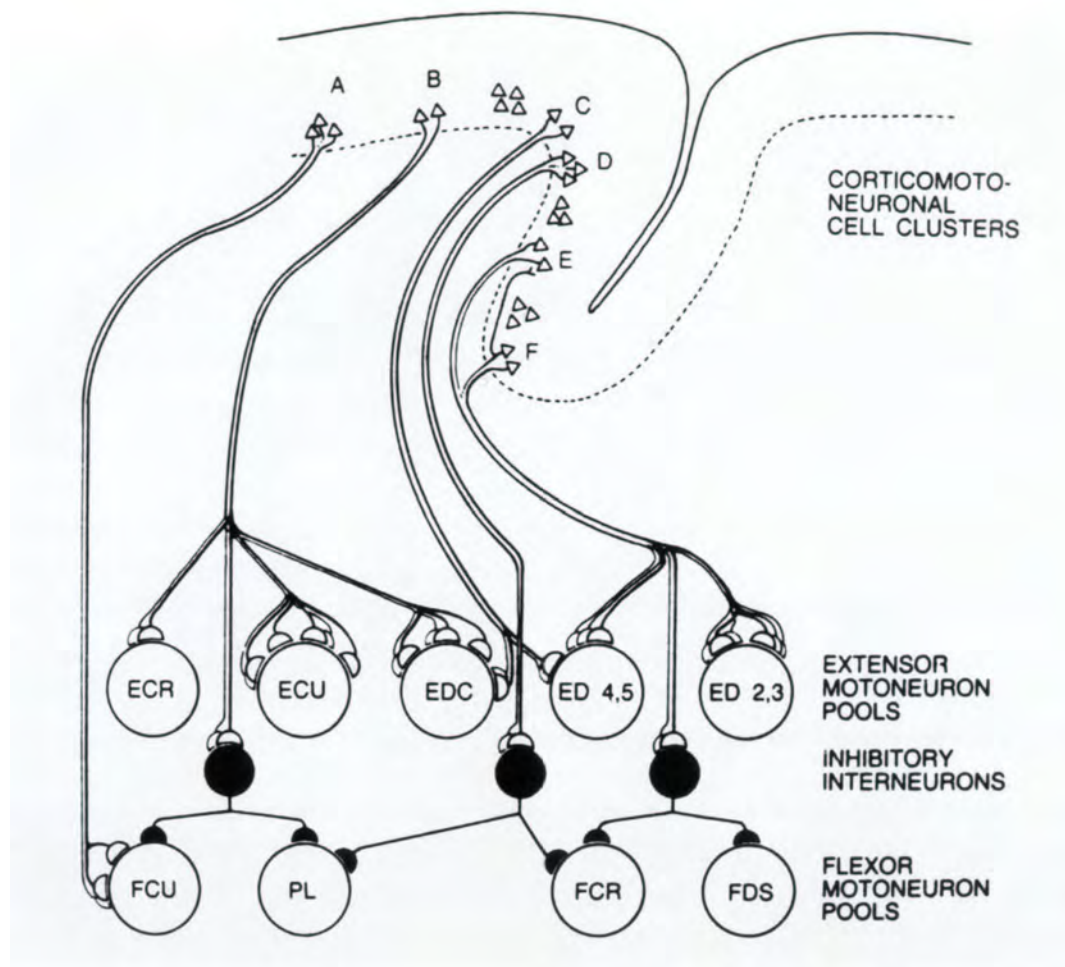
Figure 1.10

Basic features of the motor cortex output map:

- A – F: Clusters of about 5 – 20 CM cells in layer V of M1 (output module) projecting to the same muscle field
- a): facilitates a single motor nucleus (e.g. A)
- b): facilitate different combinations of synergist motor nuclei (e.g. B + F)
- c): pure facilitation no effect on antagonist muscles (e.g. A + C)
- d): simultaneous facilitation of agonist muscles and inhibition of
  antagonist muscles (via inhibitory interneurons) (e.g. B + E)

Note: 1. Cells facilitating flexors and extensors are very rare in M1 but more
        frequent in the red nucleus.
      2. c) and d) are most common in M1

Modified from Cheney and Fetz (1985).

1.4 Distribution of corticospinal neuron axons on a single alpha motoneuron

According to anatomic and electrophysiological studies (Asanuma et al., 1979; Fetz and Cheney, 1980; Shinoda, 1981) most corticospinal axons branch extensively within the spinal cord and terminate monosynaptically within multiple motoneuron pools located at one spinal level or distributed across several spinal levels. That is why within the spinal cord α-motoneurons targeted by corticospinal projections are localized in somatomotor cell columns each controlling a different group of muscles (see Figure 1.11 below).

Cell column	Muscles
Ventromedial (all segments)	Erector spinae
Dorsomedial (T1–L2)	Intercostals, abdominals
Ventrolateral (C5–C8, L2–S2)	Arm/thigh
Dorsolateral (C6–C8, L3–S3)	Forearm/leg
Retrodorsolateral (C8, T1, S1–S2)	Hand/foot
Central (C3–C5)	Diaphragm
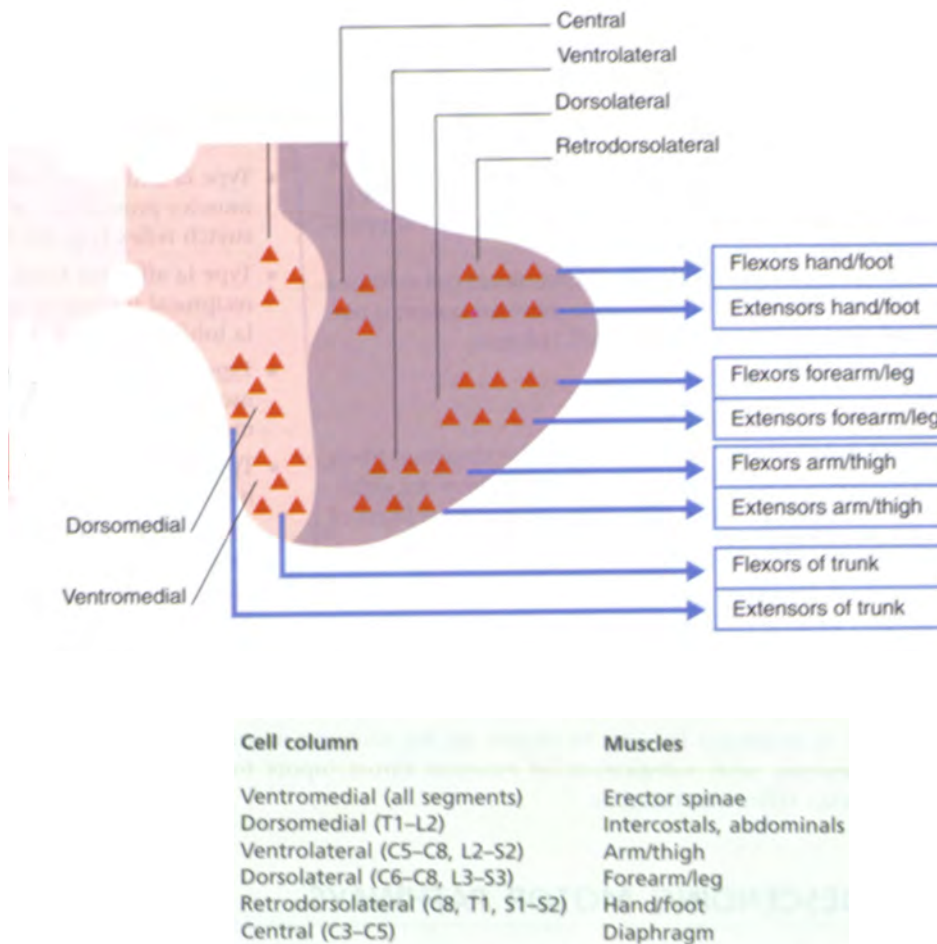
Figure 1.11

Somatomotor cell columns in the ventral grey horn of the spinal cord:
Corresponding muscle groups controlled by alpha motoneurons lying in the respective column are indicated in the table below.

Adapted from Clinical Neuroanatomy and Related Neuroscience 2002.

In order to determine the set of corticospinal neurons terminating on a single alpha motoneuron (= motor unit) different approaches were such as the study of Andersen et al. (1975) and also the experiments of Shinoda et al. (1981) based on anatomical and histological techniques. In parallel electrophysiologists tried to understand the wiring of a single alpha-motoneuron by electrical surface stimulation of the motor cortex and subsequent recordings of EPSPs, IPSPs and EMGs (e.g. Landgren et al., 1962; Clough et al., 1968; Jankowska et al., 1975). More detailed insight in the wiring of single alpha motoneurons was provided by new electrophysiological approaches with the techniques of ICMS and spike-triggered averaging in all its variants (Cheney and Fetz, 1985; Fetz and Cheney, 1980), as well as from additional recent studies (Belhaj-Saif et al., 1998; McKiernan et al., 1998). In the next two paragraphs first mainly anatomical key findings about alpha motoneurons are represented (a) followed by a brief description of the most important

electrophysiological discoveries (b) concerning corticospinal neurons terminating on single alpha motoneurons.

a) Results from anatomical studies:

Andersen et al. (1975) tried to define the cortical representation of a single alpha motoneuron. They placed anodal stimulation electrodes over the cortex at potential forelimb representations in baboon monkeys. Doing so, they were able to investigate whether there is a convergence of multiple cortical neurons to single motoneurons. It turned out that there are relatively large (5-12 mm^2) territories converging on a single alpha motoneuron. These territories even from different muscles are extensively overlapping. Inside each territory there is a "hotspot" of corticospinal cells that projects to the same alpha motoneuron or muscle, where the stimulation induces best a particular EPSP or contraction respectively. It is important to note that, although territories are overlapping, the hotspots are physically separated from each other. As there are no pure responses of only one muscle, it is evident that corticospinal neurons can not be organized in the sense that each muscle is controlled by its own piece of cortical tissue in M1. The observation of Shinoda et al. (1981) is exactly along the same line as they found terminations of individual corticospinal neurons typically branching to supply motoneurons of multiple muscles. In their work they visualized the axonal branching of single corticospinal neurons to supply multiple motoneuron pools. For this purpose the ulnar nerve and the radial nerve motoneuron pools of a monkey were retrogradely labled with intra-axonal injections of HRP. After sacrifices of the monkey 12 serial transverse sections of the spinal cord at C7 level were histologically analyzed to reconstruct the terminal arborisation of a hand area corticospinal (CS) axon (see Figure 1.12).
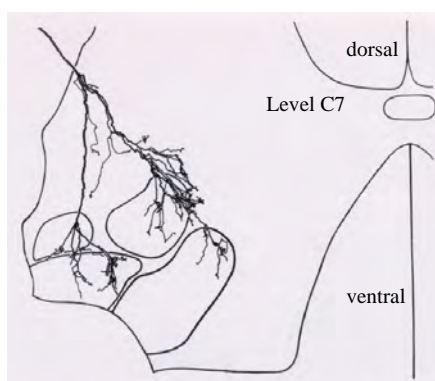
Figure 1.12
Transverse reconstruction of a single CS axon sending collaterals making connections with ulnar (upper two nuclei) and radial (lower two nuclei) nerve motoneurons.
(modified from Shinoda et al., 1981).

As can be seen in the reconstruction above the collaterals of a single CS axon is terminating on four motor nuclei. Shinoda et al. (1981) interpreted this as the anatomical basis for the functional influence of a given cortical motor fiber on its muscle field, including the possibility of actions on antagonists.

In 1985, Lawrence and colleagues (1985) combined intra-axonal injections of HRP into one or more corticospinal axons in the lateral funiculus (which originated in the hand area of the motor cortex) of the spinal cord of macaques with the intracellular injection of HRP into a number of nearby motoneurons which innervated intrinsic muscles of the hand. Compared to the study of Shinoda et al (1981) not only the corticospinal axon's terminal arborization was visualized but also the entire dendritic tree of a few motoneurons. Like this it was possible to examine their relationship. If a corticospinal axon made synaptic contacts with an identified motoneuron it could be regarded unequivocally as an axon of a monosynaptic motor cortical neuron terminating on an alpha - motoneuron (see Figure 1.13) below.
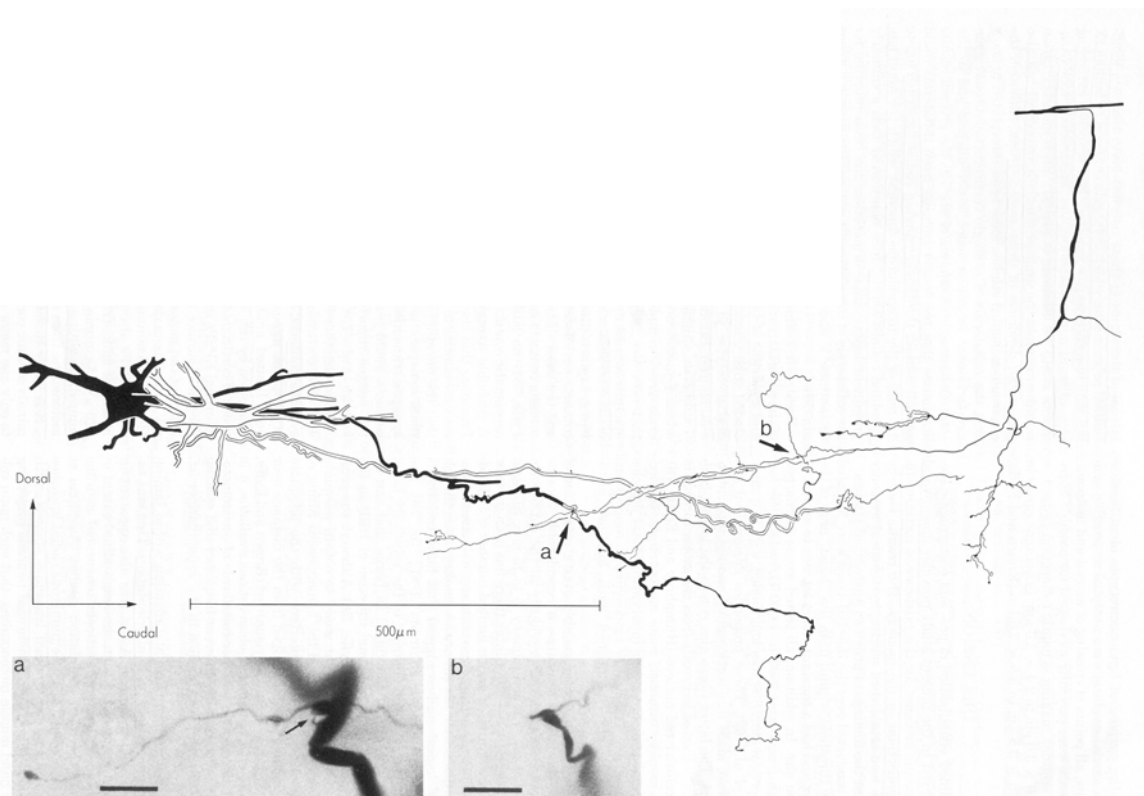
Figure 1.13

Reconstruction of collateral branches of a corticomotoneuronal axon which establish one synaptic contact (arrows a and b) with a dendrite of each of the two motoneurons (black and white). The corresponding pictures a and b show the synaptic sites (scale bars = 10 µm).

Adapted from Lawrence et al. (1985).

The main finding of this study was that each main collateral of a corticomotoneuronal axon in the monkey establishes very few synaptic contacts, and possibly only one, with the dendrites of a particular intrinsic hand muscle alpha-motoneuron. This implies that for the recruitment of a particular alpha-motoneuron by corticomotoneuronal activity, convergence from a large number of corticomotoneuronal neurons is needed, because individual EPSPs are too small to depolarize enough alpha-motoneurons for firing an action potential.

b) Results from electrophysiological studies:

To investigate the distribution of corticospinal neuron axons on a single alpha motoneuron has always been the subject of intense research. Because scientists were convinced, that these neurons are at the basis of voluntary motor control, especially of fine individuated finger movements. In earlier studies the motor cortex was stimulated by surface electrodes and the effects of such stimulation was measured by EMG recordings in target muscles as well as by first extra- and intracellular recordings of corresponding motoneurons in the ventral horn of the spinal cord. All these early studies were done in anesthetized animals mainly in cats but later also in baboon monkeys. In more recent studies more sophisticated investigations were done by intracellular recordings in the motor cortex of awaken primates. Most often the technique of spike or stimulus triggered averaging in combination with EMG recordings was used while the animal was performing a motor task. In addition the newly developed ICMS technique was especially suited to focus the electrical stimulation of the motor cortex on very small areas. So ICMS technique evokes contractions in a more limited number of muscle fibers from which EMGs can be recorded (Asanuma and Rosen, 1972; Lemon et al., 1987; Donoghue et al., 1972). In spite of this advantage there are still important limitations of the ICMS technique: Jankowska et al. (1975) showed that indirect activation of pyramidal cells occurs more frequently than in surface stimulation experiments. Later, Asanuma et al. (1976) confirmed this as they reported that ICMS did not activate single cells but rather depolarized a potentially large group of cells that were either in the vicinity of the stimulating electrode or lied in the current path. Although ICMS also has its limitations, it is clear that surface stimulations activated bigger cortical areas simultaneously and consequently evoked twitches of more numerous muscle fibers. Therefore it is evident that EMG recordings of surface stimulations were less suited to discover the pattern of corticospinal neurons terminating on a single alpha motoneuron. In spite of all technical limitations a lot about what we know from the distribution of corticospinal neurons on single alpha motoneurons was already found by the mean of the older surface stimulation technique and later confirmed and refined by more recent methods. So it is worth to briefly introduce the reader of my thesis in the evolution of the knowledge about the fascinating and clinically important topic of "alpha motoneurons and voluntary individuated finger movements in primates".

Figure 1.14 below represents a schematic illustration of the electrophysiological network in which alpha motoneurons are embedded during voluntary movement execution:

Descending CM projections

MN

IaIN

αMN

γMN

5

4

Ia fiber

Passive stretch
of spindle

Antagonist relaxing

Active stretch of spindle

Agonist contracting

3

Flexion of knee
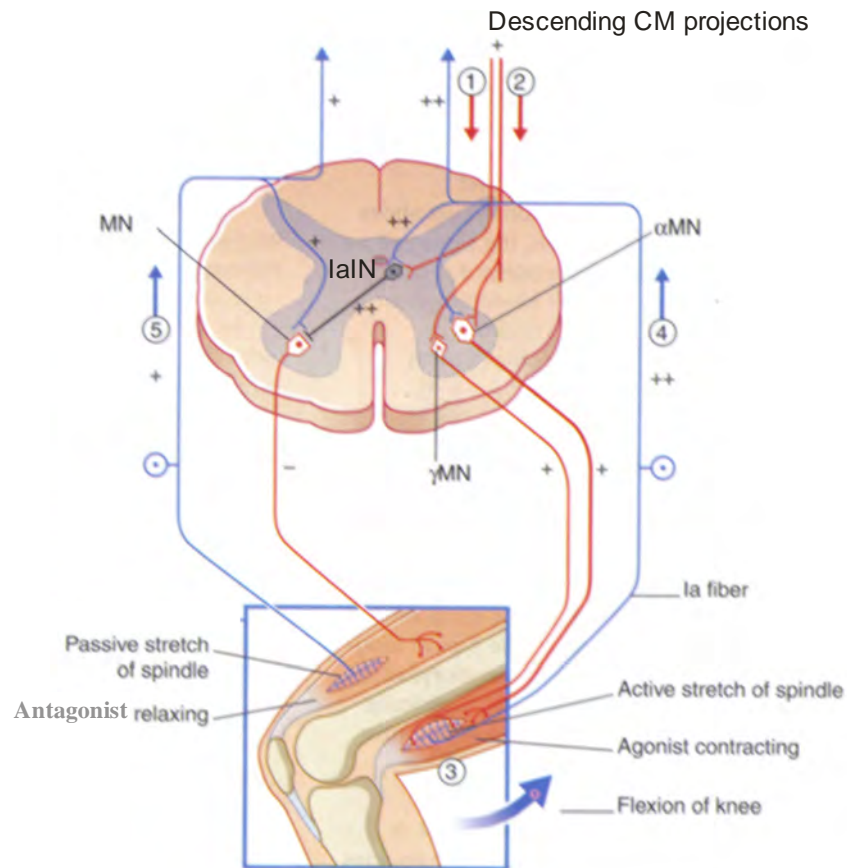
Figure 1.14

Schematic illustration of the electrophysiological network in which alpha motoneurons are embedded during voluntary movement execution:

Sequence of events:

1: Activation of Ia internuncial neurons (IaIN) to inhibit antagonist α motoneurons (αMN) through corticospinal projections
   (Kasser and Cheney, 1985)
2: Coactivation of agonist α and γ motor neurons through corticospinal projections (Clough et al., 1968, 1971)
3: Activation of extrafusal and intrafusal muscle fibers
4: Feedback from actively stretched spindles increases excitation of agonist α motor neurons and inhibition of antagonist α motor neurons
5: Ia fibers from passively stretched antagonist spindles find the respective α motor neurons refractory. *Note:* The sequence, γ motor
   neuron-Ia fiber- α motor neuron is known as the ***gamma loop***.

+ = Excitation
 - = Inhibition

Adapted from Clinical Neuroanatomy and Related Neuroscience 2002.

Using basically anatomical approaches, Shinoda (1979, 1981, 1986) concluded already that corticospinal axons terminating within motoneuron pools that innervate distal muscles branch less and have a more restricted field of influence than other pyramidal-tract axons. But because of technical reasons he was not able to define the cells on which the fibres terminate. Nor he was able to report whether the physiological influences on such cells are exerted directly or indirectly. Post-spike facilitation in spike-triggered averages of muscle's EMG is the method to functionally define the muscle field that is influenced by a particular CM cell (Fetz and Cheney, 1980). Branching of axons as proposed by Shinoda implies that an individual CM cell exerts a divergent excitatory influence on different motoneurons. Fetz and Cheney (1978) confirmed that view as they found

that a given CM cell facilitates motoneurons of several synergistic acting muscles. Further on, they reported a greater divergence for extensor-related CM cells than for flexor-related CM cells. Buys et al. (1986) found that CM cells terminating on motoneurons of intrinsic muscles of the hand or muscles acting on the distal joints of the fingers have a more restricted muscle field, as proposed by Shinoda (1981). The corresponding CM cells were mainly active during precision grip. Because the magnitude of post-spike facilitation in spike-triggered averaging can be used as a measure of CM excitatory influences on motoneurons, strong post-spike facilitation is the result of strong connections from the motor cortex to alpha-motoneurons. This approach leads to the important finding that the excitatory influence of CM cells on extensor motoneurons innervating the distal forelimb is stronger than that exerted on corresponding flexors. As post spike-facilitation is weaker in more proximal muscles (in both flexors and extensors) it can be concluded that CM projections on alpha-motoneurons innervating distal muscles are more numerous than CM projections on alpha-motoneurons innervating more proximal muscles. This idea is not new, because older studies with surface stimulation of the motor cortex already showed that EPSPs were smaller and more infrequent in motoneurons of proximal muscles than distal muscles (e.g. Landgren et al., 1962).

The pioneer work in this field was done by Clough et al. (1968) by measuring the CM EPSPs in different motoneurons of the hand in the baboon's cervical spinal cord. They demonstrated that motoneurons of intrinsic hand muscles and EDC receive larger quantities of monosynaptic pyramidal (CM) excitation than those innervating other muscles in the forearm. This observation is in accordance with the concept of controlling voluntary fine finger movements through direct monosynaptic corticospinal projections. In addition to that they were of the first researchers demonstrating that the mean size of maximal CM EPSPs for extensor motoneurons of the hand was bigger than for corresponding flexor motoneurons. This result was the first to proof that motoneurons of extensors of the hand receive more monosynaptic pyramidal excitation than motoneurons of flexors. In their study Clough et al. (1968) were also interested in the distribution of monosynaptic pyramidal excitation to "fast" and "slow" motoneurons. From their findings they concluded that the pattern of distribution of pyramidal excitation to motoneurons with "fast" and "slow" axons might be different within different motoneuron pools.

Today we distinguish two principle types of alpha-motoneurons targeted by direct CM projections:

- *Tonic* alpha-motoneurons innervate slow, oxidative-glycolytic muscle fibres; they are readily depolarized and have relatively slowly conducting axons with small spike

amplitudes. They are usually first recruited when voluntary movements are initiated, even if the movement is to be fast.

- *Phasic* alpha-motoneurons innervate squads of fast oxidative and fast oxidative – glycolytic muscle fibres. Phasic alpha-motoneurons are larger, have higher thresholds, and have rapidly conducting axons with large spike amplitudes (Clinical Neuroanatomy and Related Neuroscience 2002 p. 123).

Whilst the study of Clough et al. (1968) concentrated on the forelimb of monkeys, Jankowska et al. (1975) investigated the problematic of direct monosynaptic corticospinal projections from motor cortex to alpha-motoneurons in the hind limb of monkeys. Basically they used the same techniques as Clough et al. (1968) namely cortical surface stimulation of the motor cortex and intracellular EPSP recording of alpha-motoneurons. In addition the motor cortex was alternatively stimulated by intracortical stimulation through micro-electrodes filled with NaCl solution (similar to the ICMS technique described in the method part of this thesis). Looking at the main findings of Jankowska's study we can conclude that they are in good accordance with results from similar studies of the forelimb (see points 1-6 below (modified from Jankowska et al., 1975).

1. The proportion of motoneurons in which monosynaptic EPSPs of cortical origin were evoked and the amplitudes of the latter indicate a more extensive cortical projection to motor nuclei for distal than for proximal muscles.

2. Cortical areas from which monosynaptic EPSPs were evoked in individual motoneurons most often ranged between 3 and 7 mm^2. Individual motoneurons can have several separate areas within the hindlimb territory of the motor cortex.

3. Pyramidal tract cells projecting to various motoneurons innervating *one* muscle usually do not originate from the same cortical area. There is only partial or even no overlap of such areas.

4. Areas of location of pyramidal cells projecting to motor nuclei of *different* muscles often show an extensive overlap. When it occurred, various motoneurons of a given motor nucleus had common cortical projection areas with motoneurons of other motor nuclei, either to synergistic or antagonistic muscles.

5. The rise times of cortically evoked EPSPs indicate that the corticospinal tract fibres terminate on motoneurones at approximately similar distances from the soma as group Ia afferents. The small amplitudes of the majority of EPSPs evoked by near threshold cortical stimulation therefore suggest that unitary EPSPs of cortical origin are small and that the

density of pyramidal tract cells projecting to individual motoneurones is usually low, even in the centrum of projection areas.

6. Effects of intracortical stimulation depended on the stimulus strength. With currents of 2-3 µA, EPSPs were usually evoked in one motoneuron species or in close synergists. With currents of 5-10 µA, largest EPSPs were evoked in one or two motoneuron species and smaller EPSPs in a number of other motoneurones. Latencies of descending volleys in the lumbar corticospinal tract indicated that intracortical stimuli activated pyramidal tract cells *indirectly*; the effects of these stimuli could thus not be used to indicate the location of pyramidal tract cells responsible for them.

Most of the above mentioned studies concentrated on the analysis of an isolated small muscle group or were done by electrophysiological techniques of which the results were difficult to interpret. In order to overcome these difficulties, Mc Kiernan and colleagues (1998), combined the most adapted and most powerful electrophysiological technique to investigate the monosynaptic connections between CM neurons and alpha-motoneurons, spike-triggered averaging, with a natural reach and prehension task of the forelimb in awake monkeys. For this purpose they recorded post spike or post stimulus effects in EMGs of 24 separated forelimb muscles at both proximal (shoulder, elbow) and distal (wrist, digits, intrinsic hand) joints while the animal executed the task. Subsequently they measured post spike/stimulus latencies, magnitude of facilitation/inhibition for all muscles recorded. This approach provided more detail about the input to specific muscle groups. For the first time Mc Kiernan et al. (1998) were able to show that approximately 45% all recorded CM cells facilitate at least one proximal and one distal forelimb muscles in the monkey. Their work also helped a lot to understand the confusing and sometimes contradictory results from previous studies. For example they found a stepwise increase in the peak magnitude of PSpF from the muscles of the shoulder joint through the intrinsic muscles of the hand. This clearly supports the conclusions of older above mentioned studies that CM terminations on alpha-motoneuron pools of distal muscles are more frequent and / or more potent than those in motoneuron pools of proximal muscles. Conflicting data from different studies exist about whether extensor muscles are more strongly and more frequently facilitated than flexor muscles (Fetz and Cheney, 1980) or if the contrary is true. The findings of McKiernan et al. (1998) rather confirm the results of Fetz and Cheney. Although the approach of McKiernan et al. (1998) makes their results more plausible than those of precursor studies, they still leave open the question whether contrasting results are just motor task dependent and therefore also correct (e.g. Schieppati et al., 1996).

1.5 Properties of the corticospinal system

In this chapter, based on a few selected studies the aim is to describe how neuronal activity in the primate motor cortex is related to various parameters of movements (e.g. force, direction, etc.) while monkeys perform voluntary movements of the forelimb.

1.5.1 Force coding

It is well known that the control of force by motoneurons in the spinal cord is based on two principles: i) recruitment of a variable number of motor units ii) within each motor unit, a fine control of force is possible by modulating the number of action potentials generated by the corresponding motoneuron. As the spinal motoneurons receive inputs from the motor cortex, one may ask how force is coded by motor cortical neurons. This issue was addressed by Wannier et al. (1991). They recorded the activity of single cortical neurons in S1 and M1 in adult macaque monkeys conditioned to control force isometrically on a transducer held between the thumb and the index finger in a visual step tracking paradigm. The paradigm was as follows. The monkey had to displace a horizontal bar (blue bar in Figure 1.15) on a screen inside a target area (delimited by two horizontal red lines in Figure 1.15) corresponding to a defined force level exerted on the transducer by opposing the thumb and the index finger as during precision grip. First the monkey had to produce a force ramp to reach the low target force (W1). After maintaining the force for 1.5 seconds the target area was moved up vertically (FO2) indicating the monkey to exert a higher force on the transducer to reach the higher target force (W2). Again the monkey had to hold this force for about 1 second to get a liquid reward (REW).
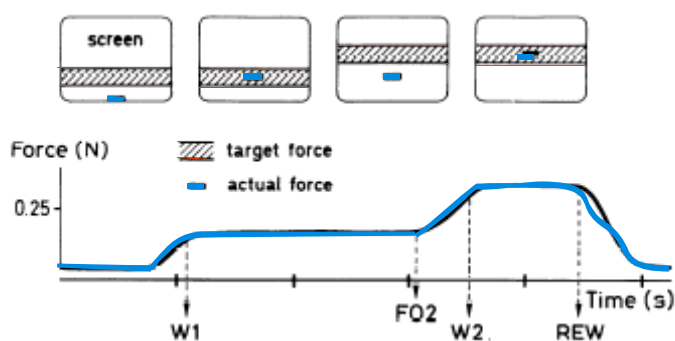
Figure 1.15

Visual step-tracking paradigm in the precision grip task (Wannier et al., 1991).

This task was particularly suited to investigate various aspects of the properties of force related activity in M1 as well as in S1. Although the task is isometric, it consists of holding phases and "dynamic" phases in which the animal either has to increase or decrease the force intensity. Potentially these different phases activate various groups of cortical cells implicated in different

motor functions. Table 1.4 briefly describes the most important findings about force coding of corticospinal neurons in M1 and S1 as revealed by the study of Wannier et al. (1991). Some of them are illustrated for representative neurons of M1 in Figure 1.16 below.
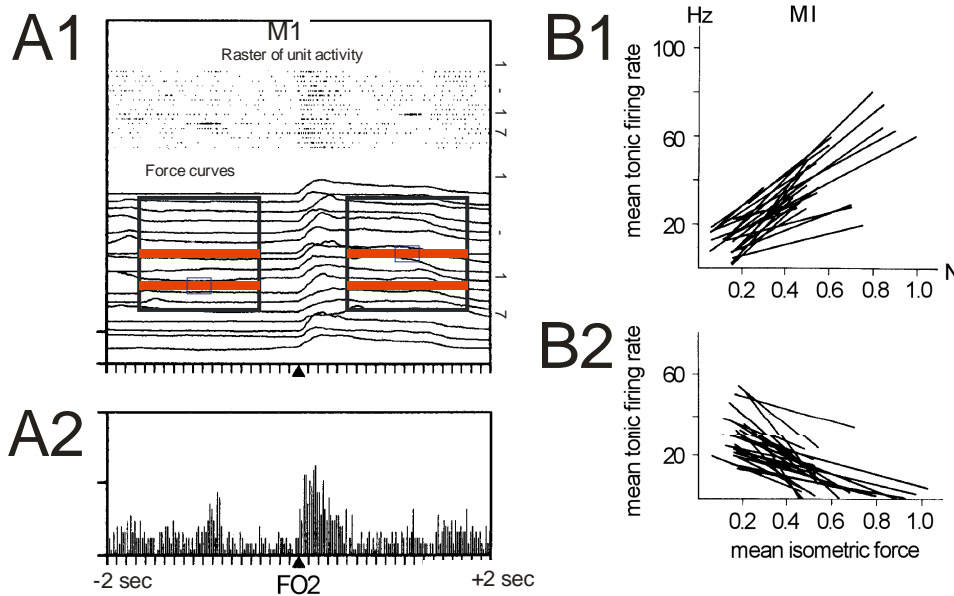
modified from Wannier et al 1991

Figure 1.16
A1: Raster of unit activity and corresponding force curves of a representative M1 neuron two seconds before and after the onset of force increase (FO2) from level W1 to W2 (1-17 chronological order of recordings)
A2: Histogram of representative changes in the discharge pattern of a phasic M1 neuron two seconds before and after the onset of force increase (FO2) from level W1 to W2 constructed from the dot display in A1.

B: Regression lines in firing rates as a function of isometric force exerted by the thumb and the index finger on the transducer.
         Two groups of neurons were observed, the first ones exhibiting an increase of firing rate for increasing forces (B1) whereas cells in the second group showed a decrease of firing rate (B2).

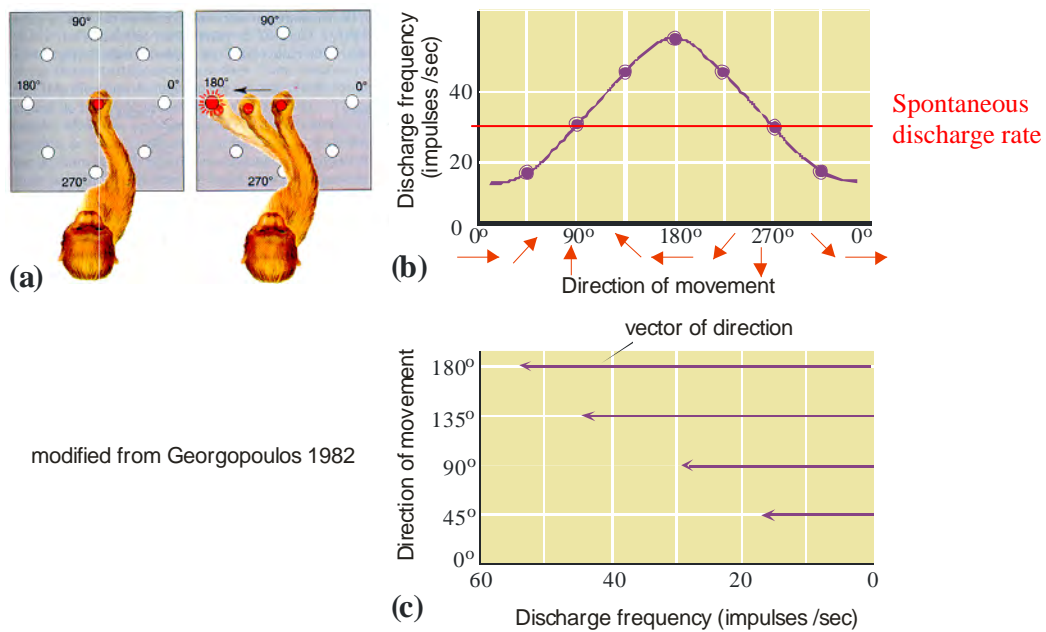|	**M1 neurons**	**S1 neurons**
ICMS	low threshold stimulations mainly induce motor reactions in thumb and/or index finger (87% of sites)	low threshold stimulations induce finger movements occasionally coupled with wrist movements (25% of sites)
Corresponding **Receptive fields**	Sensory afferent input: **73 % from deep receptors** 19 % from skin receptors 8% from both receptor types	Sensory afferent input: **68 % from skin receptors** 24 % from deep receptors 8 % from both receptor types
Discharge patterns observed	7 different types (details see Wannier et al. 1991)	7 different types (details see Wannier et al. 1991)
Distribution of the firing patterns	Most frequent are neurons with **de**creasing discharge patterns (42 %)	Most frequent are neurons with **in**creasing discharge patterns (61 %) with differences among the 4 subareas of S1 (Wannier et al 1991)
Latency distribution and mean **onset (FO2) of activity changes** with respect to the onset of force increase from the low (W1) to the high level (W2)	Tendency towards an activity change **before** force increase (FO2). 56% of M1 neurons tested	Tendency towards an activity change **after** force increase (FO2). 81% of S1 neurons tested
Relation activity static force	Clear relation of force and activity for both neurons with increasing and decreasing discharge patterns (see figure XX B1,B2)	Clear relation of force and activity for both neurons with increasing and decreasing discharge patterns

Table 1.4

   Properties of cortical neurons in M1 and S1 derived from a visual-step tracking task of
      precision grip in macaque monkeys (from Wannier et al., 1991).

1.5.2 Coding of movement direction

As already described above, the motor cortex possesses neurons differently active during force application. In addition to them, M1 neurons change their activity with respect to the direction of a specific movement. To investigate in more detail the population of direction coded neurons, Georgopoulos et al. (1982) trained adult rhesus monkeys to move a lightweight frictionless manipulandum over a plane surface and capture a lighted target out of 8 forming a fictive circle in a reaction time paradigm. In this task, the monkey started holding the manipulandum in the center of the circle. Then a LED on the circle at 1 of 8 different positions was turned on and the monkey had to catch it by displacing the manipulandum using one hand. Doing so the monkey was instructed to make movements in different directions of which the angle with respect to the starting position could be calculated (see Figure 1.17 a). Recordings of the activity of corresponding neurons in M1 (area 4 and 6) during task performance could be correlated with particular movement directions. Analysis of the recorded data revealed the following correlations:

a) Relations between changes in the frequency of discharge and direction of movement

First it has to be mentioned that almost all of the neurons investigated showed changes in discharge frequency with more than one, and commonly with all directions of movements. But each cell had a directional preference. If the monkey made a movement in this preferred direction the cell discharged at the highest discharge rate whereas the movements was made in other directions corresponded to lower discharge rate if not inhibition for certain directions of movement. This leads to a particular bell shaped directional "tuning curve" for each individual neuron mathematically corresponding to a sinusoidal function where the frequency of discharge varies with respect to the angle of the movement (Figure 1.17 b and c).

Figure 1.17 Response of a M1 neuron recorded while the monkey executed arm movements in different directions

   a) Setup of the motor reaction task described above
   b) Bell shaped directional tuning curve for a single M1 neuron
   c) Direction vectors derived from neuronal activity with respect to the angle of the arm movement

The neuron represented in panels (b) and (c) is the same one for which the activity is represented by dot raster in the Figure 1.18 below.

b) Relations between movement direction and how neuronal discharge first changes

If the movement direction was at or near the cell's preferred direction (180° in Figures 1.18 and 1.19) neuronal discharge was maximal (strong excitation) whereas for movements in directions progressively away from the preferred direction neuronal discharge decreased, reached the spontaneous activity (close to 270°) and the cell was even inhibited for movements opposite to the preferred direction (see Figures 1.18 and 1.19 below). The onset time of either excitation or inhibition with respect to movement initiation also depended on the direction. The closer the direction was to the cell's preferred direction the earlier an increase (excitation) in cell discharge occurred. In contrast the farther the movement direction was from the cell's preferred direction the earlier a decrease (inhibition) in cell discharge occurred.
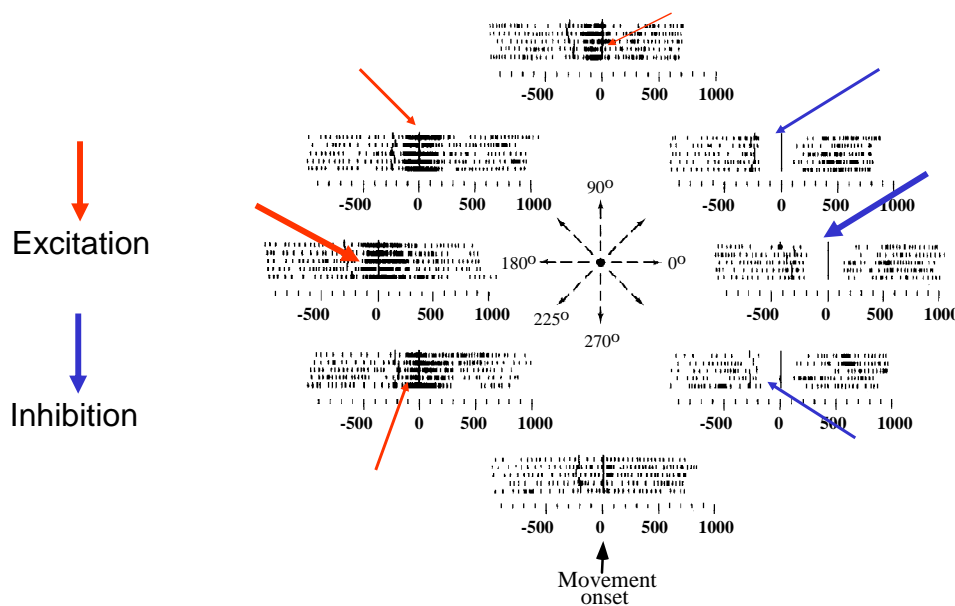
Figure 1.18 Rasters of unit activity during five repetitions of movements made in each of the eight directions indicated by the center diagram for a single neuron in M1. The width of the blue (inhibition) and red (excitation) arrows indicate the of discharge rate induced by a particular movement in one of the eight directions (modified from Georgopoulos, 1982).

Although neurons in M1 (and also in PM) show a tuning curve reflecting some selectivity for movement direction, the tuning curves are broad and at least two directions of movements may correspond to the same discharge rate. As a consequence, a single neuron in M1 does not represent unambiguously the direction of movement. Therefore, Georgopoulos et al. (1982) proposed a concept of representation of direction of movement passed on "population coding" (Figure 1.19).

As a consequence of the above coding characteristics movement directions can be predicted from the sum of the direction vectors (representing individual neuronal activities see Figure 1.19 C) from a population of neurons active in a specific moment of time as demonstrated in Figure 1.19 below.
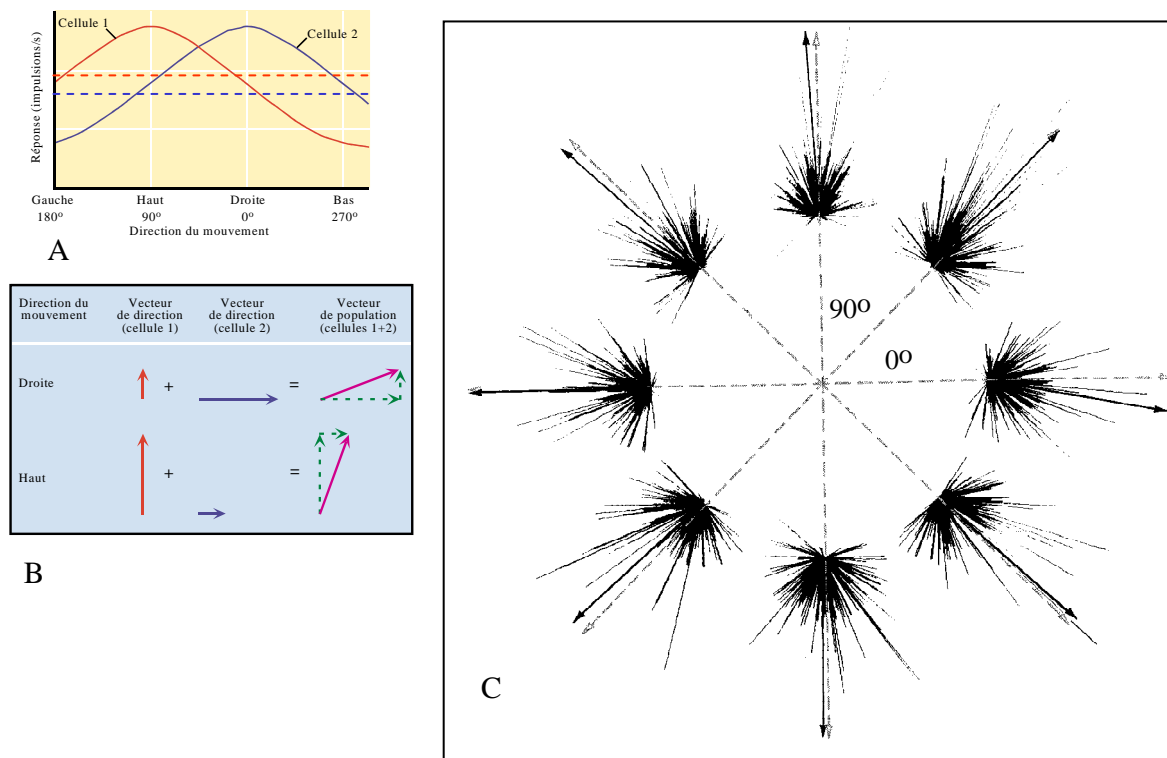
Figure 1.19 Vectors of direction, population vectors and prediction of movement direction from population vectors.

A)   Curves representing the evolution of discharge rate (tuning curves) of two cells in M1 with respect to movement direction. Cell 1 preferentially discharges during upward movements whereas cell 2 preferentially discharges during movements from left to right.

B)   The discharge of both cells can be represented as vectors oriented to the preferred direction of the corresponding cell. The length of the vectors corresponds to the discharge rate related to movement direction. For a particular movement direction, the sum of the respective vectors representing all neurons recorded is equal to the population vector.

C)   At each target location ($n \leq 8$) vectors show the discharge rate observed in neurons recorded from M1. The discharge rate is indicated by the length of each vector. For each direction of movement the individual vectors can be summed to a "sum population vector" (solid line arrow) predicting the direction (doted arrows) of the movement actually executed by the monkey (modified from Georgopoulos 1983 and Neuroscience à la découverte du cerveau; 2002; ISBN:2-913996-11-6).

1.5.3 What is represented at a neuronal level in M1: Muscles or movements?

To address this question, Kakei et al. (1999) recorded the activity from M1 neurons in a monkey, in parallel to EMG recordings from 27 muscles in the forearm, upper arm, and shoulder, trained to perform a task which dissociates three major variables of wrist movement: muscle activity, direction of movement at the wrist joint, and direction of movement in space. Briefly, the monkey had to move a manipulandum from a central start position to capture 8 targets positioned on a fictive plane surface as in the task of Georgopoulos et al., 1982. An important difference however was that the position (posture) of the wrist was taken into account in the present task. Namely that the monkey had to hold its wrist in one of 3 randomly instructed positions (postures) while capturing one of the 8 targets in individual trials. The wrist was either constantly pronated, supinated or held in an intermediate position. More details about the task are described in two other articles from the same laboratory (Hoffman and Strick, 1986, 1995). This ingenious paradigm allows distinguishing between two possible reference systems of coordinate to represent the direction of movements. First, if the system coordinate is <u>centered on the wrist</u>, then the preferred directions of the cells in M1 (and of the muscles in the EMG) should vary with the posture. Second, if the system of coordinate is <u>extrinsic</u> (outside the body), then the preferred directions of the cells in M1 (and of the muscles in the EMG) should not be influenced by the posture. Seven of the 27 muscles of which EMGs were recorded were active before movement onset while performing the task with the wrist joint held in a pronation (posture 1), intermediate (posture 2) a supination (posture 3) position. Their activity also varied for the 8 different directions of arm movement in the task. This is why for these 7 muscles the preferred direction (PD) was determined while the limb was in each of the three separate postures while performing the task. The authors observed that, as a consequence of a clockwise rotation of the forearm posture from pronation to intermediate and finally to supination, the preferred directions of all seven muscles rotated clockwise as well. However the shift in the preferred direction for the individual muscles was always less than 90° for the full 180° of forearm rotation (Figure 1.20 panel 1 D). As far as the muscles are concerned, the data do not support neither hypothesis one (system of coordinate centered on wrist) nor hypothesis two (extrinsic system of coordinate) but support a more complex mode of representation of direction of movements. Shifts of preferred direction (derived from activity recordings of neurons) of individual neurons can also be used to reveal how movements in space are represented at a neuronal level. Here again, the data are more complex than expected. First some neurons show an influence of the posture as they behaved like the muscles with a shift of the preferred direction (by about 70°) when the wrist changed from pronation to supination (180°), as shown in Panel 2 A in Figure 1.20 for a representative "muscle-like" neuron. In contrast (Panel 2B in Figure 1.20), some

neurons did not show any shift of their preferred direction and thus can be considered as "extrinsic-like". Kakei et al. (1999) found about 30% and 50% of "muscle-like" and "extrinsic-like" neurons, respectively. They found in addition about 20% of neurons with unsystematic shift of preferred direction.

In summary the findings of this study, described in Figure 1.20 below, show that both muscles and movements seem to be strongly represented in M1, as the data suggest that both systems of coordinates (body centered and extrinsic) are present in M1.

Panel 1
Kakei et al., 1999

Panel 2
Kakei et al., 1999

Panel 1:
- 3 wrist postures
- Movement trajectories to 8 targets
- EMG: preferred direction of 3 wrist muscles
- Prediction for ideal preferred direction vector fixed to the extrinsic coordinate system
- Prediction for ideal preferred direction vector fixed to the wrist joint coordinate system

Panel 2:
- P.D. shift=79 degrees "Muscle-like neuron" about 30%
- No P.D. shift "Extrinsic-like neuron" about 50%
- Unsystematic PD shift

Figure 1.20

Panel 1:
A: Three wrist postures (pronation (pro), intermediate (mid), and supination (sup)).
B: Comparable movement trajectories in extrinsic space to the 8 targets with the wrist held in each of the three postures.
C: Preferred directions (PD) of 3 wrist muscles derived from corresponding EMG recordings.
D: Normalized shifts of preferred direction of the three muscles (see C) with wrist rotations from pro to mid and pro to sup leading to PD shifts between 46° and 90° (mean value 79°) neither fixed to the joint nor to the extrinsic space coordinate system; preferred direction in the pro position is set to 0°.

Panel 2:
Representative raster activity recordings from multiple trials of 3 neuron in M 1 (A, B and C) showing task related PD shifts fixed to the muscle coordinate system (A), the extrinsic space (= movement) coordinate system (B) and of neurons with unsystematic PD shifts (C).

Up = up
Dn = down
Rt = right
Lf = left

1.5.4 Additional features of corticospinal neurons

With no doubt the motor cortex is mainly implicated in movement execution. But the corticospinal neurons of M1 are also modulated by sensory inputs from the body part that comprises the cell's motor field. The input-output processing in the motor cortex is based on particular characteristics. Stimulating the motor cortex normally elicits movement in the body part harboring the receptive field of the stimulated cortical area. Second all movements induced by such stimulation concern the body parts which enclose the cutaneous receptive fields implicated in the cutaneous feedback – loop of the corresponding movement. This feedback information is of great importance in manipulative movements involving the hand. As in the spinal cord reflex pathways there are proprioceptive sensory inputs which stimulate motor cortex neurons to respond in a similar reflexive way to muscle stretch and movement perturbations (Cheney and Fetz, 1984). Strick and Preston (1978) found that the sensory input to M1 is organized in a particular way. In primates cutaneous inputs preferentially target the caudal part of M1, whereas inputs from muscle spindles associateted to passive joint movements and movement perturbations dominate in the rostral part of M1. Probably Golgi tendon organs and other sensory afferents also contribute to rostral M1 input. Not only exist areas with different sensory inputs in M1 but also corticospinal output neurons targeting functionally different muscle fields. Belhaj-Saif et al. (unpublished data) developed three different tasks in a primate model to test how cortical cells of formerly identified muscle fields are implicated in a specific movement. For this purpose they recorded the activity of the corresponding cortical cells while the monkey was performing one of the three following tasks:

a) Isolated wrist movement task (preferential activation of only distal muscles)

b) Forelimb push-pull task (preferential activation of only proximal muscles)

c) Reach-to-grasp task (co-activation of distal and proximal muscles)

The results of this study demonstrated that the activity of cortical cells belonging to either the distal or proximal muscle field were modulated most during task a) or b) respectively whereas task c) modulated activities of both cortical cell groups. There is strong correlation between the cortical neurons activation and the the target musclesEMG activity, which is particularly depending of the taskt.

That corticospinal neurons are of particular importance in distal skilled movements and independent use of digits was already described in details elsewhere in the present thesis manuscript.

1.6 Cortical motor maps

Although the following chapter mainly concentrates on maps of the motor cortex (M1), the Figure 1.21 below is thought to remind the reader the most important cortical areas in primates also implicated in movement execution. Figure 1.22 demonstrates the obvious similarities of these cortical areas in nonhuman primates and humans making the nonhuman primate a pertinent animal model for investigating how movements are controlled by the brain in primates.
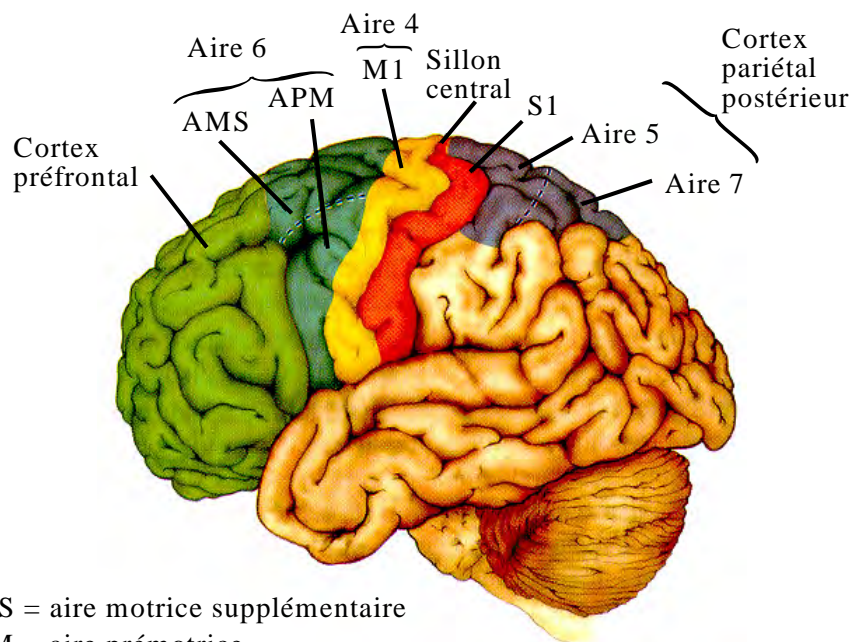
AMS = aire motrice supplémentaire
APM = aire prémotrice
M1 = cortex moteur primaire
S1 = aire somatosensorielle primaire

Figure 1.21 Cortical areas implicated in control of movement in primates.

A Human
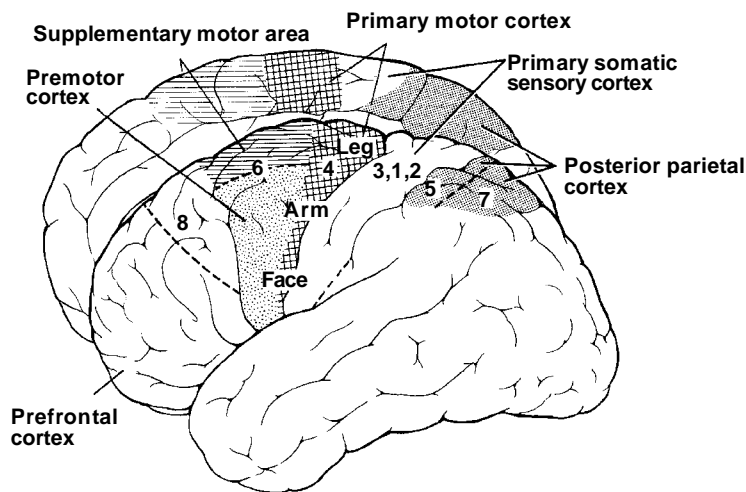
B Macaque monkey

Figure 1.22   Similarities of human and monkey cortical areas controlling movements.
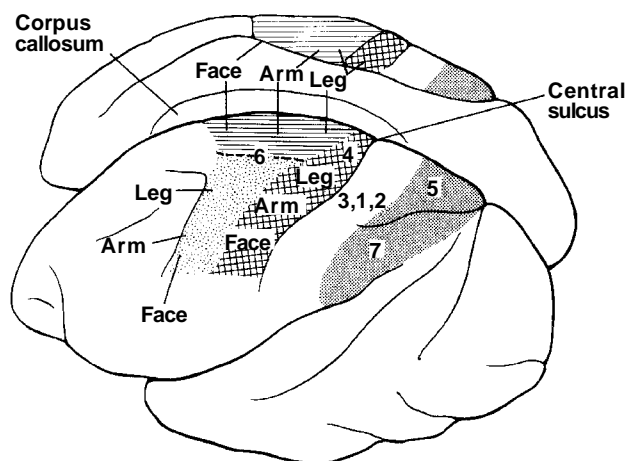
Since the first hypothesis by Hughlings Jackson (1873) assuming that the motor cortex could be systematically organized to control movements of different body parts, researchers of several epochs developed various techniques to better or more precisely map the motor cortex. Looking at their findings until today one has to realize that none of theses maps represents all features of the effective structure and functional organization of the motor cortex. Rather each type of map is better suited to demonstrate one of the various features of real motor cortex organization. So unfortunately the universal map representing the real physiological organization of motor cortex is not found yet but the knowledge about how movements are controlled by the brain has significantly increased since the first attempts of understanding. In order to categorize the multitude of maps different criteria can be chosen. In the following paragraph, I made groups of maps obtained by the use of the same electrical stimulation technique because stimulation parameters strongly influence the type of
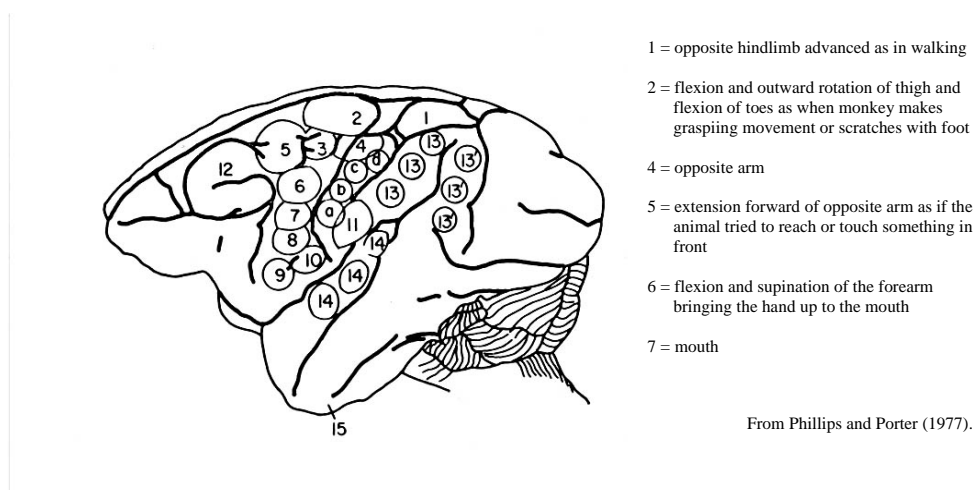
map obtained. Table 1.5 below summarizes the most important electrical parameters of the techniques used to stimulate the motor cortex. Within each group maps are basically represented chronologically with respect to the year a specific map was first published. Each map is commented to provide information about the particular features represented of the motor cortex in a specific map as well as eventual limitations and constraints of the approach used.

Cortical surface stimulation	ICMS				modified ICMS
	electrical parameters as proposed by Asanuma (1972)	threshold ICMS mapping	beyond threshold ICMS mapping	prolonged ICMS mapping (e.g. Graziano 2002) thought to induce complete natural movement sequences	Stimulus triggered averaging (StTA) mapping used to detect effects related to the most direct output pathways Cheney and Fetz (1985)
e.g. 10 ms pulses of 0.5 – 1.5 **m**A at threshold	repetitive 0.2 ms pulses of max 80 **µ**A in trains of 10 – 12 pulses at approximately 300 Hz → train duration less than 20 ms (*)	same range of electrical parameters (*); but movements are only mapped if on half of the stimulation trials the discharge of some motor units is just detected either by EMG recordings or by having enough motor units discharge to produce externally observable movement.	Mapping of ICMS responses at intensities higher than threshold intensity for a given position in the motor cortex	similar electrical parameters (*) except that trains of biphasic (+/- to prevent tissue damage) pulses used are much longer (500 ms approximating the time course of reaching and grasping movements) than in standard ICMS (max 20 ms)	similar electrical parameters (*) but single ICMS pulses acontinuously delivered at much lower frequencies (10 – 20 Hz avoiding temporal summation of high frequency used in conventional ICMS) while awake animals perform active movements. StTA is used to extract the effect of these pulses from ongoing voluntary EMG activity in the recorded muscles. Theneafter EMGs are used to map the "ICMS" induced "movements" of the corresponding muscles.→PStF maps (see below)

**Table 1.5**   Characteristic electrical parameters of different cortex stimulation methods.

a) Cortical surface stimulation

The epoch of cortical stimulation was strongly pruned by the theory of somatotopy. The idea of this theory, after several early precursor maps of the motor cortex in monkeys and apes (see Figures 1.23 and 1.24 below), culminated in the simiusculus (Figure 1.25) of Woolsey and the homunculus (Figure 1.26) of Penfield and Rasmussen. These two icons are generalized somatotopic representations derived from data recordings from several monkeys and human patients respectively. These cortical maps show a systematic, spatially organized, point – to –point mapping of control of different body parts by different pieces of M1 cortex. The size of each body part is drawn to indicate the amount of cortical tissue devoted to movements of that part. The final form of Penfield and Rasmussen's homunculus as represented in Figure 1.26 included a line representing the mediolateral ribbon of M1, broken into sequential line segments representing different body parts, down to different segments for the thumb, index, middle, ring, and little finger. Until now it remains clear that the head, upper extremity, and lower extremity have sequential and largely separated regions although the strict somatotopic representation in M1 has been challenged by recent findings revealing that representations of smaller body parts are widely distributed within these three major regions (Schieber and Hibbard, 1993). Still valid is also the view that body parts involved in the most skilled movements have the most cortical tissue devoted to their control.

1 = opposite hindlimb advanced as in walking

2 = flexion and outward rotation of thigh and flexion of toes as when monkey makes graspiing movement or scratches with foot

4 = opposite arm

5 = extension forward of opposite arm as if the animal tried to reach or touch something in front

6 = flexion and supination of the forearm bringing the hand up to the mouth

7 = mouth

From Phillips and Porter (1977).

Figure 1.23   David Ferrier's map of <u>monkey</u> brain (1876). The legend to the right only describes the muscle representations observed in the precentral gyrus corresponding to M1. Although Ferrier already at his time explored other cortical areas in the monkey brain as can be seen from the figure above.
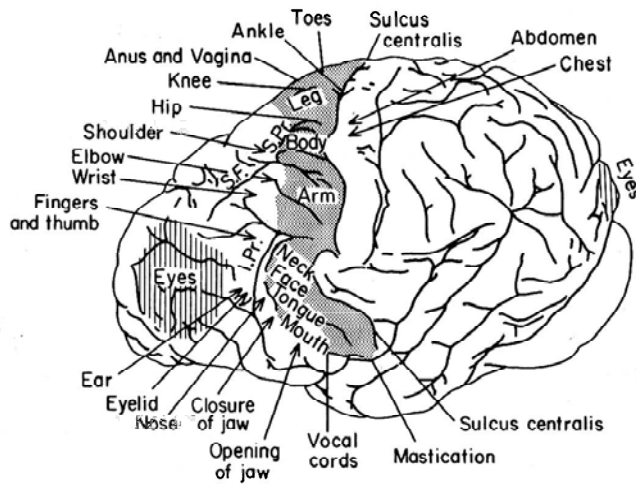
Motor map of the left hemisphere of a chimpanzee (Sherrington, 1906)

From Phillips and Porter, 1977

Figure 1.24   Sherington's map of <u>ape</u> brain (1906).

One of the earliest maps representing in detail the somatotopical representation of muscles in the precentral gyrus (M1 corresponding to area4) of non human primates.
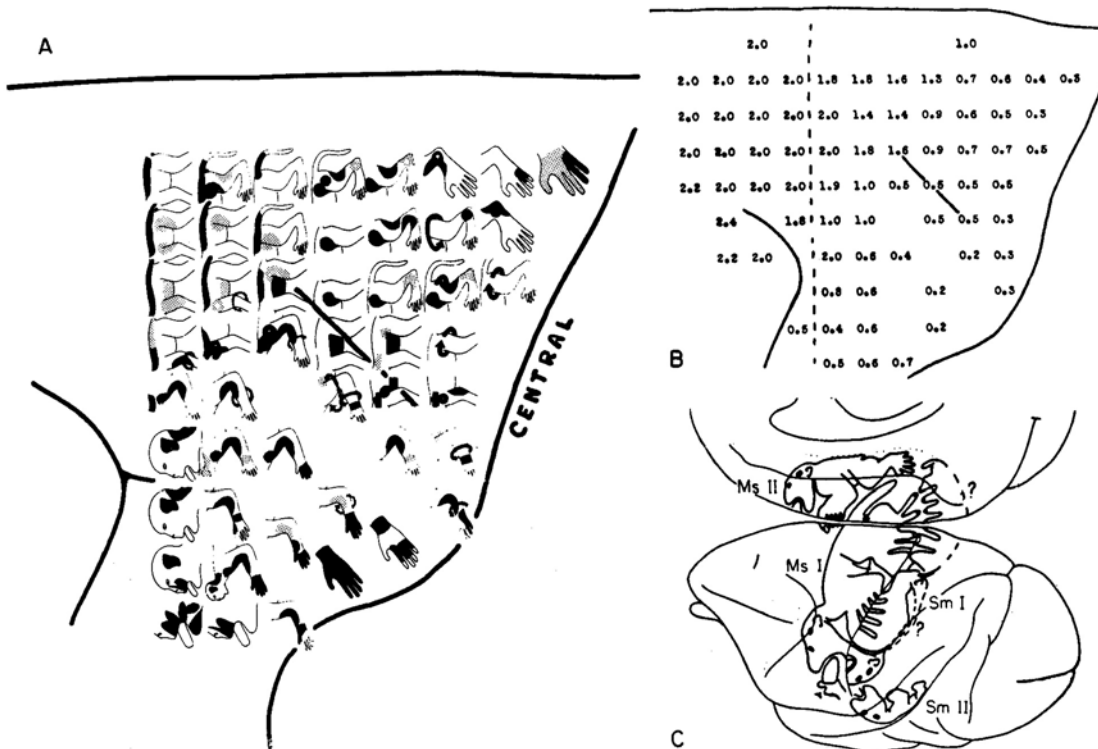

Figure 1.25 (A) Motor figurines showing responses evoked by near threshold stimulation of the surface of the monkey's cortex with sinusoidal alternating current in trains of 2-sec duration at 2-min intervals. (B) Near threshold current intensities in mA (RMS) used to evoke the movements illustrated in A. (C) "Simunculus" overlying the dorsolateral and medial surfaces of the monkey brain showing representations in primary motor (Ms I) and supplementary (Ms II) motor areas. Sm I and Sm II indicate somatosensory receiving areas. Areas marked eyes yielded conjugate movements of the eyes when faradic stimulation was applied. Data from Woolsey *et al.* (1952) and Woolsey (1964) as redrawn in Phillips and Porter (1977), used with permission.

Figure 1.2   Simiusculus of Woolsey (1952).
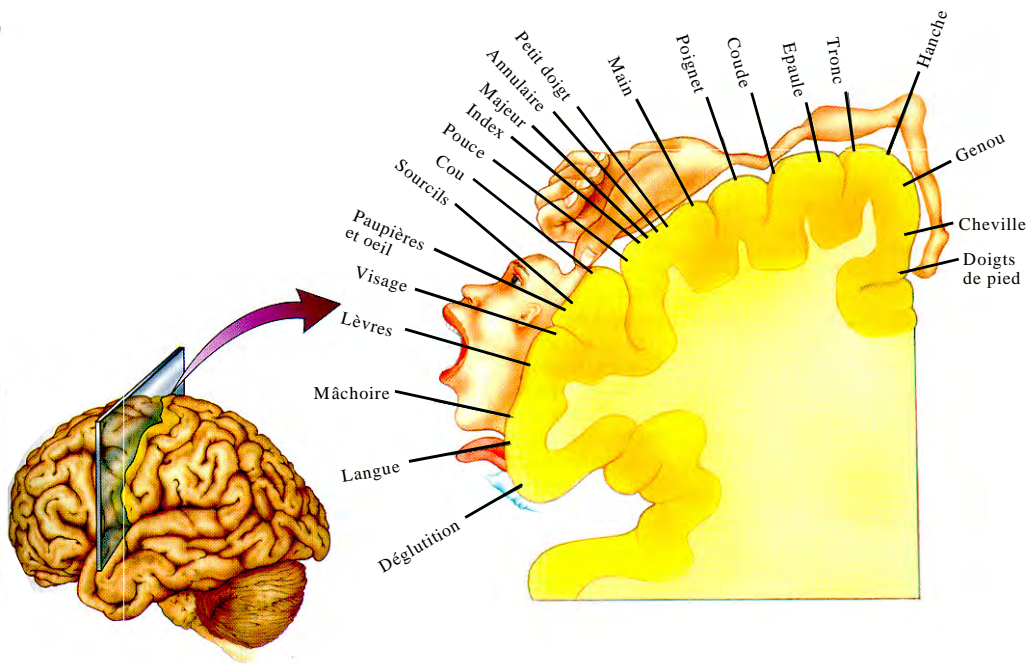
Figure 1.26   Homunculus of Penfield and Rasmussen (1950).

Somatotopic representation of muscles in the precentral gyrus controlling different body parts as derived from weak electrical stimulations in humans in the primary motor cortex (area 4).The representations of face and hand muscles cover more than the half of the surface in the precentral gyrus. The muscles of the arm, the trunk and the leg are situated more medial and are clearly less represented.

b) Classical ICMS as proposed by Asanuma (1972)

Classical ICMS technique was developed because the formerly used cortical surface stimulation had a limited resolution because of current spread. So, one of the aims was to reduce the current spread to a minimum with the intention of stimulating only direct corticospinal pathways originating in layer V of the motor cortex. Comparing maps produced by ICMS with older maps of cortical surface stimulation one has to conclude that they resemble each other in many features although the resolution in ICMS is clearly better. But in both only 3 somatotopic distinct regions (head, forelimb, and hindlimb) can be distinguished whereas the intra-territorial overlap persists also in maps derived from ICMS data. So Penfield's homunculus (Figure 1.26) is a legitimized simplification applicable also to ICMS maps. Naturally researchers wondered why they could not eliminate the overlaps within the 3 cortical territories. There are technical as well as physiological and anatomical reasons for the overlaps. From a technical point of view Stoney et al. (1968) demonstrated that in cat ICMS indeed excitates a small limited cortical area within a radius of 88 µm consisting of about 28 pyramidal neurons. But three other mechanisms constrain this: First intracortical collaterals of pyramidal tract axons (spread up to 1 mm away from the soma (Asanuma et al., 1976) and second indirect trans-synaptic excitation over much greater distances inducing the

44

greatest part of the descending volleys produced by ICMS (Jankowska et al., 1975). Third the frequency of stimulation used in ICMS (200-400 Hz) produces a temporal summation of such trans-synaptic excitation (Jankowska, 1975; Asanuma et al., 1976). But in spite of these constraints today ICMS is one of the most frequently and most reliable techniques to map rapidly and with good resolution the motor cortex of mammals.

c) Modified ICMS techniques

- #### Stimulus – triggered averaging (StTA) as proposed by Cheney and Fetz 1985

    In 1993, Schieber and Hibbard showed that the *neuronal activity* related to individuated finger *movements* or individuated joint movements is not compatible with somatotopy inside the forearm area of macaque monkeys. Rather there was a complete overlap of cortical regions activated during such movements. These findings led to the hypothesis of a cortical within limb representation in the form of a nonstandard piano keyboard better suited to represent the multidimensionality of limb movements (see Figure 1.27 below). In such a representation each joint or finger movement is represented several times allowing many more and even new combinations of movements than in an arrangement in which every single movement is only represented ones. In addition to that in the case of cortical injury a particular movement is not completely lost because healthy regions representing the same movement can compensate for the lost function. In contrast to these findings *activity of individual muscles (EMGs)* belonging to different forelimb joints induced by cortical stimulations in StTA revealed a consistent intra – forelimb somatotopy in macaque monkeys as represented in Figure 1.28 below from Park et al. (2001). Maps are derived from StTA of EMG activity from 24 muscles of the forelimb in macaque monkeys performing a reach and prehension task. The two maps in which the cortical surface was unfolded and represented two-dimensionally (see Method part of this thesis) show a consistent pattern in the representation of distal (wrist, digit, and intrinsic hand) and proximal muscles (shoulder and elbow).

Figure 1.27: Cortical pianos. *A*: the standard piano keyboard constitutes a well-ordered map of musical notes. Here the 42 white keys have been colored to distinguish each of them. Although the strict order and single representation make it easy to locate each note, these same features make it impossible for a pianist to play certain combinations of notes, such as the 5 notes marked by black dots beneath. *B*: a nonstandard keyboard can be created by re-representing each note at multiple locations and in a wide variety of orders. While this arrangement appears more complex, with each note represented over a wide territory that overlaps with the territories representing many other notes, this distributed organization provides ready access to many more combinations of notes than the standard keyboard. The 5 adjacent notes marked by black dots in *B,* for example, are the same notes indicated in *A*.

From Schieber (2001).
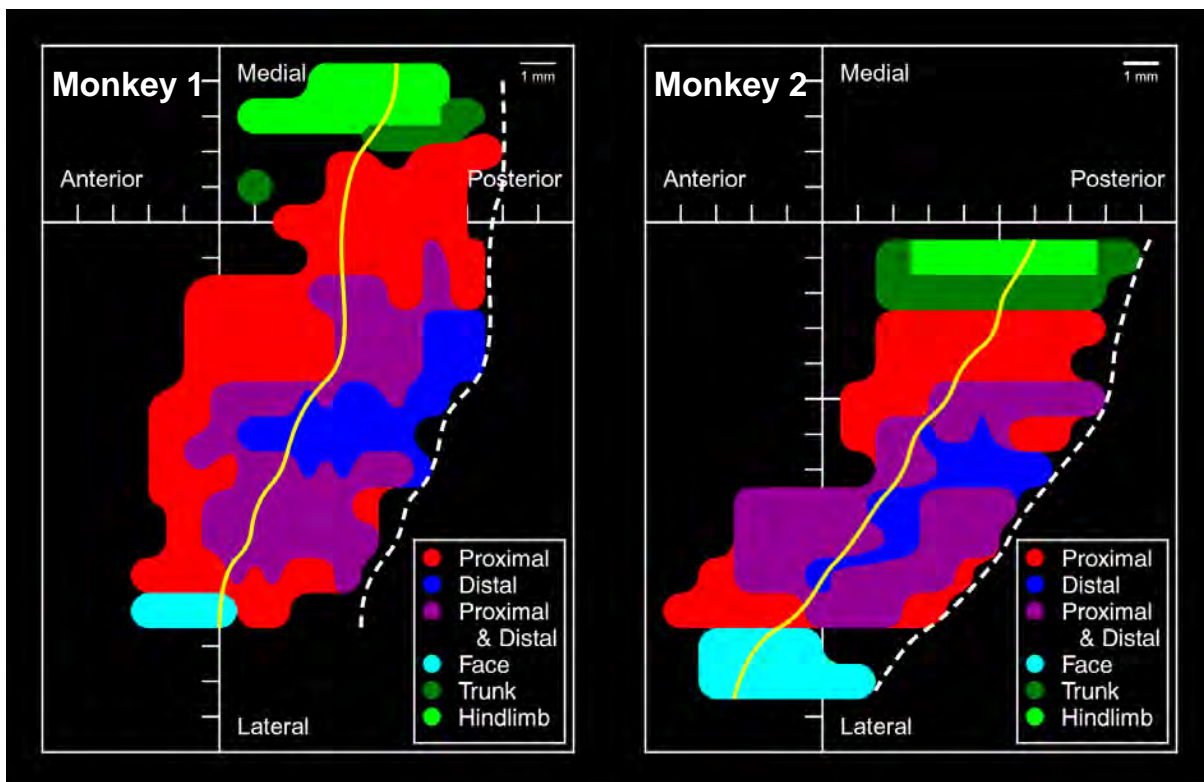
Figure 1.28   Motor cortical PStF maps of two monkeys (Park et al., 2001).

The maps of monkey 1 and monkey 2 are represented in two dimensional coordinates after unfolding the precentral gyrus. The yellow lines indicate the fundus of the central sulcus whereas the white doted lines indicate the caudal border of the central sulcus at the surface of the brain. Note the core distal representation (blue) located largely in the bank of the precentral gyrus and extending to the border of cortical area 3a (S1). The distal representation is surrounded by a horseshoe-shaped representation of proximal muscles (red). The two zones are separated by a large zone where sites produced facilitation of both distal and proximal muscles (purple). Maybe this zone is implicated in muscle synergies during coordinated multijoint movements (e.g. extending the limb)

46

- *Prolonged ICMS as proposed by Graziano (2002)*

Different from all other maps presented in this part the maps in Figure 1.29 below were obtained by high frequency ICMS applied for long durations (500 ms). The authors stimulated M1 as well as premotor areas of monkeys by this method. Such stimulations induced complex quiet natural movement sequences of the upper limb and the head. The resulting maps were completely different from all what has been seen before. In spite of cortical movement or muscle representations by this method the motor cortex (M1 and premotor areas) has to be seen as a central representation of a unified workspace around the monkey's body. Graziano et al. (2002) defined three subregions within this workspace with different functions.

1.   Subregion bringing the contralateral hand to locations in front of the chest matching the natural behavior of monkeys manipulating objects within the central space. The area corresponds to the forelimb representation of M1.

2.   Subregion corresponding to hand locations at the mouth coupled with opening of the mouth. This area reflects feeding behavior of the monkey and corresponds to the cortical area defined as PMv (F5).

3.   Subregion named polysensory zone responding to tactile stimuli on the face and arms, and visual stimuli near the face and arm in a defensive manner.
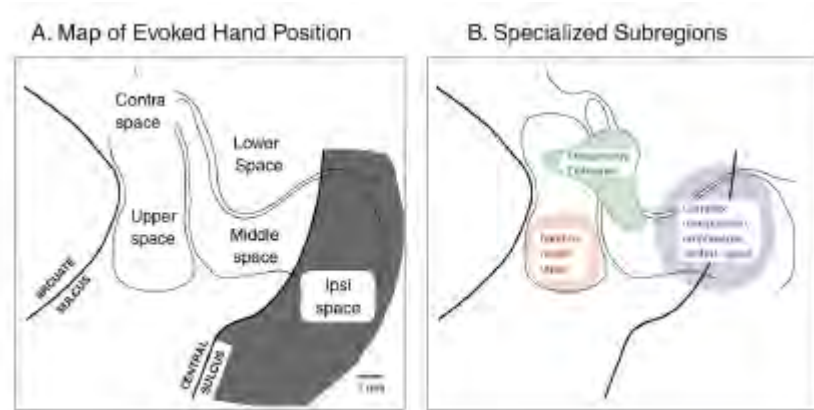
Figure 1.29   Posture maps obtained with prolonged high frequency ICMS in monkeys (Modified from Graziano et al. 2002).

(A) Stimulation at different cortical sites caused the hand to move to different positions in the space around the body. The shaded region indicates the buried cortex in the anterior bank of the central sulcus.

(B) Subregions within the map of hand position that had specialized properties. The region labeled "Polysensory, defensive" (green) may correspond functionally to the dorsal part of area F4. The region labeled "Hand-to-mouth, grasp" (red) may correspond to part of area F5. The region labeled "Complex manipulation, emphasizes central space" (blue) may correspond to the representation of the fingers in Woolsey's map (see Figure 1.25 above). It also may correspond to the primary motor forelimb representation.

d) Activity recording derived maps

Details about what information can be deduced from this type of maps were already described elsewhere in this thesis (see 1.2.1; Schieber and Hibbard, 1993).

e) Cortical maps derived from retrograde tracing studies

As demonstrated by He et al. (1993) and Dum and Strick (1991), it is also possible to map the motor cortex by the mean of anatomical tracing. From their studies they were only able to map connections to the forelimb representations of the motor cortex, because their histological analyses were limited to the cervical segments of the macaque monkey. Maps summarizing the data from both studies are represented in Figure 1.30 A and B below. But the present examples show that anatomical tracing techniques are particularly suited to reveal *connections* between the cortex and corresponding motoneurons in the spinal cord rather than to proof functionality of such connections. From this point of view electrophysiological mapping and anatomical mapping are complementary techniques crucial for the understanding of the motor system in primates.
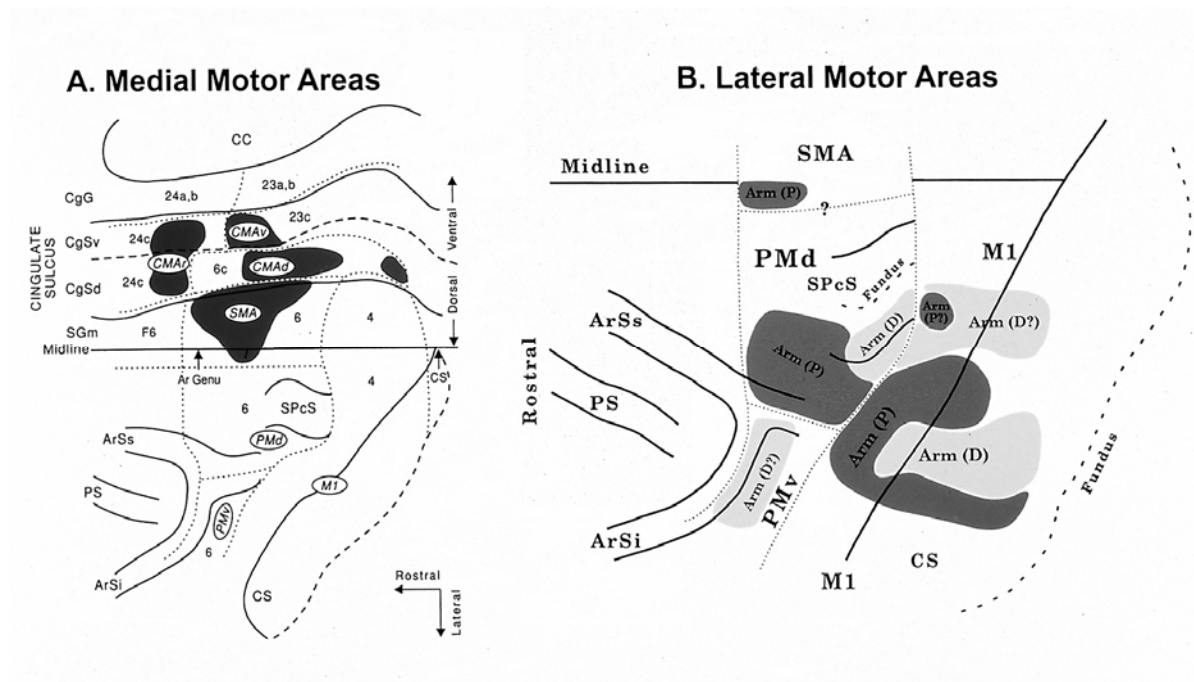
Figure 1.30 Origin of corticospinal projections from motor areas targeting forelimb motoneurons in the macaque monkey (from Cheney et al 2002).

(A)   Origin of corticospinal projections from the motor areas on the *medial* wall of the hemisphere.

This reconstruction of the frontal lobe of a macaque brain indicates the origin of corticospinal neurons (*shaded regions*) that project to the cervical segments of the spinal cord. In this view, the medial wall is unfolded and reflected upward to reveal the cingulate sulcus. The anterior bank of the central sulcus is also unfolded. A *dashed line* marks the fundus of each unfolded sulcus. The centers of the different cortical motor areas are designated by the *circled letters*. The boundaries between the motor areas and cytoarchitectonic areas (identified by *numbers*) are denoted with *dotted lines*. *Ar Genu* (with *arrow*), Level of the genu of the arcuate sulcus; *ArSi*, inferior limb of the arcuate sulcus; *ArSs*, superior limb of the arcuate sulcus; *CC*, corpus callosum; *CgG*, cingulate gyrus; *CgSd*, dorsal bank of the cingulate sulcus; *CgSv*, ventral bank of the cingulate sulcus; *CMAd*, cingulate motor area on the dorsal bank of the cingulate sulcus; *CMAr*, rostral cingulate motor area; *CMAv*, cingulate motor area on the ventral bank of the cingulate sulcus; *CS*, central sulcus; *M1*, primary motor cortex; *PMd*, dorsal premotor area; *PMv*, ventral premotor area; *PS*, principal sulcus; *SGm*, medial portion of the superior frontal gyrus; *SPcS*, superior precentral sulcus; *SMA*, supplementary motor area. Adapted from Dum and Strick (1996).

(B) Proximal and distal representation in the arm areas of the primary motor cortex and the premotor areas on the *lateral* surface of the hemisphere. This map is based on the peaks in the distribution of corticospinal neurons labelled following tracer injections into lower cervical and upper cervical segments. Abbreviations as in A, (Modified from He et al 1993 and Dum and Stick 1996).

f) Findings from a anterograde tracing study

Dum and Strick (1996) used the anterograd tracer wheat germ agglutinin – horseradish peroxidase in macaque monkeys, to examine the pattern of spinal termination of efferents from M1, SMA and CMAd and CMAv. They only investigated the termination pattern in the cervical segments. Originating from all four areas investigated they found direct connections terminating in the ventral horn (region of α-motoneurons) as well as in the intermediate zone of the spinal cord.

Consequently they concluded that all four motor areas injected with anterograd tracer must have direct connections with spinal motoneurons, particularly those innervating muscles of the fingers and wrist. Therfore SMA, CMAd and CMAv have the potential to generate and control movement at the level of the spinal cord and may provide an anatomical substrate for the recovery of motor function that follows damage to M1.

1.7 Plasticity of motor cortical maps

The "phenomenon" plasticity alone has always been a subject of conflicting discussion in neuroscience, in terms of when during life span it can occur and which anatomical parts of the CNS could potentially participate or not in such plastic changes. More recently the mechanisms of plasticity became more important in the context of recovery after CNS damage. In 1981, Tsukahara published a review entitled "Synaptic plasticity in the mammalian central nervous system", describing the basic principles, mechanisms and the morphological correlates of plasticity (for details see Table 1.6 below).

Type of plasticity	Description, physiology and morphology	Time course of reorganization after induction	Effect

Plasticity of synaptic transmission	*Long-term potentiation:*
	Produced by relatively low frequency stimulus trains (10 to 20 Hz)
	Possible mechanisms:
	    increase in the size of afferent volleys
	    increase in the excitability of the cell population
	    increased synchrony of cell firing
	    increased efficacy of synaptic transmission due to: higher postsynaptic sensitivity to transmitters, increased transmitter release or increased postsynaptic membrane resistance
	Morphological correlates:
	    Enlargement of dendritic spines and spine stems
		immediately	persists Minutes, hours up to several days

Axonal sprouting and formation of new synapses	*First discovery / evidence of sprouting in the central nervous system:* (Liu, C. N., Chambers, W. W. 1958. Intraspinal sprouting of dorsal root axons. *Arch. Neurol. Psychiatry* 79:46-61)
	
	Morphology:
	    Degree and extent of sprouting are more marked in the neonatal CNS than in the adult CNS in which sprouting is limited to the territory of the dendritic field of the deafferented neurons.
	    Sprouting is also less extensive in adult than in young animals
	    New synapses are formed on partially deafferented spinal neurons after **spinal hemisections** in adult rats, monkeys and humans. (Bernstein, J. J., Bernstein, M. E. 1971. Axonal regeneration and formation of synapses proximal to the site of lesion following hemisection of the rat spinal cord. *Exp. NeuroL* 30:336-51
	Bernstein, J. J., Bernstein, M. E. 1973a. Neuronal alteration and reinuervation following axonal regeneration and sprouting in mammalian spinal cord. *Brain Behav. Evol.* 8:135-61 Bernstein, M. E., Bernstein, J. J. 1973b. Regeneration of axons and synaptic complex formation rostral to the site of hemisection in the spinal cord of the monkey, *lnt. J. Neurosci.* 5:15-26)
	
	    Sprouting and synaptic reorganization in the motor part
		Two phases:
		    initial rapid phase: initial signs of sprouting can be observed within two weeks post lesion
		    Slower second phase: lasting for several months
		    *Attention!! Priming lesions can modify the time course (*Scheff, S. W., Bernado, L. S., Cotman, C. W.
		1978. Effect of serial lesions on sprouting in the dentate gyms: Onset and decline of the catalytic effect. *Brain Rex*
			can persist for the whole live span

	of CNS occur at a **spinal level** as well as at a **cortical level**	150:45-53)	
	Degeneration is not necessary for induction of sprouting (Brown, M. C., Ironton, R. 1977. Motor neurone sprouting induced by prolonged tetrodotoxin block of nerve action potentials. *Nature* 265:459-61; Tsukahara, N., Fujito, Y. 1976. Physiological evidence of formation of new synapses from cerebrum in the red nucleus neurons following cross-union of forelimb nerves. *Brain Res.* 106:184-88). and occurs widely in the central nervous system. Sprouting provides an important neuronal basis for recovery after brain damage, learning and memory *Physiological importance:* New formed synapses are functionally effective and synaptic transmission is comparable to normal synapses, although slight differences can be observed (.Tsukahara, N. 1980. Synaptic plasticity in the red nucleus neurons. *Proc. 28th Int. Congr. Physiol. Sci. Budapest, 1980.* In press ; Murakami, F., Tsukahara, N., Fujito, Y. 1977b. Properties of synaptic transmission of the newly formed corticorubral synapses after lesion of the nucleus interpositus of the cerebellum. *Exp. Brain Res.* 30:245-58 Spontaneous rewiring of CNS as a consequence of axonal sprouting is functional and responsible for the observed recovery (ex Florence M Bareyre et al; The spinal cord spontaneously forms a new intraspinal circuit in adult rats; Nature Neuroscience Volume 7 Number 3 March 2004)		
Plasticity of neuronal networks	Is defined as the plasticity that can not be attributed to changes at cellular level. Reverberating circuits as proposed by Forbes in 1922 (Forbes, A. 1922. The interpretation of spinal reflexes in terms of present knowledge of nerve conduction. *PhysioL Rev.* 2:361-414) for the spinal cord may be one mechanism at its basis. Short term memory may also be based on such circuits.		

Table 1.6   Basic principles, mechanisms and morphological correlates of plasticity (Tsukahara, 1981).

Approximate time course of morphological changes in the motor cortex opposite the lesions
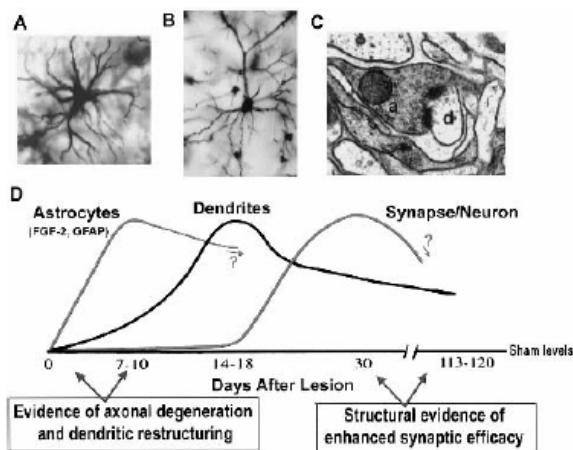
(A) Astrocyte (a subtype of glial cell) immunostained with glial fibrillary acidic protein (GFAP).

(B) Dendritic processes of a pyramidal neuron in the motor cortex.

(C) Synaptic connection including an axonal (a) and dendritic (d) process.

(D) Unilateral lesions of the sensorimotor cortex result in a sequence of glial and neuronal changes, including increases in the astrocytic expression of the neurotropic factor fibroblast growth factor-2 (FGF-2) GFAP increas es in dendritic processes and increases in synapse number per neuron.

Modified from
Theresa A. Jones, Scott D. Bury, DeAnna L. Adkins-Muir, Linslee M. Luke, Rachel P. Allred, and Jon T. Sakata
Importance of Behavioral Manipulations and Measures in Rat Models of Brain Damage and Brain Repair
ILAR, Volume 44, number 2, 2003 p 146

Figure 1.31 above shows in a representative graphic (D) the time course of morphological changes occurring in the motor cortex as a consequence of a cortical lesion. The post-lesion changes are illustrated in the motor cortex opposite to the lesion. Note, that in the ipsilesional motor cortex, similar morphological changes occur in the intact cortical tissue just adjacent to the lesion core. Typical morphological changes are illustrated by 3 photomicrographs (A-C).

Later, Donoghue (1995) defined plasticity as the ability of the nervous system to adapt to environmental challenges or to compensate for lesions. The mechanism of plasticity is crucial for the observed reorganization of sensory and motor systems of primates and other mammals after any type of damage. To correctly interpret and compare normal and reorganized maps of sensorimotor cortex, assessment should include both the changes in the somatotopic pattern and the current intensity used to produce that pattern. This is because low currents and short sequences of pulses elicit movements and twitches in individual muscles whereas high currents and long trains of pulses rather elicit complex sequences of movements involving multiple muscles (Graziano et al., 2002). Last but not least, plasticity is also the basis of different forms of learning in continuously varying contexts.

## 1.7.1 Injury induced plasticity

1.7.1.1 Amputation

As amputations fortunately are very rare events in primate research, all our knowledge about them is based on a limited number of studies in which the motor cortex contralateral to the amputation was compared to normal animals. This type of injury induced a major loss of motor neuron targets for M1 as well as a loss of somatosensory feedback to area 3a (from muscle spindles, thalamus) and 3b = S1 proper (cutaneous receptors).

The organization of M1 of monkeys with longstanding amputations was explored by means of ICMS. In one study (Wu and Kaas; 1999), changes in area 3a and PMd were investigated, in a limited number of animals. The common findings of one study in squirrel monkeys and galagos (Wu and Kaas, 1999) and two studies in macaques (Qi et al., 2000; Schieber and Duel, 1997) can be summarized as follows:

First, the age at which the amputation happened does not seem to have an influence on the post-injury reorganization in M1, area 3a and PMd. Second, primates do not differ in mechanisms of motor system reorganization as similar results were obtained in prosimians (galagos), new world monkeys (squirrel monkey) and old world monkeys (macaques). Third, extensive losses of motor neuron targets induced by limb amputations are followed by alterations in the motor system that allow the deprived forelimb or hindlimb portion of the corresponding motor area (M1, area 3a, PMd) to become fully devoted to stump movements. So muscles of the remaining stump are overrepresented as compared to normal animals. Fourth, the threshold currents needed with ICMS to induce movements in the muscles of the stump were comparable to the threshold currents for the same cortical areas in normal animals. The figure below summarizes these findings.
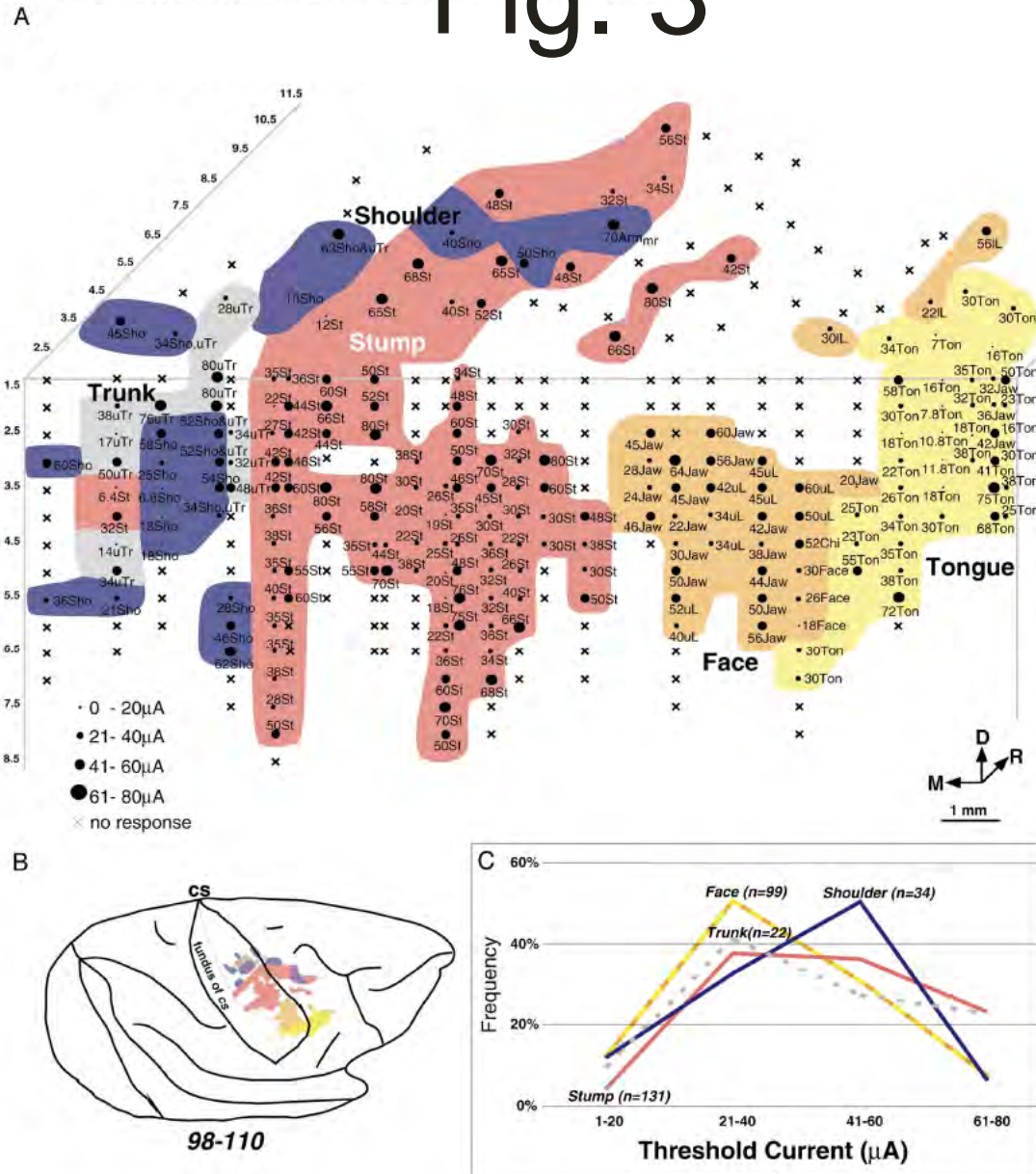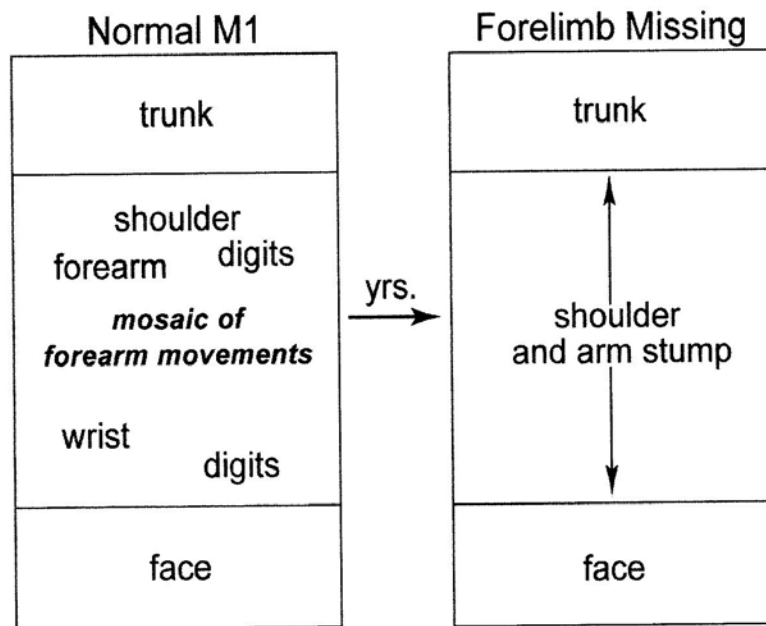
Fig. 1
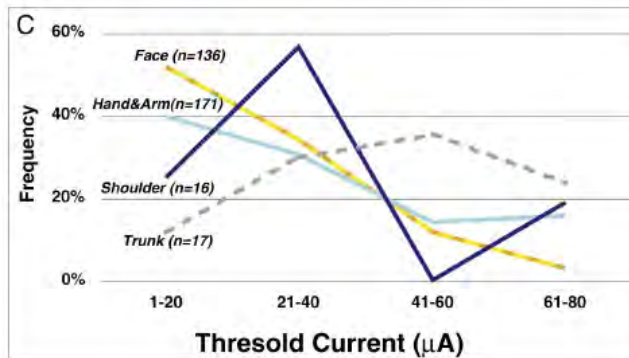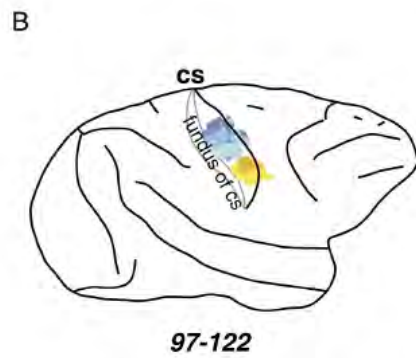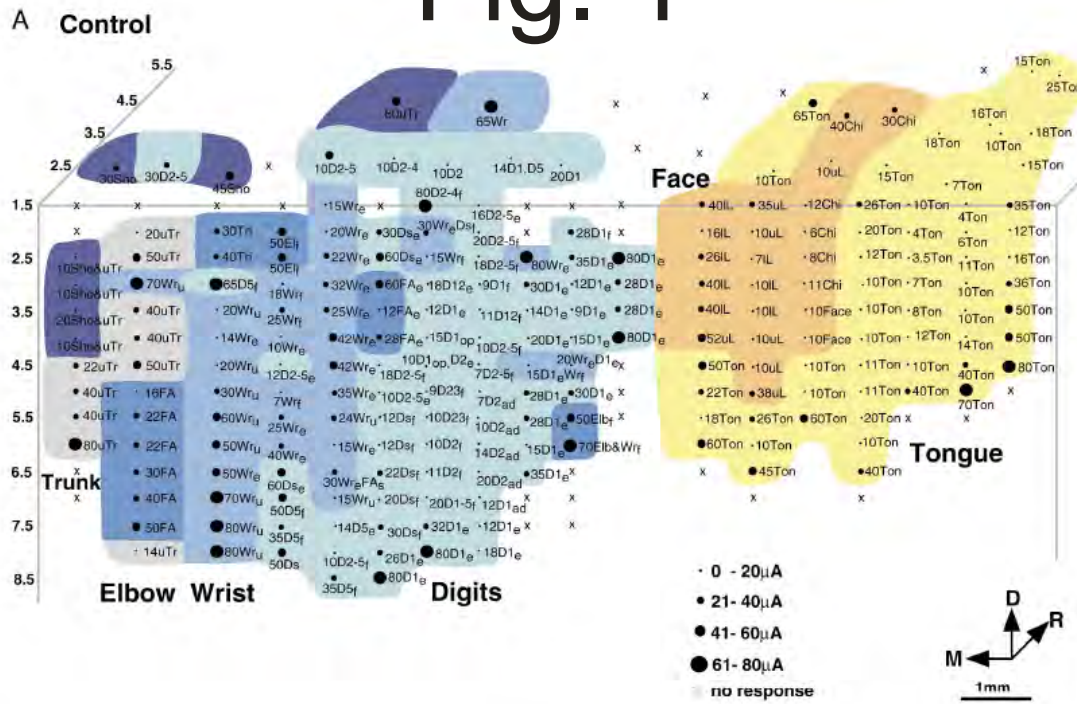
Fig. 2
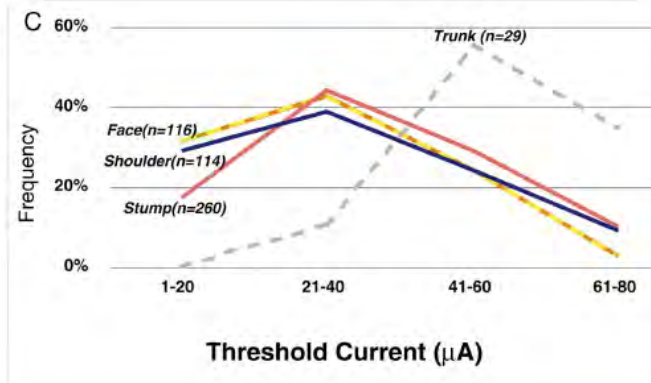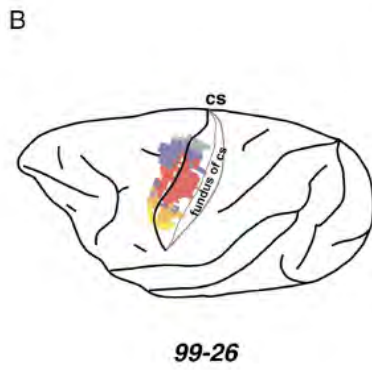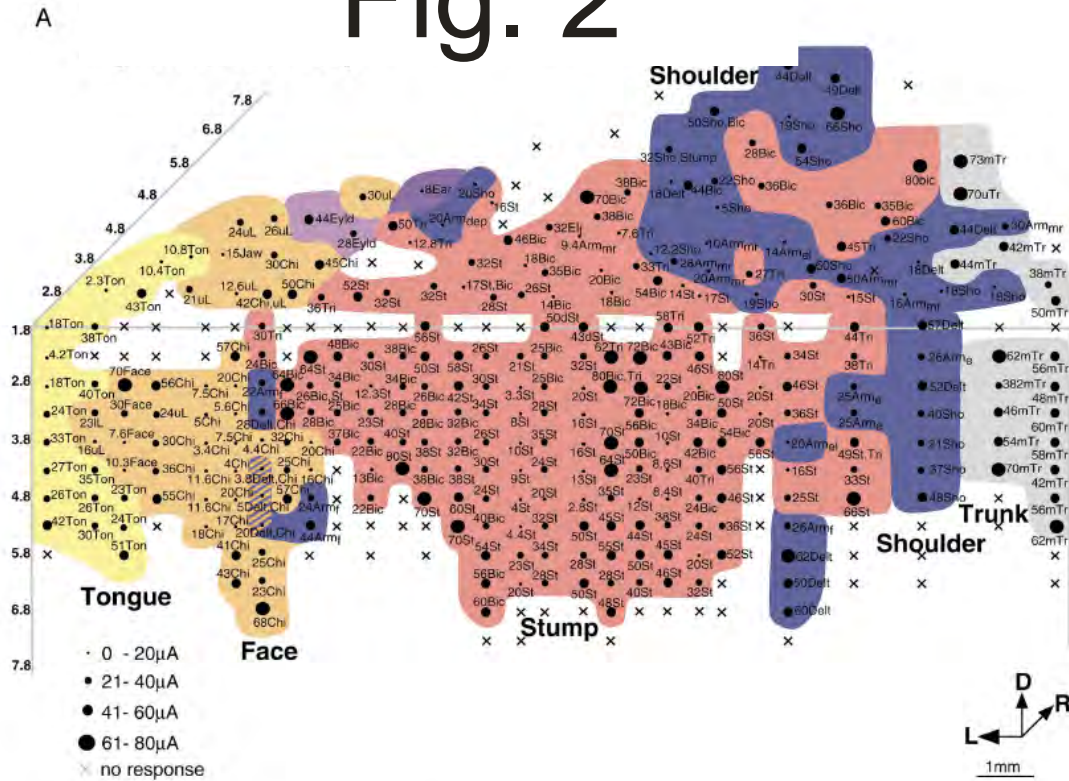
Fig. 3

Fig. 4

Figure 1.32

A (Fig.1). Motor cortex organization in a normal macaque monkey.
B (Fig.2). Motor cortex organization in a macaque monkey amputated at the age of 5 months (infant).
C (Fig.3). Motor cortex organization in a macaque monkey amputated at the age of 2 years (CNS entirely developed).
D (Fig.4). Long-term changes in M1 somatotopic pattern in forearm amputated primates.

A: movement and current thresholds for stimulation sites throughout lateral M1. This partial motor output map includes the representation of the face to the upper trunk. Microstimulation sites are marked by dots. For each mapping site, size of the dot indicates the current threshold in µA and the type of response elicited at threshold.
An, ankle; cs, central sulcus; Bic, biceps; Chi, chin; Che, cheek, D, dorsal; D1-5, digit 1, 2, 3, 4, 5; El, elbow; Eyld, eyelid; FA, forearm; Glu, gluteus; H, hip; Kne, knee; L, lateral; lL, lower lip; lTr, lower trunk; M, medial; mTr, middle trunk; Nec, neck; R, rostral; Sho, shoulder; Tri, triceps; uArm, upper arm; uL, upper lip; uTr, upper trunk; Ton, tongue; Wr, wrist; ab,abduction; ad, adduction; dep, depression; e, extention; el, elevation; f, flexion; mr, medial rotation; opp, opposition; p, pronation; r, radial deviation; s, supination; u, ulnar deviation.
B: a lateral view of the brain with central sulcus opened showing the region investigated with microstimulation.
C: distributions of threshold currents for different body representations. The number in parentheses indicates the number of mapping sites for movement of that body part.
 (Modified from Qi et al., 2000)

1.7.1.2 Spinal cord lesion

Similar to amputations (see above) and peripheral nerve cuts (Sanes et al., 1988), spinal cord lesions can be considered as triggers for limited self repair in the adult central nervous system of higher vertebrates. The mechanisms behind the observed recovery are linked to the plasticity of the adult CNS in all its variants as already described in detail above. The plastic changes are not only induced at spinal level, but also at a cortical level. As a consequence, rearrangements of the sensory

and motor representation maps of the cortex parallel plastic changes. Because these rearrangements are often the basis of partial recovery, research communities all over the world are interested in better understanding how cortical plasticity and post spinal lesion recovery are linked. For this purpose most studies compared a normal map of the sensorimotor cortex to a modified post injury map and attempted to relate changes to the observed behavioural recovery. For example, Galea and Darian-Smith (1997a,b) described the deficits and recovery of motor control associated with a hemisection of the cervical spinal cord at C3 level in new born and juvenile monkeys. Monkeys were trained in a reach-and-retrieve manual task. To get a reward the monkeys had to use precision grip opposing the pads of index finger and thumb. Immediately after a unilateral cervical spinal cord section between C3 and C6 a severe flaccide hemiparesis of the lesion attained hand was observed. But in spite of that a rapid but incomplete of the hand function was observed. Within about 30 days monkeys started to use the impaired hand to pick up objects. Within another 60 days monkeys were quite dexterous although an impairment persisted all over the 150 weeks of post-lesion follow-up. The main impairments were the following:

- Less direct trajectory used in reaching.

- Loss of preshaping of the separated index finger and thumb prior to grasping the target object.

- Weakening of the oppositional force that could be developed between the pads of the index finger and thumb.

At a histological level the persistent post – lesion impairment could be attributed to the subsequent observation:

- Profound reduction in the corticospinal and rubrospinal projections to the hemicord caudal to the lesion.

Nevertheless few corticospinal axons spared by the lesion were observed to bypass the lesion by descending in the contralteral hemicord and the passing the midline caudal to the lesion. The authors also reported that a few corticospinal axons may also have bypassed the lesion in the ipsilateral ventromedial column when this was not fully interrupted by the lesion. In contrast contralateral to the lesion no significant alterations in the corticospinal projections were detected as compared to normal monkeys. The corticospinal patterns just described remained stable throughout the whole recovery period of 2 years. The authors therefore concluded that in both juvenile and adult monkeys post-lesion there was no substantial reconstruction of corticospinal projections. The authors hypothesized that the initial remarkable but not complete recovery could be explained by

two mechanisms: First, optimizing the transmission of information from the cortex to the spinal cord by the substantially reduced populations of corticospinal neurons and corticobulbospinal projections and/or second, by a more effective use of the spinal circuitry regulating the more stereotyped elements of the manual task.

The study of Galea and Darian-Smith (1997) did not address the issue of how functional recovery and progressive plastic changes are correlated. This could be done by comparing maps at different times of the recovery period. In a first incomplete attempt in this direction, Jain et al., (1998) studied the reorganization of the sensorimotor cortex maps after spinal cord injury in monkeys at several times but unfortunately without parallel analysis of functional recovery. To address the question of reorganization in M1 after spinal cord injury, Fouad et al. (2001) studied rats in which the corticospinal tract was cut at the lower thoracic spinal cord. The findings of this study attribute the observed slow reorganization in M1 to the growth of new connections so that corticospinal axons reached new motor neuron pools. The mechanism underlying such plasticity was axonal sprouting of corticospinal axons of the reorganized hindlimb portion of M1 into the cervical spinal cord. This conclusion was based on the observation that ICMS of the former hindlimb cortex produced whisker, forelimb and trunk movements only after 4 weeks of recovery excluding other potential more rapid mechanisms.

Later, Schmidlin et al. (2004) investigated the time course of M1 reorganization by studying on a weekly time interval the correlation between functional recovery and progressive plastic changes of the M1 hand representation contralateral to a lesion of the cervical pre- and post- cord of macaque monkeys. The two ICMS maps on the left in Fig. 1.5.2 show the consequences of the cervical hemi-section on the hand representation in the contralesional motor cortex, as seen at two time points pre-lesion and 4 months post-lesion. Obviously the hand area in the contralesional hemisphere was substantially reduced in size as a result of the cervical lesion, as seen 4 months post-lesion. During 1-2 weeks post-lesion, the hand area disappeared and then, in parallel to the functional recovery, a few digit ICMS sites progressively re-appeared as indicated by the red marked post lesion hand area. In the right part of Fig. 1.5.2, the changes in ICMS responses with time of two representative electrode tracks, one within the post-lesion hand area (track A) and one outside this area (track B) are represented more in detail. In contrast to track B, in which post-lesion finger responses disappeared, in track A finger movements reappeared on day 27 post-lesion and persisted over time. The time course of these changes is in accordance with the results of Fouad et al. (2004) in the rat. Therefore, the reported plastic changes by Schmidlin et al. (2004) may also be the effect of axonal sprouting of corticospinal axons of the reorganized hand area of M1 into the cervical spinal cord.

Dynamic plasticity of the hand area in M1 following cervical lesion parallels spontaneous recovery of manual dexterity
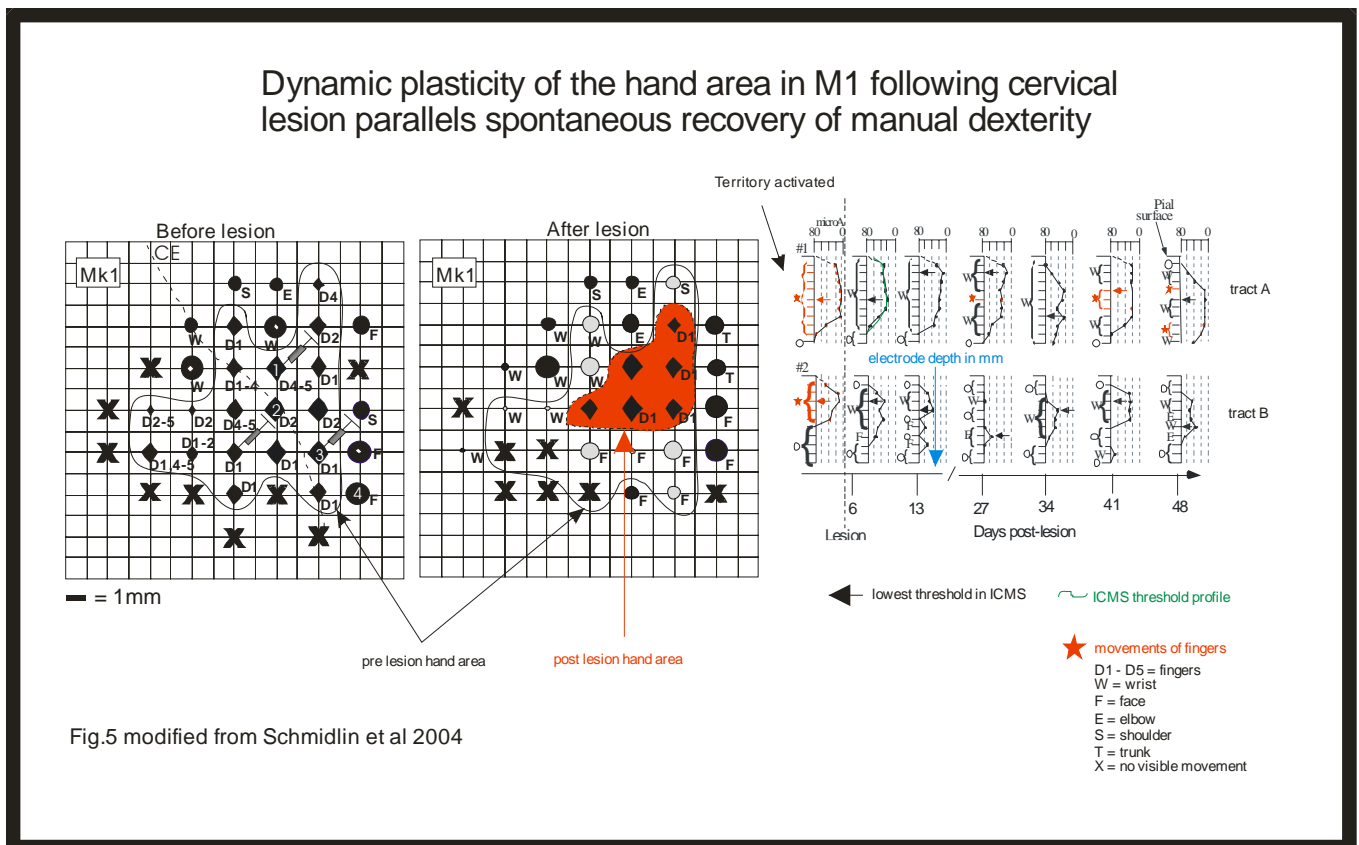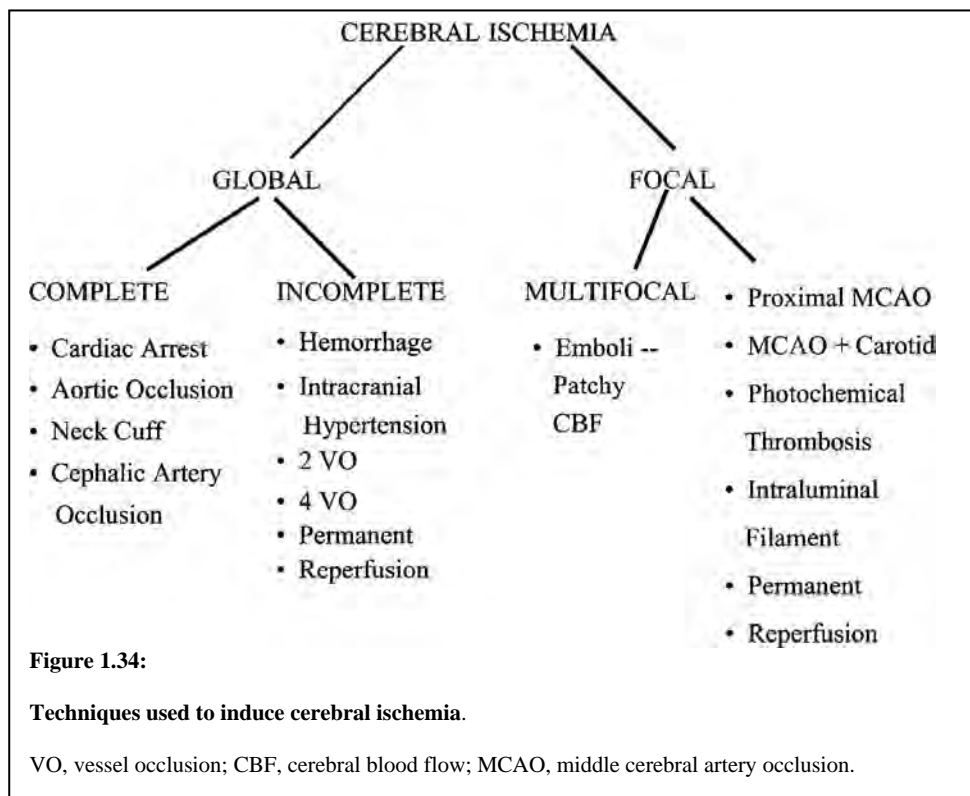
Fig.5 modified from Schmidlin et al 2004

Figure 1.33

Illustration of spinal lesion induced plasticity in the motor cortex opposite to the lesion. As can be seen from the maps, pre-lesion both tracks A and B are within the hand area. Post-lesion track B belongs to newly found wrist area whereas track A remains in the reduced hand area.

Whereas the study of Schmidlin et al. (2004) investigated cortical changes induced by unilateral spinal cord lesion using ICMS mapping, the study of Wannier et al. (2005) used histological analysis to explore post-lesion changes in two areas of the motor cortex in macaque monkeys. Application of this technique allowed investigations at a cellular level in the motor cortex. Pyramidal neurons in layer V of the hindlimbe areas of M1 and SMA-proper were visualized using the marker SMI 32. Thus subpopulations of corticospinal neurons were selectively marked. In contrast to the electrophysiological study of Schmidlin et al. (2004) implicating a loss of axotomized neurons in the motor cortex, Wannier et al. (2005) reported that the vast majority of the axotomized corticospinal neurons in the motor cortex analyzed did not degenerate but their soma shrank, as compared to the opposite intact hemisphere or to control monkeys. In fact post-lesion neurons survived although becoming smaller. This survival of most corticospinal axotomized neurons was consistent with the observation of numerous corticospinal axons 1 mm above the cervical hemi-section.

1.7.1.3 Stroke

As already described in detail (see appendix), stroke from a clinical point of view is induced by different mechanisms, amongst them the most frequent cause being cerebral ischemia. Otherwise stroke itself is a potent trigger of motor cortical plasticity. In order to study the mechanisms underlying such plasticity and with the intention to look for treatments amplifying and controlling the "natural" post-lesion plasticity towards beneficial behavioral recovery many animal models in rats and subhuman primates were developed. In addition to that, clinical studies on stroke patients were conducted to emphasize knowledge about human stroke. As almost in all research fields, most of our detailed knowledge about the basic mechanisms comes from fundamental animal research. There is a huge body of studies in which different approaches were used to create cerebral ischemia (see Fig. 1.34 below, taken from ILAR Animal models of stroke and rehabilitation, Volume 44, Number 2, 2003; p 87).

Figure 1.34:

Techniques used to induce cerebral ischemia.

VO, vessel occlusion; CBF, cerebral blood flow; MCAO, middle cerebral artery occlusion.

In contrast, another model used by Liu and Rouiller (1999) did not induce a cerebral ischemia, but a cortical lesion produced by injection of ibotenic acid, which mimics in part (the excitotoxicity) the consequences of an ischemia in the damaged portion of the cerebral cortex. In his 2006 review, Nudo considered post-injury plasticity not only as an phenomenon that has been documented at the molecular, synaptic, cellular, network and systems levels in experimental animals but also insisted that many of these plasticity events have been correlated with alterations in cortical function using neuroimaging and stimulation techniques in humans. Furthermore he reported that focal cortical

injury results in specific neurophysiological and neuroanatomical changes in both adjacent and remote cortical tissue. The mechanisms described so far are briefly summarized in Figure 1.35 and the related Table 1.7 below.
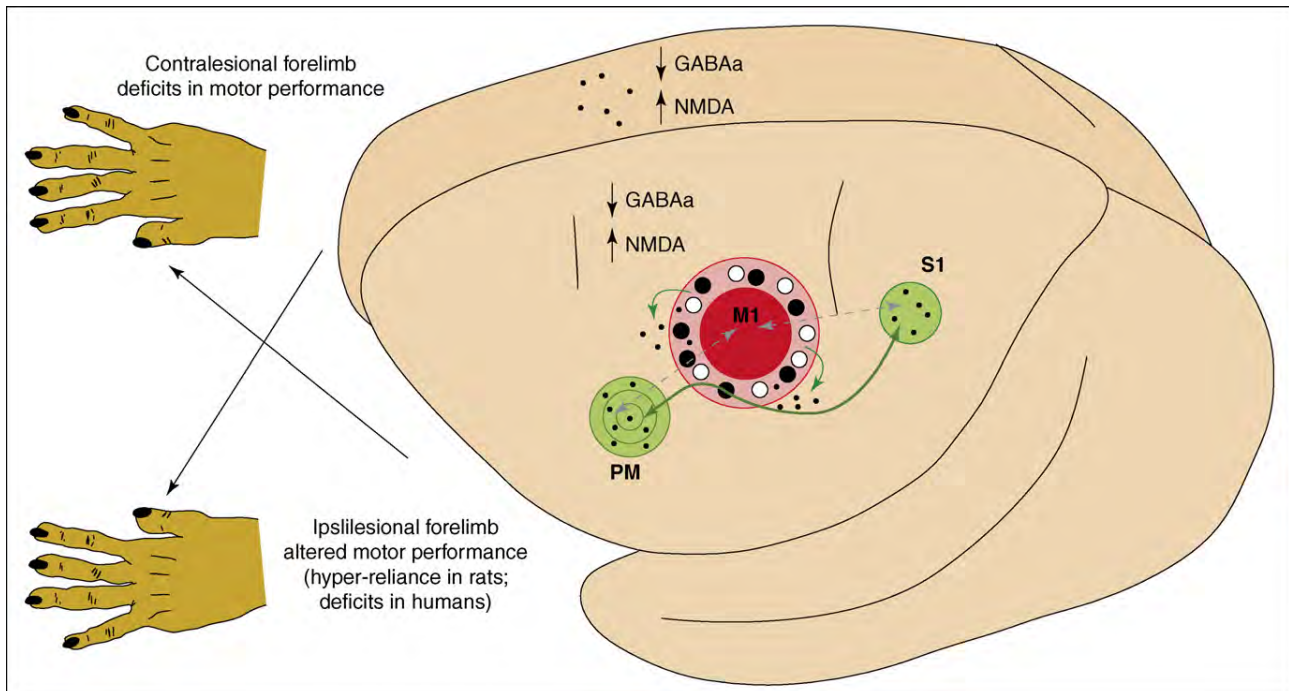
Schematic illustration of the effects of a unilateral cortical lesion (red circle) on spared cortical tissue as depicted in a nonhuman primate brain. Time-dependent neurophysiological and neuroanatomical alterations occur in the peri-infarct region (pink region surrounding lesion) and remote cortical areas. These include alteration in neurophysiological maps of motor representations, neurotransmitter receptor regulation, dendritic sprouting (not shown), local and remote axonal sprouting (short and long green arrows, respectively) and synaptogenesis (small black dots). These changes are accompanied by waves of growth-promoting and growth-inhibiting proteins (large white and black circles, respectively) that might trigger axonal sprouting and provide guidance to regenerating axons. Similar changes have been documented in the contralesional (undamaged) cortex, and are thought to be related to behavioral compensation in the ipsilesional forelimb, and possibly recovery of function by the contralesional forelimb. Recent studies suggest that lesion size is an important factor in determining the role of remote cortical plasticity. Concentric circles in PM denote expanded motor representations. Abbreviations: M1, primary motor cortex; PM, premotor cortex; S1, primary somatosensory cortex

Figure 1.35   (taken from Nudo, 2006).

| Stroke induced changes in peri –infarct / penumbra region and remote cortical areas	Time point post infarction (if defined)	Reference
Increased **GAP-43** immunoreactivity → neurite outgrowth (axonal sprouting)	3 – 14 days	Stroemer RP, Kent TA, Hulsebosch CE: Neocortical neural sprouting, synaptogenesis, and behavioral recovery after neocortical infarction in rats. Stroke 1995, 26:2135-2144.
Elevated **Synaptophysin** staining → increased synaptogenesis (axonal sprouting)	14 – 60 days	Stroemer RP, Kent TA, Hulsebosch CE: Neocortical neural sprouting, synaptogenesis, and behavioral recovery after neocortical infarction in rats. Stroke 1995, 26:2135-2144.
Hyperexitability of local surviving neurons → **NMDA** receptor up- regulation → **GABAa** receptor down- regulation	?	Schiene K, Bruehl C, Zilles K, Qu M, Hagemann G, Kraemer M, Witte OW: Neuronal hyperexcitability and reduction of GABAA-receptor expression in the surround of cerebral photothrombosis. J Cereb Blood Flow Metab 1996, 16:906-914.
Expression of specific and highly coordinated set of **growth associated genes** in surviving neurons	?	Carmichael ST: Cellular and molecular mechanisms of neural repair after stroke: making waves. Ann Neurol 2006, 59:735-742. Carmichael ST, Archibeque I, Luke L, Nolan T, Momiy J, Li S: Growth-associated gene expression after stroke: evidence for a growth-promoting region in peri-infarct cortex. Exp Neurol 2005, 193:291-311.
Growth programs are turned on in young individuals as well as in aged individuals. But there is a reduced and later expression of genes and proteins in aged brains as compared to young brains.	?	Li S, Carmichael ST: Growth-associated gene and protein expression in the region of axonal sprouting in the aged brain after stroke. Neurobiol Dis 2006, 23:362-373.

Table 1.7

All these molecular and cellular changes are reflected by a significant reorganization of the post-lesion motor cortical maps. The pattern of the post-lesion maps greatly depends on the initial lesion size and on its precise position in the brain. Frost et al. (2003) showed that the smaller the damage to M1, the less compensatory reorganization was seen in PMv. Another study has even demonstrated that destroying 33% of the M1 hand area does not promote observable changes in PMv, as seen with larger lesions (Dancause et al., 2006). As a consequence of that, reorganization of motor cortical maps induced by small M1 lesions are not necessarily easy to detect by custom stimulation techniques outside the core of the lesion. Nevertheless, many post-lesion stimulation studies with ICMS (monkeys, rats) or TMS (humans) revealed interesting features about motor cortical reorganization. PET and fMRI technique were also used in humans, as well as in animals to obtain additional information about the evolution of post-stroke reorganization. Trans-cranial magnetic stimulation (TMS) is a non-invasive method of stimulating cortical motor neurons through the scalp and skull. Neurons are depolarized within a certain area of the cortex by an electric current flowing through the cortex. This current is induced by a stimulating coil placed over the scalp which generates a local magnetic field. The techniques of TMS and fMRI can be used to produce functional maps of motor areas by detecting the activated cortical areas while a subject is performing a relatively simple motor task. Recently, researchers became more interested in the time course of changes in the penumbra zone just adjacent to the lesion, as well as in changes with time in remote cortical areas, because these areas are obviously the substrate/target for neurological recovery and future treatments.

In the following part, some of the findings from five interesting studies concerning cortical reorganization after damage to M1 will be lined out more in detail. All five studies did not only investigate cortical reorganization but also attempted to correlate the observed changes with recovery over time. The study of Dijkhuizen et al. (2001) aimed at correlating temporal sensorimotor function alterations with the evolution of changes in brain activation patterns in relation to the cerebral pathophysiological status after stroke. Stroke was induced by electrocoagulation of the right middle cerebral artery (MCA) in adult rats. MRI and histology revealed a clear ischemic lesion in the right cerebral hemisphere involving the lateral cortex and underlying subcortical structures such as the striatum. As the sensorimotor cortex lies at the border of this type of lesion, it became more or less severely affected paralleling the severity of the ischemia. Post-lesion behavioural performance in the forelimb placing test was measured and compared to pre-lesion performance. Within the first 24 hours after stroke onset, there was a marked impairment of placing of the contralesional (left) forelimb indicating sensorimotor dysfunction. In the following two weeks the performance gradually improved to reach subnormal levels (see Fig. 1.36 below). Functional recovery was paralleled by temporal changes of the cortical

activation pattern during stimulation of the impaired forelimb. But the authors were not able to establish a statistically significant correlation between the pattern of brain activation and functional recovery. Nevertheless Dijkhuizen et al. (2001) showed that dysfunction of the hemiplegic forelimb was associated with loss of brain activity in M1 and S1 as revealed by fMRI. The following recovery of sensorimotor functions was accompanied by changes in the activation and recruitment pattern of cortical areas. First, when the sensorimotor function was still severely impaired, mainly contralesional activation and recruitment of penumbra region were observed. Later, post-lesion, the relative involvement of the ipsilesional cortex increased as performance partially recovered (see Figure 1.37 below).

Performance in forelimbe placing test affected limb

0 = no impairment
12 = maximally impaired
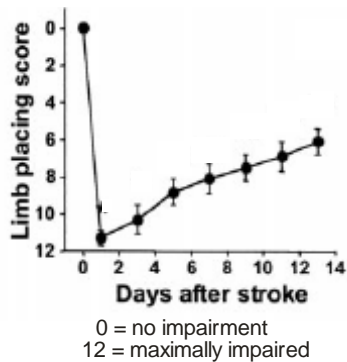
Figure 1.36 Illustration of the recovery in the forelimb placing test as measured by a score from 0 – 12. Specifically, the forelimb placing test measures sensorimotor function in the forelimb as the animal places the limb on a tabletop in response to visual, tactile, and proprioceptive stimuli Maximal impairment corresponds to a score of 12 (Modified from Dijkhuizen et al. (2001)).

Distribution of regions that exhibited significant activation response on stimulation of the left (impaired) forelimb
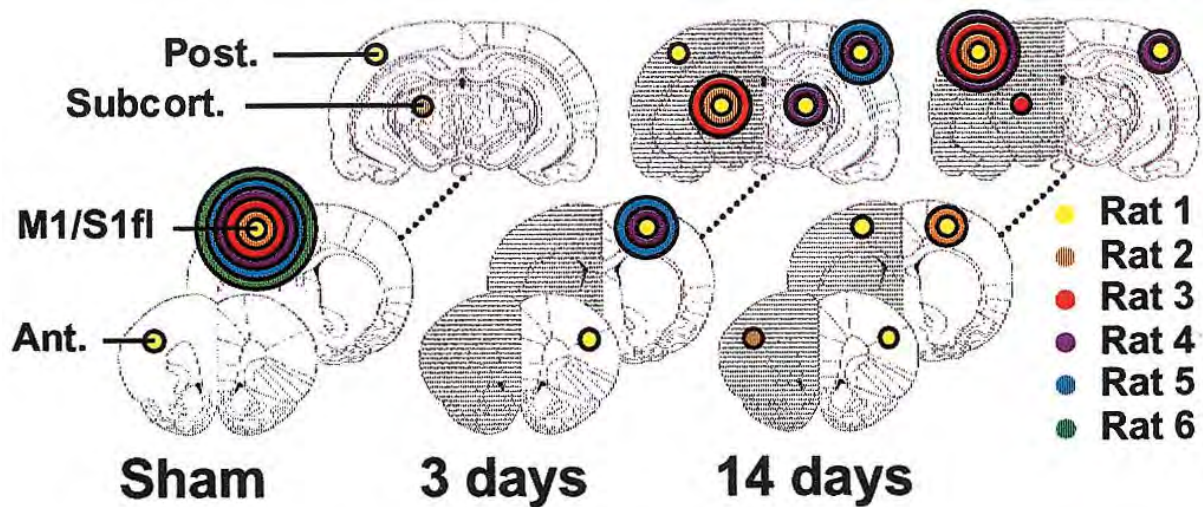
For the sake of clarity, regions are divided into four main areas:
(*i*) M1yS1fl

(*ii*) anterior (Ant.) vicinity of M1yS1fl (i.e., face region of S1; cingulate cortex; insular cortex)

(*iii*) posterior (Post.) vicinity of M1yS1fl (i.e., hindlimb, barrel field,dysgranular, and trunk region of S1; parietal association cortex; visual cortex)

(*iv*) subcortical (Subcort.) (thalamus; superior colliculus)
The radius of the colored circles corresponds with the number of animals that showed significant activation responses in the specific brain region ($P < 5*10-5$ was considered significant). The different colors represent individual animals in the sham-operated group, the 3 days stroke group, and the 14 days stroke group. The ipsilesional (right) hemisphere is shaded.
Modified from Dijkhuizen et al 2001

Figure 1.37

In their ICMS study, Liu and Rouiller (1999) investigated the mechanisms of recovery of dexterity following unilateral lesion of the sensorimotor cortex in adult monkeys. In fact, this study was the continuation of the initial work by Rouiller et al. (1998) in which evidence for compensatory reorganization of the cerebral cortex adjacent to the lesion in the hand area in infant monkeys was reported. In contrast to the infant monkey study, the adult monkey study Liu and Rouiller (1999) did not report such peri-lesional plastic changes in M1 as revealed by ICMS mapping at 9 months post-lesion. The authors reported, in the adult, remote plastic changes in the premotor cortex (PM) responsible for the partial behavioural recovery. A substantial loss of cortical function in the M1 lesion site was confirmed by ICMS (see Figure 1.39 below). Behavioural recovery was quantified with similar standard Brinkman board tasks as described in the method part

of the present thesis. The particular functional importance of remote plastic changes in PM was demonstrated by transient inactivation experiments (see Figure 1.38b below). 15 minutes after the infusion of Muscimol in the ipsilesional PM (PMv + PMd) there was loss of the recovered manual dexterity whereas no effect was observed after ipsilesional infusions in PMv alone, PMd alone, M1 core of lesion, M1 penumbra zone and different infusions in the contralesional sensorimotor cortex. The whole time course of the behavioural recovery is represented in Figure 1.38a below. Basically, immediately after the chemical lesion of M1 by infusing ibotenic acid, the hand contralateral to the lesioned cortex showed a complete deficit of movement (flaccid paralysis). The recovery of manual dexterity started after 4-6 weeks following the lesion and progressively increased over 4-5 months to reach a plateau of behavioural performance representing about 30% of the pre-lesion score. This score remained stable until 9 months post-lesion. In summary, this study supports the notion of a substantial "spontaneous" recovery and the implication of remote cortical areas (PM) in post-lesion recovery.
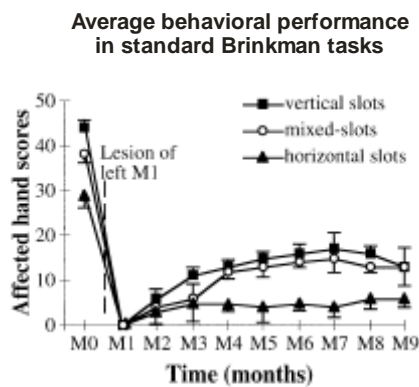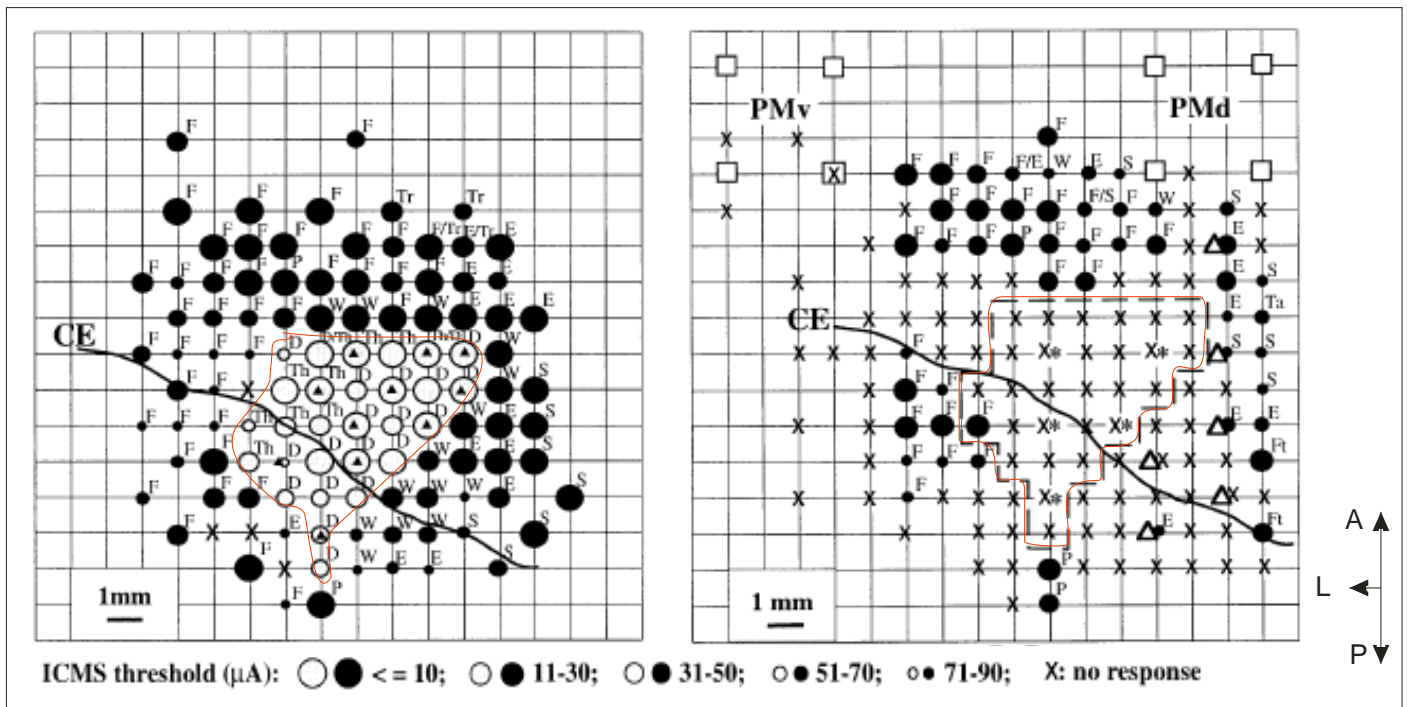

Figure 1.38a
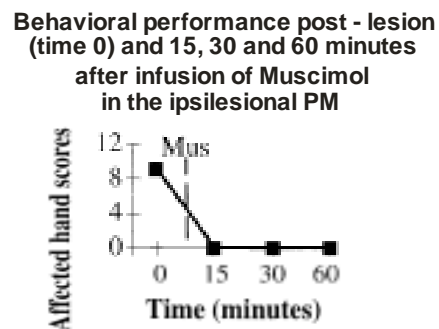
Figure 1.38b

Figure 1.38a: *M0* is the averaged scores (and SDs) collected during behavioral sessions before the cortical lesion: this data point is derived from 14 and 25 sessions in monkeys 1 and 2, respectively. *M1-M9* are averaged scores (and SDs) collected during 9 consecutive months after the lesion. For each month, the data point is the average value of the scores established during the corresponding month in 4-6 sessions for each slot orientation.

Figure 1.38b: The dexterity scores obtained before muscimol infusion are given at time point 0, whereas the three other values give the scores at time points 15, 30 and 60 min after muscimol infusion. The *vertical dashed line with abbreviation Mus* separates the scores before and after inactivation. (Modified from Liu and Rouiller, 1999).

CE is the contour corresponding to the position of the central sulcus, as it appears on this surface view of the cortex. Each *dot* (*gray* or *black*) represents the location on the brain surface of one electrode penetration. The threshold needed to induce a visible body movement is indicated by the diameter of the dot (see *key* at bottom of figure). The movement elicited at the threshold is given at the top-right of each dot: *D* digit, *E* elbow, *F* face, *Ft* foot, *H* hip, *L* leg, *P* pinna, *S* shoulder, *Ta* tail, *Tg* tongue, *Th* thumb, *Tr* trunk, *W* wrist, *X* no visible movement at the highest intensity tested (90 µA). Triangles = Site where ibotenic acid was injected after pre esion mapping to achieve chemical lesion of the hand representation. The hand area (where pre lesion ICMS elicited at threshold finger movements) is circumscribed in red. *A* Anterior, *P* posterior, *L* lateral. The brain midline is located approximately 7–8 mm from the medial limit of the grid underlying the ICMS maps.

Figure 1.39   Pre- and post-lesional ICMS map of affected M1 (taken from Liu and Rouiller, 1999).

The human study of Feydy et al. (2002), based on single fMRI sessions at different time points after stroke, showed a large variety of functional cortical reorganization. Because the time point of investigation may in part explain the different cortical activation patterns reported, their time course during recovery was followed in three fMRI sessions over a period of 1 to 6 months after stroke. The motor tasks used during fMRI were the following: Self-paced closing and opening of the hand (10 patients) and, for patients unable to perform hand movements, repetitive flexion/extension of the elbow (2 patients) or repetitive abduction/adduction of the shoulder (2 patients). The impact of the type of lesion on the recovery and the activation pattern was also

investigated. As reorganization of the descending motor pathways after stroke, especially in the pyramidal tract, is another important parameter influencing recovery, two methods were used to evaluate the deficits in the corticospinal system: First, an analysis of EMG responses from the left and right first dorsal interossei to TMS stimulation of the affected and non affected hemispheres. Second the degree of Wallerian degeneration of the corticospinal tract was assessed from MRI images. Investigations were conducted in 14 stroke patients, amongst them four with M1 lesion affecting the grey matter. Wallerian degeneration of the pyramidal tract was present and increased over time in all 14 patients. The degree of Wallerian degeneration was negatively related to functional recovery (supported by more delayed or missing responses to TMS stimulation of the affected hemisphere in patients with inferior recovery) whereas this study did not reveal a significant relation between the type of lesion (M1 normal or lesioned) and functional recovery. But the evolution of the cortical activation pattern was only related to the severity of the M1 injury. So the key element of this study is the proposed hypothesis for the evolution of the pattern of cortical activation after stroke as represented in the Figure 1.39b below.
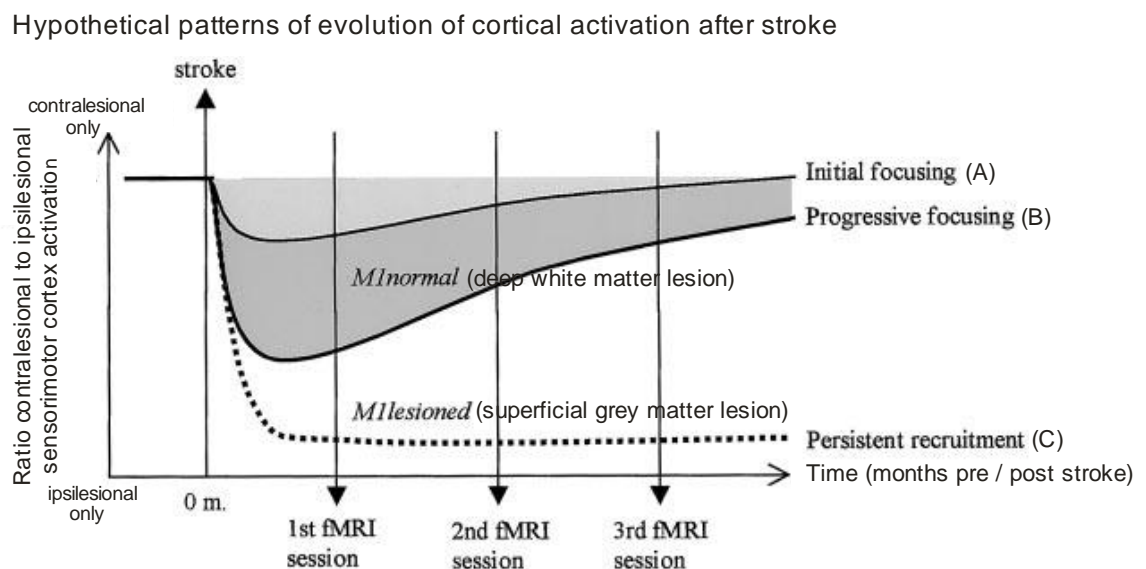
Figure 1.39b

With respect to extent of lesion, the authors propose three different patterns of evolution of cortical activation after stroke (A – C). *Initial focusing* is when activation remains contralesional from the very beginning. In the case of *progressive focusing*, first bihemispheric activation is observed but with time the activation is focused back to contralesional areas. Both types of focusing are most often seen in patients with normal M1 corresponding to deep white matter lesions. Probably the focusing is due to a gradually exerted inhibition by M1 over initially recruited areas. The third type, *persistent recruitment*, is usually seen in M1 lesioned patients in whom the gray

69

matter is affected by the lesion. Such activation pattern involving more ipsilesional and contralesional brain areas may be due to disinhibition by the lesion in M1 and the reciprocal corticocortical connections from M1 to the secondary motor areas. For details about this mechanism, compare with a corresponding study in rats (Jacobs et al., 1991).

In summary it can be said that immediately after the lesion all potentially available neurons to counteract the loss of control by the lesion are recruited. Later, if possible, focusing may select the neurons that potentially improve the efficiency of the impaired motor control relayed by the corticospinal tract. The results of this study support the idea that the degree of functional recovery of the sensorimotor system does not uniquely depend on the type of cortical plasticity but also on the number of surviving fibres in the corticospinal tract after stroke.

So far most studies investigating the consequences of motorcortical lesions focused on changes either in the core of the lesion or in the peri-infarct regions. The group of Nudo was one of the first to publish papers about changes in cortical areas remote from the lesion site. In 2005, Dancause et al. examined changes in cortical connections of PMv after injury to the primary motor cortex (M1) in a squirrel monkey model. PMv was chosen because one mechanism for recovery after a cortical infarct in M1 is the remodelling of other intact, more distant regions of the brain, such as premotor areas. A second important feature of PMv is that it shares extensive connections with M1 (Dum and Strick, 2005). Consequently, after M1 injury, targets of PMv intracortical axons degenerate. Therefore the authors hypothesize that these PMv neurons would seek novel targets during the postinfarct period. To reveal the potential rewiring, BDA (anterograde and retrograde) tract tracer was injected into PMv hand area of 4 lesioned animals. This was done at least 5 months after ischemic injury to the M1 hand area. Additionally BDA was also injected into PMv hand area of 4 control animals. Histological analysis of the BDA labeling in control versus experimental animals revealed two main findings:

In each of the lesioned monkeys, but none of the control monkeys, a very large number of labeled terminals as well as labeled cell bodies were observed in the area 1 / 2 hand representation of S1. The differences between the numbers of labelled extrinsic terminals (*out*put of PMv) and cell bodies (*in*put to PMv) in ipsilesional S1 in experimental animals compared to those in control animals were statistically significant, whereas no ipsilesional area outside of S1 as well as no other regions in S1 (area 3a / 3b) showed a statistically significant difference between control and experimental animals (see Figure 1.40 below).
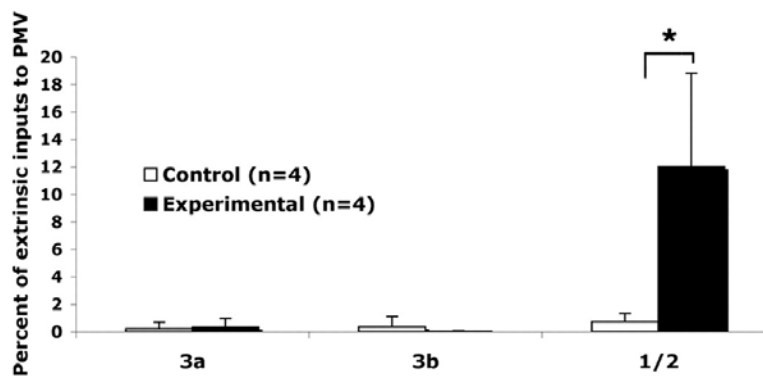
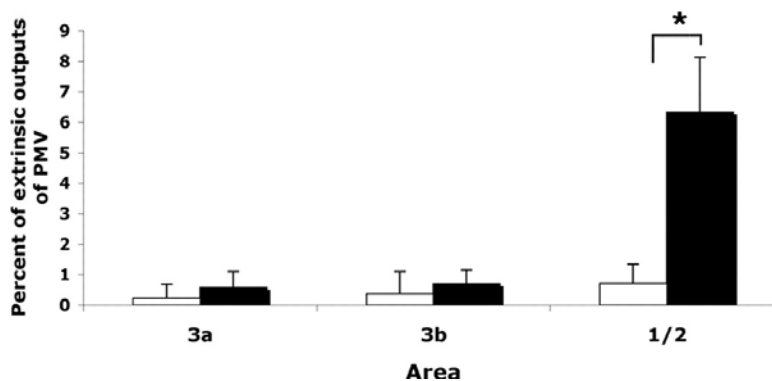**A** Distribution of labeled cell bodies in ipsilateral hemisphere (excluding S1)
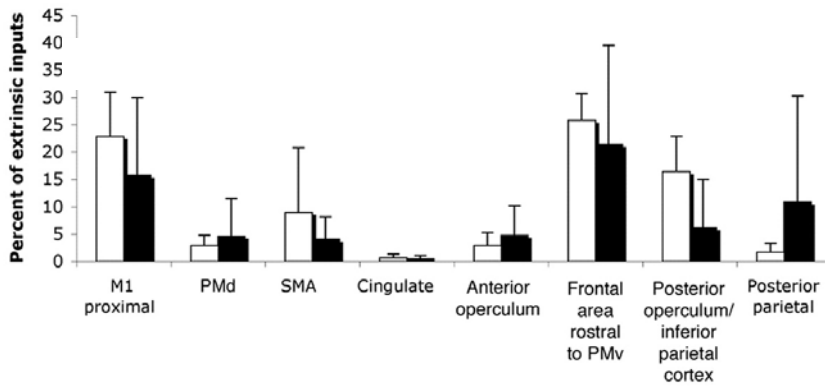
B Distribution of labeled terminals in ipsilateral hemisphere (excluding S1)
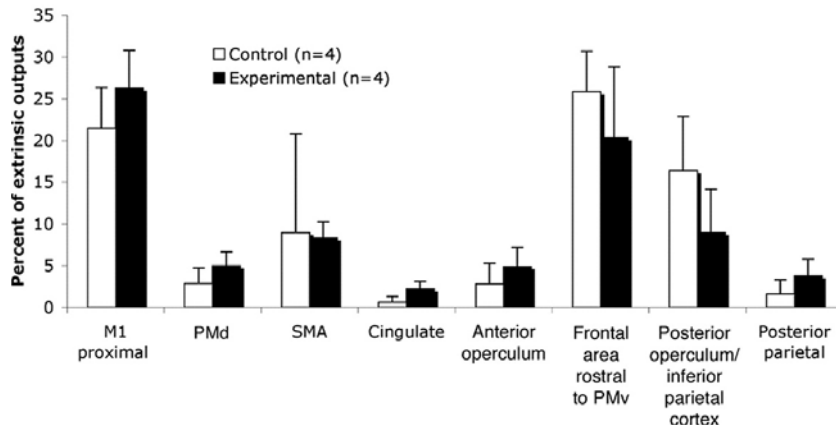
C Distribution of labeled cell bodies in ipsilateral S1

D Distribution of labeled terminals in ipsilateral S1

Figure 1.40

Distribution of labeling in the ipsilateral hemisphere .

A, Cell body distribution (excluding S1) in experimental group
  compared with control group.

B, Distribution of terminal labeling (excluding S1) in
  experimental monkeys compared with control monkeys.

C and **D**:

  Distribution of ipsilateral labeled cell bodies and terminals in
  areas 3a, 3b, and 1/2 of S1 of control and experimental monkeys.

 Proportions of extrinsic PMv inputs and outputs are shown.

  *p < 0.05, statistically significant differences.

  modified from Dancause et al 2005

A second finding of this study was that an alteration of average axonal orientation occurs at the border of M1. Intracortical axons from PMv normally targeting M1 are redirected to new targets as illustrated in Figure 1.41.
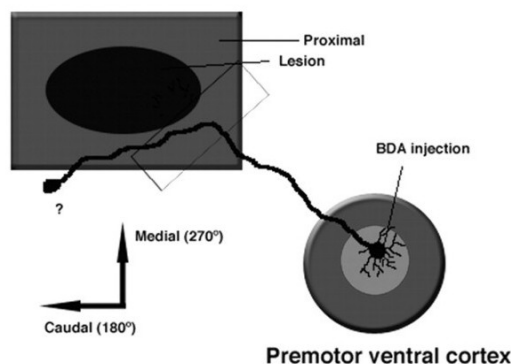

A Normal trajectory of intracortical connections between PMv and M1
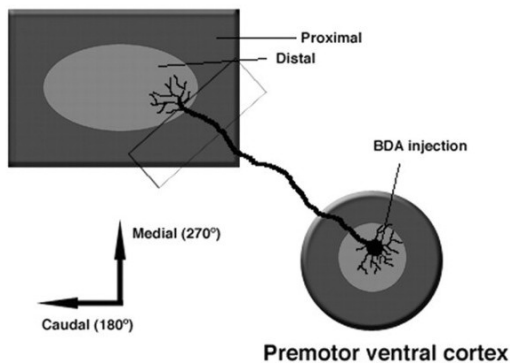
B M1 injury induced redirected trajectory of intracortical connections between PMv and M1

Figure 1.41

Schematic illustration of the presumed alterations in PMv intracortical connections after M1 injury.
After PMv targets in M1 are destroyed, PMv intracortical fibers are thought to seek new targets; axons abruptly change orientation near the lesion border and begin to course more caudolaterally, sweep around area 3b, and finally terminate in area 1/2.

Modified from Dancause et al. (2005).

The authors concluded that their results provide evidence for proliferation of novel, injury induced corticocortical connections between PMv and area 1/2 of S1 after an infarct in M1. These morphological alterations are accompanied by functional recovery and expansion of the PMv hand representation (Frost et al., 2003). Furthermore, they provide evidence for altered trajectories of axons originating in PMv. Thus, they hypothesize that, when a principal cortical target of PMv axons is destroyed, intracortical axons seek new targets in surviving, intact tissue.

In a more recent study from the same laboratory using a similar squirrel monkey model (Stowe et al., 2007), significantly increased association of vascular endothelial growth factor (VEGF) protein to neurons in the remote cortical PMv region was shown. VEGF is thought to contribute to both neuroprotection and angiogenesis. As it has been suggested that peri-infarct angiogenesis in human stroke survivors is implicated in long-term recovery (Krupinski et al., 1994) it could also be responsible for the observed post M1 injury plasticity in PMv. Although in a first step neurons in PMv may initiate molecular cascades that release VEGF for immediate neuroprotection. At long-term VEGF may play an angiogenic role during chronic stages of stroke, because post - lesion remodelling in PMv induces higher metabolic demands on the local cell population which in turn induces angiogenesis. Therefore one could imagine a direct or indirect contribution of VEGF to functional recovery. As Stowe et al. (2007) observed an increased VEGF association in the same remote cortical region where Dancause et al. (2005) described remote plastic changes after a comparable lesion in M1, these results strongly supports the idea that remote cortical areas are implicated in functional recovery after stroke.

Furthermore, as the findings of both studies are in accordance with functional recovery and expansion of the PMv hand representation reported by Frost et al. (2003) using the same squirrel monkey model.

1.7.1.4 Pyramidal lesion

So far, I have described the influence of amputations, spinal cord lesions and finally cortical lesions on brain plasticity. As illustrated a lesion or an injury to the peripheral or central nervous system does not only destroy functions of the central nervous system but also induces either new or normally suppressed functions. Most of them are of compensatory nature and seek to compensate for the lost function. Lesioning the pyramidal tract in mammals, especially in nonhuman primates, gave insight in the complex plastic events which are induced after injury to the pyramidal tract and how these changes could be implicated in the observed post lesion functional recovery. Before analyzing and even interpreting the consequences of such lesion one has to be aware that the pyramidal tract besides M1 arises from a large number of regions in the frontal cortex, even including the cingulate gyrus (areas 23 and 24) (Dum and Strick; 1991). It also contains fibres of

different functional characteristics targeting various subcortical brain stem nuclei with its collaterals while passing through the brain stem. So there are numerous points at which impulses generated in the corticospinal neurons may be fed into descending pathways *other* than the pyramidal tract. The part of the pyramidal tract leaving the brain stem is called pyramidal tract *proper* or corticospinal tract (Phillips and Porter, 1977) or *bulbar* pyramid or *medullary* pyramid. Finally at spinal level the pyramidal tract fibres terminate in three distinct areas of the spinal grey matter. In the nucleus proprius of the dorsal horn, in the intermediate zone and deeper layers of the dorsal horn and directly upon motoneurons particularly those innervating the distal muscles of the limb (Lawrence and Hopkins, 1976). There may be a large variability across pyramidal lesions, as the consequences of a particular lesion vary with respect to the level at which the lesion was made; it is also important to assess whether the lesion was unilateral or bilateral and whether fibres were spared. This makes analysis and interpretation again more complicated. In addition to that, the expression of this pathway is age related (Lawrence and Hopkins, 1976). Last but not least, there are enormous interspecies differences in the development and expression of the pyramidal tract in different mammals. Although there is a huge body of literature dealing with pyramidal lesions most of it concentrated on development, species, functional, behavioural and anatomical aspects rather than directly on plasticity induced at the level of the motor cortex. So the information about the effect of pyramidal lesions on plasticity of motor cortical maps provided is rather indirect. Therefore in the following paragraphs I rather concentrate on important findings from selected studies about how pyramidal lesions induce plasticity in the central nervous system.

The characteristic feature of the motor performance of primates in which corticomotoneuronal (CM) connections are well developed are fractionated movements especially of the arm and hand. From these movements the relatively independent finger movements (RIFM) are in particular permanently impaired or lost as a consequence of a pyramidal lesion in adult monkeys (Tower, 1940; Lawrence and Kuypers, 1968). That the pyramidal tract *proper* is indispensable for RIFM was shown in both an anatomical study and a behavioural study.

First Kuypers et al. (1962) showed that there are clearly less pyramidal fibres terminating in lower cervical segments of infant rhesus monkeys than in adult monkeys of the same species. This finding is in accordance with the observed gradual appearance of RIFM during the first several months of normal postnatal development in rhesus monkeys (Lawrence and Hopkins, 1976). The same authors also reported that a complete pyramidal lesion in infant rhesus monkeys leads to a permanent loss of RIFM too. So it seems that potential lesion induced plasticity at any level of the CNS is not able to compensate for this loss. In contrast to the permanent loss of RIFM in infant and adult pyramidotomized animals there is reappearance of the ability to reach out and grasp objects by

closure of the fingers all together. Motor recovery in infant monkeys was better than in adults confirming an impact of age. This partial recovery also allows a precision grip as defined by Napier (1960), because the only criterion for this type of movement is that an object is gripped by opposing thumb and index without taking into account the activity in the other fingers. That is probably why Hepp-Reymond and Wiesendanger (1972) reported only transitory abolishment of this grip following complete pyramidal lesion. Such partial functional recovery strongly supports the hypothesis of pyramidal lesion induced plasticity. Potential targets for plastic changes are alternative pathways to motoneurons of finger muscles. In this context the rubrospinal tract is the best candidate as axons of the rubrospinal and the corticospinal tract possess very similar branching patterns (Shinoda et al., 1988). Their terminals may overlap and synapse on the same motoneurons. Comparative analysis of the influences of the descending corticospinal and rubrospinal tracts revealed many similarities in the functional properties of these two motor systems, especially in the context of regulation of velocity, direction and the force of movements (Hepp-Reymond and Wiesendanger, 1972; Cheney and Fetz, 1980; Cheney et al., 1988). Studies which investigated the participation of neurons of both tracts during the training of an animal for new motor tasks and during the execution of already learned movements found a "switch" from the corticospinal to the rubrospinal tract after the movement was learned. The switch must be possible in both directions as lesions of either one of the two systems induced only transitory loss of motor function (e.g. Lorincz and Fabre-Thorpe, 1997) whereas lesions of both systems lead to permanent loss of function (e.g. Lawrence and Kuypers, 1968). So, plasticity operates by changing the position of the virtual switch in the CNS part of the motor system.

The mechanism of how the position of the virtual switch is changed activating either on or the other of the two parallel systems was investigated by a study of Fanardjian et al. (2000) in a rat model. For this purpose rats of three experimental groups were conditioned for the reflex of equilibrium by putting them on a slowly rotating horizontal bar.

Rats of group 1:
Rats were first trained on the task. Afterwards a unilateral pyramidotomy was carried out and the rats were retrained until they reached again stable performances in the reflex task. Then after an aspiration lesion of the ipsilateral sensorimotor cortex was performed. After this second operation training sessions on the equilibrium task continued and the evolution of the performances was measured.

Rats of group 2:

After they were completely trained on the equilibrium task a unilateral aspiration lesion of the sensorimotor cortex was performed. Post operation they were retrained as the animals in group 1 and again the evolution of the performances were quantified.

Rats of group 3:

Before starting training sessions on the equilibrium task, in these rats unilateral ablation was performed. Subsequently the training was started and performances in the task were monitored in parallel.

Comparing the results of the three experimental groups revealed that a unilateral transection of the bulbar pyramid performed before the ablation of the ipsilateral sensorimotor cortex (group 1) lead to significant better recovery of the conditioned equilibrium reflex as well as to a stronger induction of compensatory processes than it could be observed in animals of group 2 or 3. The authors conclude that a preliminary lesion of a peripheral part in the cortico-rubrospinal system, represented by a descending spinal projection (pyramidal tract), facilitates the recovery processes to develop during the subsequent destruction of its central part (sensorimotor cortex). The induced functionally more effective post-ablation plasticity in group 1 animals can be explained as follows: In healthy animals and animals of group 2 and 3 the rubrospinal system is inhibited by collaterals of the fast conducting pyramidal tract neurons (see Figure 1.42 below). This inhibition disappears in the case of a unilateral bulbar pyramidotomy. As a consequence the corticorubrospinal system in group 1 animals receives a greater volume of freedom, switching for the compensation of the effects of the pyramidal tract leading to the observed better performances. The concept of this compensatory switching is represented in Figure 1.42 below.
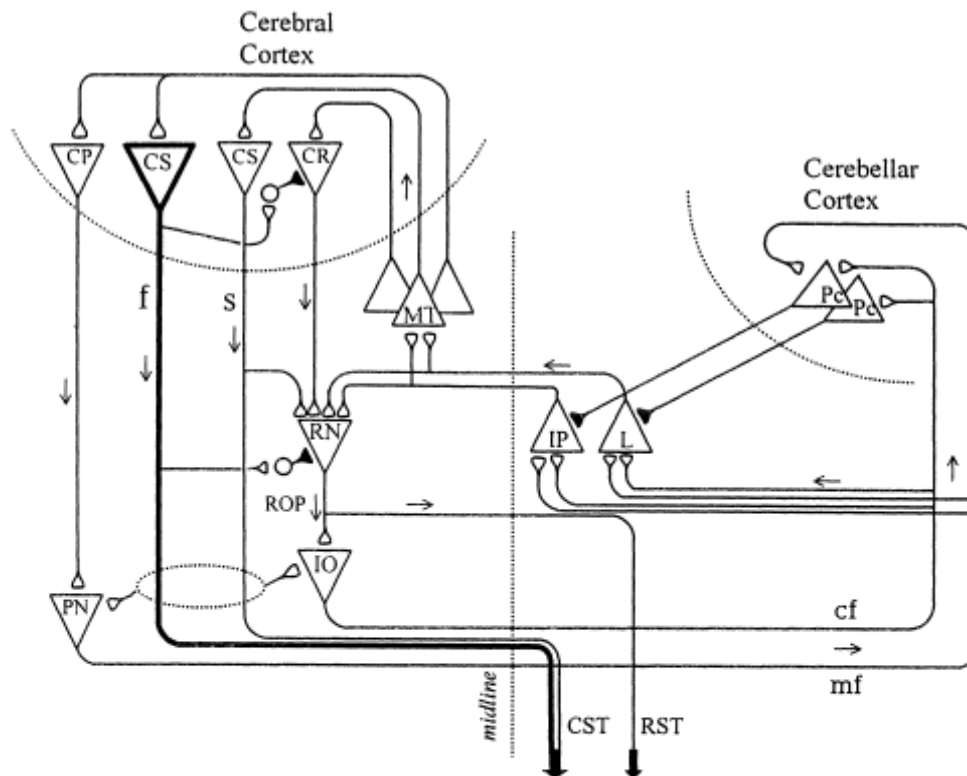
Diagram of neuronal circuitry of interrelation and substitution of corticispinal and cortico-rubrospinal systems. Corticispinal (CST) projections arise from fast-conducting (CSf) and slow-conducting (CSs) pyramidal tract cells. Cortico-rubral projections arise from coricorubral (CR) cells in the cerebral cortex. CSs and CR are connected monosynaptically with rubrospinal tract (RST) cells of the red nucleus (RN). Neurons of RN receive cerebellar inputs via contralateral n.interpositus (IP) and n. lateralis (L), which are projected also to the cerebral cortex through the motor thalamus (MT). Rubro-olivary projection (ROP) are terminated on the inferior olive (IO), which sent olivo-cerebellar fibres (climbing fibres, cf) to Purkinje cells (Pc) and neurons of cerebellar nuclei (IP,L). CSf exert inhibitory influences via interneurons on CR and RST cells. Corticopontine projections (CP) to the pontine nuclei (PN) provides polysynaptic connections from the cerebral cortex to the cerebellum, since efferent neurons of the PN projects onto the cerebellar cortex and its nuclei as mossy fibres (mf). CSf are indicated by thick line. Excitatory and inhibitory projections are indicated by open and filled knobs. Arrows show direction of information flow.

Figure 1.42   From Fanardjian et al. (2000).

That pyramidotomy is an inductor of plasticity in the CNS was also observed by Z'Graggen et al. (2000). They investigated the reorganization of the corticofugal projections rostral to a unilateral lesion of the corticospinal tract at the level of the medullary pyramid and the contribution of this reorganization and other descending systems to functional recovery in two day old and adult rats. In contrast to the above study three months post-lesion this approach only lead to reorganization in infant rats. But although reorganization was limited to infant rats their results, showing a relatively large number of corticorubral and corticopontine fibres crossing the midline from the lesioned side and establishing an additional contralateral innervation of the red nucleus and the pons, also suggest an important role of the corticorubrospinal system in the reconnection of the cortex to the periphery after pyramidotomy supporting the concept of switching (see Figure 1.42 above).

Implication of the corticorubrospinal system in plastic changes after pyramidotomy was also demonstrated in adult macaque monkeys. As in the rat several weeks post pyramidal lesion there is

considerable recovery of manual dexterity although digit movements remain clumsy. If the pyramidal tract and the rubrospinal tract are lesioned both there is either little or no recovery even after extensive postoperative training indicating a major contribution of the corticorubrospinal system in recovery (Lawrence and Kuypers, 1968). Belhaj-Saif et al. (2000) investigated the contribution of the magnocellular red nucleus to compensation for motor impairments associated with lesions of the pyramidal tract. Despite the similarities of the corticospinal and the corticorubrospinal system (see above) there is one difference: In healthy adult monkeys the rubrospinal system exhibits a very prominent extensor preference in the distribution of excitatory output effects that is not characteristic of the corticospinal system (Belhaj-Saif et al., 1998). So if the corticorubrospinal system takes over the function of the corticospinal system consequently rubrospinal neurons would show appropriate changes in synaptic output organization and/or functional activity during the performance of a forearm reach and prehension task. In fact stimulus triggered averaging of electromyographic activity recorded from 11 forearm muscles revealed a remarkable reorganization of rubrospinal output after recovery from pyramidotomy. The normal extensor preference was largely lost in favor of a distribution more closely matching that of the corticospinal system. So this study provides clear evidence that pyramidotomy can induce plasticity in CNS of adult nonhuman primates confirming results from rat studies.

### 1.7.2 Learning induced plasticity

From a neurophysiological point of view a multitude of various events during lifespan can be implicated in learning. The reason for that is that at the basis of learning induced plasticity are many at first instance completely different inductors. For example enriched and impoverished environments can stimulate plastic events in the CNS (e.g. ILAR Journal S. 110-124; Volume 44 Number 2, 2003). In the past, the most popular research field to demonstrate plasticity in the adult CNS was the investigation of changes in the somatosensory cortex (S1) as a consequence of input modulation, either by learning of adapted tasks or by experimental manipulations at different levels of the somatosensory input pathway (for review see Kaas, 1991; Dinse and Merzenich, Adaptations of inputs in the somatosensory system; Chapter 2, pp. 19-42; In: Perceptual learning, 2002; ISBN 0-262-06221-6). Only more recently, evidence was accumulated indicating that such plastic changes also occur in the adult motor cortex. As my thesis deals with lesion at a cortical level of the primate motor system and also evaluates which mechanisms besides an anti-NoGo treatment could be implicated in post lesion recovery, in the following paragraph I will concentrate on learning induced plasticity in the motor cortex.

1.7.2.1 Training

Training can be considered as a variant of learning, if an animal is trained for a novel skilled movement. If the trained task is just a more extensive daily repetition of a natural already known movement sequence then plastic changes in motor cortical maps to be expected over time are not significantly different as compared to control animals. In other words training does only induced plastic changes in M1 if the acquired motor task is new to a subject. That skilled learning is essential to drive neurophysiological changes in motor cortex was shown by Plautz et al. (2000). They showed that in a squirrel monkey trained to retrieve pellets from the smallest well of the Kluver board, forcing the monkey to use only one or two fingers, the post training motor maps showed a significantly increased finger area as compared to controls. This task is a novel skilled movement to squirrel monkeys and has to be learned as they naturally can not effectuate individuated finger movements in order to oppose thumb and index or even use only one finger. This is because squirrel monkeys do not possess monosynaptic corticospinal projections. The above mentioned study was a succeeding study of the pioneer work about training induced motor cortical plasticity in adult nonhuman primates (Nudo et al., 1996).

The aim of Nudo's study was to document plastic changes in the functional topography of primary motor cortex (M1) which are generated in motor skill learning in the normal adult intact primate. For this purpose squirrel monkeys were trained on two different tasks that either encouraged skilled use of the digits (same Kluver board task as described above) or pronation and supination of the forearm. In the second task the monkey had to turn a rotable eye-bolt to receive food pellets. ICMS was used to derive detailed pre- and post training maps of the representation of movements in the distal forelimb zone of M1. There was a post training increase in digit representations for the monkeys trained on the Kluver board task at the expense of wrist/forearm representations (see Figure 1.43 a below). The observed plastic changes were progressive and reversible indicating that M1 is alterable by use throughout the life. In addition to that the performance in the Kluver board task paralleled the plastic changes in the motor cortex. Therefore it can be concluded that plasticity in M1 is of functional importance during motor learning. In the monkey trained on the eye-bolt turning task similar training induced changes were reported but in this animal the area of the wrist/forearm representations increased at the expense of digit representations (see Figure 1.43 b below). It is important to note that the total size of the forelimb representation remained constant throughout this plastic changes. So plasticity is the product of use-dependant M1 reorganization. In this context the authors found a post training increase in multiple-joint movements elicited by ICMS stimulations. Such simultaneous execution of digit and wrist or

digit and proximal movements from stimulations at intensities less than 20µA were observed more frequently *after* training. The observation was only made for the Kluver board task (see Figure 1.43 c). The mechanism responsible for this could be a Hebbian-like strengthening of horizontal fibres connecting the two corresponding areas through repetitive co activation (Hess et al., 1994) as well documented for the somatosensory cortex (e.g. Allard et al., 1991).
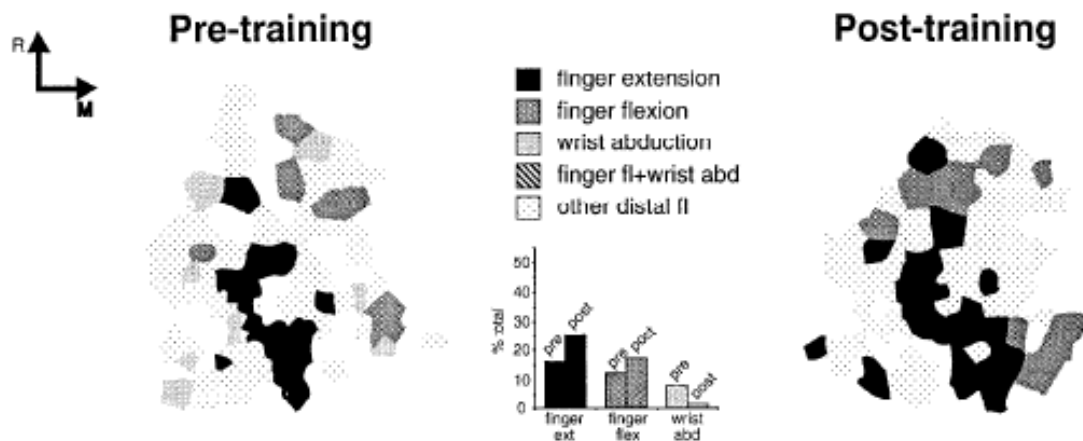

modified from Nudo et al 1996

Figure 1.43a

Representation of finger extension, finger flexion, and wrist abduction movements in cortical area 4 derived from pre- and post- Kluver board training mapping sessions.

Observations:

1) Relative area devoted to both finger extension and finger flexion movements increased
2) Relative area devoted to wrist abduction movements decreased

   Note: In bar graphs, finger flexion + wrist abduction dual- responses are included in each individual movement categories
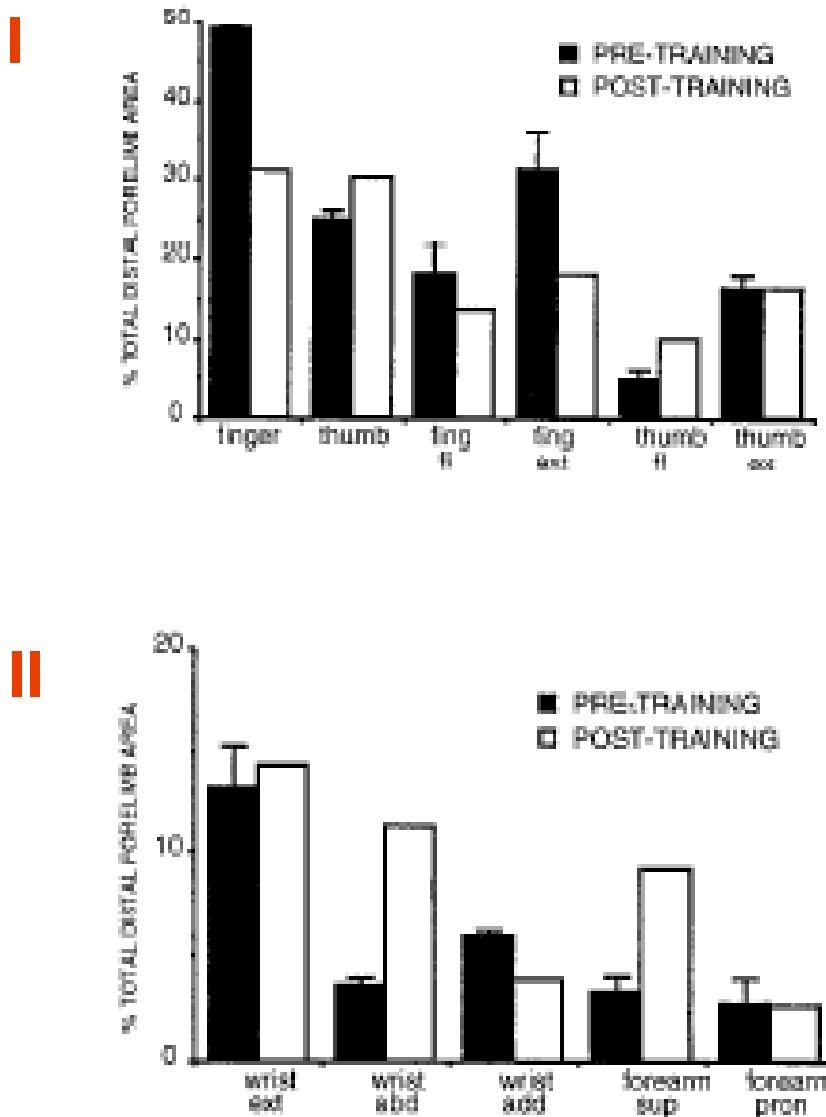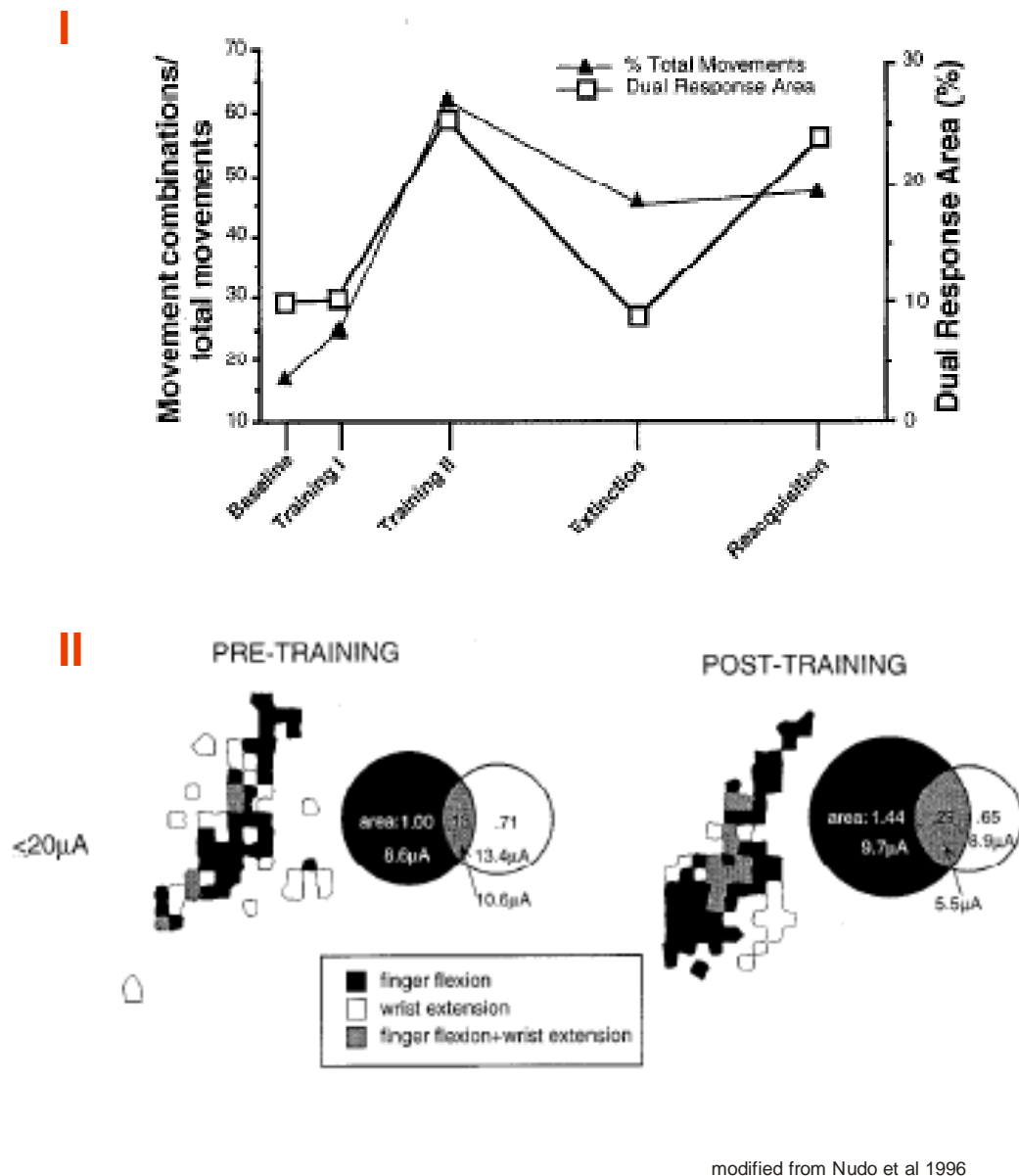
Figure 1.43 b

Proportions of selected forelimb movements in area 4 before and after a training task requiring repetitive forearm supination and pronation (eye-bolt task)

Plot I represents the plastic changes in the finger controlling area whereas plot II shows the corresponding changes in the wrist and forearm area of M1.
In sum there is a substantial loss of finger representations at the expense of wrist and forearm representations although some individual movements show an inverse tendency.

Note: fingers = D2-D5; thumb = D1

Modified from Nudo et al. (1996).

I

II PRE-TRAINING   POST-TRAINING

finger flexion
wrist extension
finger flexion+wrist extension

modified from Nudo et al 1996

Figure 1.43c

I: Proportion of total movements elicited by ICMS comprising movement combinations.

   Representational area is the percentage of distal forelimb area from which dual responses were evoked.

   Note, that dual responses are the electrophysiological correlate of multiple – joint movements elicited in ICMS.

II: Pre and post training representation of M1 forelimb areas of finger flexion, wrist extension, and combined (dual

   responses) finger flexion + wrist extension. Note that in this representation only sites at which threshold was ≤ 20 µA were considered. After training, the finger flexion zone as well as the combined finger flexion + wrist extension zone increased substantially in total areal extent. Training also resulted in a decrease in the average threshold for evoking wrist extension indicating learning induced motor cortex plasticity.

1.8 Functional recovery

1.8.1 Spontaneous recovery

After a lesion to the motor part of the CNS, functional recovery may occur, based on different mechanisms to re-establish the lost motor abilities (Xerri et al., 1998; Rouiller and Olivier, 2004). Thereby, most often, the lost abilities are compensated by alternative movement strategies (Friel et al., 1998; Roby-Brami et al., 2003) rather than a complete recovery of the original movement. As this type of recovery of function occurs in absence of therapeutic interventions, it is called spontaneous recovery. Unfortunately such recovery often leads to movement patterns which are coupled with the so called learned nonuse phenomenon (Taub et al. 2006). This means that, although an impaired body part is functionally still enough connected to the motor system to be controlled; however, the animal or the patient uses a compensatory movement pattern excluding the impaired body part. Such compensatory movements can be sufficient for an attained individual to handle daily life but clearly has the potential to be improved by rehabilitative strategies activating the hidden motor potential achieving better post lesion recovery closer to the prelesion situation. How different post lesion "therapies" can influence plasticity in the M1 hand area either to induce recovery towards use or nonuse of the attained limb was demonstrated in two ICMS studies of Nudo and collaborators (Nudo et al., 1996; Nudo and Milliken, 1996), (see Figure 1.44 below; for details about the first study see paragraph 1.8.2). In other words, corresponding therapies should aim to optimize/direct natural spontaneous recovery processes to reach maximal functional recovery. The following two paragraphs line out different post-lesion therapies in more detail.
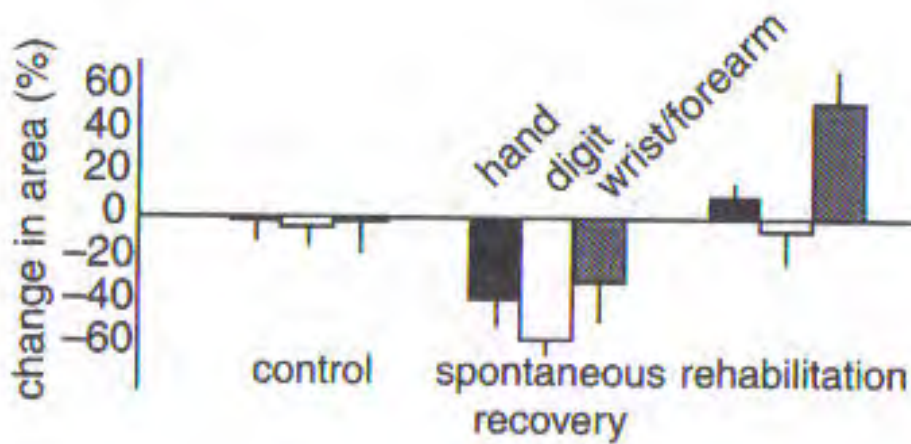
Figure 1.44

Reorganization of M1 hand area after subtotal infarct in squirrel monkeys.
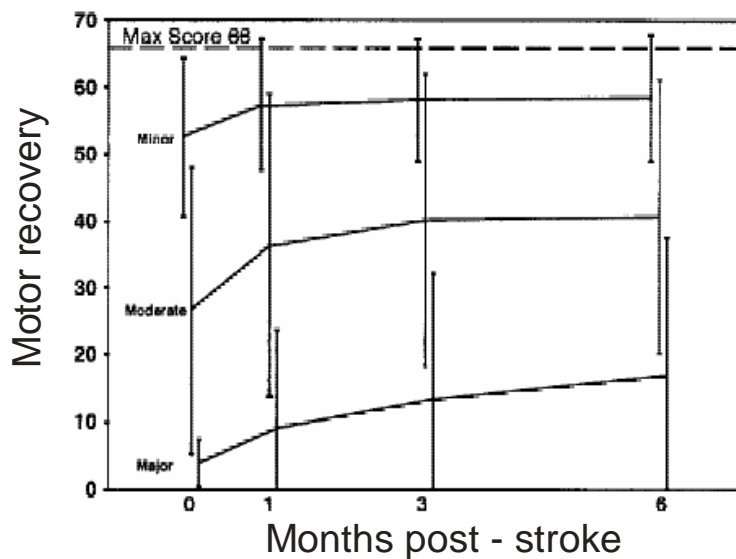
Control: Only ICMS mapping
Spontaneous recovery: No specific training after infarct
Rehabilitation: Daily repetitive training on Kluver board for two to three weeks after infarct.
Modified from Nudo et al. (1996).

1.8.2 Training induced recovery

a) Constraint induced recovery

Figure 1.45

Evolution of post stroke functional recovery in humans as a function of initial severity.

Modified from Duncan et al. (2000).

As indicated in the Figure 1.45 above, spontaneous functional recovery plateaus about 6 months post-lesion at a performance inferior as compared to the pre-lesion situation. Even patients with minor lesions do not reach the normal maximal score of 68. More disturbing in daily life are these chronic impairments in patients suffering from major lesions reaching a performance level of only 15. But since Taub and colleagues (2002) introduced the *constraint-induced movement therapy,* there is hope for patients chronically suffering from post stroke handicaps. This type of therapy was especially successful for the reinstatement of skilled use of the hand in patients that have entered treatment with chronic deficits.

As in quiet every research field first attempts to document neurophysiological plasticity associated with constraint-induced, repetitive, training of the impaired limb were done in experimental animals. To do so, Nudo et al. (1996) trained squirrel monkeys in the same Kluver board task as in the study described in paragraph 1.5.2.1. After a preinfarct training of about one month to reach stable performances in the task, a small lesion in the caudal M1 hand region was introduced. In contrast to the former study immediately after the infarct, monkeys were fitted with a soft mesh jacket restricting the unaffected hand. As a consequence, during the one month post-lesion training, monkeys were forced to use the impaired hand. Data analysis revealed that the trained animals returned to pre-lesion scores on the smallest, most difficult food-well ever attained by spontaneous post-lesion recovery. The better performance was paralleled by maintenance of the pre-lesion distal hand area initially spared by the infarct. This means no further loss of distal hand representations, as well as no expansion of the proximal hand area adjacent to the lesion as it was seen in spontaneous recovery (see Figure 1.44 above). The results of this study strongly supported the idea that constraint induced therapies (CI therapy) are the "key" towards a better more physiological recovery in stroke patients.

In clinics, the CI therapy is most frequently used to counteract the learned nonuse phenomenon in stroke patients. The idea that such a therapy could improve post-lesion recovery has its origin in clinical observations. Numerous patients, when asked to execute skilled movements with the attained limb, succeed although when ask without trying, they would say that they cannot do a particular movement. This discrepancy has its explanation in the fact that immediately after stroke, patients really cannot make use of the attained limb. As a consequence of this, they are convinced that the limb is "lost" for ever although constant effort and trials throughout a longer period of time would be successful. So, nearly all individuals give up making efforts to regain pre-lesion motor performance. The positive feedback provided by physiotherapists and neurologists resulting from encouraging patients to do a potentially impossible movement with the attained limb is one important component for successful CI therapy. Another key element for improvement is the

permanent repetition of such movements. Many clinicians report that most of the therapeutic progress is made on the first few days after the initiation of CI treatment. It is also very common for the greatest progress to be made the first day, even when the lack of use of the limb has been present for years or decades. Figure 1.46 below shows a typical CI therapy induced amelioration of motor performance in humans.
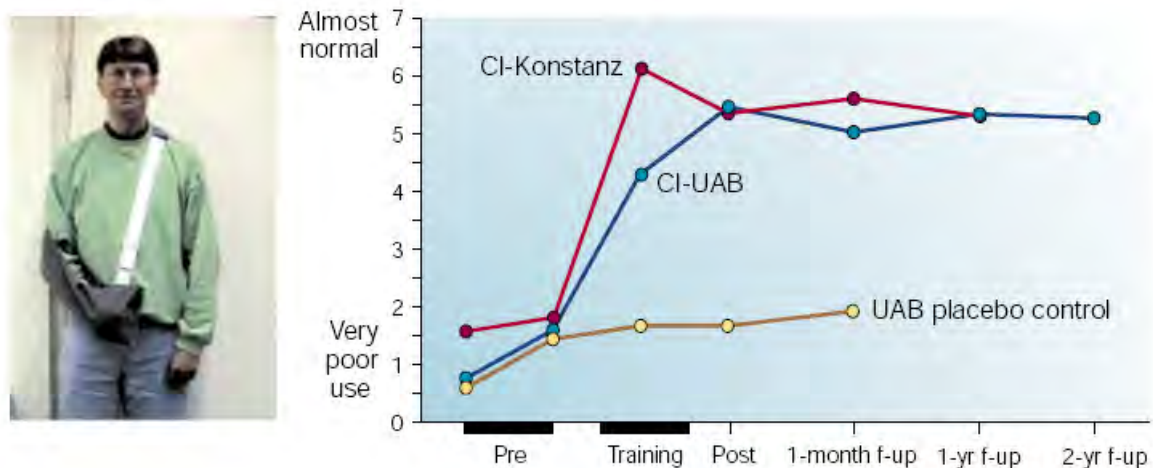
Figure 1. 46 Constraint-Induced Movement therapy. Constraint-Induced (CI) Movement therapy involves constraining the movement of the extremity that is less affected by cerebral nervous system injury and, more importantly, 'shaping' the affected limb (an arm in this case) for many hours a day for two or three consecutive weeks. The constraint, by a sling or a mitt, forces the individual to make use of the more affected extremity. The quality or skill of the movements is systematically improved by a shaping procedure. This method was derived from work with monkeys that would not make use of a deafferented arm, but readily learned to use this extremity either through shaping or when the constraining device prevented movements of the intact arm. The data show a large increase in real-life arm use in a CI therapy group trained at the University of Alabama at Birmingham (UAB), and the close replication of this result in a group treated at the University of Konstanz. A placebo group that received a general fitness programme did not show a significant change over time. (f-up, follow-up study.)

From Taub et al; New treatments in neurorehabilitation founded on basic research;
Nature reviews neuroscience Volume 3 pp. 228 – 236: 2002

Nowadays it becomes also more and more clear that tasks representing movements of daily use are more effective because patients are more easily motivated to repeat the exercise, as it makes sense to them. In contrast to animals, it seems not to be crucial to completely restrain the unimpaired limb in humans if they themselves pay attention to exclusively use the attained limb. In spite of the positive influence of CI therapy on recovery, one should not forget that a substantial part of the respective impairment in a patient comes from the permanently destroyed part of the CNS. Miracles are not expected in the sense that CI therapy-induced improvements could restore the motor status patients had before stroke. Although impairment and disability can be meaningfully reduced, there is typically still a deficit. The most important elements about CI therapy are represented in the Schema 1.1 below (Taub et al., 2006).
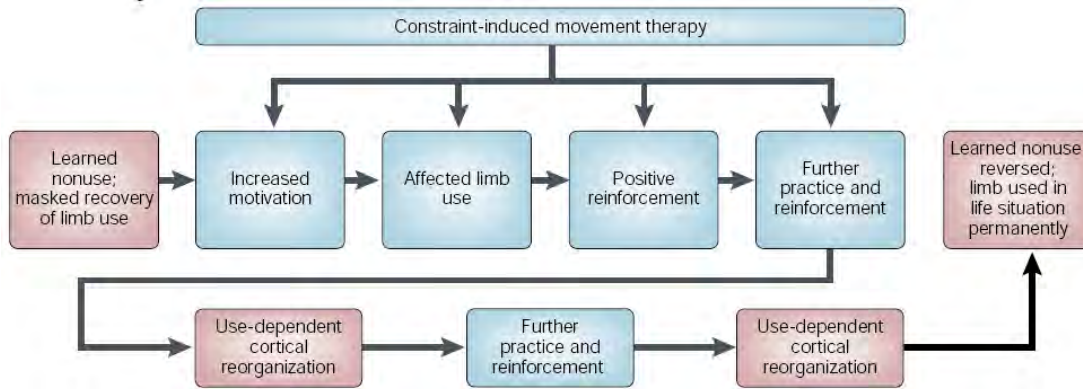
Schema 1.1   Overcoming learned non-use by constraint induced movement therapy
                    (From Taub et al., 2006).

Note also, that CI therapy should not be too severe, otherwise it may be detrimental as the lesion may become bigger (see Nudo, 1999 for review).

b) Physiotherapy and robotic devices

Achieving maximal post-stroke recovery strongly depends on the quality of rehabilitation. As recovery processes are reflected or temporally stored in cortical reorganization, it is of great importance to guide these plastic changes the way to nearly restore natural movement sequences. Therefore physiotherapists have a great impact on the outcome of rehabilitative training. Two factors are limiting in this context: First, a physiotherapist has limited time he can dedicate to a given patient. Second, movements practiced under the survey of physiotherapists are never completely optimized to an individual patient. So herein lies another potential to ameliorate post-lesion recovery. In order to profit from this potential, robotic devices such as the LOKOMAT and ARMIN were developed. In contrast to physiotherapists, they never get tired and are easily perfectly individualized to a patient.

Basically both devices are similar from a technical point of view the only difference is that the LOKOMAT is thought for patients with leg and foot impairments and ARMIN for patients with impairments of the arm and hand. Because stroke survivors often show problems with skilled movements of arm and fingers the next paragraph will briefly line out some important features of ARMIN which makes it a future oriented therapeutic device for stroke patients. ARMIN belongs to the so – called patient – cooperative controllers. Such robotic devices have the advantage that they can take into account the patient's intention and efforts rather than imposing any predefined movement by the help of measuring sensors.

Because of these constant feedback measurements, the robot "knows" the amount of force the patient can produce himself to make a particular movement. Consequently ARMIN supports the patient's impairment only as much as needed to complete the intended movement. So the therapeutic aid is precisely adapted to individual patients. The advantage of this type of rehabilitative training is that patients can repeat movements much longer and more precisely than it can be achieved with classical physiotherapy. In addition, audiovisual displays in combination with ARMIN can be used to present a virtual environment and let the patient perform different motor tasks and activities of daily life. This makes rehabilitative training more interesting and understandable for patients. Therefore, the positive impact of motivation can be increased (compare with key elements for successful CI therapy in Schema 1 above) (Riener, 2004).

1.8.3 Cortex stimulation induced recovery

As already mentioned several times, plasticity is one of the crucial mechanisms underlying post stroke recovery in mammals as well as in humans. Therefore it is not surprising that the observation that ICMS can induce additional plastic changes in the cortex of adult rats (Nudo et al., 1990) culminated in the innovative idea to make use of this side effect of cortex stimulation techniques in post stroke rehabilitation. Basically, the future application of such stimulation therapies is thought to lie in the chronic post-stroke phase where performances of patients plateau at a level substantially below normal resulting in persistent impairments. One could also imagine combining rehabilitative training such as CI therapy with cortex stimulation to generate cumulative positive effects on post-lesion motor performances. Several approaches along this line were made of which representative studies are briefly discussed in the next two paragraphs.

a) Electrical stimulation

Probably inspired by the findings of Nudo et al. (1990) and other pre-clinical and clinical studies of the same type, DeAnna et al. (2003) investigated whether performance of a reaching task after focal ischemic cortical lesions is improved in experimental rats as compared to controls, as a result of combining rehabilitative training on this task with concurrent electrical surface stimulation of the cortex. They chose the Montoya staircase task which is especially suited to evaluate both forelimb skill acquisition and sensorimotor impairments. The lesion in the primary somatic-sensory and motor cortex (SMC) was created by the endothelin-1 vasoconstriction method. Post lesion control animals did not receive any electrical stimulation but were trained in the Montoya staircase task. In experimental animals a stimulating surface electrode was placed subdurally over the forelimb representing area of SMC. Two experimental groups during post-lesion training received additional sub-threshold stimulations (threshold = forelimb movements evoked in 50% of 10 pulse

trains) by 3 second trains of 1 msec pulses at either 50 Hz or 250 Hz. Behavioural data from the post lesion training revealed that rats from the 50 Hz group had a significantly greater improvement over days of post-lesion training in comparison to the 250 Hz group and controls. It is interesting that there was no detectable improvement in the 250 Hz group indicating a frequency dependence of cortical stimulation therapies. The authors also looked for evidence of cortical plasticity paralleling better behavioural improvement. Immunostaining for MAP2 (more expressed during peri-lesion plasticity indicating compensatory dendritic restructuring in remaining neurons) of dendritic processes was significantly increased within layer V of the cortex contiguous to the lesion of the 50 Hz group. Although the mechanisms of the cortical stimulation therapy (CST) remain uncertain the above findings support the idea that CST may promote restorative plasticity at multiple levels ranging from cytoskeletal proteins to neuronal networks.

Plautz et al. (2003) tested whether the findings from the above rat study can be confirmed in squirrel monkeys and if there are substantial post-lesion plastic changes in the motor cortex paralleling behavioural recovery. Cortical stimulation parameters were close to those used in the 50 Hz rat group of DeAnna et al. (2003) (continuous sub-threshold stimulation at 50 Hz with pulses of 100 μsec duration) having the greatest positive impact on recovery in rats. In this squirrel monkey model, the ischemic injury in the M1 hand representation was created by bipolar electrocoagulation. Attention was paid to spare as much as possible of the lesion surrounding cortical tissue potentially taking over the function of the destroyed hand area. The stimulating surface electrode was placed to include as many spared hand representations in the peri-infarct motor cortex as possible beneath the electrode to provide an initial neural substrate for facilitating recovery. Experimental as well as control monkeys were submitted to a pre-lesion training on the Kluver board task until they reached stable performances. Then the lesion in the M1 hand representation was introduced. Cortical stimulation therapy was started after spontaneous recovery reached the plateau phase (at least 3 months post-lesion) indicating that the persisting impairments were chronic. Control animals were only retrained on the Kluver board task. Experimental animals received cortical stimulation starting 5 minutes before rehabilitative training began and was maintained throughout the 35 min training session. Animals were trained twice a day on a daily basis for 11-24 days. Pre- and post-infarct ICMS maps of M1 movement representations were made. In addition, a post-therapy motor mapping of the peri-infarct motor cortex was done in each animal. Behavioural analysis revealed that each monkey of the experimental group showed substantial improvements in task performance during the course of therapy. Nevertheless the combination therapy (electrical stimulation + training) produced only incomplete recovery from chronic motor performance deficits. In spite of that, it has to be mentioned that the improvement was clearly higher than spontaneous or only rehabilitative training-induced recovery. The 4 month follow up of the attained performance level

showed no relapses in the absence of the combination therapy. So the effect persisted over time and was paralleled by the persistence of map changes over this same period. The authors found extensive regions of newly-emerged hand representations in the peri-infarct cortex, with the majority of expansion occurring in cortex beneath the stimulating electrode. In summary, this study confirms the finding of the rat study in monkeys and therefore electrical stimulation therapies have the potential to be a new effective tool in clinical rehabilitation programs for stroke survivors.

b) TMS

Historically TMS (transcortical magnetic stimulation) was rather developed to track cortical reorganization following/during clinical rehabilitation of stroke patients as it is done by ICMS in experimental animals (e.g Liepert et al., 2000). Because TMS is a non-invasive, low risk technique, it is particularly suited for frequent routine use in clinics. As in ICMS, motor cortical neurons can be stimulated to induce muscle twitches all over the body. The advantage of TMS is that neurons are stimulated by an electric current which is passed through a stimulating coil that is positioned over the scalp. No craniotomy is thus necessary; neither does an electrode have to be lowered in the brain. The generated magnetic field of the coil causes an electric current flowing through the cortex. As a consequence, neurons are depolarized in a small area of the cortex. The resolution of this technique is reasonable, although lower than ICMS, as the coil can be moved across the scalp in 1 cm or even 0.5 cm increments. So TMS as ICMS and cortical surface stimulation induces movements by electrical stimulation of the motor cortex. That is why researchers thought that the phenomenon of use-dependent plasticity fundamentally important in neurorehabilitation may also be improved by repetitive application of TMS as observed for the two other techniques. Several studies were conducted in this context and revealed that the outcome was intensity, frequency and duration dependent as observed in ICMS and surface stimulation experiments (Siebner and Rothwell, 2003).

The study of Bütefisch et al. (2004) demonstrated for the first time that TMS of the cortex combined with motor training can enhance human cortical plasticity leading to better performances in the corresponding motor task. They also provided evidence that the effect of TMS sessions on plasticity may depend on whether stimulation is applied synchronous or asynchronous with movements. In addition, their results show the impact of TMS targeting the ipsilateral M1 (cortex not involved in movement) versus such targeting the contralteral M1 (directly implicated in movements). For this purpose, 11 healthy right-handed young volunteers were studied during training of a motor task under four different conditions:

a) Training alone

b) Training + TMS synchronous in contralateral M1

c) Training + TMS synchroneous in ipsilateral M1

d) Training + TMS asynchroneous in contralateral M1

TMS was applied in single pulses at subthreshold (80% of resting motor threshold) intensities with a frequency of 0.1 Hz. TMS at such subthreshold intensities preferentially activates corticocortical connections targeting pyramidal tract neurons (Day et al., 1987). Furthermore this intensity was shown to be effective in modulating cortical plasticity (Ziemann et al., 1998). To quantify the effect of training and TMS induced plasticity, first, for each subject, the preferred direction of thumb movements induced by TMS was defined (baseline = any movement in the direction of the training target zone (TTZ)). Second, for the subsequent 30 minutes training, subjects were told to mentally move (without execution) the thumb exactly in the opposite direction as compared to the preferred direction (training target zone (TTZ)). At the end of the different training sessions the motor cortex was again stimulated by TMS in order to evaluate whether the proportion of thumb movements within the TTZ had increased. So, the higher the proportion of movements within the TTZ, the stronger was the effect on cortical plasticity of the corresponding treatment (a-d). In the Figure 1.47 below, effects of each type of "treatment" a) to d) are represented.
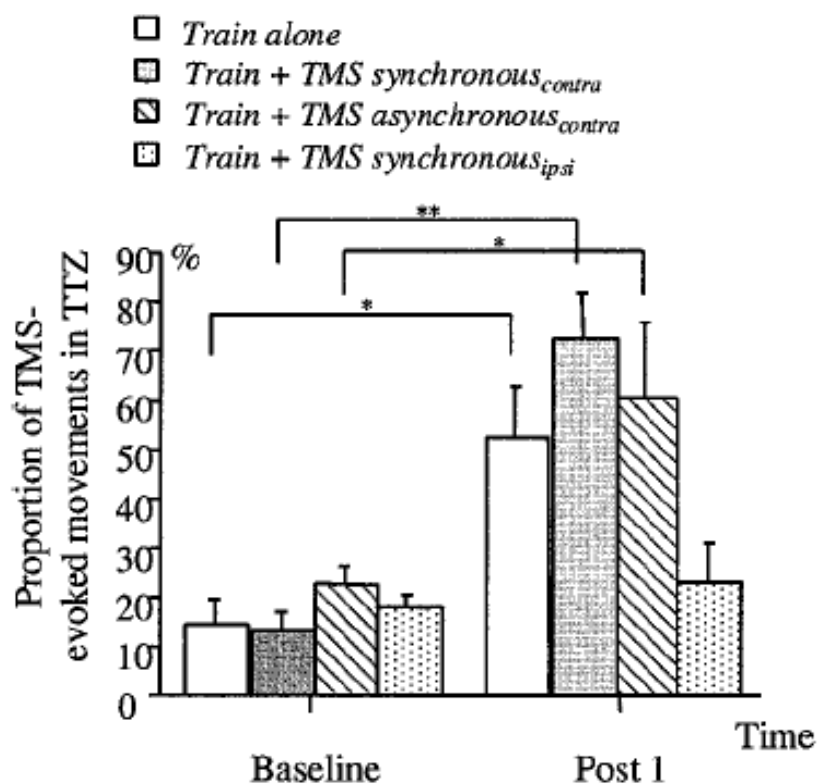
Figure 1.47 Proportion of TMS – evoked movements in the TTZ before (baseline) and after (post 1) training. All interventions except Training + TMS synchronous ipsilateral led to a significant increase in the proportion of TMS evoked movements in the TTZ.

The authors also investigated how long the effect persists after the 30 minutes training session. Depending on the intervention, the training effect lasted about 20 minutes (training alone) to even ≥ 60 minutes (training + TMS contralteral synchroneous). In summary, this study shows in spite of limited short training sessions, that TMS can induce motor cortical plasticity, enhance the effects of motor training, and prolong the duration of this memory and that the ipsilateral hemisphere is differently implicated in such training than the contralateral movement executing hemisphere. As visible in Figure 1.47 above, the more synchronized stimulations and motor movements are, the higher is the effect. This is in accordance with different studies claiming that the more inputs converge onto a target neural structure in temporal synchrony, the more they enhance cortical plasticity (e.g Baranyi and Feher, 1981). Differences in the longevity can be explained by the Hebbian principle that potentiation of synaptic efficacy (LTP) is higher when its pre- and postsynaptic elements are simultaneously active. The fact that ipsilateral TMS reduced the training effect is in accordance with the theory of interhemispheric competition resulting in balanced interhemispheric interactions necessary to generate proper voluntary movements (Murase et al., 2004; Ferbert et al., 1992).

1.9 Nogo

As the subject of Nogo by itself could be the theme of an entire thesis, this chapter concentrates on most important aspects about Nogo and anti-Nogo-treatment relevant to understand how the idea of treating cortical lesions in monkeys by anti-Nogo-A came into play. Second, this chapter is thought to provide arguments why such a treatment has the potential for future successful clinical application in stroke patients. Looking at this chapter, the reader has to keep in mind that Nogo is not the only inhibitory factor leading to failure of CNS regeneration but one of the most potent (see for review Schwab, 2004; Yiu and He, 2003).

In contrast to the peripheral nervous system (PNS) and the immature central nervous system (CNS) where injured nerve fibres can regenerate or react with structural plasticity, lesions in the adult CNS always lead to severe and irreparable disabilities. So what is different in the adult CNS as compared to immature CNS or PNS? At a first glance, not much, as nerve fibres in the adult CNS after lesion initially start to sprout. So, the most important requirements for regeneration of the injured axons seem to be met: namely, the survival of the nerve cell body and its capacity to induce gene expression, leading to axonal re-growth and re-innervation of the original targets. But although genes are expressed, unfortunately what is crucial for the final lack of regeneration in CNS is that nerve fibres of the adult CNS fail to regenerate over long distances and cannot contact appropriate target cells, finally resulting in the observable permanent loss of function. As a consequence of this, any therapeutic approach to induce successful regeneration in adult CNS somehow has to mimic the

physiological environment of either the PNS or the developing CNS. A task particularly difficult as first, a multitude of cellular and molecular factors is implicated and second, re-induction of normally suppressed growth processes in adult mammals always has the potential of malign tissue formation, for example tumours.

### 1.9.1 Can Anti-Nogo-A treatment partially mimic immature CNS?

It is well known that embryonic CNS axons can regenerate quite readily and that they lose this capacity postnatal with age (e.g. Dusart et al., 1997) leading to an abortive regenerative response. This loss of adequate axonal growth capacity is paralleled by the maturation of CNS glial cells, both astrocytes and oligodendrocytes. Myelin was detected as key factor in limiting the regenerative capacity of CNS with aging. For example Keirstead et al. (1992) showed in chick embryos that a suppression of the onset of myelination extends the permissive period for functional repair of embryonic spinal cord. Such experiments attribute a decisive role to the presence of extrinsic factors in the adult CNS microenvironment of neurons in terms of whether regeneration after lesion is permitted or suppressed. Caroni and Schwab (1988) detected two major myelin-associated neurite growth inhibitors **NI-35** and **NI-250** in the adult CNS myelin. In vitro, tests with these two proteins induced long-lasting growth cone collapse and inhibited neurite growth. Application of the monoclonal antibody **IN-1** directed against these two proteins allowed neurite outgrowth on adult CNS myelin or cultured oligodendrocytes in vitro. That adult CNS reacts similar to injury, if the inhibitory effect of myelin is blocked by IN-1 antibody, as neonatal CNS not yet expressing NI-35 and NI – 250 was demonstrated in a in vivo study by Wenk et al. (1999) (details about this study are represented below). So, in fact as hypothesized in the introducing lines of this chapter, successful regeneration should partially be attributable to a repetition of developmental processes.

1.9.2   Differences between CNS and PNS milieu in adult mammals leading to failure of CNS regeneration (first observations by Schwab et al.)

To test whether failure of adult CNS regeneration is due to different intrinsic properties of CNS neurons as compared to neurons of the peripheral nervous system or rather to a different extracellular milieu in these two systems, Schwab et al. (1985) used a tissue culture dish setup as represented in figure 1.48 below. This experiment was one of the first decisive steps in the 20 years history of NoGo research of Schwab and collaborators leading to the present understanding of CNS regeneration failure after injury. In fact the findings of this study were particularly important in "accusing" *central* myelin playing a crucial role in the lack of regeneration after CNS injury. In contrast to central myelin produced by oligodendrocytes, myelin of the PNS is the product of

Schwann cells. Oligodendrocytes are only one type of central glial cells, fundamentally different from PNS glial cells. In addition, there is an exclusive presence of basement membrane in the PNS. In their experiment Schwab et al. (1985) in a three compartment arrangement put in the middle compartment either dissociated newborn rat sympathetic or sensory neurons. The central chamber was connected by two small bridges of either an adult sciatic or an adult optic nerve explant to two adjacent chambers. Neurons were grown in the presence of optimal concentrations of nerve growth factor (NGF). This type of setup was suited to give neurons the choice to grow along PNS milieu (sciatic nerve explant) or CNS milieu (optic nerve explant) into the respective side chamber. Irrespective of the presence and number of Schwann cells in the PNS explant, a large number of axons could be observed inside the sciatic nerve explant whereas in the optic nerve explant no axon could be found under any tested condition. Axons in the PNS explant preferentially grew on Schwann cell membranes and on the Schwann cell side of the basal lamina. This is exactly what happens after peripheral nerve injury in vivo. So, even under optimal growth conditions (NGF is a strong axon growth inductor) the extremely poor and non-permissive milieu of CNS explants cannot be overcome. This early observation motivated Schwab and colleagues to put enormous effort in research to find the inhibitory factors inside central myelin. They were rewarded in 1988 by the discovery of NI-35 and NI-250 already introduced above.
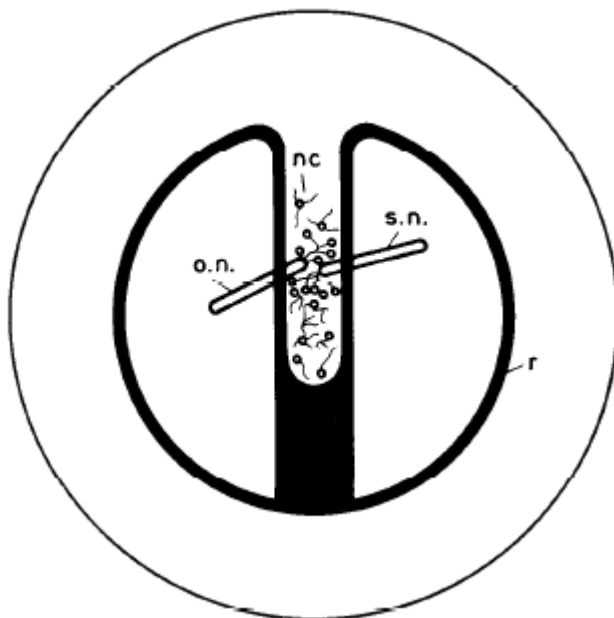
Figure 1.48   Chamber culture arrangement demonstrating the inhibitory effect of central myelin.

r: Teflon ring
o.n.: optic nerve explant (CNS milieu)
s.n.: sciatic nerve explant (PNS milieu)
nc: dissociated neurons

(From Schwab et al., 1985).

1.9.3. Different influence of CNS white and grey matter on axonal growth in healthy animals

So far I have described the great lines about lack of CNS recovery. But, as in all domains, knowledge about details is often more crucial to resolve a problem than first expected. A long this line for successful future clinical application it is not enough to know that CNS is non - permissive for axons but more important is to know whether there are parts within adult CNS tissue naturally allowing axonal growth. One then could think about copying these favourable conditions to induce therapeutic axonal growth in non-permissive tissue. Probably it was this spirit, together with the recent discovery of IN-1 antibody (see above), that encouraged Savio et al. (1989) to study neuronal cell adhesion and fibre outgrowth in adult CNS white and gray matter. For their investigation they used frozen sections of adult rat CNS and PNS as culture substrates for neuroblastoma cells and for sympathetic and dorsal root ganglia. Because, in contrast to higher vertebrates, in lower vertebrates such as fish and amphibians significant axonal re-growth after CNS lesion is also possible in adults, trout CNS white and grey matter was also used as alternative culture substrates. Last but not least, spinal cord sections from newborn rats, injected with an anti-mitotic agent selectively reducing the oligodendrocyte population and, as a consequence also, the myelin content of the spinal cord, and IN-1 antibody pre-treated spinal cord sections from adult rats were as well used as culture substrate. The results of the individual preparations are represented and commented in Figure 1.49 below.
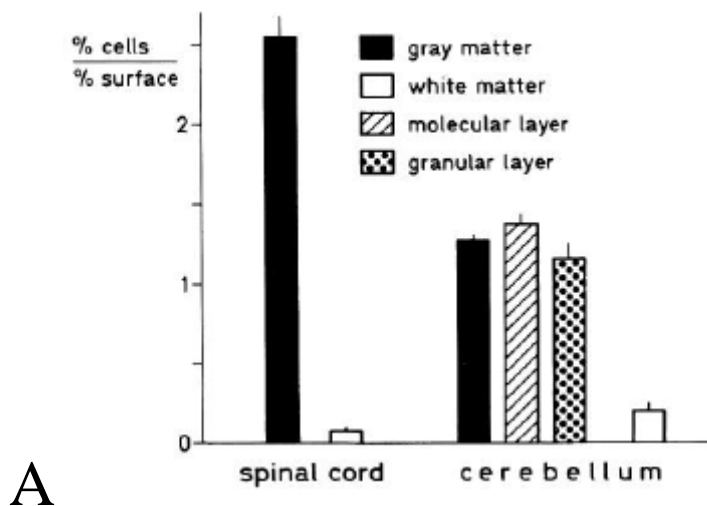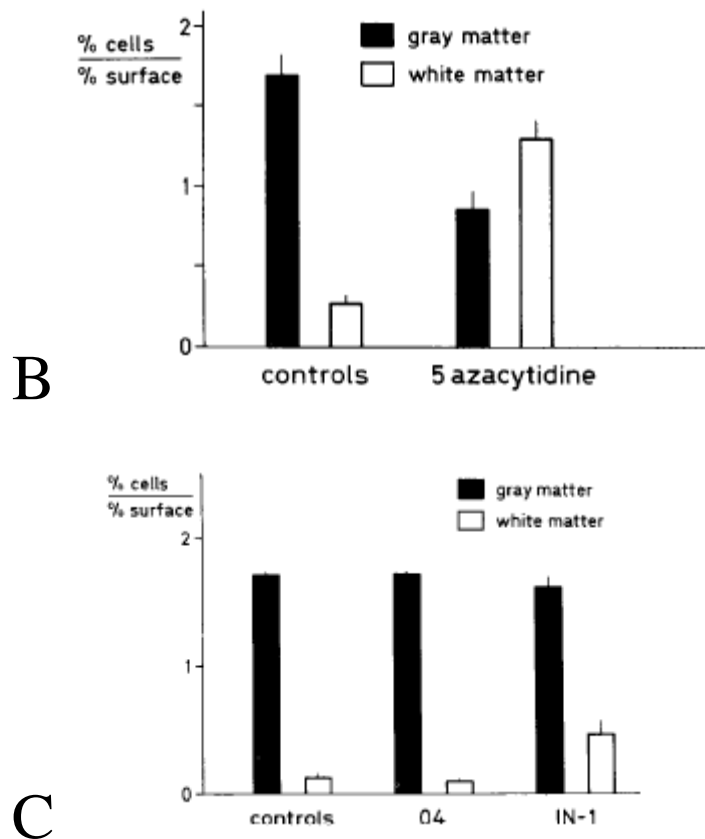
Figure 1.49   Neuroblastoma cell density on white and gray matter of adult rat spinal cord and

cerebellar sections resulting from different preparations.

A: Preparations clearly demonstrating the strong inhibitory characteristics of adult CNS white matter
in the spinal cord and the cerebellum. In contrast grey matter of any part of the adult CNS
does not show inhibitory effects.
B: This preparation demonstrates that 2 (oligodendrocytes and myelin) of the 3 main components of
white matter regions are responsible for the non-permissive character of adult CNS white
matter whereas the third component (astrocytes) is of secondary importance.
C: Comparing the three preparations reveals an increase of neuroblastema cell density on white
matter regions incubated with IN -1 antibody but not with control antibody 04.
Y – axis: percentage of neuroblastema cells related to the percentage of the corresponding region
surface (white, grey matter, molecular or granular layer) of a particular culture substrate.
X – axis: respective culture substrate of neuroblastema cells

04: control antibody strongly labelling myelin and oligodendrocytes

5 azacytidine: antimitotic agent selectively reducing oligodendrocytes

(Modified from Savio et al., 1989).

From this study, the authors concluded that adult rat CNS white matter (oligodendroctes and
myelin), but not astrocytes and gray matter, from various parts of brain and spinal cord is a non-
permissive substrate for adhesion of neurons and neuroblastoma cells and for axonal elongation.
This property is linked to the presence of oligodendroglia and adult CNS myelin and is significantly
reduced by IN -1 antibody against CNS myelin inhibitory substrate components (NI-35 and NI-

250). In addition neuroblastoma cells adhered approximately equally well to grey and white matter of adult trout spinal cord sections. It is not clear whether the absence of laminin in the adult fish CNS is responsible for the observed permissive properties.

1.9.4 Inhibitory power of CNS white matter on axon growth is related to maturation and injury

The Figure 1.50 below is thought as an introductory summary of the changes in CNS environment related to injury and maturation. The next parts of this chapter will explain in more detail the here briefly described alterations focussing on the ones induced by CNS injury.

Figure 1.50 Changes in CNS environments after maturation and injury (from Yui and He; Nature reviews 2006)

During embryonic development, unmyelinated axons with motile growth cones can extend, retract and respond to various trophic and guidance molecules. This dynamic process allows the neural circuitry to be fine-tuned (**a**). As the nervous system matures after birth, myelination is finalized with oligodendrocytes ensheathing axons to prevent aberrant sprouting and astrocytes secreting chondroitin sulphate proteoglycans (CSPGs) to further limit structural plasticity in the adult (**b**). After CNS injury, axons become transected and reactive astrocytes further upregulate their secretion of CSPGs. The distal endings of severed axons form dystrophic growth cones and become exposed to CSPGs from the glial scar, as well as myelin-associated inhibitors from oligodendrocytes and myelin debris (**c**). As similar mechanisms prevent short-range plasticity in the adult and long-distance axon repair after injury, relieving these inhibitory influences might not only enhance the regeneration of severed axons, but might also promote compensatory sprouting. EphA4, the cognate neuronal receptor for ephrin B3; MAG, myelin-associated glycoprotein; NgR, Nogo-66 receptor; OMgp, oligodendrocyte myelin glycoprotein; Trk, tyrosine receptor kinase.

1.9.5 Cellular components of inhibition

Because neurons themselves seem not to have crucial inhibitory effects on axonal growing after damage to the CNS, the inhibitory action must be dedicated to the CNS glia consisting of oligodendrocytes, astrocytes and microglia cells. Fully differentiated oligodendrocytes have a permanent inhibitory effect on axonal growth, whereas astrocytes in healthy adult CNS do not inhibit axonal growth. Bandtlow et al. (1990) demonstrated this in an elegant in vitro experiment. They used video time-laps microscopy to analyze the interaction of growth cones of newborn rat

dorsal root ganglion cells with dissociated young rat CNS glial cells present in the culture at low density. When a growth cone encountered astrocytes it maintained its normal configuration and growth velocity. In contrast, when encountering differentiated oligodendrocytes, firm filopodia contact was sufficient to induce a rapid long lasting arrest of the growth cone motility. Often a subsequent collapse of the growth cone structure was observed. One third of the paralyzed growth cones were observed to retract. This behaviour could be prevented by the monoclonal antibody IN-1 directed against the main inhibitors of myelin (NI-35 and NI-250) produced by differentiated oligodendrocytes. Figure 1.51 below represents the influence of astrocytes, differentiated oligodendrocytes and differentiated oligodendrocytes in the presence of IN-1 antibody on growth cone velocity.
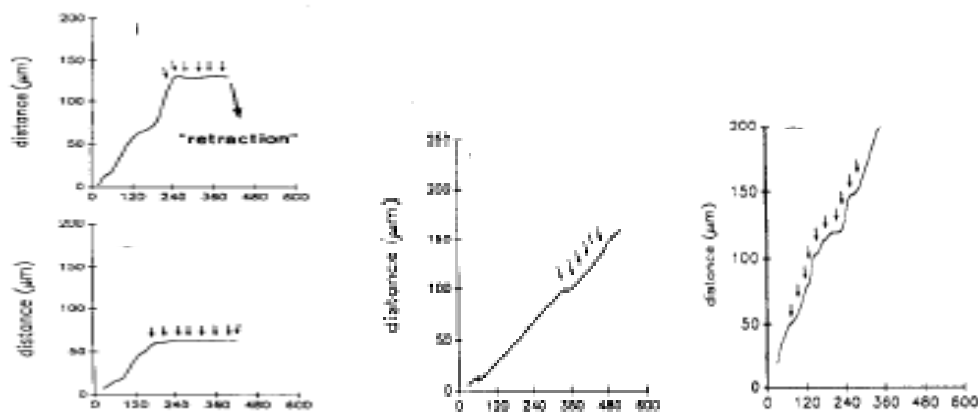
Figure 1.51   Growth cones encountering different CNS glia cells.

> **Left top:** Growth con encountering a differentiated oligodendrocyte first reacting with arrest
>   followed by retraction
> **Left lower:** Growth con encountering a differentiated oligodendrocyte reacting with arrest
> **Middle:** Growth con encountering an astocyte reacting with a minimal reduction in growth
>   velocity but then continuing growing with the previous velocity
> **Right:** In the presence of the IN – 1 antibody growth cones, though sometimes reducing their
>   growth rate, continue to move along oligodendrocyte processes
> **X –axis:** Time in minutes
> **Y – axis:** Distance travelled in μm

From this study, it can be concluded that the oligodentrocyte itself is not responsible for the observed axon growth inhibition but its product myelin. Following CNS lesion associated with degenerating fiber tracts i.e. where axons have been damaged, oligodendrocytes around the lesion site undergo apoptotic cell death. But this is not the decisive step concerning inhibition. More important is the fact that following CNS lesion, the myelin sheaths are degraded by proteases

leaving myelin debris at the lesion site. Unfortunately, in contrast to PNS where macrophages immediately clean this debris, in the CNS the number of macrophages is considerably lower. Instead resident microglia cells acquire full macrophage competence only after long time resulting in long term persistence of myelin debris at the lesion site. As a consequence axonal re-growth is strongly impaired. In addition to myelin debris deposition and invasion of microglia cells, astrocytes at the lesion site transform into *reactive* astrocytes. Reactive astrocytes become hypertrophic, greatly increase their expression of vimentin (intermediate filament protein), GFAP (glial fibrillary acidic protein), up-regulate their expression of scar-associated inhibitory CSPGs (neurocan, phosphocan and versican). The sum of these three post lesion events is known as reactive gliosis finally leading to non-permissive scare tissue at the lesion site. Glial scar formation starts within hours of injury and forms both a mechanical and molecular barrier to axon growth. At a molecular level the glial scar does not only act as a diffusion barrier for growth-promoting-molecules but as listed above contains active inhibitors of axonal re-growth.

1.9.6 Collateral sprouting: A "natural" way of the injured CNS to partially recover after injury?

Besides re-growth of damaged axons after CNS injury, the CNS reacts by a second important mechanism to re-establish the lost functions. Uninjured axons can respond to denervation of neighbouring areas by developing new fibre branches that innervate the denervated tissue. This reaction is considered as *collateral sprouting* and has been reported to occur in both the PNS and the CNS. Unfortunately, as axonal re-growth, this regenerative mechanism also becomes strongly impaired in the adult CNS. Although in some regions of the CNS, where myelination is low, a considerable degree of collateral sprouting in the adult was reported, for example in the hippocampus, the olfactory bulb and the substantia gelationsa of the spinal cord. In contrast, in the developing CNS and lesioned PNS, collateral sprouting is markedly enhanced. This leads to the conclusion that collateral sprouting as well as fibre re-growth is negatively correlated to myelination implicating the same myelin associated inhibitory substances. This hypothesis was confirmed by Schwegler et al. (1995). By the mean of x-ray irradiation in neonatal rats at lower thoracic and lumbar spinal cord level they strongly suppressed myelination in the white and grey matter creating animals with locally myelin - free spinal cords. Their results revealed that lesion induced collateral sprouting was strongly enhanced in the myelin-free spinal cords as compared to normal spinal cords. This suggests that myelin and myelin-associated neurite growth inhibitors are involved in the restriction of sprouting in the adult CNS. For future clinical application it is extremely important to overcome this inhibition of collateral sprouting, as this local event is probably more important in terms of plasticity or conditions such as stroke.

1.9.7 Events occurring after damage to CNS
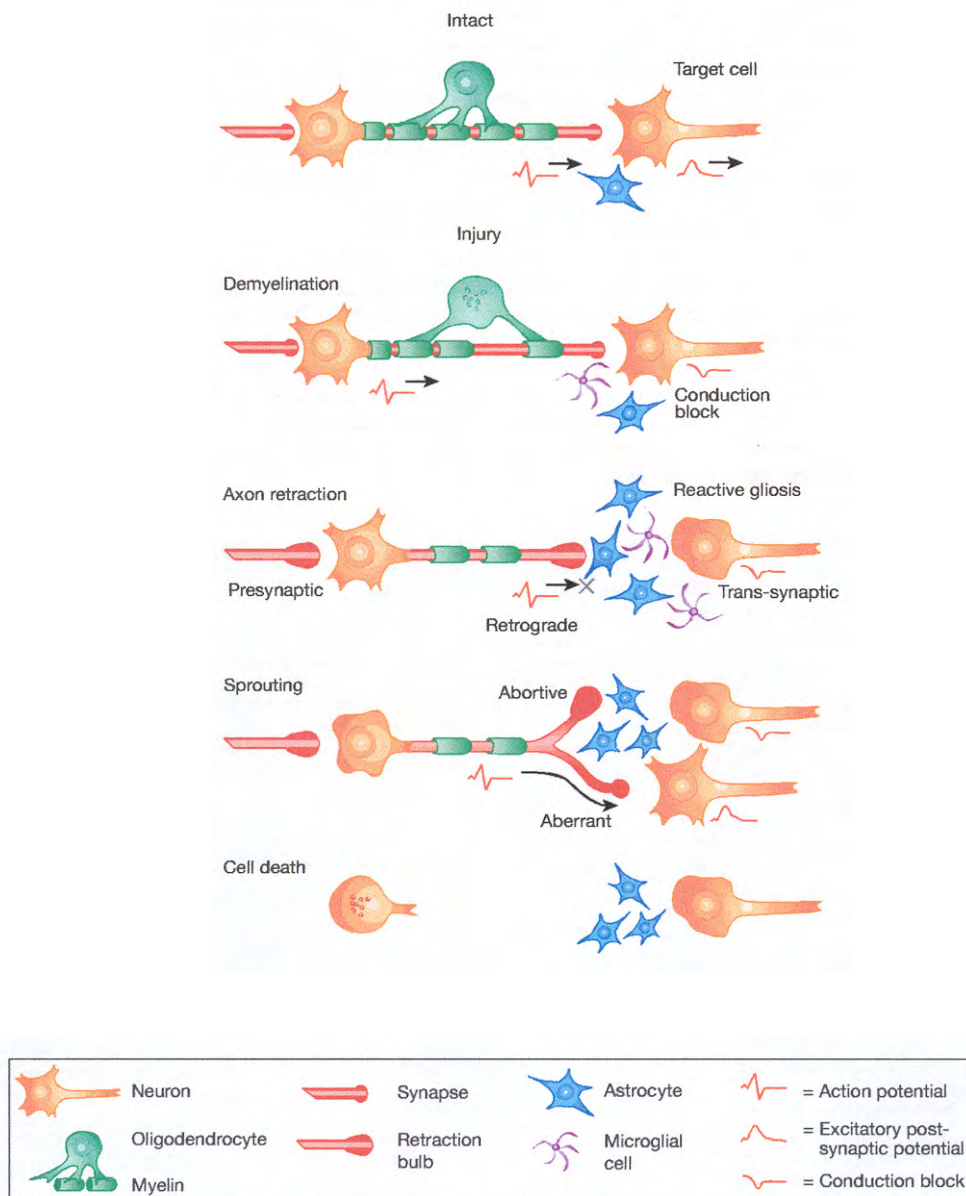
Following a specific traumatic or chemotoxic event, or as a result of ongoing degenerative processes, long-term structural and functional deficits occur in the adult CNS. In severe cases, these insults are not repaired or compensated for by surviving systems. On a cellular level, these deficits include demyelination, degeneration, abortive or aberrant sprouting, and cell death.

Demyelination. A demyelinated axon may maintain both its afferent and efferent connections but, due to a loss of myelination, poor or failed conduction results.

Axonal retraction. Injury to an axon itself or to the original cellular target of the axon can result in degeneration. Presynaptic, retrograde and trans-synaptic degeneration can occur. Synaptic conduction across a pathway is lost and a reactive cellular response, including astrocytes and microglia, forms.

Sprouting. Axonal sprouting has been described for surviving neurons. It is typically abortive when a sprouting axon encounters an inhibitory matrix or scar, loss of neurotrophin support, or the presence of continuing inflammation or toxicity. Aberrant sprouting can occur when an axon reconnects to an inappropriate target. Synaptic conduction is restored but this pathway does not result in functional restoration.

Cell death. When a neuron is completely deprived of its source of growth factors and exposed to high levels of toxic molecules or inflammatory attack, it can undergo cell death. These patterns

represent the anatomical correlates of brain dysfunction but also the
specific processes that must be targeted for repair.

Figure 1.52   Summary of the different events that can occur after damage to CNS neurones.

(Modified from Horner et al., 2000).

1.9.8 Molecular components of inhibition

a. Glial scar-associated inhibitors

In addition to myelin-associated inhibitors there is a progressive response from glial cells surrounding the CNS injury site. Mainly this process of glial scarring is characterized by the proliferation and migration of astrocytes into the lesion site. Once arrived there, they deposit extracellular matrix creating a mechanical barrier for regeneration, as already described above. In addition reactive astrocytes within the glial scar express chondroitine sulphate proteoglycans (CSPGs) which chemically inhibit axonal outgrowth. After injury, CSPG expression is rapidly upregulated, forming an inhibitory gradient that is highest in the centre of the lesion and diminishes gradually into the penumbra. CSPGs appear to be the main class of inhibitory molecules produced by activated astrocytes in the scar tissue. They belong to a family of extracellular matrix glycoproteins characterized by a protein core to which large, highly sulphated glycosaminoglycan (GAG) chains are attached.

b. Myelin-associated inhibitors

- **Nogo**

From all myelin associated axon growth inhibitors, most is known about Nogo. Nogo was discovered after sophisticated analysis of the inhibitory fraction of myelin against which the antibody IN-1 was originally directed (see above). Searching the putative antigen in the inhibitory fraction of myelin finally led to the discovery of Nogo. Further analysis revealed three distinct isoforms of Nogo, Nogo-A, -B and -C generated by alternative splicing. All isoforms are members of the reticulon family of membrane proteins. The three isoforms share a common C-terminal domain of 188 amino acids homologuos to the reticulon homology domain of reticulon family proteins (RTN). These proteins are anchored to the endoplasmatic reticulum via a C-terminal ER retention signal. In addition all isoforms have a 66 amino acid loop (Nogo-66) in common. Nogo A is the most potent inhibitory isoform mainly expressed by white matter oligodendrocytes and by subpopulations of large projecting neurons in the CNS. In contrast Nogo-A is not or little expressed in Schwann cells of the PNS. Strong inhibitory effect on neurite outgrowth and induction of growth cone collapse were shown for the Nogo-A specific region as well as for Nogo 66. Figure 1.53 below schematically represents the three isoforms of Nogo. Although the Nogo-66 domain is thought to be situated on the extracellular surface and the amino-Nogo intracellularly (see Figure 1.54 below) the

exact topology of Nogo-A remains still controversial. For more molecular biology details about Nogo, see Oertle and Schwab (2003).
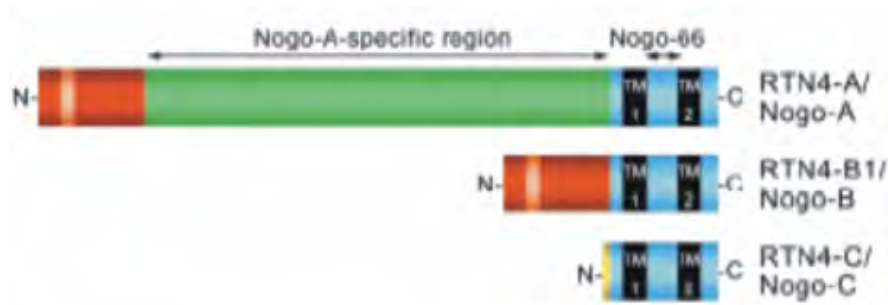
Figure 1.53   Drawing representing the three isoforms Nogo A, B and C.
(modified from Oertle and Schwab, 2003).

- **Myelin Associated Glycoprotein (MAG)**

MAG is one of the myelin-associated components which either promotes or inhibits neurite outgrowth depending on the age and type of neuron. Unlike Nogo, it is expressed by both CNS oligodendrocytes and PNS Schwann cells. It belongs to a sub-family of the immunoglobulin super-family of cell adhesion molecules but has no role in the immune system. Changes in the endogeneous cAMP levels of CNS neurons are thought to account for the sharp transition from promotion to inhibition at around the time of birth of axon growth. The inhibitory contribution in the CNS may be minor because MAG is also present in the highly regenerative PNS, although one can argue that in the PNS the inhibitory effect is masked by the rapid and efficient cleaning of myelin debris after lesion to peripheral nerve tissue (Schäfer et al., 1996).

- **Oligodendrocyte Myelin Glycoprotein (OMgp)**

OMgp is the most recently identified myelin associated protein inhibiting axonal growth in vitro. It is a GPI-anchored protein that contains a leucin-rich repeat (LRR) domain. Mouse and human OMgp are structurally very similar. It is not only expressed in the white matter of CNS but also in diverse groups of neurons (e.g. pyramidal cells, motoneurons in the brainstem and the spinal cord) (Wang et al., 2002). Recent evidence suggests that it is enriched in membranes of oligodendroglia-like cells that encircle nodes of Ranvier, and might act to prevent collateral sprouting (Huang et al., 2005).

1.9.10 Transduction of axon growth-inhibitory signals

Nowadays it becomes more and more clear, that the three main myelin-associated inhibitors present at the outer side of the oligodendrocyte membrane act through the same receptor (NgR) to induce growth cone collapse of neurons. In spite of that MAG and Nogo-A have slightly different binding site on the NgR. In addition to that, MAG also binds to a second receptor on the surface of neurons (GD1a and GT1b). GT1b complexes with the non-selective neutrophin receptor p75 and then binds to MAG, whereas GD1a can bind itself to MAG. Nogo-A itself has also a receptor on the neuronal surface with which it can interact alternatively. Although there are alternative receptors for different myelin – associated inhibitors the first common point of convergence is at the NgR. Furthermore regardless of its mechanism of activation, intraneuronally the Rho signalling pathway seems to be the point of convergence for all presently identified myelin (Woolf and Blöchlinger, 2002; McGee et al., 2003) and scar (Borisoff et al., YYYY) derived inhibitors. The Figure 1.54 below summarizes the main pathways of myelin -associated inhibitors. The CSPG pathways are not indicated. The two photomicrographs represent on the right neurons grown on laminin (permissive for growth) and on the left neurons grown on a CNS myelin substrate that prevents growth.
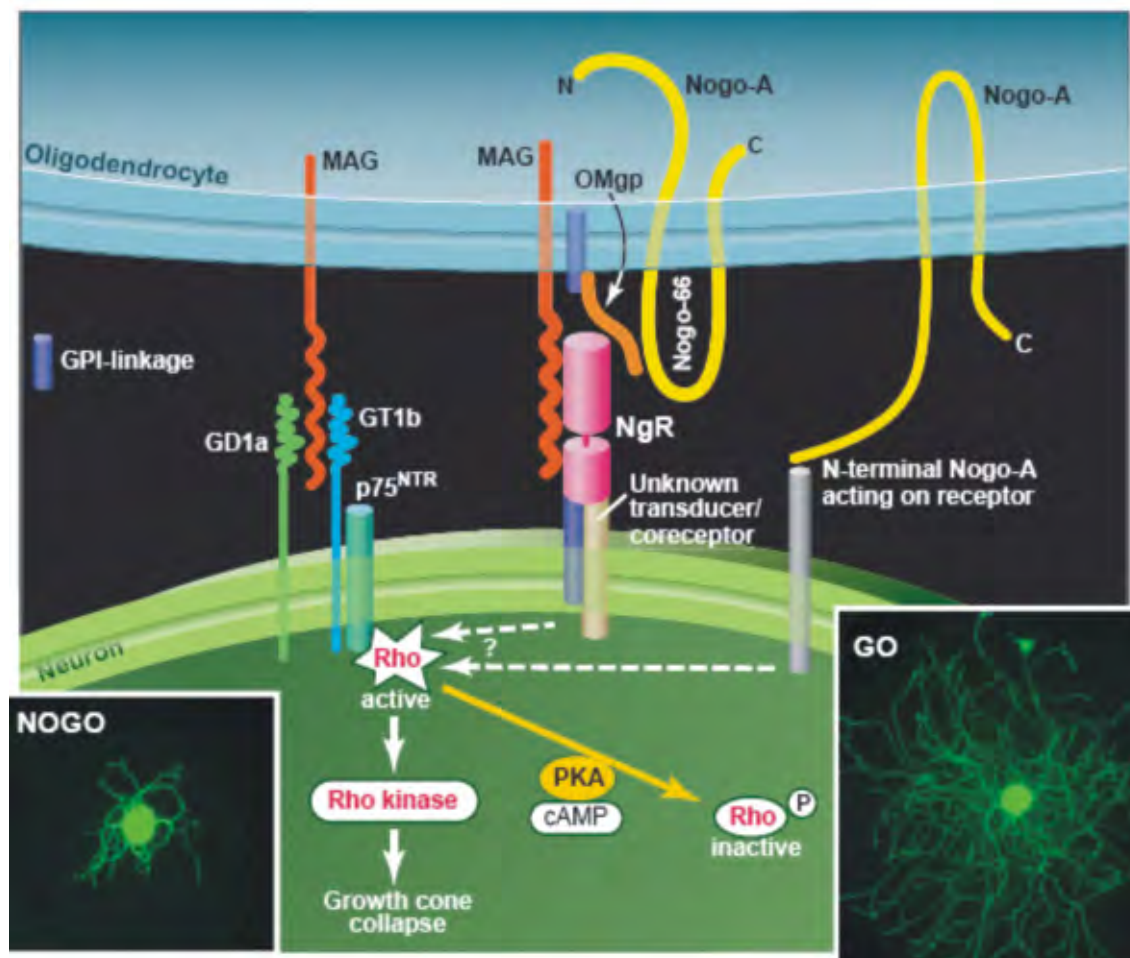
Figure 1.54   Drawing representing the interaction between the three different trans-membrane proteins of oligodendrocytes having an inhibitory role in neurite growth and the receptor NgR (in pink) of the neurones

of central nervous system. Myelin Associated Glycoproteins (MAG) are in red, Oligodendrocyte Myelin Glycoprotein (OMgp) in orange and the 66 domain of Nogo A in yellow. Even if there are two pathways or more outside the cell in the myelinic protein and the receptor, all seem to interact through the Rho kinase cascade inside the neurone, leading to an inhibition of neurite growth (modified from Woolf and Bloechlinger, 2002).

1.9.11 Strategies to overcome regeneration failure in adult CNS

So far, neutralizing every identified step in axon growth inhibition, from ligands to receptors, to intracellular substrates has been targeted to promote regeneration. Figure 1.55 below represents a survey of potential targets whereas Table 1.8 summarizes the most important reagents that have been developed to target and antagonize inhibitory molecules involved in the inhibition of adult CNS regeneration. Most of these reagents have either been tested in in vitro assays of neurite outgrowth and growth cone collapse or in animal models of spinal cord injury. Other treatment strategies such as Knock-out of corresponding genes (e.g. Zheng et al., 2006), application of high dosed growth factors competing with regeneration inhibitors, vaccination with Nogo-A derived peptide, myelin or MAG (e.g Hauben et al., 2001) as well as cellular and semi-artificial transplants to bridge scar tissue respectively the gap between the upper and lower part of damaged axons have also been tested (e.g. Fouad et al., 2005). Furthermore some studies demonstrate that the genetic background can be decisive whether a particular treatment is successful or not (e.g. Simonen et al., 2003). As in my thesis work I used the monoclonal antibody 11C7 acting directly against Nogo-A, in the following I will mainly report the findings of studies which evaluated different aspects of slightly different anti-Nogo-A treatments under different circumstances and in different animals up to non – human primates. In the last part of this chapter, I will provide arguments for a future application of anti-Nogo-A treatment after cortical lesion in primates.
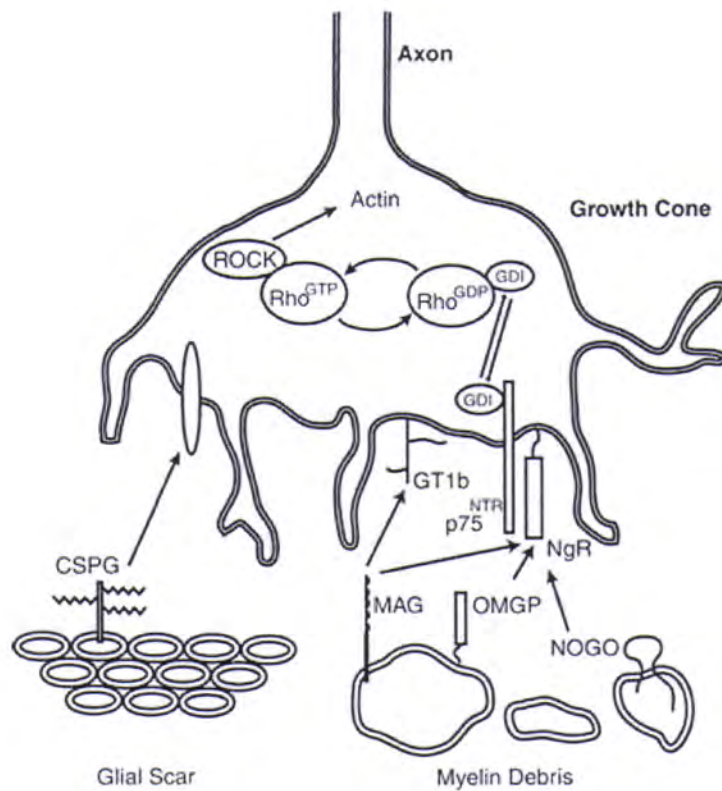
Fig. (1). Potential molecular targets to promote CNS regeneration. Schematic representation of CNS inhibitory molecules, their receptors and intracellular targets. The growth cone of a severed axon encounters inhibitory cues present in the glial scar and CNS myelin debris. Binding of MAG, Nogo and OMgp to NgR, as well as exposure to CSPGs, leads to Rho activation and actin cytoskeleton rearrangements that in turn cause growth cone collapse and neurite retraction.. (CSPG, chondroitin sulfate proteoglycan; MAG, myelin-associated glycoprotein; GDI, guanine nucleotide dissociation factor; ROK, Rho-associated kinase; NgR, Nogo-66 Receptor).

Figure 1.55 (from Ferraro et al; 2004)

Antagonist	Target
C3 transferase [1, 2, 3]	Rho A
Chondroitinase ABC [4, 5]	Chondroitin Sulfate Proteoglycans
cytosine-D-arabinofuranoside [6]	Proliferating Glial Cells
db-cAMP [7, 8, 9, 10]	Protein Kinase A
IN-1 Ab [11, 12, 13]	NI35/250
IN-1 F(ab) [14]	NI35/250
Myelin Vaccination [15]	Myelin Inhibitors
NEP1-40 [16, 17]	NgR
NgREcto [18]	NgR
Nogo-66/MAG vaccination [19]	Nogo-66/MAG
p75^{NTR} antibody [20]	p75^{NTR}
p75^{NTR} siRNA [21]	p75^{NTR}
PEP5 [22]	p75^{NTR}
Y-27632 [23, 24, 25]	Rho Kinase

([1] Lehmann et al., 1999, [2] Dergham et al., 2002, [3] Fournier et al., 2003, [4] Moon et al., 2001, [5] Bradbury et al., 2002, [6] Rhodes et al., 2003, [7] Cai et al., 2002, [8] Neumann et al., 2002, [9] Qiu et al., 2002b, [10] Cui et al., 2003, [11] Caroni and Schwab, 1988b, [12] Schnell and Schwab, 1993, [13] Schnell et al., 1994, [14] Fiedler et al., 2002 [15] Huang et al., 1999, [16] GrandPre et al., 2002, [17] Li and Strittmatter, 2003, [18] Fournier et al., 2002 [19] Sicotte et al., 2003, [20] Wong et al., 2002, [21] Higuchi et al., 2003 [22] Yamashita and Tohyama, 2003 [23] Dergham et al., 2002, [24] Fournier et al., 2003, [25] Borisoff et al., 2003).

Table 1.8 Most important reagents developed to target and antagonize inhibitory molecules involved in the inhibition of adult CNS regeneration with corresponding references (From Ferraro et al., 2004).

1.9.12 Different types of antibodies against Nogo-A

1.9.12.1 Common features of all anti-Nogo-A antibodies

All of the subtypes mentioned below are derived from the relatively low stability monoclonal antibody against Nogo-A (mAb IN-1) belonging to the subclass of the IgM /κ immunoglobulins. Each of them acts against slightly different sites of Nogo-A. As the first antibody (mAb IN-1) was successfully used against Nogo-A of different animals (rat, mouse, frog, opossum, bovine, monkey) as well as the mAb 11C7 (rat, monkey), it seems that the antigen against Nogo-A is highly conserved among different species. In order to reach a higher stability of the antibody, instead of using whole length IgM antibodies, engineered recombinant Fab fragments (rxFab; x stands for the engineered subtype) were used. Figure 1.56 represents schematically the engineering of such recombinant Fab fragments. In addition to a direct neutralizing effect by binding to and sterically covering the active sites of Nogo-A, a fraction of cell surface Nogo-A is directly removed by antibody-induced internalization and subsequent degradation allowing long distance regeneration of lesioned spinal axons and the widespread occurrence of compensatory sprouting (wide distribution of the CSF anti-Nogo-A antibodies see below) following spinal, brainstem or cortical lesions in anti-Nogo-A antibody-treated animals (Schnell and Schwab, 1990; Wenk et al., 1999; Brosamle et

al., 2000; Merkler et al., 2001; Papadopoulos et al., 2002; Emerick et al., 2003; 2004; Lee et al, 2004 ; Seymour et al, 2005).
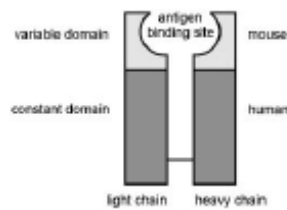
Figure 1.56 Example of a recombinant IN-1 Fab carrying the variable domains of the original (murine) IgM/κ mAb IN-1 determining the antigen specificity and constant domains of human origin, IgG1/κ subclass. (Modified from Brösalme et al., 2000).

1.9.12.2 The most important engineered subtypes

- **mAb IN – 1 (whole length IgM; rFab)** (Caroni and Schwab, 1988; Chen et al., 2000).

  Raised against a myelin fraction enriched in Nogo-A that is able to bind Nogo-A and neutralize its growth inhibitory properties.

- **mAb 7B12 (rFab)** (Oertle et al., 2003; Liebscher et al., 2005).

  Has an epitop towards the C-terminus of the Nogo-A specific region; Binds to the outer surface of living cultured oligodendrocytes.

- **mAb 11C7 (rFab)** (Oertle et al 2003).

  Directed against a 18 amino acid peptide (aa 623-640) close to the active site of the rat Nogo-A specific region. Binds to the outer surface of living cultured oligodendrocytes.

- **mAb hNogo – A (rFab)** is a humanized monoclonal antibody raised against the Nogo-A specific region of the human Nogo-A sequence. Recognizes human and primate Nogo-A specifically on Western blots.

1.9.12.3 Antibody delivery systems in vivo

- Implantation of antibody producing hybridoma cells either encapsulated or directly as suspension leading to immunological problems and tumor growth. The disadvantage of this method is the poor control of the production and secretion of the antibody in the CNS. Only short periods of treatment are possible.

- Intrathecally or intraventricular antibody infusion by Alzet® osmotic pumps (only for rFab antibodies). This method offers better control of antibody delivery, possibility to treat CNS damage secure over long periods of time. Application in patient would not create any problems as the same infusion technique is already used in human patients for application of

substances like balcofen to the spinal cord after spinal cord lesion to prevent severe spinal spasticity (e.g. Penn et al., 1989; Lazorthes et al., 1990).

1.9.12.4. Distribution in the CNS

Following intrathecal administration of anti-Nogo-A at cervical level, anti-Nogo-A antibodies are distributed all over the CNS in rat and monkey, as shown in Figure 1.57 in macaque monkeys, as reported by Weinmann et al. (2006).
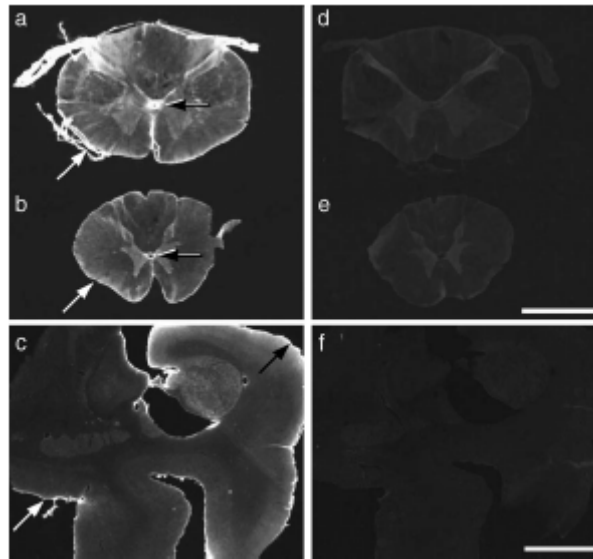
Figure 1.57   Distribution of mAb hNogo-A in macaque CNS.

Sections of cervical (a, d) and thoracic (b, e) spinal cord and forebrain (c, f) of adult Macaque monkey infused intrathecally with a humanized antihuman Nogo-A antibody for 7 days. High levels of the anti-Nogo-A antibody are visible throughout the cervical spinal cord close to the infusion site (a), as
well as in the thoracic spinal cord 6 cm caudal to the infusion site (b). The antibody also reaches and penetrates into the large forebrain of this animal (c). Central canal and CNS surface are most strongly labeled (arrows). Staining is specific as seen by omitting the secondary antibody on adjacent sections (d–f). Calibration bars: a, b, d, e: 3 mm; c, f: 5 mm. (From Weinmann et al., 2006).

1.9.13 Relation of dose and effect

For a future clinical application, it is very important to know the minimal therapeutic dose of each anti-Nogo-A antibody. Otherwise an effective therapy is not possible. The Figure 1.58 below represents the relation of dose and effect for the mAb 11C7.
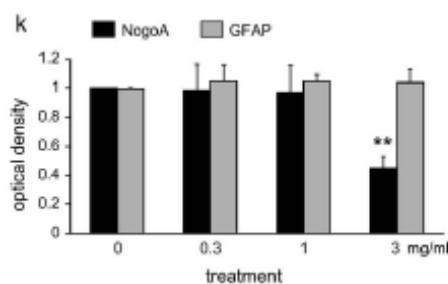
Figure 1.58: Down-regulation of Nogo-A (measured by the respective optical density) after 7 days of **mAB 11C7** infusion requires 15 µg/h (3mg/ml; 5 µl/h) as an effective <u>minimal</u> antibody dose. In contrast, the amount of astrocytes was not changed (GFAP) by either concentration (Modified from Weinmann et al., 2006).

1.9.14 In vivo degradation of anti-Nogo-A antibodies

In contrast to the known rapid turnover of IgGs in the CSF (Zhang and Pardrige, 2001), the engineered anti-Nogo-A antibodies infused either in the lateral ventricle or into spinal subdural liquor space reached the entire CSF circulation and diffused well into grey and white matter of the whole neuraxis in rats as well as in macaque monkeys without being degraded immediately (Weinmann et al., 2006). These results contrast with earlier findings (Merkler et al., 2003) where circulating antibodies against Nogo-A penetrated very poorly in the CNS due to rapid resealing of the blood brain barrier. Therefore the two infusion techniques (intraventricular and intrathecal) seem to be excellent in terms of application of therapeutic antibodies to CNS.

1.9.15 Cellular targets

The Figure 1.59 below shows that anti-Nogo-A antibodies (11C7 and 7B12) are highly specific in CNS, only down regulating significantly the level of Nogo-A on the cell surface of oligodendrocytes but having no effect on MAG level and the number of astrocytes (revealed by measuring the optical density of astrocyte specific marker GFAP). In contrast application of a control antibody (IgG) does not affect the astrocyte number, MAG level nor Nogo-A concentration in CNS. Nogo-A level, MAG level and astrocyte number were measured by the respective optical density.
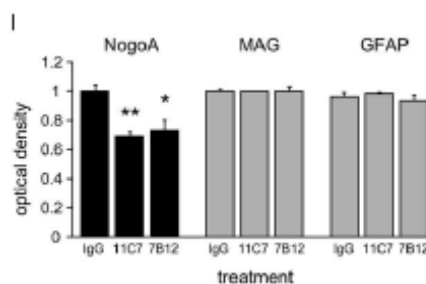
Figure 1.59   Downregulation of endogenous Nogo-A levels in the CNS (measured by the respective optical density) by anti-Nogo-A antibodies in vivo by different subtypes of antibodies without affecting MAG levels as well as astrocyte numbers, showing the specificity of anti-Nogo-A antibodies for Nogo – A (Modified from Weinman et al., 2006).

1.9.16 Subcellular mechanism of action

Specific Nogo-A antibodies are probably retained in the CNS tissue by binding to Nogo-A on the cell surface of oligodendrocytes, CNS myelin and some types of neurons but not on astrocytes

(see Figure 1.59 above). Afterwards antibodies are internalized as complex together with their binding partners by large endosomes and afterwards degraded in secondary lysosoms. Probably because such antibody induced internalization and subsequent lysosomal degradation of Nogo-A protein affects Nogo-A protein levels in CNS and its availability for receptor interactions and neurite growth inhibitory functions the action of Nogo-A antibodies is dose dependent as explained in Figure 1.58 above.

1.9.17 Consequence of anti-Nogo-A treatment

The two photomicrographs below show induced excessive neurite outgrowth on adult CNS myelin when pre-treated with Nogo-A neutralizing anti-Nogo-A antibody 11C7. In contrast, pre-treatment with the control antibody IgG does not block the inhibitory effect of Nogo-A in adult CNS myelin, resulting in a lack of neurite growth. As indicated in the Figure 1.60 below, the same Nogo-A neutralizing effect can be observed if other anti-Nogo-A antibodies, than the 11C7 antibody, are used for pre-treatment.
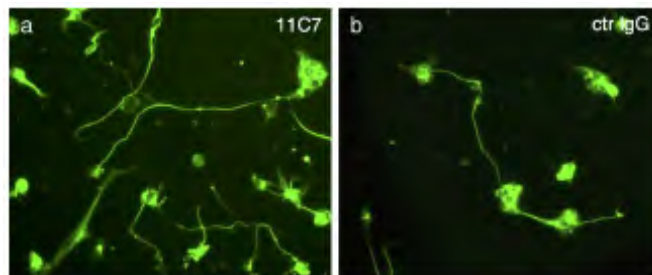
Figure 1.60   Effect of 11C7 on neuron growth in adult CNS

Monoclonal antibodies against rat Nogo-A (mAB 11C7, 7B12, and human Nogo-A (mAB hNogo-A)) improve neurite outgrowth on culture dishes coated with inhibitory adult monkey brainstem membrane protein extract. Figure a) representing the growth pattern resulting from 11C7 treatment (excessive neurite outgrowth and b) neurites growing on the same substrate without previous 11C7 treatment. (Modified from Weinmann et al., 2006).

1.9.18 From mouse and rat to nonhuman primates and humans

1.9.18.1 Treating spinal cord lesions with Anti-Nogo-A antibody in rats

The application of the neutralizing antibody (anti-Nogo-A) in spinal cord lesioned rats showed rostro-caudal regeneration of axons of the CS tract and sprouting of uninjured collaterals (Schnell and Schwab, 1990; Thallmair et al., 1998; Brösamle et al., 2000; Fouad et al., 2001; Merkler et al., 2001), correlated with better functional recovery as compared to untreated rats.

On of the hallmark first study demonstrating enhanced axonal regeneration and sprouting induced by anti-Nogo-A was the study by Schnell and Schwab (1990). Two to six week old rats, after complete section of the corticospinal tract, were treated by intracerebral application of the monoclonal antibody IN-1. IN-1 antibody acting against NI-35 and NI-250 was delivered by cortical tumors resulting from intracerebral injections of antibody-secreting mouse IN-1 producing hybridoma cells. As a result IN-11 treated rats showed massive sprouting at the lesion site, and fine axons and fascicles could be observed up to 7-11 mm caudal to the lesion within 2-3 weeks post lesion. In contrast, in control rats, a similar sprouting reaction occurred but the maximal distance of elongation rarely exceeded 1mm in accordance with former studies investigating axonal sprouting and re-growth in the adult CNS (e.g. Vidal-Sanz et al., 1987). Although growth was enhanced in IN-1 antibody treated rats, fiber plexus and fine bundles were seen in and across the lesion area most often circumventing the scar tissue ventrally or laterally as in control rats. The number of axons caudal to the lesion in IN-1 treated animal was always small, best a few percent of the total CST axons. But anatomically, these CST fibers were often close to or in the original CST location. There were also some fibers passing through the grey matter. Regenerating fibers were easily to distinguish from unlesioned fibers as they grew in an irregular way with frequent branching as described by Brösamle et al. (2000). In conclusion, these results demonstrated for the first time, in vivo, the capacity of CNS axons to regenerate and elongate within different CNS tissue after the neutralization of myelin-associated neurite growth inhibitors. The Figure 1.61 below briefly summarizes the findings of this very important study.

Strategy of Nogo neutralization in rat spinal cord (Schnell and Schwab, 1990.)

<u>Control rats</u>: limited regeneration rostral to the lesion site (→) no regeneration of CS tract caudal to the lesion site

<u>IN – 1 antibody treated rats</u>: CS tract regeneration /sprouting rostral and far caudal to the lesion site (→)

r: rostral
c: caudal
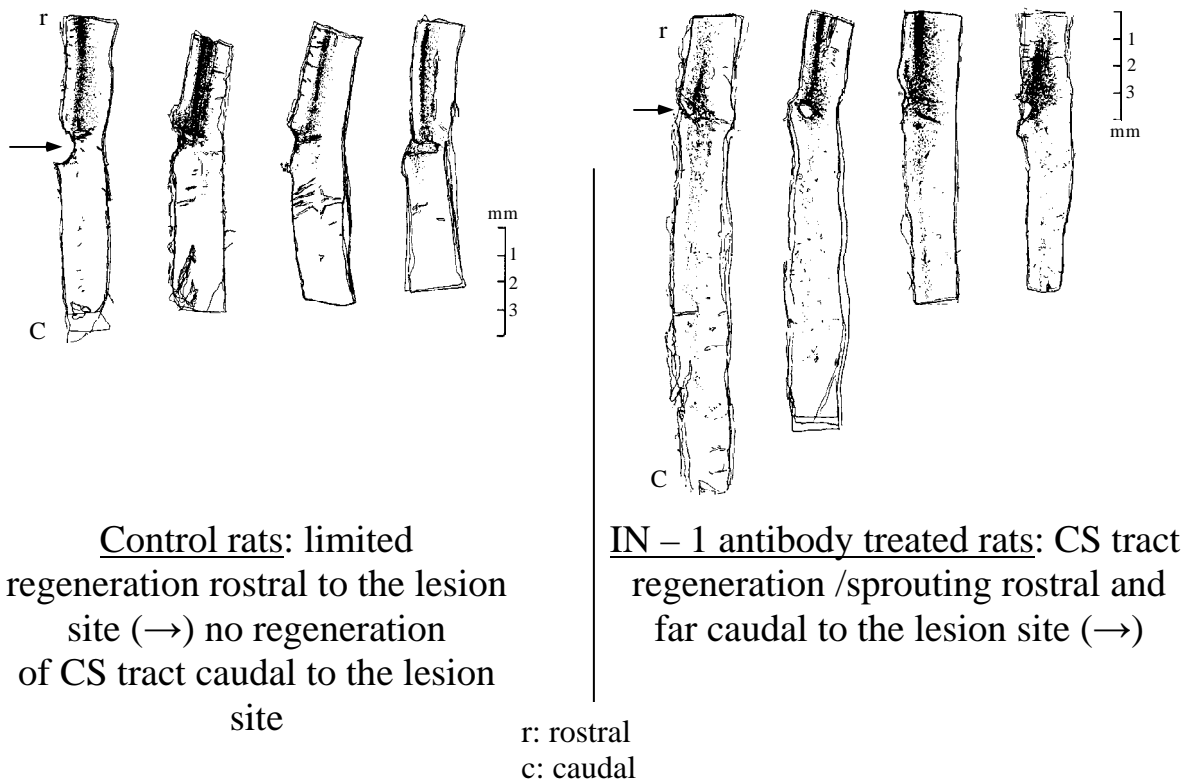
Figure 1.61

Whereas the study by Schnell et al., (1990) was purely anatomical, subsequent studies aimed to proof the functionality of re-grown fibers. Indeed, researchers were very interested in demonstrating the functional importance of augmented post lesion CNS plasticity in recovery, resulting from enhanced compensatory collateral sprouting of *intact* fibers in anti-Nogo-A antibody treated animals (Thallmair et al., 1998). At this time, it was clear that neurite growth inhibitory proteins prevent regenerative fiber growth but whether they also prevent reactive sprouting of unlesioned fibers in spinal cord lesioned rats was less clear. To investigate this plastic fiber growth and functional recovery of the mature rat corticospinal tract (CST) in response to a complete unilateral section at the lower brainstem (pyramidotomy), IN-1 treated and control animals were histologically analyzed. In addition to that, both groups of animals were tested for their post lesion performance in several motor behavioral tasks. The authors also investigated whether behavioral performance paralleled post - lesion plastic changes in CNS. In neonatal rats, where myelin is almost missing, lesion induced sprouting of the CST and other descending tracts are well described. In contrast, in adult animals, such sprouting is absent after damage of CNS. Because in rat spinal cord the normal CST innervation pattern is very specific, as well as its central projections changes

112

in these patterns can be attributed to plastic events such as collateral compensatory sprouting of intact fibers and aberrant fiber growth to new targets within the lesioned CNS. In control animals, lesion of the CNS led to permanent functional impairment on each of the tasks, and anatomical studies revealed only limited anatomical changes in response to the lesion. In sharp contrast, IN-1 antibody treated rats showed full functional recovery in all behavioral tasks. Functional recovery was paralleled by plastic sprouting of both the lesioned and the contralateral unlesioned CST as represented schematically in Figure 1.62 below. The authors thus concluded that neutralization of myelin-associated neurite growth inhibitors restores in adult the structural plasticity and functional recovery normally found only at perinatal ages (Thallmair et al., 1998).
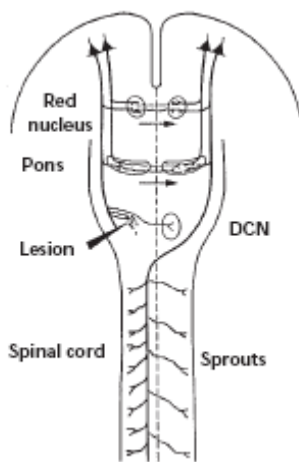
Figure 1.62   Schematic representation of the lesion site and the corticospinal projections that were examined in Thallmair et al. (1998).
Gray lines represent newly sprouted fibers after the unilateral CST lesion and IN-1 treatment. The arrows indicate the growth direction of the sprouts. The intact CST showed collaterals that recrossed the midline at spinal cord levels to branch into the denervated hemicord. The lesioned tract increased its innervation to the contralateral red nucleus and pontine nuclei and reinnervated the dorsal column nuclei. (From Thallmair et al 1998).

Studies described so far here, used rat anti-Nogo-A antibodies administered by antibody producing tumor cells. It is self-evident that neither rat antibodies nor tumor cells can be introduced in human patients without risk. In addition to that, the antibody used in the studies of Schnell and Schwab (1990) and of Thallmair et al. (1998) was biochemically not very stable (for details about that, see above). For this reason, Brösamle et al. (2000) used a partially humanized, recombinant Fab fragment (rIN-1 Fab) derived from the original mAb IN-1. This type of antibody is more stable over time and can be administered by an Alzet® 2002 osmotic mini - pump placed under the skin in the back of the animal with the tip of a small catheter sub-durally placed close to the lesion site in the spinal cord. Basically the concept of this study is similar to the one of Schnell and Schwab (1990) except that, this time, the effect of a new type of anti-Nogo-A antibody on axonal growth and sprouting was analyzed. As represented in the Figures 1.63 and 1.64 below, in rIN-Fab treated

rats, regenerating fibers grew for > 9 mm beyond the lesion site and arborized profusely in the distal cord. Note that the inter-individual variation is large. This may for example result from growth-adverse effects of the scar, growth inhibitory molecules produced by the scar tissue itself, inflammation or blood – brain barrier breakdown. It is also noteworthy that the bulk of regenerating transected fibers was found to sprout rostral from the lesion site bypassing the injury through remaining ventral grey and white matter.
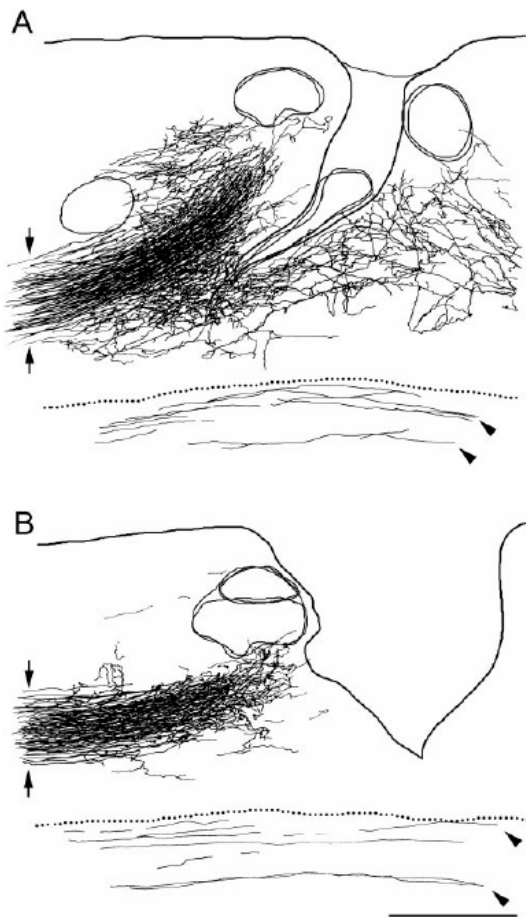
Figure 1.63 Reconstruction of a few adjacent sagittal sections of rat spinal cord in two rats subjected to a spinal
lesion using camera lucida.

In **A**, the animal has been treated with rIN-1 Fab directed against Nogo A, while in **B** the animal received the control inactive antibody. Note that in **B**, the stained CS axons do cross or turn around the lesion to migrate distally on several millimetres, in contrast to the untreated animal (**B**). Resulting cysts in the scar can be seen (Modified from Brösamle et al., 2000).
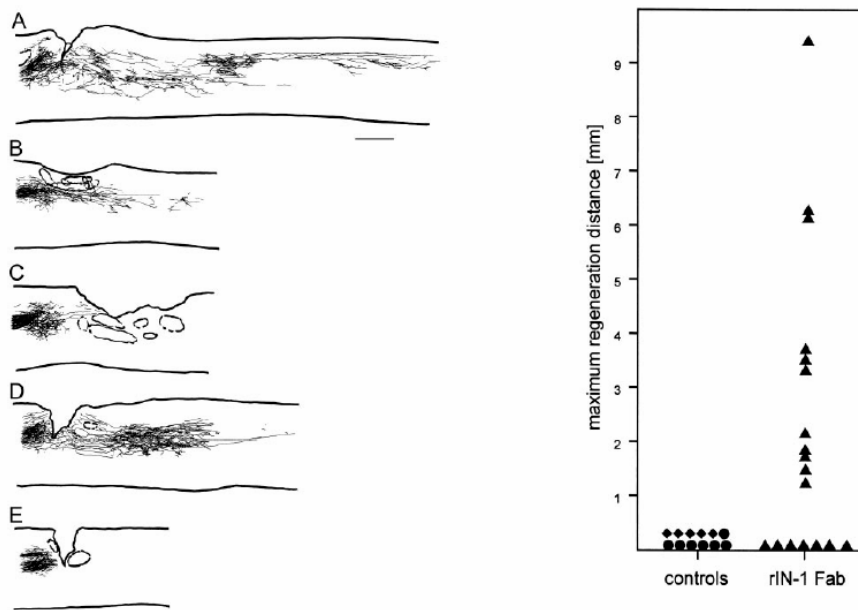
Figure 1.64

<u>Left</u>: Reconstruction from photomicrographs showing in 5 rats that regenerated CST fibres can growth over a long distance.
<u>Right</u>: length of regenerated CST axons in different spinal cord injured rats, control versus treated (rIN-1 Fab) rats. Scale bar in A: 1mm (Modified from Brösamle et al., 2000).

In the context of stroke and restorative post - lesion plasticity, it is interesting to note that, in rIN-1 Fab treated rats, besides long-distance re-growth of injured axons in the spinal cord, regenerated fibres formed terminal arbors with varicosities in the spinal cord grey matter. They strongly resembled new synaptic points of contact to neurons in the spinal cord distal to the lesion. Such mechanisms could also positively influence regenerative processes inside the penumbra zone of a stroke. Figure 1.65 below shows detailed photomicrographs of potential new formed synaptic boutons and arborizations.
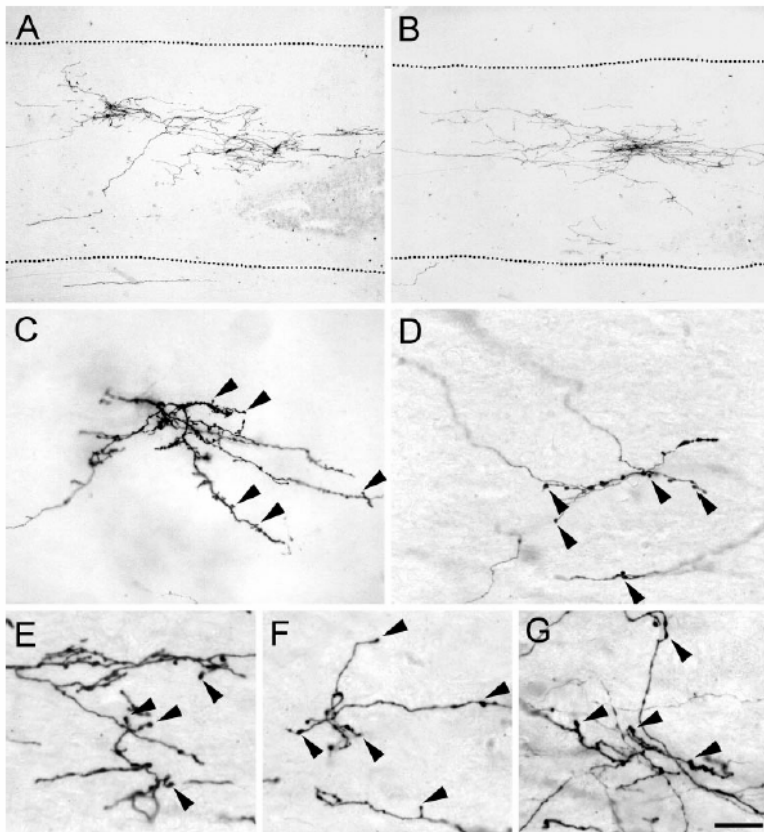
Figure 1.65: Photomicrographs showing in A and B the arborisation of regenerated CST fibres caudally to the spinal cord lesion. Higher magnification in panels C-F of these arborisations showing a large number of varicosities (arrowheads) that could be synaptic *boutons*. At even higher magnification (G), the authors conclude that these varicosities are presynaptic *boutons*. Scale bar: In A-B: 250 μm, in C-F: 30 μm and in G: 15 μm (Modified from Brösamle et al., 2000).

A major question arising from anatomical studies is whether the functional recovery observed in behavioural tests after anti-Nogo-A antibody treatment can be attributed directly to anatomical changes. In this context it is of major interest to test whether regenerating or plastically growing neurons are reconnected in a functionally meaningful way in the adult CNS. This was tested by Merkler et al. (2001) in a rat spinal cord injury model. Before a laminectomy of half a vertebra, performed at the thoracic level Th8 (dorsal over-hemisection, sparing just parts of the ventral funiculus) to induce impairment in hindlimb use, rats were trained in various motor tasks to define the baseline pre-lesion performance. In the following, I only report the findings of EMG recordings acquired in control antibody treated and IN-1 antibody treated rats at post – lesion day 40 during treadmill walking. Animals were implanted with bipolar electrodes in each hindlimb into the vastus lateralis muscle (VL) (knee extensor) and the tibialis anterior muscle (TA) (ankle flexor). A ground electrode was implanted subcutaneously on the back of each animal. EMG recordings were performed while rats were walking on the treadmill (running at a speed of 10.5 m/min). EMGs of approximately 20 step cycles were analyzed per rat. The step-cycle duration and burst duration of the TA and the VL muscles were measured. The deviation between step cycles was used as marker for rhythm. Uncoupling of the stepping pattern of the hindlimbs (irregular alternation between the

muscle activity) was counted and set in relation to the number of performed steps (n = 20) as represented in Figure 1.66 below. Stepping frequency was significantly higher in IN-1 antibody treated animals as compared to controls. A significant better recovery of rhythm in IN – antibody treated animals was seen as well. In addition, uncoupling of the two hindlimbs in IN – 1 treated rat was significantly less frequent (see figure 1.67 below). The authors therefore concluded that the increased plastic and regenerative capabilities of the adult CNS after Nogo-A neutralization result in a functionally meaningful rewiring of the motor system.
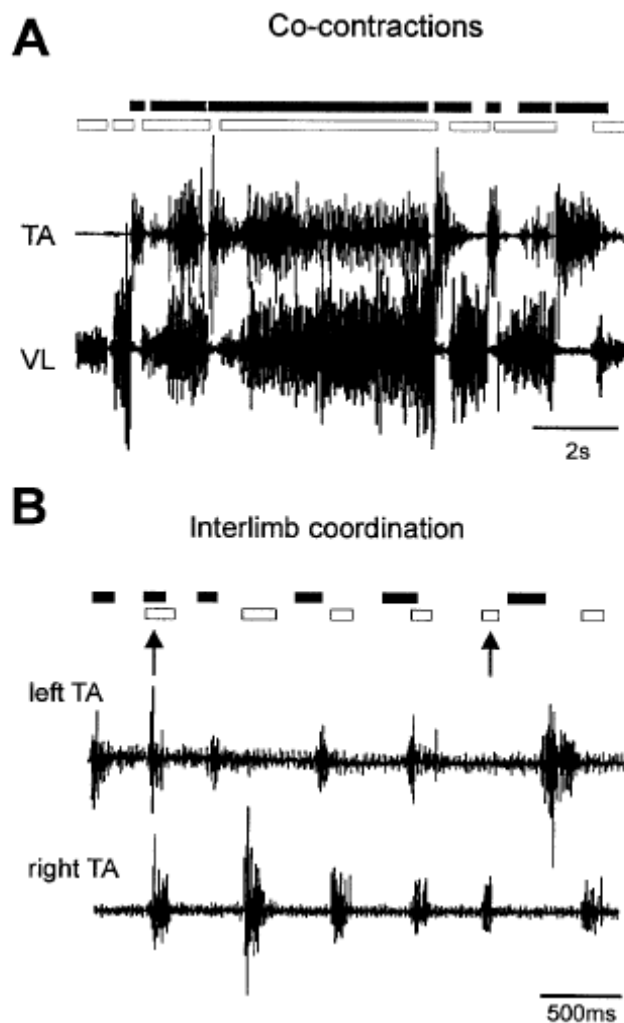
Figure 1.66   *A*, Cocontractions between the VL (extensor) and the TA (flexor). The *black bars* and *white bars* represent the activity pattern of the TA and the VL muscles, respectively.
B, Uncoupling of the rhythmically active hindlimbs (*arrows*). An example for the right and left TA is shown. The *black bars* and *white bars* represent the activity pattern of the left TA and the right TA muscle, respectively (Modified from Merkler et al., 2001).
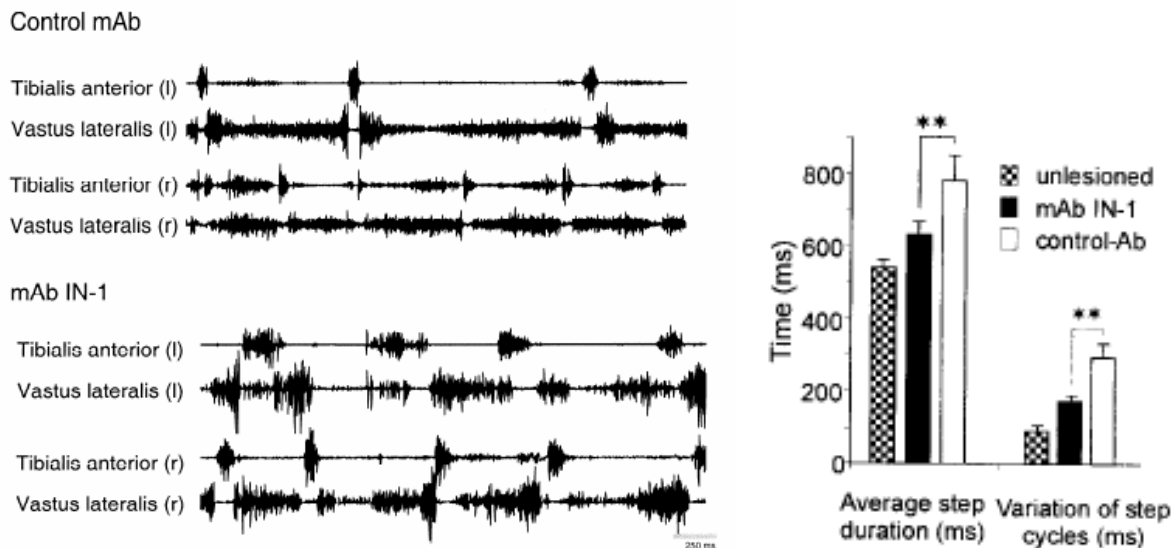
Figure 1.67

Left: Figure showing a comparison of EMG activity recorded in rats after a spinal cord section during locomotion in (A) animals treated with a control antibody compared to (B) animals treated with the IN-1 antibody. The pattern of EMG activity in (B) is much closer to the normal alternated pattern of electrical activity of locomotor muscles than in (A) (modified from Fouad, K. et al., 2001).

Right: Comparison of the average step-cycle duration as well as its variation (shown as SD) between IN-1-treated and control Ab-treated rats shows a highly significant improvement in the mAb IN-1 group. **$p <$ 0.01 (Modified from Merkler et al., 2001).

1.9.18.2 Treating spinal cord lesion with anti-Nogo-A antibody in monkeys

In 2004, the IN-1 antibody was successfully tested in spinal cord lesioned marmoset monkeys. The study by Fouad et al. (2004) was the first to provide anatomical evidence that neutralization of the myelin-associated inhibitor Nogo-A results in increased regenerative sprouting and growth of lesioned spinal cord axons in sub – human primates. As in former studies in rat, a partial hemi-section mainly targeting the lateral funiculus with the corticospinal tract (CST) was performed at thoracic segment 8. Antibodies were delivered by hybridoma cells grafted unilaterally into the hippocampus according to the method of Merkler et al. (2001). In both in control animals and IN-1 antibody treated marmosets, the lesioned CST fibers ended sharply rostral to the lesion and many retraction bulbs were noted. Fibers sprouting into the grey matter rostral to the lesion were also seen in both groups. Only in IN-1 antibody treated marmosets, very few fine fibers arising from the proximal stump of the lesioned CST were seen. Such fibers grew either around or through the lesion site and were characterized by a winding appearance unlike straight fibers of the intact CST (Steward et al., 2003). Caudal to the lesion these fibers could be followed up to 5 mm. In general, in IN-1 treated marmosets, the number of regenerated fibers was 5-10 fold increased as compared to controls (Fouad. et al., 2004).

Two recent studies from our laboratory (Freund et al., 2006; 2007) investigated the effect of anti-Nogo-A antibody treatment on recovery, axonal regeneration and compensatory sprouting after spinal cord lesion at C7-C8 level in adult macaque monkeys. The lesion was aimed to unilaterally interrupt the CST caudal to the biceps motor nucleus, but rostral to the nuclei of triceps forearm, and intrinsic hand muscles (illustrated in Freund et al 2006; Jenny and Inukai, 1983). Immediately after the lesion, the monkeys received an anti-Nogo-A antibody treatment by either mouse mAB 11C7 or mAB hNogo-A (see above) for four weeks, intrathecally infused by an ALZET® osmotic pump as described in the method part of this thesis. In addition to that, my colleagues tested whether in anti-Nogo-A antibody treated monkeys the observed anatomical changes were paralleled by better recovery of the post - lesion manual dexterity and higher force generation with the lesion attained fingers (Freund et al., 2006). To assess manual dexterity, the standard Brinkman board task (see methods) was used. In order to quantify the force generated with the lesion impaired fingers the "reach and grasp" drawer test was used (supplementary Figure 2a; Freund et al., 2006). In this test, the monkey had to open a drawer by gripping the knob on the front side of the drawer with its finger. Then after, the monkey had to grasp a small reward pellet out of a small well inside the drawer forcing the monkey to use precision grip. Either hand can be tested individually. Adapted laboratory developed computer software permits to measure the rapidity with which the monkey is able to open the drawer as well as the time of grasping the pellet. The higher the grip force to hold the knob of the drawer the more rapid the drawer can be opened. The better the precision grip recovers the less time consuming is the pellet grasping. Results revealed that the performance of anti-Nogo-A antibody treated monkeys recovered faster and significantly better as compared to controls (Freund et al., 2006). In a third task, ballistic arm movements tested the capacity of pre-shaping the lesion attained hand to catch food: anti-Nogo-A antibody treated monkeys also recovered markedly better (supplementary Figure 2b; Freund et al 2006). Accordingly, the study of Freund et al., (2006) is the first to show in primates Nogo-A specific antibody treatment leading to considerable functional recovery after spinal cord injury. Whether the anti-Nogo-A antibody enhanced functional recovery was paralleled by plastic and regenerative changes in the spinal cord was investigated by labeling corticospinal axons with anterograde BDA tracer injections in the contralesional motor cortex (Freund et al., 2006; 2007). The BDA tracing revealed the following main findings:

Caudal to the lesion site, the corticospinal axonal arbors were more numerous in anti-Nogo-A antibody treated monkeys than in controls as well as the cumulated axonal arbor length was larger in anti-Nogo-A antibody treated animals. The authors observed sprouting for a total distance of about 10 – 12 mm occurring from *axotomized* corticospinal axons. In addition, the number of

corticospinal axonal swellings caudal to the lesion was significantly higher in anti-Nogo-A antibody treated animals.

Rostral to the lesion site a more detailed histological analysis was performed showing the following:

A:

In anti-Nogo-A antibody treated animals, the cumulated numbers of corticospinal axons exhibiting terminal retraction bulbs were significantly lower (ca fourfold on average) than in control monkeys. Instead of the standard retraction bulbs, outgrowing sprouts being torturous in shape and decorated with varicosities, strongly resembling boutons en passant and terminaux that approached the lesion border were observed. If retraction bulbs of transected corticospinal axons were observed, in anti-Nogo-A antibody treated monkeys, the average retraction distance from the lesion border was markedly reduced and most retraction bulbs were found very close to the lesion (within 100 µm) whereas retraction bulbs were very frequent and also more distant (within 600 µm) from the lesion in controls, indicating a further retraction.

B:

In the grey matter, a non significant tendency of enhanced axon sprouting rostral to the cervical lesion site in anti-Nogo-A antibody treated monkeys was found.

C:

In anti-Nogo-A antibody treated monkeys, a significantly higher number of corticospinal axons entering the scar tissue as compared to control monkeys was found but none of the axons reached the caudal border of the lesion. This observation indicates that the caudally observed axons rather are regenerating axons which have grown around the lesion on bridges of spared white and grey matter as formerly observed in rat (see above).

D:

Axons growing around the lesion in attempt to reinnervate the denervated spinal cord caudal to the lesion were found in a higher number in anti-Nogo-A antibody treated monkeys than in controls.

E:

Collateral sprouting was more frequent in anti –Nogo-A antibody treated monkeys than in controls.

Axonal regeneration and sprouting rostral and caudal to the lesion site are schematically illustrated in the four reconstruction drawings (A-D) in Figure 1.68 below, A and C from control monkeys B and D from anti-Nogo-A antibody treated monkeys. The corresponding lesion extent (controls in blue, anti-Nogo-A treated in red) of each monkey is indicated in a small drawing on the right side of each reconstruction. Rostral to the lesion the densely packed brown lines represent the BDA labeled CS axons in the white matter interrupted by the transection (vertical black arrows) of the dorsolateral funiculus. The black line segments represent the CS axon arbors traced rostrally in the grey matter and caudally to the lesion.
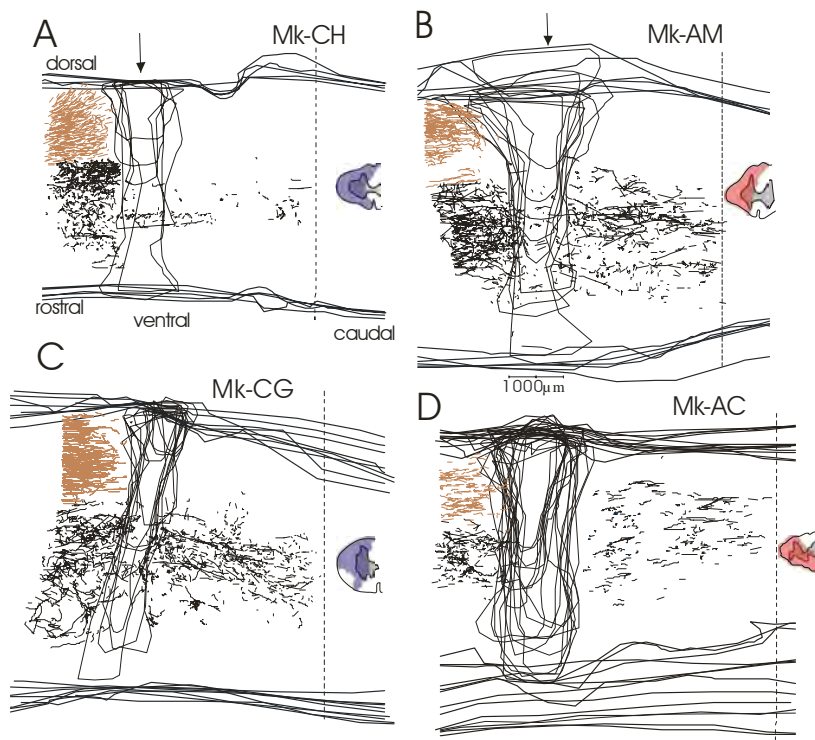
Figure 1.68   Superimposed reconstructions of para-sagittal sections of the cervical-thoracic cord showing the lesion (vertical black arrows) as well as the density of BDA-labeled CS axon arbors present around the lesion in two control monkeys (A and C) and two anti-Nogo-A treated monkeys (B and D) subjected to a complete lesion of the dorsolateral funiculus (Taken from Freund et al., 2007).

121

Taken together, the results from all three studies discussed (Fouad et al., 2004; Freund et al., 2006; 2007), application of the neutralizing antibody (anti-Nogo-A) in spinal cord lesioned monkeys confirmed the findings of the rat studies. Confirmation was obvious at an anatomical as well as at a functional level. In addition to that, the findings of Freund et al., (2006 and 2007) demonstrate that the anatomical changes are strongly related to post - lesion functional recovery after damage to the adult CNS in primates.

1.9.18.3 Anti-Nogo-A: A strategy to better treat stroke patients in the future?

A: Rat cortical lesion model

An increased behavioral recovery was observed in rats subjected to motor cortex lesion and treated with anti-Nogo-A antibodies (e.g. Wenk et al., 1999; Papadopoulos et al., 2002; Emerick et al., 2003; 2004; Lee et al, 2004 ; Seymour et al, 2005). After unilateral ablation of the sensorimotor cortex and treatment with monoclonal antibody IN-1 in adult rats by implantation of antibody producing hybridoma cells, Wenk et al., (1999) demonstrated structural plasticity that is normally restricted to a short postnatal period. In fact, they observed that the remaining corticospinal tract from the intact hemisphere sprouted into the denervated contralateral red nucleus and pons in a somatotopically correct manner. Such aberrant sprouting normally is only seen in neonatal rats subjected to cortical lesions but not in adult animals. These data indicate that the IN-1 antibody reestablished a plasticity and regeneration friendly environment in adult CNS similar to the neonatal situation. Whether the observed increased plastic and regenerative processes were functionally meaningful was not tested in this study.

Functional recovery was tested in a similar approach by Papadoupolos et al. (2002) but, instead of an ablation of the sensorimotorcortex, adult rats were subjected to a middle cerebral artery occlusion mimicking the most frequent type of stroke in humans (see addendum at the end of the thesis). The effect of the IN-1 antibody treatment was tested with the skilled forelimb reaching task, already described above, that requires an intact CST and the integration of the rubrospinal tract. Post - lesion functional recovery in IN-1 antibody treated rats was significantly better (80% of pre - lesion score) and faster than in controls (50 % of pre - lesion score) over time as represented in the Figure 1.69 below. In addition, this enhanced recovery was paralleled by a significant higher degree of plasticity in the corticorubral pathway originating from the intact hemisphere. At the level of the brainstem the authors examined the red nucleus that receives direct input from the primary motor cortex, i.e., the corticorubral projection. In normal healthy adult animals, this projection from the primary motor cortex ends primarily in the ipsilateral parvocellular part of the red nucleus with

only a small number of fibers crossing the midline to project to the contralateral red nucleus. The authors reported significantly more corticorubral fibers crossing the midline and terminating in the contralateral red nucleus in appropriate target areas mirroring the non-deafferented red nucleus in IN-1 antibody treated animals as compared to controls (see Figure 1.70 below). This compensatory bilateral innervation seems to be responsible, at least in part for the observed better recovery in these animals. This is very likely, as the corticorubral as well as the corticospinal pathway in rats are extremely important for skilled forelimb movements in rat.

Figure 1.69

Following stroke, the monoclonal antibody (mAb) IN-1treatment resulted in better functional recovery as demonstrated by the success rat and percent of recovery of pre-lesion score in the forelimb reaching task. (Modified from Papadopoulos et al., 2002).
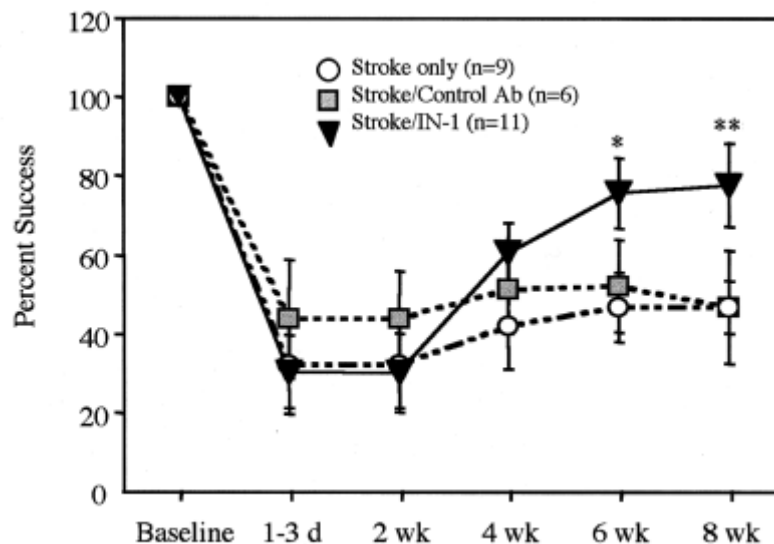
mAb IN-1 treatment after stroke lesion improved the success score (the percentage of pellets obtained in the 20-pellet test in relation to baseline), reaching significance 6 weeks postoperatively. *, $p \leq 0.05$; **, $p \leq 0.01$ in a one-way analysis of variance (ANOVA) of IN-1–treated animals compared with controls. Error bars indicate standard error.
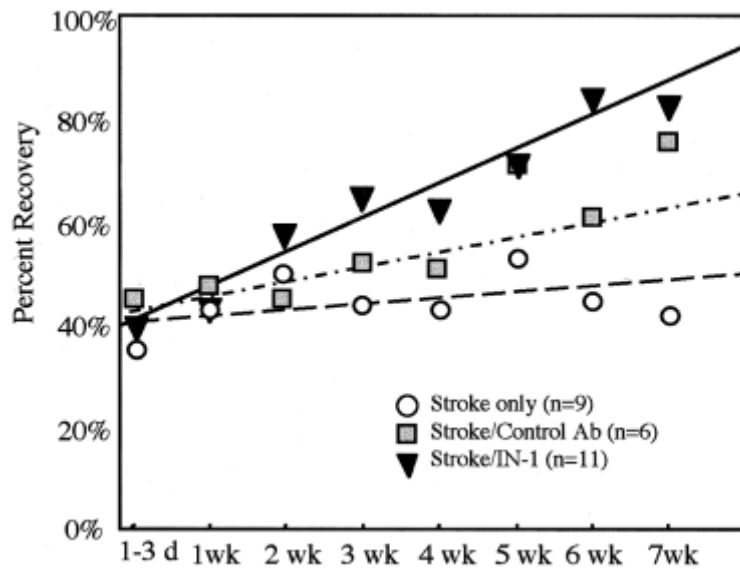
In a repeated-measures one-way ANOVA between experimental groups, animals in the stroke/mAb IN-1 treatment group had a higher rate of recovery (captured by the respective slopes) in the pellet-reaching test, measured by the percentage of successes in a given week compared with the baseline percentage ($p < 0.0001$), whereas the recovery rates did not differ between the two control lesion groups ($p < 0.05$).
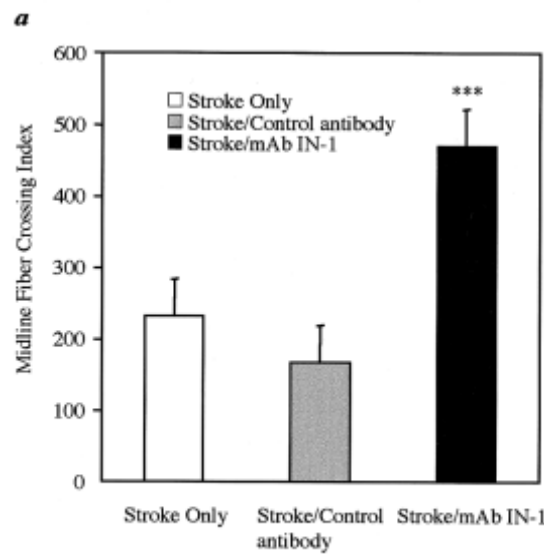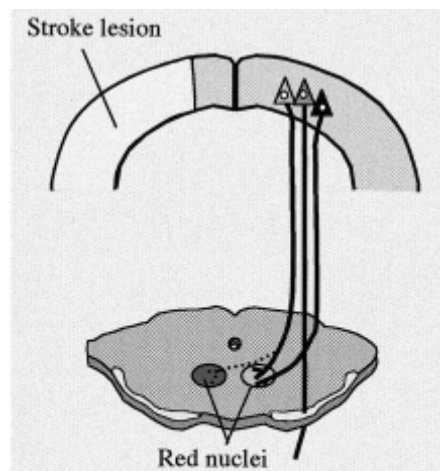
Figure 1.70   Monoclonal antibody (mAb) IN-1 treatment after stroke enhanced corticorubral plasticity.

(a) Scheme of the new projection from the intact primary motor cortex to the contralateral(dashed lines) red nucleus.
(b) Midline fiber crossing index: number of midline crossing fibers in the area of the red nucleus divided by the total labeled cerebral peduncle fibers (to correct for the difference in the tracing) and multiplied by 10,000.
***, $p \leq 0.001$, log-linear Poisson regression analysis. Error bars indicate standard error.
(From Papadopoulos et al., 2002).

Whereas the study of Papadopoulos et al. (2002) examined subcortical changes, Emerick et al. (2003) tested in the influence of an IN-1 antibody treatment on the post-lesion functional reorganization of the opposite motor cortex spared by the lesion. For this purpose, adult rats were subjected to unilateral sensorimotor cortex (SMC) aspiration lesion. The forelimb and hindlimb motor cortex was aspired unilaterally. Immediately after the lesion, hybridoma cells secreting either mAb IN-1 or a control antibody were injected posterior to the lesion site into the hippocampus. A third group of rats was only lesioned without being treated. ICMS mapping of both the lesioned and intact forelimb motor cortex was performed six weeks after SMC lesion. All stimulation sites were screened by maximal stimulation intensity of 80µA and if there was a movement, threshold current was defined as the lowest current needed to reliably produce a visible movement. Forelimb movements were grouped as follows: Distal: digit or wrist, proximal: shoulder or elbow. Finally, individual forelimb motor maps from each animal where then combined to make a representative map for each experimental group. Analysis of the ICMS maps revealed a significantly higher number of ipsilateral movements in IN-1 antibody treated rats as compared to both control groups (see Figure 1.71 below), confirming the results of Papadoupolos et al. (2002) reporting more rubrospinal fibers originating in the intact sensorimotor cortex innervating the contralateral red nucleus after unilateral MCA occlusion. In contrast, although treatment with mAb IN-1 increased the frequency of evoked ipsilateral movements, it did not change the proportion of proximal and distal movements evoked by ICMS in the ipsilesional forelimb. The authors concluded that mAb IN-1 (i.e., Nogo-A blockade) after adult cortical injury results in a physiological reorganization of the motor cortex that is functionally meaningful. Accordingly, this observed functional reorganization could be important for recovery of motor control after cortical damage resulting from stroke or traumatic brain injury.
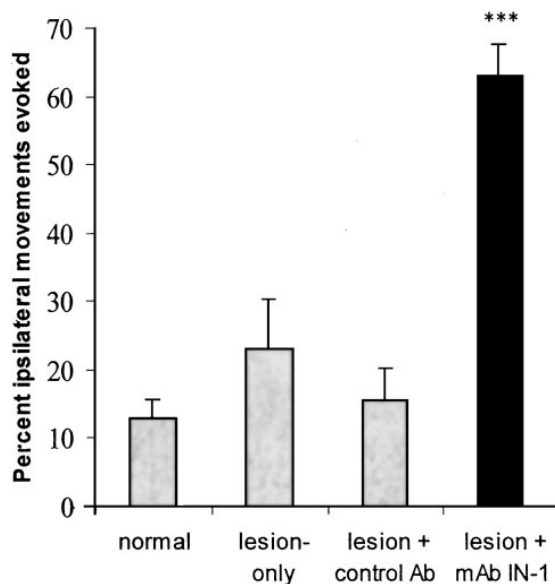
Figure 1.71

Treatment with mAb IN-1 after SMC lesions (filled bar) significantly increased ipsilateral output from the nonlesioned motor cortex when compared with all other groups (gray bars). Percentage values represent the average number of ipsilateral points/total forelimb points. Error bars indicate mean SEM. Asterisks indicate significance compared with all of the groups: ***$p \leq 0.001$, one-way ANOVA, *post hoc* Bonferroni's multiple comparison. Ab, Antibody (from Emerick et al., 2003).

In a subsequent study of the same type by Emerick et al. (2004), in spite of investigating the rubrospinal tract, they investigated the effect of mAb IN-1 treatment after adult sensorimotor cortex aspiration on behavioral recovery and neuroanatomical plasticity of the corticospinal tract. The authors investigated the corticospinal connections from the non – injured cortex to the α-motoneurons that innervate muscle groups implicated in different motor tasks and whether new growth paralleled recovery. In the anatomical analysis, BDA tracer was injected in the intact sensorimotor cortex (SMC) opposite to the lesion. The percent of CST fibers projecting into the lateral (distal muscles) and medial (proximal muscles) α-motoneuron columns of the ventral motor horn ipsilateral to the injection site was determined. There was no significant difference between IN-1 treated and control animals for CST projections to the lateral α-motoneurons, but in IN-1 antibody treated animals a significant increase of the percentage of CST fibers projecting to the medial α-motoneuronal column was observed as compared to controls. (see Figures 1.72 and 1.73). As a consequence, mAb IN-1 treated animals have more CST connections to α-motoneurons facilitating movements in the impaired forelimb related to proximal (i.e. shoulder) muscles but not distal (i.e. digit) muscles. In this sense the study also revealed that treatment with mAb IN-1 after cortical aspiration lesion induces remodeling of motor pathways resulting in recovery in only certain behavioral tasks. Anatomic results were in line with data obtained from a battery of different motor tasks designed to quantify functional recovery of proximal muscle groups, distal muscle groups represented in Figure 1.74. Overall coordination revealed by the skilled ladder rung walking test (for description, see Emerick et al., 2004) evaluated by counting the number of

misplaced forepaws was also significantly better in IN-1 antibody treated animals. As the IN-1 antibody treated animals of Emerick et al. (2004) conflict with previous reports in animals treated with IN-1 antibodies following unilateral ischemic stroke (Papadopoulos et al., 2002) showing an excellent recovery in digit grasping, the question arises as to whether behavioral outcome after CNS injury and mAb IN-1 treatment depends in part on the lesion type.
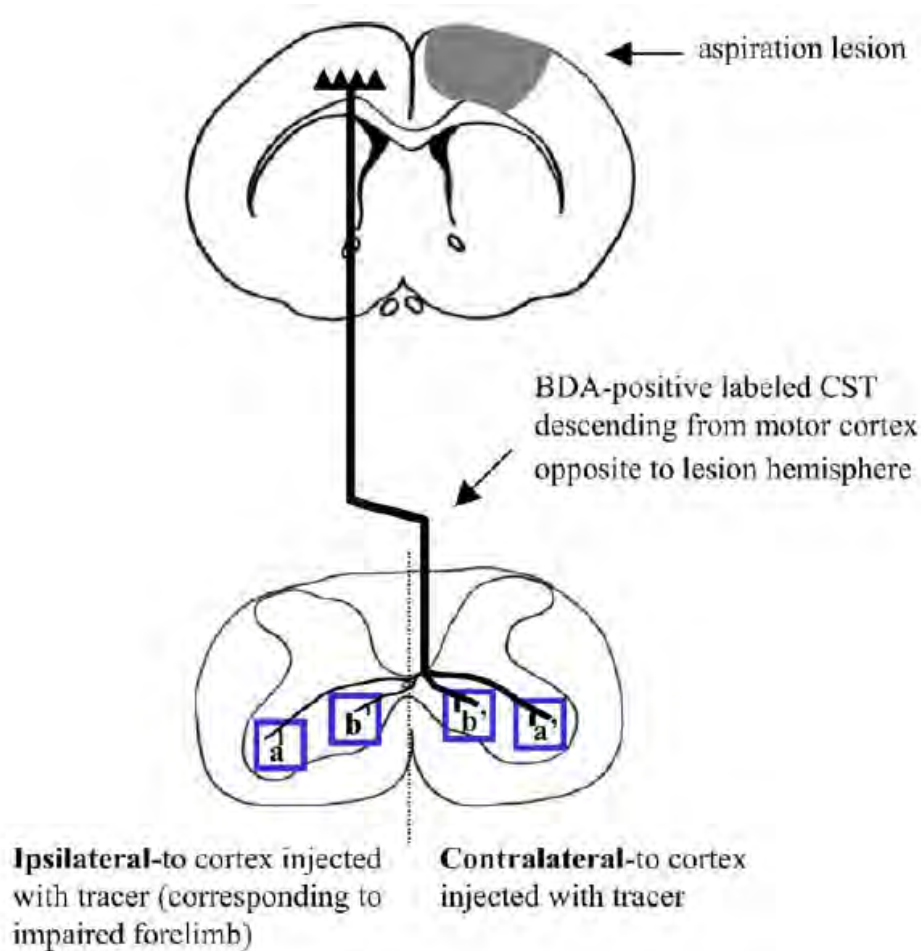
Figure 1.72   Neuroanatomical plasticity was examined in the cervical spinal cord.

The BDA-positive labeled CST fibers projecting from the non-injured cortex were counted in the *lateral α-motoneuron cell column* (box a, a'*)* and *medial α- motoneuron cell column* (box b, b') on both ipsi- and contralateral sides (from Emerick et al 2004).
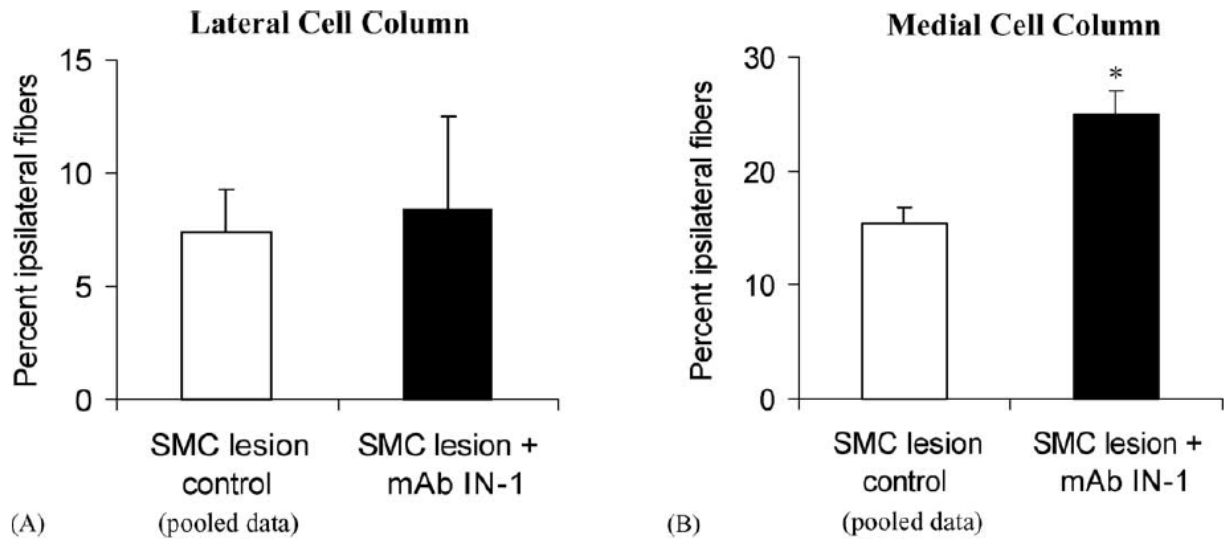
Figure 1.73

Treatment with mAb IN-1 after SMC lesion results in an increase in CST fibers projecting to the α-motoneurons that innervate proximal muscles of the impaired forelimb. The percentage of CST fibers projecting to the ipsilateral (lesion-affected) lateral α-motoneuron cell column did not change after SMC lesion and treatment with mAb IN-1 as compared to SMC lesion control (pooled data from lesion-only and lesion + control Ab) (P > 0.05, Mann–Whitney) (A). However, there was a significant increase in the percentage of CST fibers projecting to the medial α-motoneuron cell column (B) in animals treated with mAb IN-1 as compared to lesion-control animals. Error bars indicate mean ± S.E.M. Asterisk (∗) indicates P < 0.05, Mann–Whitney. (from Emerick et al 2004)
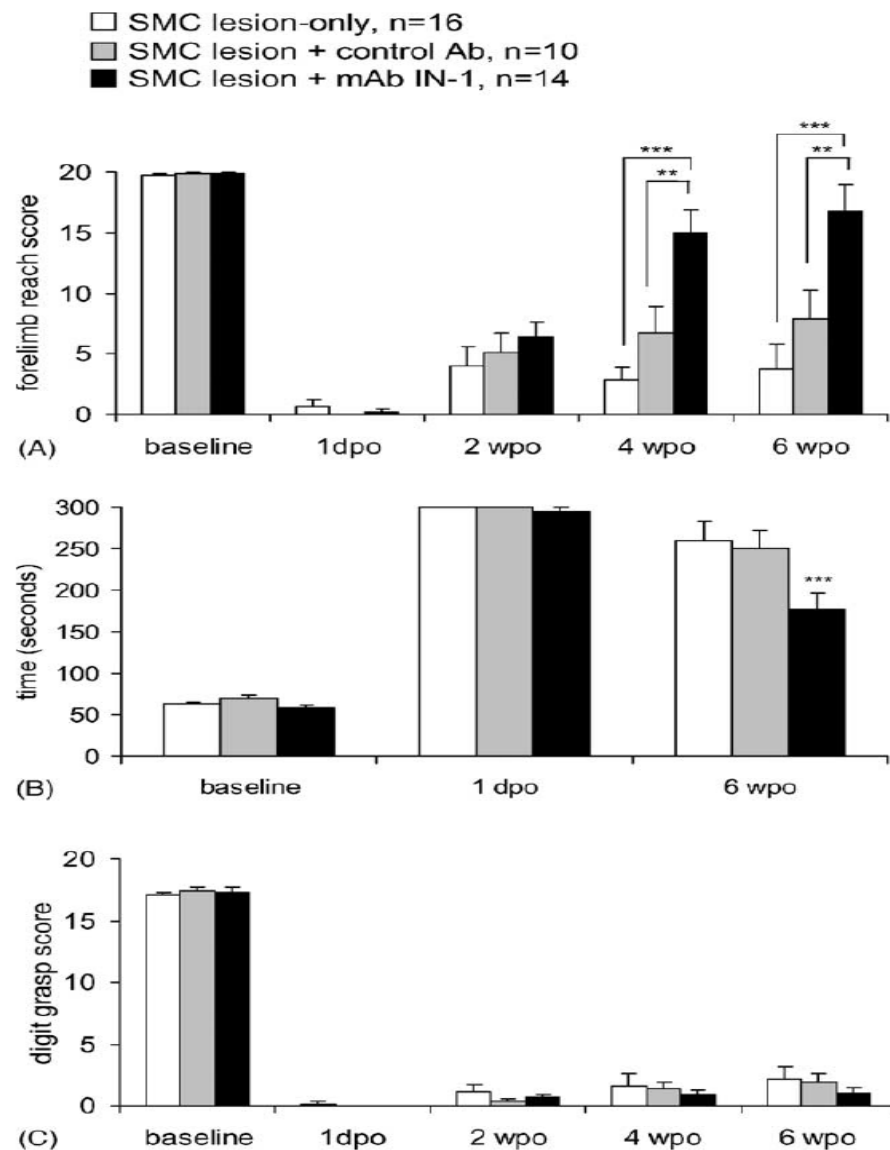
Figure 1.74

Treatment with mAb IN-1 leads to behavioral recovery in the skilled forelimb use test as measured by the number of successful forelimb reaches using the impaired forelimb in a 20-pellet test (A). At 4 weeks following surgery, animals treated with mAb IN-1 were significantly improved compared to control treatment animals. This recovery was sustained through postoperative week 6 at which time point animals treated with mAb IN-1 showed no statistical difference from preoperative baseline scores ($P > 0.05$, unpaired t-test). SMC lesion-only and SMC lesion + control AB were not significantly different throughout the course of the study ($P > 0.05$). Treatment with mAb IN-1 improves the time it takes animals to complete the 20-pellet test (B) Time (seconds) to reach was significantly faster in the mAb IN-1 treatment group as compared to the SMC lesion-only and SMC lesion plus control Ab groups at postoperative week 6 ($P < 0.001$). Digit grasping abilities showed little or no recovery in all treatment groups (C). At postoperative week 6, animals treated with mAb IN-1 were not significantly different from SMC lesion-only or SMC lesion plus control Ab animals ($P > 0.05$). Data shown are mean ±S.E.M. Asterisks indicate significance compared to SMC lesion-only and SMC lesion + control Ab treatment groups: $**P < 0.01$; $***P < 0.001$, one-way ANOVA, followed by Bonferroni's Multiple Comparison for post hoc evaluation of group differences (dpo: days postoperative; wpo: weeks postoperative). (from Emerick et al 2004)

B: Monkey cortical lesion model

Monkey M1 injury model without treatment: the first important observation about the subject of cortical lesions in untreated monkeys was that infant monkeys do recover better than adult monkeys (Rouiller et al., 1998). These data are in line with the notion of increasing inhibitory effects of myelin in adult monkeys blocking substantial recovery after cortical injury similar to what was observed in rats (see above).

A chemical lesion in the hand area of M1 by injection of ibotenic acid in adult macaque monkeys generated a severe paresis of the hand contralateral to the injection side (Liu and Rouiller, 1999). However, there was a spontaneous recovery reaching 30% after 3 to 4 months suggesting that probably limited plastic changes based on collateral sprouting and regenerative axon re-growth were spontaneously induced by the lesion. These results inspired us to enhance the spontaneous recovery in adult monkeys by an anti-Nogo-A treatment similar to what was formerly done in rats subjected to cortical lesions. In my thesis work, I adapted and tested the effect of an anti-Nogo-A treatment in a monkey model. Adult macaque monkeys were subjected to chemical lesions in the hand area of M1 and subsequently treated with the 11C7 anti-Nogo-A antibody. The promising anatomical, behavioral, and electrophysiological results of this approach are presented in chapter 3 of this thesis.

Aims of the present study

As outlined above, the goal of the present thesis work was to test whether anti-Nogo-A antibody treatment can enhance functional recovery from motor cortex lesion in adult monkeys. More specifically, the aims were:

I. To assess the effect of anti-Nogo-A antibody treatment on the monkey behavioural recovery of manual dexterity after motor cortex lesion.

II. To assess the effect of anti-Nogo-A antibody treatment in the reorganization of the hand representation in M1 post-lesion.

III: To assess the role of this reorganization in the behavioural recovery of the monkey by inhibiting its action by infusing Muscimol.

1.11   Bibliography for the Introduction

Allard T, Clark SA, Jenkins WM, Merzenich MM. 1991. Reorganization of somatosensory area 3b representations in adult owl monkeys after digital syndactyly. J Neurophysiol 66:1048-1058.

Alstermark B, Isa T, Kummel H, Tantisira B. 1990. Projection from excitatory C3-C4 propriospinal neurones to lamina VII and VIII neurones in the C6-Th1 segments of the cat. Neurosci Res 8:131-137.

Andersen P, Hagan PJ, Phillips CG, Powell TPS. 1975. Mapping by microstimulation of overlapping projections from area 4 to motor units of the baboon's hand. Proc R Soc London SerB 188:31-60.

Andlin-Sobocki P, Jonsson B, Wittchen HU, Olesen J. 2005. Cost of disorders of the brain in Europe. Eur J Neurol 12 Suppl 1:1-27.

Asanuma H, Rosén I. 1972. Topographical organization of cortical efferent zones projecting to distal forelimb muscles in the monkey. Exp Brain Res 14:243-256.

Asanuma H, Arnold A, Zarzecki p. 1976. Further study on the excitation of pyramidal tract cells by intracortical microstimulation. Exp Brain Res 26:443-461.

Asanuma H, Zarzecki p, Jankowska E, Hongo T, Marcus S. 1979. Projection of induvidual pyramydal tract neurons to lumbar motor nuclei of the monkey. Exp Brain Res 34:73-89.

Bandtlow CE, Zachleder T, Schwab ME. 1990. Oligodendrocytes arrest neurite growth by contact inhibition. J Neurosci 10:3837-3848.

Baranyi A, Feher O. 1981. Long-term facilitation of excitatory synaptic transmission in single motor cortical neurones of the cat produced by repetitive pairing of synaptic potentials and action potentials following intracellular stimulation. Neurosci Lett 23:303-308.

Belhaj-Saïf A, Karrer JH, Cheney PD. 1998. Distribution and characteristics of poststimulus effects in proximal and distal forelimb muscles from red nucleus in the monkey. J Neurophysiol 79:1777-1789.

Belhaj-Saïf A, Cheney PD. 2000. Plasticity in the distribution of the red nucleus output to forearm muscles after unilateral lesions of the pyramidal tract. J Neurophysiol 83:3147-3153.

Bentivoglio M, Rustioni A. 1986. Corticospinal neurons with branching axons to the dorsal column nuclei in the monkey. J Comp Neurol 253:260-276.

Borisoff JF, Chan CCM, Hiebert GW, Oschipok L, Robertson GS, Zamboni R, Steeves JD, Tetzlaff W. 2003. Suppression of Rho-kinase activity promotes axonal growth on inhibitory CNS substrates. Mol Cell Neurosci 22:405-416.

Brösamle C, Huber AB, Fiedler M, Skerra A, Schwab ME. 2000. Regeneration of lesioned corticospinal tract fibers in the adult rat induced by a recombinant, humanized IN-1 antibody fragment. J Neurosci 20:8061-8068.

Butefisch CM. 2004. Plasticity in the human cerebral cortex: lessons from the normal brain and from stroke. Neuroscientist 10:163-173.

Buys EJ, Lemon RN, Mantel GW, Muir RB. 1986. Selective facilitation of different hand muscles by single corticospinal neurones in the conscious monkey. J Physiol 381:529-549.

Caroni P, Schwab ME. 1988. Antibody against myelin-associated inhibitor of neurite growth neutralizes non-permissive period for functional repair of embryonic spinal cord. Neuron 1:85-96.

Chen MS, Huber AB, Van der Haar ME, Franck M, Schnell L, Spillmann AA, Christ F, Schwab ME. 2000. Nogo-A is a myelin-associated neurite outgrowth inhibitor and an antigen for monoclonal antibody IN-1. Nature 403:434-438.

Cheney PD, Fetz EE. 1984. Corticomotoneuronal cells contribute to long-latency stretch reflexes in the rhesus monkey. J Physiol (Lond) 349:249-272.

Cheney PD, Fetz EE. 1985. Comparable patterns of muscle facilitation evoked by individual corticomotoneuronal (CM) cells and by single intracortical microstimuli in primates: Evidence for functional groups of CM cells. J Neurophysiol 53:786-804.

Cheney PD, Mewes K, Fetz EE. 1988. Encoding of motor parameters by corticomotoneuronal (CM) and rubromotoneuronal (RM) cells producing postspike facilitation of forelimb muscles in the behaving monkey. Behav Brain Res 28:181-191.

Cheney PD, Hill-Karrer J, Belhaj-Saif A, McKiernan BJ, Park MC, Marcario JK. 2000. Cortical motor areas and their properties: implications for neuroprosthetics. Prog Brain Res 128:135-160.

Clough JFM, Kernell D, Phillips CG. 1968. The distribution of monosynaptic excitation from the pyramidal tract and from primary spindle afferents to motoneurons of the baboon's hand and forearm. J Physiol 198:145-166.

Clough JFM, Phillips CG, Sheridan JD. 1971. The short latency projection from the baboon's motor cortex to fusimotor neurons of the forearm and hand. J Physiol (London) 216:257-279.

Dancause N, Barbay S, Frost SB, Plautz EJ, Chen DF, Zoubina EV, Stowe AM, Nudo RJ. 2005. Extensive cortical rewiring after brain injury. J Neurosci 25:10167-10179.

Dancause N, Barbay S, Frost SB, Zoubina EV, Plautz EJ, Mahnken JD, Nudo RJ. 2006. Effects of small ischemic lesions in the primary motor cortex on neurophysiological organization in ventral premotor cortex. J Neurophysiol 96:3506-3511.

De Noordhout AM, Rapisarda G, Bogacz D, Gerard P, De P, V, Pennisi G, Delwaide PJ. 1999. Corticomotoneuronal synaptic connections in normal man: an electrophysiological study. Brain 122 (Pt 7):1327-1340.

Dijkhuizen RM, Ren J, Mandeville JB, Wu O, Ozdag FM, Moskowitz MA, Rosen BR, Finklestein SP. 2001. Functional magnetic resonance imaging of reorganization in rat brain after stroke. Proc Natl Acad Sci U S A 98:12766-12771.

Donoghue JP, Leibovic S, Sanes JN. 1992. Organization of the forelimb area in squirrel monkey motor cortex: Representation of digit, wrist, and elbow muscles. Exp Brain Res 89:1-19.

Donoghue JP. 1995. Plasticity of adult sensorimotor representations. Curr Opin Neurobiol 5:749-754.

Dum RP, Strick PL. 1991. The origin of corticospinal projections from the premotor areas in the frontal lobe. J Neurosci 11:667-689.

Dum RP, Strick PL. 1996. Spinal cord terminations of the medial wall motor areas in macaque monkeys. J Neurosci 16:6513-6525.

Dum RP, Strick PL. 2005. Frontal lobe inputs to the digit representations of the motor areas on the lateral surface of the hemisphere. J Neurosci 25:1375-1386.

Duncan PW, Jorgensen HS, Wade DT. 2000. Outcome measures in acute stroke trials: a systematic review and some recommendations to improve practice. Stroke 31:1429-1438.

Dusart I, Airaksinen MS, Sotelo C. 1997. Purkinje cell survival and axonal regeneration are age dependent: an in vitro study. J Neurosci 17:3710-3726.

Emerick AJ, Neafsey EJ, Schwab ME, Kartje GL. 2003. Functional reorganization of the motor cortex in adult rats after cortical lesion and treatment with monoclonal antibody IN-1. J Neurosci 23:4826-4830.

Emerick AJ, Kartje GL. 2004. Behavioral recovery and anatomical plasticity in adult rats after cortical lesion and treatment with monoclonal antibody IN-1. Behav Brain Res 152:315-325.

Fanardjian VV, Papoyan EV, Hovhannisyan EA, Melik-Moussian AB, Gevorkyan OV, Pogossian VI. 2000. The role of some brain structures in the switching of the descending influences in operantly conditioned rats. Neuroscience 98:385-395.

Ferbert A, Priori A, Rothwell JC, Day BL, Colebatch JG, Marsden CD. 1992. Interhemispheric inhibition of the human motor cortex. J Physiol 453:525-546.

Ferrier D. 1876. The functions of the brain. XV. London: Smith Elder & Co.

Fetz EE. 1968. Pyramidal tract effects on interneurons in the cat lumbar dorsal horn. J Neurophysiol 31:69-80.

Fetz EE, Cheney PD. 1980. Post-spike facilitation of forelimb muscle activity by primate corticomotoneuronal cells. J Neurophysiol 44:751-772.

Feydy A, Carlier R, Roby-Brami A, Bussel B, Cazalis F, Pierot L, Burnod Y, Maier MA. 2002. Longitudinal study of motor recovery after stroke: recruitment and focusing of brain activation. Stroke 33:1610-1617.

Fouad K, Volker D, Schwab ME. 2001. Improving axonal growth and functional recovery after experimental spinal cord injury by neutralizing myelin associated inhibitors. Brain Res Rev 36:204-212.

Fouad K, Klusman I, Schwab ME. 2004. Regenerating corticospinal fibers in the Marmoset (*Callitrix jacchus*) after spinal cord lesion and treatment with the anti-Nogo-A antibody IN-1. Eur J Neurosci 20:2479-2482.

Fouad K, Schnell L, Bunge MB, Schwab ME, Liebscher T, Pearse DD. 2005. Combining Schwann cell bridges and olfactory-ensheathing glia grafts with chondroitinase promotes locomotor recovery after complete transection of the spinal cord. J Neurosci 25:1169-1178.

Foundas AL, Hong K, Leonard CM, Heilman KM. 1996. The human primary motor cortex. Neurology 46:1491.

Freund P, Schmidlin E, Wannier T, Bloch J, Mir A, Schwab ME, Rouiller EM. 2006. Nogo-A-specific antibody treatment enhances sprouting and functional recovery after cervical lesion in adult primates. Nature Med 12:790-792.

Freund P, Wannier T, Schmidlin E, Bloch J, Mir A, Schwab ME, Rouiller EM. 2007. Anti-Nogo-A antibody treatment enhances sprouting of corticospinal axons rostral to a unilateral cervical spinal cord lesion in adult macaque monkey. J Comp Neurol 502:644-659.

Friel KM, Nudo RJ. 1998. Recovery of motor function after focal cortical injury in primates: compensatory movement patterns used during rehabilitative training. Somatosens Mot Res 15:173-189.

Frost SB, Barbay S, Friel KM, Plautz EJ, Nudo RJ. 2003. Reorganization of remote cortical regions after ischemic brain injury: A potential substrate for stroke recovery. J Neurophysiol 89:3205-3214.

Galea MP, Darian-Smith I. 1994. Multiple corticospinal neuron populations in the macaque monkey are specified by their unique cortical origins, spinal terminations, and connections. Cereb Cortex 4:166-194.

Galea MP, Darian-Smith I. 1997. Manual dexterity and corticospinal connectivity following unilateral section of the cervical spinal cord in the macaque monkey. J Comp Neurol 381:307-319.

Galea MP, Darian-Smith I. 1997. Corticospinal projection patterns following unilateral section of the cervical spinal cord in the newborn and juvenile macaque monkey. J Comp Neurol 381:282-306.

George G, Griffin JW. 1994. Delayed Macrophage Responses and Myelin Clearance during Wallerian Degeneration in the Central Nervous System: The Dorsal Radiculotomy Model. Exp Neurol 129:225-236.

Georgopoulos AP, Kalaska JF, Caminiti R, Massey JT. 1982. On the relations between the direction of two-dimensional arm movements and cell discharge in primate motor cortex. J Neurosci 2:1527-1537.

Georgopoulos AP, Caminiti R, Kalaska JF, Massey JT. 1983. Spatial coding of movement: a hypothesis concerning the coding of movement direction by motor cortical populations. In: Massion J, Paillard J, Schultz W, Wiesendanger M, editors. Neural Coding of Motor Performance. Berlin: Springer Verlag. p 327-336.

Graziano MSA, Taylor CSR, Moore T. 2002. Complex movements evoked by microstimulation of precentral cortex. Neuron 34:841-851.

Hauben E, Ibarra A, Mizrahi T, Barouch R, Agranov E, Schwartz M. 2001. Vaccination with a Nogo-A-derived peptide after incomplete spinal-cord injury promotes recovery via T-cell-mediated neuroprotective response:comparison with other myelin antigens. Proc Natl Acad Sci 98:15173-15178.

He S-Q, Dum RP, Strick PL. 1993. Topographic organization of corticospinal projections from the frontal lobe: Motor areas on the lateral surface of the hemisphere. J Neurosci 13:952-980.

He S-Q, Dum RP, Strick PL. 1995. Topographic organization of corticospinal projections from the frontal lobe: Motor areas on the medial surface of the hemisphere. J Neurosci 15:3284-3306.

Hepp-Reymond MC, Wiesendanger M. 1972. Pyramidotomy in monkeys: effect on force and speed of a conditioned precision grip. Brain Res 36:117-131.

Hess G, Donoghue JP. 1994. Long-term potentiation of horizontal connections provides a mechanism to reorganize cortical motor maps. J Neurophysiol 71:2543-2547.

Hoffman DS, Strick PL. 1986. Activity of wrist muscles during step-tracking movements in different directions. Brain Res 367:287-291.

Hoffman DS, Strick PL. 1995. Effects of a primary motor cortex lesion on step-tracking movements of the wrist. J Neurophysiol 73:891-895.

Horner PJ, Power AE, Kempermann G, Kuhn HG, Palmer TD, Winkler J, Thal LJ, Gage FH. 2000. Proliferation and differentiation of progenitor cells throughout the intact adult rat spinal cord. J Neurosci 20:2218-2228.

Huang JK, Phillips GR, Roth AD, Pedraza L, Shan W, Belkaid W, Mi S, Fex-Svenningsen A, Florens L, Yate JR, Colman DR. 2005. Glial Membranes at the Node of Ranvier Prevent Neurite Outgrowth. Science 310:1813-1815.

Hughlings J. 1873. On the anatomical and physiological localisations of movements in the brain. In: Clinical and Physiological Researches on the Nervous System. Churchill. p 2-25.

Jacobs KM, Donoghue JP. 1991. Reshaping the cortical motor map by unmasking latent intracortical connections. Science 251:944-947.

Jain N, Florence SL, Kaas JH. 1998. Reorganization of somatosensory cortex after nerve and spinal cord injury. News Physiol Sci 13:143-149.

Jankowska E. 1975. Identification of interneurons interposed in different spinal reflex pathways. In: Santini M, editor. Golgi Centennide Symposium: Perspectives in Neurobiology. New York: Raven Press. p 235-246.

Jankowska E, Padel Y, Tanaka R. 1975. The mode of activation of pyramidal tract cells by intracortical stimuli. J Physiol 249:617-636.

Jankowska E, Padel Y, Tanaka R. 1975. Projections of pyramidal tract cells to α-motoneurones innervating hind-limb muscles in the monkey. J Physiol 249:637-667.

Jankowska E, Padel Y, Tanaka R. 1976. Disynaptic inhibition of spinal motoneurones for the motor cortex in the monkey. J Physiol 258:467-487.

Jenny AB, Inukai J. 1983. Principles of motor organization of the monkey cervical spinal cord. J Neurosci 3:567-575.

Jones EG, Wise SP. 1977. Size, laminar and columnar distribution of efferent cells in the sensory-motor cortex of monkeys. J Comp Neurol 175:391-438.

Jones TA, Bury SD, dkins-Muir DL, Luke LM, Allred RP, Sakata JT. 2003. Importance of behavioral manipulations and measures in rat models of brain damage and brain repair. ILAR J 44:144-152.

Kaas JH. 1991. Plasticity of sensory and motor maps in adult mammals. Annu Rev Neurosci 14:137-167.

Kakei S, Hoffman DS, Strick PL. 1999. Muscle and movement representations in the primary motor cortex. Science 285:2136-2139.

Kasser RJ, Cheney PD. 1985. Characteristics of corticomotoneuronal postspike facilitation and reciprocal suppression of EMG activity in the monkey. J Neurophysiol 53:959-978.

Keirstead HS, Hasan SJ, Muir GD, Steeves JD. 1992. Suppression of the onset of myelination extends the permissive period for the functional repair of embryonic spinal cord. Proc Natl Acad Sci U S A 89:11664-11668.

Krupinski J, Kaluza J, Kumar P, Kumar S, Wang JM. 1994. Role of angiogenesis in patients with cerebral ischemic stroke. Stroke 25:1794-1798.

Kuypers HGJM. 1962. Corticospinal connections: postnatal development in the Rhesus monkey. Science 138:678-680.

Kuypers HGJM. 1981. Pyramidal Tract. In: Handbook APS. p 1018-1020.

Lacroix S, Havton LA, McKay H, Yang H, Brant A, Roberts J, Tuszynski MH. 2004. Bilateral corticospinal projections arise from each motor cortex in the macaque monkey: A quantitative study. J Comp Neurol 473:147-161.

Landgren S, Phillips CG, Porter R. 1962. Cortical fields of origin of the monosynaptic pyramidal pathways to some alphamotoneurones of the baboon's hand and forearm. J Physiol (Lond) 161:112-125.

Lawrence DG, Kuypers HGJM. 1968. The functional organization of the motor system. I. The effects of bilateral pyramidal lesions. Brain 91:1-14.

Lawrence DG, Hopkins DA. 1976. The development of motor control in the Rhesus monkey: evidence concerning the role of corticomotoneuronal connections. Brain 99:235-254.

Lawrence DG, Porter R, Redman SJ. 1985. Corticomotoneuronal synapses in the monkey:light microscopic localization upon motoneurons of intrinsic muscles of the hand. J Comp Neurol 232:499-510.

Lee Jung-Kil et al, 2004. Nogo Receptor Antagonism Promotes Stroke Recovery byEnhancing Axonal Plasticity. The Journal of Neuroscience 24(27):6209–6217

Lemon RN, Muir RB, Mantel GW. 1987. The effects upon the activity of hand and forearm muscles of intracortical stimulation in the vicinity of corticomotor neurones in the conscious monkey. Exp Brain Res 66:621-637.

Lemon RN. 2004. Cortico-motoneuronal system and dexterous finger movements. J Neurophysiol 92:3601.

Lemon RN, Griffiths J. 2005. Comparing the function of the corticospinal system in different species: Organizational differences for motor specialization? Muscle Nerve 32:261-279.

Liebscher T, Schnell L, Schnell D, Scholl J, Schneider R, Gullo M, Fouad K, Mir A, Rausch M, Kindler D, Hamers FPT, Schwab ME. 2005. Nogo-A antibody improves regeneration and locomotion of spinal cord-injured rats. Ann Neurol 58:706-719.

Liepert J, Storch P, Fritsch A, Weiller C. 2000. Motor cortex disinhibition in acute stroke. Clin Neurophysiol 111:671-676.

Liu Y, Rouiller EM. 1999. Mechanisms of recovery of dexterity following unilateral lesion of the sensorimotor cortex in adult monkeys. Exp Brain Res 128:149-159.

Lorincz E, Fabre-Thorpe M. 1997. Effect of pairing red nucleus and motor thalamic lesions on reaching toward moving targets in cats. Behav Neurosci 111:892-907.

Maier MA, Illert M, Kirkwood PA, Nielsen J, Lemon RN. 1998. Does a C3-C4 propriospinal system transmit corticospinal excitation in the primate? An investigation in the macaque monkey. J Physiol (Lond) 511:191-212.

Matelli M, Luppino G, Rizzolatti G. 1985. Patterns of cytochrome oxidase activity in the frontal agranular cortex of the macaque monkey. Behav Brain Res 18:125-136.

Matelli M, Luppino G, Rizzolatti G. 1991. Architecture of superior and mesial area 6 and the adjacent cingulate cortex in the macaque monkey. J Comp Neurol 311:445-462.

Mazzocchio R, Rothwell JC, Day BL, Thompson PD. 1994. Effect of tonic voluntary activity on the excitability of human motor cortex. J Physiol (Lond) 474:261-267.

McGee AW, Strittmatter SM. 2003. The Nogo-66 receptor: focusing myelin inhibition of axon regeneration. Trends in Neurosciences 26:193-198.

Merkler D, Metz GAS, Raineteau O, Dietz V, Schwab ME, Fouad K. 2001. Locomotor recovery in spinal cord-injured rats treated with an antibody neutralizing the myelin-associated neurite growth inhibitor Nogo-a. J Neurosci 21:3665-3673.

Merkler D, Oertle T, Buss A, Pinschewer DD, Schnell L, Bareyre FM, Kerschensteiner M, Buddeberg BS, Schwab ME. 2003. Rapid induction of autoantibodies against Nogo-A and MOG in the absence of an encephalitogenic T cell response: implication for immunotherapeutic approaches in neurological diseases. FASEB J 17:2275-2277.

Murase N, Duque J, Mazzocchio R, Cohen LG. 2004. Influence of interhemispheric interactions on motor function in chronic stroke. Ann Neurol 55:400-409.

Murray EA, Coulter JD. 1981. Organization of corticospinal neurons in the monkey. J Comp Neurol 195:339-365.

Nakajima K, Maier MA, Kirkwood PA, Lemon RN. 2000. Striking differences in transmission of corticospinal excitation to upper limb motoneurons in two primate species. J Neurophysiol 84:698-709.

Napier J. 1962. The evolution of the hand. Scientific Amer 207:56-62.

Nelson RJ, Sur M, Felleman DJ, Kaas JH. 1980. Representations of the body surface in postcentral parietal cortex of Macaca fascicularis. J Comp Neurol 192:611-643.

Nudo RJ, Jenkins WM, Merzenich MM. 1990. Repetitive microstimulation alters the cortical representation of movements in adult rats. Somatosens Motor Res 7:463-483.

Nudo RJ, Milliken GW. 1996. Reorganization of movement representations in primary motor cortex following focal ischemic infarcts in adult squirrel monkeys. J Neurophysiol 75:2144-2149.

Nudo RJ, Milliken GW, Jenkins WM, Merzenich MM. 1996. Use-dependent alterations of movement representations in primary motor cortex of adult squirrel monkeys. J Neurosci 16:785-807.

Nudo RJ. 1999. Recovery after damage to motor cortical areas. Curr Opin Neurobiol 9:740-747.

Nudo RJ. 2006. Mechanisms for recovery of motor function following cortical damage. Curr Opin Neurobiol 16:638-644.

Oertle T, Van der Haar ME, Bandtlow CE, Robeva A, Burfeind P, Buss A, Huber AB, Simonen M, Schnell L, Brösamle C, Kaupmann K, Vallon R, Schwab ME. 2003. Nogo-A inhibits neurite outgrowth and cell spreading with three discrete regions. J Neurosci 23:5393-5406.

Olivier E, Baker SN, Nakajima K, Brochier T, Lemon RN. 2001. Investigation into non-mono synaptic corticospinal excitation of macaque upper limb single motor units. J Neurophysiol 86:1573-1586.

Papadopoulos CM, Tsai SY, Alsbiei T, O'Brien TE, Schwab ME, Kartje GL. 2002. Functional recovery and neuroanatomical plasticity following middle cerebral artery occlusion and IN-1 antibody treatment in the adult rat. Ann Neurol 51:433-441.

Park MC, Belhaj-Saïf A, Gordon M, Cheney PD. 2001. Consistent features in the forelimb representation of primary motor cortex in rhesus macaques. J Neurosci 21:2784-2792.

Penfield W, Rasmussen T. 1950. The Cerebral Cortex of Man. New York: McMillan.

Penn RD. 1989. Intrathecal medications for spasticity. In: Emre M, Benecke R, editors. Spasticity: the Current Status of Research and Treatment. p 125-129.

Phillips CG, Porter R. 1977. Corticospinal neurones, their role in movement. In: Monographs of the Physiol. Soc. - No. 34. London, New York, San Fancisco: Academic Press. p 450pp.

Picard N, Strick PL. 1996. Motor areas of the medial wall: A review of their location and functional activation. Cereb Cortex 6:342-353.

Plautz EJ, Milliken GW, Nudo RJ. 2000. Effects of repetitive motor training on movement representations in adult squirrel monkeys: Role of use versus learning. Neurobiol Learn Mem 74:27-55.

Plautz EJ, Barbay S, Frost SB, Friel KM, Dancause N, Zoubina EV, Stowe AM, Quaney BM, Nudo RJ. 2003. Post-infarct cortical plasticity and behavioral recovery using concurrent cortical stimulation and rehabilitative training: A feasibility study in primates. Neurol Res 25:801-810.

Qi HX, Stepniewska I, Kaas JH. 2000. Reorganization of primary motor cortex in adult macaque monkeys with long-standing amputations. J Neurophysiol 84:2133-2147.

Ralston DD, Ralston HJI. 1985. The terminations of corticospinal tract axons in the macaque monkey. J Comp Neurol 242:325-337.

Riener R, Lunenburger L, Colombo G. 2004. Cooperative strategies for robot-aided gait neuro-rehabilitation. Conf Proc IEEE Eng Med Biol Soc 7:4822-4824.

Roby-Brami A, Jacobs S, Bennis N, Levin MF. 2003. Hand orientation for grasping and arm joint rotation patterns in healthy subjects and hemiparetic stroke patients. Brain Research 969:217-229.

Rouiller EM, Yu XH, Moret V, Tempini A, Wiesendanger M, Liang F. 1998. Dexterity in adult monkeys following early lesion of the motor cortical hand area: the role of cortex adjacent to the lesion. Eur J Neurosci 10:729-740.

Sanes JN, Suner S, Lando JF, Donoghue JP. 1988. Rapid reorganization of adult rat motor cortex somatic representation patterns after motor nerve injury. Proc Natl Acad Sci USA 85:2003-2007.

Sasaki S, Isa T, Pettersson LG, Alstermark B, Naito K, Yoshimura K, Seki K, Ohki Y. 2004. Dexterous finger movements in primate without monosynaptic corticomotoneuronal excitation. J Neurophysiol 92:3142-3147.

Savio T, Schwab ME. 1989. Rat CNS white matter, but not gray matter, is nonpermissive for neuronal cell adhesion and fiber outgrowth. J Neurosci 9:1126-1133.

Schäfer M, Frutiger M, Montag D, Schachner M, Martini R. 1996. Disruption of the Gene for the Myelin-Associated Glycoprotein Improves Axonal Regrowth along Myelin in C57BL/Wld^s Mice. Neuron 16:1107-1113.

Schieber MH, Hibbard LS. 1993. How somatotopic is the motor cortex hand area? Science 261:489-492.

Schieber MH. 1995. Muscular production of individuated finger movements: The roles of extrinsic finger muscles. J Neurosci 15:284-297.

Schieber MH, Deuel RK. 1997. Primary motor cortex reorganization in a long-term monkey amputee. Somatosens Mot Res 14:157-167.

Schieber MH. 2001. Constraints on somatotopic organization in the primary motor cortex. J Neurophysiol 86:2125-2143.

Schieppati M, Trompetto C, Abbruzzese G. 1996. Selective facilitation of responses to cortical stimulation of proximal and distal arm muscles by precision tasks in man. J Physiol 491 (Pt 2):551-562.

Schmidlin E, Wannier T, Bloch J, Rouiller EM. 2004. Progressive plastic changes in the hand representation of the primary motor cortex parallel incomplete recovery from a unilateral section of the corticospinal tract at cervical level in monkeys. Brain Research 1017:172-183.

Schnell L, Schwab ME. 1990. Axonal regeneration in the rat spinal cord produced by an antibody against myelin-associated neurite growth inhibitors. Nature 343 no 6255:269-272.

Schwab ME, Thoenen H. 1985. Dissociated neurons regenerate into sciatic but not optic nerve explants in culture irrespective of neurotrophic factors. J Neurosci 5:2415-2423.

Schwab ME. 2004. Nogo and axon regeneration. Curr Opin Neurobiol 14:118-124.

Schwegler G, Schwab ME, Kapfhammer JP. 1995. Increased collateral sprouting of primary afferents in the myelin-free spinal cord. J Neurosci 15:2756-2767.

Seymour A. B. et al, 2005. Delayed treatment with monoclonal antibody IN-1 1 week after stroke results in recovery of function and corticorubral plasticity in adult rats. Journal of Cerebral Blood Flow & Metabolism 25, 1366–1375

Shinoda Y, Zarzecki p, Asanuma H. 1979. Spinal branching of pyramydal tract neurons in the monkey. Exp Brain Res 34:59-72.

Shinoda Y, Yokota JI, Futami T. 1981. Divergent projection of individual corticospinal axons to motoneurons of multiple muscles in the monkey. Neurosci Letters 23:7-12.

Shinoda Y, Yamaguchi T, Futami T. 1986. Multiple axon collaterals of single corticospinal axons in the cat spinal cord. J Neurophysiol 55:425-448.

Shinoda Y, Futami T, Mitoma H, Yokota J. 1988. Morphology of single neurones in the cerebello-rubrospinal system. Behav Brain Res 28:59-64.

Siebner HR, Rothwell J. 2003. Transcranial magnetic stimulation: new insights into representational cortical plasticity. Exp Brain Res 148:1-16.

Simonen M, Pedersen V, Weinmann O, Schnell L, Buss A, Ledermann B, Christ F, Sansig G, Van der Putten H, Schwab ME. 2003. Systemic deletion of the myelin-associated outgrowth inhibitor Nogo-A improves regenerative and plastic responses after spinal cord injury. Neuron 38:201-211.

Stoney SD, Thompson WD, Asanuma H. 1968. Excitation of pyramidal tract cells by intracortical microstimulation: effective extent of stimulating current. J Neurophysiol 31:659-669.

Stowe AM, Plautz EJ, Eisner-Janowicz I, Frost SB, Barbay S, Zoubina EV, Dancause N, Taylor MD, Nudo RJ. 2007. VEGF protein associates to neurons in remote regions following cortical infarct. J Cereb Blood Flow Metab 27:76-85.

Strick PL, Preston JB. 1978. Sorting of somatosensory afferent information in primate motor cortex. Brain Res 156:364-368.

Taub E, Uswatte G, Elbert T. 2002. New treatments in neurorehabilitation founded on basic research. Nat Rev Neurosci 3:228-236.

Taub E, Uswatte G, Mark VW, Morris DM. 2006. The learned nonuse phenomenon: implications for rehabilitation. Eura Medicophys 42:241-256.

Thallmair M, Metz GAS, Z'Graggen WJ, Raineteau O, Kartje GL, Schwab ME. 1998. Neurite growth inhibitors restrict plasticity and functional recovery following corticospinal tract lesions. Nature Neurosci 1:124-131.

Tower SS. 1940. Pyramidal lesion in the monkey. Brain 63:36-90.

Tsukahara N. 1981. Synaptic plasticity in the mammalian central nervous system. Annu Rev Neurosci 4:351-379.

Vidal-Sanz M, Bray GM, Villegas-Perez MP, Thanos S, Aguayo AJ. 1987. Axonal regeneration and synapse formation in the superior colliculus by retinal ganglion cells in the adult rat. J Neurosci 7:2894-2909.

Wang KC, Koprivica V, Kim JA, Sivasankaran R, Guo Y, Neve RL, He Z. 2002. Oligodendrocyte-myelin glycoprotein is a Nogo receptor ligand that inhibits neurite outgrowth. Nature 417:941-944.

Wannier TMJ, Maier MA, Hepp-Reymond M-C. 1991. Contrasting properties of monkey somatosensory and motor cortex neurons activated during the control of force in precision grip. J Neurophysiol 65:572-587.

Weinmann O, Schnell L, Ghosh A, Montani L, Wiessner C, Wannier T, Rouiller E, Mir A, Schwab ME. 2006. Intrathecally infused antibodies against Nogo-A penetrate the CNS and downregulate the endogenous neurite growth inhibitor Nogo-A. Mol Cell Neurosci 32:161-173.

Wenk CA, Thallmair M, Kartje GL, Schwab ME. 1999. Increased corticofugal plasticity after unilateral cortical lesions combined with neutralization of the IN-1 antigen in adult rats. J Comp Neurol 410:143-157.

Widener GL, Cheney PD. 1997. Effects on muscle activity from microstimuli applied to somatosensory and motor cortex during voluntary movement in the monkey. J Neurophysiol 77:2446-2465.

Wiesendanger M. 1981. The pyramidal tract.   Its structure and function. Hand behav neurobiol 5:401-491.

Woolf CJ, Bloechlinger S. 2002. It takes more than two to NOGO. Science 297:1132-1134.

Woolsey CN, Settlage PH, Meyer DR, Spencer W, Pinto Hamuy T, Travis AM. 1952. Patterns of localization in precentral and "supplementary" motor areas and their relation to the concept of a premotor area. Res Publ Assoc Res Nerv Ment Dis 30:238-264.

Woolsey CN. 1964. Cortical localization as defined by evoked potential and electrical stimulation studies. In: Schaltenbrand G, Woolsey CN, editors. Cerebral Localization and Organization. Madison and Milwaukee: The University of Wisconsin Press. p 17.

Wu CWH, Kaas JH. 1999. Reorganization in primary motor cortex of primates with long-standing therapeutic amputations. J Neurosci 19:7679-7697.

Xerri C, Merzenich MM, Peterson BE, Jenkins W. 1998. Plasticity of primary somatosensory cortex paralleling sensorimotor skill recovery from stroke in adult monkeys. J Neurophysiol 79:2119-2148.

Yiu G, He ZG. 2003. Signaling mechanisms of the myelin inhibitors of axon regeneration. Curr Opin Neurobiol 13:545-551.

Z'Graggen WJ, Fouad K, Raineteau O, Metz GAS, Schwab ME, Kartje GL. 2000. Compensatory sprouting and impulse rerouting after unilateral pyramidal tract lesion in neonatal rats. J Neurosci 20:6561-6569.

Zheng B, Lee JK, Xie F. 2006. Genetic mouse models for studying inhibitors of spinal axon regeneration. Trends Neurosci 29:640-646.

Ziemann U, Tergau F, Wassermann EM, Wischer S, Hildebrandt J, Paulus W. 1998. Demonstration of facilitatory I wave interaction in the human motor cortex by paired transcranial magnetic stimulation. J Physiol (Lond) 511:181-190.

Content of Methods

2. Methods

For the purpose of this study the data were collected from 5 monkeys (*macaca fascicularis*, 3 males and 2 females, weighted between 3 and 6 kg, and aged between 4 and 6 years old at the time of starting recording electrophysiological data (see Table 3.1; page 208). For some aspects, the two untreated monkeys of the study by Liu and Rouiller (1999) will be included in the data (Table 3.1, page 208). All the behavioral, surgical and electrophysiological procedures were approved by the ethical committee, in accordance with the Guidelines for the Care and Use of Laboratory Animals (ISBN 0-309-05377-3; 1996) and approved by local (Swiss) veterinary authorities. In this chapter we will describe in detail the different behavioral, surgical, electrophysiological, and histological methods used in the present study.

2.1 Behavioral procedures

Five monkeys were trained daily to perform various behavioral tasks involving hand dexterity. During each data collection session, including training, the monkeys were seated in a custom primate chair (Fig. 2.1C). The primate chair is a Plexiglas box with an opening on top through which the monkey can put out its head. Using a sliding Plexiglas piece around the neck, the monkey can be restrained while allowing free head movements. The monkey is seated on horizontal bars that can be adapted to its size, making its position comfortable. During the entire study each primate chair was dedicated to a specific monkey. On the front panel of the primate chair, two sliding doors allow testing separately the left or the right hand during the performance of a specific task. For the behavioral tests the monkey was placed into an experimental chamber equipped with four digital recording cameras. The behavioral measurements consisted of quantitative and qualitative tests. The quantitative test allowed direct assessment of the hand dexterity of the monkey during the behavioral tasks conducted in the experimental chamber whereas the qualitative data of the monkey were derived from observations outside the experimental chamber, such as in the cage or in the animal room.

2.1.1 Quantitative tests

In their early work Brinkman and Kuypers (1973) have developed a behavioral test to assess the manual hand dexterity recovery after brain split in rhesus monkeys. The Brinkman board consisted of circular food wells which could just accommodate a food pellet (Fig. 2.1A). The food wells communicated by two or three radial grooves 5 mm wide. These grooves allow the monkey

to dislodge the pellet from the well. Moreover, in their study, Brinkman and Kuypers used two different food pellets: a small pellet which was even with the board surface or a larger pellet which stuck out. In the present study, we used a modified version of their test board ("modified Brinkman board). Instead of cylindrical wells, we chose oval wells (slots) which, in comparison to the original Brinkman board, consisted of a combination of two cylindrical wells and a groove (Fig. 2.1B). Such slots permit the monkey to remove the food pellet using one finger to dislodge it and opposing to a second finger, to pick it up. The slot was 14 mm long, 7mm large and 6 mm deep (Fig. 2.1C). The slot dimension was just large enough for the monkey to place the distal phalange of the index finger and flex it to get the pellet out. The size of the slot was the same for all tasks. The size of the pellet was about 4 mm in diameter. The monkeys were trained to perform two different modified Brinkman board tests: the standard Brinkman board, and the hidden Brinkman board. Brief sequences of these two tasks can be seen on internet (http//www: unifr.ch/neuro/rouiller/motorcadre.htm)

A

View from above

24 cm

B

22 cm

14 cm   12 cm

Pellet

7 mm

4mm

1.4 cm

Pellet

Side view

1.2 cm   Pellet   6 mm

1.4 cm

NORMAL BRINKMAN BOARD
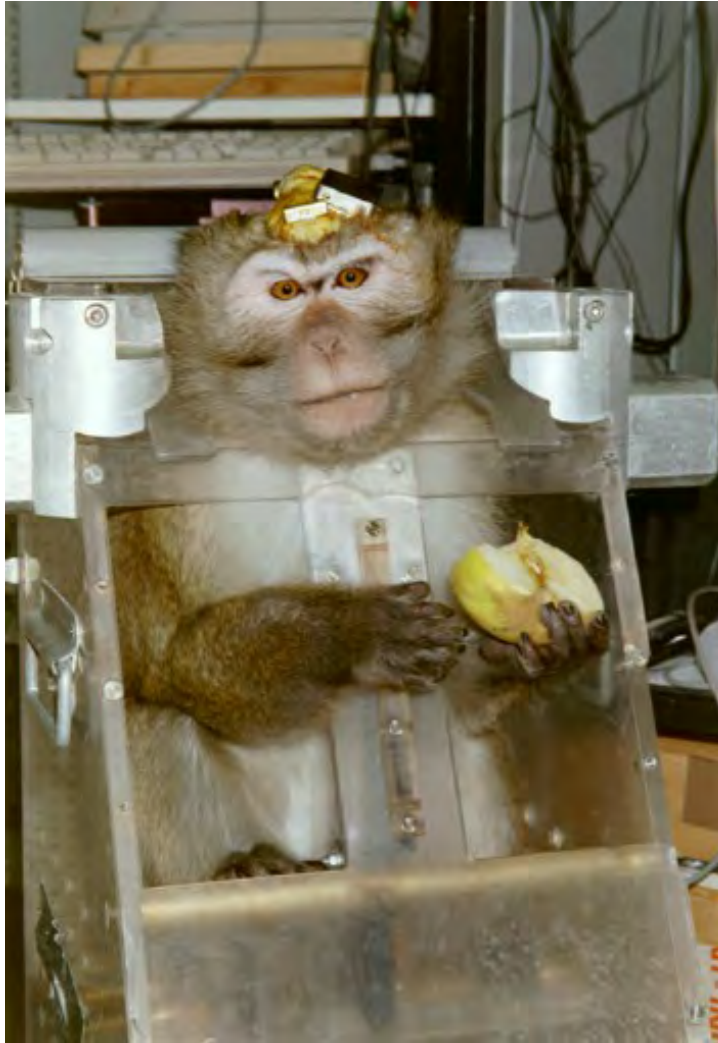
Figure 2.1   Brinkman behavioral board.
   A) Original Brinkman board as introduced by Brinkman and Kuypers (1973).
   B) Modified Brinkman board used in the present study, as seen from above (top) or from the side (bottom).
   C) View of the primate chair, with a monkey in it.

2.1.1.1 Modified Brinkman board

The modified Brinkman board consists of a green Plexiglas board in which 25 horizontally oriented and 25 vertically oriented slots were milled (Fig. 2.1). The green board is inserted within a black plastic frame. This setup is held by an aluminum rod in the experimental chamber in order to keep it in a stable position with respect to the primate chair. The modified Brinkman board is positioned in front of the monkey with 40 degree inclination. The setup can either be aligned to the left or the right primate chair window in order to separately test the left or the right hand of the monkey. During each recording session the right and the left hands were always tested separately. The standard Brinkman board can be used to test the monkey's hand skill resulting from the combination of tactile, proprioceptive and visual inputs. This board is suited to determine whether the monkey is able to perform the so-called precision grip, namely grasping of a small object between the thumb and index finger. The width of the slots is slightly larger than the width of the monkey's fingers. For the vertical slots, most of the time the monkeys used the index finger, as seen in Figure 2.2, to dislodge the pellet and then grasped it by opposing the thumb. Grasping pellets out of horizontal slots needed in addition a rotation of the wrist (Fig. 2.3).

Figure 2.2   **Figure 2.3**

Figures 2.2 /3   The hand dexterity, as tested by the pellet retrieval, from vertical slot (Fig. 2.2) and horizontal slot (Fig. 2.3).

2.1.1.2 Hidden Brinkman board

As described in the review of Naito (2004), the primary motor cortex receives sensory information especially during limb movements. Along this line one can imagine that monkeys subjected to M1 lesions will have not only motor deficits, but also sensorimotor dysfunctions. The hidden Brinkman board consists of a plastic box (Fig. 2.4). The top, back and side panels were

made from non-transparent PVC. In contrast, the bottom of the box was made of transparent Plexiglas, allowing video-recording of the hand from below. The top panel of the box is movable (sliding panel). When it was open, the monkey had visual control of its hand and when it was closed, the monkey had no visual feedback and could count only on its tactile and proprioceptive inputs. As for the standard Brinkman board, the box was placed in front of one of the two primate chair windows. The width of the entrance of the Hidden Brinkman box was large enough for the monkey to place its hand inside and rotate its wrist easily. The monkey was trained to reach inside the Hidden Brinkman box first with visual feedback and then without visual control. The Hidden Brinkman board consisted of 20 slots, 10 oriented vertically and 10 horizontally (Fig. 2.5)

Hidden Brinkman Board
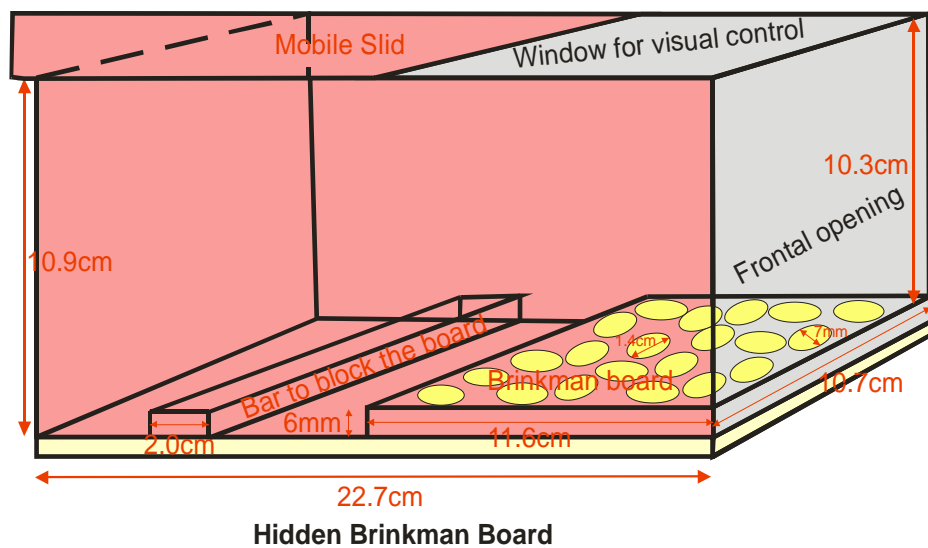
Figure 2.4   Drawing of the hidden Brinkman box.

Frontal opening
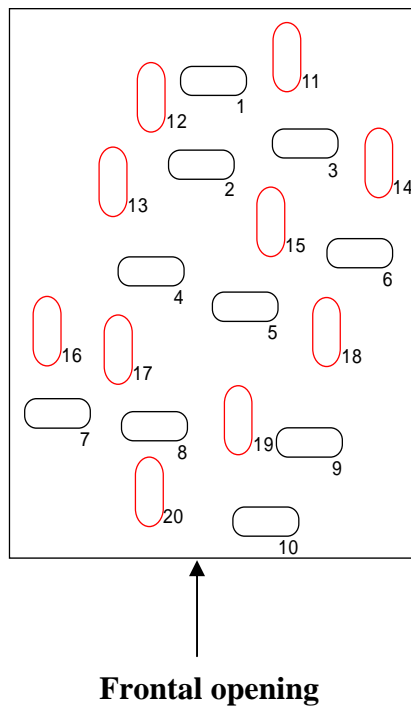
Figure 2.5   "Hidden Brinkman board" slots' arrangement.

In red the vertical slots and in black the horizontal slots. Each slot has a number in order to register the monkey's strategy, if there is any, for retrieving the pellets.

2.1.2 Qualitative observations in the primate chair and in the animal house

These observations served as a complement to the quantitative tests and were **not** performed systematically during the whole experimental phase for a given animal. They were rather conducted at time points after the lesion at which one could expect to gain important additional information about the monkey's behavior and the manual dexterity. Video taping of treated and control monkeys thus took place either in the primate chair or in the animal room, usually during the recovery phase and in the hours following the muscimol injections. Videos of the freely moving monkeys in the animal room were especially useful to better evaluate which limbs or which parts of a limb were affected by the lesion, because a monkey often avoided using an impaired limb for climbing or feeding. Investigating the monkey's behavior, while sitting in the primate chair, was mainly helpful for approximately evaluating its remaining force to grasp a morsel of food. In general the piece of food was restrained by the experimenter in order to force the monkey to pull it out of his hand. By this method one can have an estimate of the force of the proximal muscles and the power of the grip of the impaired hand. To further asses the hand dexterity, a sweet, in the form of spaghetti, was presented to the monkey. The monkey could

successfully reach with both hands only if the monkey used them alternately to pull the spaghetti. These tests were useful to better describe the performance of the monkeys in different environments after a lesion of the hand representation in M1.

2.2. Surgical Procedures

For all implant surgeries, the monkeys were tranquilized initially with ketamine (Ketalar®; Parke-Davis, 5 mg/kg, i.m.), atropine was administered (0.05 mg/kg, i.m.) in order to reduce bronchial secretions and, subsequently, the monkey was anesthetized with intravenous perfusion of 1% propofol (Fresenius®) mixed with a 5% glucose solution (1 volume of propofol and 2 volumes of glucose solution). To prevent oedema of the CNS, 60 mg of Solu - Medrol® were added to 120 ml of the above propofol/glucose solution. The level of anesthesia was kept at an optimal level with a perfusion rate of the propofol/glucose mixture of 0.1ml/min/kg. Before taking the monkey to the surgery room, it was prepared by shaving the operative site, cleaning it with betadin and after with alcohol. Before the incision, the operative site was covered with antimicrobial incision drape (Steri-drape 3M^{TM} Ioban^{TM} 2) to thoroughly dry the intact skin. All monkeys received, before and after surgery, subcutaneous injections of the antibiotic Albipen® (Ampiciline 10%, 30mg/kg) and of the analgesic Carprofen (Rymadil®, 4mg/kg). All surgeries were performed in a facility approved by the local cantonal veterinarian, with strict attention to sterile technique. Blood pressure, expired CO_2, inhaled O_2 and rectal temperature, were carefully monitored throughout the surgery. After each surgery, the monkey was under observation until it came out of the anesthesia and started eating, drinking and behaving as usual.

2.2.1 Cortical Chamber Implant

On completion of training and once the monkey reached a behavioral plateau in all the behavioral tasks, each monkey was implanted with a cortical recording chamber. A rectangular stainless steel "recording" chamber was stereotaxically implanted over the forelimb area on the left hemisphere of each monkey as described in previous studies from this laboratory (Liu and Rouiller 1999). The recording chamber was centered at anterior 15 mm and lateral 15 mm (Fig. 2.6), and its shape was adapted to fit the profile of the monkey's skull allowing for perpendicular penetrations with microelectrodes in the brain. The skull was opened at a location and an area corresponding to the inner dimension of the recording chamber. The recording chamber was anchored to the skull with titanium screws (Synthes®, Cortex screw). A head fixation device consisting of a stainless steel cylinder was anchored over the occipital zone of the skull to allow attachment of a flexible

head restrain system during electrophysiological recording sessions. The whole implant was secured to the skull by dental acrylic cement and/or by orthopedic cement (Palacos® 40 Gentamicin 500 mg). The size of the recording chamber was 22 x 22 x 15 mm for one monkey (MK3-V) and 22 x 17 x 15 mm for the other monkeys (MK1-G, MK2-L, MK4-S and MK5-R). Three monkeys (MK1-G, MK2-L and MK3-V) were implanted with two chambers over both the left and right hand areas of the motor cortex. However, ICMS data of the right M1 were limited to only two of these monkeys (MK1-G and MK2-L). For the other two monkeys (MK4-S and MK5-R), a single recording chamber was implanted on the left side only.
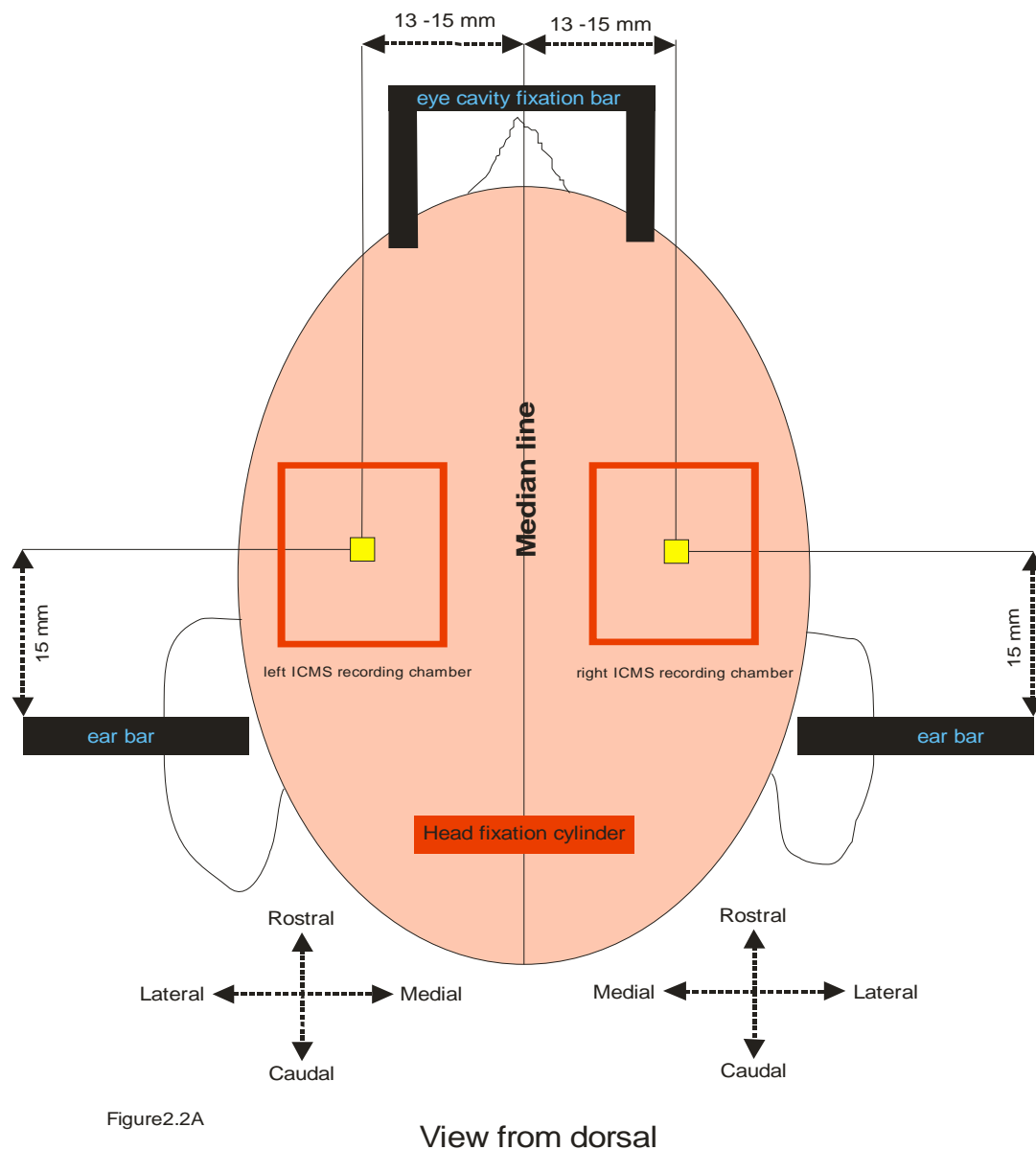
Figure 2.6   Illustration of the implantation of the recording chamber over the M1 forelimb area bilaterally.

2.2.2 Anti-Nogo Pump Implant

Once the pre-lesion ICMS mapping was completed (see below), a lesion of the representation of the M1 hand was performed (see 2.5). For the three treated monkeys, just after the lesion two osmotic pumps (Alzet® osmotic pump, model 2ML2, 5µl per hour), containing the anti-Nogo-A antibody 11C7, were implanted, one at cervical level and the other at cortical level. The antibody diffusion study conducted in monkeys and rats (Weinmann et al., 2006) showed that a subarachnoidal infusion at cervical level generated amounts of 11C7 antibodies in the brain detectable by antibody staining, but it is not yet known if the detected concentration in the brain was high enough to be therapeutically efficient. The strategy of implanting two pumps in the present study was aimed at making sure to reach a concentration of 11C7 high enough for treatment at the lesion site in the motor cortex.

The surgery to implant osmotic pumps is well described in previous reports from our laboratory related to spinal lesion studies (Freund et al., 2006, 2007; Schmidlin et al., 2004; 2005). The surgery procedures followed the same protocol as described for the cortical recording chamber implantation. The monkey was anesthetized first with Ketamine, followed by perfusion with Propofol solution. To implant the pumps, the back of the monkey was shaved and cleaned with Betadine solution and with alcohol solution. A surgical tape covered the whole area.

The implantation of the osmotic pumps was done by a neurosurgeon (Dr. Jocelyne Bloch, CHUV, University of Lausanne). The monkey was placed in the stereotaxic apparatus with the head fixed with ear bars, but no eye bars or mouthpiece. A pillow was placed under the monkey's chest to elevate it and to obtain a rounded back. An incision along the median line in the skin of the back above the dorsal spinal processes from C2 to Th1 was made. Paravertebral muscles were retracted on both sides. The spinal processes from C2 to Th1 were exposed. The tissue around the vertebra was retracted and the laminae of the segments C6 to Th1 were dissected. As a next step, the dorsal arc of segment C7 was removed in order to expose the dura mater, which was incised longitudinally under binocular. Through this small incision a thin wall catheter connected to the first pump was pushed in the subarachnoidal space 3-5mm rostral to C6, allowing direct delivery of the antibody 11C7 into the cerebral-spinal-fluid (CSF). Several sutures to the catheter were done to assure certain stability and limit its movement. The catheter of the second pump was tunneled under the skin to the head of the monkey. A small trepanation close to the cortical chamber implant and a small incision of the dura were made. Through this opening, a thin wall catheter was slipped underneath the dura. Histologic glue (Histoacryl®) was placed to cover the dura opening and the catheter was secured with dental acrylic cement. Once the catheters were in place, the muscles were sutured, a subcutaneous small pouch lateral to the spinal cord was made and the pumps were

placed inside it. Before suturing the skin a local antibiotic was applied into the incision and a subcutaneous injection of Albipen® (Ampiciline 10%, 30mg/kg) was administered to prevent infections, before bringing the monkey back to the animal room. The monkey was then kept in a separate cage for few days until it fully recovered from surgery. Once the monkey recovered and the sutures were healed, the monkey rejoined its group. Following the surgery, the monkey received an antibiotic and analgesic treatment for up to 10 days and was taken to the laboratory daily to clean the surgery incision and apply local antibiotic. The pumps allowed delivery of the antibody treatment during 14 days. Two others surgeries were needed for replacing (for 2 more weeks treatment) and finally removing the pumps. These procedures were similar to those described above. The treatment lasted 4 weeks, and the monkeys received a total volume of anti-Nogo-A antibody ranging from 13 to 23 mg (see below). In this study, three monkeys were treated (MK2-L, MK3-V and MK4-S). The two control monkeys (MK1-G and MK5-R) did not receive any treatment and therefore they were not subjected to this surgical procedure. The choice of the treated or untreated monkey was done randomly, but whether a given monkey was treated or not was known to the experimenter.

The three treated monkeys received the monoclonal antibody 11C7 (antibody 11C7, 3.7mg / ml; kindly supplied by Novartis Pharma AG) directed against Nogo-A. Monkey MK2-L was treated over a period of 16 days corresponding to a total amount of 13.19 mg 11C7, whereas monkeys MK3-V and MK4-S received a similar 11C7 treatment lasting for about 28 days corresponding to 23.07 mg.

2.3 Data Recording

2.3.1. Behavioral data

The experimental chamber in the laboratory is equipped by four digital recording cameras (Fig. 2.7) that allow video-taping of the hand dexterity tests. One digital camera is positioned in the ceiling of the experimental chamber and permitted having a broad view from the top of the whole hand during the task. Two other digital cameras were mounted one at the left and the other one at the right of the monkey, allowing a side view of the digit movement during the task. For the Hidden Brinkman board task, a digital camera was placed below the Hidden Brinkman board. Figure 2.7 shows the setup inside the experimental chamber.
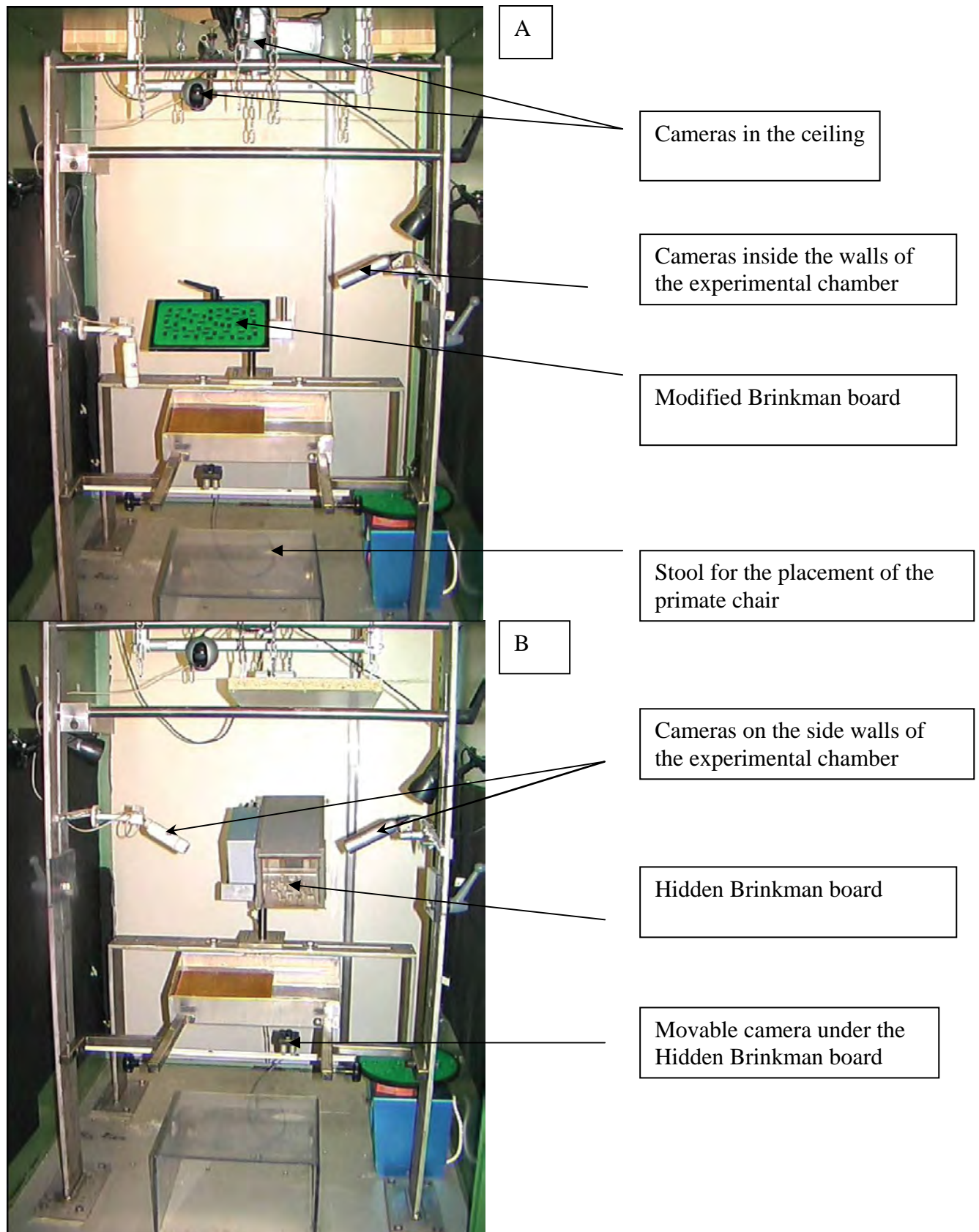
Figure 2.7   Experimental chamber setup for behavioral assessment, during Standard Brinkman Board (A) or during Hidden Brinkman board (B) tasks.

2.3.2 Motor cortex mapping

The motor cortex of each monkey was electrophysiologically (ICMS) mapped twice, once before the lesion and once a few months after the lesion. The pre-lesion mapping started when the monkey reached the behavioral plateau and recovered from the cortical surgery implantation. The post-lesion mapping started when the monkey showed no more behavioral improvement (plateau of recovery). Tungsten Mylar insulated electrodes with impedances between 0.7-1.5 MΩ (Frederick Haer & Co., Bowdoinham, Maine, USA) were used for ICMS mapping. Electrode penetrations were systematically made mainly in the precentral and in some cases also in the postcentral gyri, using a 1 mm grid interval for four monkeys and 2 mm grid interval for one monkey (MK2-L). The electrode was advanced with a manual hydraulic microdrive (Narishige group, Japan, Model MO-95). Stimulation was performed at 1 mm intervals, starting from 2 mm bellow the dura and stopped at 12 mm depth.

For the purpose of this study, we used a classical intracortical microstimulation paradigm (ICMS) in awake monkeys as initially reported by Asanuma (1976). The ICMS consisted of trains of 12 pulses delivered at 330Hz. The stimulation was applied through the microelectrode. Individual stimuli are 0.2 ms negative pulse generated by a "WPI" stimulator and a stimulus isolation unit ("WPI"). The highest intensity was limited in this study to 80 µA. By using ICMS, the aim was to activate corticospinal neurons that will bring motoneurons to discharge, which will activate one or several muscles, thus producing a visible movement or muscle contraction detectable by palpation. At the first stimulation site of a given track, the highest intensity was used until it produced a movement or muscle contraction; after that, the stimuli intensity was reduced to a level below which no effect was observed. This value was considered as the threshold for that given stimulation site. The experimenter needed to hold the monkey's arm during the lowest stimulation intensities to have a better feeling of the movement and muscle contraction. Moreover, by manipulating the arm in different positions it was possible to facilitate a joint movement which was not obvious in the other arm positions. Depending on the monkey's cooperation, 2 to 5 tracks were made daily. Once the monkey became impatient, the ICMS session was stopped, and the monkey was brought back to the animal room. In general, the ICMS mapping lasted about 20-30 days.

2.4. Data Analysis

2.4.1 Behavioral

Two methods were used to assess the hand dexterity. First, we used the number of pellets that the monkey retrieved in a certain time window and, second, the pellet retrieval time. These analyses were done offline by replaying the video tapes.

2.4.1.1 Modified Brinkman board

For all subtypes of data analysis we used **general guidelines.** These guidelines, summarized in Table 2.1, mainly describe the most frequent errors the monkeys made while retrieving the pellets out of the slot of the Standard Brinkman board. If a pellet was retrieved by means of an incorrect manipulation (see Table 2.1) or left in a slot, indicating that the animal was not able to pick it out or was just not motivated to complete the task, these events were rated as errors and not taken into account for further statistical analysis.

Possible Errors	Type of Error	
	Real Error	Subsequent Error
pellet displaced to an other slot	X	
formerly displaced pellet but correctly retrieved		X
pellet jumped out of the slot during manipulation and fell on the floor	X	
pellet retrieved with the hand not tested (right hand tested but pellet retrieved with left hand)	X	
Pellet bimanually retrieved	X	

Table 2.1   Guidelines of possible errors made by the monkey during pellet retrieval.

2.4.1.2 Measuring the performance of the Modified Brinkman board task

For each monkey, the performances of the left and the right hands were analyzed individually. In order to compare pre- and post-lesion data, we generally selected the time span to analyze as follows: Analyses were conducted on recorded data during 150 days pre-lesion, as well as on recorded data during 150 days post-lesion. We considered that this time window covered the different behavioral pre- and post-lesion phases. Pre-lesion data were analyzed 2 to 3 times a week

and every day two weeks before the lesion. Post-lesion data recordings were analyzed every day until the monkey reached and maintained a stable performance (plateau of recovery). From there on, again 2 to 3 weekly sessions were analyzed. The video recordings from each day were used as basic data source for generating graphics and charts with graphic softwares (EXCEL, Sigma Plot). Some analyses were done by viewing the videos and others by using automatic analysis homemade software programs (Monkey Cam Software, Blackdot.net). The parameters we first investigated were the following:

- Number of correctly retrieved pellets from vertical and horizontal slots during the first 15 seconds.

- Number of correctly retrieved pellets from vertical and horizontal slots during the first 30 seconds.

- Number of correctly retrieved pellets from vertical and horizontal slots during the first 45 seconds.

- Number of correctly retrieved pellets from vertical and horizontal slots during the first 60 seconds.

- Number of correctly retrieved pellets from all slots of the Modified Brinkman board.

- Total number of errors for each time period indicated above.

2.4.1.3 Retrieval time

Instead of analyzing the entire Standard Brinkman board, six selected positions were analyzed in detail. First, the contact time with the pellet was computed for the first vertical and the first horizontal slots successively retrieved. Second, contact times were measured in 4 additional, peripheral slots, namely the most peripheral vertical and horizontal on top left (3, 4) and the most peripheral vertical and horizontal on bottom right (1, 2) slots (Fig. 2.9). Figure 2.8 shows two successive images, first one when the monkey entered the slot and second when the monkey retrieved the pellet. For each slot the retrieval time (RT) or contact time of the pellet was measured using a frame by frame analysis as indicted by the formula:

$$\textbf{RT} = \textbf{T}_1 \textbf{-} \textbf{T}_0$$

T_1 = frame at which the monkey exits the slot with a pellet

T_0 = frame at which the monkey enters the slot
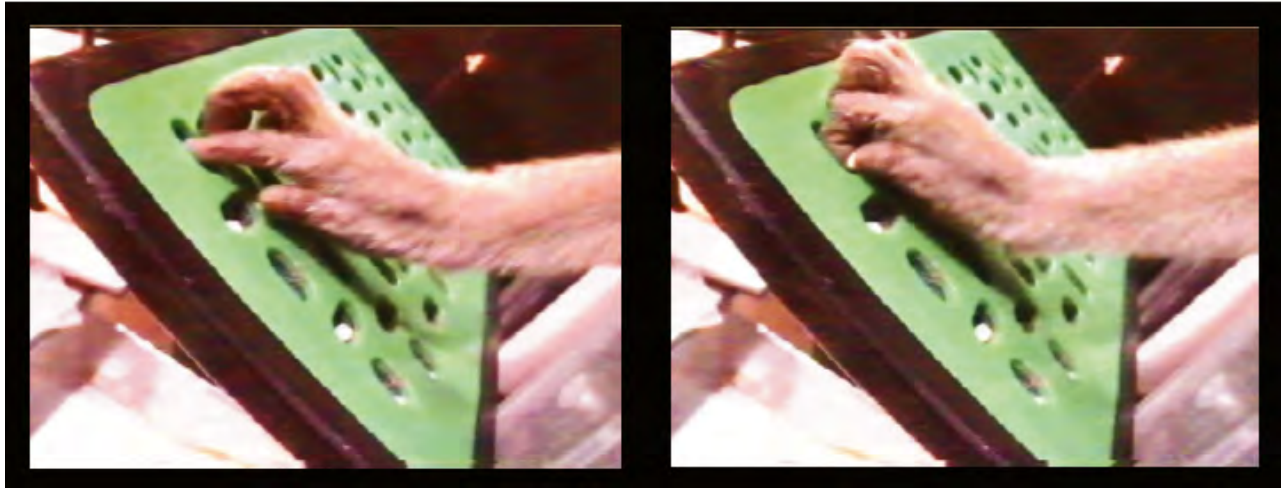
Figure 2.8   Pellet retrieval time (contact time). Left panel: the monkey entered the slot at time (T_0). Right panel: the monkey exits the slot with the pellet between its fingers (index and thumb) at time (T_1).

To evaluate the monkey's strategy used during the Modified Brinkman board task, the following analysis was conducted to determine which of the vertical slots and which of the horizontal slots the monkey preferred to empty first. In order to simplify the analysis, the Modified Brinkman board was divided into three zones: A (in front of the monkey), B (left to the monkey) and C (right to the monkey) (Fig. 2.9). This analysis allowed assessing any changes of the monkey's strategy before and after the lesion (Analysis of data currently underway in our laboratory, therefore not yet presented in chapter 3 of this thesis).
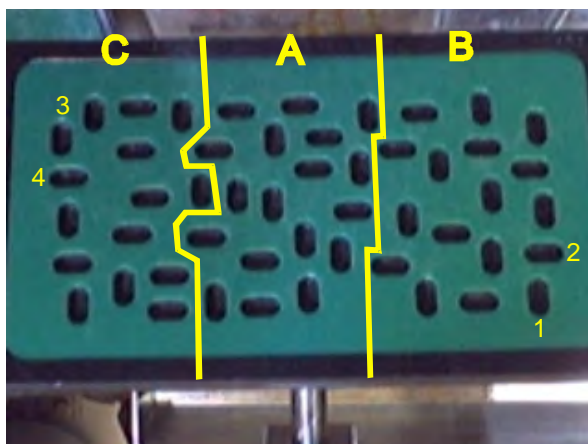
1 = position 1 vertical
2 = position 2 horizontal
3 = position 3 vertical
4 = position 4 horizontal

Figure 2.9   The modified Brinkman board zones A, B and C. Slots 1, 2, 3 and 4 used for assessment of retrieval time. See text above for description.

2.4.1.4 Grip types

The routine analysis procedures of the Modified Brinkman board described above already quantify various aspects of the manual dexterity of the macaque monkey. Nevertheless, it is limited to detect more subtle deficits or changes in manual dexterity. This is especially the case if the deficit induced by the cortical lesion was rather weak. In order to overcome this limitation, an additional analysis of precision and power grip was performed as it was recently proposed by Spinozzi et al. (2004) for tufted capuchine monkeys (*Cebus paella*). The basic idea of this approach is to distinguish not only between precision grip, power grip and deficit to dislodge the pellets, but to go further and differentiate between 4 different types of grips. To assess the different grips used by the monkey at different pre- and post-lesion phases, the analysis was limited to 40 sessions (20 pre-lesion and 20 post-lesion). The grip type, the frequency of each grip type used were noted and then analyzed. The same was done for the success rate of each grip type, in other words, whether the pellet was retrieved and brought to the mouth or not.

2.4.2 Hidden Brinkman board

In order to analyze the recorded video data, the following guidelines had to be respected. The timer was started at the moment the monkey grasped the first pellet from the first slot and held the reward in its hand (t = 0). This means that for the first emptied slot, the searching phase for moving from one slot to the other was not considered. For the following 19 slots, searching time was included. In that manner the timing was continued for the whole board until the monkey had picked out all pellets (n=19) or given up working (0< n >19) because of loss of motivation. Doing so, one got the sequence of the slots visited and the total time spent by the monkey to complete the task. If the total time was divided by the total number of slots emptied <u>minus one</u> in one session, it gave the average time to successfully retrieve a reward. We also established how many horizontal and vertical pellets were taken during one given session. As in the other tests, displacing a pellet to another slot, making it jumping out of it or just not taking the reward were considered as errors.

2.4.3 ICMS mapping

ICMS data collected from left hand representation in M1 were represented in two different types of maps: Standard (surface) ICMS map and unfolded ICMS map. The standard ICMS maps are well described in previous studies from our laboratory (Rouiller et al., 1998a; Liu and Rouiller, 1999; Schmidlin et al, 2004, 2005). Briefly, on the standard ICMS maps, the representation of the

different parts of the forelimb take in account only the lowest ICMS threshold for each electrode penetration that elicited a movement of a particular joint as well as the depth at which the movement was observed. This site of the lowest intensity of stimulation is projected on the surface of the motor cortex in the form of circle. This representation does not reflect the exact position of the most sensitive site, especially when the ICMS tracts were located in the rostral bank of the central sulcus. The threshold current intensity of the stimulus used to elicit the movement was also indicated by the size of the circle. In fact, the larger the size, the lower the intensity of the stimulation.

Basically unfolded ICMS maps were made as described in Park et al. (2001) and in Sato and Tanji (1989). All ICMS responses elicited were represented on this type of map without indication of the stimulus intensity. The responses of each tract lying at different depths on the z axis (horizontal vertical axis) were projected into the x (rostral-caudal) - y (medial-lateral) plane. The response with the lowest threshold (supposed to lie in layer V) was placed at the x - y position of the corresponding tract. Responses lying more vertical were placed caudal and those lying more horizontal were placed rostral to this reference point. Doing so the motor cortex appeared as unfolded and one could assess the responses found close and over the central sulcus either lying medial or lateral to the fundus. This type of map was used to better define the sub-areas of M1 and PM (face, finger, wrist, elbow, shoulder, and foot). The Box 2.1 below provides detail about how unfolded maps were made.

Box 2.1:

The corticospinal neurons are located in cortical layer V of the motor cortex. A two-dimensional representation of cortical layer V in the anterior bank of the central sulcus required flattening and unfolding its curvature. First, all electrode tracks were grouped according to their M-L coordinate and within each group, the tracks were then ordered according to their A-P coordinate. On the basis of the pictures taken during chamber implant showing the position of the central sulcus and on electrophysiological data, a parasagittal diagram can be constructed to represent the cortex that was stimulated (Fig. 2.10). White matter was identified by a significant increase of the intensity of stimulation or by absence of response. For the sensory cortex the limit is identified in the convexity of the cortex by no response to stimulation and in the bank of the central sulcus by a significant increase of the intensity of stimulation or absence of response. For each electrode track, sites corresponding to cortical layer V were identified by the lower intensity used to produce a movement. The tracks made on the convexity of the gyrus the electrode penetrated cortical layers perpendicularly and in these cases layer V was relatively easy to identify by the lowest intensity used to produce a movement. For tracks made on the precentral gyrus and traversing approximately parallel to the cortical layers, it was more difficult to identify layer V. In these cases, the effects obtained from stimulation sites from different tracks at the same A-P axis were compared. Selections of stimulation sites the most closely to layer V were based on the lowest intensity used to produce a movement. This analysis yielded a series of reconstructed parasagittal cortical sections oriented along the A-P axis of the chamber in the plane of the tracks (Fig. 2.10).

The layer V was represented by a line in the horizontal plane on the convexity of the M1 and by vertical line on the gyrus, similar to those used by Park et al. (2000) and, Sato and Tanji (1989) (Fig. 2.10). The intersection of these lines, marked with an asterisk in Fig. 2.11, defined the convexity of the precentral gyrus. Stimualtion effects from sites corresponding to cortical layer V were projected onto these lines (Fig. 2.11). Then, layer V was unfolded by rotating the reference vertical line with respect to the convexity of the gyrus (Fig. 2.10). The resulting unfolded reference line then gave rise to the coordinates for each stimulation site on the two-dimensional map (Fig. 2.11).

Parasagittal Section
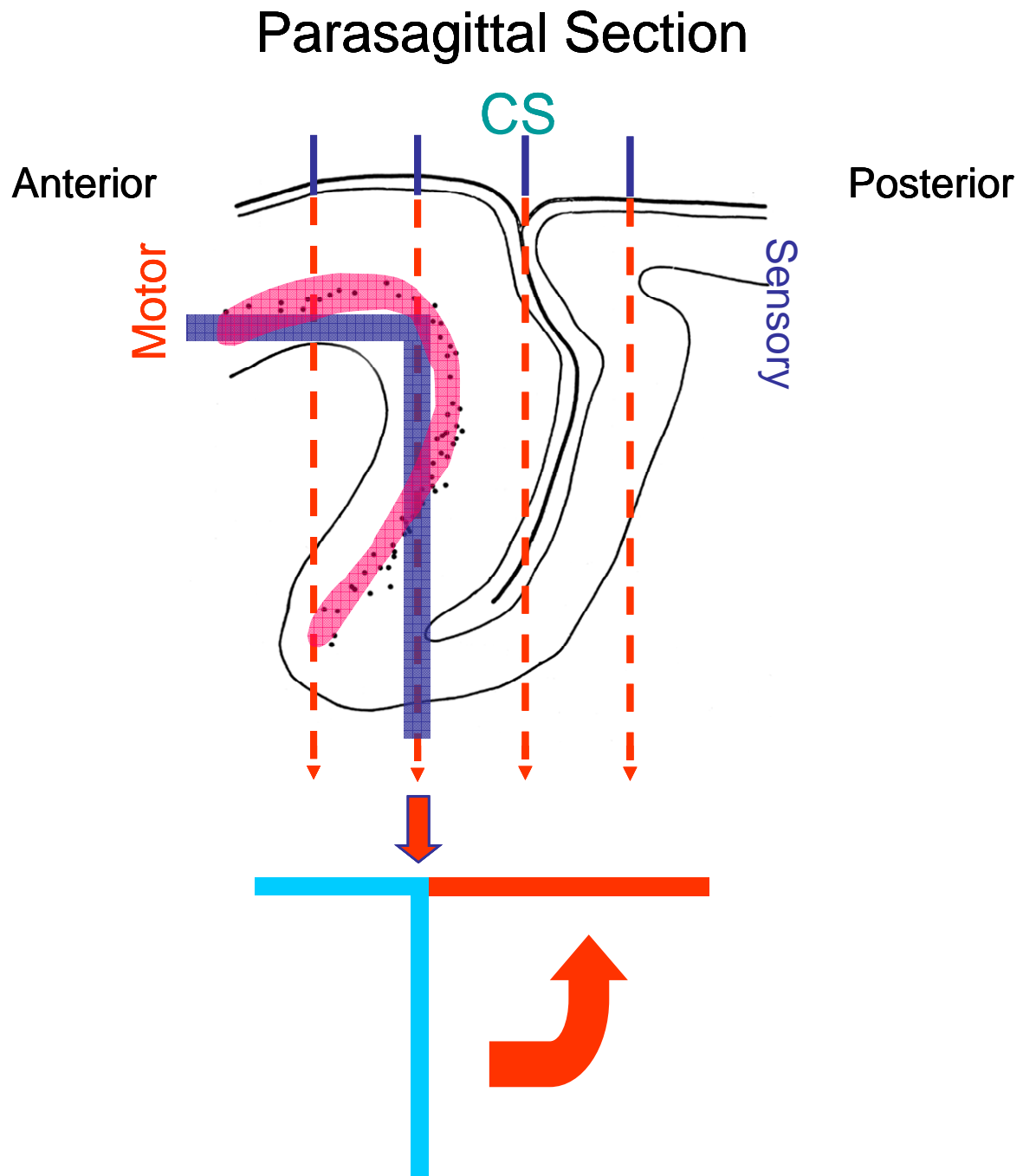
Figure 2.10

Schema of representative para-sagittal section explaining how the unfolded maps were constructed
     subsequently.
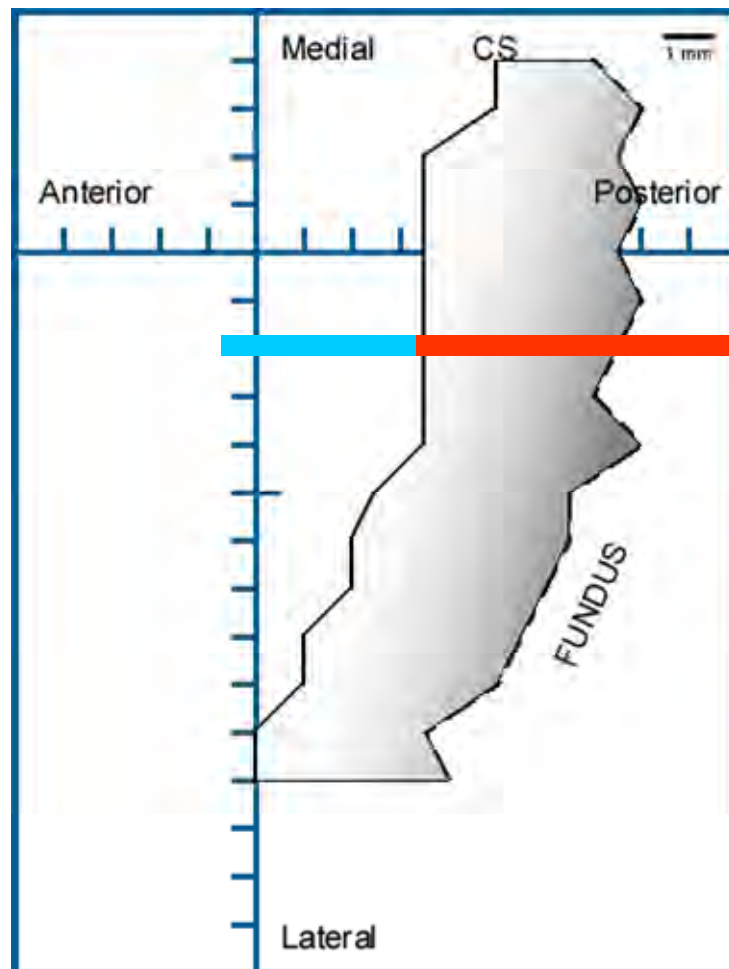
Figure 2.11   Ideal unfolded map as constructed from data recorded ICMS.

For all monkeys, a virtual x (rostral caudal axis) – y (medial lateral axis) coordinate system was projected on the surface of the motor cortex of the respectively hemisphere explored by ICMS. The resulting grid from that had intervals of 1mm x 1mm except for monkey MK2-L in which the intervals in the grid were 2mm x 2mm. With the help of this grid, all tracts explored by ICMS could be clearly positioned on the brain surface. In a first approach, with respect to the position, the intensity and the depth at which a threshold movement was found in each tract, the tracts were classified as belonging to M1, S1, PMv or PMd area. In a second step, using histological data of the brain, reconstruction of the trials was re-evaluated, the arcuate sulcus (AS) and the central sulcus (CS) were added on each map and subsequent corrections of the maps were made.

Comparison of the pre- and post-lesion forelimb maps of each monkey were made. The three anti-Nogo-A treated monkeys (MK2-L,MK3-V and MK4-S) were compared to the maps of the two untreated control animals (MK1-G and MK5-R). Post lesion maps were especially analyzed for changes in the hand representation area of M1 and PMd.

Additional ICMS data from two M1 lesioned (and untreated) monkeys taken from a previous study (Liu and Rouiller 1999) were added to give more statistical power by increasing the number of control animals investigated.

2.5 Cortical lesions in the hand representation in M1

2.5.1 Characteristics of ibotenic acid

The experimental lesion of the motor cortex, restricted to the hand area of M1 unilaterally, was performed by multiple injections of ibotenic acid, as previously reported (Liu and Rouiller, 1999). Ibotenic acid is an agonist of glutamate, the most frequent released excitatory transmitters by synapses in the mammalian brain. Ibotenic acid exerts its neurotoxic effect primarily through excessive activation of ionotropic NMDA receptors leading to a lethal over-excitation of the corresponding neurons. There is also more and more evidence that glutamate, respectively ibotenic acid, can generate oxidative stress culminating in neuronal cell death. It seems that these two actions could act in a sequential as well as a reinforcing manner in order to induce selective neuronal degeneration. As glutamate in excess, ibotenic acid is a potent and rapidly acting neurotoxin if applied continuously in low concentrations or briefly in larger amounts. Under physiological conditions, glutamate is rapidly cleared from the synaptic cleft by high affinity transport systems and a slow diffusion into the neighboring glial cells in order to maintain very low extracellular concentrations. The clearance or reuptake of glutamate is only affected indirectly by the administration of ibotenic acid but the shortly acting high concentration of ibotenic acid is enough to cause cell damage (see below). As a consequence, ibotenic acid causes postsynaptic neuronal cell damage in the tissue surrounding the injection site, as glutamate would do under pathological conditions. Studies in tissue cultures revealed two forms of neuronal degeneration mediated by glutamate receptors, an acute form and a delayed one. NMDA receptors, after a brief exposure to high concentrations of glutamate agonists such as ibotenic acid, open $Ca2^+$ permeable ion channels. This opening leads to an excessive intraneuronal $Ca2^+$ concentration, representing the starting point of a number of different pathways causing oxidative stress followed by neuronal death. An important pathway activates phospholipase A2 which mediates a subsequent release of amino acids leading to the generation of oxygen radicals. Amino acids and oxygen radicals

enhance the release of glutamate and inhibit its uptake, thus promoting a vicious circle. Reactive oxygen species are also yielded by $Ca2^+$ induced catabolism of purine bases such as xanthine and by the Fenton reaction which is favored by ATP depletion caused by ibotenic acid and the associated increase of intracellular lactic acid. Last but not least, in certain neurons, the NO synthetase is activated and can additionally cause degeneration of surrounding neurons. In the case of ibotenic acid this spread of degeneration is restricted to a very small area around the injection sites as it was shown by Schwartz and collaborators (1979). The present lesion technique generates a clearly circumscribed damage at the injection site. Another advantage of ibotenic acid compared to other neurotoxic agents is its selective toxicity for nerve cells in the injected area while axons of passage and nerve terminals of extrinsic origin do not seem to degenerate. A third advantage of ibotenic acid is the rapid degradation into muscimol after intracerebral injection which may lead to minimal general toxicity.

GLUTAMAT   IBOTENIC ACID
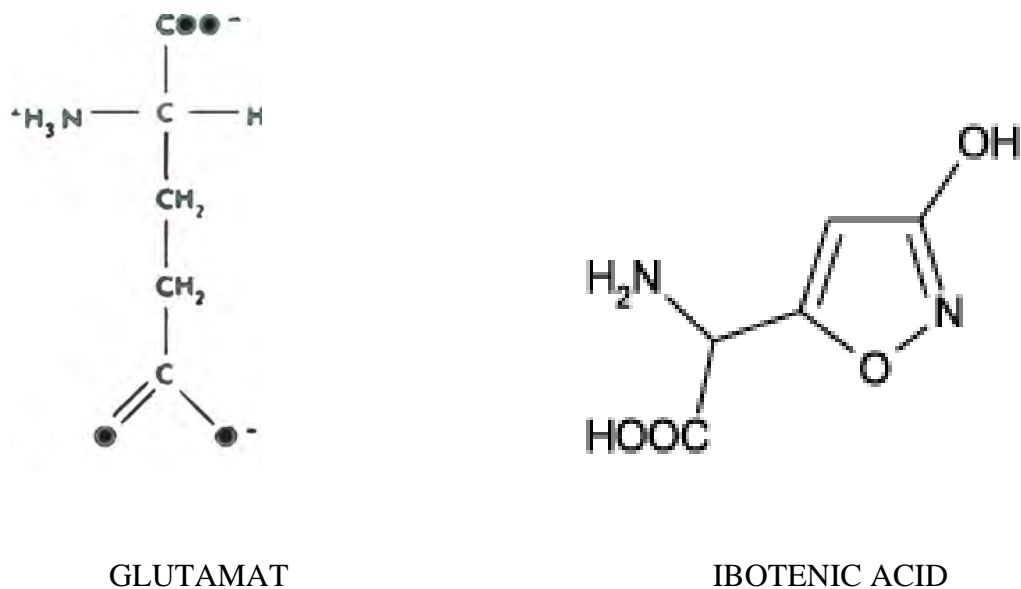
Figure 2.12   Comparison of the chemical structure of glutamate and ibotenic acid.

2.5.2 Cortical lesion

After having completed the pre-lesion mapping of the forelimb area in M1 of either both hemispheres (MK2-L and MK1-G) or of the left hemisphere (the other 3 monkeys) by ICMS, the resulting maps were used to determine the sites of ibotenic acid injections. In each monkey the lesion was made in the hand representation area of M1 of the left hemisphere. Injection sites were selected considering the type of elicited movements at each site in ICMS sessions, the stimulation intensity needed to induce a movement and site to site distances in order to cover the hand

representation area with a limited number of injections. A volume of 1µl (MK1-G, MK3-V, MK4-S, and MK5-R) or 1.5µl (MK2-L) ibotenic acid solution (10 µg/µl in phosphate-buffered saline; see Newsome et al. 1985a, 1985b; Merigan et al. 1993; Newsome and Paré 1988; Liu and Rouiller 1999) was injected at each site. The total volume of ibotenic injected in each monkey ranged from 13 µl to 16 µl (Table 3.1, page 208). The total volume of the injection depended on the extent of the hand representation in M1. Ibotenic acid is expected to diffuse approximately 1.5 mm around the center of the injection site. We anticipated that such diffusion distance would cover the target area. Depending on the surface of the hand representation, 4 to 6 syringe penetrations were made. The sites where ibotenic acid was injected corresponded to the ICMS sites that produced fingers movement. The distance between injection sites was between 1.5 to 3 mm.

During the injections of ibotenic acid, the monkeys were awake and quietly sitting in the primate chair as during a standard ICMS session. The XY positioning system was attached to the chronic implanted chamber. The tungsten microelectrode used in ICMS sessions was replaced by a 10 µl Hamilton syringe. In order to guarantee a perpendicular penetration into the cortex, the needle was secured by a guiding tube. Once the Hamilton syringe was precisely positioned at the aimed location at the surface of the dura, it was then slowly advanced into the cerebral cortex until the tip reached the deepest site in the corresponding tract, where the first injection would be made. A volume of 1 µl or 1.5 µl ibotenic acid solution was slowly injected at each site. Then the needle was left in place for at least 1 minute, just the time for the ibotenic acid to diffuse in the adjacent tissue.

While injecting the ibotenic acid at multiple sites, a progressive motor deficit of the contralateral hand in the form of flaccid paralysis was observed. Afterwards, monkeys were brought back to the animal room and videotaped regularly in the subsiding hours. This was done, to exclude or confirm possible effects of ibotenic acid on other regions of M1 than the region originally chosen, and in order to document the deficits during the first hours after the lesion.

2.6 Reversible inactivation of restricted cortical areas with muscimol

Following the lesion, several months of behavioral assessment took place in order to quantify the post-lesion deficits and to evaluate the extent and time course of recovery. When the recovery reached a plateau, ICMS sessions took place to establish the post-lesion map in the cerebral cortex in and around the lesion. Finally, to tentatively infer which cortical areas are contributing to the

recovery, reversible inactivation experiments were conducted using the GABA agonist, muscimol (see Kermadi et al., 1997).

2.6.1 Characteristics of muscimol
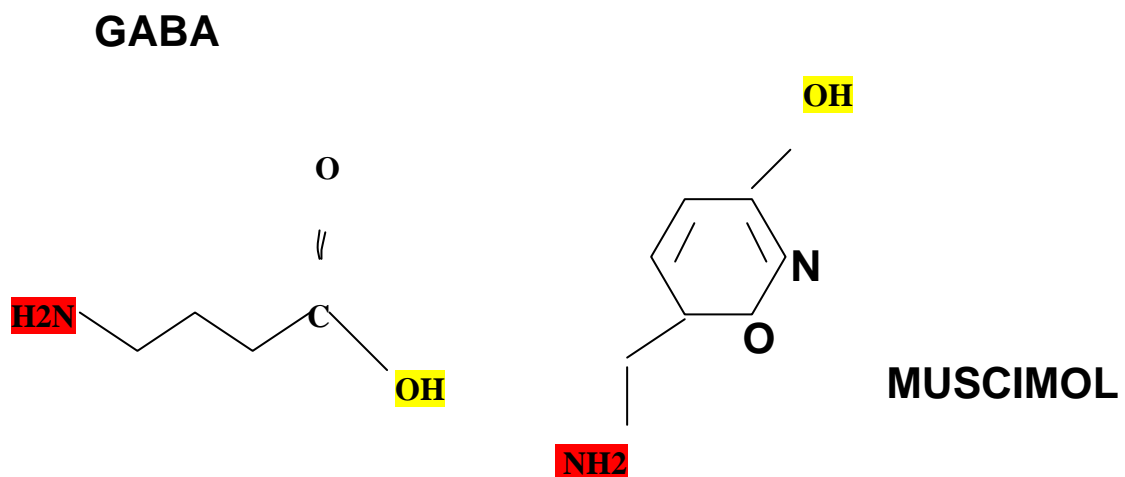
GABA

MUSCIMOL

Figure 2.13   Similar chemical structure of GABA and Muscimol. Note: the red and yellow marked functional groups are identical in both molecules

As indicated in Figure 2.13, Muscimol and GABA have two functional groups in common, namely the red marked NH2 group and the yellow marked OH group. Due to this similarity, Muscimol is able to mimic the inhibitory action of the neurotransmitter GABA in the central nervous system.

There are three subtypes of GABAergic receptors: GABA-**A**, GABA-**B** and GABA-**C**. Muscimol is acting only on two of them, namely on GABA-**A** as an agonist and on GABA-**C** as a partial agonist. In contrast, the GABA-**B** receptor is not influenced by muscimol. GABA-A as well as GABA-C are part of the ionotropic receptor group. These ionotropic receptors consist of five subunits, which form ion channels traversing postsynaptic membranes of neurons. The ion

channels are specific for Cl⁻ ions. Opening these channels leads to Cl⁻ ions influx and fast synaptic inhibition. Because Cl⁻ ions are charged negatively, the neuron is hyperpolarized with the consequence that it can no longer be excited. If the amount of muscimol injected in a cortical region is high enough, this leads to a general hyperpolarisation of many neurons around the injection site. Injections of muscimol in M1 induced after about twenty minutes a temporally limited paralysis of the corresponding muscles on the opposite side of the muscimol injected hemisphere. This paralysis lasted for two to four hours with the strongest effect occurring within the first hour, depending on the monkey's metabolic capacities to eliminate muscimol via the urine.

2.6.2 Experimental procedure of reversible motor cortex inactivation

Transient cortical inactivations using muscimol were only performed post-lesion when behavioral scores of the Modified Brinkman tests had reached the plateau phase, meaning that during the post-lesion period the monkey's behavioral score in the Modified Brinkman board tests reached a saturating value and for several days without further significant improvement. The aim of these muscimol injections was to assess indirectly the role of other premotor areas (e.g. PMd and PMv) in the recovery of hand dexterity. A muscimol injection was also made in the lesion territory. In addition to that, muscimol infusion in the core of the lesion of control animals served to prove that the damaged part of M1 was no longer functional (no loss of regained manual dexterity). The hydraulic manipulator system used to infuse muscimol was basically the same as described for ibotenic acid injections and ICMS sessions. The muscimol solution (1µg in 1µl saline) volume injected at each site was 1.5µl to 2.0µl. As shown in the rat brain study (Martin 1991), the administration of muscimol in such volumes and concentrations leads to a spread along a radius of 1 – 1.5 mm. Based on these data, the distance between individual sites of muscimol injection and syringe penetrations was between 1.5 to 2.5 mm. As for the ibotenic acid injections, the individual injection sites were placed at depths where hand movements have been elicited with ICMS after the recovery phase. Moreover, the aimed territory was confirmed by ICMS recording one day before the muscimol injections or the same day. The total volume of muscimol infused per session varied between 9µl and 20µl, depending on the dimension of the cortical hand representation post-lesion, which was variable from one monkey to the other. The course of a typical inactivation session started with the monkey performing the Modified Brinkman board test with the left and right hands; then, muscimol injections were performed at multiple selected sites. Afterwards, the behavioral performances of the monkey's left and right hands were tested 10 min and/or 20 min after the final injection of muscimol in order to describe the effects of inhibiting the

corresponding cortical territory. All behavioral sessions were videotaped, as well as the monkey's behavior while moving freely in the animal room, during 4 hours following the injections of muscimol.

2.7 Histology

Once the monkey recovered and ICMS mapping of contralesional motor cortex was completed, the anterograde tracer (BDA, Molecular Probe®, 10% in saline) was injected in the reorganized hand representation to tentatively evaluate new projections. The sites of injection were determined by the strongest effects on the hand obtained by post-lesion ICMS. After approximately 2 weeks the monkey was first anesthetized with an i.m. ketamine injection, whereas sacrifice of the animal resulted from a lethal dose of pentobarbital (90 mg/kg) injected i.p. The animal was then transcardially perfused, first with saline (300 ml) followed by 3 L g paraformaldehyde and at the end by sucrose solutions. The brain was dissected and stored in a sucrose solution (30%) for few days. The tissue was then cut in the frontal plane at a thickness of 50μm. Five series of sections were collected, one treated immunocytochemically (SMI-32 antibody) and a second series was Nissl-stained. The protocols for histological processing have been described in detail earlier (e.g. Boussaoud et al., 2005; Freund et al., 2007; Liu et al., 2002; Morel et al., 2005; Rouiller et al., 1996, 1998a,b, 1999; Wannier et al., 2005). Using Neurolucida, we reconstructed the lesion site. These reconstruction procedures are described in detail in recent publications (Freund et al., 2006; 2007; Wannier et al., 2005).

2.8 Bibliography for Methods

Asanuma H, Arnold A, Zarzecki p. 1976. Further study on the excitation of pyramidal tract cells by intracortical microstimulation. Exp Brain Res 26:443-461.

Boussaoud D, Tanné-Gariépy J, Wannier T, Rouiller EM. 2005. Callosal connections of dorsal versus ventral premotor areas in the macaque monkey: a multiple retrograde tracing study. BMC Neuroscience 6:67.

Brinkman J, Kuypers HGJM. 1973. Cerebral control of contralateral and ipsilateral arm, hand and finger movements in the split-brain rhesus monkey. Brain 96:653-674.

Freund P, Schmidlin E, Wannier T, Bloch J, Mir A, Schwab ME, Rouiller EM. 2006. Nogo-A-specific antibody treatment enhances sprouting and functional recovery after cervical lesion in adult primates. Nature Med 12:790-792.

Freund P, Wannier T, Schmidlin E, Bloch J, Mir A, Schwab ME, Rouiller EM. 2007. Anti-Nogo-A antibody treatment enhances sprouting of corticospinal axons rostral to a unilateral cervical spinal cord lesion in adult macaque monkey. J Comp Neurol 502:644-659.

Kermadi I, Liu Y, Tempini A, Rouiller EM. 1997. Effects of reversible inactivation of the supplementary motor area (SMA) on unimanual grasp and bimanual pull and grasp performance in monkeys. Somatosens Mot Res 14:268-280.

Liu J, Morel A, Wannier T, Rouiller EM. 2002. Origins of callosal projections to the supplementary motor area (SMA): A direct comparison between pre-SMA and SMA-proper in macaque monkeys. J Comp Neurol 443:71-85.

Liu Y, Rouiller EM. 1999. Mechanisms of recovery of dexterity following unilateral lesion of the sensorimotor cortex in adult monkeys. Exp Brain Res 128:149-159.

Martin JH. 1991. Autoradiographic estimation of the extent of reversible inactivation produced by microinjection of lidocaine and muscimol in the rat. Neurosci Lett 127:160-164.

Merigan WH, Maunsell JHR. 1993. How parallel are the primate visual pathways? Annu Rev Neurosci 16:369-402.

Morel A, Liu J, Wannier T, Jeanmonod D, Rouiller EM. 2005. Divergence and convergence of thalamocortical projections to premotor and supplementary motor cortex: a multiple tracing study in the macaque monkey. Eur J Neurosci 21:1007-1029.

Newsome WT, Wurtz RH, Dursteler MR, Mikami A. 1985. Deficits in visual motion processing following ibotenic acid lesions of the middle temporal visual area of the macaque monkey. J Neurosci 5:825-840.

Newsome WT, Wurtz RH, Dursteler MR, Mikami A. 1985. Punctate chemical lesions of striate cortex in the macaque monkey: effect on visually guided saccades. Exp Brain Res 58:392-399.

Newsome WT, Paré EB. 1988. A selective impairment of motion perception following lesions of the middle temporal visual area (MT). J Neurosci 8:2201-2211.

Park MC, Belhaj-Saïf A, Gordon M, Cheney PD. 2001. Consistent features in the forelimb representation of primary motor cortex in rhesus macaques. J Neurosci 21:2784-2792.

Rouiller EM, Moret V, Tanné J, Boussaoud D. 1996. Evidence for direct connections between the hand region of the supplementary motor area and cervical motoneurons in the macaque monkey. Eur J Neurosci 8:1055-1059.

Rouiller EM, Yu XH, Moret V, Tempini A, Wiesendanger M, Liang F. 1998a. Dexterity in adult monkeys following early lesion of the motor cortical hand area: the role of cortex adjacent to the lesion. Eur J Neurosci 10:729-740.

Rouiller EM, Tanné J, Moret V, Kermadi I, Boussaoud D, Welker E. 1998b. Dual morphology and topography of the corticothalamic terminals originating from the primary, supplementary motor, and dorsal premotor cortical areas in macaque monkeys. J Comp Neurol 396:169-185.

Rouiller EM, Tanne J, Moret V, Boussaoud D. 1999. Origin of thalamic inputs to the primary, premotor, and supplementary motor cortical areas and to area 46 in macaque monkeys: A multiple retrograde tracing study. J Comp Neurol 409:131-152.

Sato KC, Tanji J. 1989. Digit-muscle responses evoked from multiple intracortical foci in monkey precentral motor cortex. J Neurophysiol 62, no 4:959-970.

Schmidlin E, Wannier T, Bloch J, Rouiller EM. 2004. Progressive plastic changes in the hand representation of the primary motor cortex parallel incomplete recovery from a unilateral section of the corticospinal tract at cervical level in monkeys. Brain Research 1017:172-183.

Schmidlin E, Wannier T, Bloch J, Belhaj-Saïf A, Wyss A, Rouiller EM. 2005. Reduction of the hand representation in the ipsilateral primary motor cortex following unilateral section of the corticospinal tract at cervical level in monkeys. BMC Neuroscience 6:56.

Wannier T, Schmidlin E, Bloch J, Rouiller EM. 2005. A unilateral section of the corticospinal tract at cervical level in primate does not lead to measurable cell loss in motor cortex. Journal of Neurotrauma 22:703-717.

Weinmann O, Schnell L, Ghosh A, Montani L, Wiessner C, Wannier T, Rouiller E, Mir A, Schwab ME. 2006. Intrathecally infused antibodies against Nogo-A penetrate the CNS and downregulate the endogenous neurite growth inhibitor Nogo-A. Mol Cell Neurosci 32:161-173.

Contents of Results

3. Results

_____

3. Results

3.1 Lesion

3.1.1 Lesion reconstruction

For the present thesis work, the lesion extent in the cortex of one hemisphere, induced by infusion of the neurotoxin ibotenic acid in the hand representing area of M1, was analyzed in seven macaque monkeys. For this reconstruction analysis, histological data from two additional control monkeys (monkey MK6-J and monkey MK7-C) of the study of Liu and Rouiller (1999) were represented as well to give to the present data more statistical power. In a first step, series of photomicrographs of frontal sections of 50 μm thickness covering the lesion were taken at intervals of 500 μm along the rostro-caudal axis. Generally, the lesion extend was determined based on analysis of SMI-32 stained histological sections. In some monkeys (monkey MK1-G and monkey MK3-V), because of suboptimal SMI-32 staining, Nissl stained sections were also used to better delimit the lesion borders. Of every tenth section (corresponding to an interval of 500μm), a photomicrograph at 14 fold magnification was taken and subsequently analyzed with Neurolucida© software. For each photomicrograph analyzed, the surface of the lesioned brain tissue was determined. Care was taken to distinguishing different cortical areas damaged as well as to evaluate whether the lesion also touched sub-cortical areas. Total surfaces and the surface of each sub-area touched were calculated using Neuroexplorer© software in all seven animals. Photomicrographs of the SMI-32 sections analyzed of each monkey are represented in Figures 3.2 – 3.8 below.

Figures 3.2 – 3.5 are series of photomicrographs of the lesion site in four control (untreated) animals (monkeys MK1-G, MK6-J, MK7-C and MK5-R), whereas Figures 3.6 – 3.8 represent series of photomicrographs of the lesion site in three anti-Nogo-A treated monkeys (monkey MK2-L, MK3-V and MK4-S). In a second step, the total volume of the lesion and the sub-volumes in the corresponding cortical and subcortical areas were calculated using the Cavalieri method. The calculated values of the lesion surfaces and the lesion volumes are indicated in Table 3.1 below. To better visualize the lesion extent in each monkey, lateral views from the corresponding lesioned hemisphere were redrawn from photographs (lateral views) of the whole brain. On this schematic brain representation, individual sections analyzed were placed in a rostral to caudal manner with respect to scale and anatomical reference points for correct positioning. The total lesion size is indicated by vertical bars each representing the lesion extends on an individual section. Lateral views of the brain for all seven monkeys are represented in Figures 3.9 and 3.10 below.

_____

3.1.2 Photomicrographs of lesion site in SMI-32 material

The Figure 3.1 below is thought as an introductory orientation help for the reader looking at SMI-32 staining of the lesion site of the monkeys used in this thesis work (see Figs. 3.2 – 3.8). Figure 3.1 represents an ideal SMI32 section through the frontal cortex of an intact hemisphere showing the most important cortical areas around the potential lesion site in the hand representing area of M1. Boundaries between M1 and PM cortex were defined by using a combination of staining methods revealing cytochromoxydase (CO), acetylcholinesterase (AChE), calcium binding proteins, some of the $GABA_A$ receptor subunits and neurofilaments in pyramidal neurons (SMI-32). SMI-32 staining is particularly suited to detect the lesion site as it specifically marks pyramidal neurons in layers III and V of the motor cortex. These pyramidal cells are preferentially destroyed by ibotenic acid injections. Therefore a loss of either or both pyramidal layers in SMI-32 staining is a reliable indicator for cortical lesions induced by ibotenic acid injections. Note that the section represented in Figure 3.1 is a parasagittal section whereas the sections represented in Figures 3.2 – 3.8 are transversal sections along the rostro-caudal axis of the brain (thus perpendicularly oriented to the section represented in Figure 3.1).
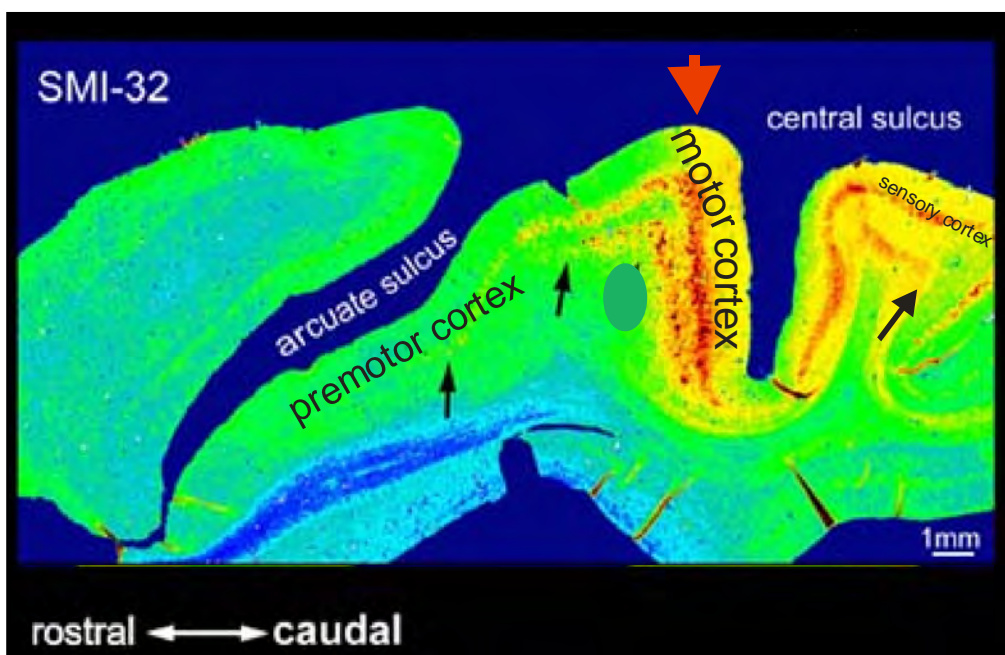
Figure 3.1: Boundaries between the most important motor cortical areas around M1 on an ideal parasagital section in the frontal cortex of a macaque monkey as revealed with different staining techniques.

($\rightarrow$ = boundaries between different cortical areas; red arrow indicates the aimed lesion site in the present study).

(modified from Hepp –Reymond: http://www.ini.unizh.ch/)

173

3.1.2.1 Reconstruction of lesion in Control (untreated) monkeys
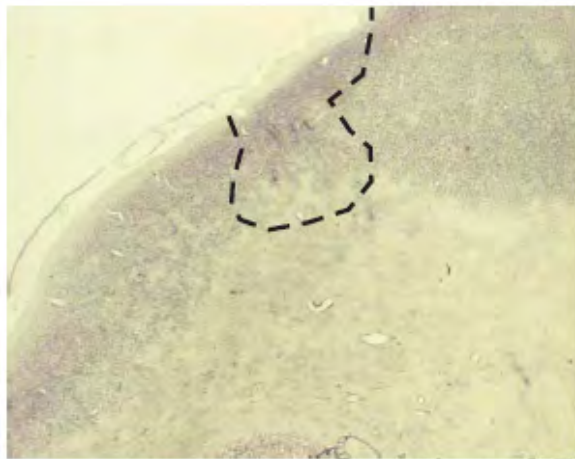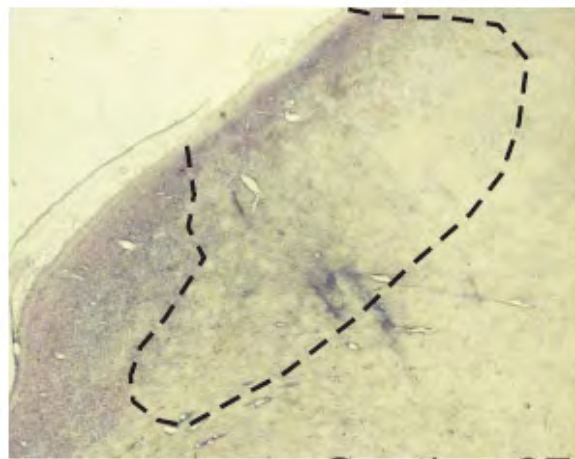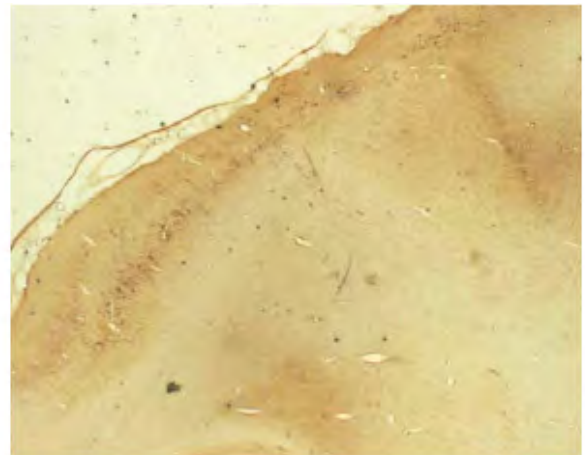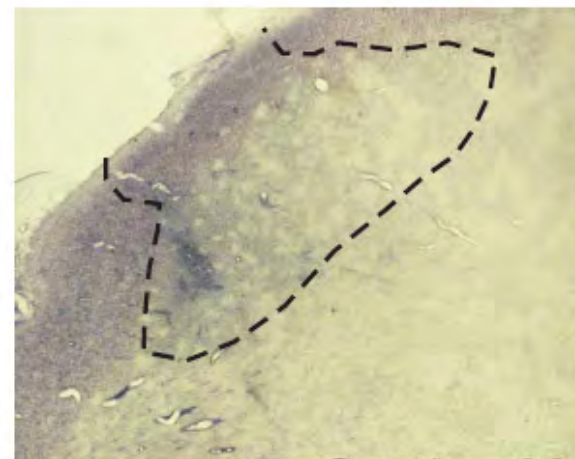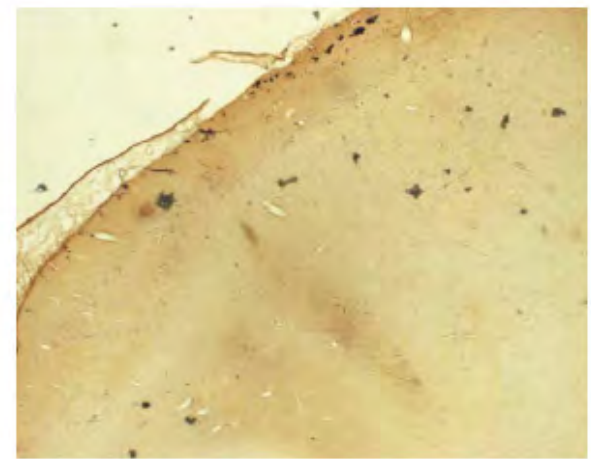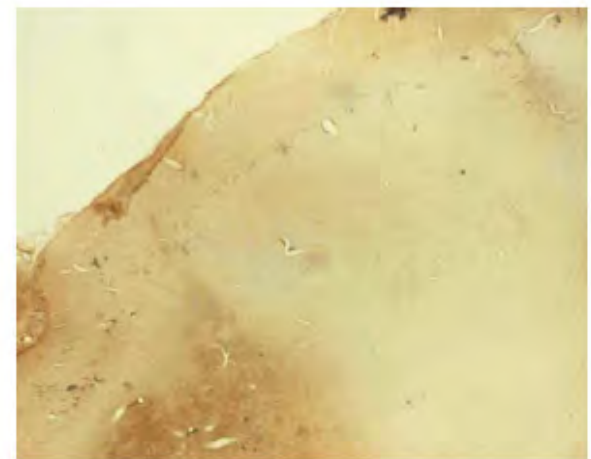
A. <u>Monkey MK1-G</u>

(Figure 3.2 – panel 1 – Monkey MK1-G)

Section 41

Section 43
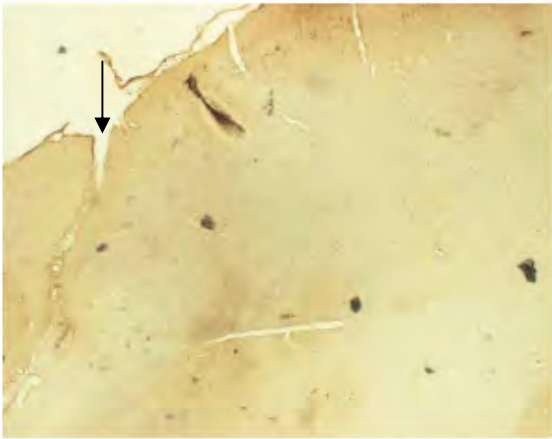
(Figure 3.2 – panel 2 – Monkey MK1-G)
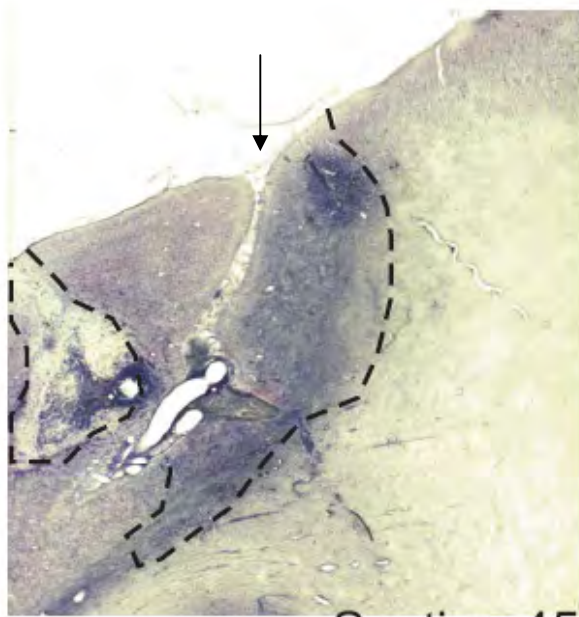
Section 45
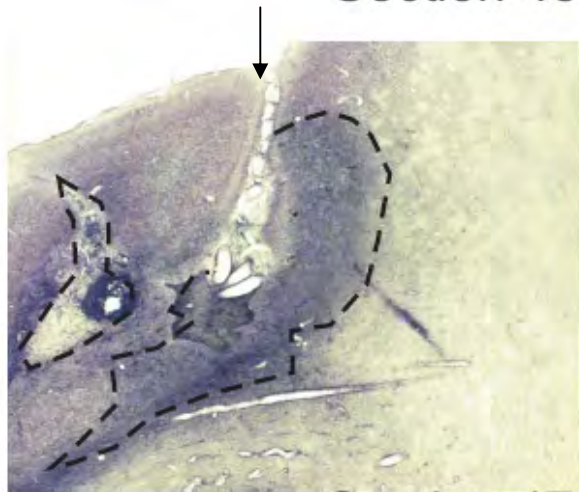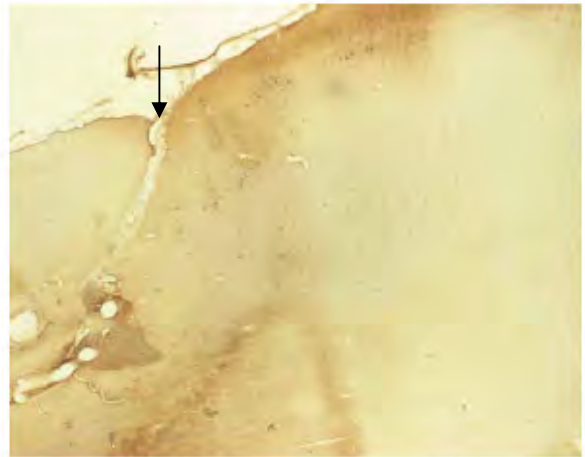
Section 47
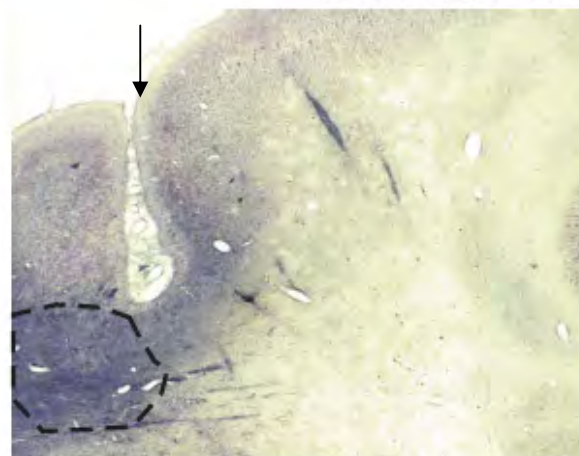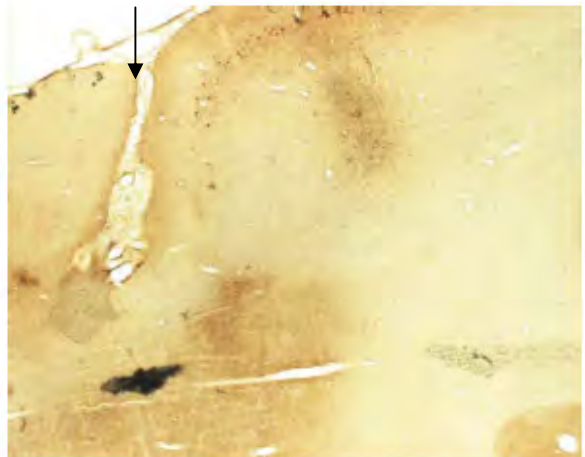
Section 49

No SMI section

(Figure 3.2 – panel 3 – Monkey MK1-G)

Section 51

section 53: no apparent lesion
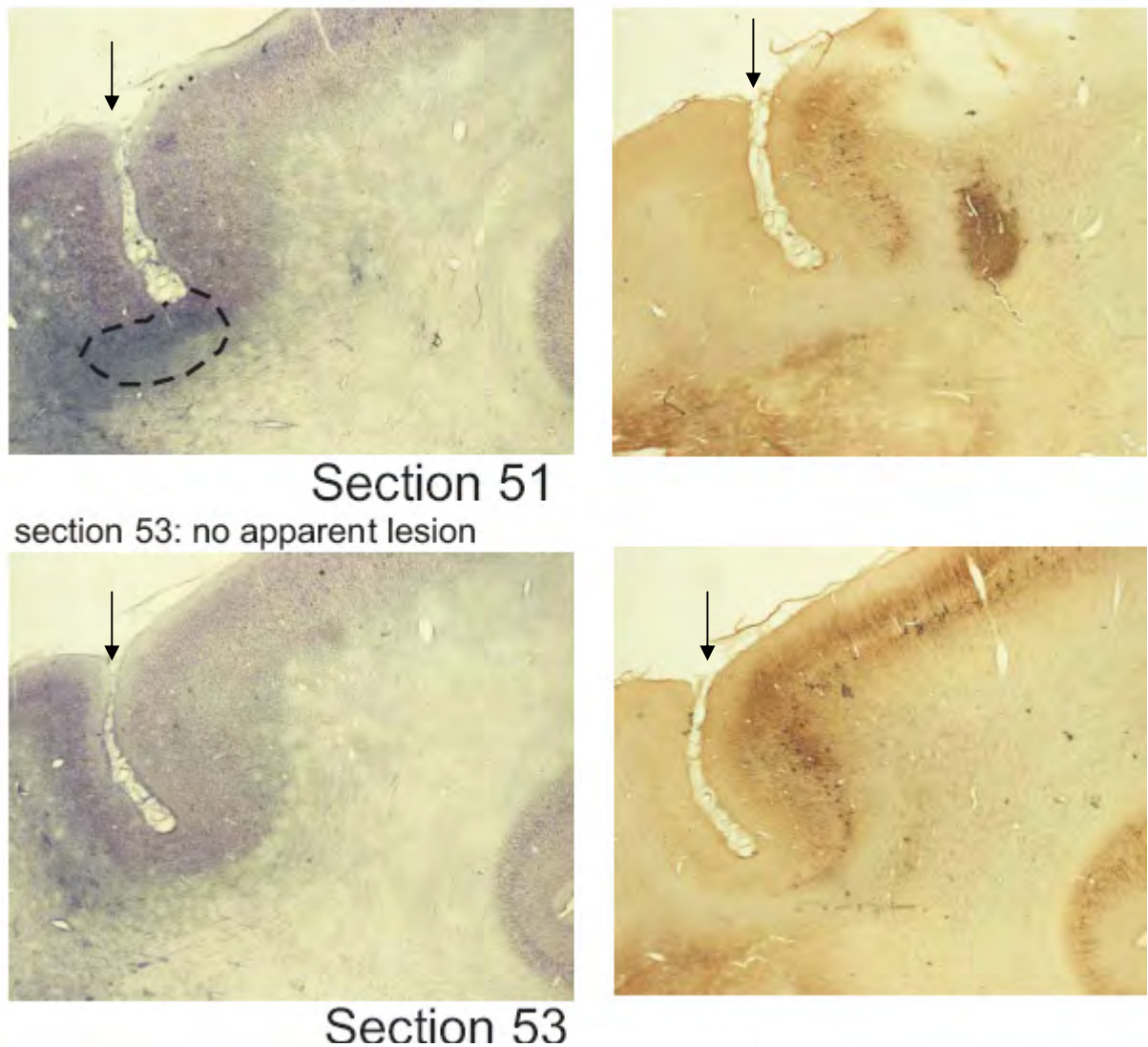
Section 53

(Figure 3.2 – panel 4 – Monkey MK1-G)

5 mm

Figure 3.2: SMI-32 and Nissl staining of frontal brain sections of the left (ipsilesional) hemisphere of monkey MK1-G. At each rostro-caudal level (sections 35-53), a photomicrograph of the Nissl staining is shown on the left, whereas the corresponding photomicrograph of the SMI-32 section is shown on the right. Black vertical arrows indicate the position of the central sulcus (CE), lateral is to the left, dorsal is to the top. M1 is right to the CE and S1 left to the CE. The lesion extent is indicated by dashed black lines.

In Monkey MK1-G, rostrally in the rostral bank of the central sulcus, (sections 35 – 39), only the hand representation of M1 was touched by the lesion (area outlined by a dashed line). More caudal, starting with section 41 up to section 47, in addition to the lesion in M1, the medial part of S1 in the caudal bank of the central sulcus was also affected by the ibotenic acid infusion. The

most caudal part of the lesion is located in S1 (sections 49 and 51). More caudal (sections 53 and higher numbers), no apparent lesion was detected.

In this monkey (MK1-G), because the tissue was in general damaged (perfusion, extensive ICMS?) and SMI32 sections were of poor inhomogeneous quality, Nissl-stained sections were used as well to detect the lesion site, whereas SMI-32 sections of the same rostro-caudal level were only used as a help to better delineate some lesion border. Nevertheless, the quality of SMI-32 sections was sufficient to detect loss of pyramidal neurons in layers III and V of the motor cortex, in comparison to adjacent intact tissue (e.g. sections 51 and 53).

B. <u>Monkey MK5-R</u>

This monkey is still alive (ICMS post-lesion and tracing experiments on-going) and therefore the lesion cannot be reconstructed at that step. After sacrifice of the animal, the corresponding lesion reconstruction will be shown in Figure 3.3.

Figure 3.3: SMI 32 sections in monkey MK5-R. Same conventions as in Figure 3.2. (next 5 pages)

Reconstruction of lesion in M1 (MK5-R)
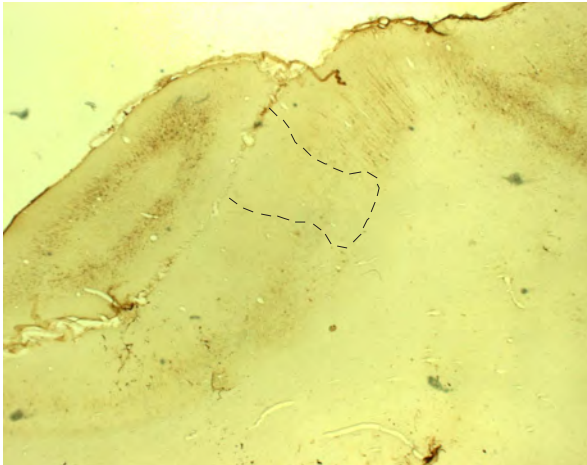
section 48
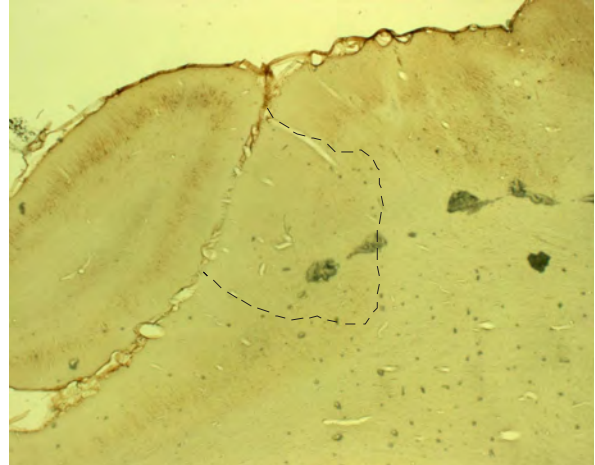
section 50
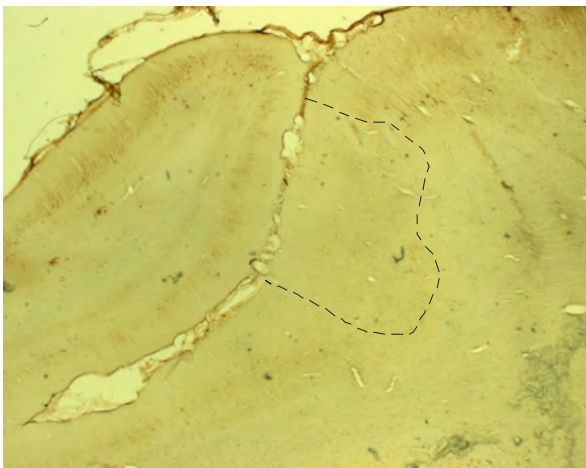
section 52
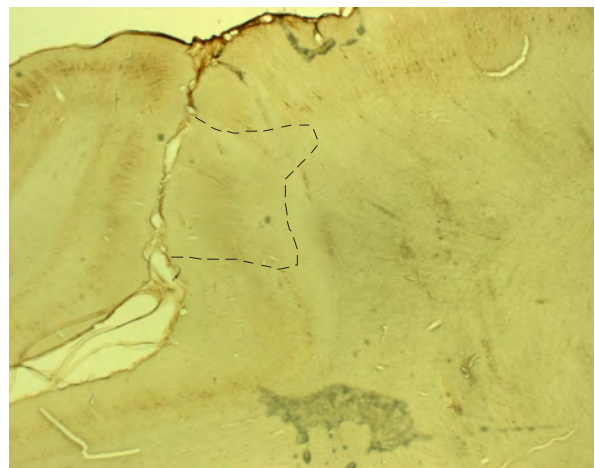
section 54
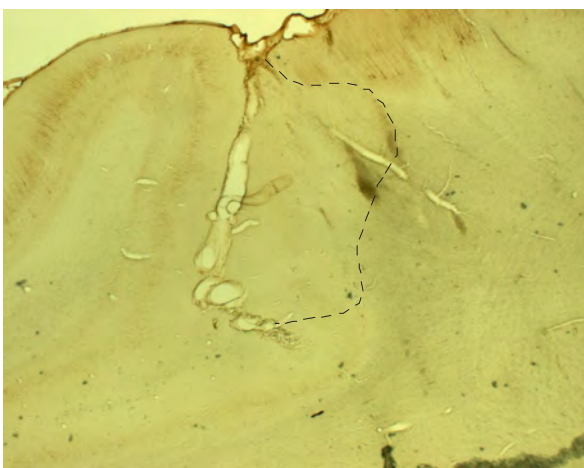
section 56
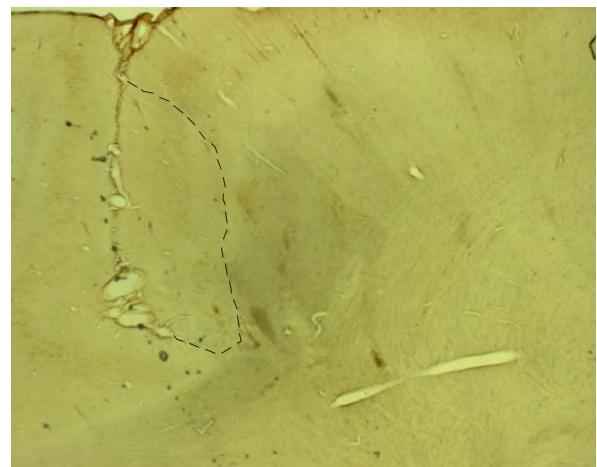
section 58

5 mm

Reconstruction of lesion in M1 (MK5-R) (con't)

CS
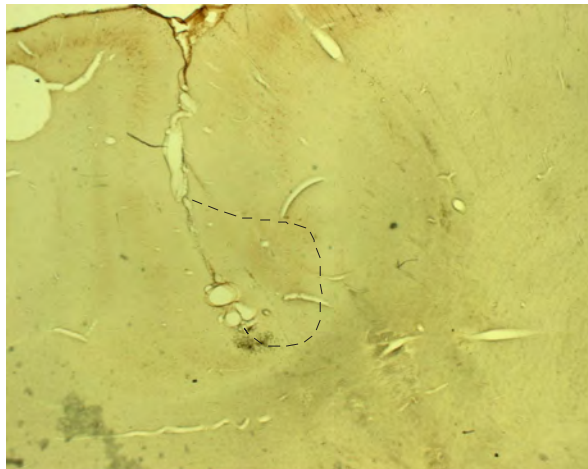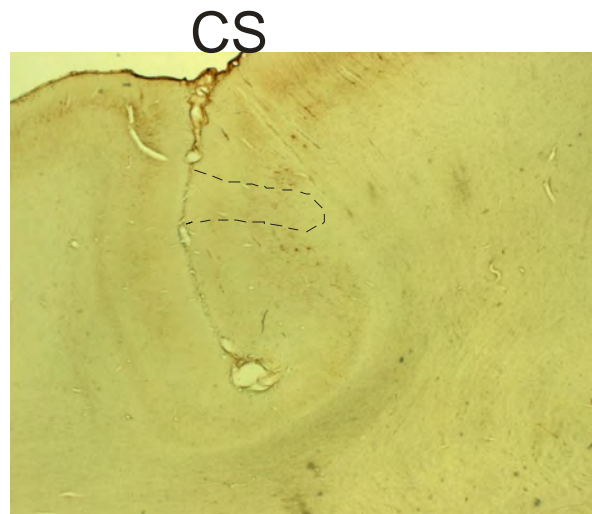
section 60

section 62
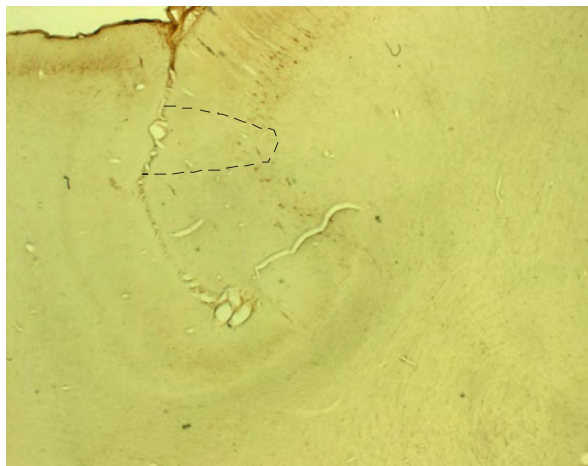
section 64
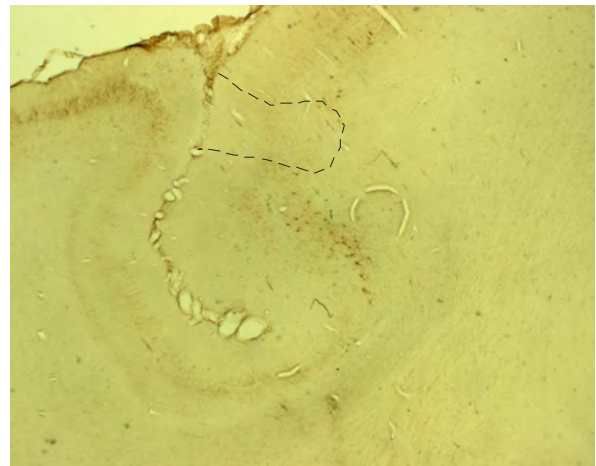
section 66
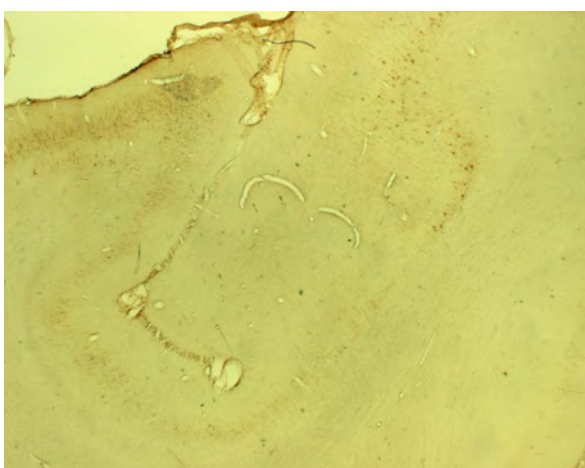
section 68
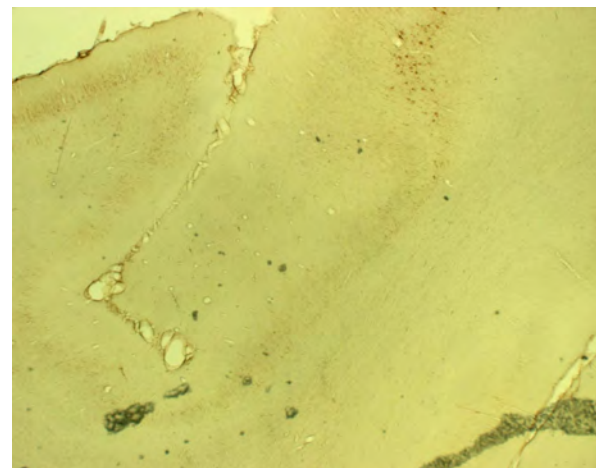
section 70

5 mm
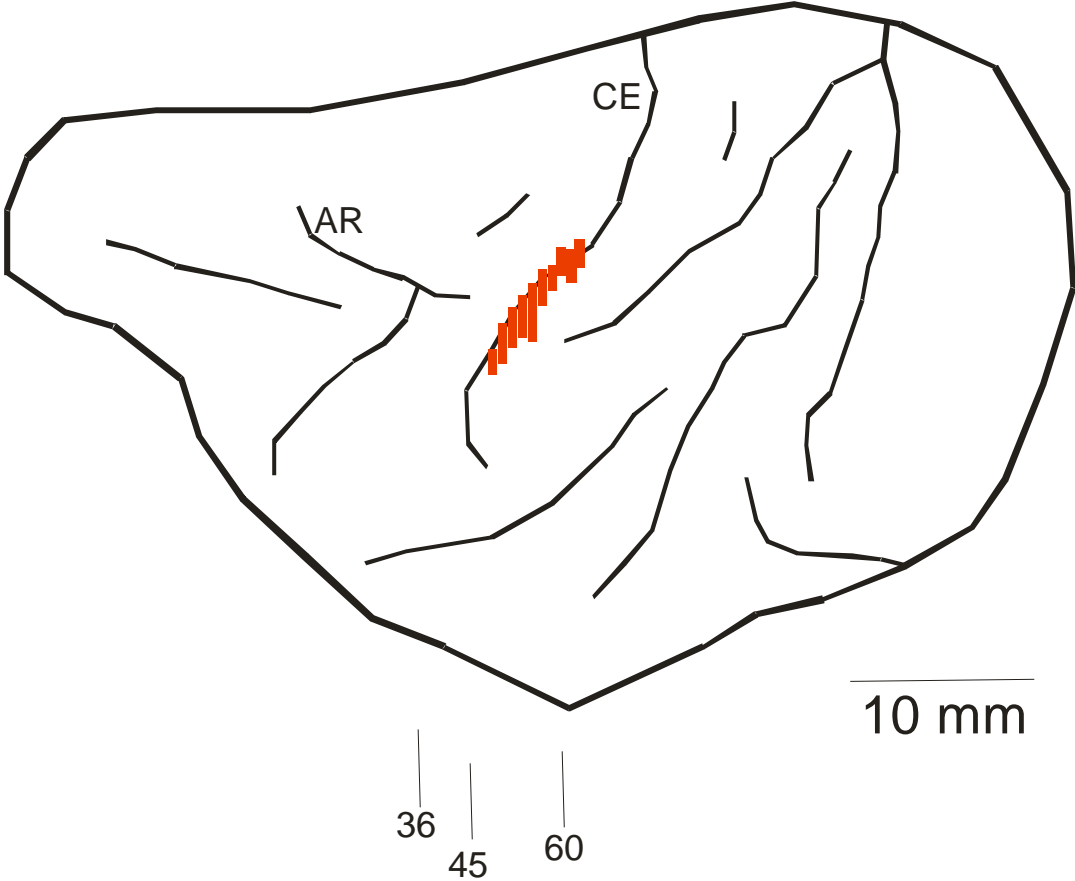
Lateral superficial view of the lesion in MK5-R
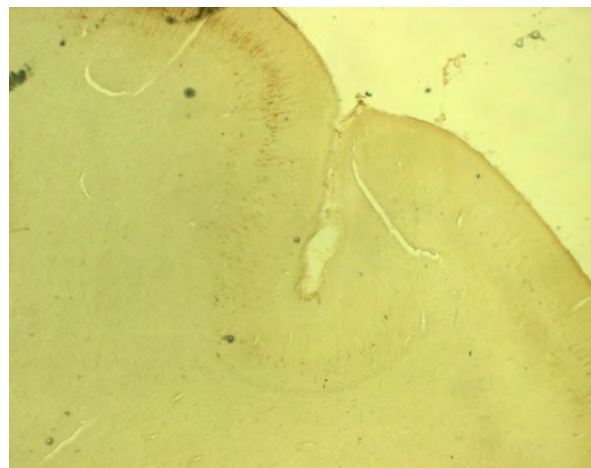
For comparison, intact hemisphere (MK5-R)
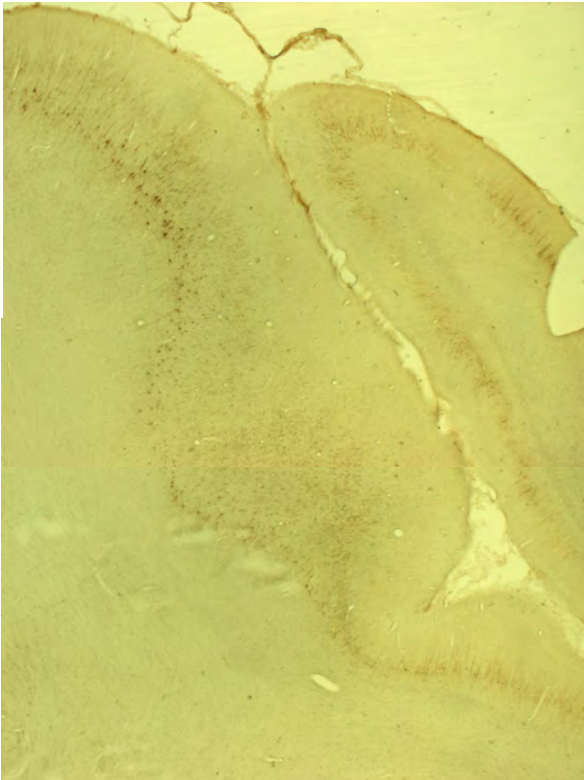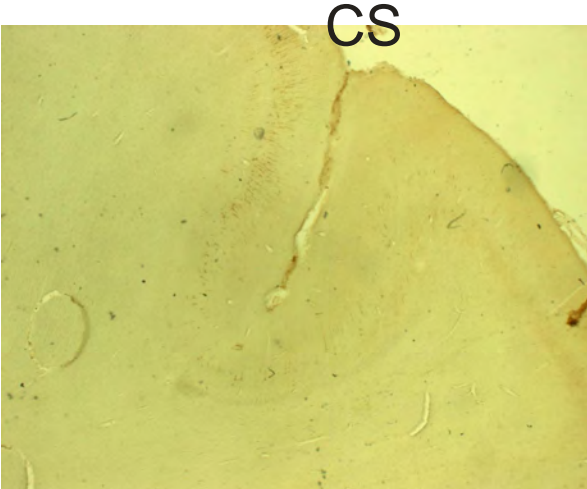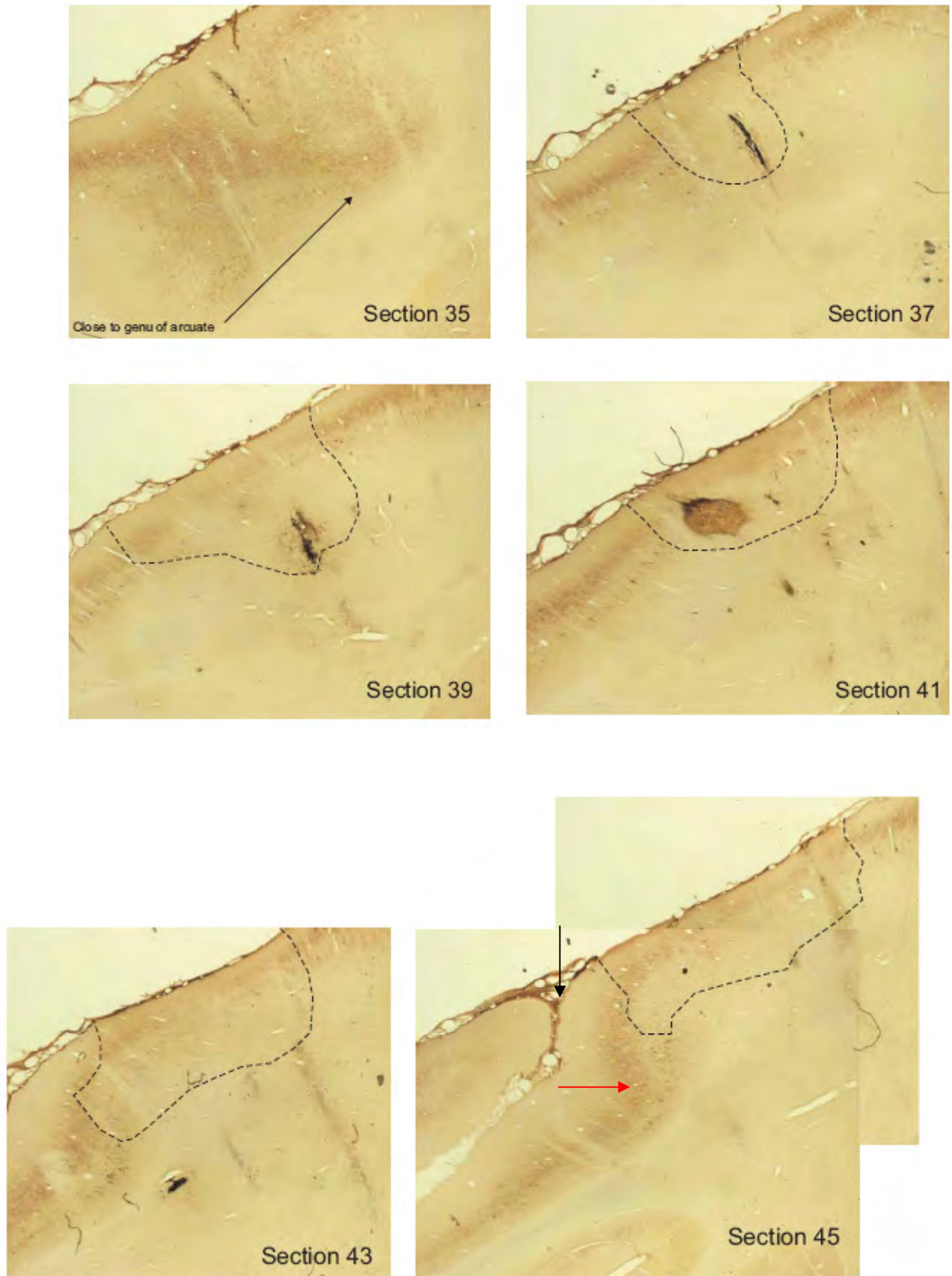

section 64
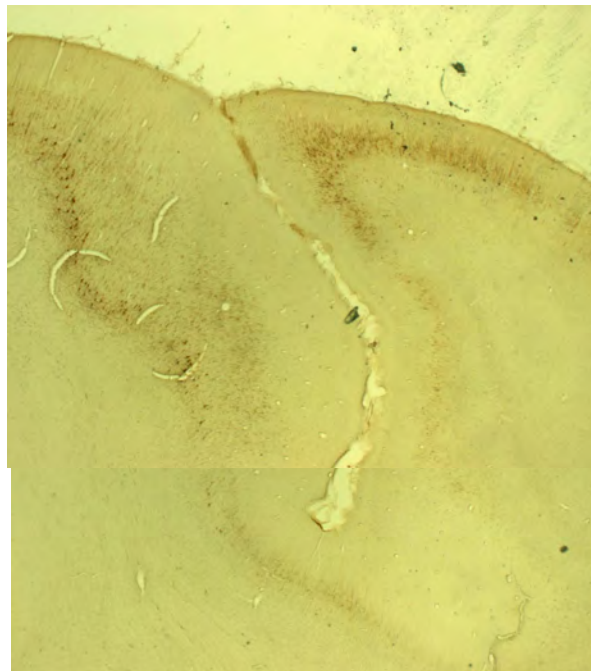
section 69
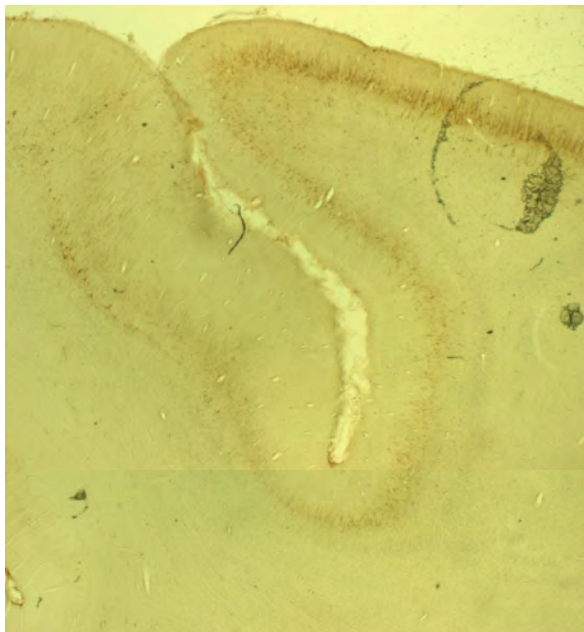
section 72

section 75

5 mm

For comparison, intact hemisphere (MK5-R) (con't)

CS
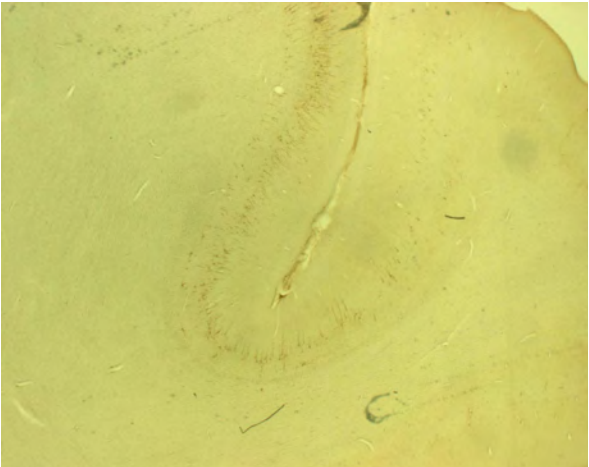
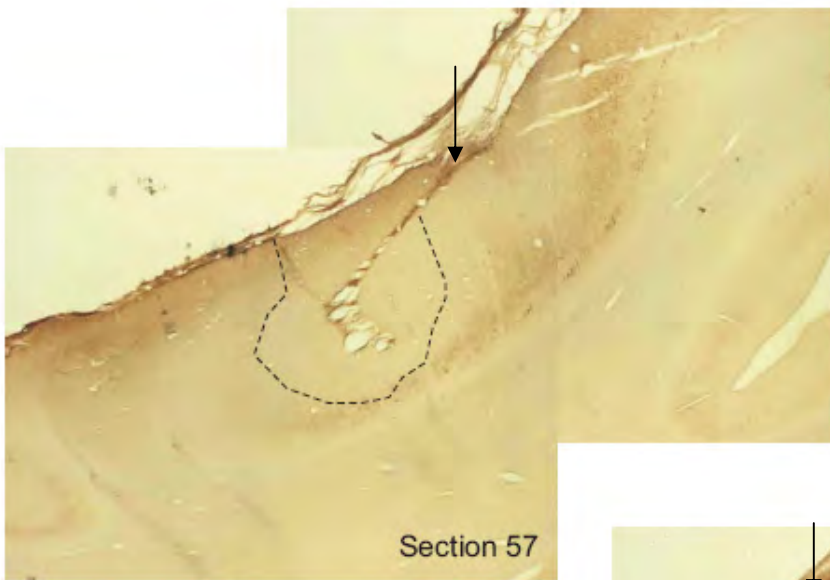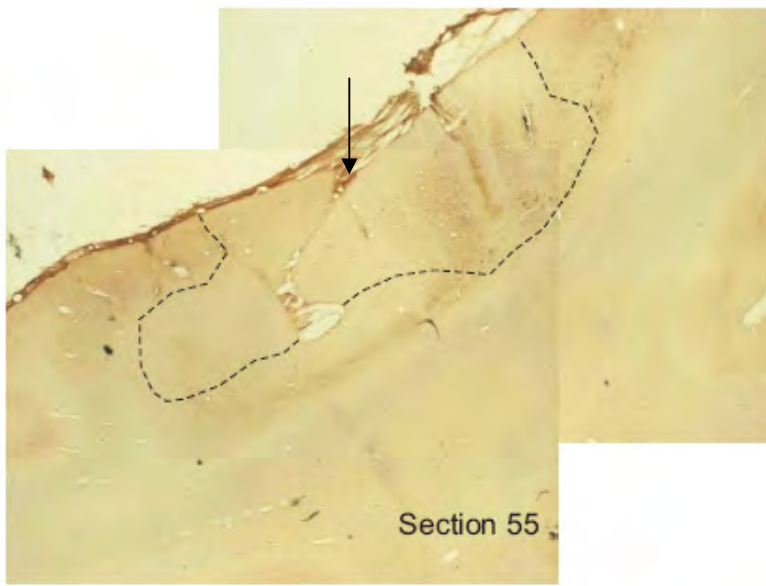

section 77

section 80

5 mm

_____

C. <u>Monkey MK6-J</u> (taken from Liu and Rouiller, 1999)

(Figure 3.4 – panel 1 – Monkey MK6-J)

(Figure 3.4 – panel 2 – Monkey MK6-J)   Black arrow points to the central sulcus

Section 47

Section 49

Section 51

Section 53

_____
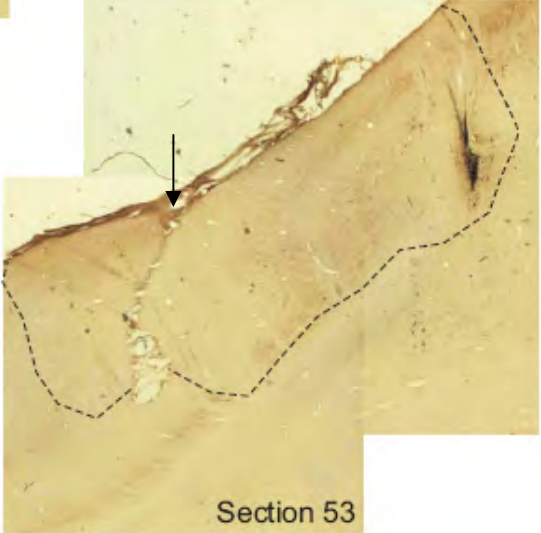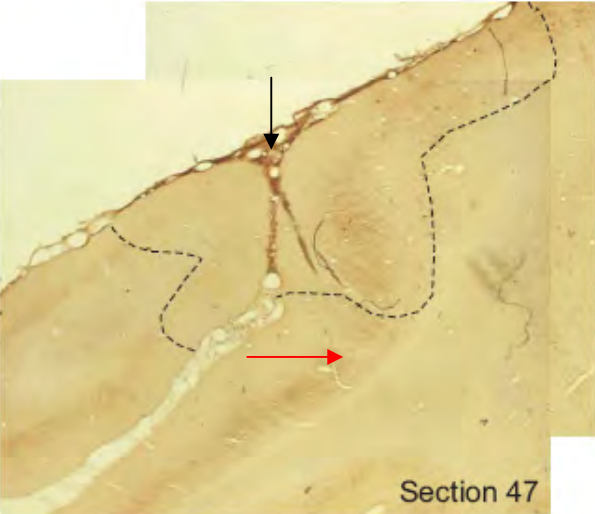
(Figure 3.4 – panel 3 – Monkey MK6-J)   Black arrow points to the central sulcus
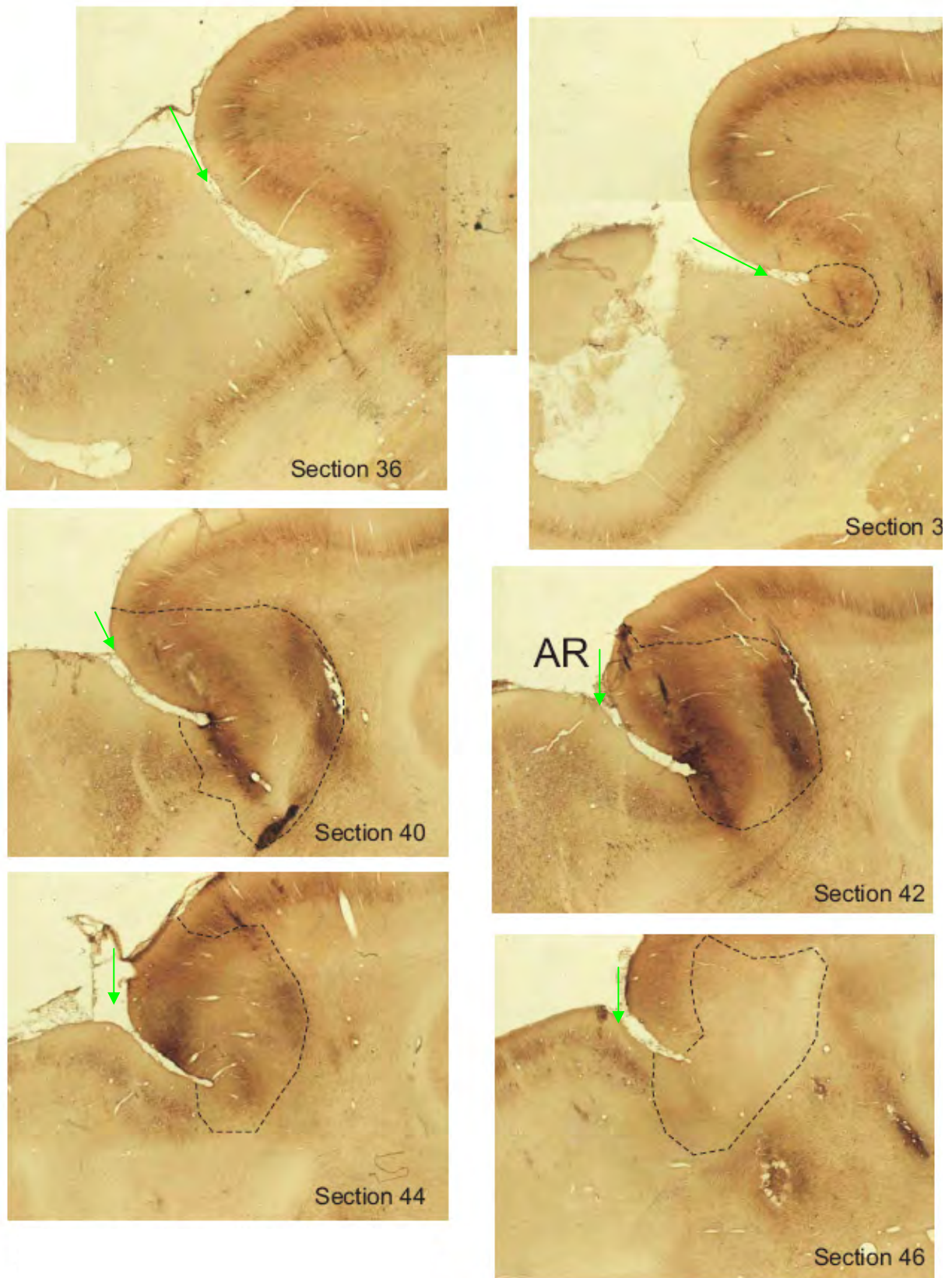
_____

(Figure 3.4 – panel 4 – Monkey MK6-J)

Figure 3.4: SMI-32 sections of the right (ipsilesional) hemisphere of monkey MK6-J (same conventions as in Figure 3.2). Small black vertical arrows indicate the position of the central sulcus (CE), lateral is to the left, dorsal is to the top. M1 is right to the CE and S1 left to the CE (except in the intact hemisphere in panel 4, where it is the other way around). The lesion extent is indicated by dashed black lines. CIN=cingulate sulcus.

In monkey MK6-J, the lesion of the right M1 hand area included the sulcus and crest regions of the M1 hand representation. The lesion extends fairly rostally, close to the genu of the arcuate sulcus (sections 35 and 37), thus possibly including a part of the premotor cortex (PM). The lesion also affects a significant portion of S1, on the left of the central sulcus (sections 47 – 59). As clearly shown in this animal, the lesion was identified as an interruption of the typical bi-layer (III and V) appearance of the motor cortex in SMI-32 material. In some cases, the lesion affected mainly the layer V, corresponding also to a lesioned territory as layer V is the origin of the corticospinal tract.

Some parts of M1, located in deep layers (red arrows), have been spared by the ibotenic acid lesion. For comparison, a representative section (section 55) of the intact left hemisphere is shown as well (panel 4 of Fig. 3.4). Note the easily visible layers III and V in the motor cortex, disappearing to some extent at the border with S1.

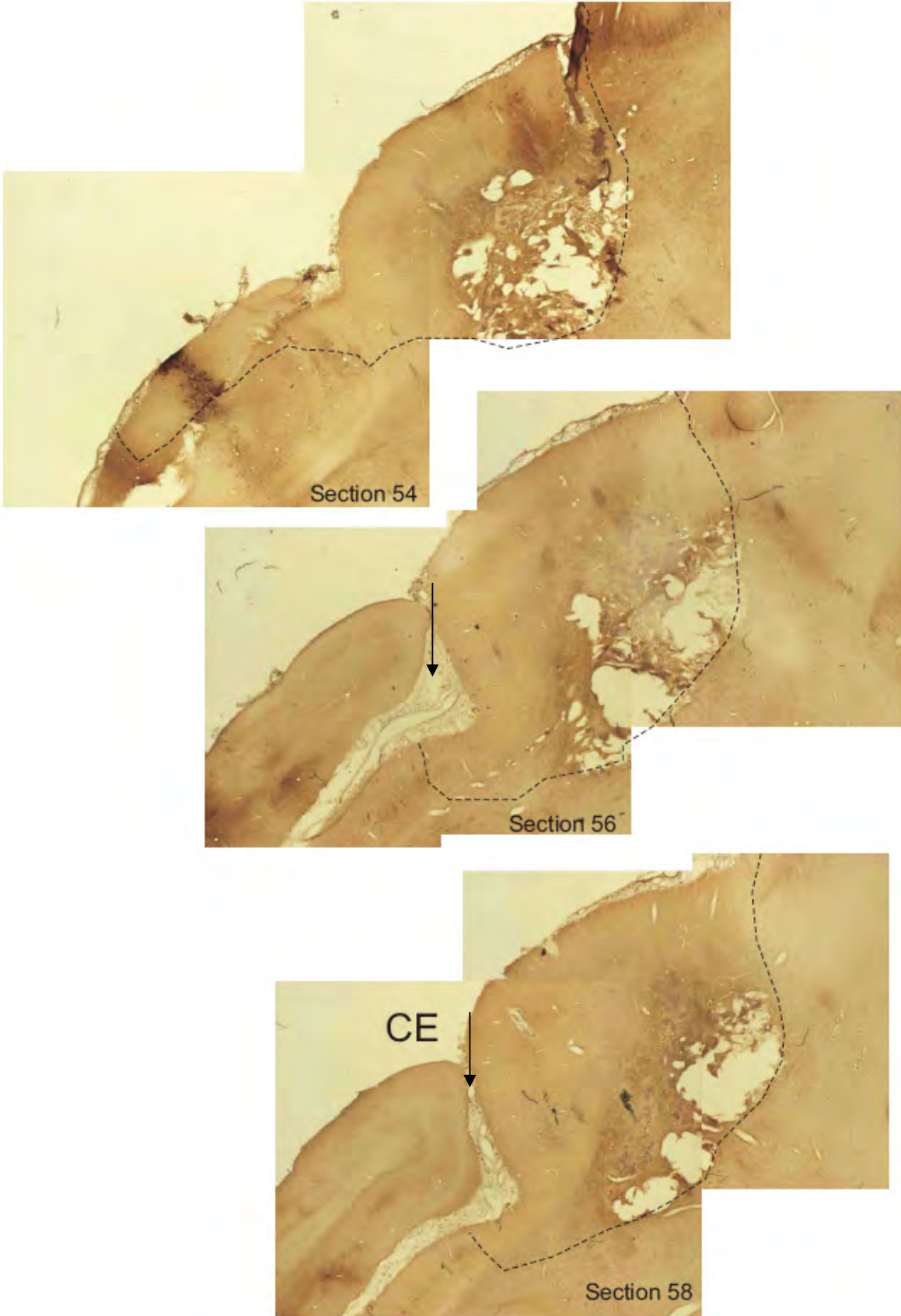**D. Monkey MK7-C** (taken from Liu and Rouiller, 1999)
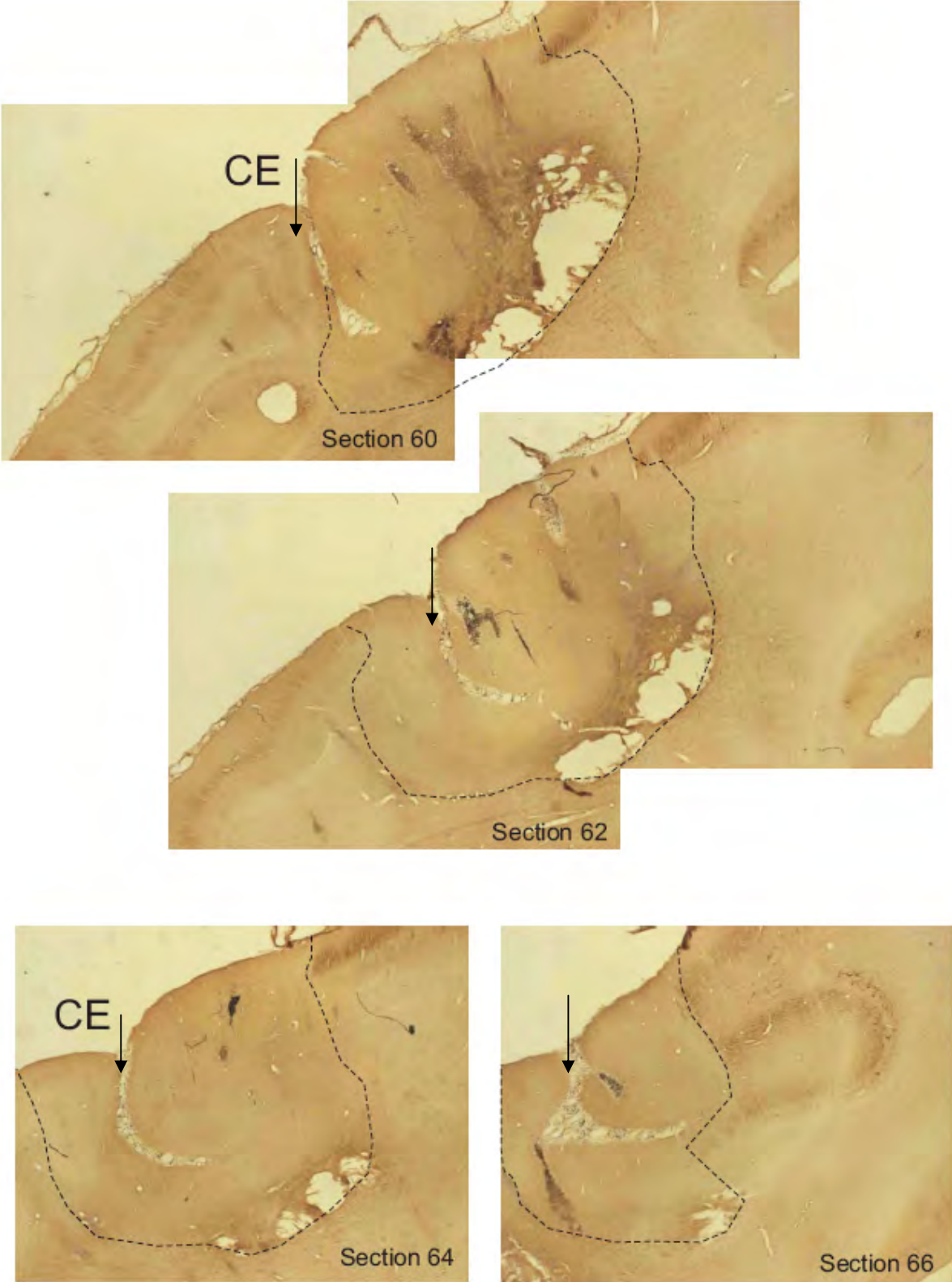

(Figure 3.5 – panel 1 – Monkey MK7-C)

_____
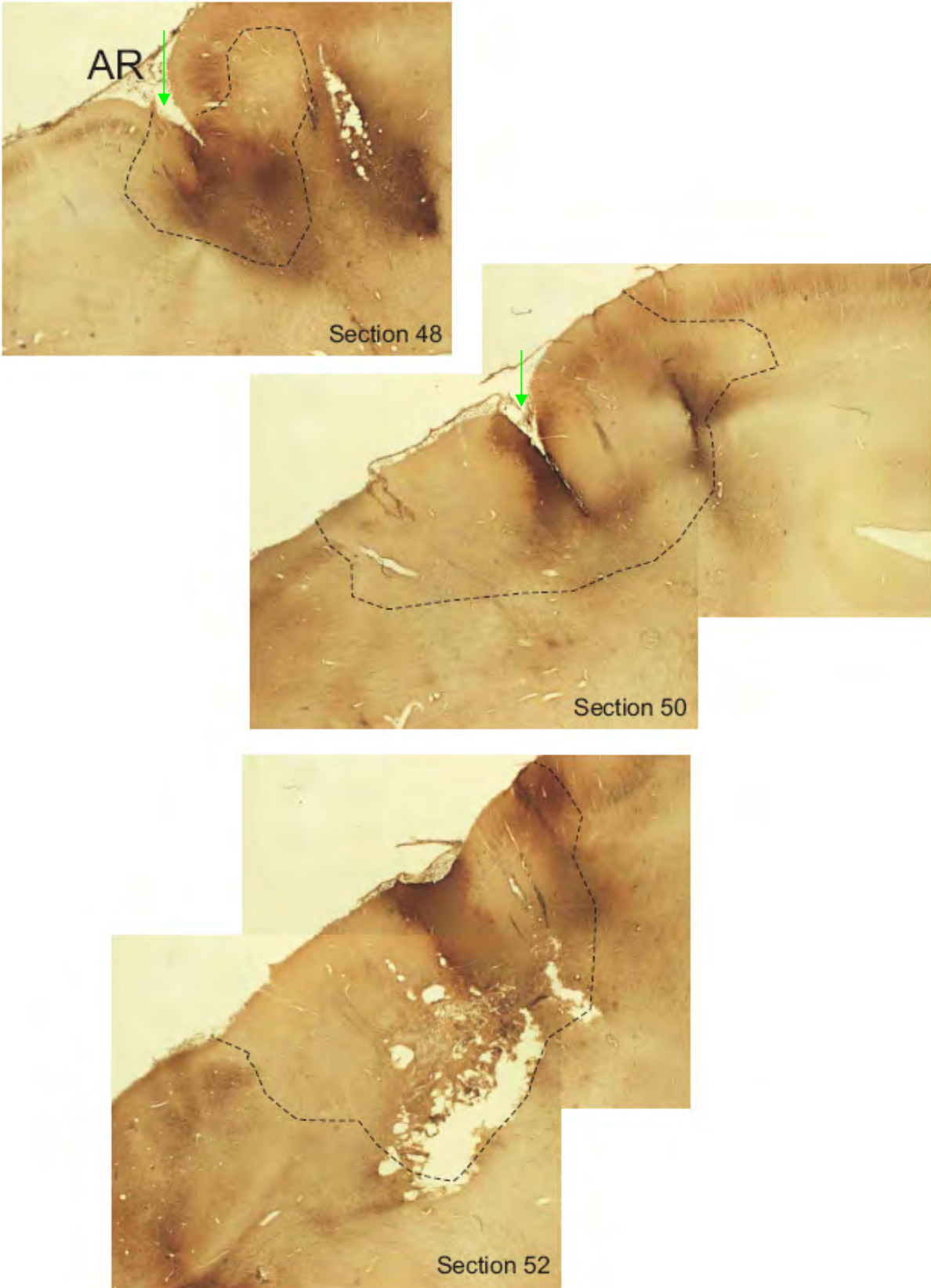
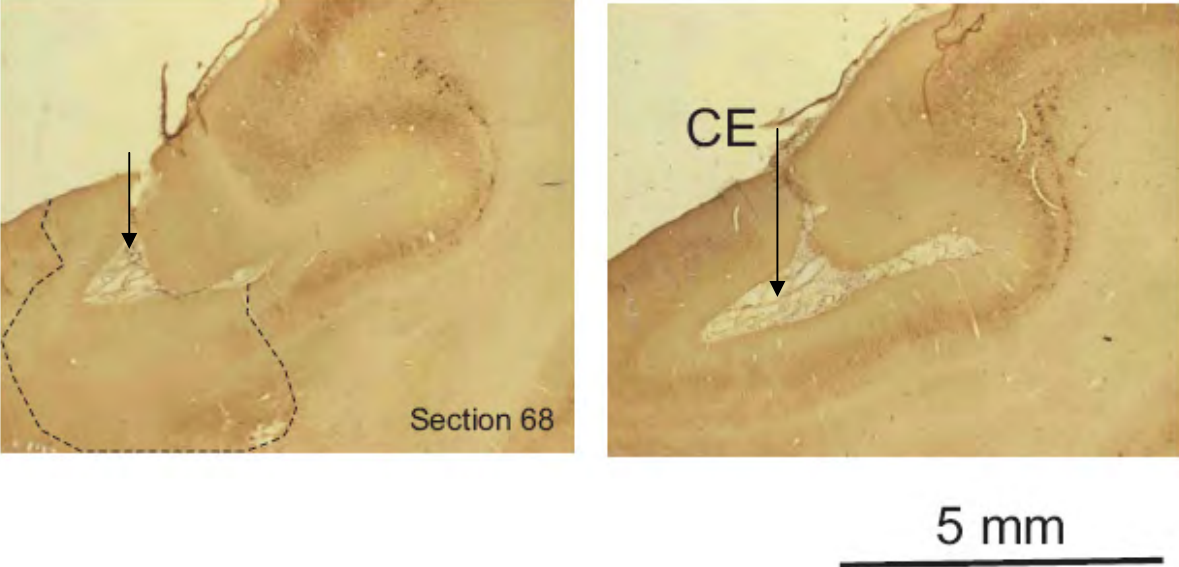(Figure 3.5 – panel 2 – Monkey MK7-C)

(Figure 3.5 – panel 3 – Monkey MK7-C)

(Figure 3.5 – panel 4 – Monkey MK7-C)

_____

(Figure 3.5 – panel 5 – Monkey MK7-C)

(Figure 3.5 – panel 6 – Monkey MK7-C)

Figure 3.5: SMI-32 sections of left (ipsilesional) hemisphere in monkey MK7-C. Same conventions as in Figure 3.2. The small black vertical arrows indicate the position of the central sulcus (CE) whereas green arrows indicate the position of the arcuate sulcus (AR), lateral is to the right, and dorsal is to the top. M1 is right to the CE and S1 left to the CE (except in the intact hemisphere in panel 6, where it is the other way around). The lesion extent is indicated by dashed black lines.

The lesion of the left hand representation in monkey MK7-C covered the rostral bank of the central sulcus, corresponding to the putative sulcus and crest regions of the M1 hand

representation. However, the lesion was not restricted to the pre-central gyrus, but also involved the caudal bank of the central sulcus, corresponding to the hand representation in the primary somatosensory cortex (S1) in the post-central gyrus (sections 54 and 62 to 68). As in the previous monkey, the lesion spreads rostrally in the region of the genu of the arcuate sulcus (sections 38 to 48), thus involving PM. In this monkey, there is also an extent of the lesion relatively deep, affecting the white matter (sections 52 to 66). For comparison two representative sections of the intact right hemisphere are shown. Note the easily distinguishable layers III and V in the motor cortex within the rostral bank of the central sulcus.

_____

3.1.2.2 Reconstruction of lesion in anti-Nogo-A treated monkeys
A. <u>Monkey MK2-L</u>
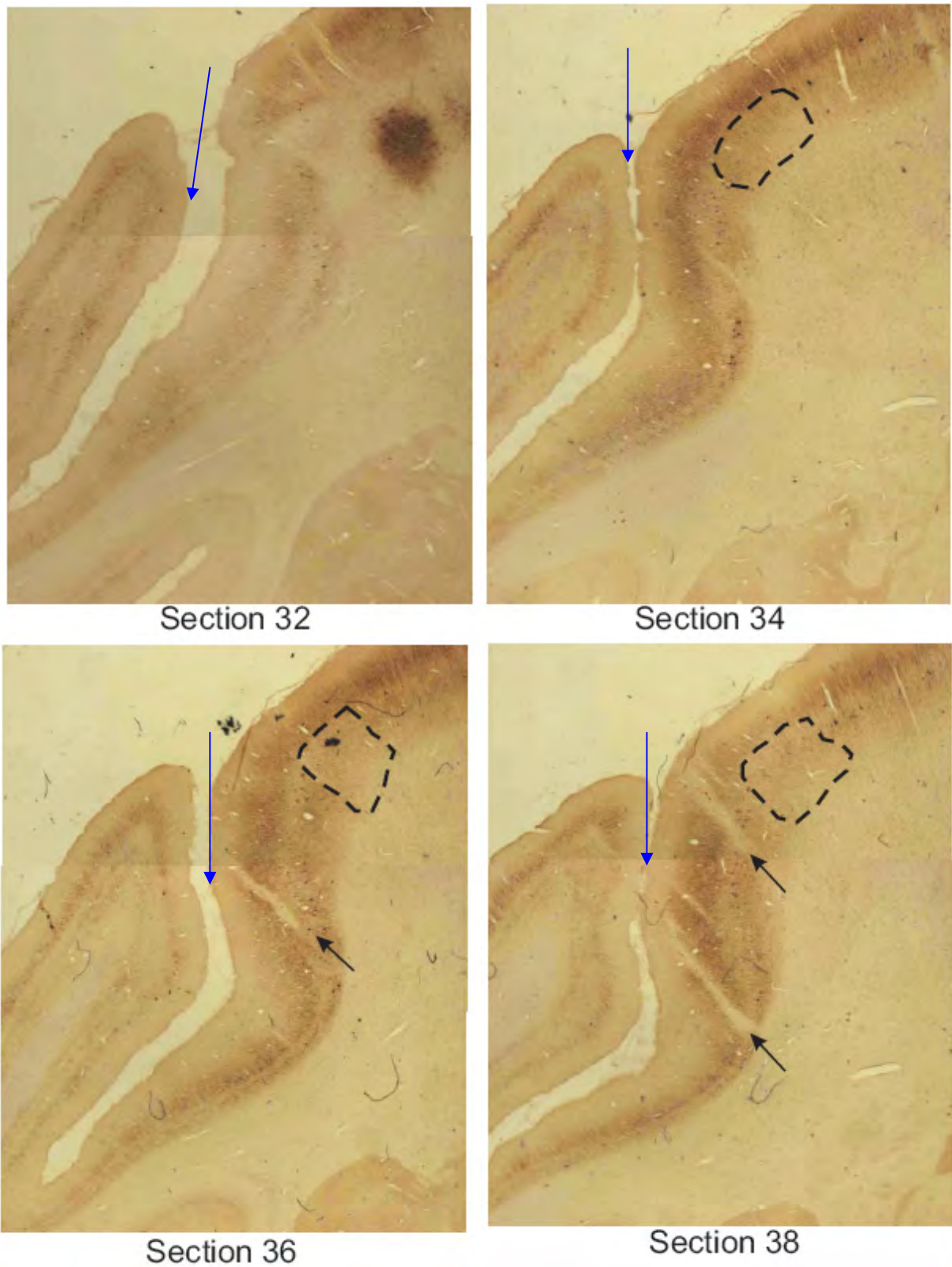
(Figure 3.6 – panel 1 – Monkey MK2-L)
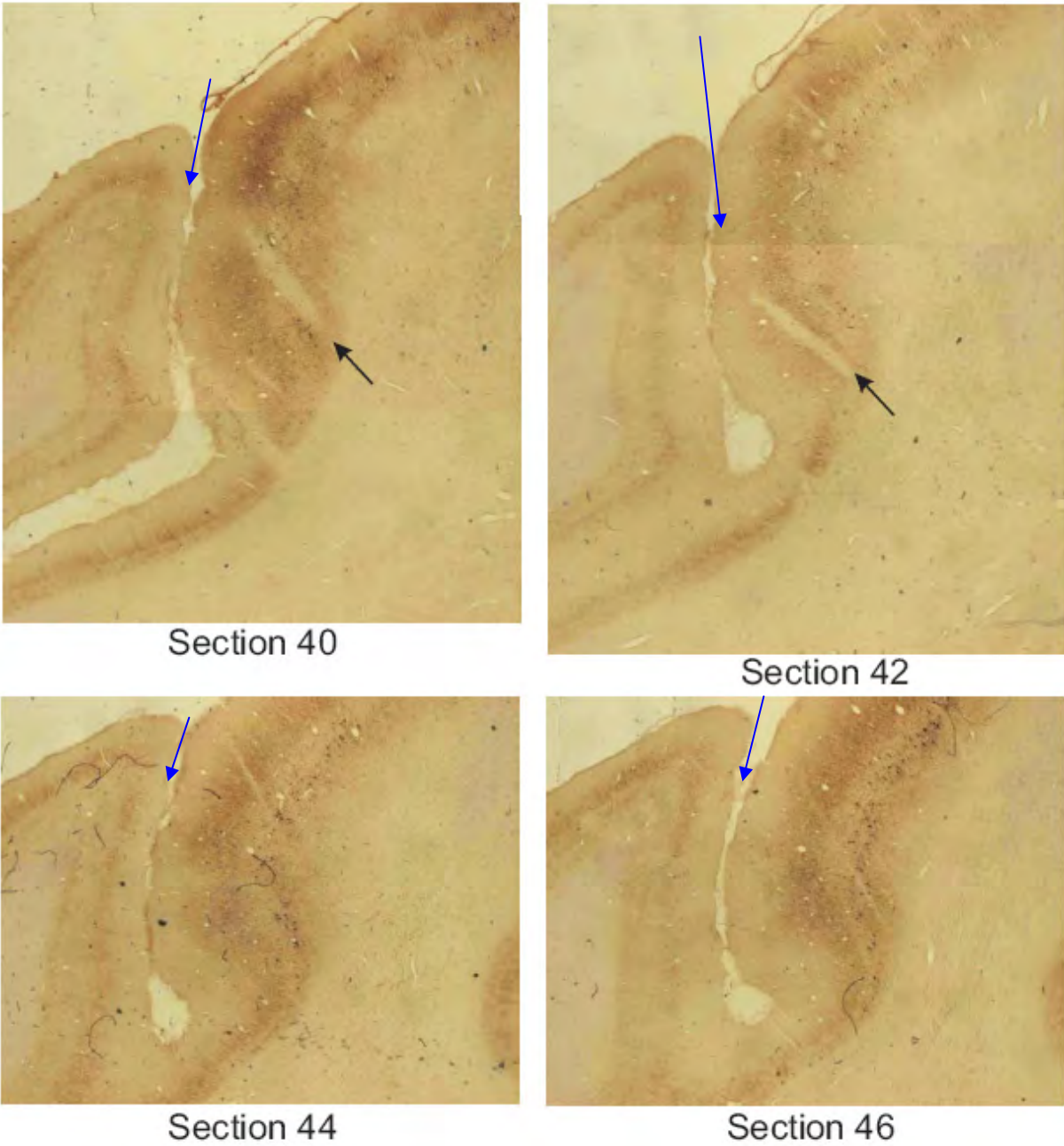
(Figure 3.6 – panel 2 – Monkey MK2-L)

_____

(Figure 3.6 – panel 3 – Monkey MK2-L)
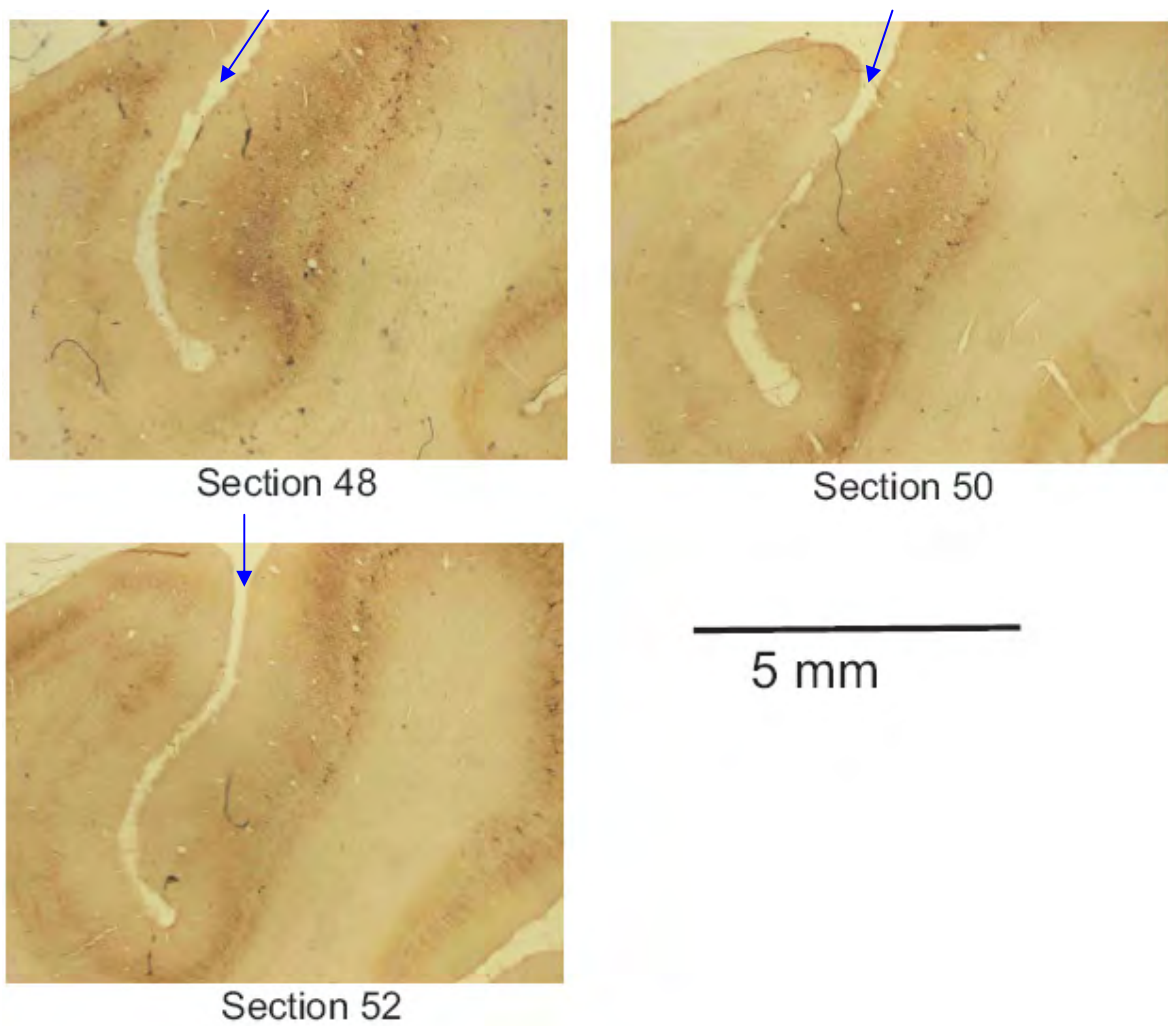
Figure 3.6: SMI-32 sections of left ipsilesional hemisphere of monkey MK2-L. Same conventions as in Figure 3.2.

In monkey MK2-L, for unknown reasons, the lesion induced by the ibotenic acid infusion was very small and limited to layer V of the hand represention of M1 in the rostral bank of the central sulcus (sections 34 – 38). The small blue arrows indicate the position of the central sulcus (CE), whereas black arrows indicate electrode traces resulting from ICMS. Lateral is to the left, and dorsal is to the top. M1 is right to the CE and S1 left to the CE. The lesion extent is indicated by dashed black lines.

B. Monkey MK3-V
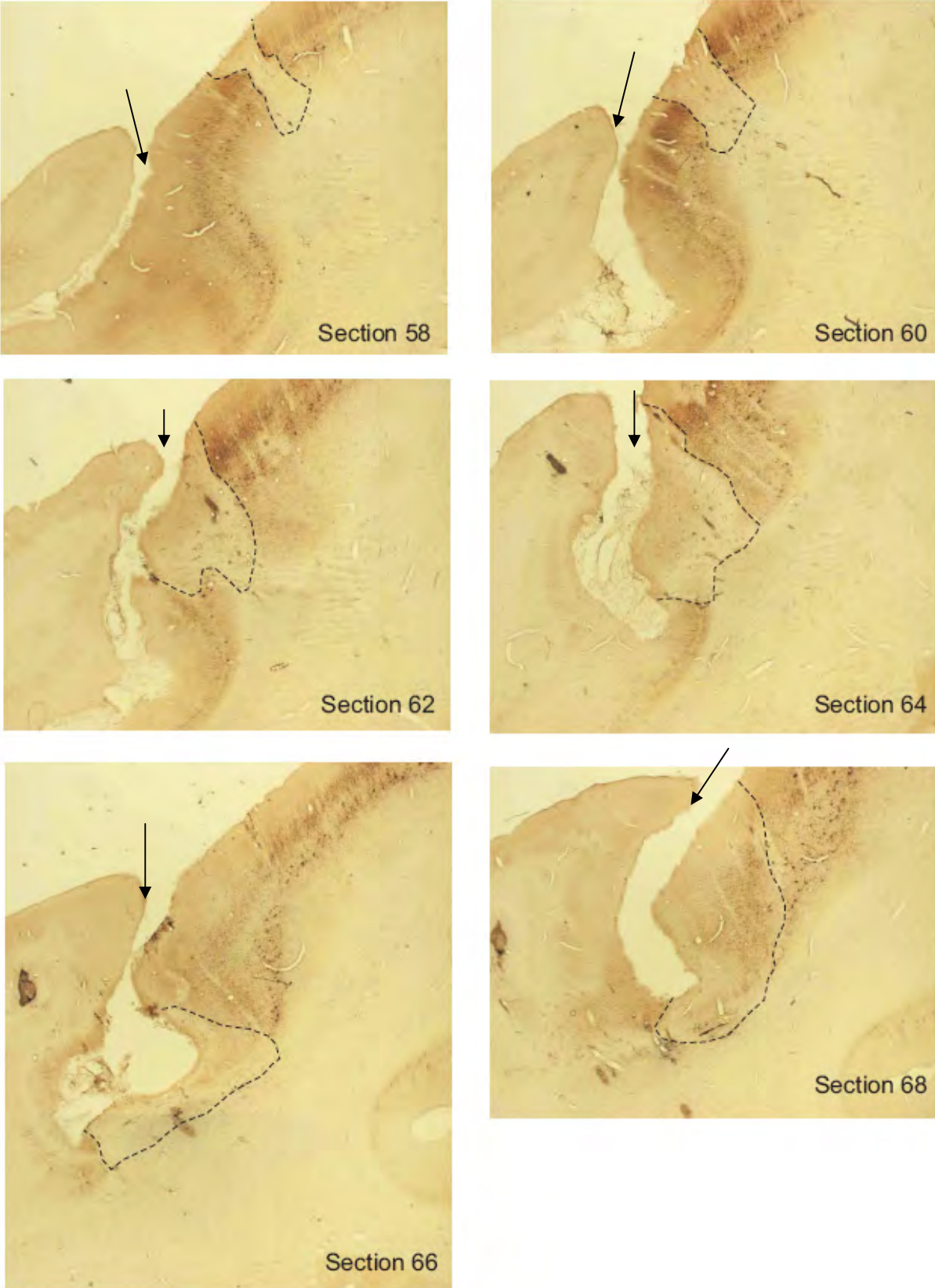
(Figure 3.7 – panel 1 – Monkey MK3-V)

(Figure 3.7 – panel 2 – Monkey MK3-V)

Section 70

Section 72

Section 74

5 mm

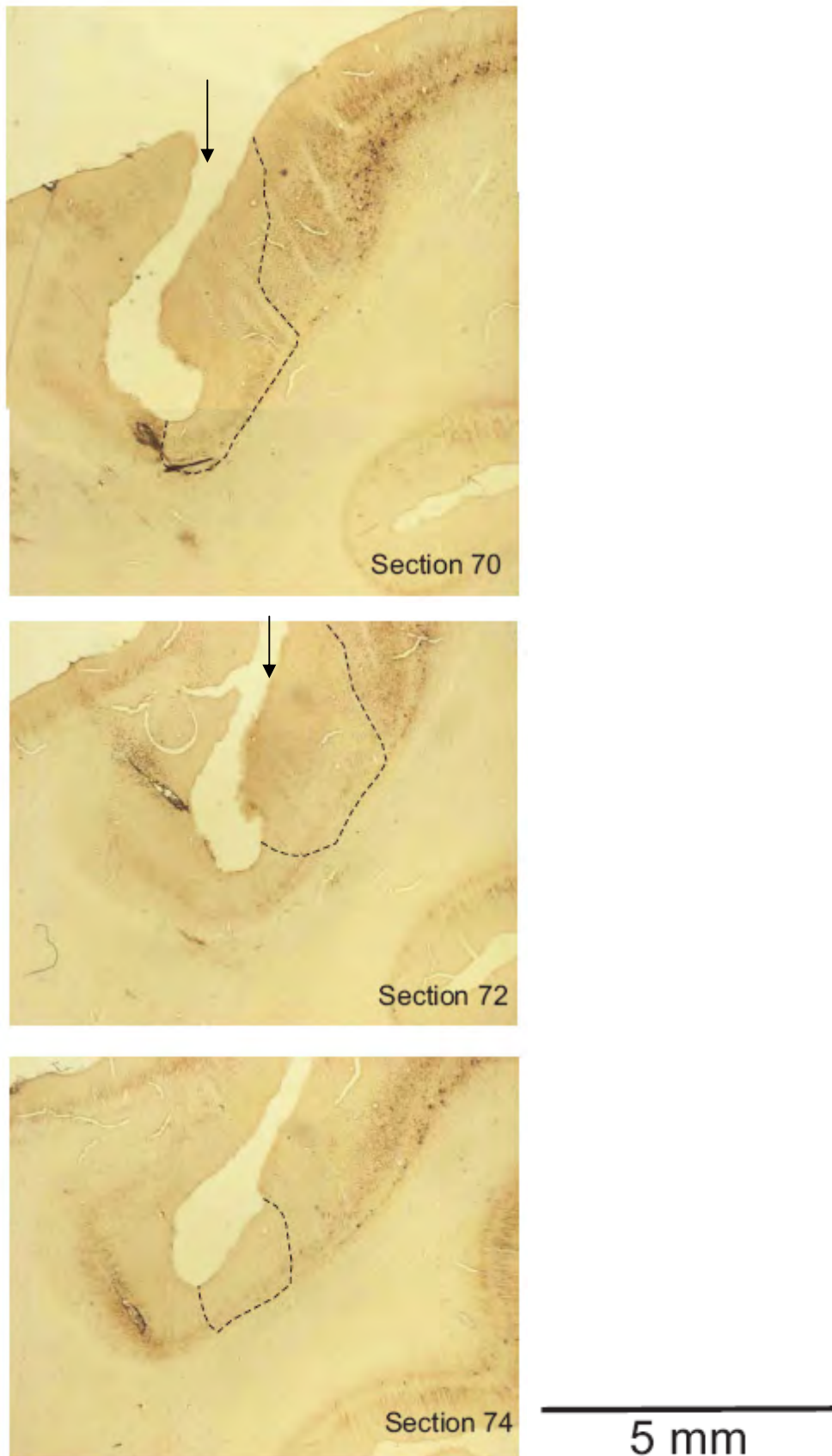**Figure 3.7:** SMI-32 sections of left (ipsilesional) hemisphere of monkey MK3-V. Same conventions as in Figure 3.2. The small black vertical arrows indicate the position of the central

_____

sulcus (CE), lateral is to the left, and dorsal is to the top. M1 is right to the CE and S1 left to the CE. The lesion extent is indicated by dashed black lines.

In monkey MK3-V, the lesion was almost perfectly situated inside the hand represention of M1, touching both layer III and layer V, but excluding S1. The lesion was limited to grey matter, sparing white matter brain tissue. Rostrally, the smaller part of the lesion was situated on the crest area of M1 (Sections 58 – 62), whereas the biggest part of the lesion was situated in the rostral bank of the central sulcus (Sections 64 – 74), starting close to the brain surface but then more caudally also reaching the fundus of the central sulcus.

_____

C. <u>Monkey MK4-S</u>

Section 20

Section 22

Section 24

Section 26
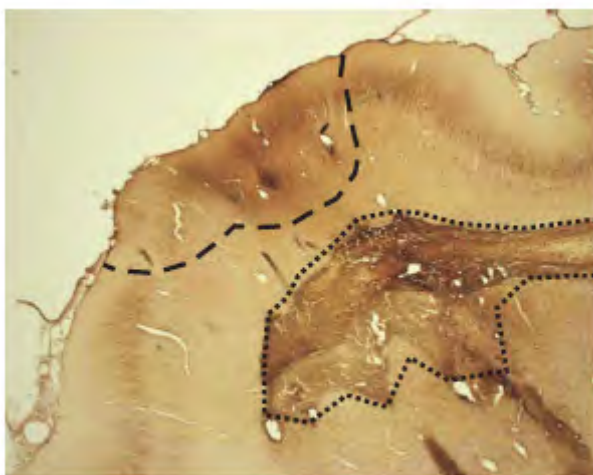
Section 28

(Figure 3.8 – panel 1 – Monkey MK4-S)

(Figure 3.8 – panel 2 – Monkey MK4-S)

Section 32

Section 34

Section 36
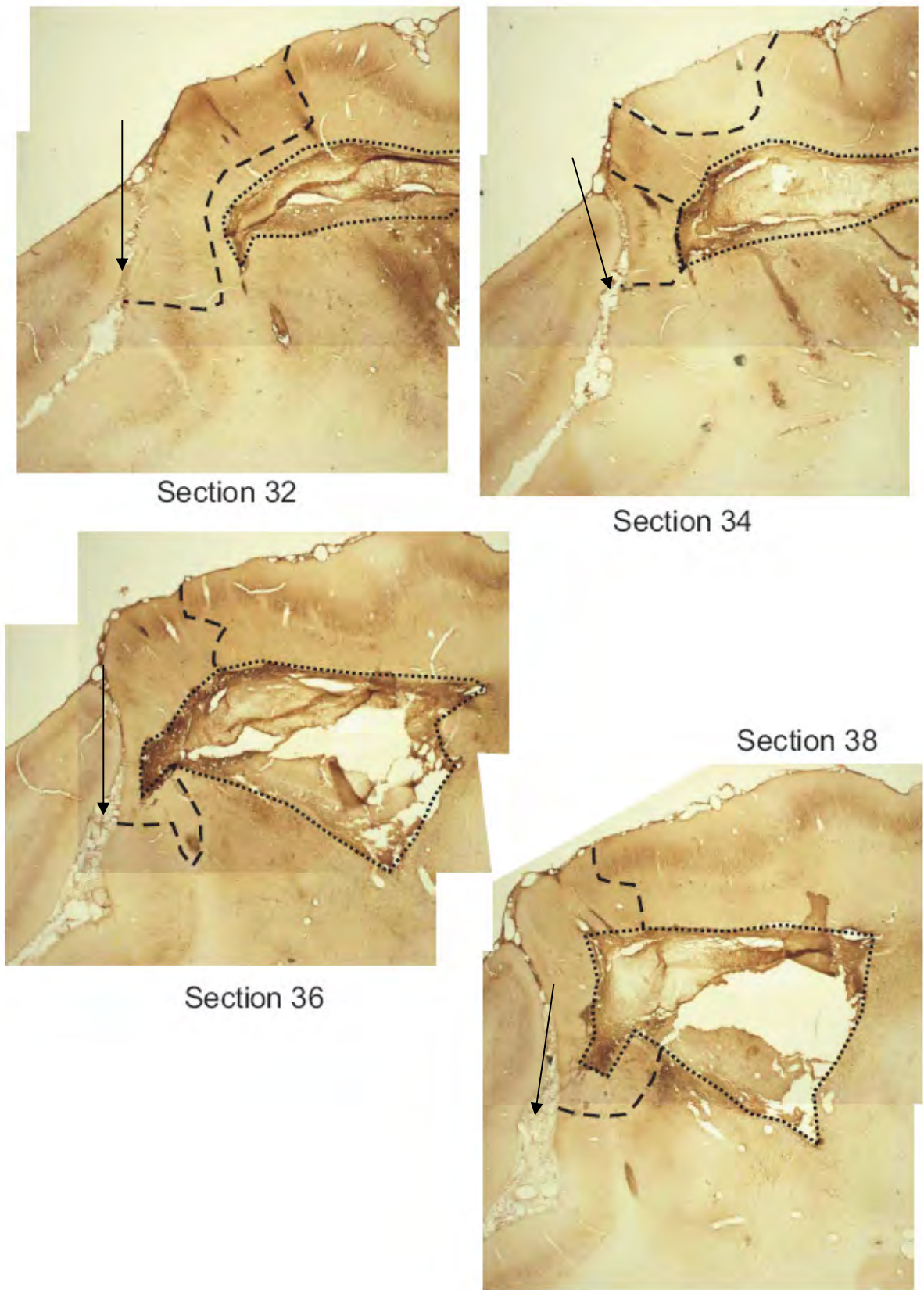
Section 38

(Figure 3.8 – panel 3 – Monkey MK4-S)
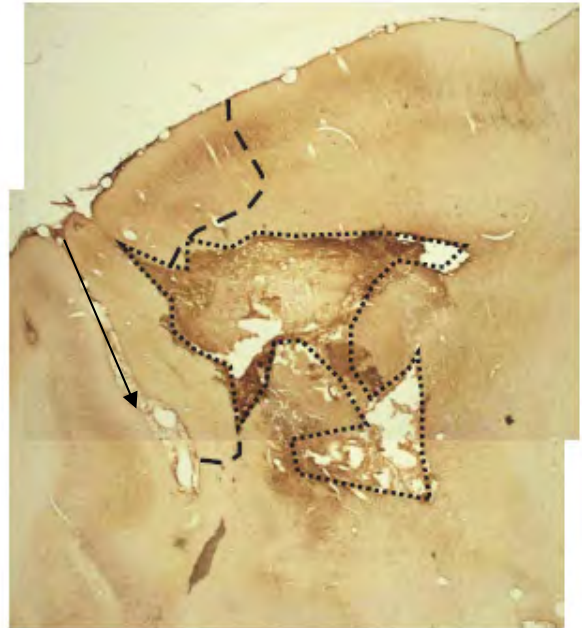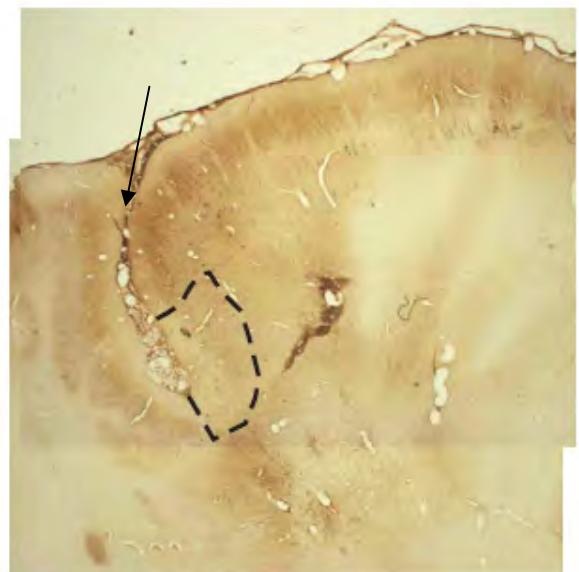
(Figure 3.8 – panel 4 – Monkey MK4-S)

(Figure 3.8 – panel 5 – Monkey MK4-S)

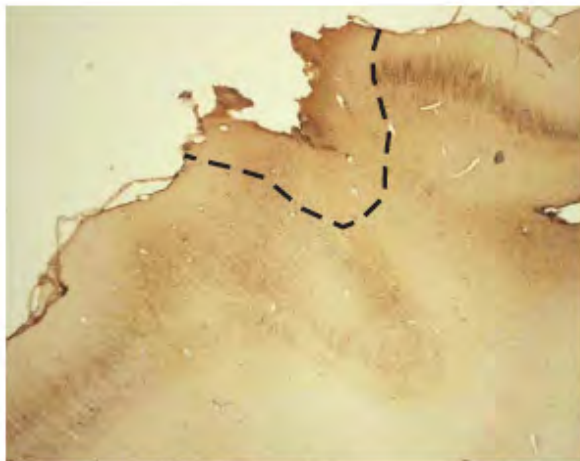Section 48

Section 50

5 mm
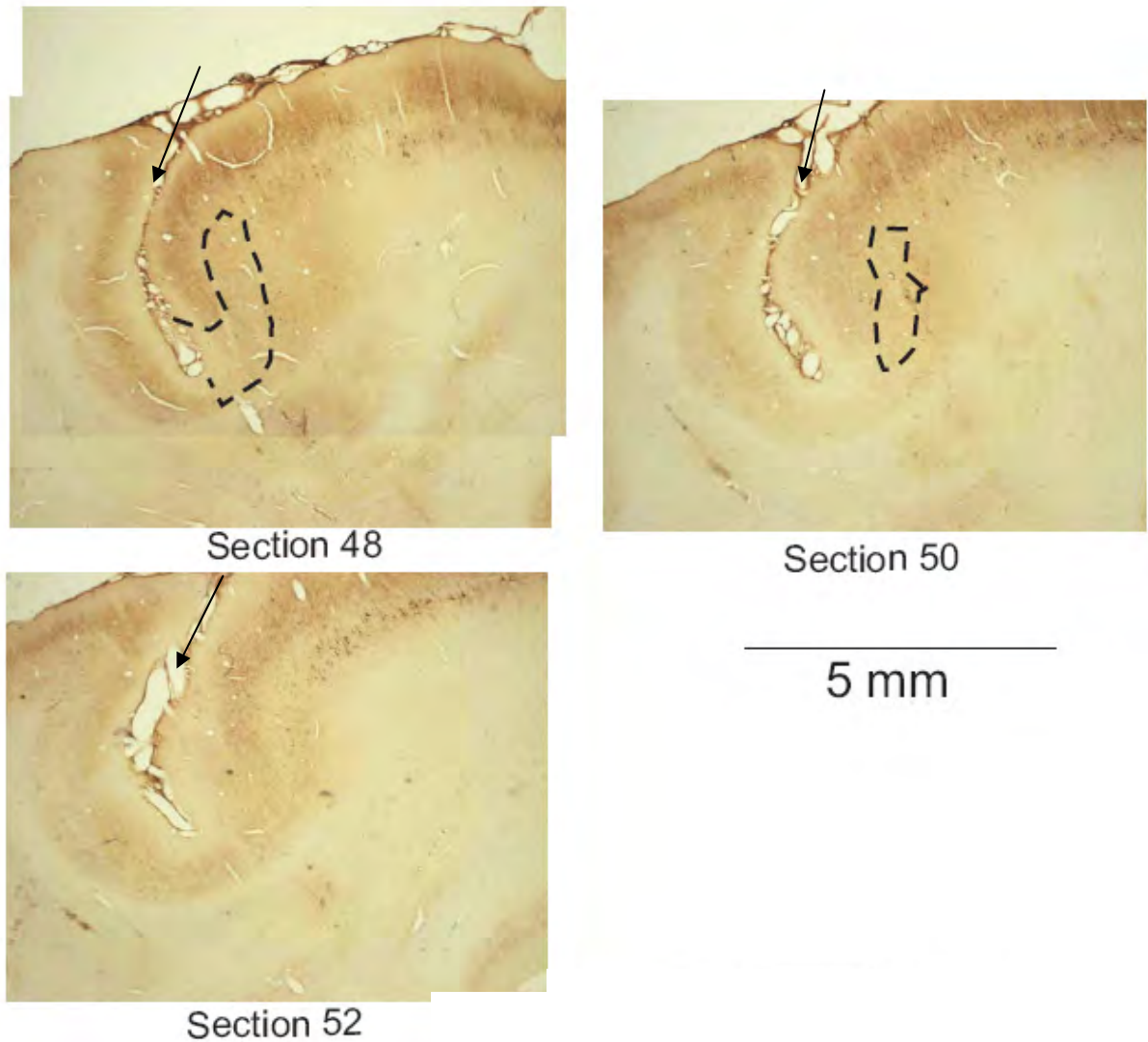
Section 52

Figure 3.8: SMI-32 sections of left (ipsilesional) hemisphere of monkey MK4-S. Same conventions as in Figure 3.2. The small black vertical arro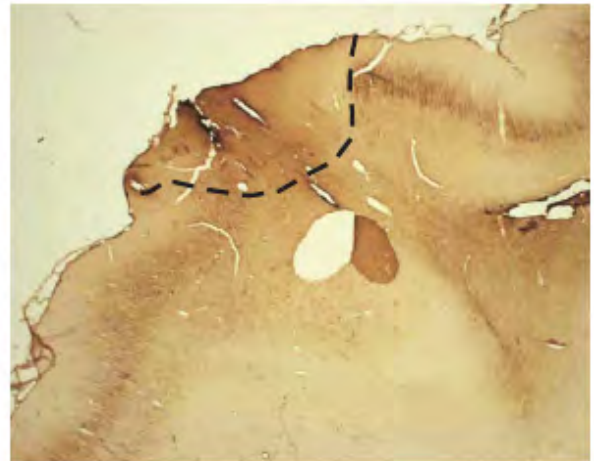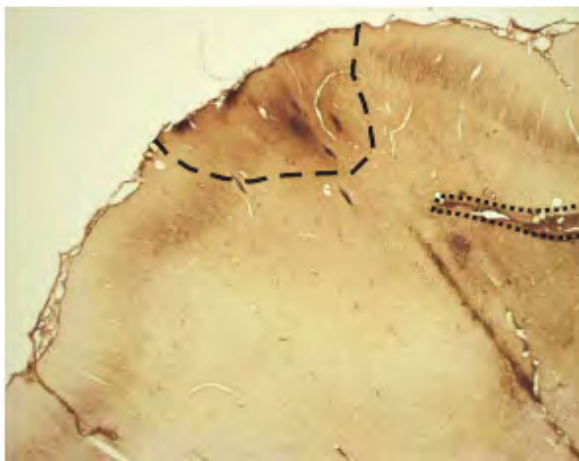ws indicate the position of the central sulcus (CE), lateral is to the left, and dorsal is to the top. M1 is right to the CE and S1 left to the CE. The lesion extent is indicated by dashed black lines (cortical lesion) and dotted black lines (sub-cortical lesion).

In monkey MK4-S, the lesion was situated inside the hand represention of M1. In contrast to most other monkeys, a fairly large subcortical region (dotted line) mainly in the white matter was substantially affecteded as well. Approximately same amounts of the cortical extent of the lesion were situated on the crest of M1 (Sections 20 – 30) and in the rostral bank (Sections 32 – 52) of the central sulcus. Rostrally, the cortical part of the lesion was mainly situated close to the brain surface whereas the caudal part covered the whole rostal bank from the brain surface to the fundus of the central sulcus.

_____

3.1.2.3 Reconstruction of lesion seen on lateral views in control (untreated) monkeys
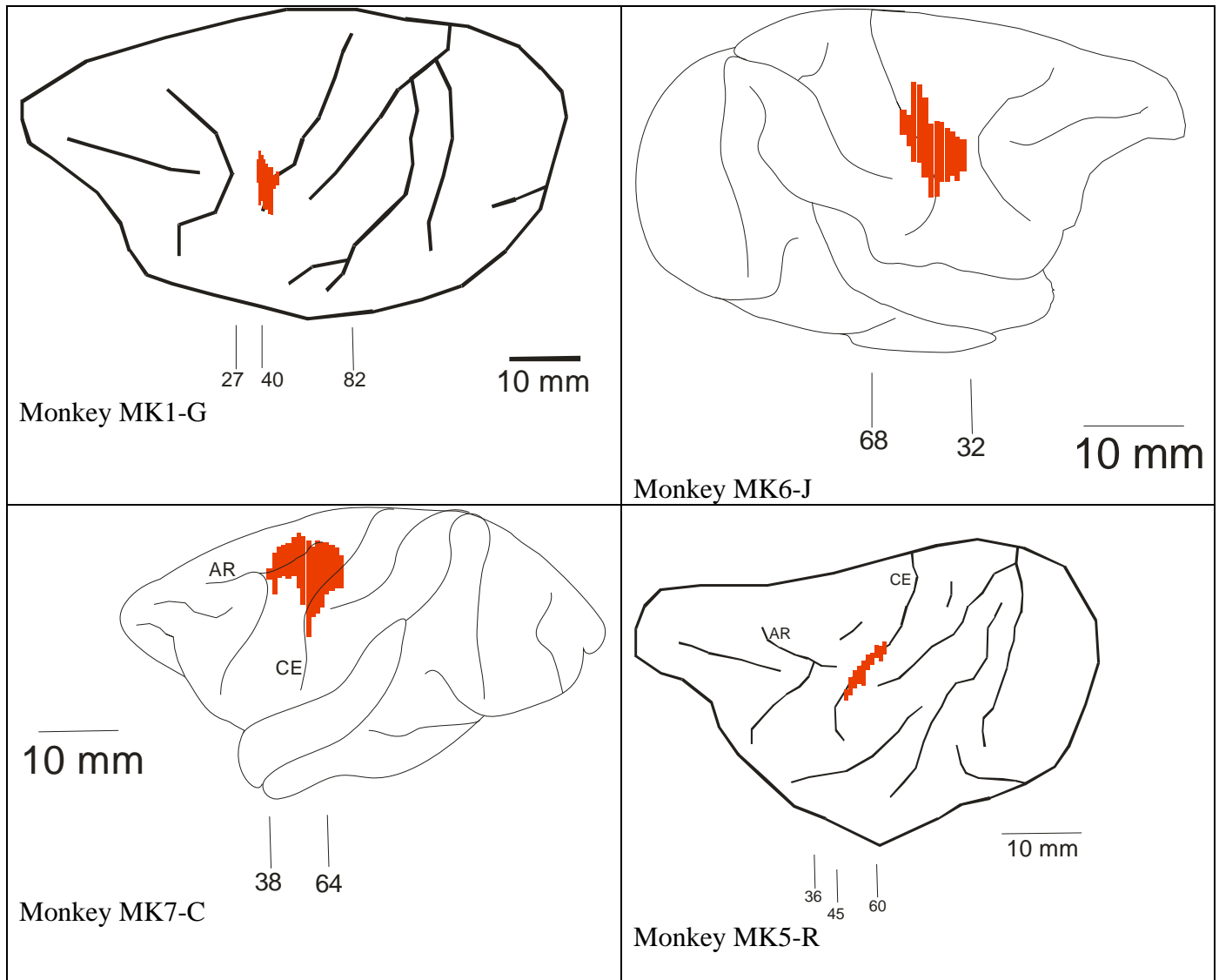
Figure 3.9: Lateral views of the hemisphere with the lesion for the four control (untreated) monkeys. The lesion is represented in red, in transparency of the cortical surface. The numbers below every lateral view correspond to the sections numbers indicated in Figures 3.2 – 3.8 above.

As expected, the two monkeys (MK6-J and MK7-C), taken from the previous study by Liu and Rouiller (1999), exhibit a larger lesion than the monkeys MK1-G and MK5-R, in line with the larger volume of ibotenic acid (more than double) injected in the two former monkeys than in the latter two monkeys (see Table 3.1 below). In monkeys MK1-G and MK5-R, the lesion is fairly well restricted to the hand area, whereas in the monkeys MK6-J and MK7-C the lesion spreads more rostrally in PM as well as more medially, thus affecting more proximal territories in M1 (wrist, elbow, etc).

_____

3.1.2.4 Reconstruction of lesion seen on lateral views in anti-Nogo-A treated monkeys
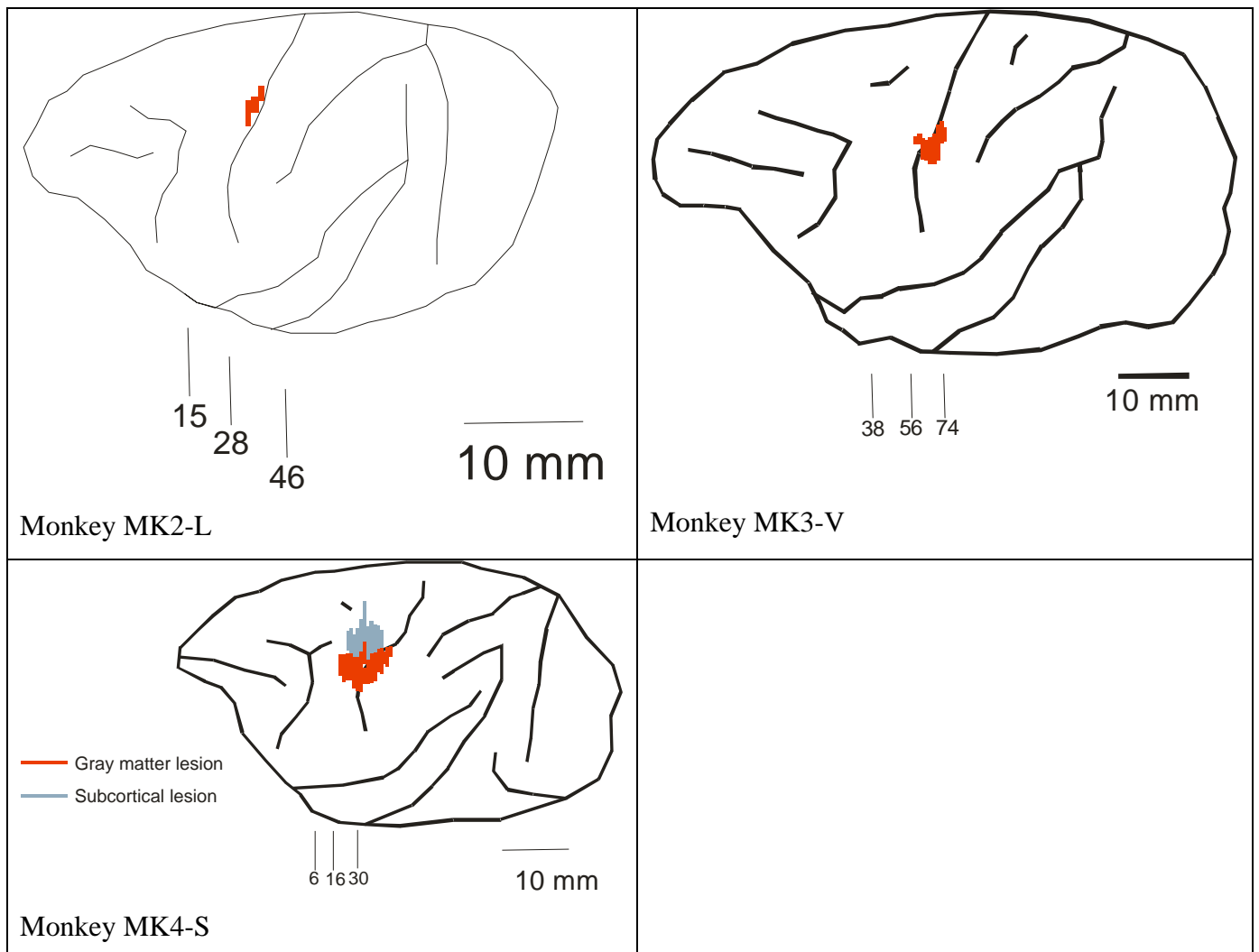
Figure 3.10: Lateral views of the hemisphere with the lesion for the three anti-Nogo-A treated monkeys. The lesion is represented in red, in transparency of the cortical surface. Note in MK4-S, a large part of the lesion located sub-cortically (grey area). The numbers below every lateral view correspond to the sections numbers indicated in Figures 3.2 – 3.8 above.

As already mentioned above, the lesion in MK2-L is very small. In this animal, for unknown reasons, the ibotenic acid was not efficient or was not properly delivered. As a consequence, this animal is not pertinent to study the functional recovery in relation to the anti-Nogo-A antibody treatment. With such a small lesion, even in absence of treatment, spontaneous recovery may well restore 100% of the hand dexterity. In contrast, the lesion is ideally placed and has the desired extent in MK3-V, corresponding to the hand representation in M1. In MK4-S, the part of the lesion

affecting the grey matter (in red) also corresponds fairly well to the hand representation but, in addition, the lesion included a large area of white matter sub-cortically, affecting more proximal territories.

3.1.3 Lesion size

In Table 3.1, the volumes and surfaces of the lesions in the cerebral cortex of the seven monkeys investigated in the present thesis work are indicated. For each monkey, the amount of ibotenic acid injected and whether the corresponding monkey was treated with anti-Nogo-A antibody (or not) is indicated as well. Table 3.2 lists several parameters having an impact on the final lesion size resulting from ibotenic acid injections in the motor cortex.

Monkey	Anti-Nogo-A	Volume of ibotenic acid injected	Cumulated lesion surface (mm^2)		Lesion volume (mm^3)	
			M1	S1 /subcortical	M1	S1 /subcortical
MK1-G	NO	13.0 µl	89.13	17.63	44.93	8.81
MK2-L	YES	13.5 µl	6.23	_	3.12	_
MK3-V	YES	16 µl	41.04	_	20.52	_
MK4-S	YES	18 µl	93.06	98.99	47.00	49.49
MK5-R	NO	18 µl *	28.76	_	14.34	_
MK6-J °	NO	40 µl	117.58	33.06	58.79	16.53
MK7-C °	NO	40 µl	116.90	34.50 112.52	58.45	17.25 56.26

* In this monkey (MK5-R), the lesion was repeated three times because anti-epileptic treatment influenced (reduced) the action of ibotenic acid (see discussion below).

° These monkeys are the same as those in the study of Liu and Rouiller (1999).

Table 3.1: Lesion extent in Anti-NoGo-A antibody treated monkeys and control (untreated) monkeys.

_____

Monkey	Amount of ibotenic acid (µl)	Amount of Anti – Nogo A (subtype 11C7)	Duration of treatment	Anesthesia (A) and anti-epileptic Medication (M) (day of lesion and days after)	Age of monkey at the moment of M1 lesion
MK1-G	13.0	Control (No treatment)	none	**A:** none **M:** none	5 years
MK2-L	13.5	Total amount **13.19** mg 11C7	2 weeks	**A**: low dose of Ketamin® **M**: none	4 2/3 years
MK3-V	16.0	Total amount **23.07** mg 11C7	4 weeks	**A:** Ketamin®/ Propofol® **M:** none	ca 5.5 years
MK4-S	18.0	Total amount **29.16** mg 11C7	4 weeks	**A:** none (animal <u>awake</u> during injection procedure) **M:** Luminal® and Depakine chrono® 300	ca 5 years
MK5-R	18.0*	Control (No treatment)	none	**A:** none (animal <u>awake</u> during injection procedure) for lesion 1, lesion 2, and lesion 3 **M:** *Lesion 1:* Depakine chrono® 300 complete dose *Lesion 2:* Depakine chrono® 300 ¼ dose *Lesion 3:* no antiepileptic drug	4 years

* In this monkey the lesion was repeated three times because anti-epileptic treatment influenced (reduced) the action of ibotenic acid (see discussion below).

Table 3.2: Parameters potentially influencing the lesion size

For comparison and completeness of information, the two untreated monkeys (MK6-J and MK7-C; derived from Liu and Rouiller, 1999) were not anesthetized when infusing the ibotenic acid and they did not receive any anti-epileptic medication. At time of lesion, they were both about 4.5 years old.

3.2. Intracortical Microstimulation (ICMS) data

3.2.1 Reproducibility of ICMS data

In this part of the study, the goal was to test the reproducibility of the ICMS method.

_____
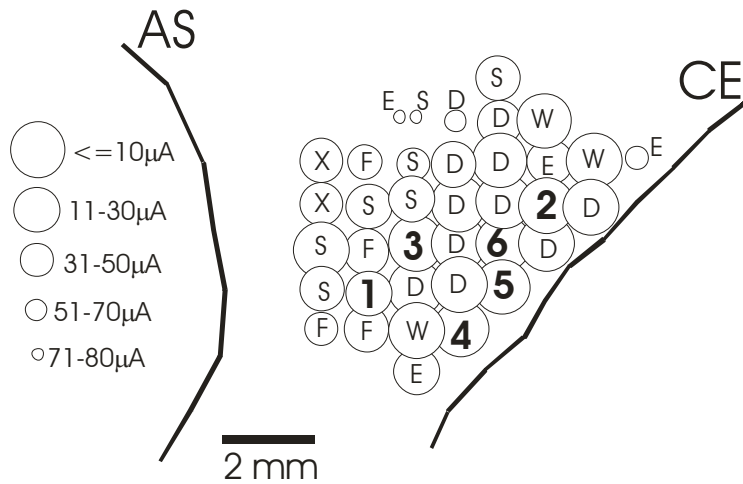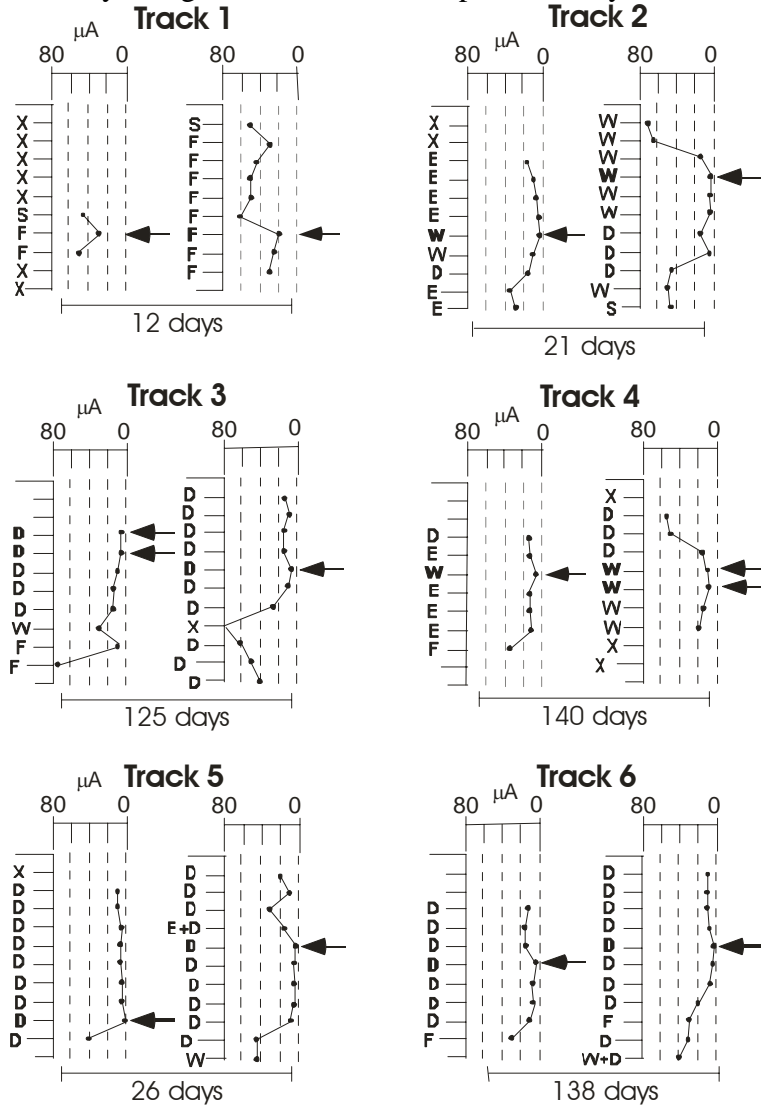
Figure 3.10: Reproducibility of the intracortical microstimulation (ICMS) method.

To investigate the variability of the method (Fig. 3.10 above), six ICMS electrode tracks (1 to 6) were each performed at two time points, separated by a time interval indicated in days (12, 21, 125, 140, 26, 138) below the horizontal bar. For each track, the penetration drawn on the left is the first one whereas the second, performed at the same location, is displayed on the right. For each penetration, the tics along the vertical line represent the sites of stimulation, at a distance of 1 mm. Usually, the first stimulation site is located 2 mm below the surface of the dura. The horizontal scale (in µAmps) indicates for each stimulation site the lowest current at which the effect was observed. The body territory activated by the ICMS is indicated as follows: "D"=digit; "E"=elbow; "F"=face; "S"=shoulder; "W"=wrist; "X"=non-microexcitable site. Along each penetration, the arrows (and bold letters) indicate the ICMS threshold for the entire penetration (criterion taken to define the body territory for the corresponding location on the surface map). The bottom panel is a surface representation of the left intact hemisphere of the monkey MK1-G before the lesion was introduced, in which the six electrode penetrations represented above were performed twice (indicated by the numbers 1–6). The other circles with the same letter code as above represent the other electrode penetrations performed in the left hemisphere of MK1-G. The size of the circles represents the ICMS threshold obtained for the corresponding electrode penetration. CE=central sulcus; AR=arcuate sulcus; rostral is to the left and medial towards top.

What is the variability of ICMS sites elicited along two electrode penetrations performed at two distinct time points in an intact monkey? This question was addressed in monkey MK1-G before the lesion, in which six electrode penetrations taken from the left hemisphere were repeated at time intervals ranging between 12 and 140 days (Fig. 3.10). For instance, three electrode penetrations located in the hand area (tracks 3, 5 and 6), in which movements of the digits were observed at the lowest threshold site when the electrode was inserted the first time (arrows in the left columns), exhibited again a movement of the digits at the lowest effective current intensity 125, 26 and 138 days later. Interestingly, note that the ICMS thresholds were highly comparable at the two time points (Fig. 3.10). Along these three electrode tracks (3, 5 and 6), the sequence of territories activated at the consecutive ICMS sites (with a step of 1mm along the penetration) remained generally comparable at the two time points.

Two other electrode penetrations were taken from the wrist representation (tracks 2 and 4) and repeated at two time points, separated by an interval of 21 and 140 days, respectively (Fig. 3.10). In both tracks, the first penetration yielded several ICMS sites at which the elbow ("E") articulation was activated, replaced in the second penetrations by wrist movements in most cases.

However, the lowest efficient current intensity corresponded to a wrist ("W") movement in the two tracks, both during the first and the second penetrations (Fig. 3.10). Again, as for digits territories, the threshold obtained for these two wrist territories remained similar at the two time points tested. Along the same line, in the electrode track located in the face representation (track 1), at the two time points tested (12 days apart), ICMS at threshold elicited movements of face muscles (Fig. 3.10). In summary, from the six electrode tracks repeated at two time points (Fig. 3.10), one can conclude that, in spite of some variability at some ICMS sites, the territory assigned to each track as defined by the effect observed at threshold did not change, even when the time interval was as long as 140 days. These observations support the notion that changes in size of the hand area observed in relation to a lesion cannot be explained by the intrinsic variability of the ICMS method and thus are indeed related to post-lesion plasticity. The above data about the variability of the ICMS data were published in a recent report (Schmidlin et al., 2005).

3.2.2 ICMS maps

3.2.2.1 Mapping strategy

The pre- and post-lesion ICMS maps represented here show threshold movements elicited by ICMS in awake monkeys. Movements were detected by muscle palpation and visual examination of all body muscles of the corresponding monkey. For each site stimulated, only the type of movement at threshold current is represented as a projection on the brain surface. The following types of movement were distinguished: foot (any type of leg and foot movement), trunk, tail, shoulder, elbow, wrist, fingers (any type of digit movement), neck, and face (any type of head movement). Movement types are color coded. Stimulation thresholds at a specific site are indicated by the diameter of the colored circles. In the post-lesion maps, ibotenic acid injection sites are indicated by an orange X or a blue I. In all monkeys, except monkey MK2-L where a 2 mm*2 mm grid interval was used, we used a 1 mm*1 mm grid interval to explore the motor cortex with ICMS. The surface covered by the grid of each map is equal to the surface of the brain exposed by craniotomy inside the chronic chambers implanted over the motor cortex. Note that, in monkeys MK6-J and MK7-C, the map is restricted to the central portion of the chronic chamber (17 mm of the 23 mm corresponding to the total inner dimension). With respect to the brain midline, the chamber was placed such that its medial wall is located approximately 7–8 mm laterally in monkeys MK6-J and MK7-C. The exact placing of the chambers in the other monkeys is indicated in the method part of this thesis.

_____

3.2.2.2 Pre- and post-lesion ICMS maps in control (untreated) monkeys

A. Monkey MK1-G

Monkey MK1-G Pre-Lesion left

Figure 3.11: Pre- and post-lesion ICMS maps for Monkey MK1-G.

On the pre-lesional map of control monkey MK1-G (Fig. 3.11), the hand area is mainly represented around the central gyrus. This hand territory is surrounded by a wrist, shoulder and elbow area. Shoulder and wrist are equally represented. The elbow is less present. There is an area for the face, just lateral to the fingers. The majority of pre-lesion ICMS thresholds are situated below 10μA.

Ibotenic acid was injected at six sites in the hand representing area of M1. Post-lesion ICMS revealed that lesioned sites now are, in majority, not responding at thresholds situated below 80μA (Fig. 3.11). There are few responding sites for digits. Their thresholds are increased to 30-80μA. There is a little expansion of the shoulder area in the digits area from the lateral site. This expansion concerns five points with low thresholds. Anyhow, there is a general tendency of the hand area to disappear from the post-lesion ICMS map of control monkey MK1-G.

B. Monkey MK5-R

Monkey MK5-R Pre-Lesion
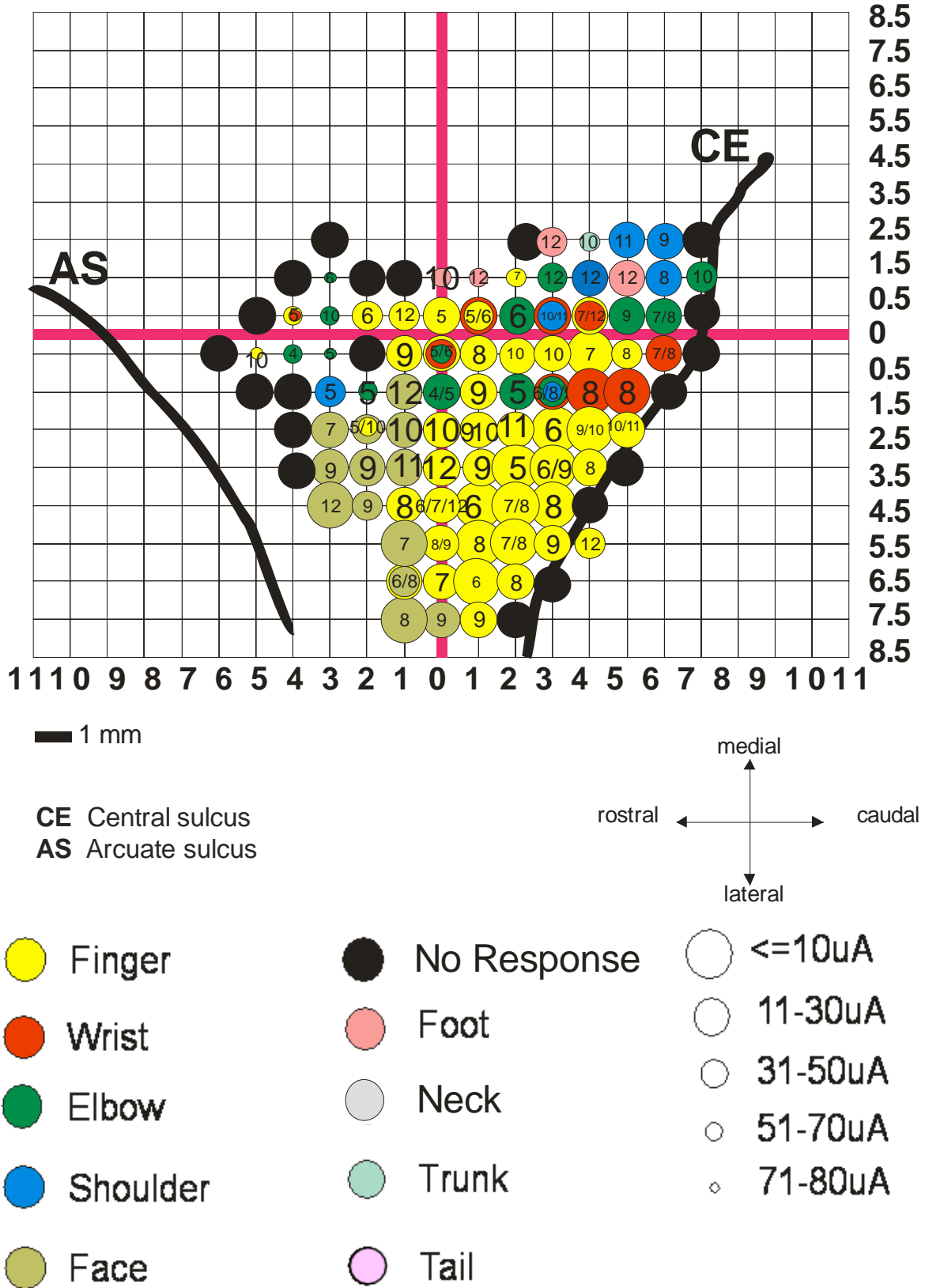
Monkey MK5-R Post-Lesion
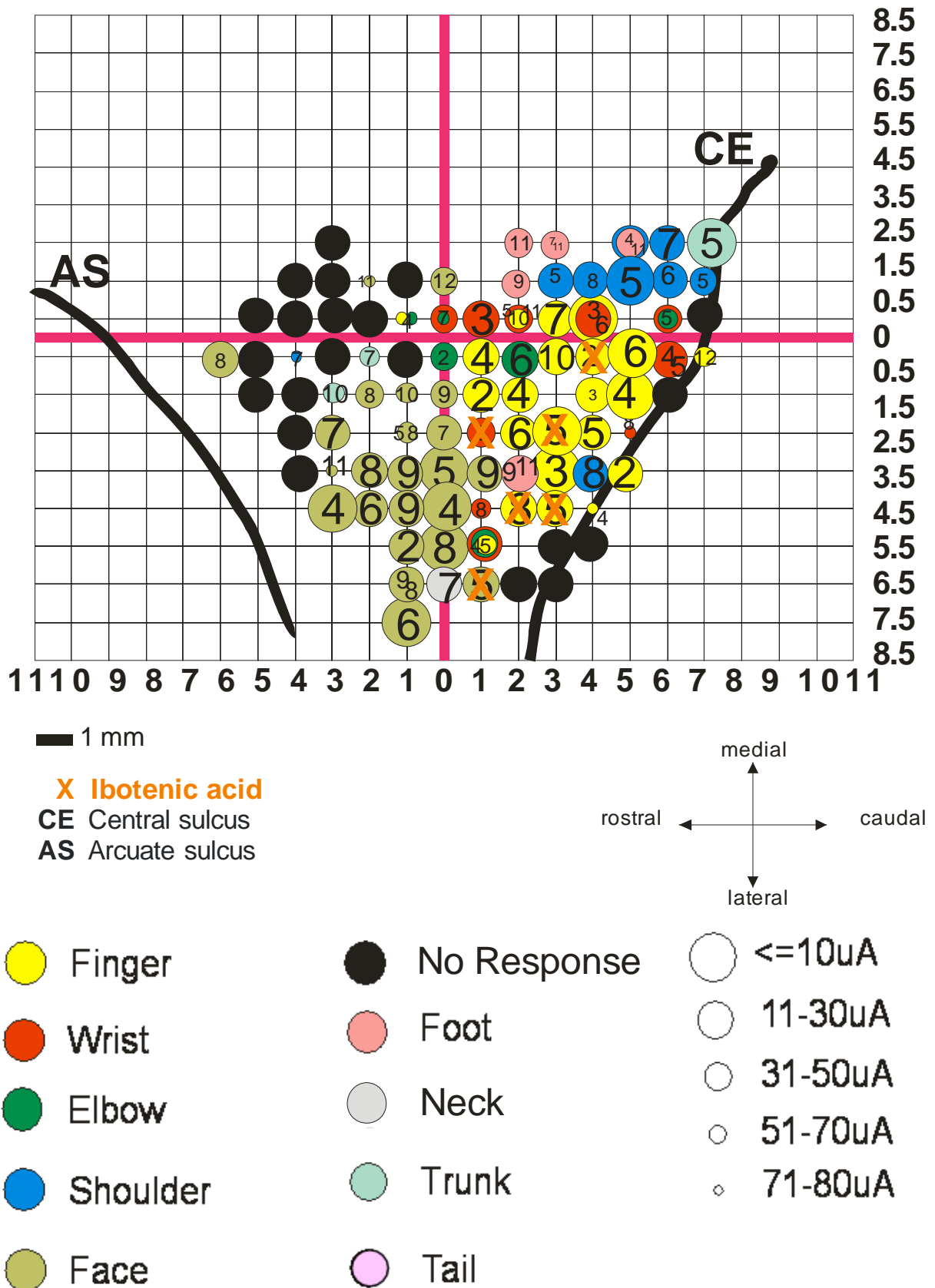
Figure 3.12: Pre- and post-lesion ICMS maps for Monkey MK5-R.

In this monkey, extensive ICMS mapping was performed in about 100 sites in M1, as well as in PM. Pre-lesion mapping shows a substantial hand representation area in the lateral part of M1, rostral to the central sulcus, mainly representing the fingers. More medial, some ICMS sites with wrist and elbow responses can be seen. A bit more caudal and medial, but still rostral to the central sulcus, some ICMS sites eliciting shoulder and foot movements are present. Rostro-lateral to the finger representation area in M1, sites evoking movements of the face are represented. Rostro-medial to M1 sites lying in the dorsal premotor cortex (PMd), representing mainly finger and elbow movements, are present. Note the slightly higher thresholds in PMd ($\geq$ 30µA) as compared to M1 ($\leq$ 10 µA).

Post-lesion, a comparable extensive ICMS mapping was performed, visiting 92 out of 100 pre-lesion sites. 8 ICMS sites were no longer accessible due to dura thickening and regrowth of the bone at the border of the craniotomy. A closer look at the post-lesion ICMS map reveals no obvious change in the area of PMv except for one site (1 rostral / 4.5 lateral) which changed from finger to face representation. In contrast the area of PMd shows various fundamental changes: First, several sites became irresponsive to ICMS whereas still responsive sites changed from finger and elbow representation to more proximal representations like shoulder or even trunk. One site kept a combined finger and wrist representation post-lesion but at a higher threshold (71 - 80µA post-lesion; 31 - 50µA pre-lesion). The pattern of changes in M1 is fairly more complex: In general changes were more prominent in the vicinity of the ibotenic acid injection sites in the lateral area of M1, where normally the fingers are represented. The area of M1 representing the proximal part of the forelimb was left uninfluenced by the injection of ibotenic acid. A detailed analysis revealed the emergence of two new high threshold finger ICMS sites at sites irresponsive to pre-lesion ICMS (51 - 80µA), both of them lying in the prospective penumbra zone of the lesion in M1. Post-lesion, 3 finger sites became irresponsive to ICMS. Several sites keeping the same threshold changed their target muscles from fingers to neck (1), to face (5), to tail (1), to shoulder (2), to elbow (3) to wrist (5). Another group of ICMS sites changed to higher thresholds, while changing in parallel the target muscle from fingers to wrist and elbow (1), to wrist (1). One ICMS site still controlled the fingers but at a higher threshold. Obviously, the core of the lesion in control monkey MK5-R was less dramatic and less clearly circumscribed than in MK1-G. Part of this observation can probably be explained by the side effects of the post-lesion antiepileptic treatment in MK5-R (see discussion Figure 4.1 and Table 4.1).

_____

C. **Monkey MK7-C**

(data taken from Lui and Rouiller, 1999).
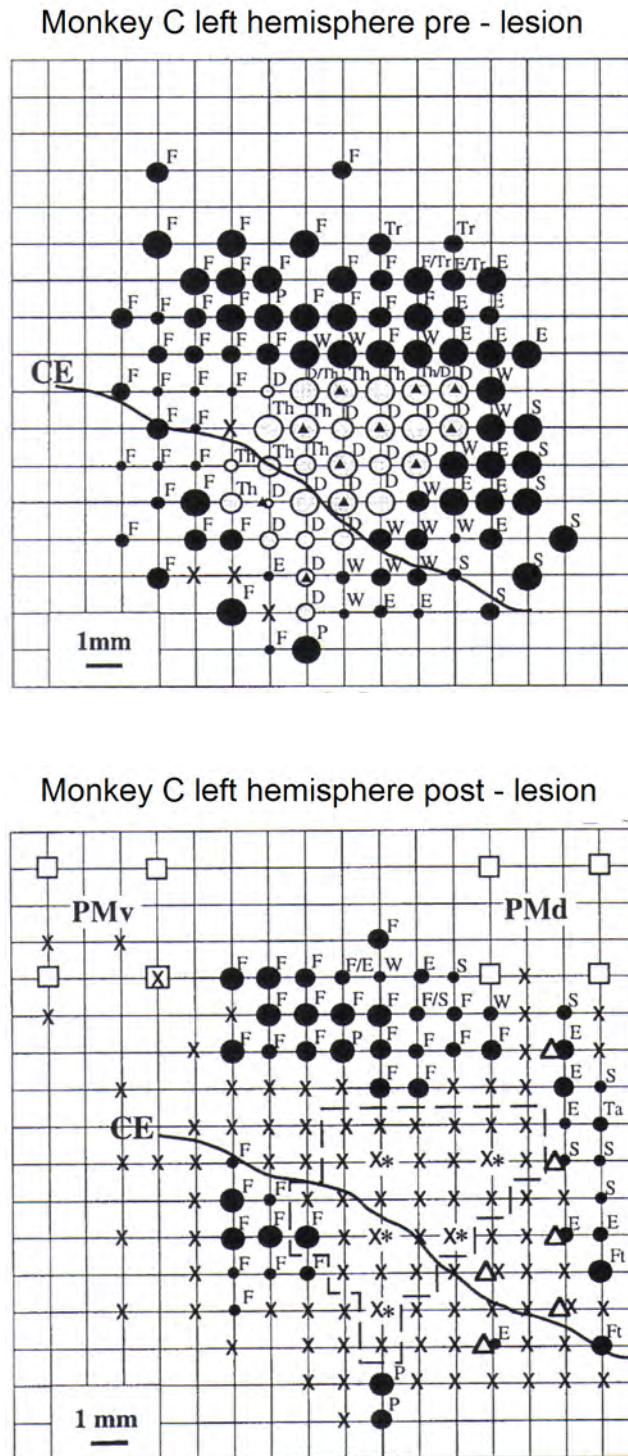
Figure 3.13: Pre- and post-lesion ICMS maps for Monkey MK7-C.

_CE_ is the contour corresponding to the position of the central sulcus, as it appears on this surface view of the cortex. Each _dot_ (_gray_ or _black_) represents the location on the brain surface of one electrode penetration. The threshold needed to induce a visible body movement is indicated by the diameter of the dot (see _key_ at bottom of figure). The movement elicited at the threshold is given at the top-right of each dot: _D_ digit, _E_ elbow, _F_ face, _Ft_ foot, _H_ hip, _L_ leg, _P_ pinna, _S_ shoulder, _Ta_ tail, _Tg_ tongue, _Th_ thumb, _Tr_ trunk, _W_ wrist, _X_ no visible movement at the highest intensity tested (90 µA). Black filled triangles=Site where ibotenic acid was injected after mapping to achieve chemical lesion of the hand representation. The hand area (where ICMS elicited at threshold finger movements) is indicated by _gray_ dots, as opposed to _black_ dots for other body parts. Anterior is to the top, posterior is to the bottom, and lateral to the left. PMd and PMv were not mapped but inferred from previous ICMS, reversible inactivation and tracing experiments (Kermadi et al 1997; Rouiller et al 1999). On the post-lesion map, for comparison, the pre-lesion hand area is outlined with a dashed line polygon.

In monkey MK7-C (Fig. 3.13), after ibotenic acid injections, as expected no response was elicited by ICMS in the left hand area delineated by pre-lesion ICMS mapping (see pre-lesion map). In addition, adjacent territories representing wrist (caudal and medial) and face (laterally) on pre-lesion map became ineffective. Pre-lesion data are not described in detail here but are comparable to those of the other monkeys presented in this thesis work.

D. **Monkey MK6-J**

(data taken from Lui and Rouiller, 1999).
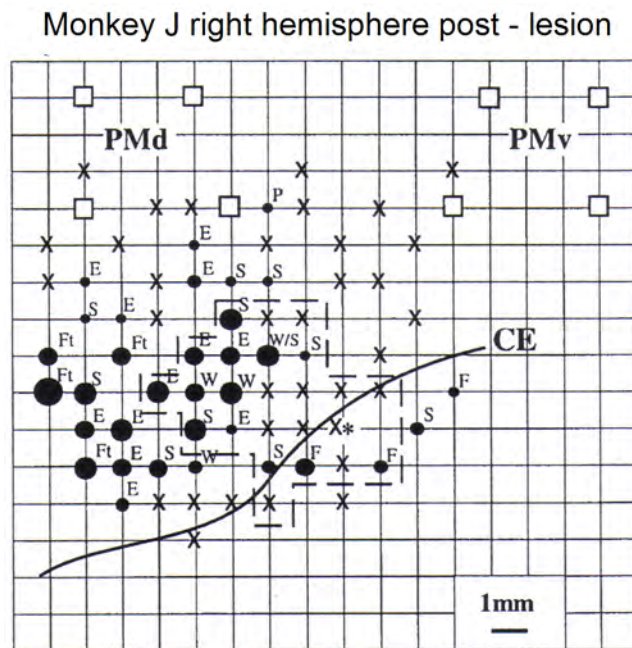
ICMS threshold (µA): ○ ● < = 10;   ○ ● 11-30;   ○ ● 31-50;   ○ ● 51-70;   ○ ● 71-90;   X: no response

Figure 3.14: Post-lesion ICMS map for Monkey MK6-J. Other conventions are the same as for monkey MK7-C, except that lateral is to the right.

In the lesioned hemisphere in monkey MK6-J, the initial hand representation was ineffective in its lateral part, whereas, surprisingly, movements of the wrist, elbow, and shoulder were elicited by ICMS in the medial part (Fig. 3.14). As in monkey C, territories surrounding the initial hand representation became less microexcitable or even ineffective, especially rostrally. The pre-lesion ICMS map of monkey MK6-J is not shown here, but it was comparable to the other monkeys.

3.2.2.3 Pre- and post-lesion ICMS maps in anti-Nogo-A antibody monkeys

A. Monkey MK2-L
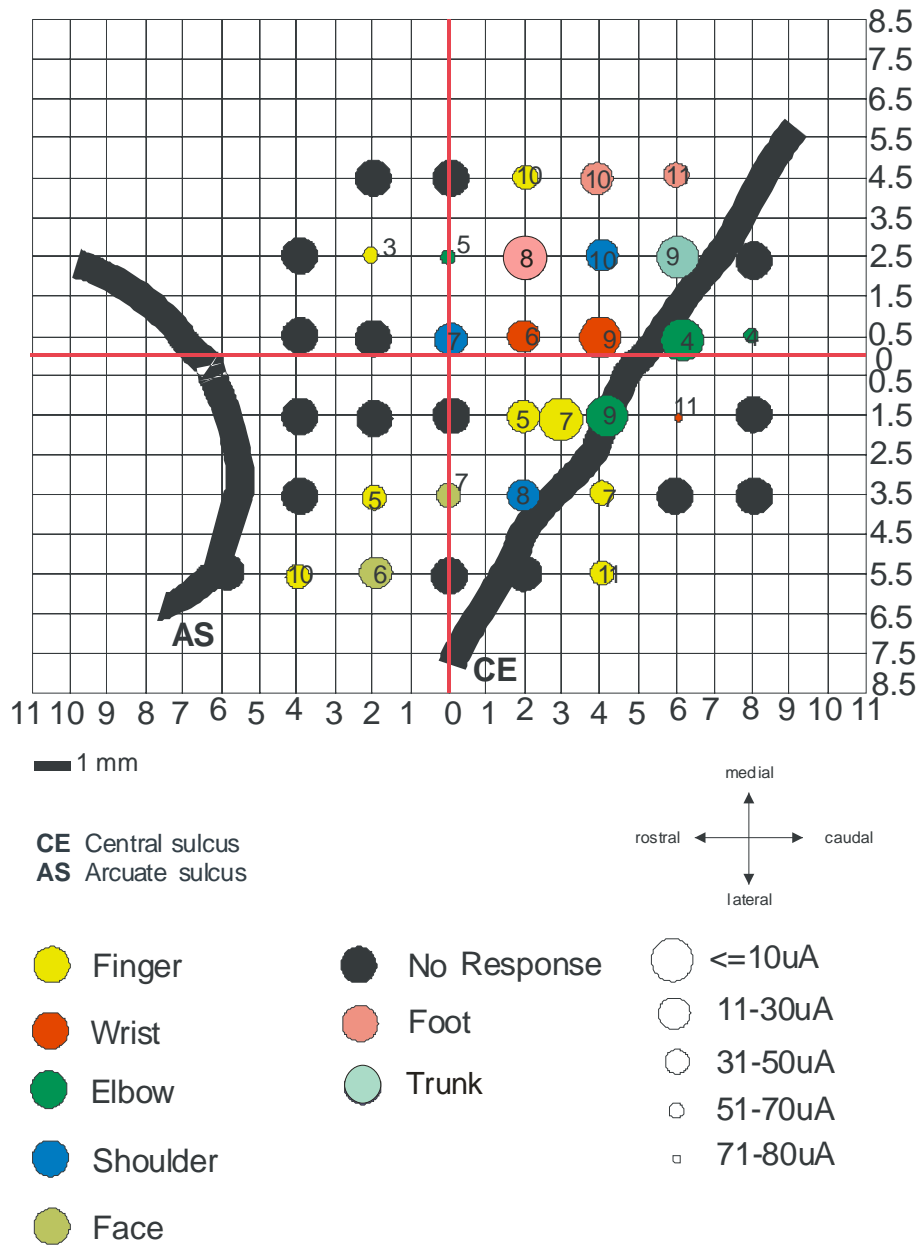
Monkey MK2-L Pre-Lesion
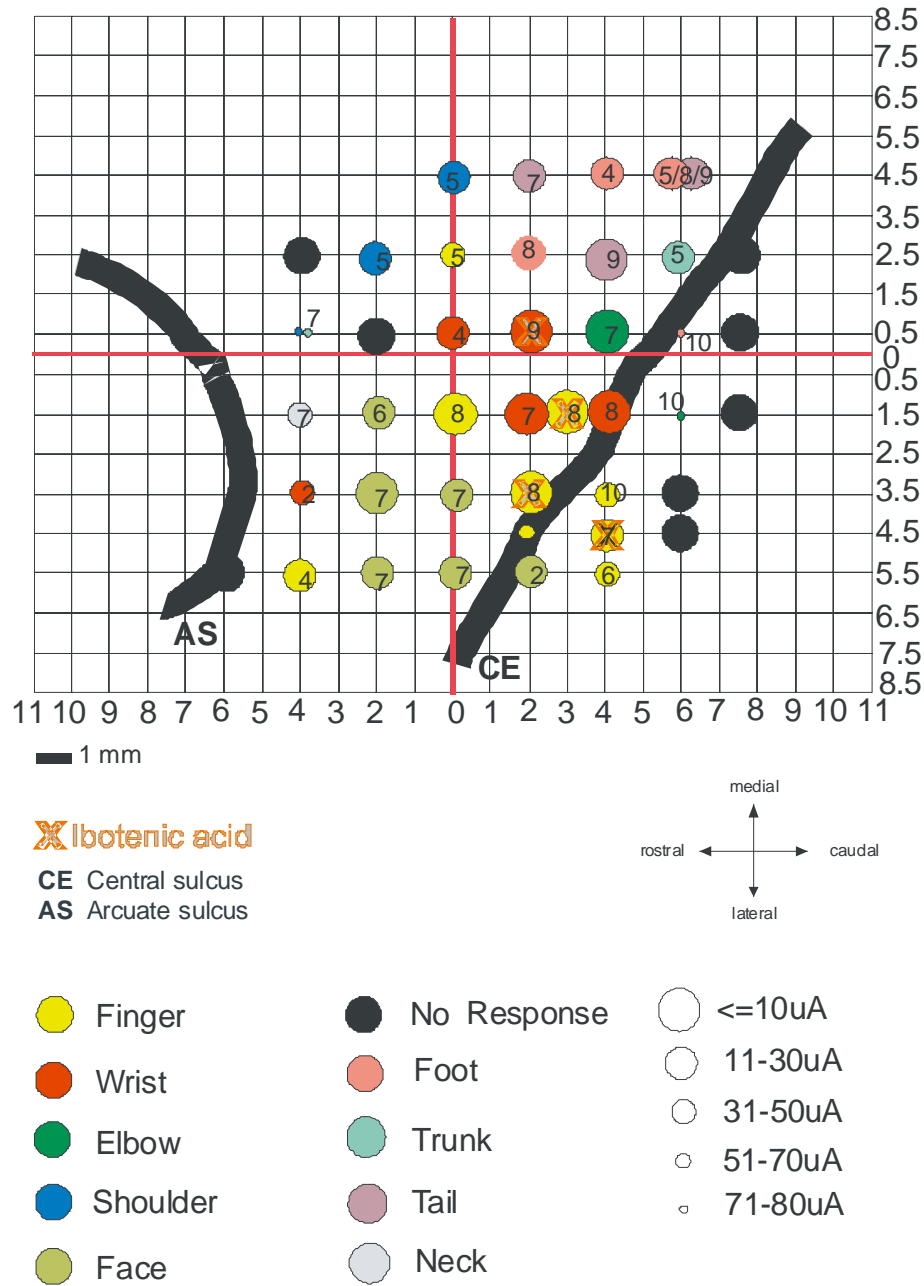
Figure 3.15: Pre- and post-lesion ICMS maps for Monkey MK2-L.

_____

In spite of the limited number of sites visited, the hand representing area in M1 could be determined in Monkey MK2-L (Fig. 3.15). Rostral and caudal, close to the central sulcus, sites eliciting finger movements can be seen. These sites are surrounded by wrist, elbow, and shoulder. Most medial, some sites evoking foot movements in ICMS are present. Rostro-medial to M1, there are two sites (finger and elbow) with higher thresholds (≥ 50 µA) close to the surface of the brain (depth of 3 – 5 mm). Probably these sites can be attributed to PMd. Two additional sites, showing higher thresholds as compared to the majority (≤ 10 µA), are situated rostro-lateral to the face represention area of M1, close to the arcuate sulcus. Maybe they already belong to PMv.

After injections of ibotenic acid in four sites inside the hand representing area of M1 targeting wrist and fingers, no obvious changes in the post-lesion mapping can be seen (Fig. 3.15). This observation is in line with the very small lesion size in this particular monkey (see chapter 3.1). However, the two sites inside PMd show reduced ICMS thresholds, as compared to the pre-lesion map. This could indicate plastic changes in PMd. Also in line with the small size of the lesion, in this monkey, the post-lesion ICMS elicited finger and wrist movements at very low thresholds (not different from pre-lesion thresholds) at the sites of ibotenic acid injection (Fig. 3.15). The latter observation suggests that the ibotenic acid was ineffective or did not reach the cerebral cortex (may injected in the thickened dura).

B. Monkey MK3-V

Monkey MK3-V Pre-Lesion
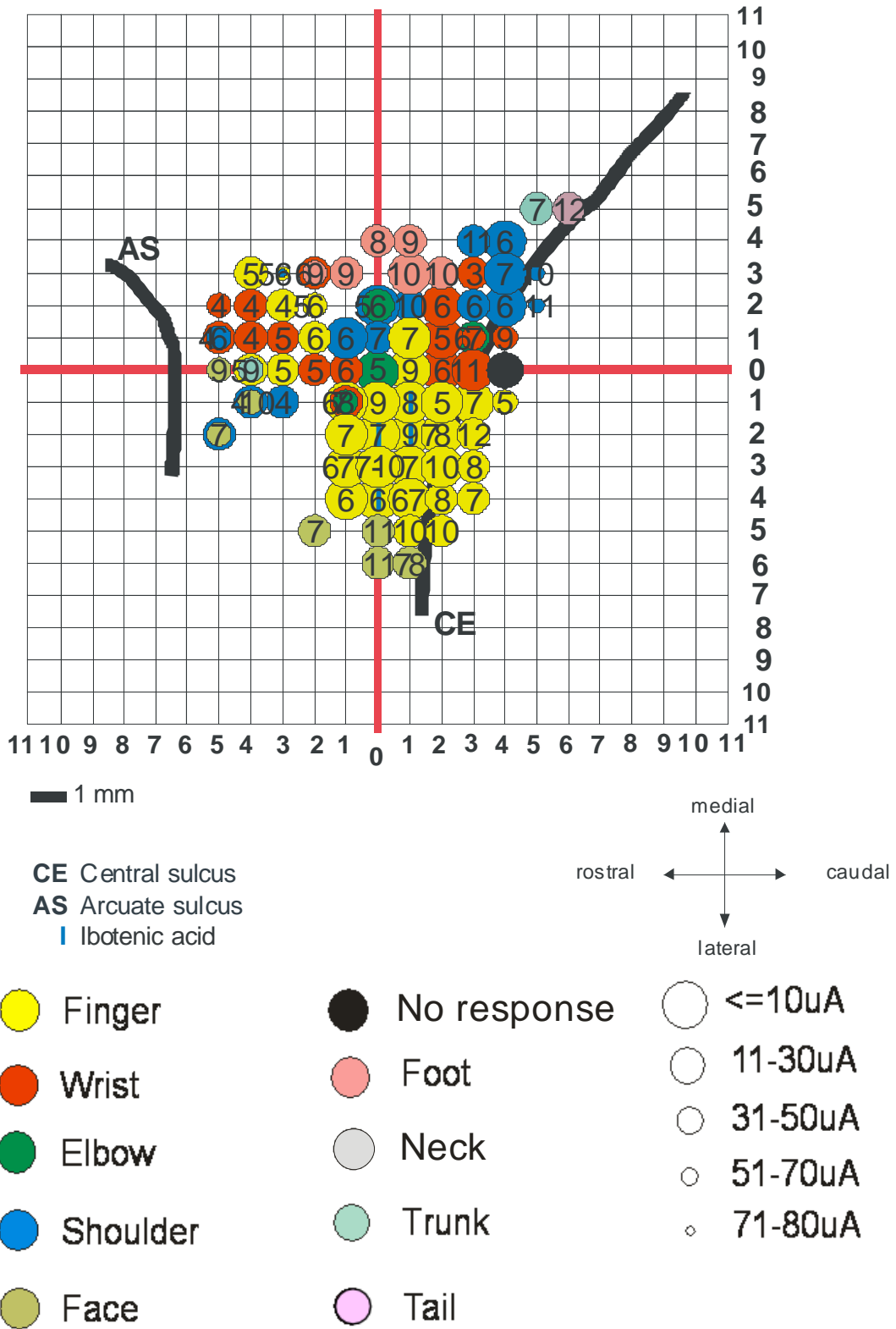
Monkey MK3-V Post-Lesion
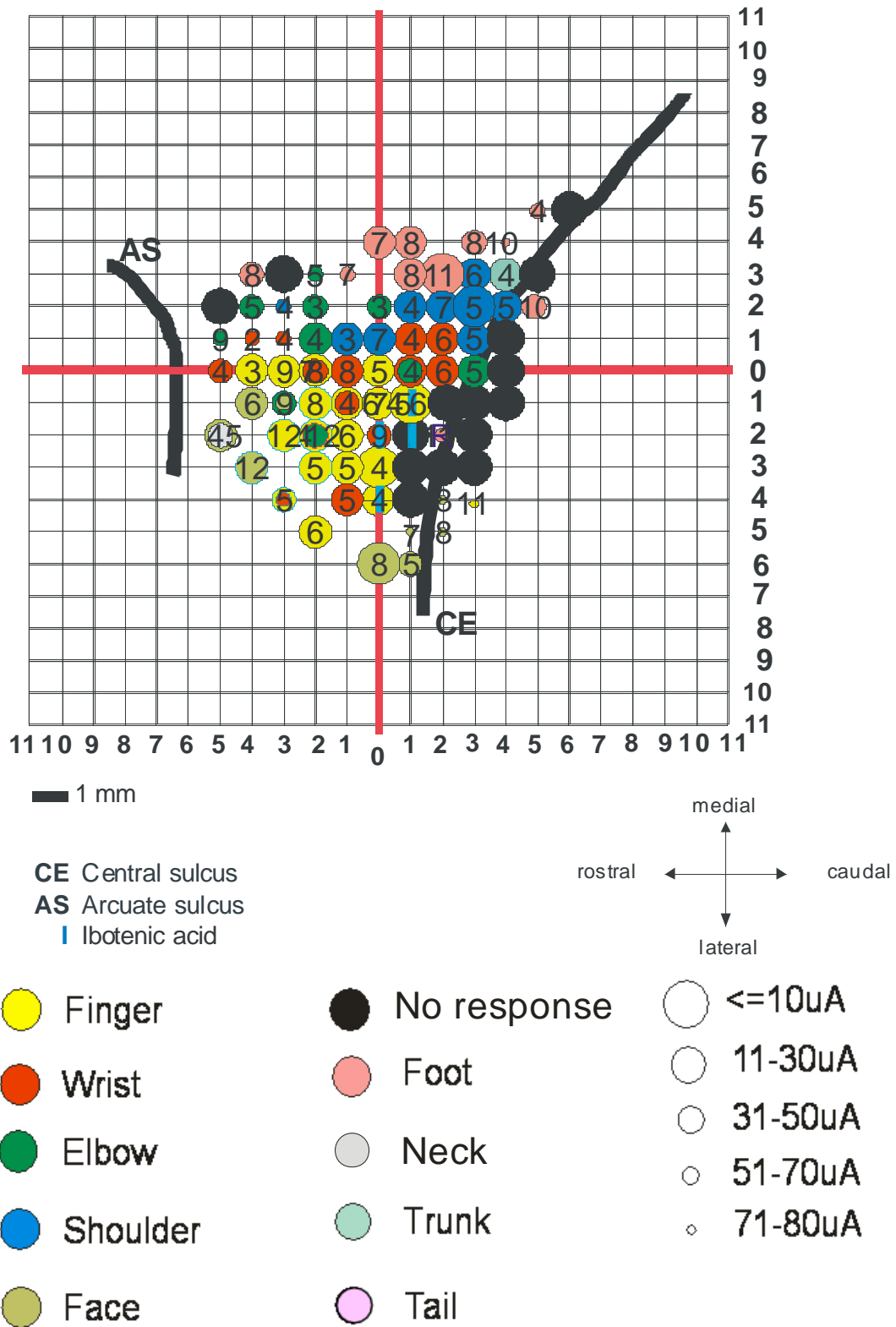
Figure 3.16: Pre- and post-lesion ICMS maps for Monkey MK3-V.

On the pre-lesion map of the anti-Nogo-A antibody treated monkey MK3-V (Fig. 3.16), the hand area is situated along the central gyrus, lateral to M1. Caudal to this area, there is a region for the wrist and the shoulder, with a small region for the elbow. ICMS thresholds are generally situated below 10μA.

After injection of ibotenic acid in five ICMS sites of the hand area and treatment with anti-Nogo-A antibody, the ICMS mapping shows a non responding area along the central gyrus. Rostral to it, there is a responding area for digits situated on sites of lesion. The hand area has not disappeared, but thresholds have been elevated up to 11-50μA. There is a reorganization of the wrist, shoulder and elbow territories lateral to their original site. The ICMS mapping of the anti-Nogo-A antibody treated monkey MK3-V shows less diminution of micro-excitable hand area and ICMS thresholds are lower than in untreated (control) monkeys.

C. Monkey MK4-S
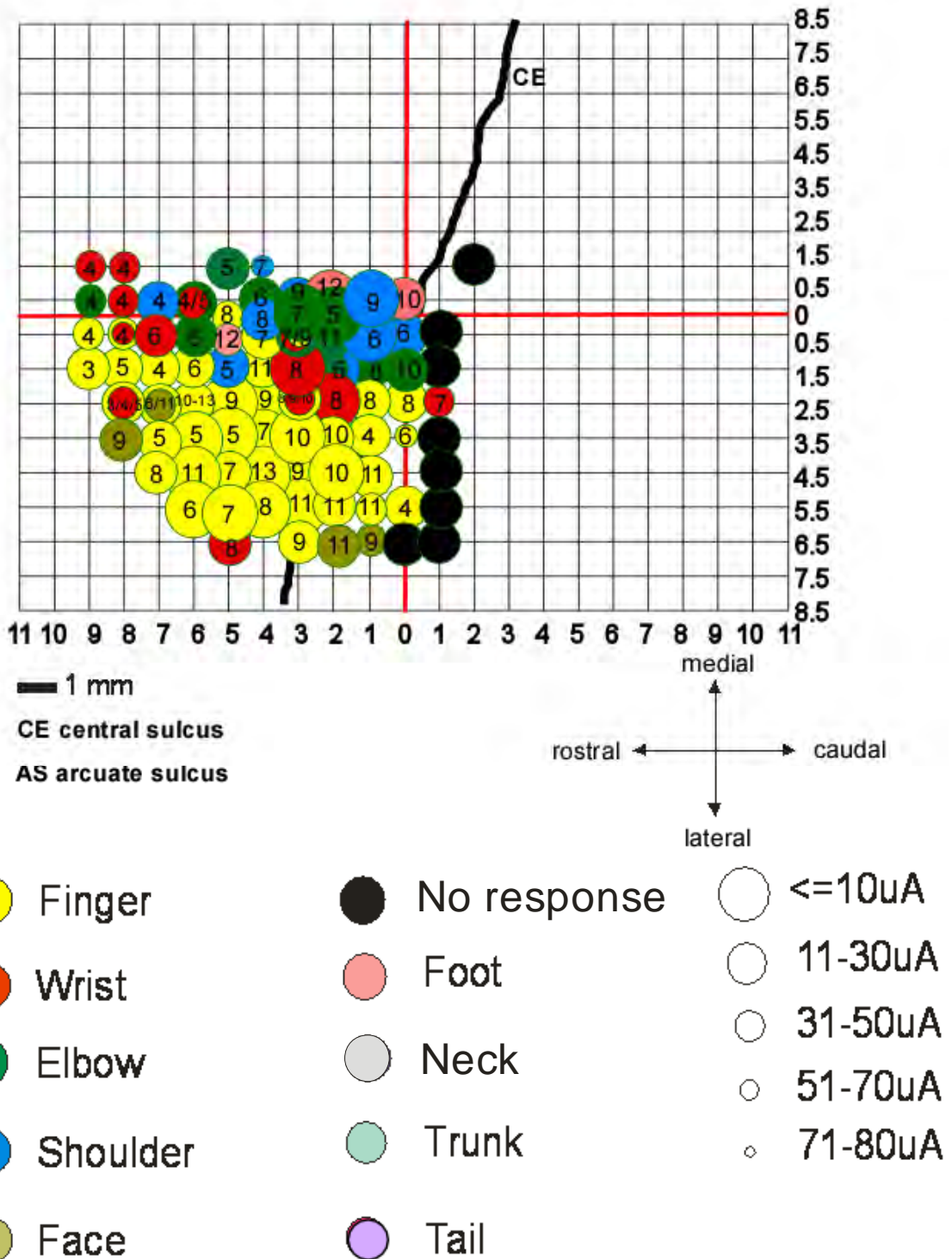
Monkey MK4-S Pre-Lesion
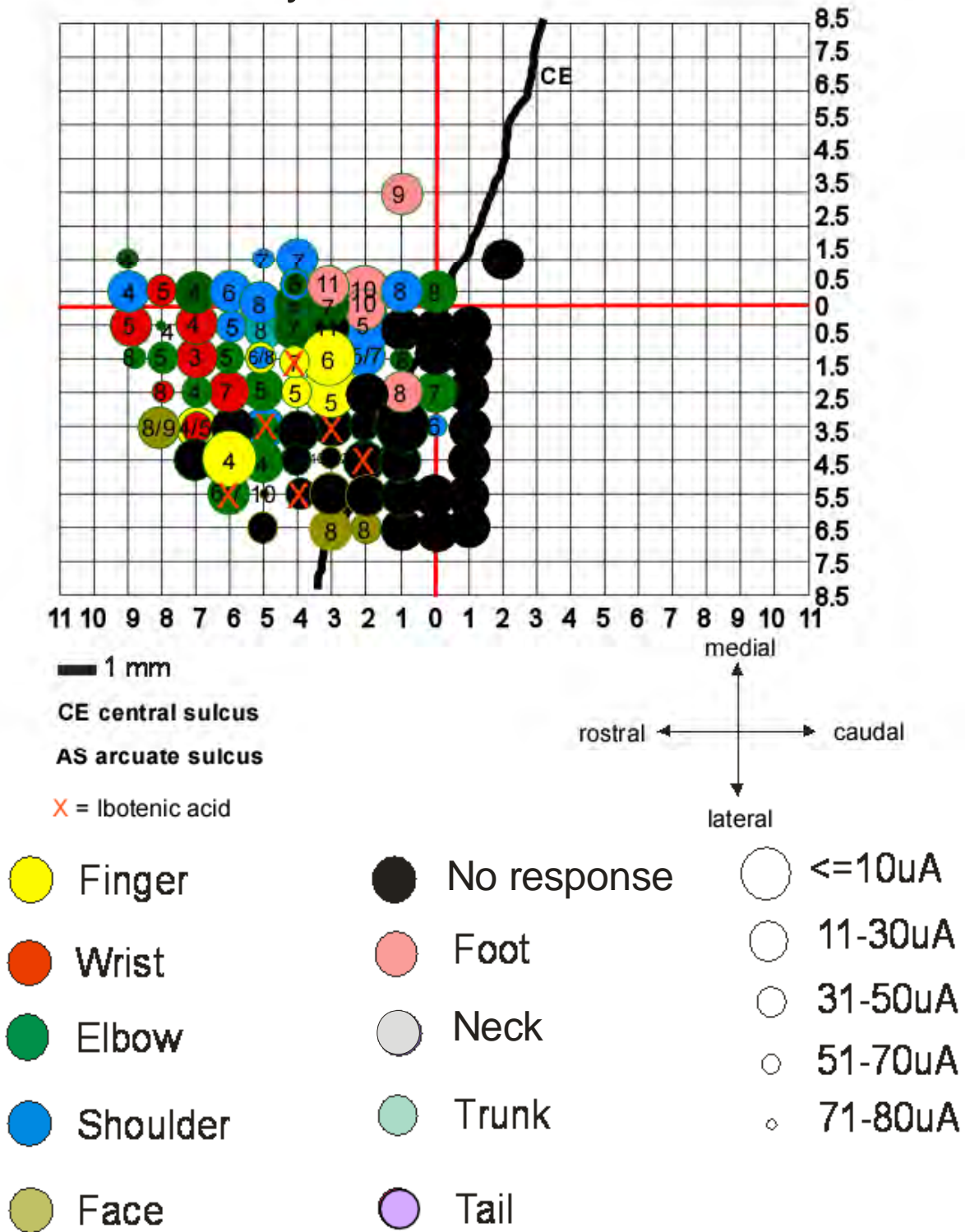
Figure 3.17: Pre- and post-lesion ICMS maps for Monkey MK4-S.

In this monkey MK4-S, because the implanted chamber was placed more caudal than in the other animals, accessing PMv by ICMS was not possible. As in monkey MK5-R, an extensive ICMS mapping was performed covering most areas of M1 as well as the more lateral parts of PMd (Fig. 3.17). ICMS thresholds in M1 are mainly at $\leq 10\ \mu A$ whereas, in PMd, movements at the majority of sites were elicited at slightly higher thresholds of about 11–30 µA. About 75% of the big finger representing area in M1 is situated rostral to the central sulcus. Approximately 15 % of the finger representation can be found caudal to the central sulcus. Towards medial, the finger representation is surrounded by wrist, elbow and shoulder representation whereas, rostro-lateral, some face representation can be seen. For sure we did not explore the complete face area of M1. Medio-rostral to the finger representation, there are sites inside PMd representing finger, wrist and elbow (Fig. 3.17).

After injection of ibotenic acid in six tracks of finger representing ICMS sites, substantial changes in the post-lesion ICMS map could be observed. As a result of the lesion, a big part of the finger sites rostral and caudal to the central sulcus became irresponsive to maximal electrical stimulation of 80 µA (Fig. 3.17). In contrast to control animals, in this anti-Nogo-A antibody treated monkey the finger representation was not completely lost. At the most medial injection site, a finger response is still present post-lesion, although the threshold is higher. At the two most rostral sites of ibotenic acid injections, ICMS elicited elbow movements instead of finger movements at slightly higher thresholds as compared to the pre-lesion situation. In the putative PMd area, in the rostro-medial corner of all responses represented in the post-lesion map, a tendency for a shift to more proximal responses and higher thresholds can be observed. This is true for the remaining responsive sites in M1 as well.

_____

3.2.2.4 Sites and diffusion pattern of ibotenic acid injections

Here only the post-lesion ICMS maps for monkeys MK1-G, MK2-L, MK3-V, and MK4-S are represented (Figs. 3.18 to 3.21). On each ICMS map, the sites where ibotenic acid was injected are indicated by an orange X. The orange circles around the corresponding injection sites delimit the theoretical maximal range of diffusion. Such theoretical diffusion extent can be used as a help to estimate the territory touched by the chemical lesion. But because the brain tissue is not a homogeneous mass, the diffusion characteristics do not exactly fit with theory. Probably varying proportions of glia cells, neuronal cells, and fibers in the white matter as well as the composition of the extracellular matrix may influence the diffusion of ibotenic acid. The gyri and sulci also have an important impact on diffusion. As can be seen on the ICMS maps of monkey MK4-S (Fig. 3.18) and MK3-V (Fig. 3.19), one gets the impression of a caudal shift of the effective lesion as compared to the theoretical diffusion range. The reason for that may be that injections were made close or even in the central sulcus. As a consequence, the ibotenic acid may have traveled longer distances in the cerebrospinal fluid. In contrast, in monkey MK1-G (Figure 3.20), the effective lesion fits well with the theoretical range of diffusion. This may indicate that injections were made less close to the central sulcus targeting sites inside the rostral bank of the central sulcus. Finally, in monkey MK2-L (Figure 3.21), there seems to be no lesion, neither inside nor outside the theoretical range of diffusion. This is consistent with the histology which showed that there was nearly no lesion in this animal.
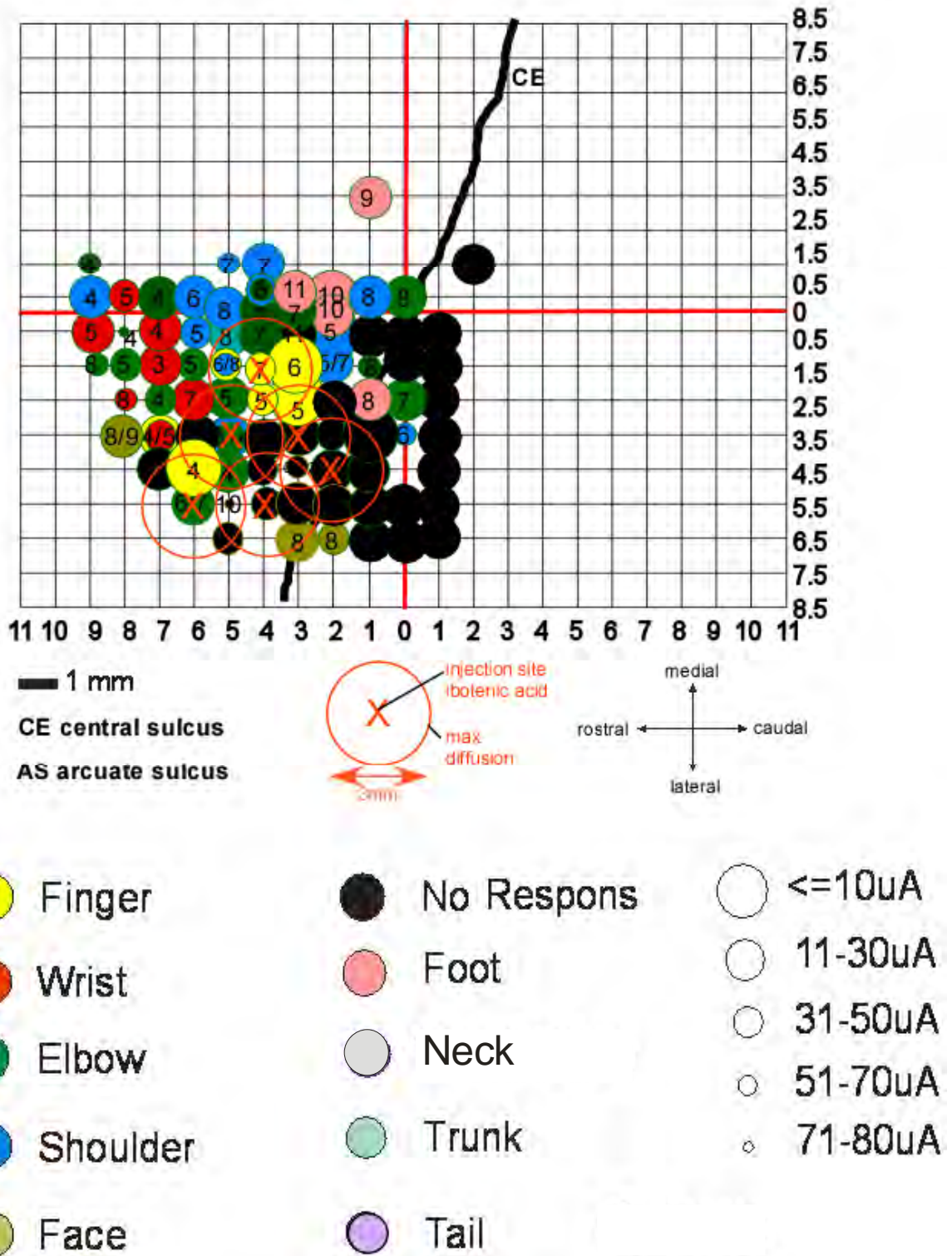
Figure 3.18: Diffusion of ibotenic acid in Monkey MK4-S.
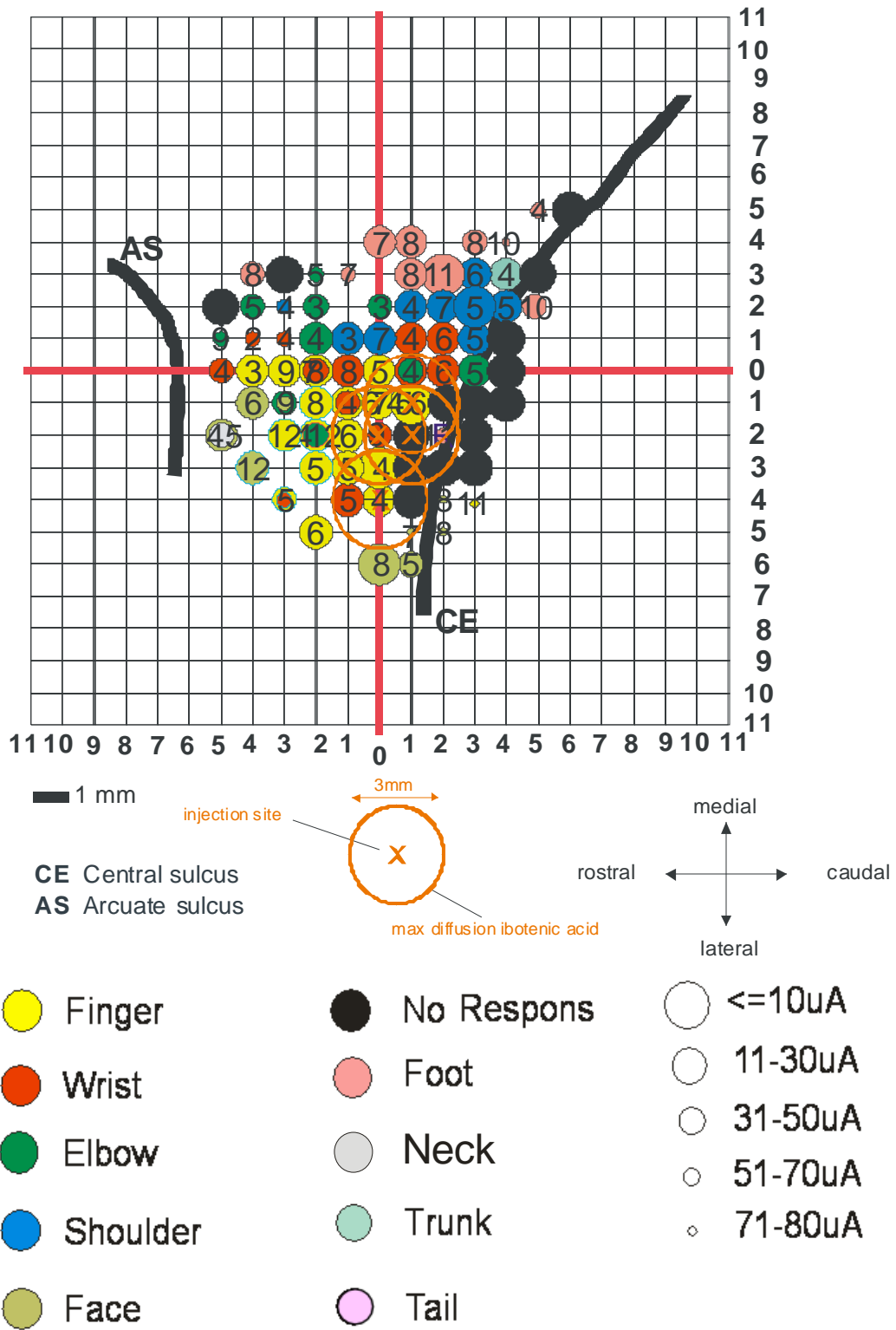
Figure 3.19: Diffusion of ibotenic acid in Monkey MK3-V.
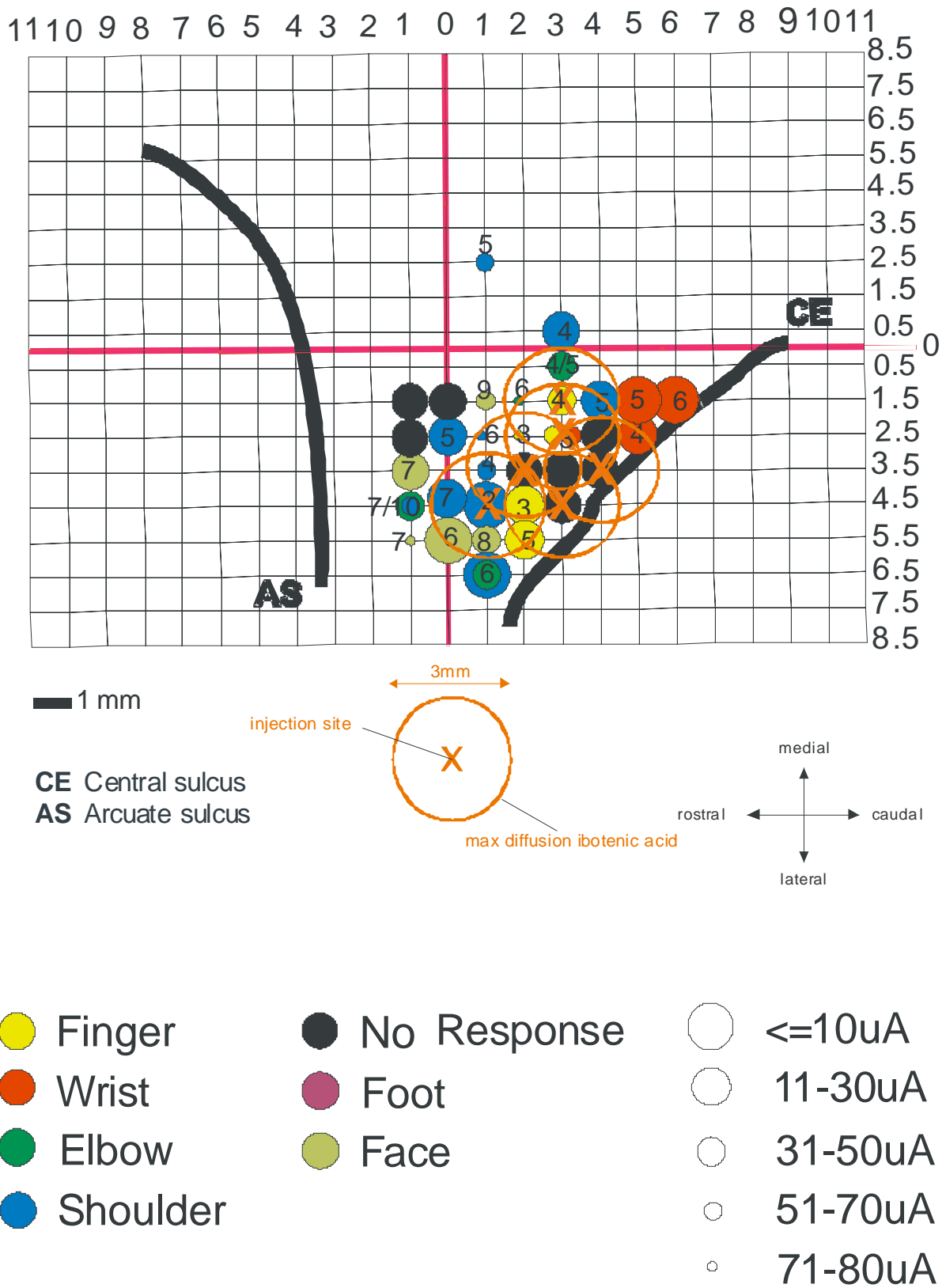
Figure 3.20: Diffusion of ibotenic acid in Monkey MK1-G.
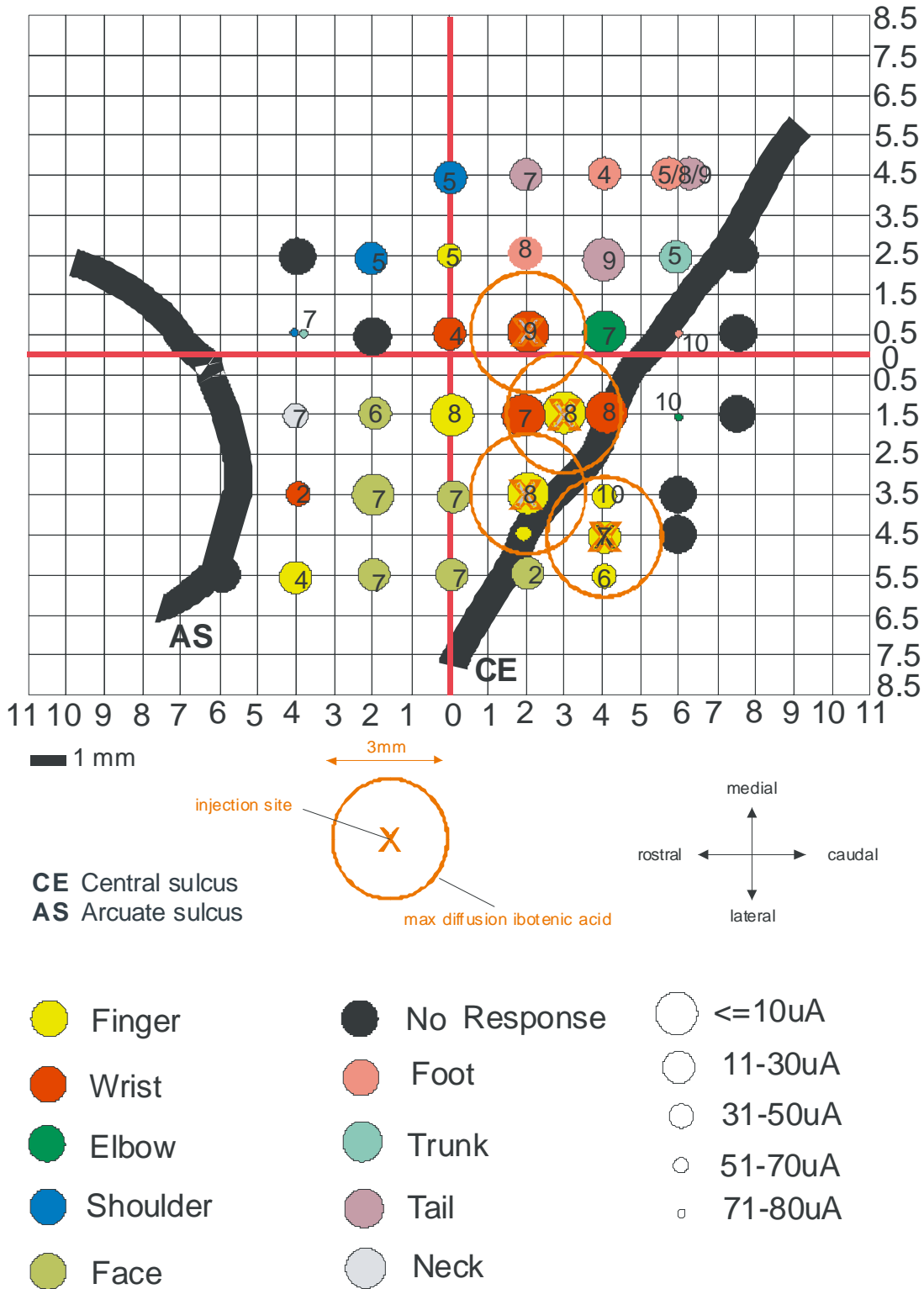
Figure 3.21: Diffusion of ibotenic acid in Monkey MK2-L.

_____

3.2.2.5 Positioning of ICMS maps on brain surface

Post mortem the whole brain of each monkey was isolated and fixated as described in the method part of this thesis work. In the Figure 3.22 below, photos of the brains of individual monkeys are shown, on which the pre-and post-lesion ICMS maps were placed. For this purpose every map was rescaled according to the scale of the entire brain. Then, each map was positioned on the brain surface with respect to anatomical reference points (arcuate sulcus and central sulcus). Panels A-E of Figure 3.22 represent the untreated control monkeys (MK1-G, MK6-J, MK7-C) whereas Panels F-K of Fig. 3.22 represent the anti-Nogo-A antibody treated monkeys (MK2-L, MK3-V, MK4-S). In general, it is important to note that the shape and the position of the approximated sulci (arcuate sulcus and central sulcus) used as references during ICMS mapping fit well with the anatomically correct shape of these sulci. This underlines the high precision of ICMS mapping conducted in all monkeys used in this thesis work. Overall, the ICMS points eliciting finger movements are located on the brain views at a location which is coherent with what is expected from previous series of monkeys.

Figure 3.22: (panels A to K on next pages).
In each Panel, except Panel C where a side-view of the right hemisphere is shown (because the lesion monkey MK6-J was on the right M1), a side-view of the left lesioned hemisphere of the entire brain is shown. In addition, the dorsal parts of the corresponding opposite hemispheres are represented as well. Note also that, in monkey MK6-J, only the post-lesion ICMS map was placed on the brain surface. In Panels C-E, the motor cortex areas were zoomed out in a separate picture for better visibility of the corresponding superimposed ICMS maps. Rostral is to the left (MK6-J to the right), caudal to the right (MK6-J to the left), dorsal to the top. Conventions for the ICMS maps are the same as lined out in paragraph 3.2.2.2.

_____

Fig. 3.22 Panel A

Monkey MK1-G pre - lesion

Fig. 3.22 Panel B
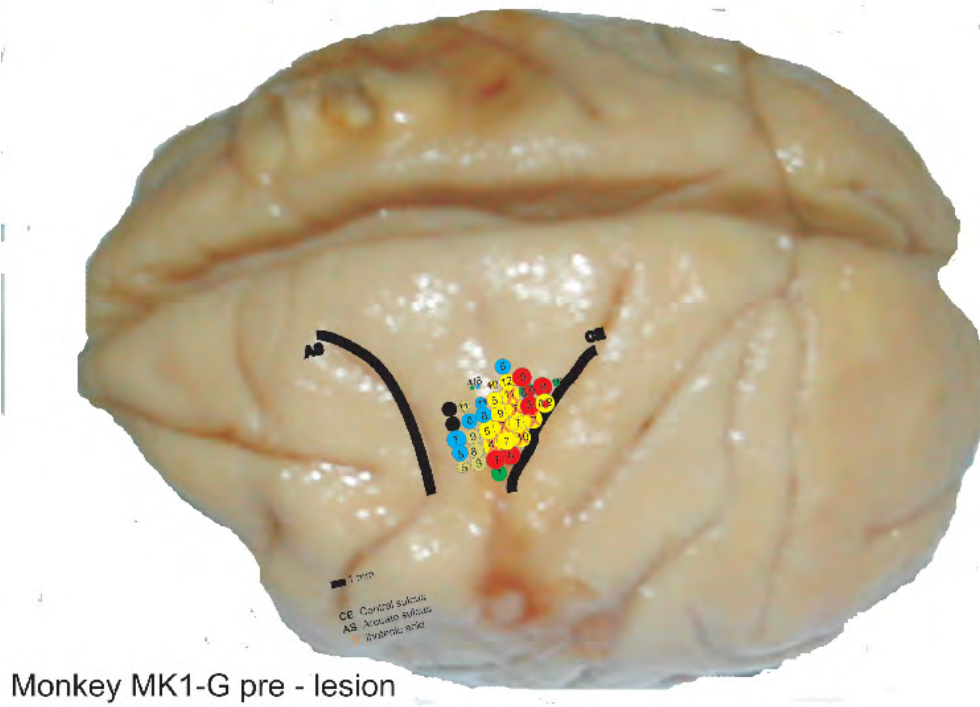
Monkey MK1-G post - lesion
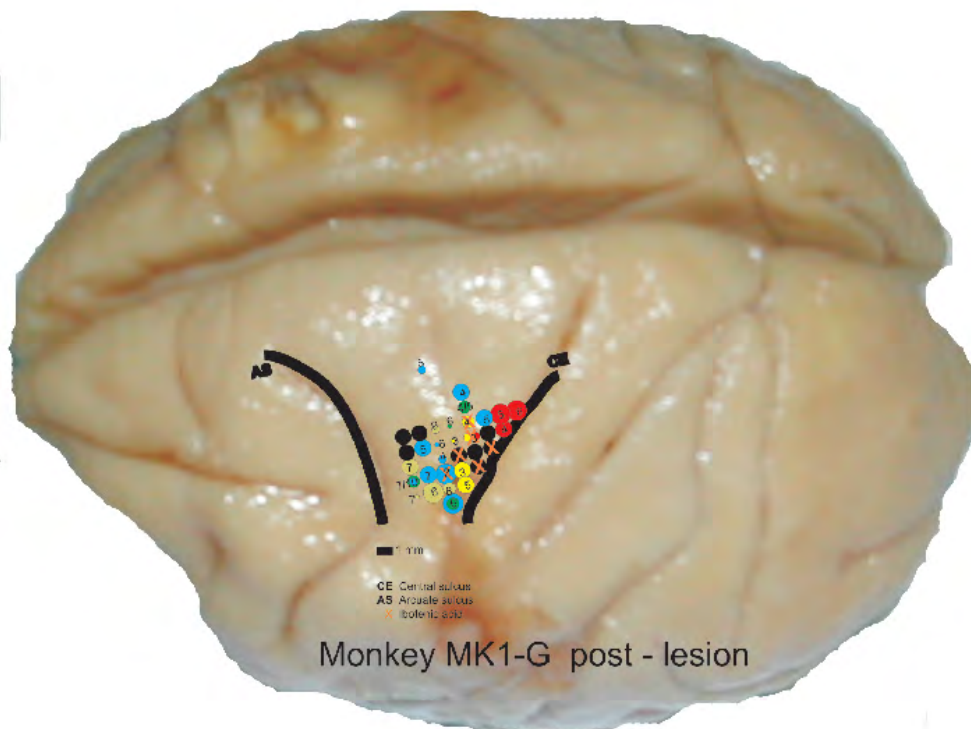
Fig. 3.22 Panel C

AS Arcuate sulcus
CE Central sulcus
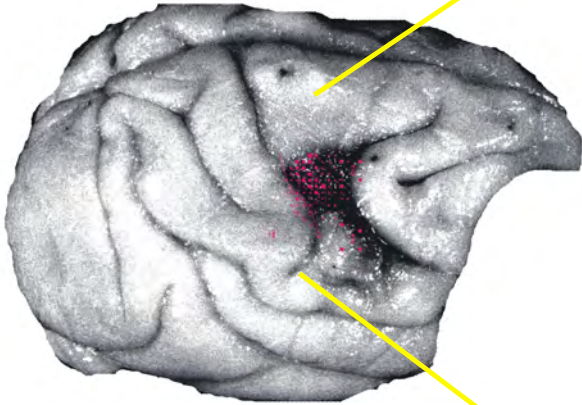
Monkey MK6-J post - lesion

_____
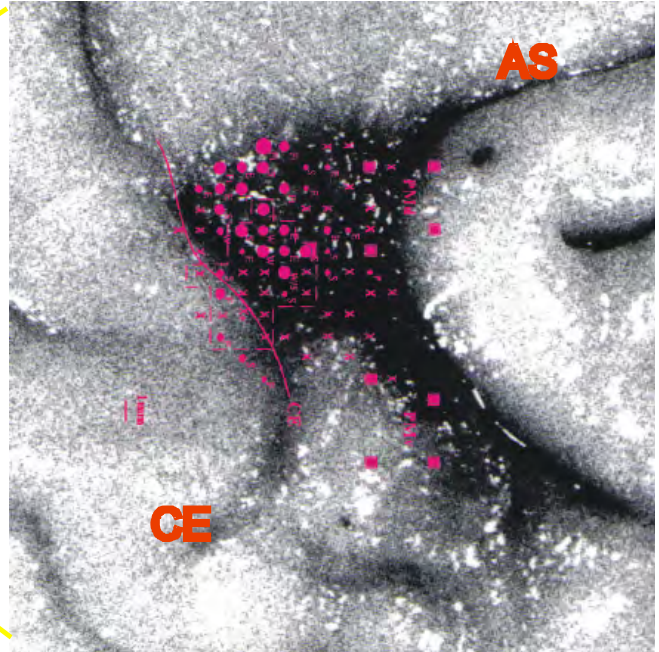
Fig. 3.22 Panel D
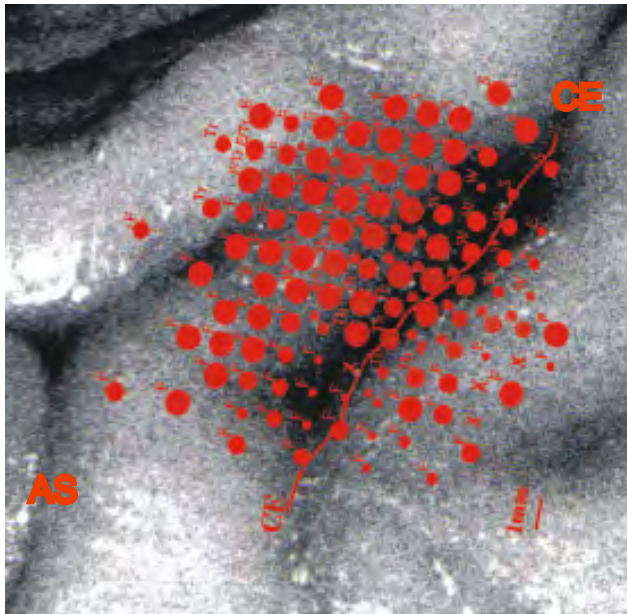
AS Arcuate sulcus
CE Central sulcus
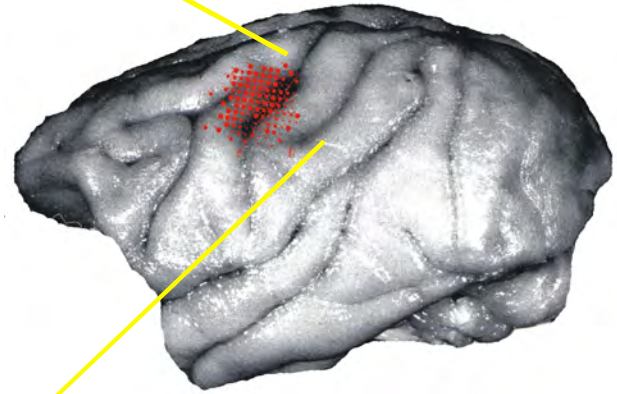
Monkey MK7-C pre - lesion

Fig. 3.22 Panel E
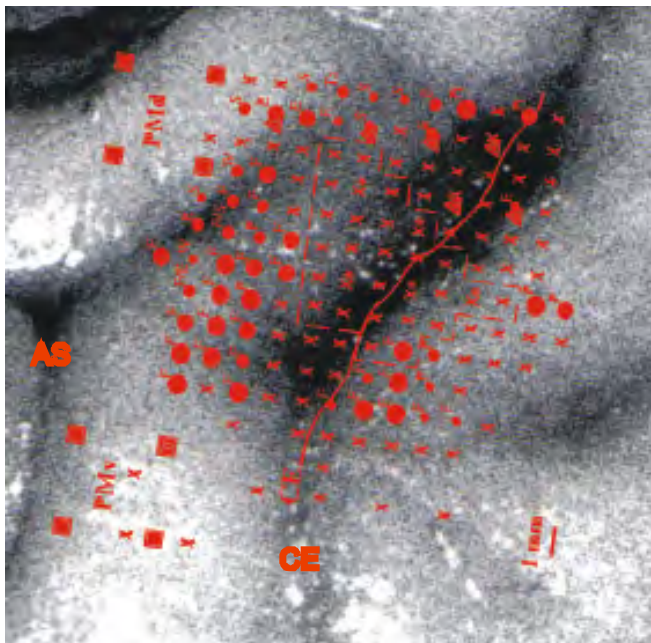
AS Arcuate sulcus
CE Central sulcus
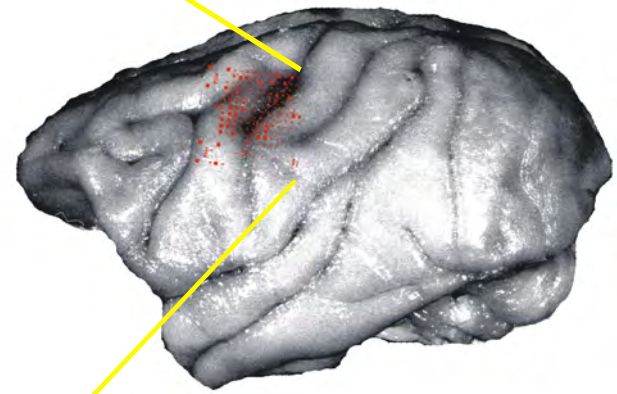
Monkey MK7-C post - lesion

_____

Fig. 3.22 Panel F

Monkey MK2-L pre - lesion

Fig. 3.22 Panel G
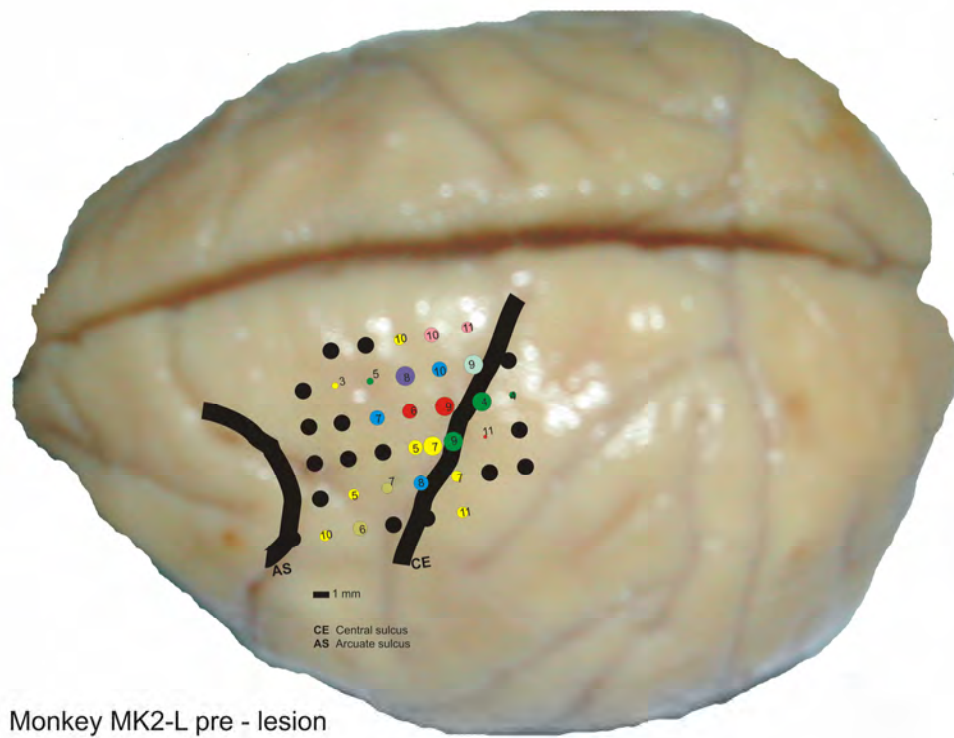
Monkey L Post - Lesion left
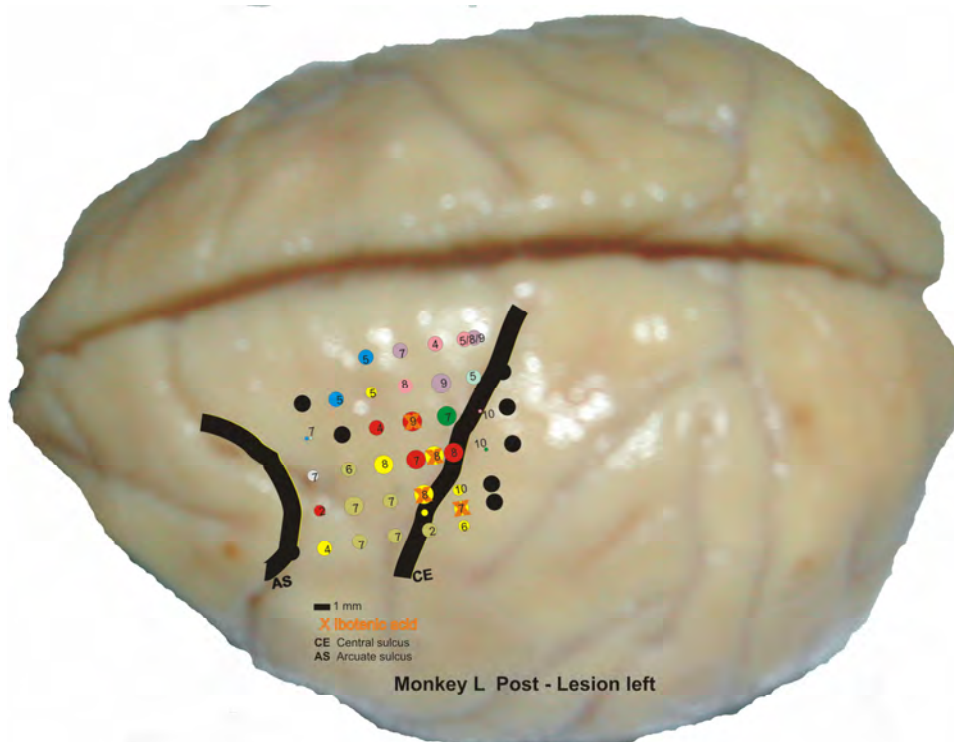
Fig. 3.22 Panel H

Monkey MK3-V pre - lesion

--- 1mm

Fig. 3.22 Panel I

CE Central sulcus
AS Arcuate sulcus
i Ibotenic acid
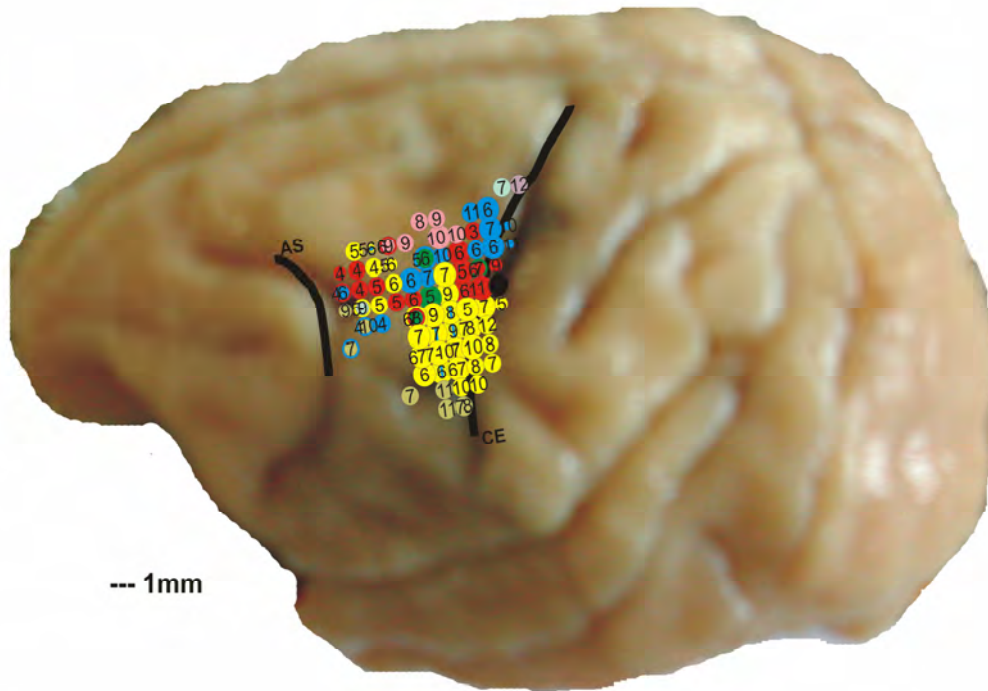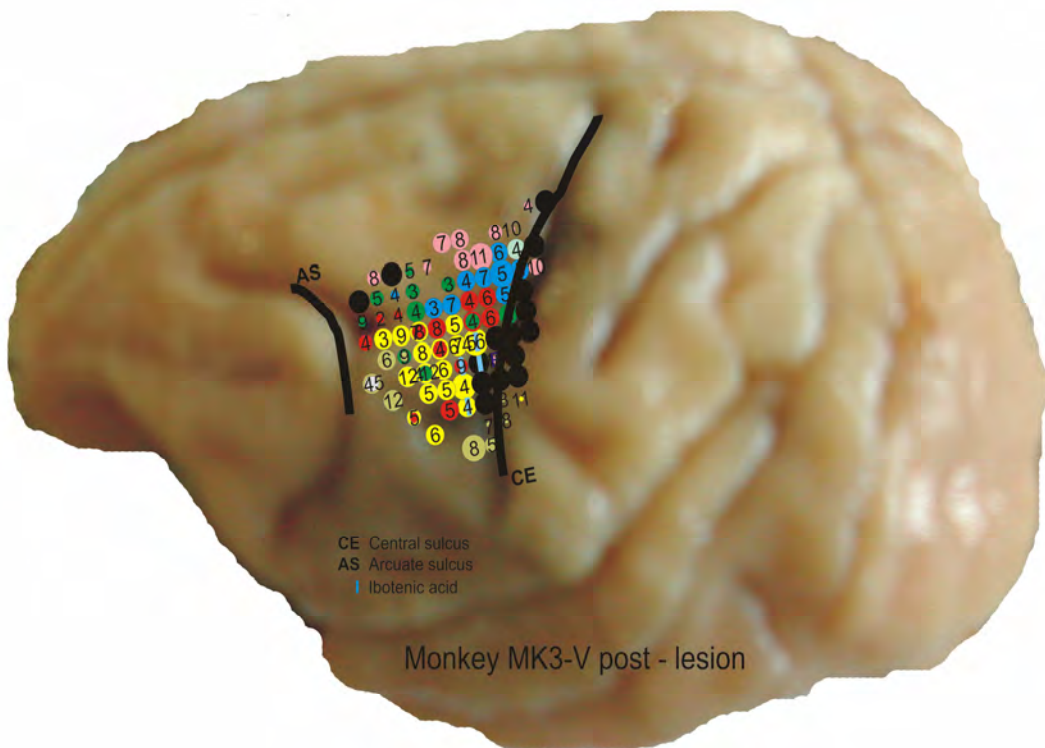
Monkey MK3-V post - lesion

— 1mm

_____

Fig. 3.22 Panel J

Monkey MK4-S pre -lesion

Fig. 3.22 Panel K

Monkey MK4-S post - lesion
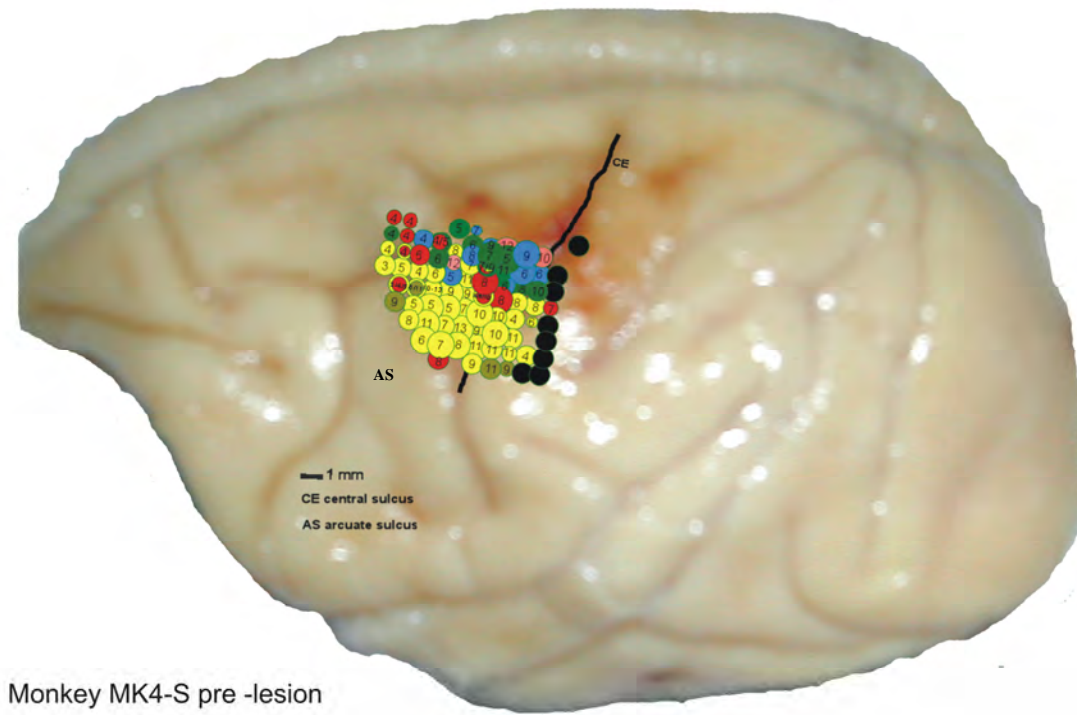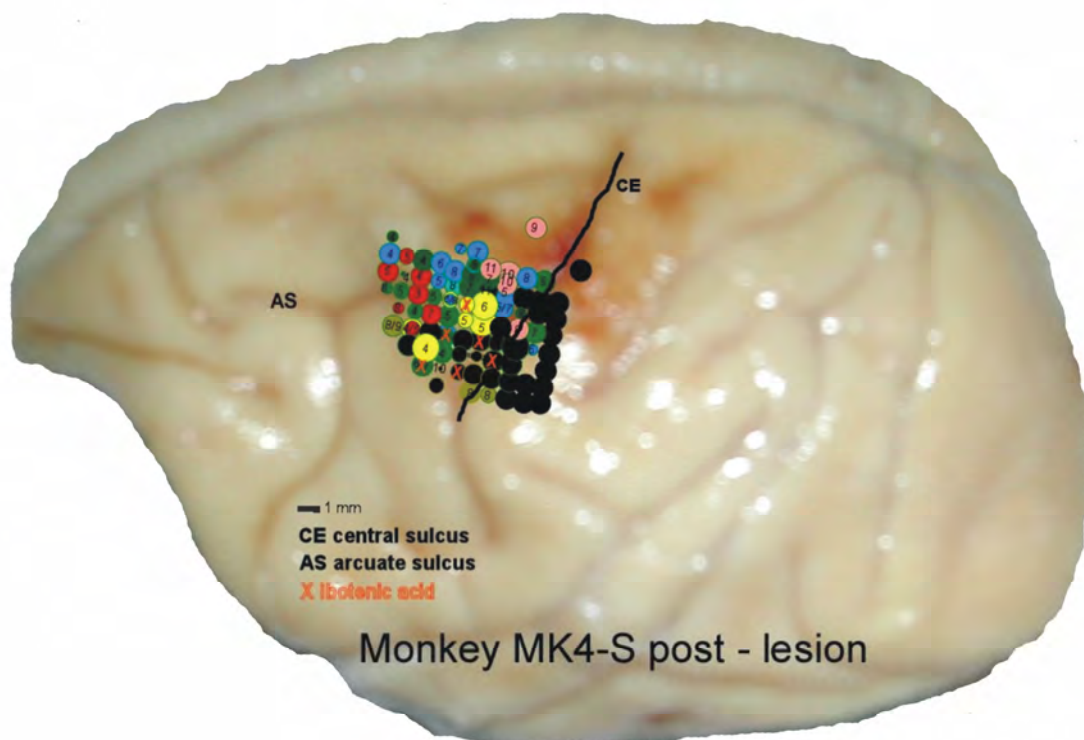
Figure 3.22: Positioning of ICMS maps on brain surface

_____

3.2.2.6 Positioning of post-lesion ICMS maps on lesion reconstructions

For this purpose, every post-lesion ICMS map was rescaled according to the scale of the brain reconstructions. Then, each map was positioned on the corresponding reconstruction with respect to anatomical reference points (arcuate sulcus and central sulcus). Panels A-C in Fig. 3.23 represent the untreated control monkeys (MK1-G, MK6-J, MK7-C) whereas Panels D-F in Fig. 3.23 represent the anti-Nogo-A antibody treated monkeys (MK2-L, MK3-V, MK4-S). The aim of these representations was to investigate whether histological data confirm the findings of ICMS mapping. In fact they do for all monkeys analyzed. As can be seen in Panels A-F of Figure 3.23, black dots (in Panels A and D-F) and X (in Panels B and C), representing non-responsive ICMS sites in the hand representing area of M1 at maximal stimulation (80µA respectively 90 µA) are in majority lying inside the lesion territory (red vertical bars). Note that the non-responsive sites in monkey MK2-L in the caudal bank of the central sulcus were already irresponsive before the ibotenic acid was infused (compare with Panels A and B in Figure 3.22). In contrast, the injection sites of ibotenic acid in monkey MK2-L are perfectly situated inside the lesion territory. One may argue, why in MK2-L it was still possible to elicit low threshold responses inside the lesioned area. As already discussed above, in this monkey, the lesion was extremely small. Thus stimulation current may have stimulated adjacent cortical areas, explaining the observed responses in ICMS sessions. For all monkeys one has to note that, because ICMS responses were projected on the brain surface, the real lesion extend may have been underestimated (especially inside the central sulcus) explaining the smaller lesion areas derived from post-lesion ICMS maps as compared to the effective lesion size revealed from histology.

Figure 3.23: (panels A-F on next pages)
In each Panel, except Panel C where a reconstruction of the right hemisphere is shown (because the lesion in monkey MK6-J was in the right M1), reconstructions of the left lesioned hemisphere are shown. Rostral is to the left (MK6-J to the right), caudal to the right (MK6-J to the left), dorsal to the top. Conventions for the ICMS maps are the same as lined out in paragraph 3.2.2.2.

_____

Fig. 3.23 Panel A

CE

AS

— Cortical lesion
CE Central sulcus
AS Arcuate sulcus
X Ibotenic acid

1 mm

27   40   82

Monkey Mk1-G post - lesion

Fig. 3.23 Panel B

1 mm

Monkey Mk6-J post - lesion

— Cortical lesion   PMd dorsal premotor cortex
CE Central sulcus   PMd ventral premotor cortex
AS Arcuate sulcus

68   32

Fig. 3.23 Panel C

AR

CE

1 mm

Monkey MK7-J post - lesion

Cortical lesion
CE Central sulcus
AS Arcuate sulcus

PMd dorsal premotor cortex
PMd ventral premotor cortex

38   64

Fig. 3.23 Panel D

AS   CE

Cortical lesion
CE Central sulcus
AS Arcuate sulcus
X Ibotenic acid

15
28
46

1 mm

Monkey Mk2-L post - lesion

Fig. 3.23 Panel E

Cortical leson
CE Central sulcus
AS Arcuate sulcus
I Ibotenic acid

38 56 74

1 mm

Monkey MK3-V post - lesion

Fig. 3.23 Panel F

Gray matter lesion

Subcortical lesion

CE central sulcus

AS arcuate sulcus

X Ibotenic acid

6 16 30   1 mm

Monkey MK4-S post - lesion

Figure 3.23 Positioning of post – lesion ICMS maps on lesion reconstructions

3.2.2.7 Unfolded ICMS maps

By representing only the effect obtained by the lower stimulation current on the surface of the motor cortex for each electrode penetration we miss the anterior bank of the central sulcus were most of the forelimb area is represented. Subsequently, stimulation sites corresponding most closely to cortical layer V in the anterior bank of the central sulcus were selected from the resultant three-dimensional matrix of stimulation site data. For each electrode track, sites corresponding to cortical layer V were identified using a combination of electrode depth and current threshold of ICMS allowing a reconstruction of unfold precentral gyrus (for more description of the method see Box 1 in Chapter 2 of this thesis). For this type of representation, data analysis was restricted to the representation on forelimb M1 of distal joints (wrist and fingers) and proximal joints (elbow and shoulder) in three representative monkeys. One untreated control monkey (MK1-G) and two anti–Nogo–A antibody treaded monkeys (MK3-V and MK4-S).

_____
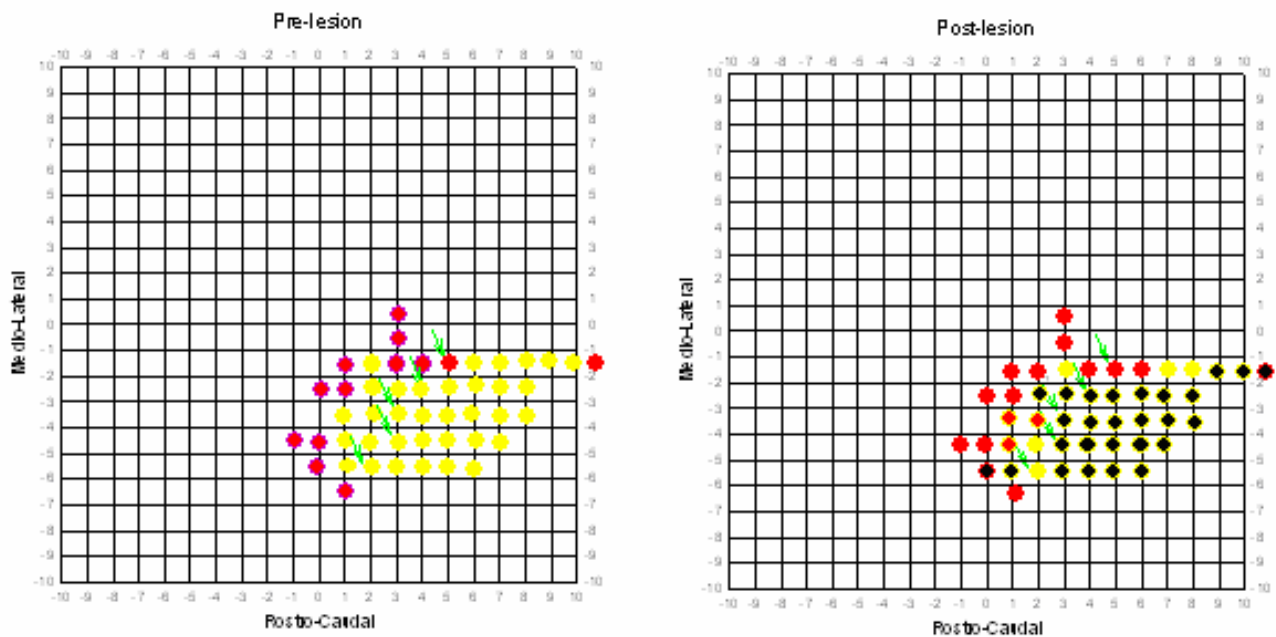
Figure 3.24: Unfolded maps of forelimb representation in M1 of untreated control monkey MK1-G. Left graph represents the pre-lesion map and Right graph represents the post-lesion map. Red circles represent proximal joints (elbow and shoulder), Yellow circles represent the distal joints (fingers and wrist) and black circles represent stimulation sites where no effect was obtained by ICMS up to 80 µA. The rostral crest of the central sulcus is indicated by small green arrows. Accordingly, responses left to the green arrows are in the cortical layer V at the surface of the rostral bank of the central sulcus. Responses right to the green arrows represent cortical layer V in the anterior bank of the central sulcus, rightmost responses partially already lying in the cortical layer of the fundus of the central sulcus (depending on the shape of the central sulcus).

On the representation shown in Figure 3.24, a central core of distal joints (finger and wrist) representation is surrounded by representation of proximal joints (shoulder and elbow). In the pre-lesion map of MK1-G, the distal forelimb area of M1 mainly lies inside the anterior bank of the central sulcus with 5 sites lying in the rostral bank close to the surface. The proximal area almost completely lies on the convexity of M1 rostral bank except one ICMS site. As can be seen from the post-lesion map, the lesion almost completely destroyed the finger representation (86%) in the rostral wall of M1, leaving only two sites intact. The proximal representation was mostly still intact post-lesion. So, in this monkey MK1-G, the chemical lesion perfectly targeted the distal representation in M1.

_____
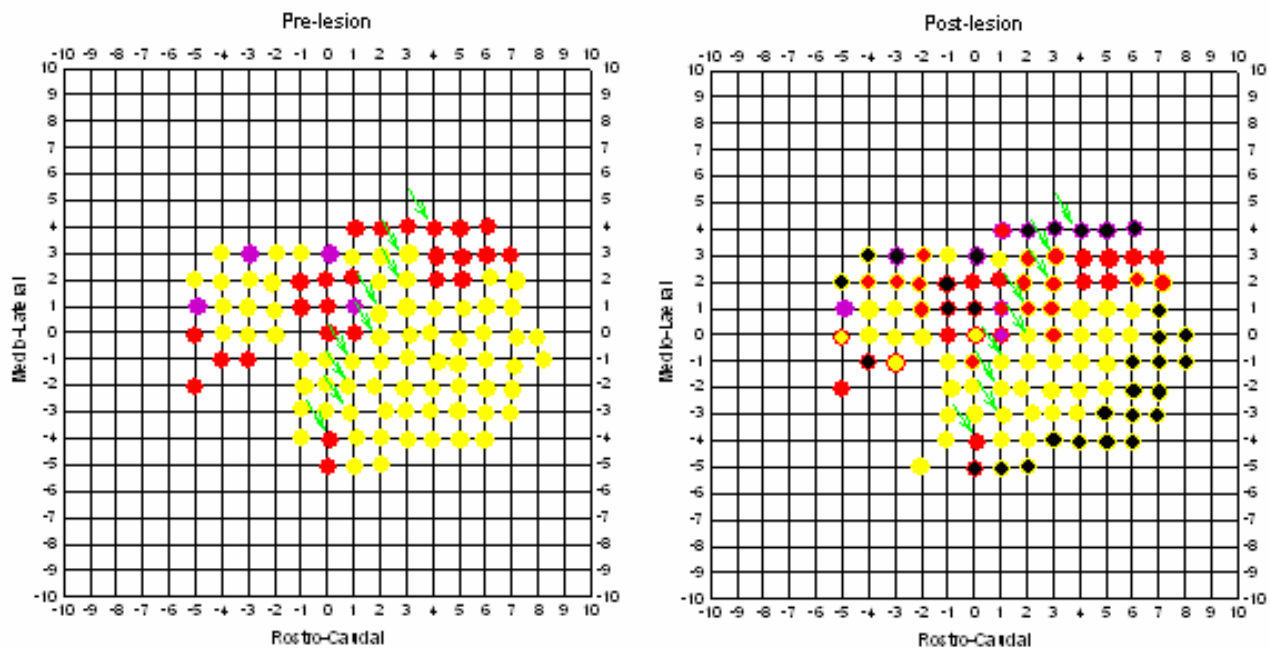
Figure 3.25: Unfolded pre- and post-lesion maps of anti-Nogo-A antibody treated monkey MK3-V. Same conventions as in Figure 3.24. The purple circles represent ICMS stimulation sites where both proximal and distal joints were represented.

As reflected by the higher number of responses in the pre- and post-lesion maps as compared to MK1-G, in this anti-Nogo-A antibody treated monkey, the mapping was more extensive, especially in the crest region of the rostral bank of the central sulcus. Therefore, the distal representation appears to be bigger and some proximal responses can be seen in the rostral bank of the central sulcus. So this leads to two pre-lesion finger representations, one in the rostral bank and one in the wall and fundus parts of the central sulcus. After the injection of ibotenic acid, the distal joints sites in the most ventral part in the rostral bank of the central sulcus were strongly touched by the lesion. The area representing the distal joint diminished by 43%. For the proximal representation, the number of stimulation sites post-lesion was comparable to pre-lesion (27 and 25 respectively). There was also some reorganization of the distal joints in the crest region of the central sulcus. This may correspond to a re-arrangement because of the anti-Nogo-A antibody treatment. Although about more than half (57%) of the distal joints representation in these monkey seems to be spared by the lesion, one has to note that the total loss of responding sites in MK3-V, in the areas representing finger and wrist (31 non-responsive sites post-lesion), is comparable to what was seen in MK1- G (27 non-responsive sites post-lesion). Therefore, the better post-lesion recovery in MK3-V as observed in the behavioural test (see Chapter 3.3) may be due to the anti-Nogo-A antibody treatment.
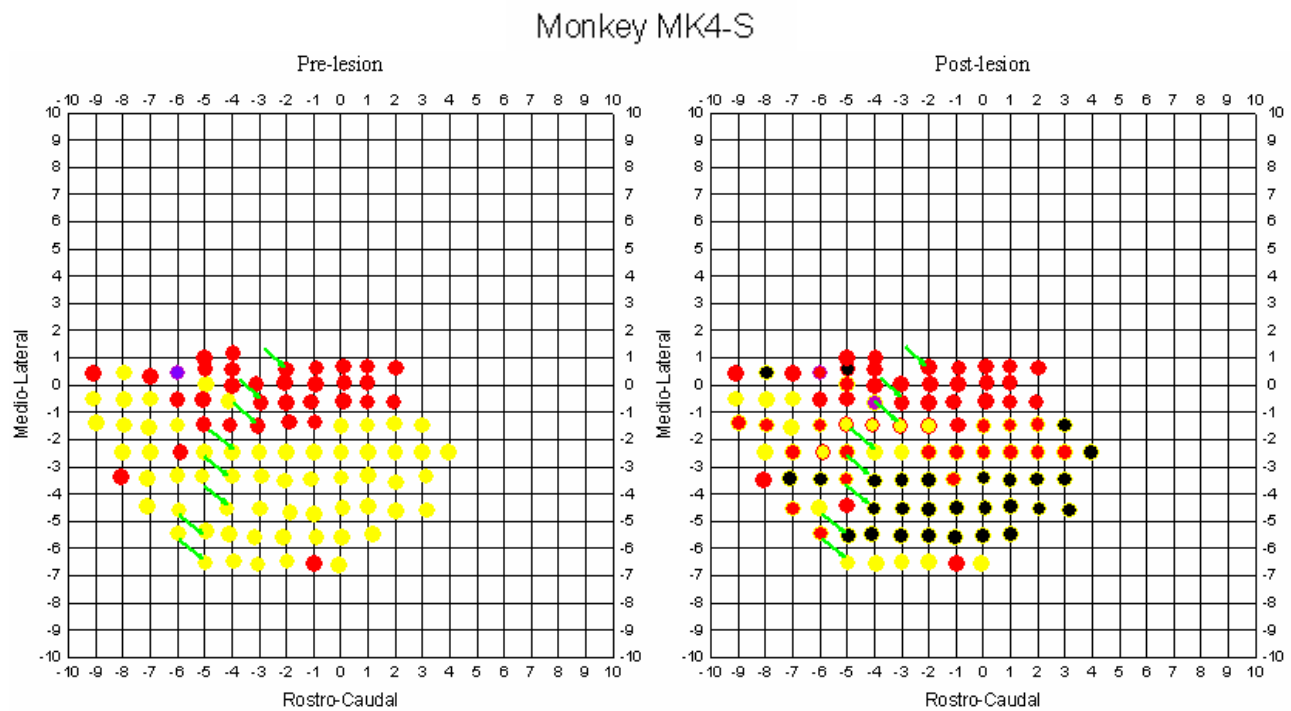
Figure 3.26: Unfolded pre- and post-lesion maps of anti-Nogo-A antibody treated monkey MK4-S. Same conventions as in Figures 3.24 and 3.25.

The number of sites explored inside the distal joints representation area of the motor cortex in monkey MK4-S is comparable to what was done in monkey MK3-V. Again, on the pre-lesion map, two distal joints representation areas can be seen: one in the crest area of the rostral bank of the central sulcus and one mainly lying in the wall of the rostral bank of the central sulcus, with some sites close to the fundus of the central sulcus. The post-lesion map revealed that the distal joints area in the wall of the rostral bank of the central sulcus was half destroyed by the lesion. The other half underwent changes in the quality of responses elicited by ICMS. In fact, distal joints responses changed to proximal joints responses, but there were also about 4 sites which changed from proximal to distal response. In general post-lesion data show a significant decrease of the distal joints representation (31%) and an increase of the proximal joints representation (142%). A limited number of sites in the wall of the rostral bank of the central sulcus were spared by the lesion (4 sites representing distal joints and 13 sites representing proximal joints). In contrast, the crest region showed only 2 non-responsive sites post-lesion, but these sites were surrounded by sites where distal joints representations became proximal joints representations. In sum, the number of non-responsive sites (28) inside the distal and proximal representing areas in monkey MK4-S was comparable to the number of non-responsive sites in monkeys MK1-G and MK3-V. Thus, as in monkey MK3-V, one can conclude that the sites, which changed the quality of response but did not become non-responsive, are likely to be the equivalent of augmented post-lesion plasticity induced

252

by anti-Nogo-A antibody treatment. Again this interpretation is in line with the observed better recovery of MK4-S in the performances of the behavioural tests as compared to MK1-G (see Chapter 3.3).

3.2.3. Quantification of ICMS data

Looking at the statistics below, the reader should keep in mind that so far about 7 monkeys were studied in this thesis work and that most of the graphics represented below are limited to only 5 animals (3 untreated control monkeys: MK1-G, MK6-J and MK7-C and 2 anti-Nogo-A antibody treaded monkeys: MK3-V and MK4-S). Monkey MK2-L was excluded because of ineffective (too small) lesion and MK5-R because this monkey was still alive and therefore comprehensive data were not available. In spite of the limited statistical power, due to the restricted number of animals, the Figures 3.27-3. 33 below show promising tendencies towards an enhancement of functional recovery post-lesion related to the anti-Nogo-A antibody treatment, which has to be however confirmed in additional monkeys.

3.2.3.1 Distribution of pre- and post-lesion ICMS effects

3.2.3.1.1 Responding sites:

Figure 3.27 shows the total number pre- and post-lesion of ICMS stimulation sites that produced effect on the forelimb joints for each monkey. There are many responding sites per track, at different depths. Four monkeys (MK-7C, MK6-J, MK4-S and MK3-V) show a higher number of responding stimulation sites, because of expansion of the mapping to the premotor areas. For the untreated monkeys, the number of stimulation sites that produced effect post-lesion decreased significantly, representing 5.6% for MK7-C, 11.1% for MK6-J and 29.2% for MK1-G of the number of pre-lesion stimulations sites. For the anti-Nogo-A antibody treated monkeys, the diminution was less drastic, the number of effective post-lesion sites representing 40.9% for MK4-S and 55.4% for MK3-V of the number of pre-lesion stimulations sites. The number of tracks post-lesion that produced effects normalized to pre-lesion tracks was low for monkeys MK7-C and MK6-J (11.9% and 28.8% respectively) and it amounted to about 58% for monkey MK1-G. For the anti-Nogo-A antibody treated monkeys (MK4-S and MK3-V), this number was about 69% and 68% respectively. Otherwise, the reduction of the number of electrode tracks that produced effects on the forelimb muscles was higher for the untreated control monkeys (MK1-G, MK6-J and MK7-C, respectively 41.67, 71.25 and 88.06%) than for the anti-Nogo-A antibody treated monkeys (MK3-V and MK4-S, respectively 31 and 32%) (Figure 3.28).

In conclusion, these values represent the amount of sites in which ICMS produced a muscular response by stimulation below to 80μA. There was a loss of responding sites after the lesion of M1. Anti-Nogo-A antibody treated monkeys recovered about half of the initial number of ICMS responding sites. For the untreated monkeys, there was only a few responding sites left after the lesion. The Figure 3.27 shows that the anti-Nogo-A antibody treatment contributed to preserve to some extent the number of ICMS responding sites in M1 after a lesion of the hand area in M1.
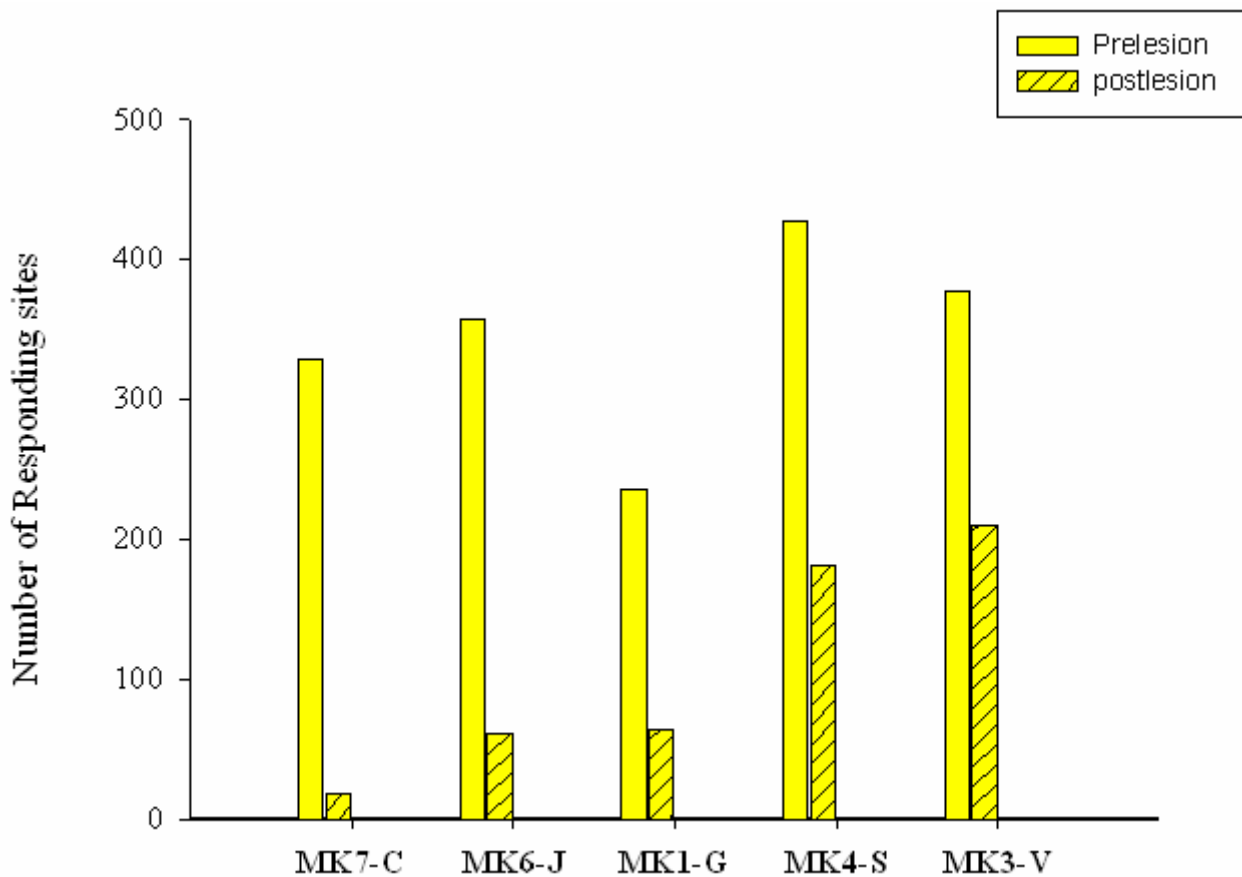
Figure 3.27: Number of ICMS stimulation sites producing joint movement of the forelimb. The number of tracks is similar for pre- and post-lesion for each monkey.
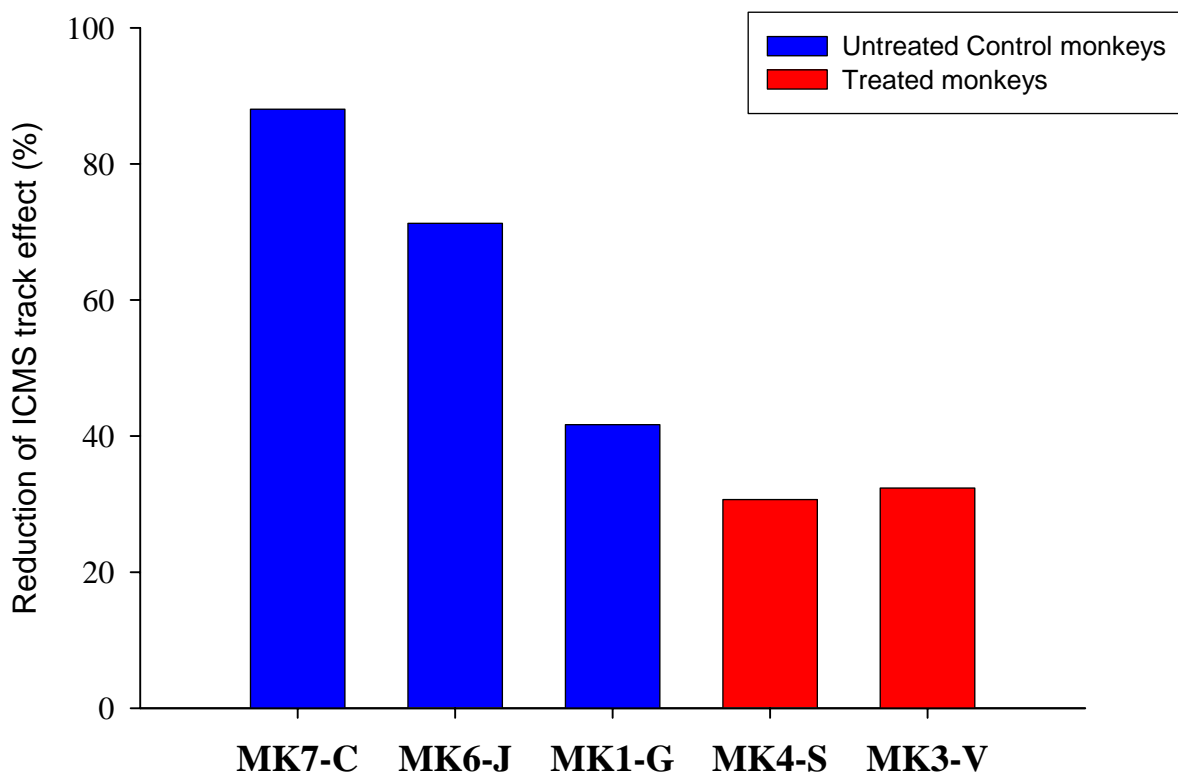
Figure 3.28: Reduction of the number of ICMS electrode tracks post-lesion that produced effects on forelimb muscles, normalized to the number of pre-lesion tracks (expressed in percent) for the untreated control monkeys (blue) and the anti-Nogo-A antibody treated monkeys (red).

3.2.3.1.2 Joints response:

Figure 3.29 shows the distribution of the number of ICMS stimulation sites that produced effects on digit, wrist and proximal joints (elbow and shoulder). The stimulation sites were considered as digit sites if ICMS produced effect in at least one finger.

The untreated monkeys showed a diminution of responses in all groups of joint muscles after the lesion. The area of digits was mainly concerned as, in two of the untreated monkeys (MK7-C and MK6-J), the representation of digits was lacking and it was limited to few sites for the third monkey (MK1-G). The wrist area was significantly diminished for all untreated monkeys. The post-lesion representation of the proximal group was more prominent than both digit and wrist representations.

The anti-Nogo-A antibody treated monkeys showed a better preservation of ICMS sites eliciting digit movements after the lesion. Proximal and wrist muscles are more represented than in untreated monkeys. There is even a case (MK4-S) in which proximal muscles are more represented

after the lesion than before. The anti-Nogo-A treatment thus enhanced cortical reorganization after a lesion in the sense of preserving a significant representation of the digits. In this graphic, all differences of ICMS thresholds between pre- and post-lesion situation were significant for the five monkeys (p<0.05).
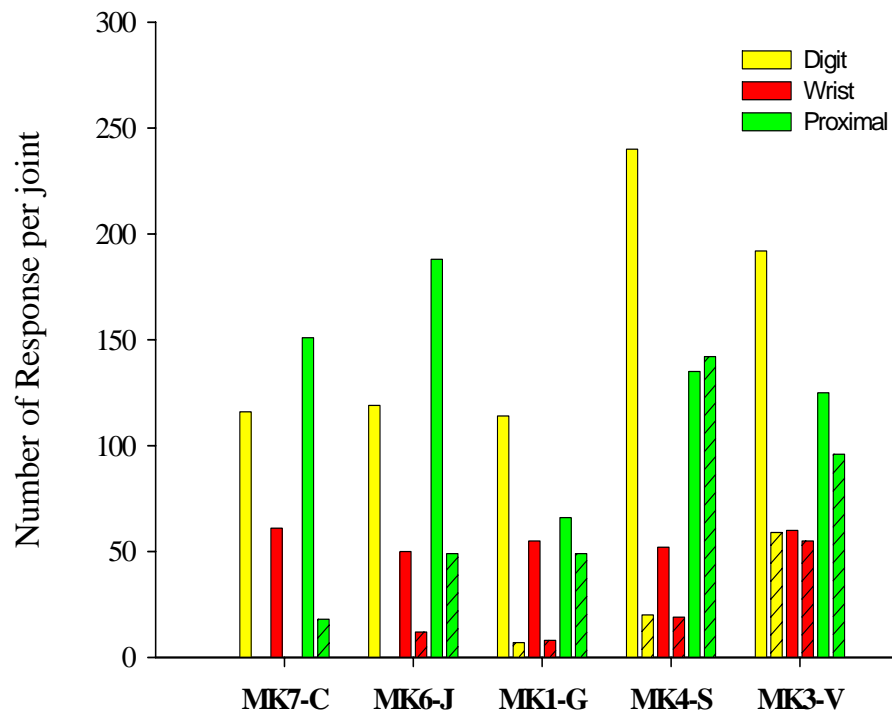
Figure 3.29: Distribution of the number of ICMS stimulation sites that produced effects on digit, wrist and proximal joints. The dashed bars show the post-lesion data to be compared with the adjacent pre-lesion data (non dashed bars).

3.2.3.2 ICMS threshold analysis

3.2.3.2.1 All ICMS thresholds

Figure 3.30 shows the differences between pre- and post-lesion of the ICMS threshold required to produce a joint movement. The ICMS thresholds in the untreated monkeys were higher post-lesion than pre-lesion. This increase was about two fold for monkeys MK7-C and MK1-G. The ICMS thresholds in the anti-Nogo-A treated monkeys post-lesion were also higher than pre-lesion, but the difference between the pre- and post-lesion stimulation threshold more prominent for the untreated monkeys (41.4, 21.2 and 18.4 µA for MK7-C, MK6-J and MK1-G, respectively) as compared to the anti-Nogo-A antibody treated monkeys (10.1 and 16.4 µA for MK4-S and MK3-V, respectively). However, the untreated monkey MK1-G exhibits a difference of ICMS thresholds

pre- and post-lesion close to that observed for the anti-Nogo-A antibody treated monkeys. Its lesion was significantly smaller than in the other untreated monkeys and the ICMS mapping was limited to M1 whereas it was extended to PMd for the other untreated monkeys (Fig. 3.30).
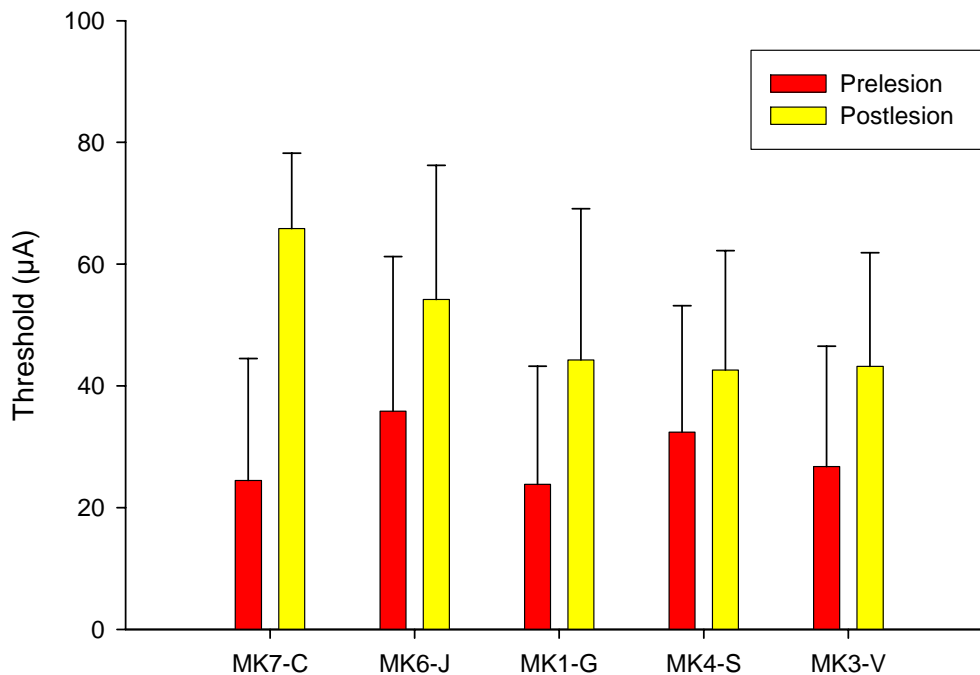
Figure 3.30: Differences of average ICMS thresholds before (red) and after (yellow) the lesion. Histograms show average value of thresholds. Muscles of digits, wrist, elbow and shoulder were grouped together in each monkey.

3.2.3.2.2 ICMS thresholds grouped by joint

The distribution of ICMS thresholds pre- and post-lesion for each monkey and by joint is represented in Figure 3.31. This figure shows that there was a general increase of ICMS thresholds after the lesion. However, the elevation of digits' ICMS thresholds are lower in the anti-Nogo-A antibody treated monkeys. This difference ranged between 22.4 and 29.8 µA for the untreated monkeys and between 9.3-15.7 µA for the anti-Nogo-A antibody treated monkeys. Pre- and post-lesion difference of wrist's ICMS thresholds was between 16.8-22.1 µA for the untreated control monkeys and between 5.3-14.3 µA for the anti-Nogo-A antibody treated monkeys. The difference of pre- and post-lesion proximal ICMS thresholds in both groups of monkeys was somewhat less prominent. The ICMS threshold differences, within a group of muscles, before and after lesion, are significant ($p < 0.05$), except in one case (wrist for monkey MK1-G), for which the number of data points was low ($p = 0.094$).

The effect of the anti-Nogo-A antibody treatment on ICMS threshold is more prominant in the hand and wrist areas of M1. In these areas, the ICMS thresholds obtained post-lesion are lower in the anti-Nogo-A antibody treated monkeys than in the untreated monkeys.
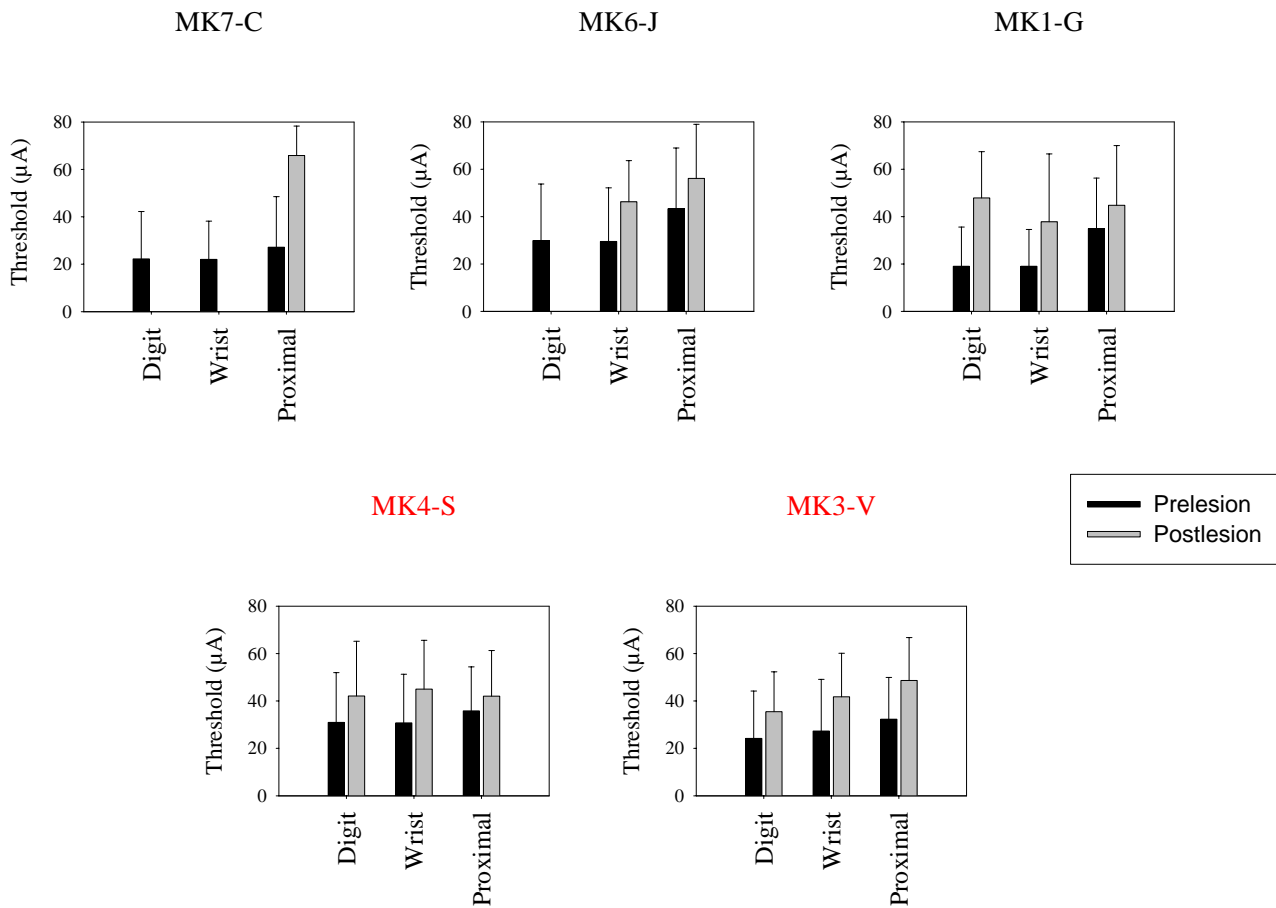
Figure 3.31: Distribution of pre- and post-lesion ICMS thresholds for each monkey and by joint. Joints are grouped in 3 categories: digits, wrist and proximal (elbow and shoulder). Note the absence of post-lesion ICMS effect for digits and wrist in MK7-C and for digits in MK6-J.

3.3 Behavioral data

3.3.1 Modified (standard) Brinkman board

3.3.1.1 Defining the ideal time span for data analysis

The Figures 3.32A and 3.32B address the question of which time span in the daily sessions should be considered for the quantitative analysis of the Modified Brinkman board in order to obtain the most reliable, reproducible and stable data. Another important point, especially addressed in Figure 3.32B, is to ask how long it takes for a monkey naïve to the Modified Brinkman board task to achieve stable daily performances. Therefore, in Figure 3.32B, the daily manual dexterity scores for monkey MK5-R, **measured as the number of pellets retrieved in 30, 45, and 60 seconds** in the Modified Brinkman board task, were plotted from the initial phase of pre-lesion training for a period of about 150 days. Two important features can be seen from Figure 3.32B: First, in monkey MK5-R, there was a training phase lasting approximately about 150 days. From there on, the behavioural score became very stable (pre-lesion plateau phase). Second, the scores obtained for monkey MK5–R are equally stable when established in time windows of 30, 45, and 60 seconds. This is expressed by the three curves (black, red and green) being parallel to each other. So, this second observation strongly supports our strategy to limit data analysis to the first 30 seconds of the Modified Brinkman board task. One may argue that monkey MK5-R was an especially well working animal and perhaps, for less cooperative animals and/or after the lesion, this may not be true anymore. To investigate this issue, we established a similar plot for monkey MK4-S, an animal which was less cooperative and more easily disturbed by environmental (uncontrolled) influences. As can be seen from Figure 3.32A, the behavioural score is less stable in monkey MK4-S than in monkey MK5-R. Nevertheless, the variability is comparable for the scores derived from the time widows of 30, 45, and 60 seconds. Even during the initial delicate post-lesion phase (days 1 -20), the three curves (black, red, and green) parallel each other in MK4-S. Therefore, we can conclude that data analysis of manual dexterity scores in the first 30 seconds only is representative for the whole performance in every monkey tested on the Modified Brinkman board task.

_____

Pre – and post – lesion scores MK4-S Standard Brinkman board
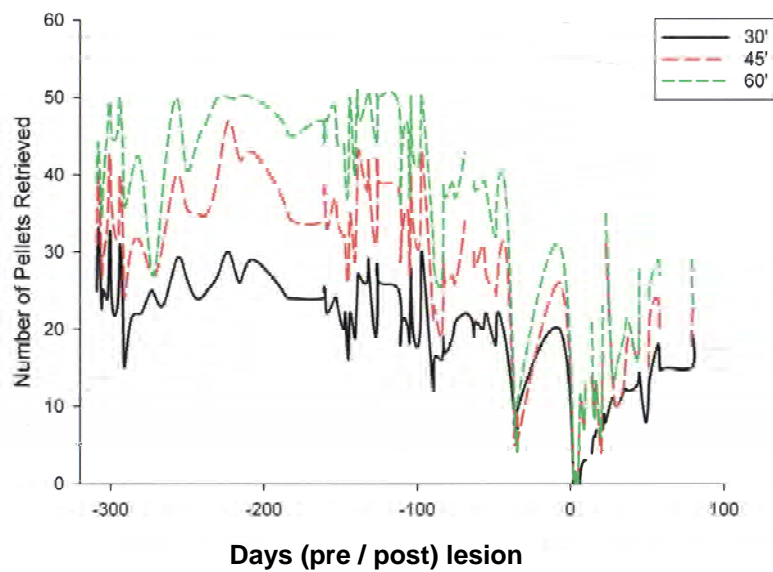
Figure 3.32A: Modified Brinkman board scores for monkey MK4-S. The number of pellets was counted during the first 30 seconds (black curve), 45 seconds (red curve) or 60 seconds (green curve).

Pre - lesion training scores MK5-R Standard Brinkman board
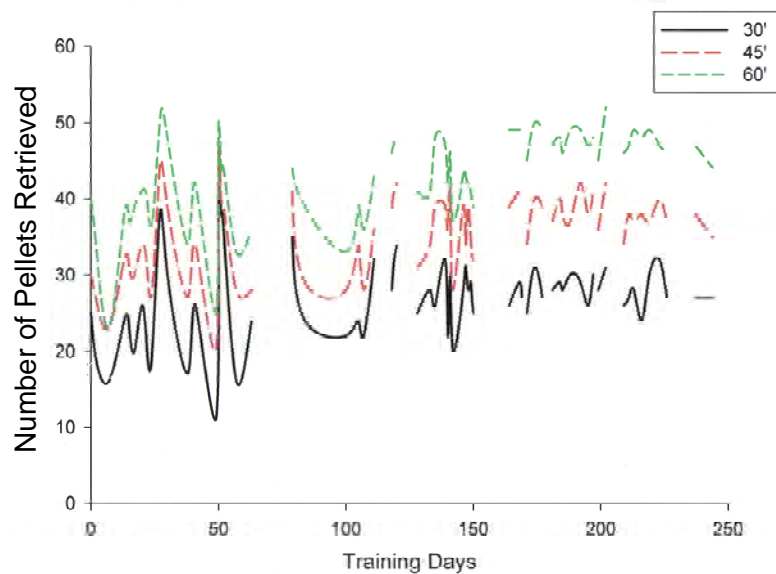
Figure 3.32B: Modified (standard) Brinkman board scores for monkey MK5-R, showing a training effect.

3.3.1.2 Modified Brinkman board scores in the first 30 seconds

The following behavioural data report only on the behavioural performance with the hand <u>affected</u> by the lesion (data for the hand opposite to the lesion will be reported elsewhere). In Figure 3.33 below (Panels A and B for control untreated monkeys MK1-G and MK5-R; Panels C-E for the anti-Nogo-A antibody treated monkeys MK2-L, MK3-V, MK5-S), the pre- and post-lesion performances in the Modified (standard) Brinkman board are represented. Although we did not yet perform sophisticated statistical analysis, because of the limited number of animals included so far, some preliminary tendencies can be deduced from the data presented in Figure 3.33. **Note that in Figure 3.33, horizontal lines were drawn to represent the average pre-lesion and post-lesion scores, respectively. However, these horizontal lines were computed on longer pre- and post-lesion periods than shown in the Figure, explaining why they do not appear to be in the middle of the respective individual values. Furthermore, post-lesion, the horizontal line does not include the scores while the monkey recovers (few weeks immediately after the lesion), but only the scores after a plateau of recovery was reached.** In other words, the post-lesion horizontal line is the stable recovered performance (plateau).

First, as previously reported by our laboratory (e.g. Liu and Rouiller, 1999), the post-lesion performances in picking out reward pellets from the vertical slots is less affected by the lesion than the ones for the horizontal slots, in both untreated control monkeys and in anti-Nogo-A antibody treated monkeys (Fig. 3.33). Second, at that step, there is a tendency that the post-lesion deficit in the scores for both types of slots (horizontal and vertical) is somewhat less strong in the group of anti-Nogo-A antibody treated monkeys as compared to the group of untreated control monkeys. The values are the following:

- Untreated control monkeys: $-\Delta H=5.5$ (horizontal slots), $-\Delta V=3$ (vertical slots).
- Anti-Nogo-A antibody treated monkeys: $-\Delta H=2.8$, $-\Delta V=2.1$.

Figure 3.33 (panels A-E): Scores for Modified Brinkman board tests conducted in five monkeys.

On the X-axis of each graph, negative values indicate pre-lesion sessions, whereas positive values indicate post-lesion sessions. 0 (red vertical line) is the day of lesion induction by ibotenic acid infusion in M1. On the Y–axis the performance is indicated as the number of horizontal and vertical pellets retrieved in the first 30 seconds of the task. In each Panel (A-E) scores of 150 pre-and post-lesion sessions are represented. For each monkey the mean pre- and post-lesion scores for horizontal and vertical slots are indicated by dashed horizontal bars. **Note that these mean score values are derived from more data (additional pre- and post-lesion sessions) than represented in the individual graphics of Panels A - E**. To better illustrate the scores obtained from sessions close to the lesion day, an additional small graphic showing the scores 20 days pre-and post-lesion at higher resolution was extracted for each monkey.

Untreated monkey (MK1-G)

Panel A

Untreated monkey MK5-R

Panel B
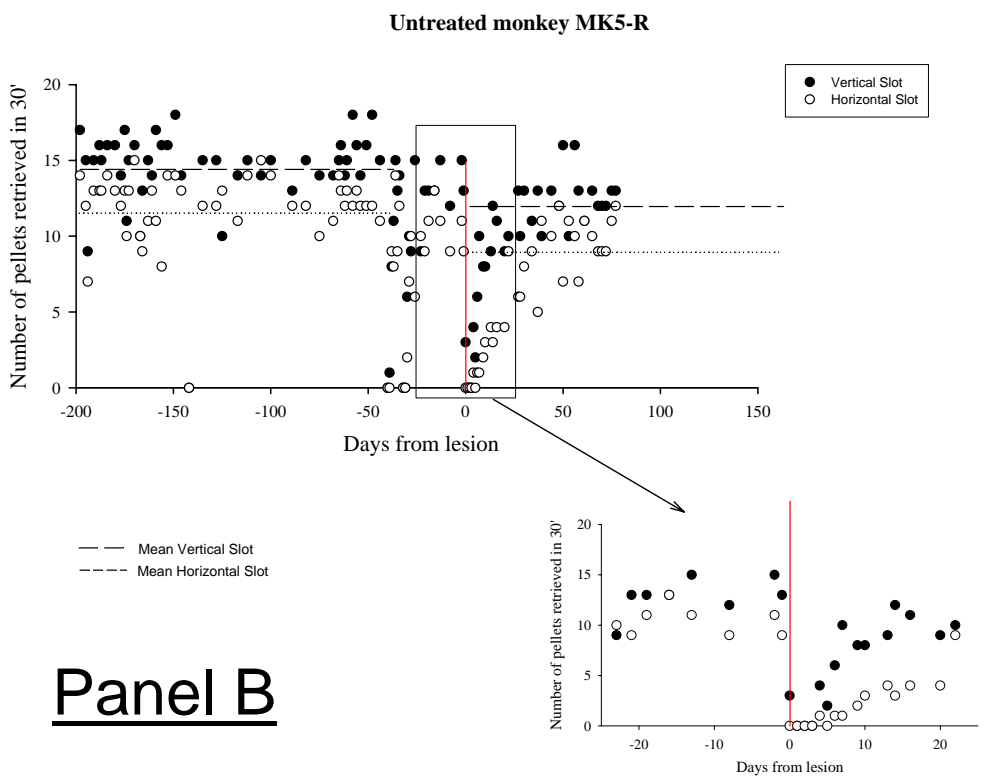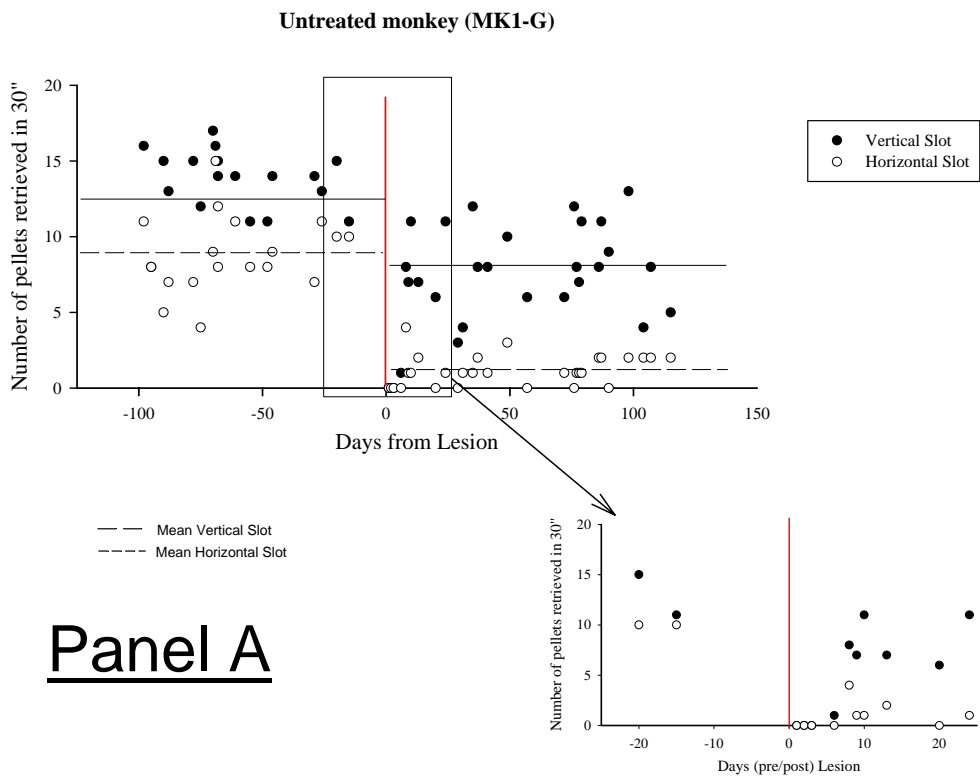
Scores for the Modified Brinkman board in the untreated monkeys MK1-G (A) and MK5-R (B).

Anti-Nogo-A antibody treated monkey (MK2-L)

Panel C

Anti-Nogo-A antibody treated monkey MK3-V

Panel D
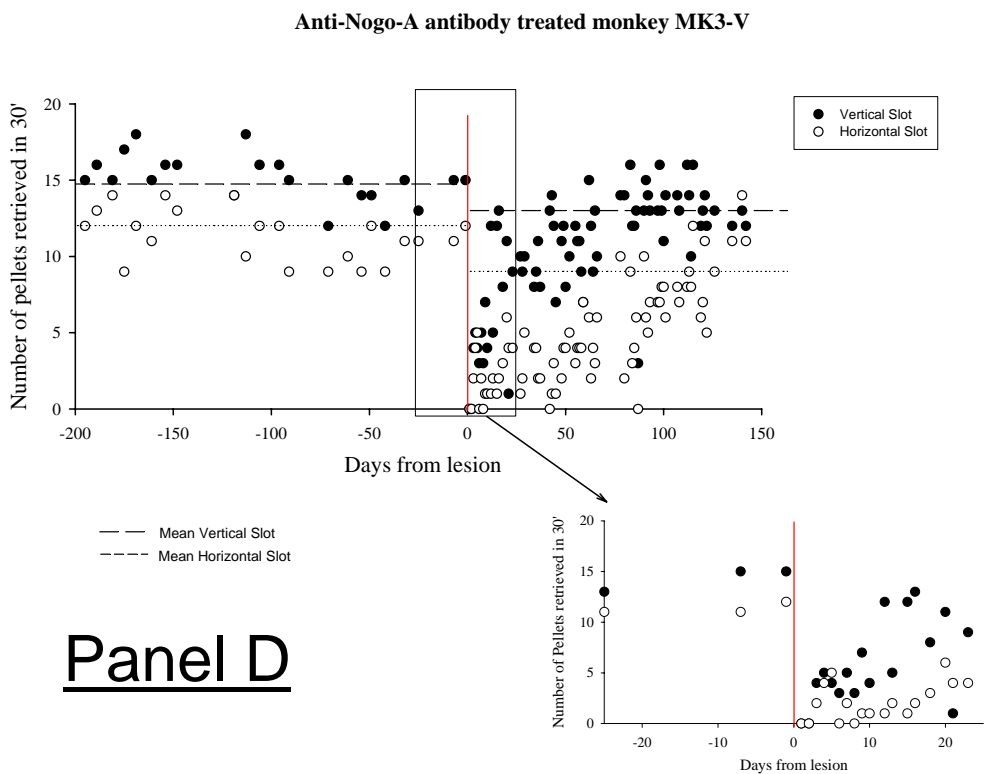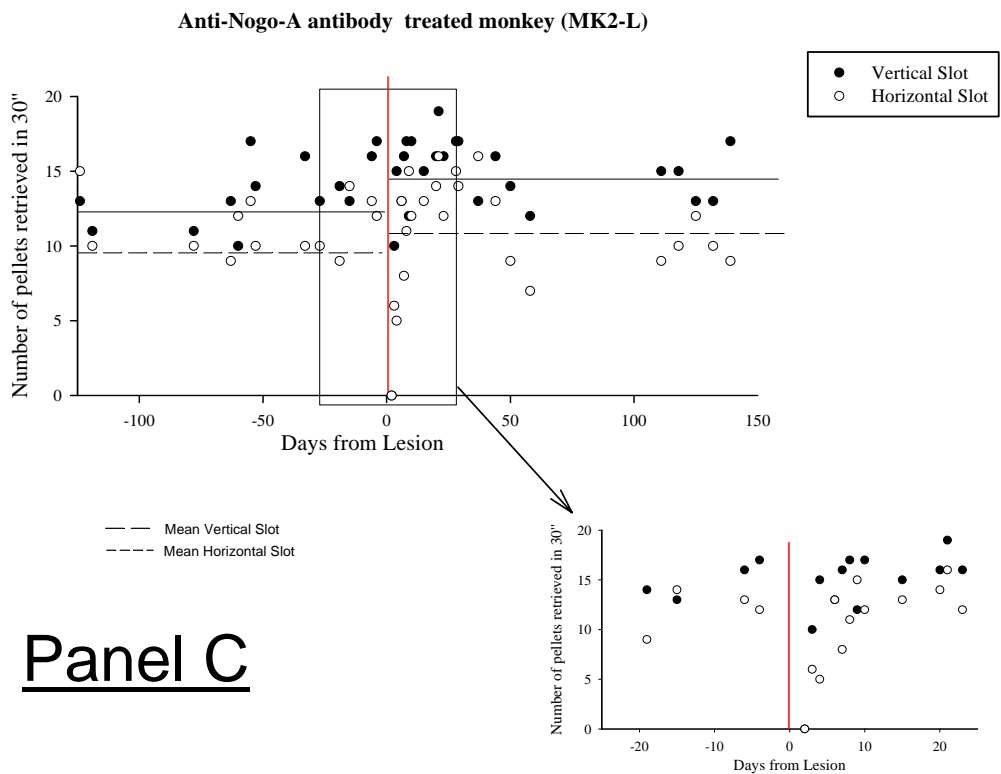
Scores for the Modified Brinkman board in the anti-Nogo-A antibody treated monkeys MK2-L (C) and MK3-V (D).

Anti-Nogo-A antibody treated monkey MK4-S

Panel E
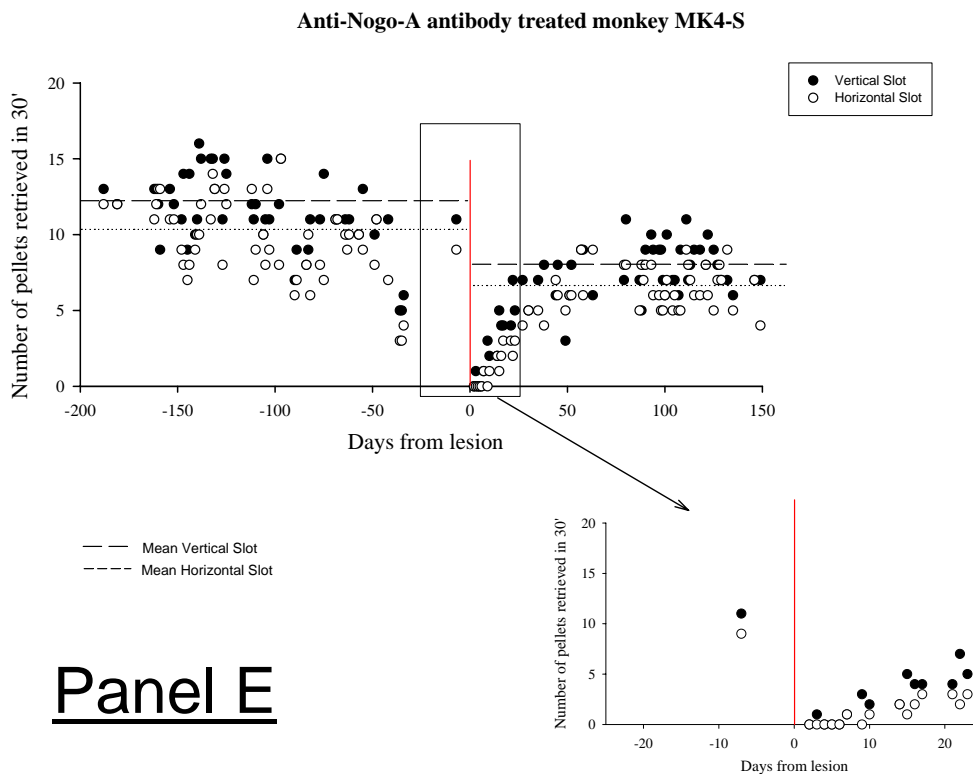
Scores for the Modified Brinkman board in the anti-Nogo-A antibody treated monkey MK4-S (E).

Immediately after the lesion, the scores in all monkeys dropped to 0 for both types of slots. About one week after the lesion, all monkeys started to be progressively able to grasp out pellets from vertical and, but to a lesser extent, from the horizontal slots. In this context, it is interesting to note that anti-Nogo-A antibody treated monkeys on average tended to recover faster and better as compared to untreated control monkeys. There seems also to be a tendency towards more stable post-lesion performances in anti-Nogo-A antibody treated monkeys during the post - lesion plateau phase. In summary the graphs show that anti-Nogo-A antibody treatment may enhance recovery of manual dexterity after a cortical lesion in M1 as compared to controls, although this tendency needs to be confronted with the lesion characteristics of each monkey (see below) and extended to a larger number of monkeys.

3.3.1.3 Contact time to retrieve individual pellets in the Modified Brinkman board
(only scores of the affected hand are shown)

General remarks

During a manual dexterity performance lasting 30 seconds (data shown in Figs. 3.32 and 3.33), the monkey may exhibit variability in terms of motivation and/or attention. Furthermore, the score established during 30 seconds include motor aspects not directly related to manual dexterity (namely finger movements), such as the reaching phase of the movement (hand toward the board and hand back towards the mouth) and time separating two consecutive wells (for instance if the monkey chews without initiating immediately the next reaching movement). To reduce variability and emphasize the finger movements, we have measured the time of contact between the finger with the first pellet aimed for by the monkey, for the vertical and horizontal slots, respectively. In other words, this corresponds to the retrieval time for the first vertical pellet and the retrieval time for the first horizontal pellet. Motivation must be maximal, as these "first" retrievals occur at the very beginning of the session. Usually, the first vertical and first horizontal slots visited by the monkey are located in the centre of the Brinkman board. To also assess performance in zones of the Brinkman board remote from the centre, the contact time was also measured for four slots (2 vertical and 2 horizontal) located at corners (see Fig. 3.34). In this case, the retrieval of the pellet from these four slots may occur at any time point during the daily session.

The graphs presented in Figure 3.34 show pre- and post-lesion data obtained from two untreated control monkeys MK1-G and MK5-R (Panel A and B) and three anti-Nogo-A antibody treated monkeys MK2-L, MK3-V and MK4-S (Panel C-E). In each panel, the pellet retrieval times for six different slots of the standard Brinkman board were plotted against days from lesion. In addition, the mean retrieval time obtained from all six slots analyzed is shown in a similar separate graph. The small picture in the right corner at the bottom of each panel indicates the position of slot 1-4 analyzed at corner areas on the Modified Brinkman board. Slots 1 and 2 were closer to the monkey than slots 3 and 4. The first vertical and the first horizontal slots are not indicated, as the monkey "defined" them itself in each session and therefore these slots were in various arbitrary positions.

The data available so far are rather complex and therefore difficult to interpret and will certainly need more detailed statistical analysis integrating data from additional monkeys from both groups (anti-Nogo-A antibody treated and controls). In spite of that, first preliminary, interesting findings can be presented here. In all monkeys tested, the pre-lesion scores for the first vertical, the first horizontal and for slots 1 and 2 appeared very stable and therefore well suited for comparison with post-lesion scores. In contrast, pre-lesion scores of slots 3 and 4 were more variable and

therefore less suited for such comparison. One explanation could be that monkeys tended to take reward pellets from theses slots towards the end of the task and therefore were less concentrated. Another factor could be that because these slots were away from the monkey, it was more difficult to pick out the pellets from these two slots, especially for small monkeys. A special remark has to be made concerning the anti-Nogo-A antibody treated monkey MK4-S: In addition to the lesion induced impairment, the fingers of this monkey grew substantially during the experimentation period, probably making the post-lesion pellet grasping even more difficult (revealed by analysis of pre- and post-lesion video recordings). This could in part explain why some post-lesion scores for the anti-Nogo-A antibody treated monkey MK4-S tend towards values typically observed in untreated control monkeys.

Comparison of untreated control monkeys and anti-Nogo-A antibody treated monkeys

Immediately after the lesion, the time needed to retrieve a pellet from any slot analyzed increased substantially in untreated control monkeys as well as in anti-Nogo-A antibody treated monkeys (Fig. 3.34). There was a tendency towards less variation during the post-lesion plateau phase in the anti-Nogo-A treated monkeys as compared to the untreated control monkeys, for all six slots analyzed. In addition to that, the mean post-lesion retrieval time for all 6 slots pooled was lower in the anti-Nogo-A antibody treated monkeys than in controls. Unexpectedly, the post-lesion retrieval times for the first vertical slot during the plateau phase (scores nearly as short as corresponding pre-lesion retrieval times) were comparable in both groups of monkeys. A reason for this could be that, as the monkeys could select themselves which slot to empty first, they probably first emptied the most easy one (usually a vertical slot) allowing a good performance (short retrieval time) for this slot, even with somewhat limited manual dexterity. In contrast, the retrieval times for the first horizontal slot were shorter in the anti-Nogo-A antibody treated animals as compared to controls. In summary, this analysis reveals a tendency towards an enhancement of recovery by the anti-Nogo-A antibody treatment after cortical lesion of M1 in macaque monkeys.

Figure 3.34: Contact time (to retrieve individual pellets) in the Modified Brinkman board in 5 monkeys (see text for details).

Pellet Retrieval Time Monkey MK1-G
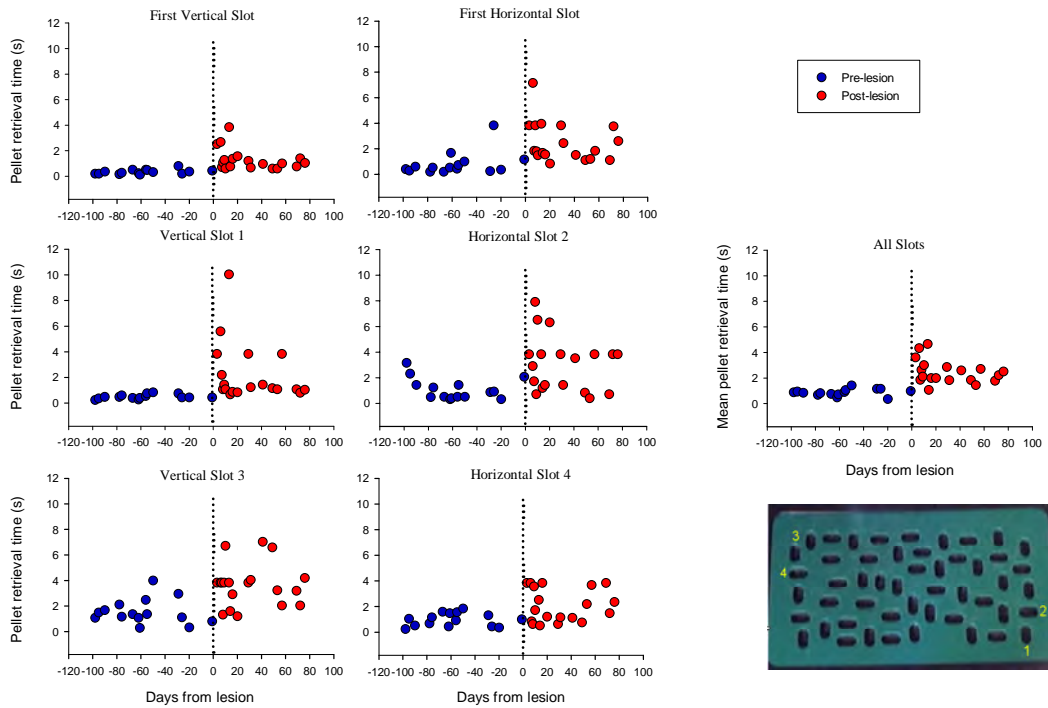
Panel A: untreated monkey MK1-G

Pellet Retrieval Time Monkey MK5-R
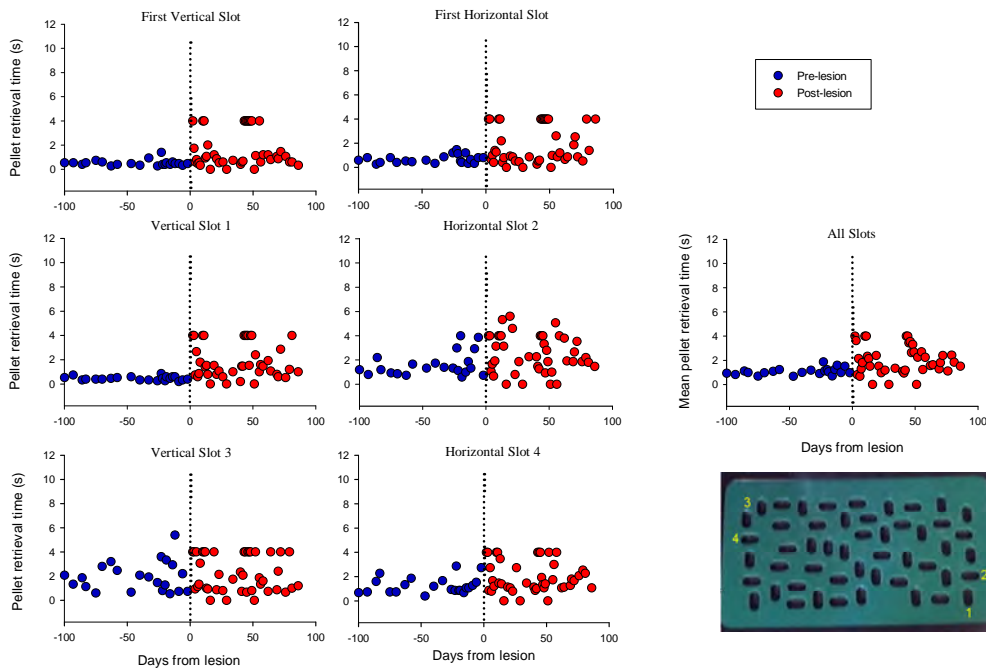
Panel B: untreated monkey MK5-R

Pellet Retrieval Time Monkey MK2-L
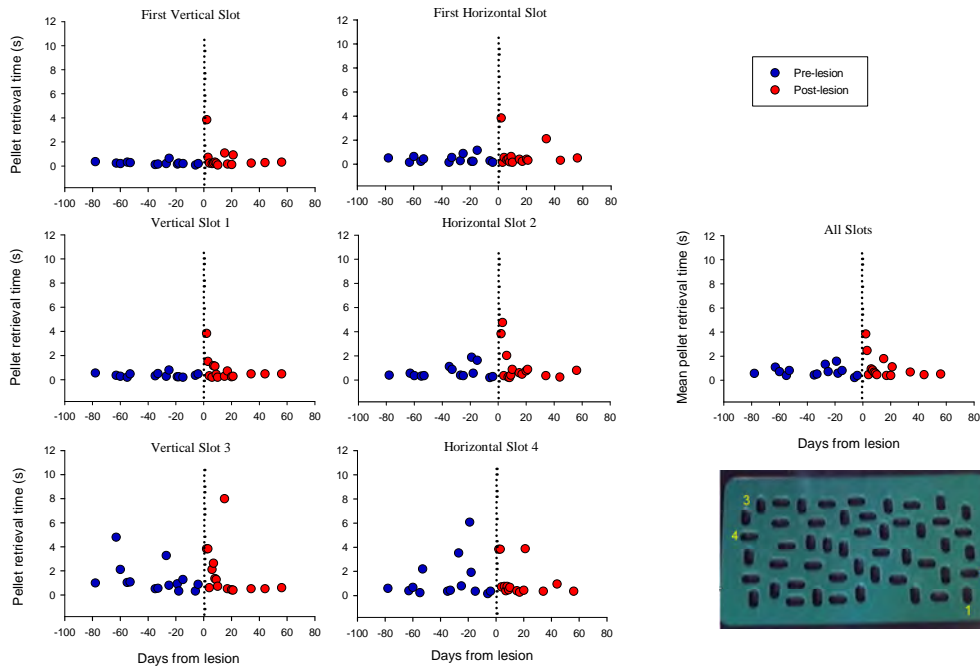
Panel C: anti-Nogo-A treated monkey MK2-L

Pellet Retrieval Time Monkey MK3-V
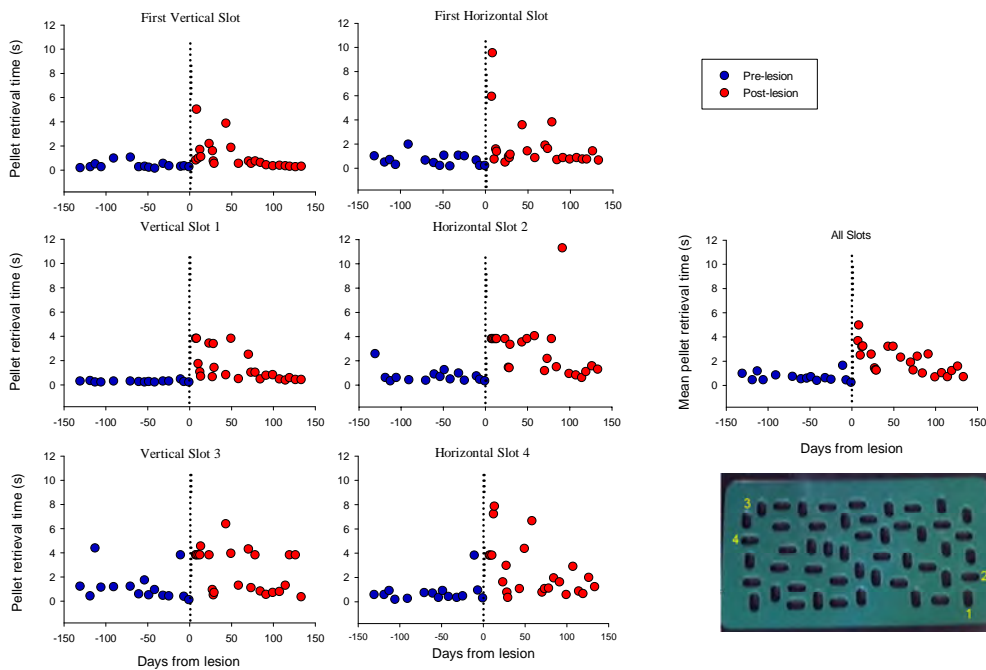
Panel D: anti-Nogo-A antibody treated monkey MK3-V

Pellet Retrieval Time Monkey MK4-S
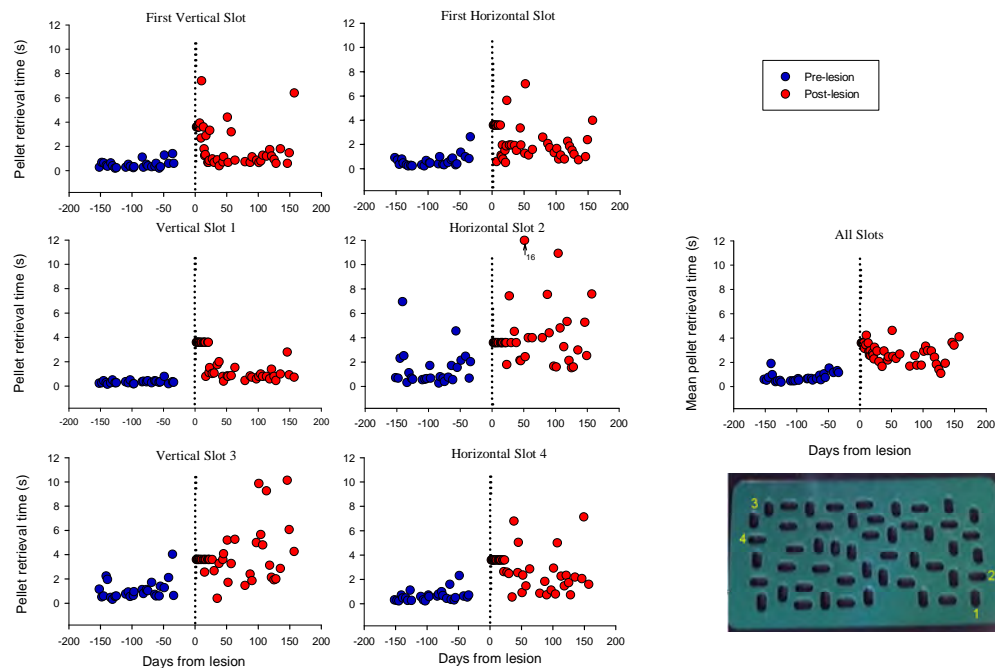
Panel E: anti-Nogo-A antibody treated monkey MK4-S

3.3.2 Hidden Brinkman board (only scores of the affected hand are shown)

3.3.2.1 Total number of vertical and horizontal pellets retrieved

The plots of Figure 3.35 below represent the total number of horizontal (max. 10) and vertical (max. 10) pellets retrieved during the entire testing time in the hidden Brinkman board task for each monkey. In panel A, the scores of two untreated control monkeys MK1-G and MK5-R are given whereas in panel B the scores of three anti-Nogo-A antibody treated monkeys, MK2-L, MK3-V, and MK4-S, are indicated. For each monkey, scores on the left are for performance with visual feedback (slid of the box open) whereas scores on the right are for performance without visual feedback (slid of the box closed).

In the pre-lesion state, both the anti-Nogo-A antibody treated monkeys and the untreated control monkeys performed similarly well for horizontal and vertical slots if the task was performed with visual feedback. This is also true for the task executed without vision (comparable performance for vertical and horizontal slots), but the scores were less stable and generally lower for both groups of monkeys, as compared to the situation with visual feedback. Immediately after

the lesion, manual dexterity scores in the hidden Brinkman board task (with and without vision) dropped close to 0, irrespective of the orientation of the slots (horizontal or vertical), for monkeys of either group. Later, post-lesion, the anti-Nogo-A antibody treated monkeys tended to perform somewhat better as compared to control monkeys in the task with visual feedback. In the two groups of monkeys, the scores did not reach pre-lesion values and pellets were more easily taken from vertical slots than from horizontal slots. Again, the control monkey MK5-R reveals a pretty good recovery nearly comparable to what was seen in the anti-Nogo-A antibody treated monkeys, whereas monkey MK1-G performed clearly less well. Post-lesion, the situation for the task without vision is less clear although the untreated control monkey MK1-G performed less well than the anti-Nogo-A antibody treated monkey MK2-L. As with visual feedback, in both groups of monkey, pellets were grasped more easily from vertical slots than from horizontal slots.

Figure 3.35: Manual dexterity scores derived from the hidden brinkman board (see text).

Panels A (top) and B (bottom): untreated control monkeys.
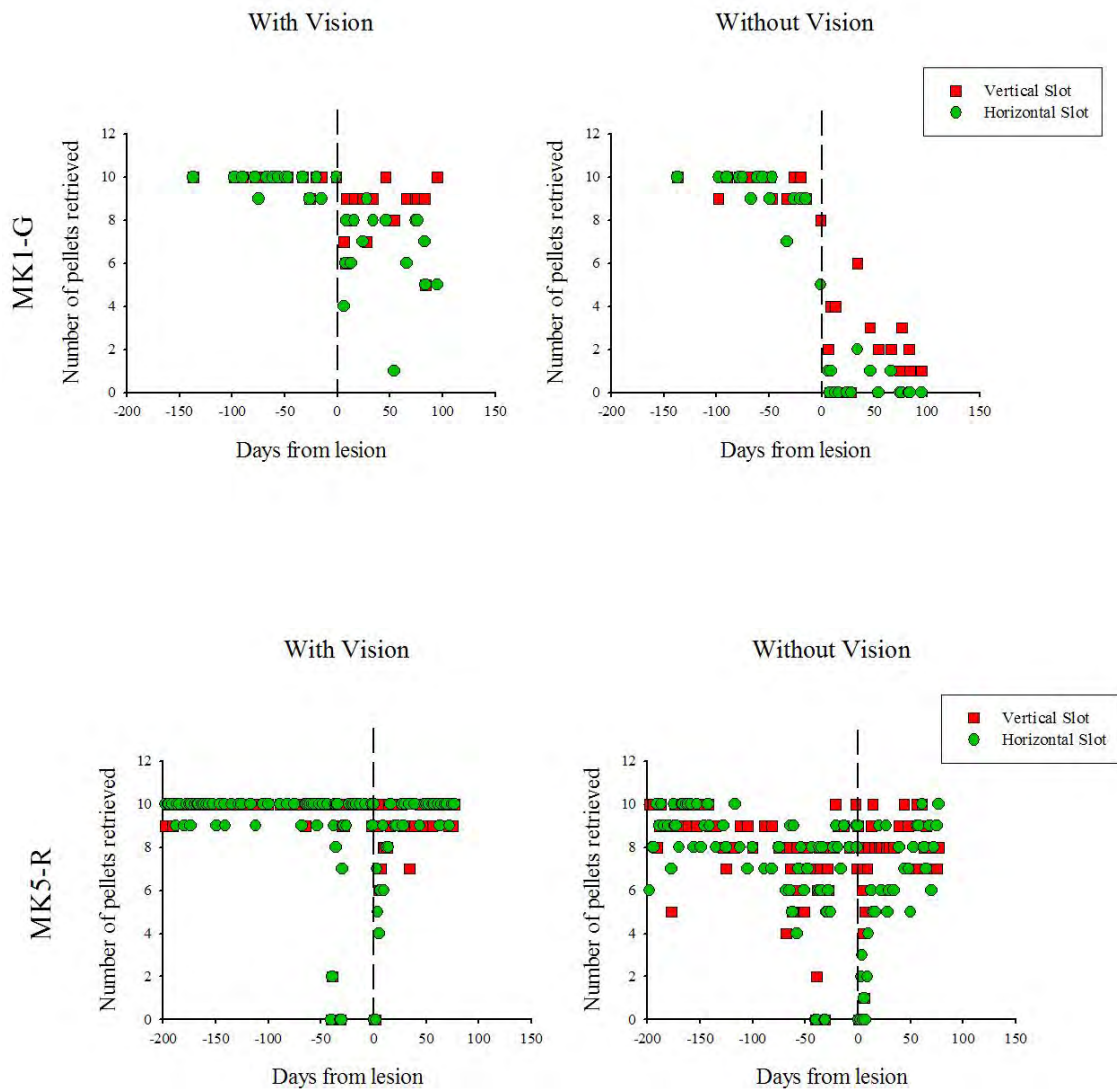
Fig. 3.35 (con't)   **Panels C (top), D (middle) and E (bottom)**: anti-Nogo-A antibody treated monkeys.
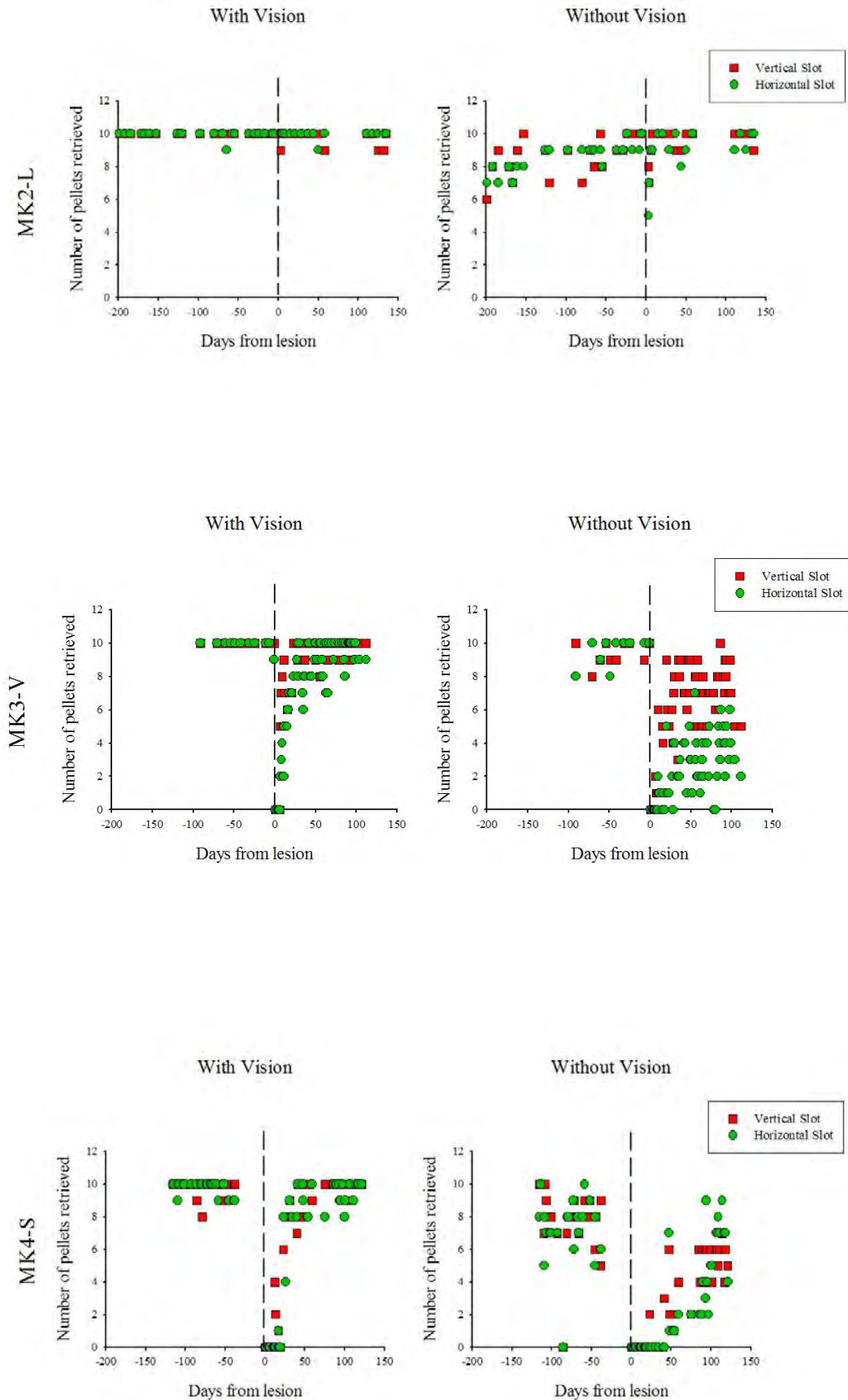
The plots in Figure 3.36 below represent the mean pre- and post-lesion pellet contact (retrieval) times needed to grasp out a pellet from either a vertical or a horizontal slot. In panel A, the mean pellet retrieval times are given for two untreated control monkeys (MK1-G and MK5-R) whereas, in panel B, the mean pellet contact (retrieval) times are indicated for the three anti-Nogo-A antibody treated monkeys MK2-L, MK3-V, and MK4-S. For each monkey, times on the left are values obtained with visual feedback (slid of the box open) whereas, on the right, values are given for performance without visual feedback (slid of the box closed). As can be seen on the individual plots, the pre-lesion performances (contact time) in both groups of monkeys are more stable with visual feedback than without visual feedback. In the first sessions analyzed post-lesion, the anti-Nogo-A antibody treated monkeys as well as the untreated control monkeys needed substantially more time to grasp out a pellet from an individual slot. In both situations, with and without visual feedback, there was a post-lesion tendency for anti-Nogo-A antibody treated monkeys to grasp out pellets more rapidly, with more constant mean contact (retrieval) times than untreated control monkeys when the hidden Brinkman board task was performed with visual feedback. Mean contact (retrieval) times in anti-Nogo-A antibody antibody treated monkeys attained nearly pre-lesion values. The difference between groups of monkeys was less clear for the hidden Brinkman task performed without visual feedback, except monkey MK2-L performing clearly better than all other monkeys (but again, the lesion in this monkey was very small).

Figure 3.36: Average contact (retrieval) time in seconds needed to pick out a reward from one well.

- *Panel A: Untreated (control) monkeys*
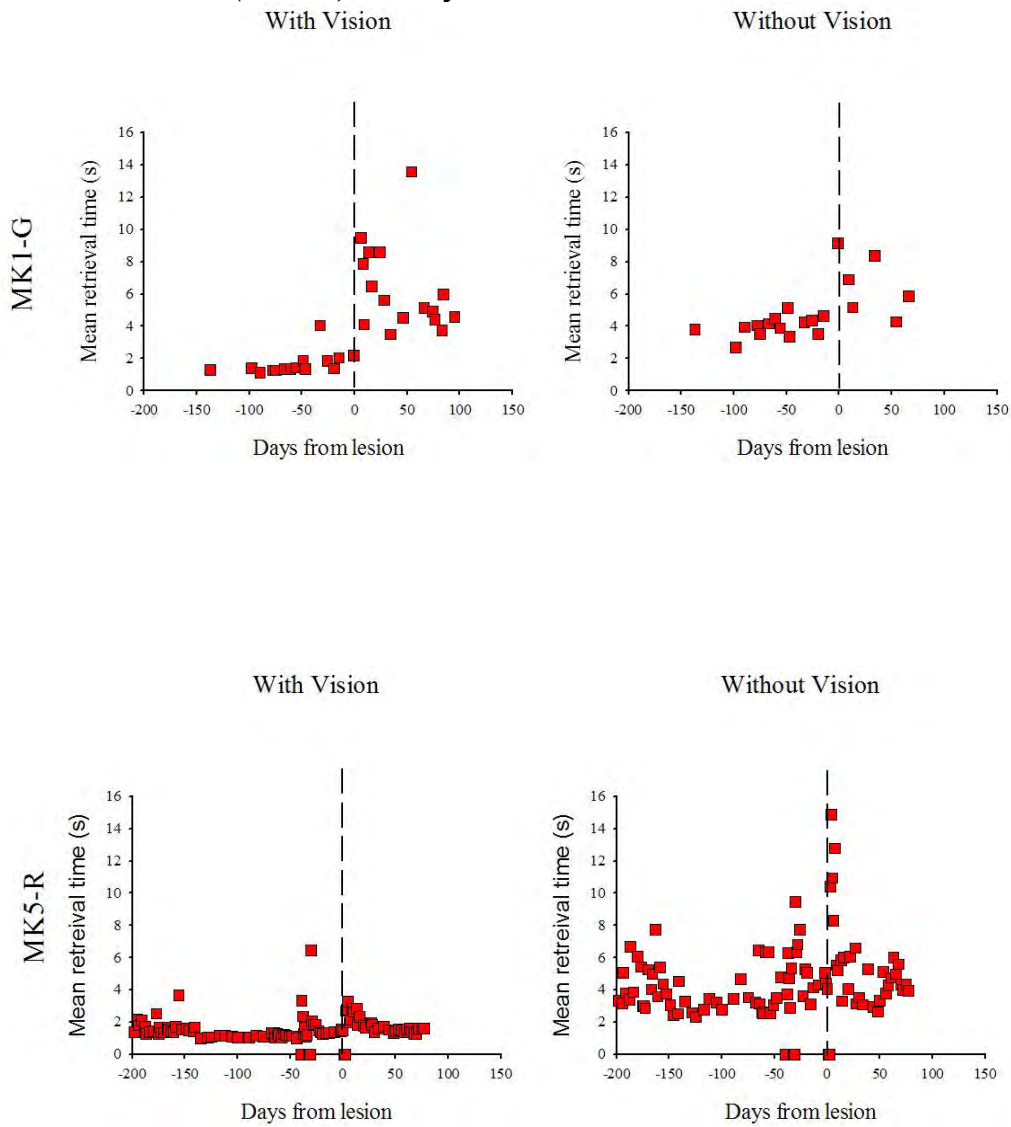
Figure 3.36 (con't), *Panel B: anti-Nogo- A antibody treated monkeys*

_____
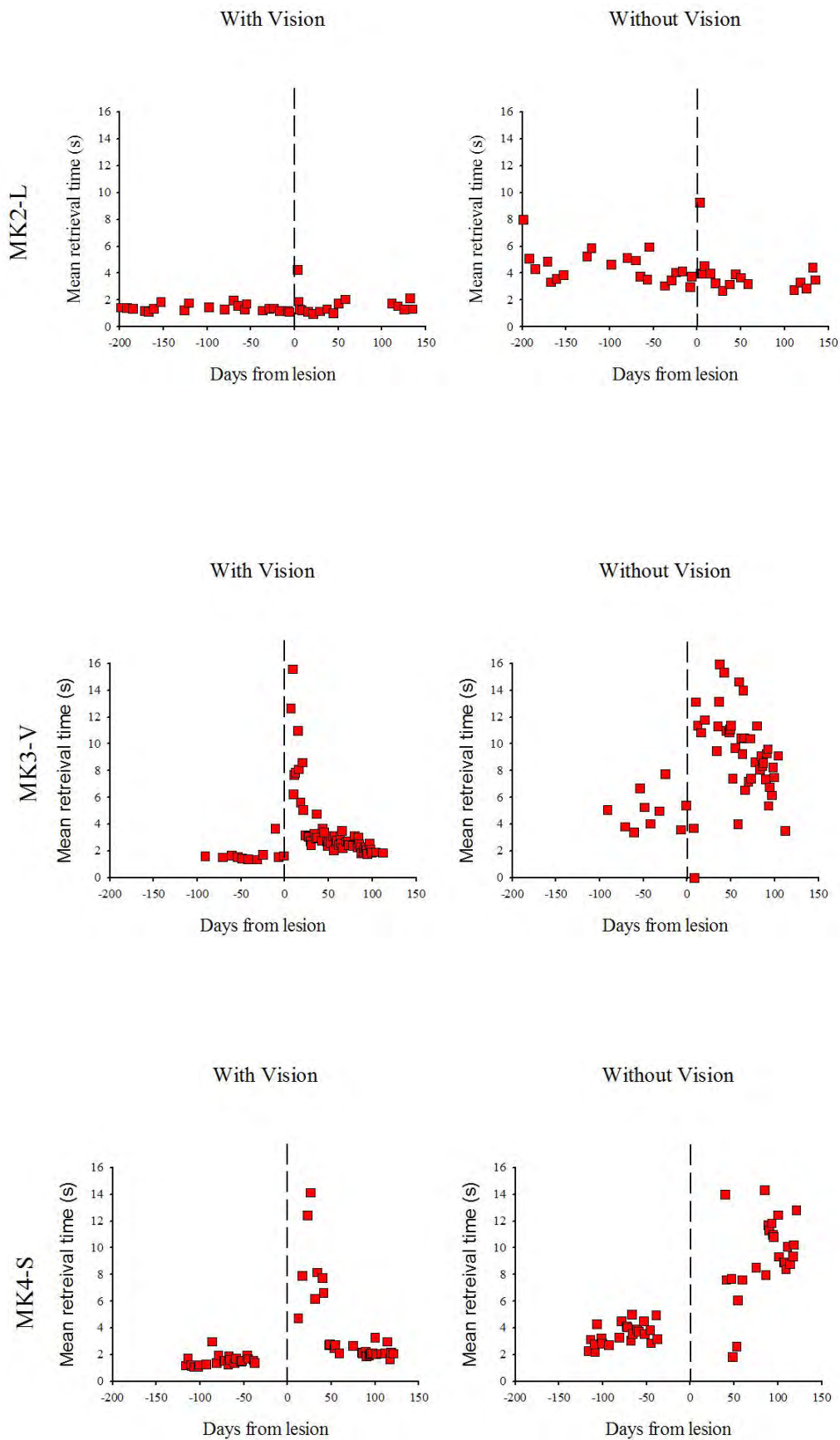
The graphs in Figure 3.37 below represent the total time needed to execute the hidden Brinkman task in pre- and post-lesion conditions. In panel A, the total time needed to complete the task, or to nearly complete the task (1. Motivation: monkey stops working because of frustration (mostly without visual feedback); (2. in post-lesion situation: monkey stops trying because manual dexterity was not good enough to get a reward) of two untreated control monkeys MK1-G and MK5-R are given. In panel B, the same total times are given for three anti-Nogo-A antibody treated monkeys, MK2-L, MK3-V, and MK4-S. For each monkey, total times on the left are with visual feedback (slid of the box open) whereas, on the right, total times are without visual feedback (slid of the box closed).

Pre-lesion, for both groups of monkeys, the total time needed to complete the task was longer and more variable without visual feedback. Immediately post-lesion, in both situations (with and without visual feedback), the total time spent to complete the task was clearly higher in both groups of monkeys. There was again a slight tendency for anti-Nogo-A antibody treated monkeys to recover better as compared to control monkeys in the task with visual feedback, although monkey MK5-R seems to perform equally well (still alive, size of lesion not known). As for the mean contact (retrieval) time, in the situation without visual feedback, the total time values post-lesion are less evident to interpret. In both anti-Nogo-A antibody treated monkeys and untreated control monkeys, the total time stayed at a higher more variable level post-lesion without any obvious difference between the two groups of monkeys.

Figure 3.37: Total time needed to complete (or nearly complete) the hidden Brinkman board task.

- *A: Untreated (control) monkeys*
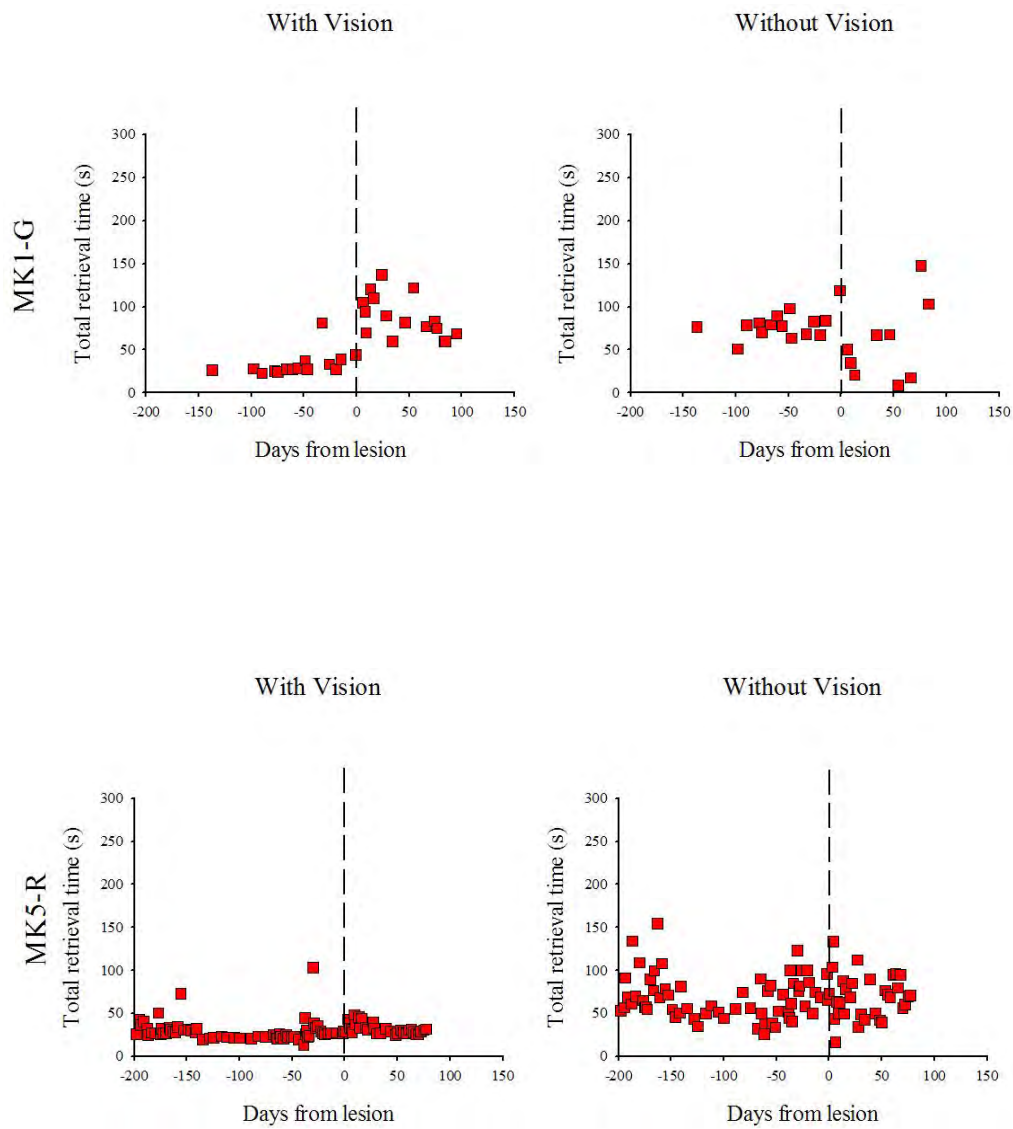
Figure 3.37, Panel *B: Anti-Nogo-A antibody treated monkeys*

_____
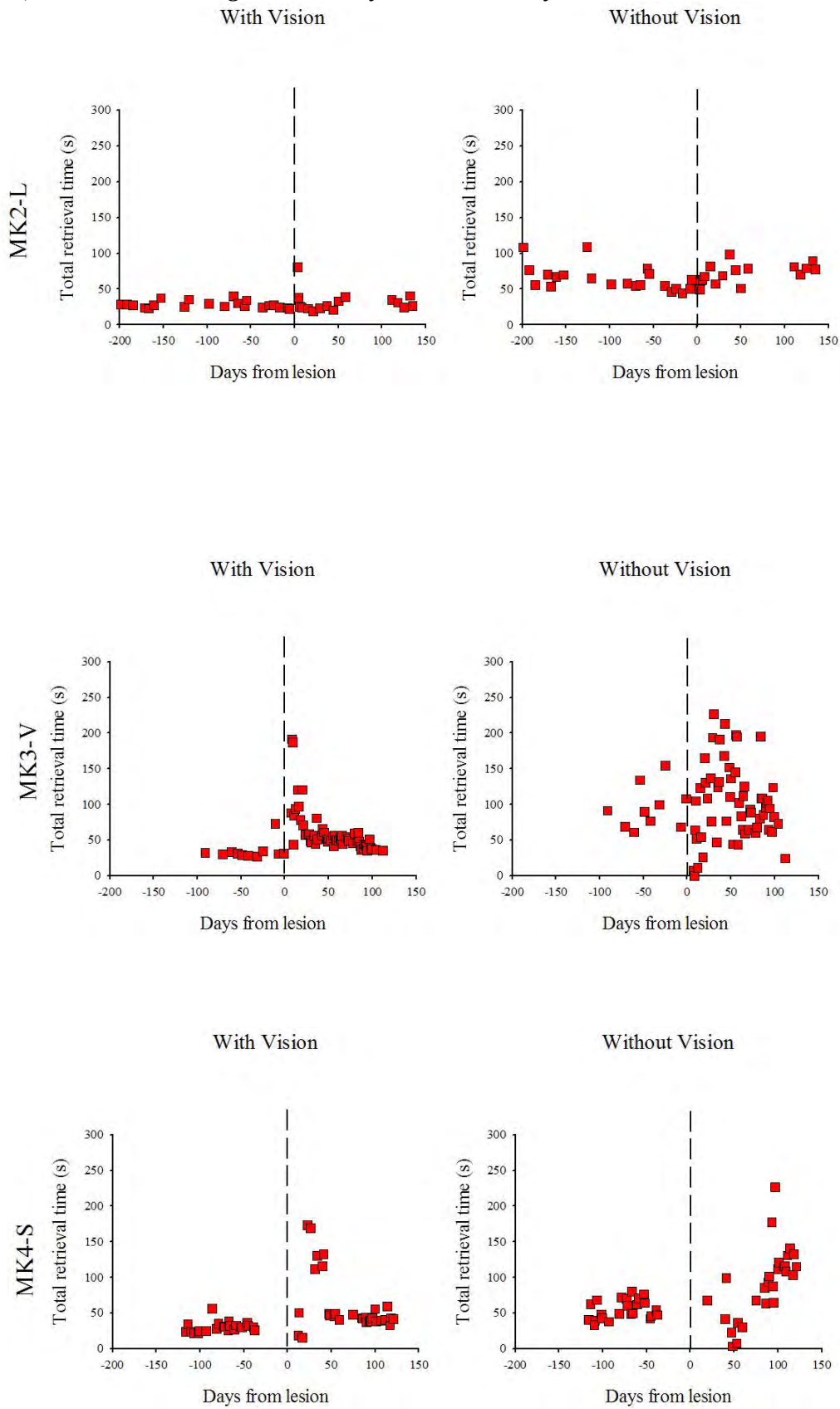
3.3.3 Relationship between behavioral data and lesion

3.3.3.1 Summary of behavioral recovery

From the Modified (standard) Brinkman board test data of each monkey, the mean pre- and post-lesion scores (sum of total number of horizontal and vertical pellets retrieved in the first 30 seconds) of the respective plateau phases were calculated. The pre-lesion behavioral score plateau of each monkey was considered as a score of 100%. On this basis, the percentage of post-lesion recovery for each monkey was calculated expressing the post-lesion scores as percentages of pre-lesion scores. This quantitative assessment in % of behavioral recovery after the lesion is represented in Figure 3.38.for untreated control monkeys and for the anti-Nogo-A antibody treated monkeys.
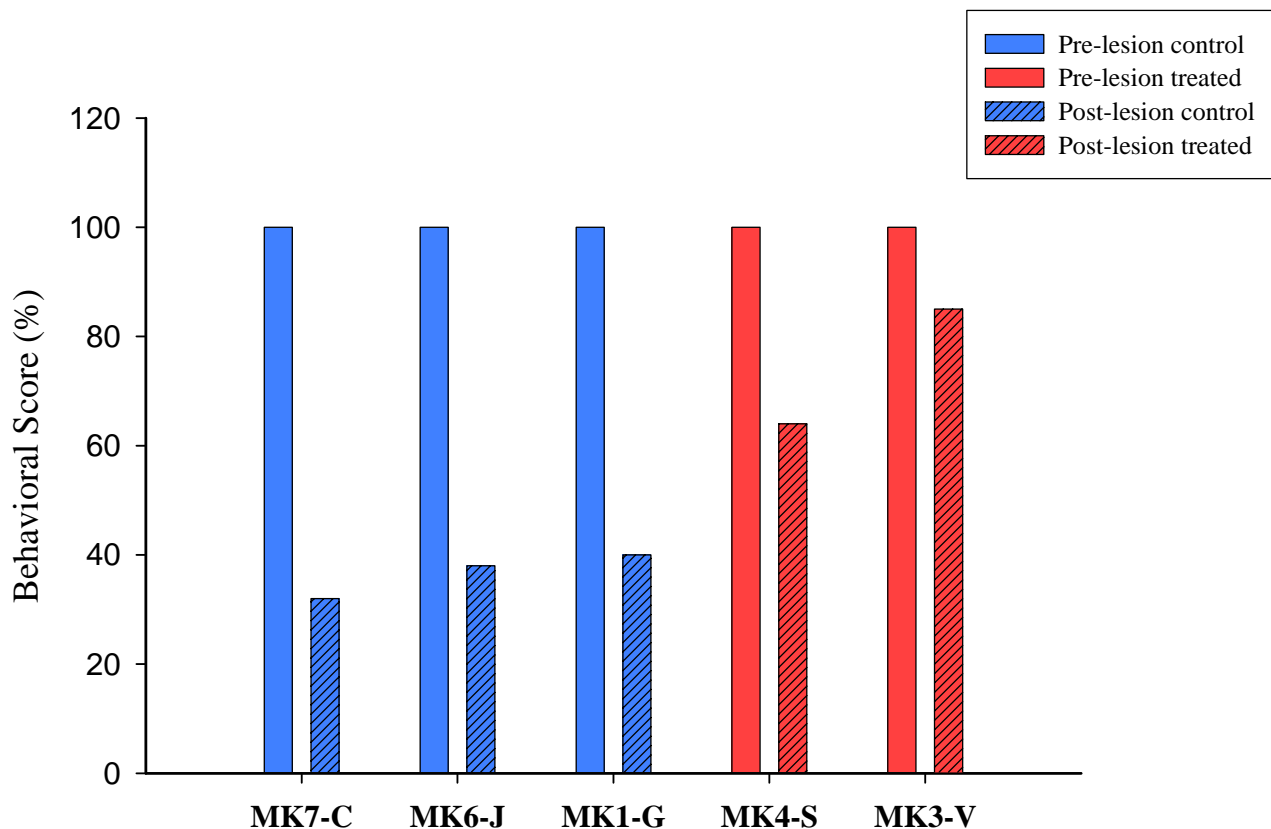
Figure 3.38: Modified (standard) Behavioral Brinkman test scores, before and after cortical lesion, expressed as percentages of pre-lesion scores. Untreated control monkeys are in blue and anti-Nogo-A antibody treated monkeys in red. The dashed plots show the post-lesion scores reached for each monkey.

The untreated monkeys recovered below 40% of manual dexterity after the lesion. The higher recovery for the untreated monkeys was for the monkey MK1-G that had a smaller ibotenic injection than the other two control monkeys (MK6-J and MK7-C), corresponding to a lesion restricted to the digit area in M1. For the anti-Nogo-A treated monkey, the recovery reached 64% for monkey MK4-S and 85% for monkey MK3-V. Figure 3.38 shows that anti-Nogo-A antibody treated monkeys recovered somewhat better their hand dexterity following the lesion than untreated control monkeys.

3.3.3.2 Correlation between behavioral recovery and lesion size

Based on the behavioral recovery in the Modified Brinkman board test, a correlation between the recovery and the lesion size can tentatively be made, as shown in Figure 3.39. In fact, it is expected that the amount of brain tissue destroyed by a cortical lesion is a key parameter impacting on post-lesion recovery of manual dexterity in monkeys, as well as in other mammals. To investigate this, two different types of correlation graphs were established. First, the mean post-lesion recovery in the Modified (standard) Brinkman task expressed in % were plotted as a function of the cumulated lesion surface in M1 (Figure 3.39, Panel A), and as a function of the cumulated lesion surface in all areas, thus including S1 for instance (Figure 3.39, Panel B). The surface values are those taken from Table 3.1 (see chapter 3.1 of results on page 208). Furthermore, a second type of correlation graphs was made, in which the mean post-lesion recovery in the Modified (standard) Brinkman task expressed in % was plotted as a function of the total lesion volume in M1 (Figure 3.39, Panel C) and in all cortical areas (Figure 3.39, Panel D). The volume of lesion values are those derived from Table 3.1. There was a tendency towards an inverse correlation between cumulated lesion surfaces and mean post-lesion performances in the Modified (standard) Brinkman board task, within the group of untreated control monkeys (MK1G, MK6-J and MK7-C) as well as in the anti-Nogo-A antibody treated monkeys (MK2-L, MK3-V, MK4-S). The same was generally true for the lesion volumes and the mean post-lesion recovery in the Modified (standard) Brinkman board task.

In general, these data are consistent with the general notion that the larger the lesion size the less good was the post-lesion recovery. Note however that lesion size does not tell the whole story as the precise position of the lesion is also a crucial parameter. In other words, two lesions of equal size in M1 may have quite different effects depending on their precise location, for instance how much of the lesion affects the hand representation. As a preliminary tendency, the anti-Nogo-A antibody treated monkeys tend to recovery somewhat better the untreated control monkeys. This tendency appears even when the lesion was bigger in an anti-Nogo-A antibody treated monkey

(MK4-S) than in an untreated control monkeys (MK1-G). However, this tendency needs to be confirmed on a larger number of animals (see discussion for more details).

Figure 3.39: Correlation between post-lesion recovery and lesion size in M1 (Panels A and C: surface and volume, respectively) and the total lesion size in all cortical areas (Panels B and D: surface and volume, respectively). Blue symbols are for untreated control monkeys whereas red symbols are for anti-Nogo-A antibody treated monkeys.

Panel A
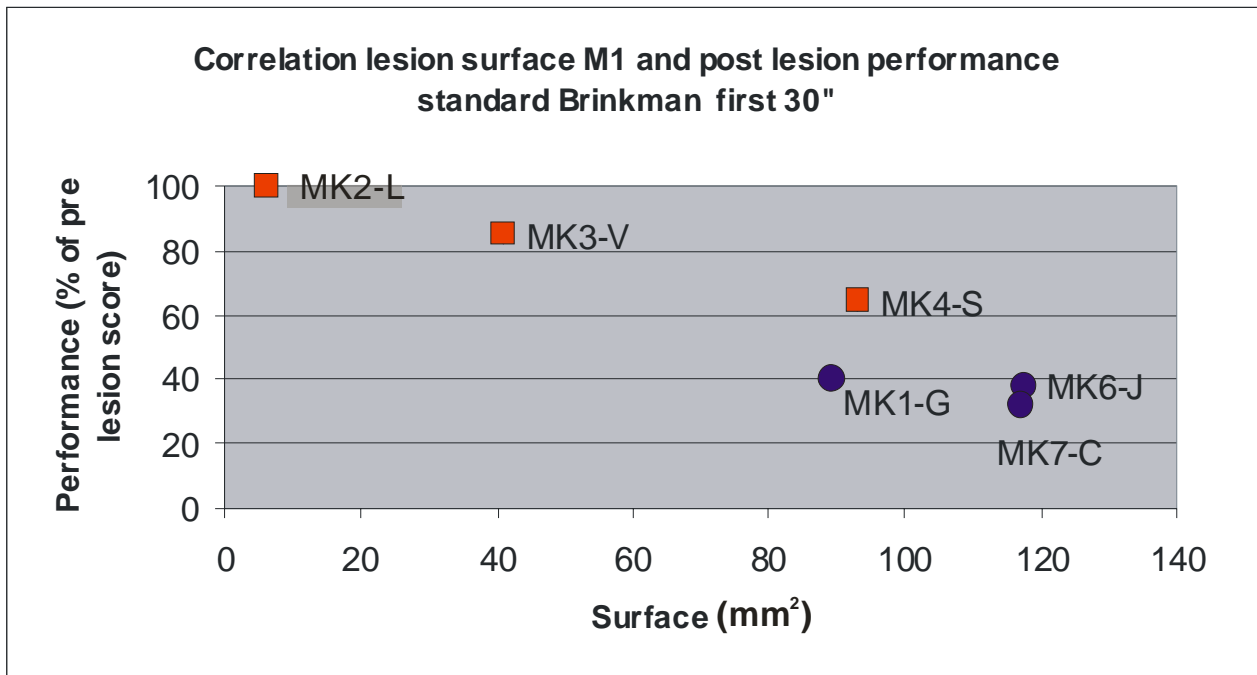
Panel B
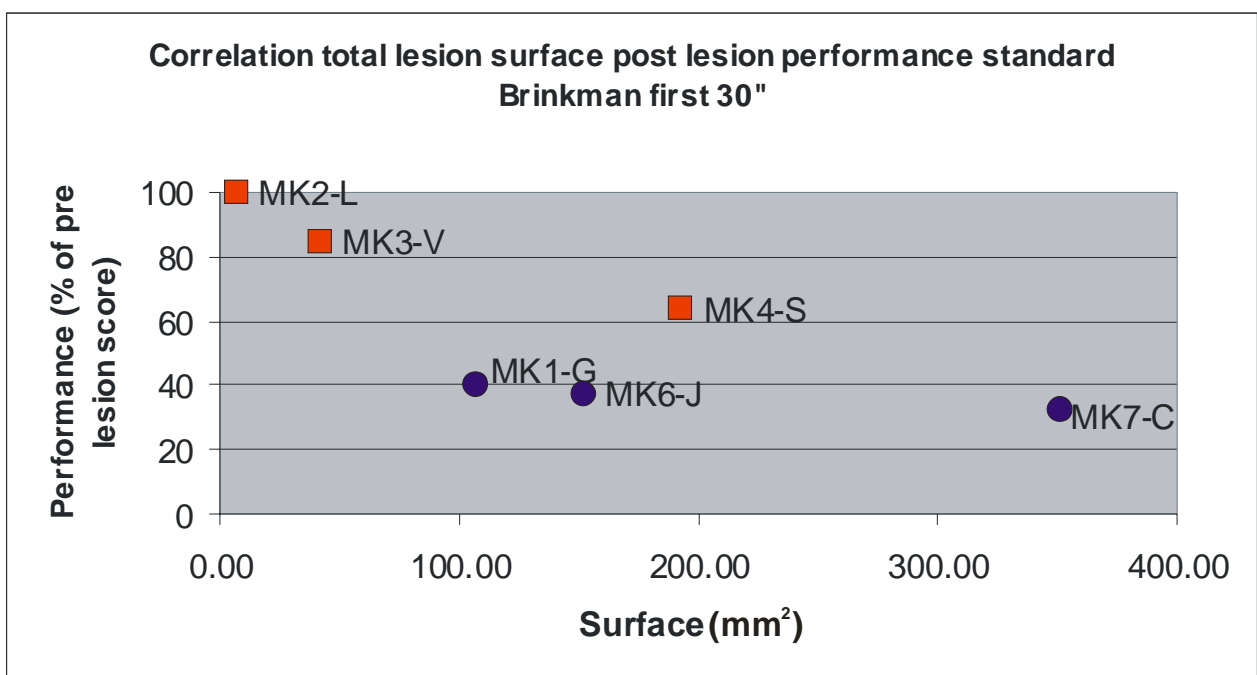
Fig. 3.39 (con't)

Panel C
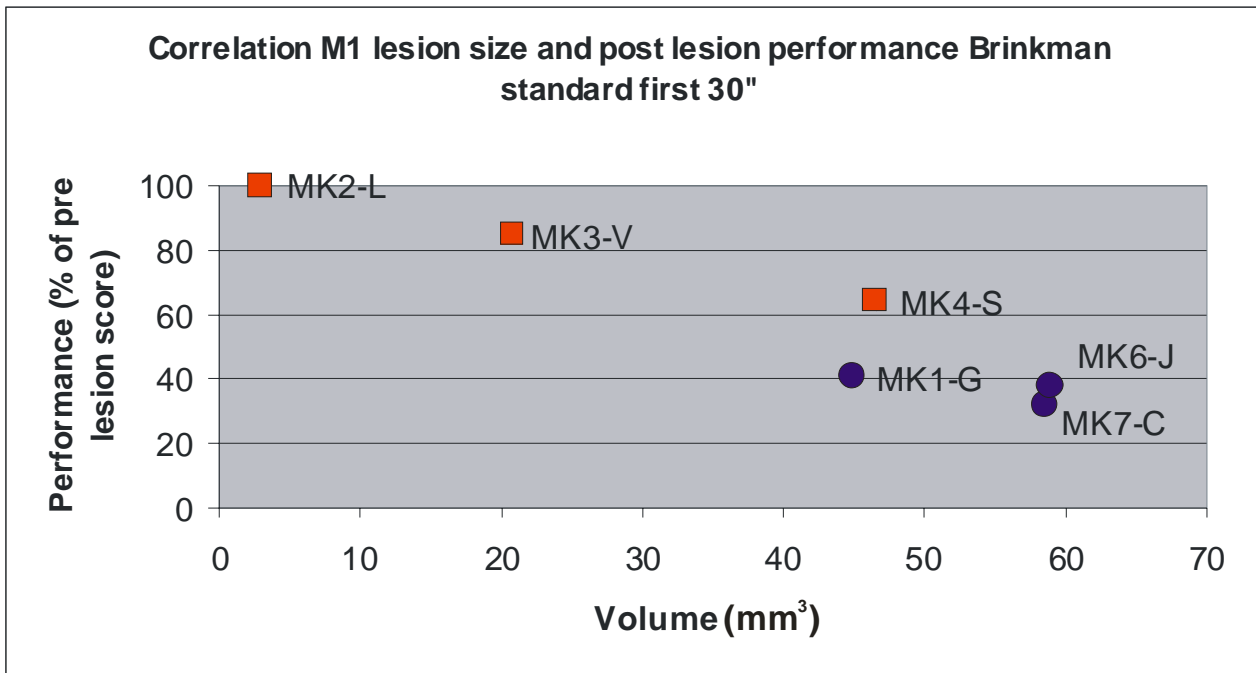
Panel D
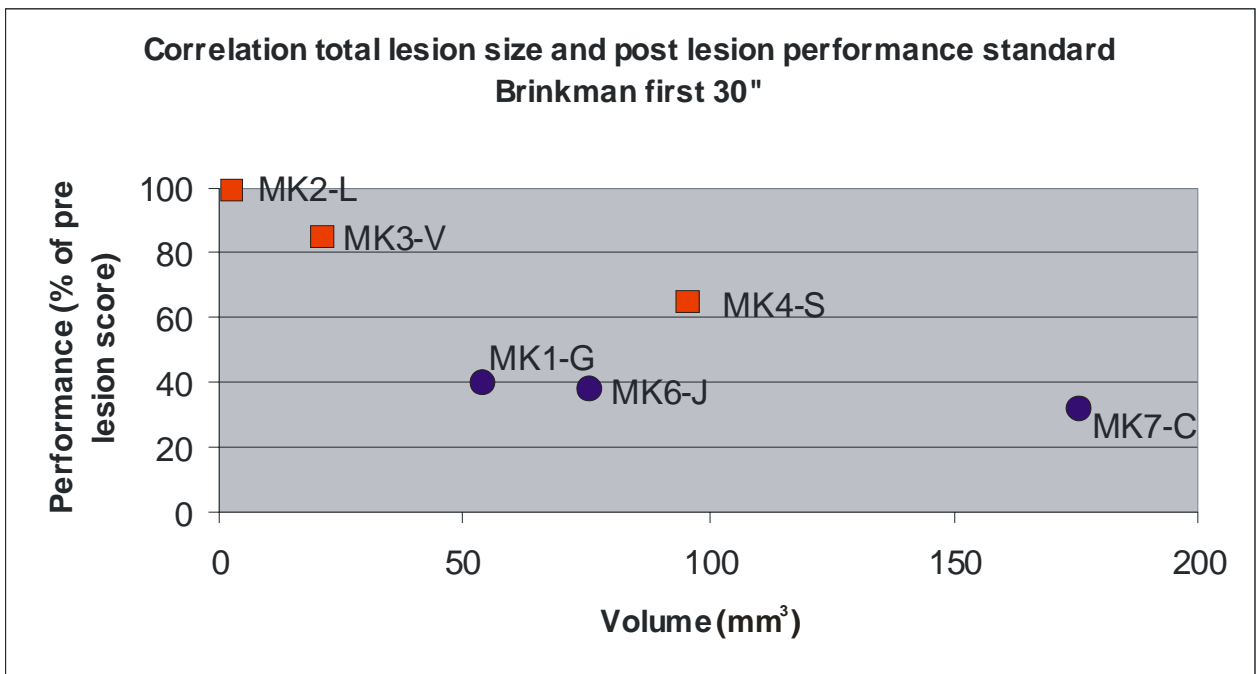
Figure 3.39: Correlation of standard Brinkman performance and the lesion size of M1 (panel A and Panel C) and the total lesion size of all motor cortical areas (Panel B and Panel D).

3.3.3.3 Statistical analysis of the behavioural data

The Table 3.3 below summarizes the results from statistical tests applied on pre- and post-lesion data from corresponding pre- and post-lesion plateau phases of the modified (standard) Brinkman task in three anti-Nogo-A antibody treated monkeys (MK2-L, MK3-V and MK4-S) and two untreated control monkeys (MK1-G, MK5-R). For each monkey, pre- and post-lesion scores in the first 30 seconds for vertical and horizontal slots individually were compared statistically. In addition, for each monkey, the mean retrieval time to grasp out a pellet from 6 specific slots (Contact time=average time needed to pick rewards from the first horizontal slot, the first vertical slot, the two most peripheral horizontal slots and the two most peripheral vertical slots see Figure 2.9 in methods) for the pre- and post-lesion plateau phases were compared. We used the parametric t-test or, if more adequate, the non-parametric Mann-Whitney-test. All pre- post-lesion differences were statistically significant, except for the horizontal slots and the contact time of MK2-L, which had a very small lesion, which did not really impaired manual dexterity. In all other monkeys, the post-lesion recovery was thus incomplete.

		Standard Brinkman Task					
		Plateau-Vertical (nb. Pellets retrieved in 30')		Plateau-Horizontal (nb. Pellets retrieved in 30')		Contact Time (s)	
		Pre-lesion	Post-lesion	Pre-lesion	Post-lesion	Pre-lesion	Post-lesion
MK3-V	Mean ± SD	14.72 ± 2.48	13.02 ± 2.74	12.04 ± 2.41	9.0 ± 2.09	0.70 ± 0.36	2.10 ± 1.13
	P value	$p \leq 0.001$		$p \leq 0.001$		$p \leq 0.001$	
MK4-S	Mean ± SD	12.16 ± 2.58	8.06 ± 1.50	10.32 ± 2.86	6.58 ± 1.39	0.78 ± 0.37	2.80 ± 0.79
	P value	$p \leq 0.001$		$p \leq 0.001$		$p \leq 0.001$	
MK2-L	Mean ± SD	13.21 ± 2.42	14.64 ± 2.13	11.53 ± 2.79	10.88 ± 2.93	0.73 ± 0.38	1.04 ± 0.97
	P value	$p = 0.013$		NS		NS	
MK1-G	Mean ± SD	12.35 ± 2.81	8.12 ± 2.73	8.94 ± 2.91	1.32 ± 0.99	0.88 ± 0.27	2.48 ± 0.93
	P value	$p \leq 0.001$		$p \leq 0.001$		$p \leq 0.001$	
MK5-R	Mean ± SD	14.31 ± 3.39	12.09 ± 1.76	11.64 ± 2.73	9.1 ± 2.05	1.03 ± 0.32	2.01 ± 1.14
	P value	$p = 0.003$		$p \leq 0.001$		$p \leq 0.001$	

Table 3.3. Summary of results of statistical analysis for the modified (standard) Brinkman board task. The corresponding values for control monkeys MK1-G and MK5-R are shaded in grey. NS: Non-significant, SD: Standard deviation.

_____

3.4 Muscimol injections (reversible inactivation experiments)

The main goal of Muscimol injections is: 1) to assess the role of the spared and/or reorganized hand area and/or premotor areas in the recovery of manual dexterity from injections of ibotenic acid, which provoked the unilateral lesion in the motor cortex and 2) to investigate a possible role played by the ipsilateral corticospinal projections to the impaired hand (originating from the intact hemisphere) in the recovery process from lesion of the opposite motor cortex.

The results presented below will describe observation derived from <u>muscimol injections</u> placed basically in the three following regions:

- In and around the site of the permanent unilateral lesion in M1, provoked several months before by the ibotenic acid injection (paragraph 3.4.1 below).

- In the premotor cortex, on the same hemisphere as the permanent lesion in M1 (paragraph 3.4.2 below).

- In the contralesional (intact) hemisphere, in its hand representation in M1 (paragraph 3.4.3 below; limited to monkey MK2-L).

The muscimol injections were made mostly in the lesioned motor cortical areas for monkeys MK2-L, MK3-V and MK4-S and in the motor cortex in the intact hemisphere for monkey MK2-L. Note that monkey MK1-G was not subjected to any muscimol injections and monkey MK5-R is still an ongoing experiment. In the lesioned motor cortex, two injections sessions were conducted, one in the "new" fingers representation and the second in the premotor areas (PMv and PMd). Only one injection session was made in the intact motor cortex fingers representation for monkey MK2-L. The sessions were at least three days apart. In monkey MK3-V, because PMv was not explored by ICMS, the positions of Muscimol injections were approximated on the basis of coordinates derived from monkeys in which PMv was explored previously. Muscimol injections were performed at the end of the post-lesion ICMS and all injection sites (indicated by **M** on maps) were determined using these maps. For better interpretation of the impact of Muscimol injections, unfolded post-lesion ICMS maps of MK3-V and MK4-S were added. Although it is interesting to analyze the Muscimol effects over time, the most representative and most precise results are obtained within 1 hour post-injection. Later, after the infusion, due to lack of detailed information about the diffusion pattern of Muscimol in the tissue adjacent to the original target sites, results of an individual experiment are more difficult to interpret. Therefore, descriptions given below are limited to 1 hour post-infusion (MK2-L and MK3-V). As an example however, for monkey MK4-S observations up to 5h post-infusion are indicated.

3.4.1 Muscimol injection in and around the permanent lesion site

Figures 3.40-3.41 summarize the effect of Muscimol injections at the same sites as where the ibotenic acid was injected to produce the permanent lesion, for the three monkeys (MK2-L, MK3-V and MK4-S). Figure 3.40 illustrate that, 20 minutes after the last Muscimol injection in the core of the lesion area in the left M1 (total volume injected was about 14µl), MK2-L showed impairment of the contralateral (right) hand. In fact, there was a clear paralysis of the fingers and a minimal paralysis of the wrist. Therefore, the monkey could no use its fingers to hold food, but the monkey compensated this impairment by using its proximal forelimb joints to support food during feeding (Fig. 3.40) and its bodyweight while moving in the home cage. This experiment demonstrates that, in this monkey MK2-L, the main control of manual dexterity for the right hand is still under control of the hand area of the left M1.

Similar observations were obtained in monkey MK3-V after muscimol injections performed in the permanent lesion site in left M1 (total volume injected was about 11µl). In fact, a paralysis of fingers of the contralateral (right) hand can be observed, thus leading to reversible loss of recovered manual dexterity in the standard Brinkman task.

Based on the post-lesional maps (Fig. 3.40A and B), it seems that for these two monkeys (MK2-L and MK3-V) the muscimol injections affected the spared and/or reorganized corticospinal neurons. As Muscimol injections were placed in the rostral bank of the central sulcus where, according to post-lesion mapping (see unfolded map), a substantial portion of the hand representation area was left intact, the loss of recovered manual dexterity by Muscimol therefore can be attributed to inhibition of this part of M1. In contrast, more proximal parts of the contralateral forelimb as well as the ipsilateral forelimb were not impaired, and the monkeys used it for feeding and moving in the home-cage (Figure 3.40 B). These observations were similar to those in monkey MK2-L. It seems that the control of the contralateral hand dexterity remains, at least in part, under the control of the M1 territory which escaped to the ibotenic acid effect (namely surrounding the permanently lesioned area).

A

Monkey MK2-L Post-Lesion

Media

Rostral ◄────────► Cauda

Latera

B
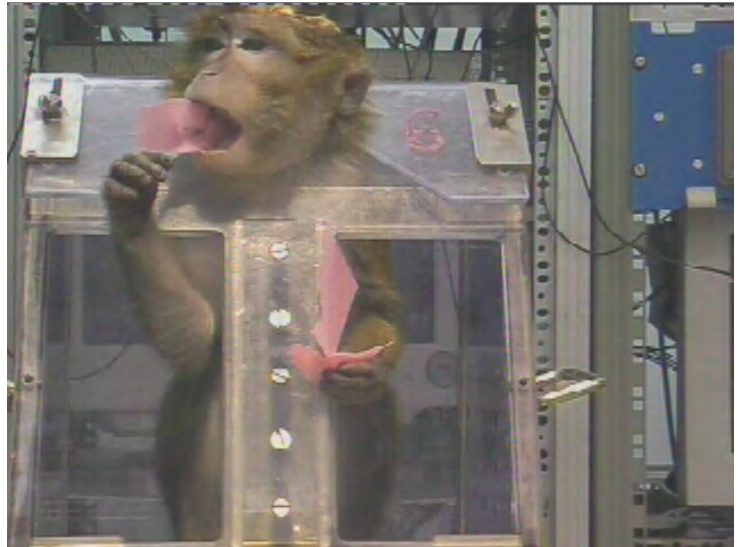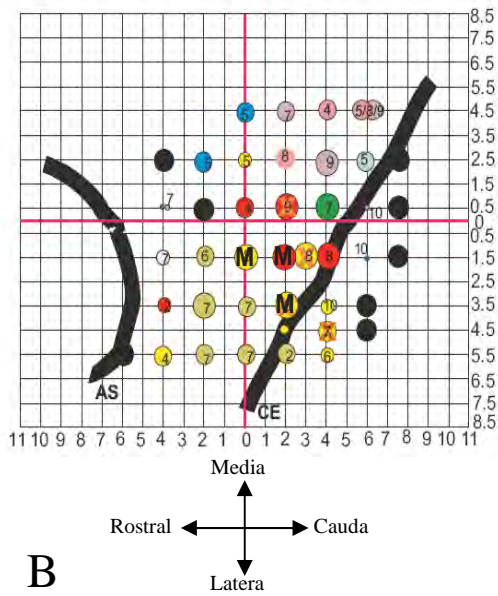
Monkey MK3-V Post-Lesion

Post-lesion
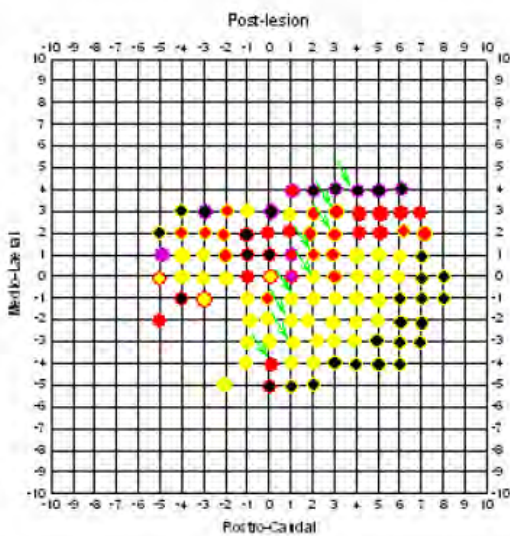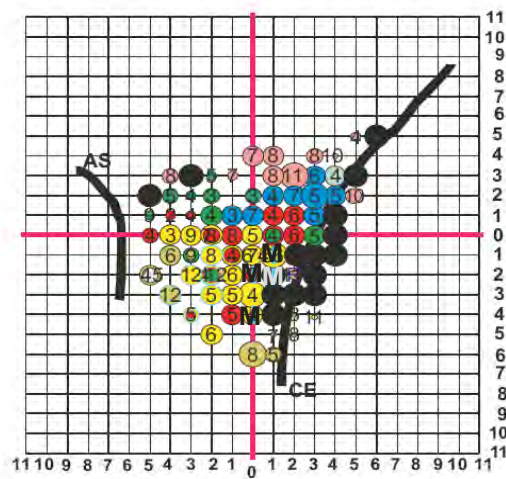
Figures 3.40: Muscimol injections in the permanent lesion site in the left M1 of monkey MK2-L (A) and of monkey MK3-V (B). Injection sites are indicated by **M** on the surface maps of left M1. Monkey MK2-L (A) used its both hand to eat but, to grasp a piece of food, the monkey used all fingers (right hand). Monkey MK3-V (B) has a similar deficit, as shown in the picture with its hand fingers spread. Legend for ICMS map is similar as in chapter 3.2.

However, the muscimol injections in the permanent lesion site in left M1 (total volume: 11 µl) for monkey MK4-S showed a rather weak effect on the right hand when the monkey was performing the standard Brinkman task as well as in its home-cage. In fact, after 15 minutes, the contralateral hand fingers showed some impairment and clumsiness. The movement was slower. Nevertheless, these deficits were not visible 45 minutes after the muscimol injections. No effects were observed on proximal joints. The minimal loss of recovered manual dexterity fits nicely with the data represented on the unfolded map of MK4-S (Fig. 3.41 A) showing irresponsive sites in the finger region of M1 no longer controlling manual dexterity. Nevertheless, when the muscimol injections were placed in spared or in the "new" hand representation near the permanent lesion site, the effect on the right hand was more evident (Fig. 3.41B). In fact, after 20 minutes, the monkey was enable to use its fingers to hold the pieces of food (see pictures in Fig. 3.41B), with little effect on the wrist. After 3 hours, the muscimol effect attained the whole forelimb which was hanging down (Fig. 3.41B).
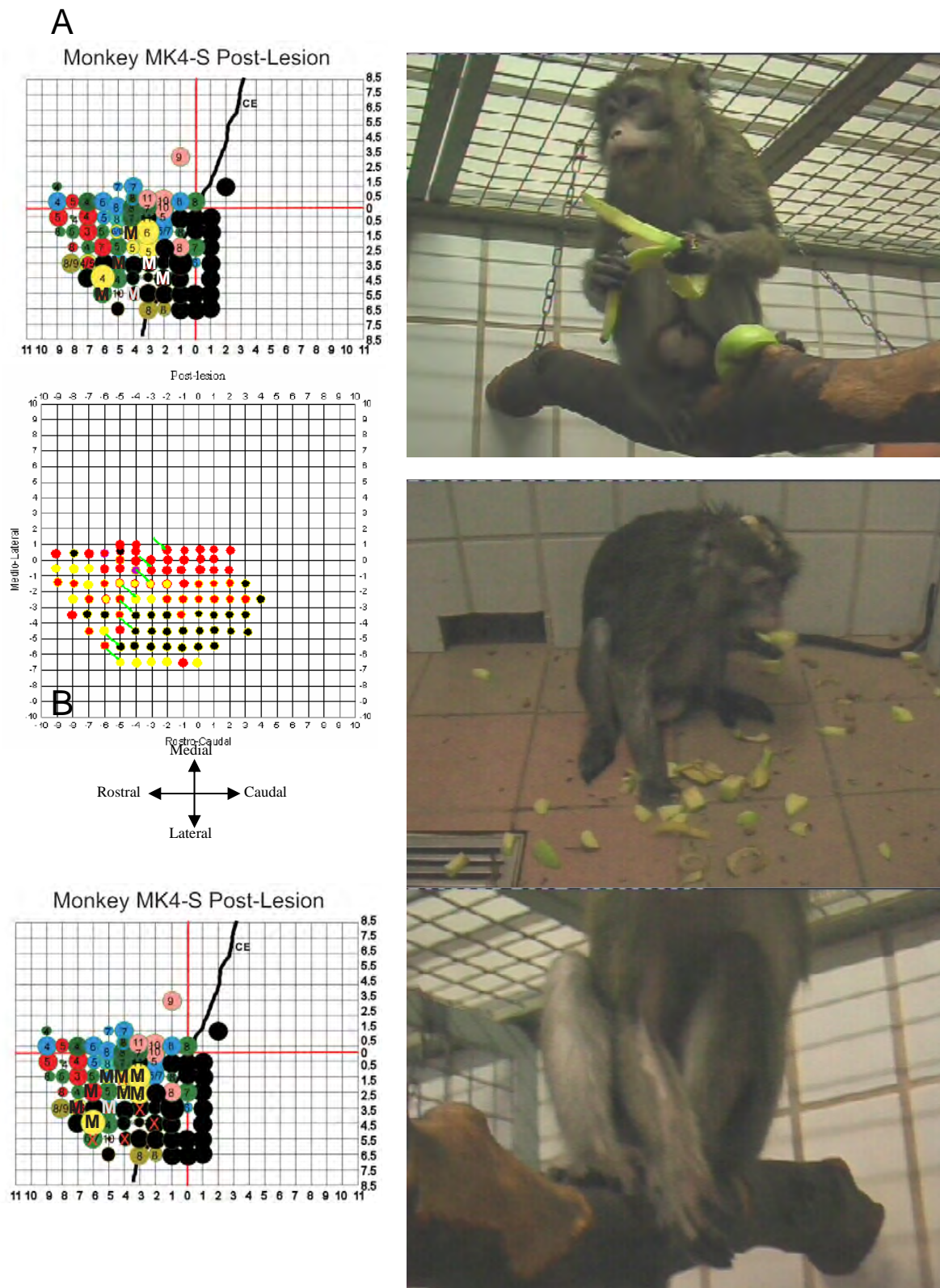
Figure 3.41: Effect of muscimol injection in monkeys MK4-S placed in the permanent lesion site (A) and in the spared fingers area (B). Legend of the ICMS maps is the same as in chapter 3.2.

_____

3.4.2 Muscimol injection in the (ipsilesional) premotor cortical areas

Muscimol injections in premotor cortical areas (on the same hemisphere as the permanent lesion in M1) showed no effects on the hand dexterity for monkey MK2-L (Fig. 3.42). In fact, the monkey used its index and thumb (precision grip) to hold pieces of food as shown in Figure 3.42. On the other hand, PMd muscimol injection in monkey MK3-V showed some effect. Figure 3.43 shows that monkey MK3-V used all its fingers to grasp a piece of food from the experimenter's hand rather than using precision grip. Such effect was not observed when the muscimol injection was placed in PMv area. In summary, the muscimol injection in premotor cortex in monkey MK2-L with a small permanent lesion in M1 does not impact on the recovered post-lesion hand dexterity whereas, in monkey MK3-V with a bigger M1 permanent lesion, the inactivation of PMd induced a modification of grasp strategy.
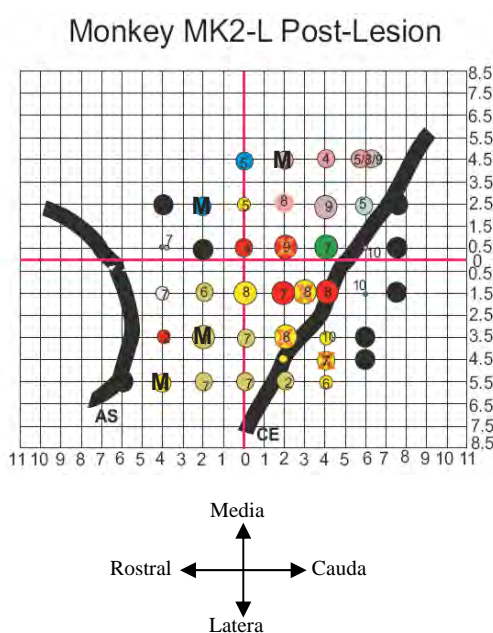
Figure 3.42: Muscimol injections in the premotor cortical areas in monkey MK2-L. Monkey used its index and thumb to tear up and hold the banana skin, as an intact monkey.

A
Monkey MK3-V Post-Lesion

Post-lesion

Medial
Rostral ← → Caudal
Lateral

B
Monkey MK3-V Post-Lesion
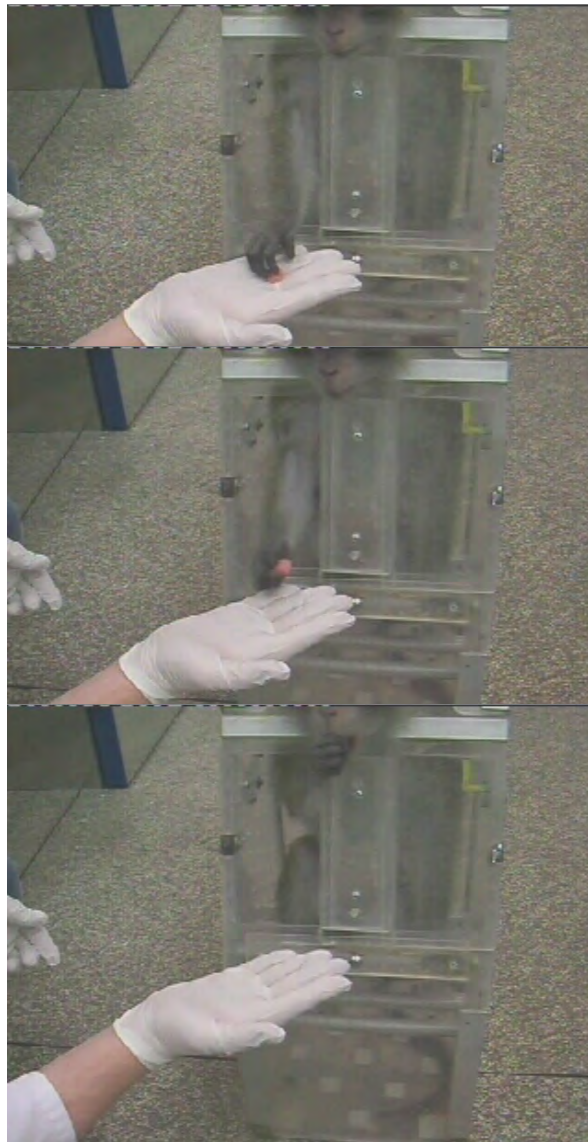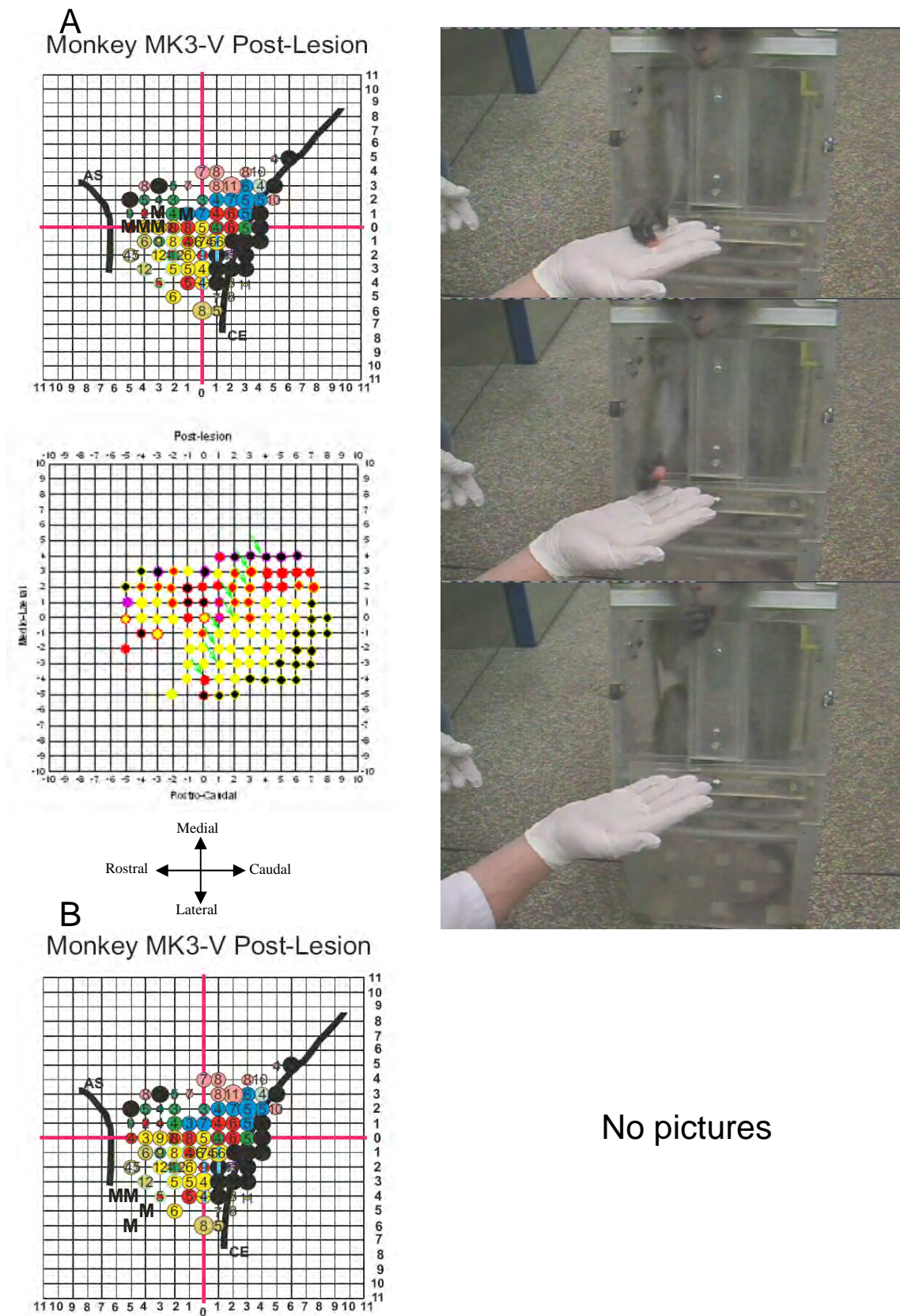
No pictures

Figure 3.43: Muscimol injections in PMd (A) and PMv (B) in monkey MK3-V. As a consequence, the monkey used all fingers to grasp a piece of food instead of only the typical precision grip (thumb and index finger).

_____

As compared to monkey MK3-V, in monkey MK4-S, the muscimol injections in PMd induced even more prominent impairment of the fingers 15 minutes after the last injection. After 20 minutes, the effect reached the proximal forelimb which most the time was just hanging down (Fig. 3.44), but the monkey was still able to hold medium size pieces of food with its fingers. Nevertheless, the force of the grip was significantly reduced as the food pieces fell most the time out of its hand. During the following hours, the muscimol effect became even more prominent. Based on these data, it is clear that PMd in monkey MK4-S played a significant role in the recovery process. Similar observations were obtained in the previous study of Liu and Rouiller (1999) on the monkeys MK6-J and MK7-C.
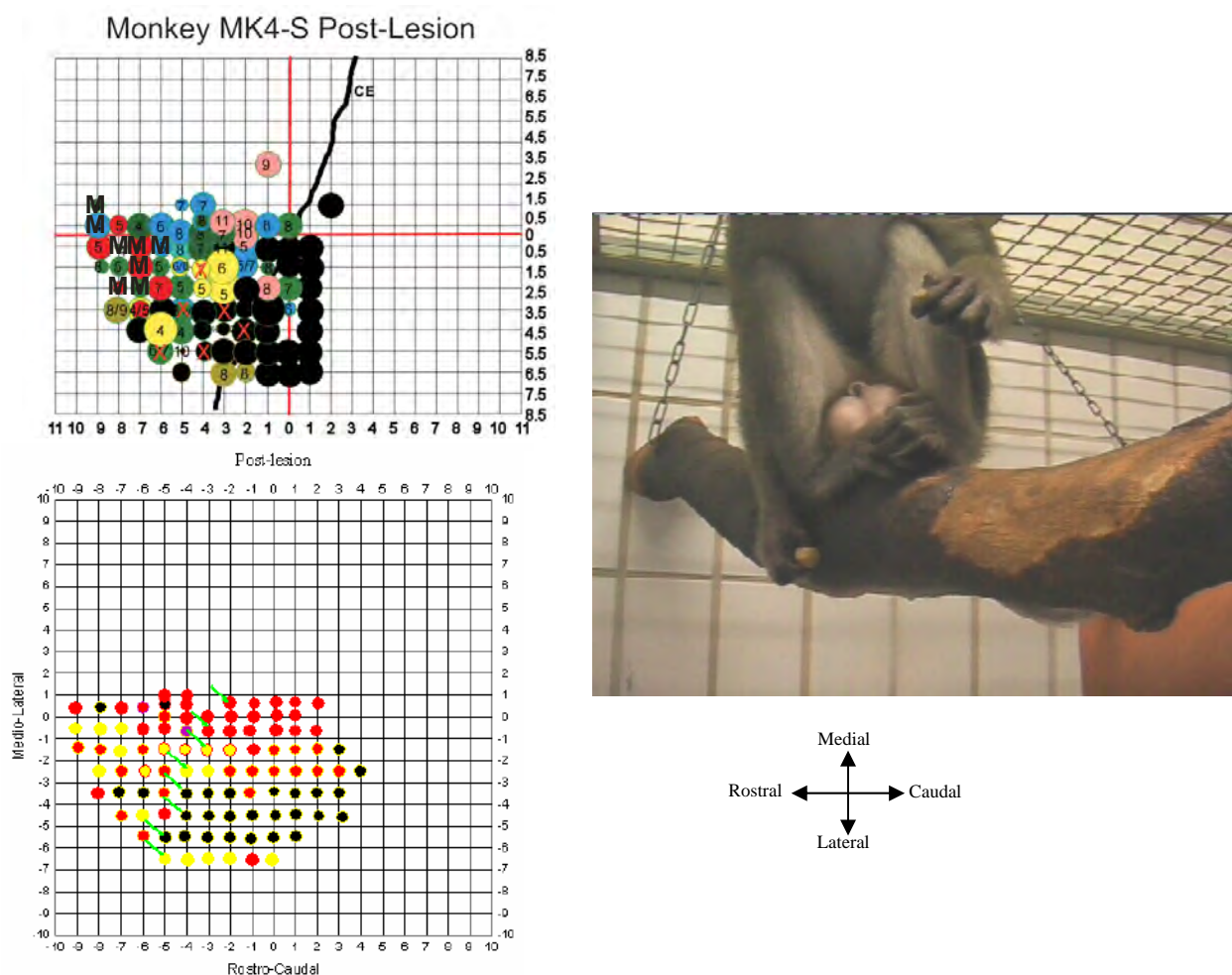
Figure 3.44: Muscimol injections in PMd (A) in monkey MK4-S. As a consequence, the monkey used all fingers to grasp a piece of food, but the force was substantially reduced.

3.4.3 Muscimol Injection in the contralesional (intact) motor cortex

As mentioned above, the goal of muscimol injection in the contralateral (intact) motor cortex (right M1) was to assess the role of the ipsilateral corticospinal projections in the recovery process of the hand affected by the permanent lesion in the left M1. From this experiment conducted on MK2-L, it seems that the muscimol injections in the intact (right) M1 did not provoke any effect on the ipsilateral (right) forelimb. In fact, when the total volume injected was about 9 µl, the effect 20 minutes after the injections was limited only the fingers and the wrist of the (left) contralateral hand (Fig. 3.45 B), without effect on the proximal forelimb muscle or the hindlimb. Again, there was no effect on the hand homolateral to the muscimol injection in the right M1. When the total volume of muscimol was about 20 µl, severe but not complete paralysis of the contralateral (left) forelimb was observed after 20 minutes post-injection (fingers, wrist and distal part of the forelimb strongly affected; proximal part of the forelimb slightly less affected). The contralateral (left) hindlimb was also substantially affected due to the relatively high amount of Muscimol infused in the intact M1, including a possible spread to the hindlimb area (see abnormal position of left hindlimb in Fig. 3.45A). So, the high dose of muscimol almost induced a transitory hemiparesis in MK2-L, indicating the well known functional importance of M1 in controlling the contralateral limb muscles. However, even at such high dose of muscimol (20 µl), no effect was observed in the ipsilateral (right) forelimb or hindlimb.

_____

A

Medial

Rostral ←——→ Caudal

Lateral

B
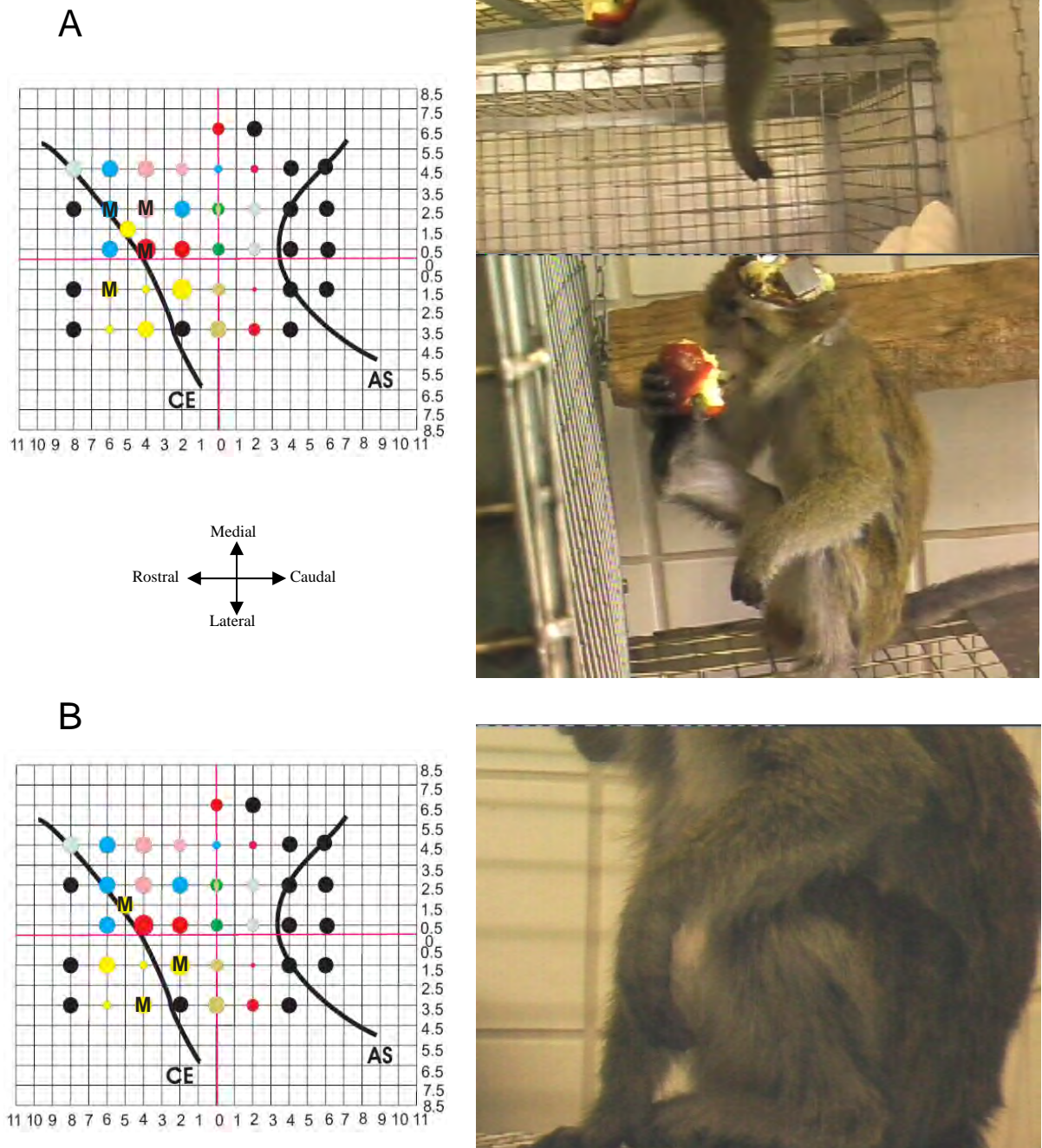
Figure 3.45: Muscimol injections in the contralesional (intact) motor cortex in monkey MK2-L. Two muscimol sessions are presented, one with a 20 ul volume (panel A) and one with 9ul (panel B).

_____

3.4.4 Conclusion on muscimol inactivation experiments

Table 3.4 summarizes the results obtained from muscimol injections either in the permanent lesion site in M1, or in the premotor cortical areas or in the contralesional (intact) motor cortex.

Injection Sites	Monkey	Volume	Effect			
			≤20'	45' (MK4-S); 1h (MK5-R)	2h	5h
Permanent Lesion sites	MK2-L	14µl	Fingers (---) Wrist (-)			
	MK3-V	11µl	Fingers (---)			
	MK4-S	11µl	Fingers (-) Hand (-)	very weak		
	MK5-R	10µl	Fingers (--) Wrist (-)	Fingers (--) Wrist (--)		
PMd/PMv	MK2-L	14µl	No effect	No effect		
PMd	MK3-V	5µl	Fingers (--)			
	MK4-S	10µl	Fingers (---)	Fingers (---) proximal (--)	Fingers (---) proximal (---)	Fingers (---) proximal (---)
	MK5-R	6µl	Fingers (-) Wrist (--)	Fingers (-) Wrist (--)		
PMv	MK3-V	4.4µl	No effect			
	MK5-R	6µl	No effect	No effect		
Spared hand area	MK4-S	9.2µl	Fingers (--) Wrist (--)	distal (---) proximal (---)		
	MK5-R	9µl	Fingers (---) Wrist (--)	Fingers (---) Wrist (--)		
Contralateral M1	MK2-L	20µl	Left forelimb (---) Left hindlimb (-)			
		9µl	Left fingers (--)			

Table 3.4: Summary of the muscimol injection sessions. The signs between parentheses indicate the severity of the limb impairment: (---) severe effect, (--) moderate effect (-) weak effect. Left forelimb is the intact one (considered here only for the muscimol injections in the intact hemisphere).

The Figure 3.46 below illustrates the main findings of the impact of muscimol injections in the lesioned motor cortex on post-lesion recovery of manual dexterity. In Panel A, the data of anti-Nogo-A antibody treated monkeys (MK2-L, MK3-V and MK4-S) are summarized whereas data of two untreated control monkeys (MK6-J and MK7-C, see Liu and Rouiller, 1999) are summarized in Panel B. It turns out that in the two monkeys MK6-J and MK7-C, the permanent lesion in M1 hand area was big and therefore muscimol injection in this territory had no additional effect. In contrast, when PM was inactivated with muscimol, the recovered performance was lost, indication that PM indeed played a major role in the functional recovery in monkeys MK6-J and MK7-C (Liu and Rouiller, 1999). For the monkeys included in the present study (MK2-L, MK3-V and MK4-S), the muscimol data are somewhat different. The lesion in M1 hand area was smaller and some territory

controlling the hand was not affected by the ibotenic acid injection. As a consequence, when muscimol was infused in the lesioned M1, an additional loss was observed as it inactivated the territory which escaped the permanent lesion. The "spared" territory in M1 hand area thus played a role in the functional recovery. Moreover, inactivation of PMd also modified the recovered performance, suggesting that PM also plays a role in the functional recovery, in parallel to the "spared" territory in M1. The difference in term of muscimol effects between these 2 groups of monkeys (MK6-J, MK7-C on one hand and MK2-L, MK3-V, MK4-S on the other hand) appears to be mostly explained by the properties of the lesion (essentially size) rather than by the treatment (anti-Nogo-A antibody). Indeed, to infer a possible role of the treatment, this would require to conduct muscimol experiments in an untreated animal with an incomplete lesion (unfortunately this was not done in monkey MK1-G). Maybe, useful data will be derived from MK5-R.

Injection of Muscimol in lesioned hand area has no effect on recovery in untreated control monkeys MK6-J and MK7-C

Ibotenic acid induced lesion

Hand

Injection of Muscimol in PMd and PMv leads to temporal limited loss of recovery of hand dexterity in untreated control monkeys
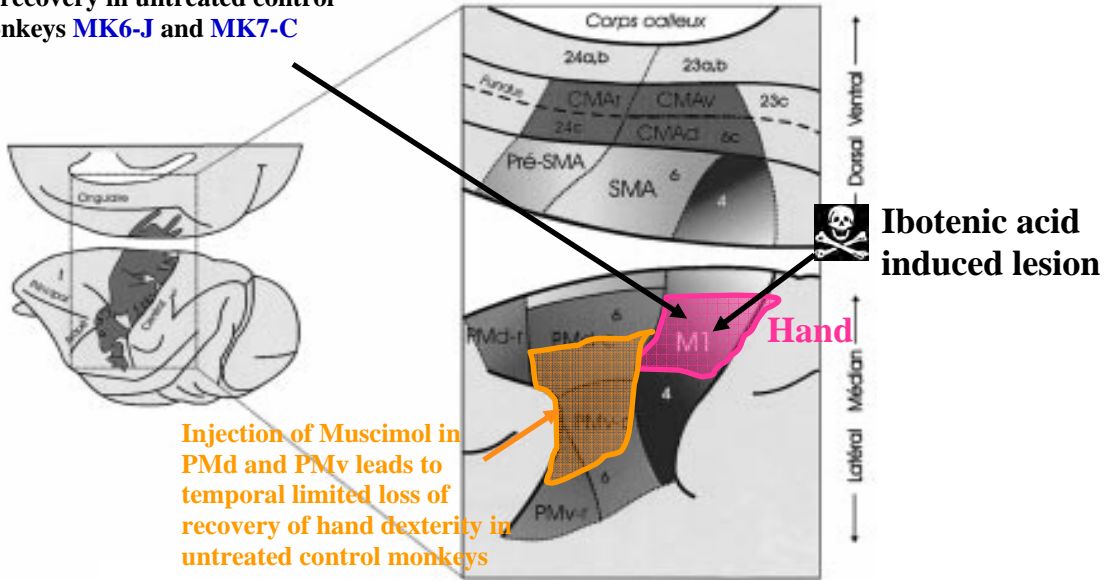
Panel A

Modified from Y. Vandermeeren et al 2003

Infusion of Muscimol in lesioned hand area leads to loss of recovery of hand dexterity in anti – NoGo-A antibody treated monkeys (MK2-L, MK3-V and MK4-S)

Ibotenic acid induced lesion

Hand

Injection of Muscimol in PMd but _not_ in PMv leads to temporal limited loss of recovery of hand dexterity in anti-Nogo-A antibody treated monkeys.
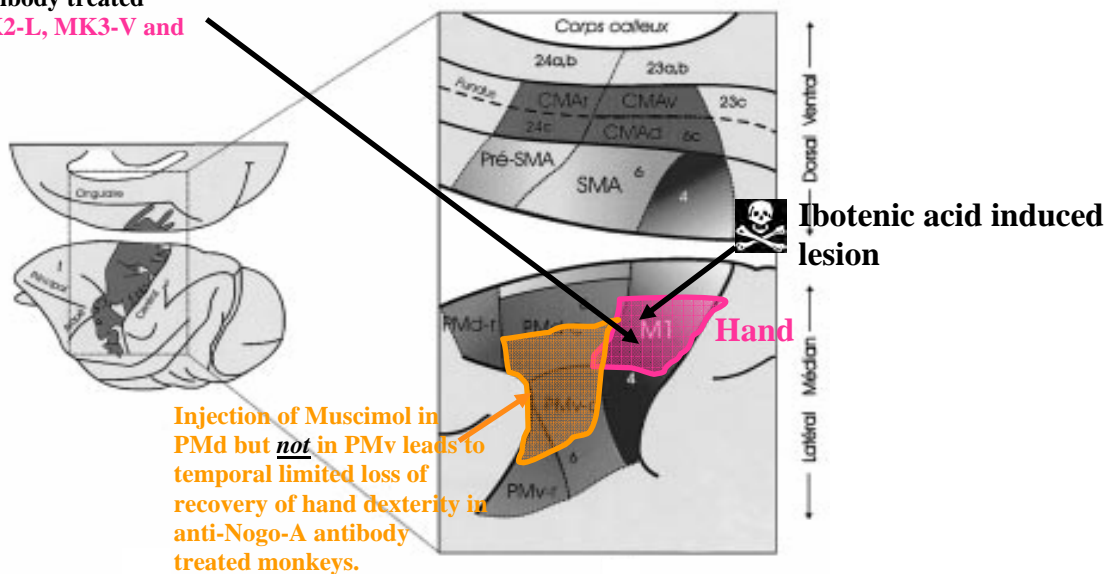
Panel B

Modified from Y. Vandermeeren et al 2003

Figure 3.46: Effects of post-lesion Muscimol infusion in untreated control monkeys (Panel A) and anti-Nogo-A antibody treated monkeys (Panel B) on recovery of hand dexterity. Note that the effects are based on a small number of animals and that the lesions in MK6-J and MK7-C were bigger than in MK2-L, MK3-V and MK4-S. Therefore the differences have to be considered as tendencies probably attributable not exclusively to anti-Nogo-A antibody treatment (see also Chapter 4 for detailed discussion).

Contents of Discussion

4. Discussion

4. Discussion

4.1 Lesions of motor cortex

The present study is a logical continuation of the pilot work of Liu and Rouiller (1999) with the aim to extend the number of monkeys subjected to motor cortex lesion and not treated (control animals). Furthermore, an additional goal was to extend the study to a treatment using an antibody against Nogo-A (based on the promising results obtained in the rat; see Emerick et al., 2003, 2004; Lee et al, 2004 ; Seymour et al, 2005). As far as the lesions are concerned, they were well placed in the two monkeys of Liu and Rouiller (1999); however they tended to be too large, as they encroached PM rostrally and S1 caudally. Furthermore, territories more proximal than the hand (wrist, elbow, shoulder) were also affected. In the present study, it was decided to tentatively better focus the unilateral motor cortex lesion to the hand representation of M1. For this reason, the volume of ibotenic acid injected was substantially reduced, from 40 μl down to 13 – 18 μl, depending on the surface of the hand area (see Table 3.1 in the results section). As expected, the lesion turned out to be considerably smaller and, to some extent, better restricted to the hand representation in M1. Adequate lesion characteristics were obtained for the monkeys MK1-G, MK3-V and MK4-S whereas, in contrast, the lesion was far too small in monkey MK2-L. In the latter monkey, the very small size of the lesion explains most of the exceptional functional recovery observed, certainly more than the treatment. Unfortunately, for this reason, the monkey MK2-L has to be excluded from further detailed discussion related to the effect of treatment.

An inherent difficulty of such lesion study is the considerable inter-individual variability in term of lesion size and lesion position. This difficulty can be circumvented in rodents by including a large number of animals in the study and eliminating the animals presenting inadequate lesion characteristics. For ethical reasons, studies conducted in monkeys include a limited number of animals, also because the experiment with a single animal is very long (about 2 years for each animal) and highly time consuming (an individual experimenter cannot supervise more than 2 monkeys simultaneously). For instance, the spinal injury study conducted in our laboratory (Freund et al., 2006, 2007; Schmidlin et al., 2004, 2005; Wannier et al., 2005) included 12 animals over a period of eight years, but involving a larger team of investigators. Due to this inter-individual variability, it is crucial to analyze the electrophysiological and behavioral data in the perspective of the lesion position and lesion extent (see below). The inter-individual variability is also due to other parameters, such as the

intrinsic motivation of the monkey, the interaction with the experimenters, seasonal variations, variable coherence within the groups of monkeys kept together in the detention boxes, possible (fortunately rare) diseases or wounds (resulting from inevitable fights between the monkeys), etc. Along this line, a very heavy constraint is the fact that a given monkey should always be supervised for the behavioral tests by the same investigator. Monkeys are indeed very sensitive to any deviation from established habits, which may dramatically affect the (behavioral) results.

Another reason to decrease the extent of the lesion in the present thesis work, as compared to the two pilot animals of Liu and Rouiller (1999) was that, in the latter two animals, the deficit was fairly considerable (loss of control of the hand and wrist, plus elbow to some extent) and the spontaneous recovery was rather modest (only 30% of the pre-lesion hand dexterity score). We felt that, for ethical reasons, the impact of the lesion could be slightly diminished and still have enough margin of progression to test the effect of the anti-Nogo-A treatment.

4.2 Post-lesion plasticity: interpretation of ICMS data

As a result of motor cortex lesion in infant monkeys (15-40 days after birth), a significant change of the motor map was observed (Rouiller et al., 1998): ICMS mapping conducted several years later at adult stage showed the appearance of a "new" hand area adjacent to the lesioned territory, medial to the original lesioned hand representation. The "new" hand area occupies a territory normally devoted to more proximal representations (wrist, elbow, shoulder), themselves shifted even more medially. This "new" hand area was demonstrated to be responsible for the extensive recovery of manual dexterity in these monkeys lesioned at neonatal stage. The question then arises as to whether such substantial re-arrangement of the motor map also takes place in M1 after a lesion taking place at the adult stage?

Based on the work of Liu and Rouiller (1999), it appears that the two monkeys lesioned in M1 at adult stage (MK6-J and MK7-C in the present thesis) do not exhibit such a profound re-arrangement of the ICMS map post-lesion around the lesioned territory. In absence of such re-appearance of a substitute of hand representation in M1, it was found that the incomplete (30%) functional recovery was under the control of the premotor cortex (PM) on the same hemisphere (Liu and Rouiller, 1999). However, the absence of substantial re-arrangement in M1 around the lesion may be due to the large extent of the lesion, spreading further than the hand area, thus leaving little space for re-arrangement in M1. We believe that the "new" animals introduced in the present thesis (MK1-G, MK2-L, MK3-V, MK4-S and MK5-R) may be more suitable to address this question of ICMS map plasticity in M1 as

the lesion was smaller, better restricted to the hand area. Considering the surface ICMS maps (Figs. 3.11 and 3.15 to 3.17), it appears that the re-arrangement of ICMS maps around the lesion are relatively modest. Indeed, substitution of initially proximal territories (wrist, elbow) by hand points are rare (1-2 points at most in each monkey). Other re-arrangements around lesion affect other territories (face, wrist, elbow, shoulder but still to a rather moderate extent). From these ICMS surface maps, one is tempted to conclude that no post-lesion substantial plasticity of the motor map took place around the lesion. However, the surface ICMS maps do not reflect the entire extent of the hand area, as most sites micro-excitable for the fingers are in the rostral bank of the central sulcus, where the consecutive sites representing the hand along an electrode penetrations appear as a single point on the surface ICMS map. For this reason, the ICMS maps were unfolded (Figs. 3.24, 3.25, 3.26), as explained in the methods section. The unfolded ICMS maps allow better assessment of the plastic changes taking place post-lesion in the motor maps in M1. However, except very few points devoted for instance to the wrist and representing the fingers post-lesions, there was no evidence for the emergence post-lesion of a "new" hand area around the lesioned territory. Indeed most ICMS points eliciting finger movements post-lesion already belonged to the hand area pre-lesion. Nevertheless, even in the unfolded maps, the individual ICMS points located on the crest of M1 still represent each several sites of microstimulation. Therefore, the unfolded maps do not represent the entire cortical sites stimulated. For this reason, our analysis also included a quantitative assessment of all ICMS sites irrespective of their depth and location (see paragraph 3.2.3: Figures 3.27, 3.28). These quantitative data aimed at investigating the proportion of ICMS sites devoted to different territories and compare across monkeys the percentage of ICMS sites eliciting "hand" movements pre- and post-lesion (Figures 3.29 – 3.31).

One limitation (imposed by the experimental protocol; see below) is that the assessment of plasticity of the motor representation in M1 in relation to the hand area lesion was derived from ICMS maps established at only two time points: one ICMS map before the lesion and one ICMS map several months after the lesion, when the recovery reached a plateau. It has to be taken into account that a complete ICMS map requires to perform about 100 electrode penetrations (or even more), corresponding to a period of extensive daily ICMS sessions of 1-2 months. As a consequence, it is not possible to establish the ICMS map more often, especially during the recovery. A controversial point is, whether it would be risky to perform extensive ICMS investigations during the recovery, as according to some authors (Freund et al., 2006; Asanuma et al. 1975) reported possible small damages due to ICMS having the potential of interfering with the recovery, thus possibly affecting the behavioral data. To be on the save side and to reduce parameters influencing post-lesion recovery, in the present study we renounced to do extensive ICMS during recovery. From our work on spinal cord injured monkeys,

in which we made a couple of electrode penetrations with ICMS during the period of recovery, it turned out that the plastic changes of motor representation in the motor cortex take place in parallel to the behavioral recovery (Schmidlin et al., 2004). How the motor map in M1 changed during the few weeks of recovery in our monkeys subjected to M1 lesion remains an open question but it may well be that most of the changes actually take place during this crucial phase of behavioral rehabilitation. Therefore, our post-lesion ICMS maps probably represent the final restored outcome of post-lesion rearrangements in the motor cortex, being only slightly different from pre-lesion situation in the case of anti-Nogo-A antibody treated animals. Behavioral data recorded during and after post-lesion ICMS mapping in some of our monkeys support this view, as performances were stable over time (post-lesion plateau phase) indicating that there were no major plastic changes occurring in the motor cortex during this period of time. An additional concern in this context is that a possible plasticity enhancing effect in anti-Nogo-A antibody treated monkeys had disappeared at the moment of the post-lesion ICMS mapping. As indicated in the method part of this thesis, post-lesion anti-Nogo-A antibody treatment in our monkeys lasted maximally 1 month, whereas post-lesion ICMS mapping normally started about five to six months post-lesion. So, major plastic changes probably occurred during the first month post-lesion and therefore may not have been documented completely by the present post-lesion ICMS maps. As our anti-Nogo-A antibody treated monkeys regained a level of manual dexterity very close to normal, the final treatment induced and training stabilized network of the motor cortex 5 to 6 months post-lesion may appear only slightly different in ICMS mapping as compared to pre-lesion ICMS mapping. This explanation seems to make sense, as anti-Nogo-A antibodies are no longer detectable in liquor or blood samples about one week after the offset of antibody administration in subhuman primates, consequently leading to fading of action. It is also important to be critical judge about the impact of the resolution of the ICMS mapping technique used in the present animals. This is a very important point as, in our monkeys, the lesions were rather small. According to Park et al. (2001), there are two main factors influencing ICMS resolution: Current intensity and the spacing in the grid used to explore a cortical area by ICMS. They report that a current intensity of only 15μA leads to current spread of a sphere with a radius of 105 – 245 μm. Consequently, at an ICMS intensity of 15 μA, the maximal resolution is obtained by a grid spacing of 0.5 mm. According to their interpretation, ICMS under such conditions would provide resolution high enough to detect all details in a specific region of the motor cortex without missing important information. In contrast to them, in the present animals, we used a grid with 1mm spacing not allowing to explore all particularly small details about the motor cortical network. As derived from post-lesion ICMS, threshold currents to elicit an observable muscle twitch became largely higher than 15μA, up to 80μA. Consequently, the radius of current spread would

have been much higher than 105 - 245 µm, thus lowering the resolution of post-lesion ICMS mapping. So, it might be possible that we missed some small post-lesion changes (induced by our small lesions) during post-lesion ICMS mapping due insufficient resolution. A possibility to investigate in more detail the post-lesion cortical rearrangements would be to use of fMRI at regular, short interval time points during recovery. This would even be possible in behaving monkeys previously trained to execute manual dexterity tasks inside an fMRI setup (Pinsk et al., 2005). Such an approach appears very promising for future experiments of the same type as presented in this thesis work, as demonstrated in recent follow-up fMRI studies in human patients documenting important changes paralleling post-lesion recovery in stroke survivors (e.g. Pineiro et al., 2001; Feydy et al., 2002; Cramer, 1997). fMRI follow-up studies in subhuman primates would certainly shed more light on the impact of anti-Nogo-A antibody enhanced recovery and changes of cortical activity. An interesting and still open issue would be to investigate whether anti-Nogo-A antibodies can excert a neuroprotective effect. In some of our monkeys, we observed a preservation of some parts in the rostral bank of the central sulcus of M1 from the toxic effect of ibotenic acid although toxin injection sites were very close. Although unlikely, one cannot completely exclude that the anti-Nogo-A antibody, infused one hour later than the ibotenic acid, may interact with the excitotoxic drug, thus reducing the lesion size. At that step, the characteristics of the lesions in the anti-Nogo-A antibody treated monkeys appears fairly well related to the injection parameters (volume, sites). Along this line, an interaction between the excitotoxic ibotenic acid and a drug used to treat the monkey at that time of the lesioning was reported. Indeed, an anti-epileptic drug was reported to reduce the lesion size after stroke (Faber et al., 2002; Kubova, 2002; Rogawski et al., 2004). In the present study, in one monkey (MK5-R), to tentatively minimize the risk of epileptic episodes, which can occur as a consequence of overexcited neurons by ibotenic acid, we introduced a preventive treatment with either Luminal® or Depakine chrono 300® in the hours and days following the infusion of ibotenic acid. Luminal® is a Barbiturate and therefore has a GABA like inhibitory effect on neurons. The action mechanism of Depakine chrono 300 is not completely understood yet, but it is very likely acting via enhancement of the inhibitory GABA activity. So, both antiepileptic drugs inhibit neuronal activity counteracting the strong excitatory neurotoxic effect of ibotenic acid. As a result, without having this indication at that time, it may well be that the impact of ibotenic acid was reduced. In the untreated control monkey MK5-R, we observed a reduced impact of ibotenic acid infusion on manual dexterity if the monkey was treated with antiepileptic drugs (first two lesions in MK5-R, see Table 3.2). It seems that this effect was dose related. The reduced neurotoxic effect was reflected in an only transitory loss of manual dexterity, as nearly normal scores were re-established within less than 10 days in the modified (standard) Brinkman task. Obviously, this period is too short

for an establishment of new plasticity related rearrangements taking over the lost function of killed neurons (Rossini et al., 2003). As a consequence, neurons may have survived the neurotoxic effect of ibotenic acid due to a reduction of the excitatory impact of anti-epileptic drugs. In contrast, the third lesion introduced in MK5-R without antiepileptic treatment led to a persistent impairment of manual dexterity. In addition, the post-lesion recovery period was extended over a longer period of time before a plateau at scores substantially lower than pre-lesion was attained. The Figure 4.1 below illustrates the evolution of the recovery of manual dexterity in MK5-R during the first 8 – 10 days post-lesion depending on the administered dose of anti-epileptic drugs. Post-lesion performances of the impaired hand were derived from the modified Brinkman board task.
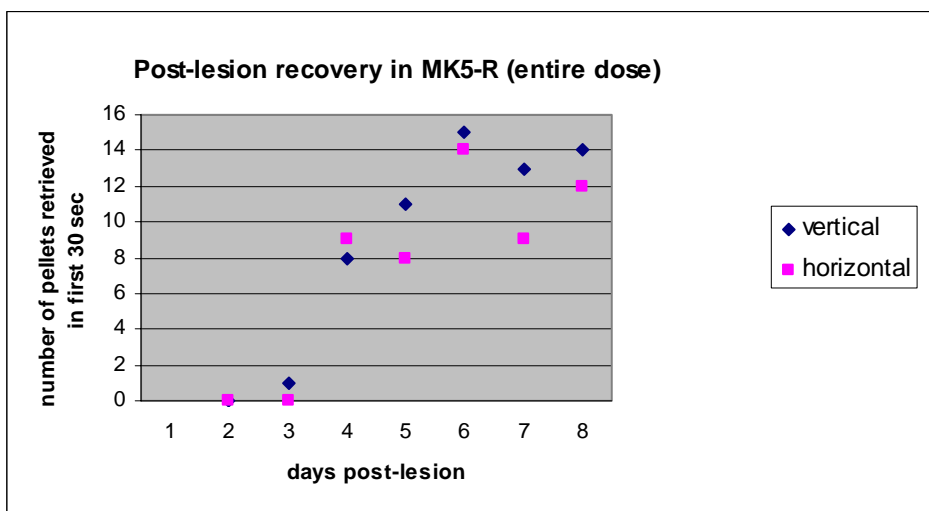
Panel A: entire dose of anti-epileptic drug was given at the moment of the lesion induction with ibotenic acid.
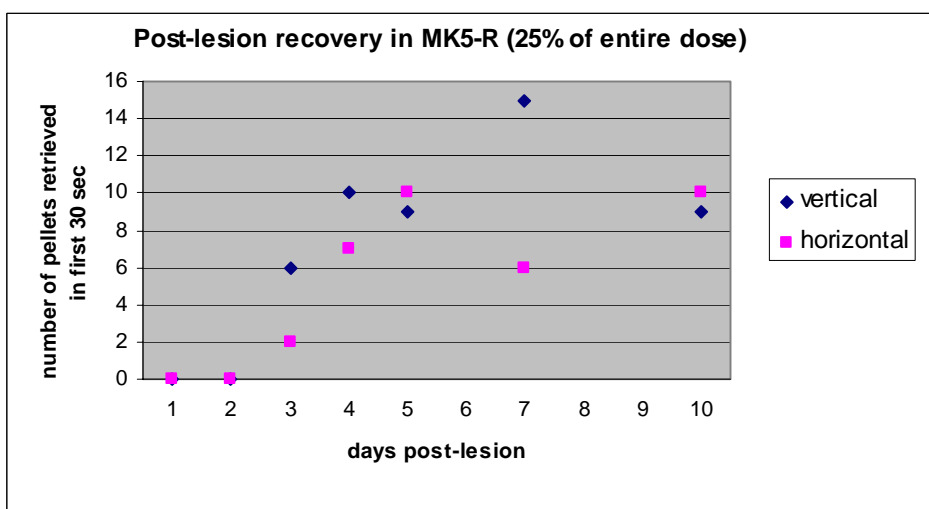
Panel B: 25% of the entire dose of anti-epileptic drug was given at the moment of lesion induction.

_____
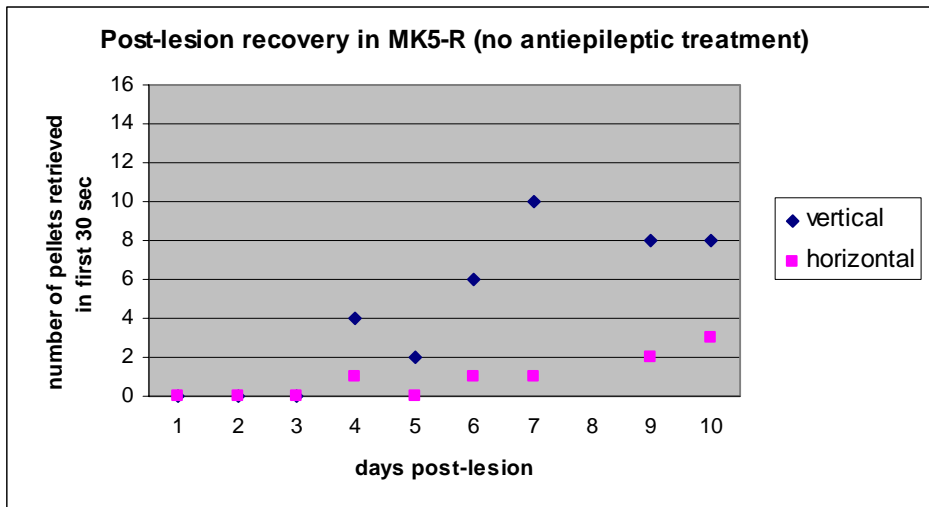
Panel C: No antiepileptic drug was given at the moment of lesion induction.

Figure 4.1: Graphs in panels A to C showing post-lesion recovery of manual dexterity over the first 10 days in untreated control monkey MK5-R with respect to different doses of anti-epileptic drugs used to prevent epileptic episodes. *Panel A* shows the recovery when a full dose of antiepileptic drug was used (75mg), *Panel B* when 25% of the above dose was administered and *Panel C* when no anti-epileptic drug was used.

The following information can be extracted from Figure 4.1: For all doses, MK5-R recovered faster and better for vertical slots than for horizontal slots. The difference between the recovery rate for vertical slots and horizontal slots became more pronounced when no antiepileptic drug was used. Note that with administration of anti-epileptic drugs, recovery achieved normal pre-lesion scores at day 8 (entire dose), respectively 10 (25% of the dose), whereas without anti-epileptic treatment pre-lesion scores were never attained, even later than 10 days post-lesion during the plateau phase (see Figure 3.33 Panel B). We made similar observations in other monkeys of our laboratory concerning the influence of anti-epileptic drugs on post-lesion recovery of manual dexterity (data not entirely analyzed yet). Scores achieved for vertical and horizontal slots in the modified Brinkman board task at day 8, respectively 10, post-lesion and corresponding mean pre-lesion scores and standard deviations from the pre-lesion mean score are indicated in Table 4.1 below.

_____

	Entire dose of anti-epileptic drug	25 % of entire dose of anti-epileptic drug	No drug
Mean ± SD vertical pre-lesion score (nb. of pellets in 30 sec.)	14.31 ± 3.39	14.31 ± 3.39	14.31 ± 3.39
Vertical slots, 8 or 10 days post-lesion	14	9	8
Mean ± SD horizontal pre-lesion	11.64 ± 2.73	11.64 ± 2.73	11.64 ± 2.73
Horizontal slots, 8 or 10 days post-lesion	12	10	3

Table 4.1: Post-lesion scores in the modified (standard) Brinkman board task for MK5-R, at post-lesion day 8 respectively 10, resulting from different anti-epileptic treatments. For comparison, the pre-lesion scores are given as well.

Along the same line, it is very likely that anesthesia may also have an impact on the final lesion size. As post-lesion neurons are very sensible to lack of energy, it seems very likely that reducing the neuronal activity by anesthetic drugs can help to rescue some additional neurons as compared to animals in which the lesion was performed in the awake state. For example, although both monkeys received the same anti-Nogo-A antibody treatment for the same period of time, the total lesion volume of 20.52 mm³ in MK3-V (anesthetized during ibotenic acid injections) was smaller than the total lesion volume of 96.49 mm³ in MK4-S (awake during ibotenic acid injections). Last but not least, it cannot be excluded that the finally relatively small lesions induced in the present monkeys did only favor limited post-lesion plasticity (Dancause et al., 2004) nor can be excluded that a lesion of the same size created by another method would have favored more dramatic post-lesion rearrangements (Voorhies et al., 2002).

4.3 Behavioral data

So far we analyzed data derived from the modified Brinkman board task and the hidden Brinkman board task. Results of these two tests (see chapter 3.3) demonstrate the following: First, in the modified Brinkman board task, all monkeys performed significantly better before the lesion as compared to post-lesion (see Table 3.3), for both vertical and horizontal slots. Anti-Nogo-A antibody treated monkeys, on average, recovered 66% of their pre-lesion score for horizontal slots whereas for vertical slots the post-lesion scores were of about 80% of pre-lesion scores. Post-lesion untreated control monkeys (MK1-G, MK6-J and MK7-C) lost completely manual dexterity for horizontal slots and recovered about the half of pre-lesion scores for vertical slots. But, to the present data, due to the limited number of animals only a tendency for better performance in anti-Nogo-A antibody treated

animals can be deduced, although the difference was more pronounced for horizontal slots than for vertical ones. Analysis of post-lesion video recordings revealed that untreated control monkeys remained incapable of performing a real precision grip with their hand opposite to the lesioned M1 hand area. Individual finger movement was limited in the sense that monkeys were not able to move the index finger and the thumb independently from the other three digits (D3-D5). Therefore, opposition of thumb and index finger in terms of a correct precision grip was not possible. Some monkeys developed alternative precision grips by opposing the thumb against the palm of the entire hand or against the external face of the thumb. The pallet of such alternative variants of precision grip is illustrated in detail in Spinozzi et al. (2004). As a consequence, untreated control monkeys had to use their entire hand to grasp the pellets. The fingers D3-D5 then often interfered with index and thumb and rendered the accurate movement of the precision grip more difficult. This difficulty was probably expressed in a larger time needed to pick out a pellet post-lesion (see Fig. 3.36). Initially, after the lesion, anti-Nogo-A antibody treated monkeys showed the same deficits of manual dexterity but, in contrast to untreated control monkeys, over the time of recovery they regained the capacity of using index and thumb without interference from the other fingers when performing the manual dexterity tasks. Detailed analyses, related to the above preliminary observations about post-lesion changes in digit use, are currently underway in our laboratory. The difference in post-lesion performances between untreated controls and anti-Nogo-A antibody treated monkeys was most pronounced comparing MK1-G with MK3-V and MK4-S, whereas the difference was less pronounced between MK5-R and anti-Nogo-A antibody treated monkeys. But, as mentioned several times, monkey MK5-R is still alive and therefore we do not yet know the permanent lesion size produced in M1.

Originally, we thought that the introduction of the hidden Brinkman board task would help to better discriminate anti-Nogo-A antibody treated monkeys from untreated control monkeys, even with a limited number of animals. The reason for this belief was that, especially when lacking visual feedback, the very limited remaining manual dexterity would create more pronounced deficits in pellet picking in untreated control animals as compared to anti-Nogo-A antibody treated monkeys, with a recovered manual dexterity close to normal. In addition, a spread of the lesion to S1 would have a higher impact on performance without visual feedback. In this situation, monkeys have to rely upon their tactile sense to detect the pellets while scanning the hidden board. Once they have found the pellet in a specific slot, retrieval success again depends on manual dexterity (motor system) and therefore animals able to do precision grip perform better. So, the hidden Brinkman board task should also be a tool to distinguish between sensory and motor deficits, especially when used without visual feedback. In fact, the post-lesion performance of monkey MK1-G (S1 substantially affected by the lesion)

without visual feedback was worse as compared to MK5-R. To attribute this difference to the lesion of S1 in MK1-G for the moment remains speculative as we do not yet know the lesion extent in monkey MK5-R. Because of possible anti-Nogo-A treatment enhancing rearrangement in the sensory as well as in the motor cortex, such animals should perform better than untreated control animals in the hidden Brinkman board task, especially without vision. To our surprise, the difference of performance between the two groups of monkeys was not substantially higher in this test than in the modified Brinkman board task. **Without** visual feedback, discrimination was even worse, although one would intuitively expect a better discriminative ability as compared to tasks **with** visual feedback, where the monkey can maximally take advantage of the spared manual dexterity. To explain this, first it has to be mentioned that in recent spinal cord injury studies (Freund 2006 / 2007) of our laboratory at this stage (only few animals), we were also only able to see tendencies, which with a higher number of analyzed monkeys became more prominent. So, one explanation for the present lack of significant difference between the two groups of monkeys tested may have its origin in the limited number of animals. This could certainly be an explanation in the case of the modified Brinkman board test and the hidden Brinkman board test **with visual feedback,** which are not complicated tasks for monkeys. In contrast, for the hidden Brinkman board task probably additional, not only task intrinsic factors, may play a crucial role, especially during the post-lesion recovery phase. Because in pre-lesion state we did not choose the monkeys for this study with respect to equal level of cooperation with the experimentator, stability in performance, motivation to explore and endurance in trying a task, which is at the limit of what a monkey can do according to its manual dexterity, these factors may have influenced more importantly the results of the hidden Brinkman board task than results derived from other tasks. Imagine, for example, in the group of anti-Nogo-A antibody treated monkeys performing generally less good as compared to untreated control monkeys under such conditions, resulting in comparable post-lesion performances of both groups. For instance, due to the limited number of animals, we can statistically not exclude such a situation. Such influences can be excluded for pre-lesion scores as we did not analyze data from sessions in which the monkey was not motivated to work. Unfortunately this was not possible post-lesion, as it is much more difficult to distinguish between sessions in which the monkey does not work because it is not motivated or sessions in which the monkey is not able to perform the task. Note that the impact of the above mentioned factors may have been most pronounced for total scores but not for the average time needed to grasp an individual pellet ("contact time"). The reason for this would be that if the monkey decides to take the pellet, the animal puts all effort in succeeding. In addition post-lesion, unsuccessful attempts to grasp a pellet were excluded from further analysis. Therefore average times needed to grasp a pellet between well working and less well working animals

are less influenced by motivational factors. That motivation can have an important impact on post-lesion recovery was also observed in human patients suffering from stroke. In fact, the positive influence of motivation is indirect by augmenting post-lesion plasticity through regular repeated execution of impaired movements. This leads to optimizing the spared cortical network to compensate for the lost function formerly controlled by the damaged part of nervous brain tissue. In the future, not only the integration of additional monkeys but also more sophisticated analysis of the present data as proposed in chapter 2, (pages 156 - 157) will certainly help to clarify the impact of anti-Nogo-A antibody treatment on post-lesion recovery of manual dexterity in M1 lesioned macaque monkeys.

4.4 Mechanisms of functional recovery of manual dexterity after M1 lesion

Thinking about potential mechanisms implicated in post-lesion recovery of manual dexterity in macaque monkeys after M1 lesion, one has to be aware that M1 is part of a very complex network controlling voluntary movement of the forelimb. As the motor system is comparable to the electrical network inside a personal computer, with the difference of being much more complex, a punctual damage will immediately have an impact on all other components in this network. The influence of cortical damage can even produce plastic rearrangements in remote areas of the motor cortex (Dancause et al., 2005). For example, inhibitory influences of the corticospinal projections originating in the damaged area of M1 may be lost. As a consequence, formerly inhibited corticospinal projections of alternative pathways may become active, notably those of the extrapyramidal system or M1 could regain access to the lost target muscles in the forelimb. A good candidate for that would be the rubrospinal tract originating in the red nucleus (Belhaj-Saif et al., 1998 and 2000; see also Figure 1.42). About that type of post-lesion rewiring, we can only speculate because corresponding anatomical analysis were not done yet in our monkeys. But the experiments of Belhaj-Saif (2000) already showed that, after unilateral pyramidotomy (disconnecting the hand muscles from the voluntary control via the M1 hand area), the rubrospinal projections to the distal forelimb muscle controlling motoneurons were importantly reorganized. Whereas in intact monkeys the rubrospinal projections preferentially control extensor muscles and inhibit flexor muscles (Belhaj-Saif et al., 1998, Mews and Cheney, 1991), the distribution pattern changed towards a more even distribution, allowing inhibition and excitation of both, extensors and flexors. Consequently, such a balanced distribution would allow a better control of distal forelimb muscles. This improved control will then be reflected in better post-lesion recovery of manual dexterity. Beside this, it would also be possible that corticocortical connections from other motor areas (PM, SMA, CMA) to the undamaged nervous tissue in M1 may become stronger. Through these newly established connections, the spared M1 could indirectly regain control over α-motoneurons

formerly directly controlled by corticospinal projections from the damaged part of M1. It is also important to mention that M1 is not the only motor cortical area projecting directly onto α-motoneurons controlling individual muscles. Therefore, any cortical area possessing such direct connections (PM, SMA, CMA, see Table 1.3 and Figure 1.7) would be a potential candidate to take over part of the lost function of the tissue damaged in M1 by ibotenic acid injections. In human patients, the primary motor cortex ipsilateral to the lesion possessing about 10% of the corticospinal fibers indirectly terminating on corresponding α – motoneurons was revealed to be more active in stroke survivors post-lesion. It is still a matter of debate whether in monkeys this is also possible. Post-lesion ICMS mapping in the ipsilesional M1 on M1 lesioned monkeys of our laboratory did not reveal major changes in the corresponding area (Liu and Rouiller 1999, MK2-L data not presented). As a consequence of the loss of function of one part of M1, not only manual dexterity is reduced but also the amount of feedback information from muscle spindles and Golgi tendon organs to M1 will be reduced, therefore leading to rearrangements in S1. It has to be investigated, whether the areas less used now, are invaded by adjacent sensory areas or if the freed space will be used for expansion of the small amount of S1 neurons directly projecting on α- motoneurons having some potential to partially take over the lost function of M1. It was demonstrated that rearrangements occur after cortical damage in S1 in monkeys (Xerri et al., 1998). Perhaps the most interesting findings about a potential function of S1 in post-lesion recovery of manual dexterity in monkeys were presented by the group of Sasaki (Sasaki and Gemba, 1984a, 1984b, 1987). Their experiments demonstrated that after temporally impairing the motor cortex (M1) by local cooling or indirectly after unilateral cerebellar hemispherectomy, S1 can partially compensate for the lost motor function. If M1 is impaired or destroyed, S1 seems particularly well placed to compensate the loss of M1 function in movement preparation and help to reduce the reaction time in visually initiated hand movements to normal. In the context of dexterity, it has to be mentioned that the authors observed a spared manual dexterity accompanied by a clumsiness of the hand. That this spared manuel dexterity was due to S1 was demonstrated by simultaneous cooling of S1 and M1. Under these circumstances, the result was a complete paralysis of the corresponding muscles. In line with a role played by S1, highly relevant is the recent observation that, after M1 lesion, the projections from PM normally aimed to M1 are re-directed to S1 (Dancause et al., 2005).

S1 plays also a crucial role in post-lesion recovery in forwarding sensory information from the impaired limb in an adequate form to stimulate plasticity in the remaining intact parts of the motor cortical system towards better functional recovery. For example in humans passive movements of impaired limbs by physiotherapists or robots positively influenced post-lesion recovery (see introduction pages 87 - 88). From Muscimol experiments of Liu and Rouiller, 1999, we know that PM

plays an important role in post-lesion recovery of monkeys subjected to large cortical lesions destroying the entire M1 (MK6-J and MK7-C). Infusion in PMd and PMv lead to transitory complete loss of the recovered manual dexterity in these monkeys (see chapter 3.4). Therefore, in the present study, we were interested to test if PM plays a similar role in post-lesion recovery in monkeys subjected to smaller lesion and subsequently treated with anti-Nogo-A antibodies. The present experiments revealed an important role of particularly PMd in MK3-V and MK4-S in post-lesion recovery, whereas in contrast Muscimol infusions in PMv in MK3-V did not lead to a transitory loss of recovered manual dexterity. Because positions of the Muscimol infusion sites in PMv in monkey MK3-V were estimated, it can not be excluded that we missed the corresponding limited number of neurons directly projecting on α-motoneurons of the forelimb. As the lesion in the present monkey MK3-V was smaller than in MK6-J and MK7-C, it is also possible that blocking the minor influence of PMv (relative to PMd and spared M1 areas; see Figure 3.25) on forelimb muscles by Muscimol infusion did not have a visible impact on the well recovered manual dexterity (86% of pre-lesion score). In contrast, in monkeys MK6-J and MK7-C, the relative importance of PMv may have been more important for post-lesion recovery (30% and 32% of pre-lesion scores). All mechanisms described above may be active in both spontaneous recovery in untreated control monkeys as well as in post-lesion recovery of anti-Nogo-A antibody treated monkeys. But such rearrangements are supposed to be more prominent in anti-Nogo-A antibody treated animals as the antibody may favor axonal sprouting by the creation of a "rewiring friendly environment" closer to the situation found during development of the CNS (see introduction, paragraph 1.9). We did not yet analyze histological slices concerning axonal sprouting, so it is too early to finally conclude about that. But from post-lesion ICMS mappings, we can speculate about some aspects of post-lesion sprouting. For example, as post-lesion thresholds in the lesion site were higher as compared to pre-lesion data in anti-Nogo-A antibody treated monkeys, this may partially due to new collaterals which were activated by ICMS. According to the work of Gustafsson et al. (1976), ICMS can activate pyramidal cells of the motor cortex either directly or indirectly through collaterals. The direct activation directly depolarizes the membrane of the pyramidal cell. Lowest thresholds for direct activation are found in the initial segment of the axon. In contrast indirect synaptic activation is made by depolarization of the membrane of axons, which make synaptic connections with a particular pyramidal cell sometimes in very remote areas. Large axons (as for example axons of pyramidal cells) are more likely to be excited within a greater radius from the stimulation site as their electrical resistance is lower than the corresponding resistance of smaller fibers (axons in great majority not belonging to pyramidal cells). As a consequence, pyramidal cells quite distant from the stimulation sites may have been activated through collaterals resulting from enhanced sprouting in anti-Nogo-A

antibody treated monkeys. In the present anti-Nogo-A antibody treated monkeys such collateral sprouting is very likely to have occurred all over the motor system including both spinal cord and motor cortical areas as the cerebrospinal fluid distributes the intrathecally infused antibodies (see Methods pages 150 - 151 and Introduction Figure 1.57, Weinmann et al., 2006) in the entire CNS. As we placed the openings of the tips of the two antibody delivering osmotic pumps at spinal level C7 (close to the α-motoneurons controlling forelimbe muscles) as well as subdurally over the lesion site in M1, hot spots of anti-Nogo-A antibody action can be expected there. But, as revealed by Weinmann et al. (2006), anti-Nogo-A antibodies can be detected all over the CNS. So, first one could expect most intense collateral sprouting at and adjacent to the lesion site in M1. Here new collaterals could be formed from pyramidal cells adjacent to the lesion (penumbra zone mainly controlling proximal movements) to the remaining intact pyramidal cells in M1 which control distal forelimb movements. Therefore distal muscle control of the impaired forelimb could be strengthened finally leading to post-lesion recovery of manual dexterity. Alternatively, new collaterals could also strengthen the connection between M1 and PM or SMA, as well as between PM and S1 (Dancause et al., 2005), allowing the use of alternative indirect pathways for distal muscle control. Through the various new collaterals, distal muscles could be controlled by formerly proximal muscle controlling pyramidal cells of M1 as well as by distal muscle controlling pyramidal cells of other motor cortical areas. It may also be possible that cortical neurons in M1 of the lesion attained hemisphere, controlling both distal and proximal muscles in healthy monkeys, compensate for the lost control of distal manual dexterity (Mc Kiernan et al., 1998). Whether in our monkeys an anti-Nogo-A antibody induced strengthening of the ipsilateral indirect corticospinal projections from the intact hemisphere had an impact on post-lesion recovery of manual dexterity as reported by others (Emerick et al, 2003; Lee et al, 2004 ; Seymour et al, 2005) has to be investigated in additional experiments.

At spinal level, anti-Nogo-A antibody treatment could have induced new projections from intact corticospinal axons to the disconnected α-motoneurons controlling distal muscles of the lesion impaired hand. This is very likely as it was demonstrated using spike triggered averaging, that almost 45% of the recorded corticomotoneuronal cells control both proximal and distal muscles (e.g. Mc Kiernan et al., 1998; see also introduction paragraph 1.3 and 1.4). Moreover, using stimulus triggered averaging to map the forelimb muscles of 24 muscles (5 shoulder, 6 elbow, 5 wrist, 5 extrinsic digits and 2 intrinsic digit muscles), Park et al. (2000) showed the existence of M1 zone that cofacilitated at least one proximal muscle (shoulder and elbow) and one distal muscles (wrist and fingers). This proximal distal co-facilitation zone (PDC zone) was located between the distal zone and proximal zone. In further histological studies, the above hypothesis about sprouting can be tested, as in recent studies

from our laboratory on spinal cord lesion model, in which we reported enhanced post-lesion collateral sprouting, reduced numbers of retraction bulbs, augmentation of synaptic buttons in anti-Nogo-A antibody treated macaque monkeys subjected to spinal cord lesion (Freund et al., 2007). Anatomical data about sprouting will soon be available as we performed BDA tracer injections in all monkeys used for this thesis work. An additional point about anti-Nogo-A antibody treatment is to ask whether, considering that anti-Nogo-A antibody treatment favors axonal re-growth, would have an impact on neuronal survival as neuronal death depends on the severity of axonal damage. If yes, anti-Nogo-A antibody treatment would have an indirect neuro-protective effect favoring post-lesion brain tissue survival. Therefore new projections from rescued pyramidal cells in M1 controlling distal muscles of the forelimb can not be excluded. However, at that step, the notion of a neuro-protective effect of anti-Nogo-A antibody treatment did not receive experimental support so far.

4.5 Does anti-Nogo-A antibody treatment enhance functional recovery after motor cortex lesion?

1. Behavioral data show that anti-Nogo-A antibody treatment tends to enhances recovery of manual dexterity following lesion of the hand area in the opposite primary motor cortex M1 although, in some part, the effect seems to be task dependent. This observation is in good accordance to previous studies in subhuman primates and rats (see Introduction, paragraph 1.9.18).

2. Post-lesion ICMS mapping shows that no movement can be induced in the lesion site of the untreated control animals, whereas in the anti-Nogo-A antibody treated animal movements can still be elicited, although at higher intensity than pre-lesion. In addition, it seems that some territories in M1 of the anti-Nogo-A antibody treated monkeys were spared from the lesion. Whether this is an effect of the anti-Nogo-A antibody treatment or not has to be analyzed in future experiments in additional monkeys.

3. Muscimol data suggest that, in anti-Nogo-A antibody treated animals, the lesioned hand area plays some role in the recovery whereas, in untreated control monkeys, the lesioned territory does not seem to contribute to the recovery process. In both groups of animals, PM also plays an important role in post lesion recovery (see chapter 3.4 and above).

4. In summary, the present data are promising, showing a positive effect of anti-Nogo-A antibody treatment, but further investigations are needed to confirm these preliminary observations. On one hand, we are very optimistic to confirm the present data in the future, as in the spinal cord injury model

we reached this goal after having considered a larger number of animals. But it has also to be taken into account that the brain is much more complex than the spinal cord. Therefore, it might be that the positive effect of anti-Nogo-A antibody treatment is less prominent in the context of cortical lesions as compared to spinal cord injury. One reason for that is that so far the anti-Nogo-A antibody treatment only is able to provide a plasticity friendly environment but it is not possible yet to specifically direct the induced rearrangements in order to repair correctly the damaged neuronal network of the motor cortical system. So, the question remains whether enhancing post- cortical-lesion sprouting is enough to repair post-stroke brain damage in the future. As it is yet not possible to limit the enhancement of rearrangement to the lesion site there is a danger of aberrant sprouting leading to malformation or malfunction of the intact part of the motor system. That anti-Nogo-A antibody treatment in fact induces transient neuronal outgrowth in adult cerebellar Purkinje cells and corticospinal neurons in the absence of a lesion was reported by Emerick et al. 2004. So far, fortunately, we did not observe negative side effects of anti-Nogo-A antibody treatment in our animals.

4.6 Limits of the present methods

As already mentioned in the introductory part of this discussion, a major problem in the context of cortical lesion studies is to produce standardized lesions of comparable size. Therefore in this part of the discussion, I will mainly focus on factors having an impact on the lesion extents of the monkeys of which data were analyzed for the present thesis work. Although varying lesion size can be a problem in terms of analyzing, comparing and interpreting results obtained, one has to be aware that clinicians are confronted with exactly this situation in clinics. As partially discussed in the addendum, today it is often very difficult to translate and confirm results from basic research in clinics (Perel et al., 2006). The reason for that is in part that often results from basic research are derived from over-idealized experiments or models. Such experiments may distract the attention of the researchers from some clinically relevant aspects of a specific treatment. Maybe this is why often newly developed treatments fail to succeed in clinical application. Nevertheless standardizing and controlling most parameters of an experiment has many advantages in terms of facilitating the understanding of mechanisms involved in a more complex and wider context. For example, the motor system in primates after cortical lesion in M1 is an enormous neuronal network far from being understood today.

Although for the present thesis work, we invested a lot of effort in controlling lesion size, finally histological analysis revealed still important differences between individual monkeys. Because we are aware of the fact that lesion size, position of the lesion, inside a specific motor cortical area as well as when touching different cortical areas of the sensory motor system (Irle, 1990), has a great impact on

post-lesion recovery we carefully planed lesion induction by ibotenic acid. Immediately before we injected ibotenic acid we re-stimulated the motor cortex in the corresponding lesion sites in order to exclude missing the targets in the hand representing area of M1 or to inject ibotenic acid in the central sulcus. But even doing so, one can not exclude different diffusion characteristics in individual monkeys affecting the effective territory of action of ibotenic acid. In addition, liquor circulation in individual monkeys might be different, therefore affecting the final concentration of ibotenic acid at target sites by removing the toxin slower or faster from the extracellular space and consequently lowering the neurotoxic action. Damage in adjacent brain regions can occur from ibotenic acid transported from the original injection sites to more remote cortical areas, although probably diluted and consequently less toxic for remote neurons. Unfortunately, in spite of all precautions in monkey MK2-L, we may have missed the target sites (see small lesion revealed from histology). The reason for this failed injection leading to a too small lesion has to be attributed to the fact that, in this monkey, ICMS mapping was done at lower resolution than in all other monkeys (grid of 2mm * 2mm; see Chapter 3 Figure 3.15). Besides the optimal positioning of the needle of the Hamilton syringe used to inject ibotenic acid there are other factors having an impact on lesion size. In monkey MK1-G immediately after the lesion, we observed an epileptic crisis. Such extreme additional activation of partially damaged neurons adjacent to the original lesion site (penumbra) may have induced additional neuronal cell death due to energy brake down in the already weakened neurons (see addendum) making the final lesion bigger. In addition in MK1-G we observed a hemorrhage close to the lesion site which may have had an impact on final lesion size of this monkey.

Looking at histological data one has to keep in mind that in all monkeys when all experiments were completed and all data recorded we made Muscimol injections (see Chapter 3.4) using Hamilton syringes and about two weeks before sacrifice BDA injections were made using the same type of syringes. So, as the needles of the Hamilton syringes are of relatively large size, we can not exclude that some brain tissue was destroyed mechanically. This was probably the case in MK4-S where we observed an important sized subcortical lesion not really attributable to ibotenic acid injections. From a developmental point of view one may argue whether the age of individual monkeys had an impact on final lesion size as younger animals show more intrinsic plasticity of the CNS than older animals. This factor can be excluded as all animals were too old at the moment of lesion induction (older than 2.5 to 3 years; see Table 3.2) to show major regeneration of lesioned brain tissue as formerly reported for lesions in neonatal monkeys (Rouiller et al., 1998). In fact, the post-natal CNS development in macaque monkeys, in particular that of the corticospinal system, is complete at the age of 2.5 to 3 years

(Rouiller et al., 1998; Olivier et al., 1997). Furthermore, it cannot be excluded that the original lesion size in our monkeys was smaller and better focused to the M1 target sites and became only bigger with time, because of secondary neuronal tissue damage, which can occur much later by apoptotic processes (see addendum).

4.7 Future directions

4.7.1 Fields of interest for future investigations

The present experiments are preliminary in the sense that more monkeys have to be analyzed to augment statistical power of the so far positive effect of anti-Nogo-A antibody treatment observed. Furthermore, analysis at the behavioral (see propositions in Chapter 2) electrophysiological and histological level has to be refined to detect perhaps now hidden positive and negative effects of the treatment. For example, results from the behavioral analysis of the study of Friel and Nudo (1998) provide evidence that compensatory movement patterns are used during the recovery of motor function following cortical injury, even after relatively small lesions that produce mild, transient deficits in motor performance. Therefore, additional more sophisticated analysis of post-lesion manual dexterity might be very fruitful to shed more light on how anti-Nogo-A antibody treatment ameliorates post-lesion manual dexterity. In addition, examination of electrophysiological maps of evoked movements by the same authors suggests that the mode of recovery (re-acquisition of pre-infarct movement strategies versus development of compensatory movement strategies) may be related to the relative size of the lesion and its specific location within the M1 hand representation. In particular it would be interesting to evaluate whether the compensatory movement pattern or the original pre-lesion movement pattern is enhanced by the anti-Nogo-A antibody treatment.

As our monkeys were trained and tested on a daily basis post-lesion it might also be interesting to compare the quantitative impact of such a training in anti-Nogo-A antibody treated monkeys and in untreated control monkeys. This could be done by pairs of monkeys of either group where one monkey restarts training immediately after the lesion, whereas the other monkey starts post-lesion training only about 3 months post-lesion when most regenerative processes are thought to be complete. The question to ask would be if the training effect is favored by anti-Nogo-A antibody treatment (what would be expected) or not. Along this line, it would also be interesting whether training differently influences the percentage of additionally spared brain tissue in anti-Nogo-A antibody treated monkeys and whether the position of the lesion (rostral or caudal in M1) has no impact on spared brain tissue as reported for untreated monkeys in a recent report (Friel et al., 2007).

_____

        In a clinical context it would also be interesting to see whether the anti-Nogo-A treatment shows different efficiency depending on the function of a specific cortical area damaged by the lesion. Such evaluations are of high importance for later safe clinical application. Another aspect to be tested is to start the anti-Nogo-A antibody treatment delayed to the moment of lesion induction. This aspect is very crucial as most patients can only be stabilized about two weeks after the cerebral accident happened. As for spinal cord injury a particular final treatment of cortical lesions will probably only be successful in some patients showing characteristics of damage compatible with the corresponding treatment. Therefore, in the future, different combinatorial treatments should be tested in subhuman primates in order to find treatments adapted to most frequent clinical cases of brain injury. I am very optimistic that the contributions of all researchers and clinicians in the field will lead to a first therapy helping patients suffering from stroke in the nearer future.

4.7.2 Two hypothetic concepts derived from the present preliminary results

        The Figures 4.2 and 4.3 below are hypothetical concepts for two major aspects of cortical lesions. The first figure (Figure 4.2) points to the crucial question where to search the neuronal substrate for post-lesion functional recovery. This aspect is of very high importance as the future treatments preferentially should help to enhance the naturally occurring "efforts" of the CNS to repair itself. In order to make the natural mechanism more effective we need to know the target area for such treatments. Therefore Figure 4.2 proposes target areas as substrates for functional recovery depending on the lesion size in M1. Depending on the lesion size, as explained in the Figure 4.2 itself, different territories may come into play in order to contribute to the functional recovery from motor cortex lesion.

Figure 4.2 (next page): Scenarii for recruitment of alternative brain regions to compensate for lost motor function depending on lesion extent of the motor cortex: a hypothetic concept derived from preliminary data on five monkeys. Panels A-E represent different lesion extents in the motor cortex and their impact on post-lesion recruitment of intact brain regions to compensate for the lost motor functions.
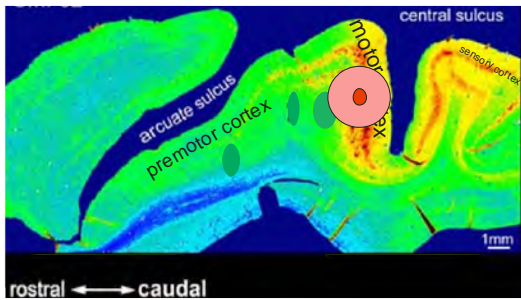
Panel A

Lesion size:+
monkey: MK2-L
Zones recruted for functional recovery:
intact neuronal tissue close to the lesion site inside M1
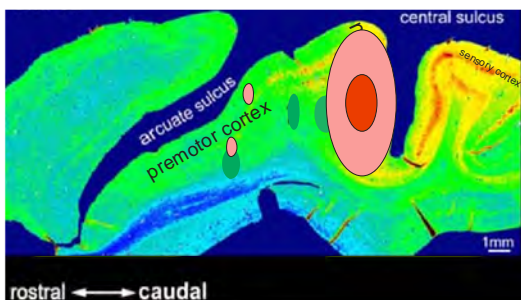
Panel B

Lesion size:++
monkey: MK3-V
Zones recruted for functional recovery: remaining
intact neuronal tissue in M1 and more
remote small areas in PM
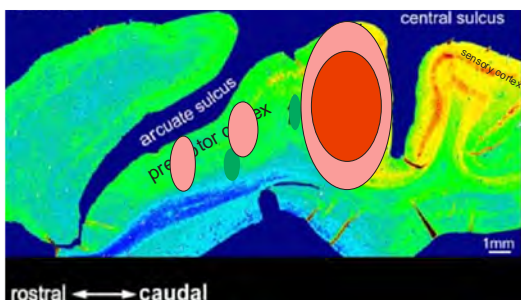
Panel C

Lesion size:+++
monkey: MK4-S
Zones recruted for functional recovery:remaining intact
neuronal tissue in M1 and bigger areas of PM
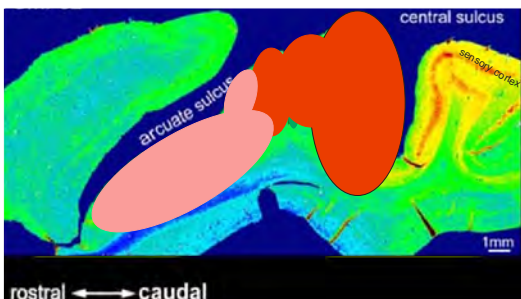
Panel D

Lesion size:++++
monkey: MK6-J, MK7-C
Zones recruted for functional recovery:
entire PM
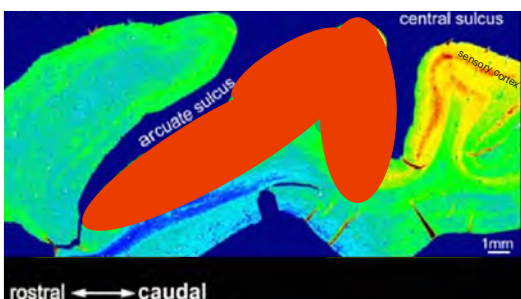
Panel E

Lesion size:+++++
monkeys:hypothetic monkey
Zones recruted for functional recovery:
SMA, CMA, intact motor cortex in opposite hemisphere
and red nucleus

Lesion size:

+ very small
++ small
+++ medium
++++ big
+++++ very large

● core of lesion   ● zone implicated in post-lesion functional recovery

318

The schematic Figure 4.3 (below) is an estimation of the impact of an anti-Nogo-A antibody treatment on functional recovery after cortical lesion in M1 in relation to the effective lesion size (panel B) and a comparison with the same strategy applied to our model of spinal cord injury (panel A) in monkeys. As reported in Freund et al. (2006), in the spinal cord lesion model, the impact of the lesion size is marginal in anti-Nogo-A antibody treated animals (Panel A in Figure 4.3). In other words, as expected, in control antibody treated monkeys subjected to spinal cord lesion, the percent of recovery was inversely correlated to the lesion extent (blue line in panel A). In contrast, in anti-Nogo-A antibody treated monkeys subjected to a spinal cord lesion, the percent of recovery was 100%, irrespective of the lesion extent (red line in panel A). From the present data on motor cortical lesion, the situation appears somewhat different. In fact, in both groups of monkeys (untreated control and anti-Nogo-A antibody treated monkeys), the percent of recovery is inversely correlated with the lesion size but, in anti-Nogo-A antibody treated monkeys (red line in panel B), the recovery is less affected by the lesion size than in untreated control monkeys (blue line in panel B). In other words, in panel B, the red line (anati-Nogo-A treated monkeys) has a slope less steep than the blue line (untreated control monkeys), suggesting that the anti-Nogo-A treatment enhanced functional recovery, but to a lesser extent than in the spinal corf injury model. Hopefully, in the future, the diminished power of anti-Nogo-A treatment in the case of cerebral cortex lesion (as compared to spinal cord lesion) may be compensated by the combination of anti- Nogo-A with additional treatment agents in order to obtain a recovery more independent of the lesion size (hypothetic green line in Fig. 4.3). However, repairing the brain is a challenge even far more ambitious that repairing the spinal cord and therefore it may be expected that successful treatments for cerebral cortex lesion will be far more sophisticated and require more basic research before clinical application.
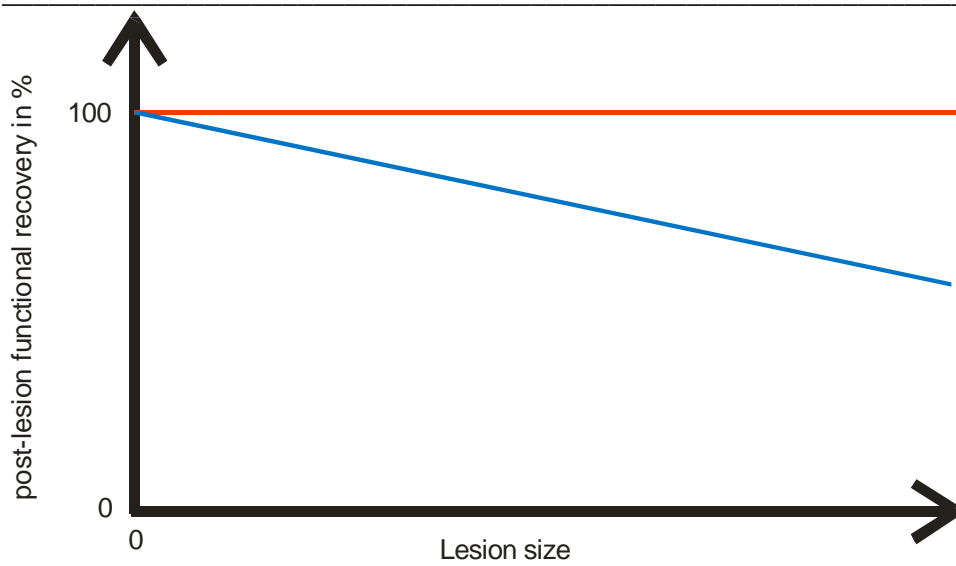
Panel A: Spinal cord lesion model
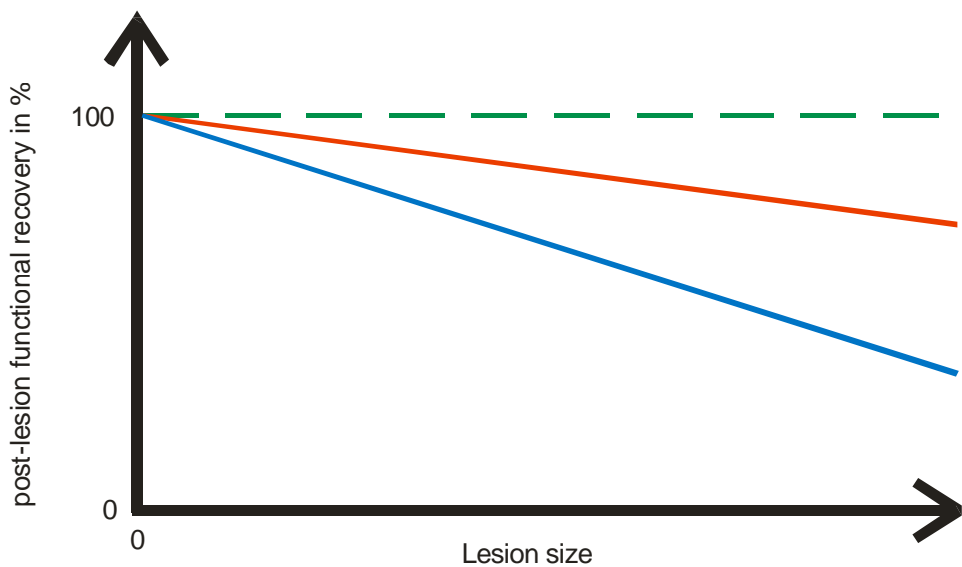
Panel B: Cortical lesion model

Figure 4.3: The impact of lesion size on the efficacy of the anti-Nogo-A antibody treatment on post-lesion functional recovery in a spinal cord lesion model (taken from Freund et al., 2006 in Panel A) and a cortical lesion model (present thesis work in Panel B) in non-human primates.

Blue lines are for untreated control monkeys, red lines are for anti-Nogo-A antibody treated monkeys and the green dashed line is "hopefully" for future monkeys subjected to cortical lesions and then treated with a combination of anti-Nogo-A antibodies and additional neural repair enhancing drugs.

_____

Bibliography for chapter 4

Asanuma H and Arnold AP. 1975. Noxious effects of excessive currents used for intracortical microstimulation.Brain Res. 96: 103-107.

Belhaj-Saïf A, Karrer JH, Cheney PD. 1998. Distribution and characteristics of poststimulus effects in proximal and distal forelimb muscles from red nucleus in the monkey. J Neurophysiol 79:1777-1789.

Belhaj-Saïf A, Cheney PD. 2000. Plasticity in the distribution of the red nucleus output to forearm muscles after unilateral lesions of the pyramidal tract. J Neurophysiol 83:3147-3153.

Cramer SC. 1997. A functional MRI study of subjects recovered from hemiparetic stroke. Stroke 28:2518-2527

Dancause N. Barbay S, Frost SB, Plautz EJ, Chen D, Zoubina EV, Stowe AM, Nudo RJ. 2004. Minimal lesion size in the primary motor cortex for the initiation of recovery associated physiological changes in the ventral premotor cortex. 4th Forum of European Neuroscience (Lisbon).

Dancause N, Barbay S, Frost SB, Plautz EJ, Chen D, Zoubina EV, Stowe AM, Nudo RJ. 2005. Extensive cortical rewiring after brain injury. J Neurosci 25:10167-10179.

Emerick AJ, Neafsey EJ, Schwab ME, Kartje GL. 2003. Functional reorganization of the motor cortex in adult rats after cortical lesion and treatment with monoclonal antibody IN-1. J Neurosci 23:4826-4830.

Emerick AJ, Kartje GL. 2004. Behavioral recovery and anatomical plasticity in adult rats after cortical lesion and treatment with monoclonal antibody IN-1. Behav Brain Res 152:315-325.

Farber NB, Jiang XP, Heinkel C, Nemmers B. 2002. Antiepileptic drugs and agents that inhibit voltage-gated sodium channels prevent NMDA antagonist neurotoxicity, Molecular Psychiatry 7:726-733.

Feydy A, Carlier R, Roby-Brami A, Bussel B, Cazalis F, Pierot L, Burnod Y, Maier MA. 2002. Longitudinal study of motor recovery after stroke: recruitment and focusing of brain activation. Stroke 33:1610-1617.

Freund P, Schmidlin E, Wannier T, Bloch J, Mir A, Schwab ME, Rouiller EM. 2006. Nogo-A-specific antibody treatment enhances sprouting and functional recovery after cervical lesion in adult primates. Nature Med 12:790-792.

Freund P, Wannier T, Schmidlin E, Bloch J, Mir A, Schwab ME, Rouiller EM. 2007. Anti-Nogo-A antibody treatment enhances sprouting of corticospinal axons rostral to a unilateral cervical spinal cord lesion in adult macaque monkey. J Comp Neurol 502:644-659.

Friel KM, Nudo RJ. 1998. Recovery of motor function after focal cortical injury in primates: compensatory movement patterns used during rehabilitative training, Somatosens Mot Res 15(3): 173-189.

Friel KM, Barbay S, Frost SB, Plautz EJ, Stowe AM, Dancause N, Zoubina EV, Nudo RJ. 2007. Effects of a rostral motor cortex lesion on primary motor cortex hand representation topography in primates, Neurorehabil Neural Repair. 21: 51-61.

Irle E. 1990. An analysis of the correlation of lesion size, localization and behavioral effects in 283 published studies of cortical and subcortical lesions in old-world monkeys. Brain Res Brain Res Rev. 15: 181-213.

Gustafsson B. 1976. Direct and indirect activation of nerve cells by electrical pulses applied extracellularly. J. Physiol. 258: 33-61.

Kubova H. 2002. Antiepileptic drugs in neuroprotection Department of Developmental Epileptology, Institute of Physiology Academy of Sciences of the Czech Republic.

Lee Jung-Kil et al, 2004. Nogo Receptor Antagonism Promotes Stroke Recovery by Enhancing Axonal Plasticity The Journal of Neuroscience 24(27):6209–6217

_____

Liu Y, Rouiller EM. 1999. Mechanisms of recovery of dexterity following unilateral lesion of the sensorimotor cortex in adult monkeys. Exp Brain Res 128:149-159.

Mews K Cheney PD. 1991. Facilitation and suppression of wrist and digit muscles from single rubromotoneuronal cells in the awake monkey. J Neurophysiol 66: 1968-1977.

Olivier E, Edgley SA, Armand J, Lemon RN. 1997. An electrophysiological study of the postnatal development of the corticospinal system in macaque monkeys, J. Neurosci. 17: 267 – 276.

Perel P, Roberts I, Sena E, Wheble P, Briscoe C, Sandercock P, Macleod M, Mignini LE, Jayaram P, Khan KS. 2006 Comparison treatment effects between animal experiments and clinical trials: systematic review, BMJ. 334:197.

Pineiro R, Pendlebury S, Johansen-Berg H, Matthews PM. 2001. Functional MRI detects posterior shifts in primary sensorimotor cortex activation after stroke: evidence of local adaptive reorganization? Stroke 32: 1134 -1139.

Pinsk MA, Moore T, Richter MC, Gross CG, Kastner S. 2005. Methods for functional magnetic resonance imaging in normal and lesioned behaving monkeys; J. Neurosci. Methods 143:179-195.

Rogawski MA, Loscher W. 2004. The neurobiology of antiepileptic drugs for the treatment of nonepileptic conditions, Nat Med. 10:685-92.

Rossini PM, Calautti C, Pauri F, Baron JC. 2003. Post-stroke plastic reorganisation in the brain. Lancet Neurol. 2:493-502.

Rouiller EM, Yu XH, Moret V, Tempini A, Wiesendanger M, Liang F. 1998. Dexterity in adult monkeys following early lesion of the motor cortical hand area: the role of cortex adjacent to the lesion. Eur J Neurosci 10:729-740.

Sasaki K, and Gemba H. 1984a. Compensatory motor function of the somatosensory cortex for the motor cortex temporally impaired by local cooling in the monkey, Exp Brain Res 55: 60-68.

Sasaki K, and Gemba H. 1984b. Compensatory motor function of the somatosensory cortex for dysfunction of the motor cortex following cerbellar hemispherectomy in the monkey, Exp Brain Res 56: 532-538.

Sasaki K, and Gemba H. 1987. Plasticity of cortical function related to voluntary movement motor learning and compensation following brain dysfunction, Acta Neurochir Suppl (Wien) 41:18-28.

Schmidlin E, Wannier T, Bloch J, Rouiller EM. 2004. Progressive plastic changes in the hand representation of the primary motor cortex parallel incomplete recovery from a unilateral section of the corticospinal tract at cervical level in monkeys. Brain Research 1017:172-183.

Schmidlin E, Wannier T, Bloch J, Belhaj-Saïf A, Wyss A, Rouiller EM. 2005. Reduction of the hand representation in the ipsilateral primary motor cortex following unilateral section of the corticospinal tract at cervical level in monkeys. BMC Neuroscience 6:56.

Voorhies AC, Jones TA. 2002. The behavioral and dedritic growth effects of focal sensorimotor cortical damage depend on the method of lesion induction; Behav Brain Res 133: 237-246.

Wannier T, Schmidlin E, Bloch J, Rouiller EM. 2005. A unilateral section of the corticospinal tract at cervical level in primate does not lead to measurable cell loss in motor cortex. Journal of Neurotrauma 22:703-717.

Xerri C, Merzenich MM, Peterson BE, Jenkins W. 1998. Plasticity of primary somatosensory cortex paralleling sensorimotor skill recovery from stroke in adult monkeys. J Neurophysiol 79:2119-2148.

Contents of Addendum

5. Addendum

5 Addendum

5.1 The macaque monkey in medical research

5.1.1 Systematic classification of macaque monkeys

```
                              ┌─────────────┐
                              │  PRIMATES   │
                              └─────────────┘
          ┌──────────────────────────┼──────────────────────────┐
          ▼                          ▼                          ▼
   ┌─────────────┐           ┌─────────────┐           ┌─────────────┐
   │  Prosimii   │           │ Anthropoidea│           │    Apes     │
   └─────────────┘           └─────────────┘           └─────────────┘
                                    │
                                    ▼
                            ┌─────────────────┐
                            │ Oldworld monkey │
                            └─────────────────┘
                                    │
                                    ▼
                            ┌─────────────────┐
                            │ Cercopithecini  │
                            └─────────────────┘
                                    │
                                    ▼
                            ┌─────────────────┐
                            │    Macaques     │
                            └─────────────────┘
          ┌──────────────────────────┴──────────────────────────┐
          ▼                                                      ▼
   ┌─────────────┐                                    ┌──────────────────────┐
   │   MACACA    │                                    │  MACACA FASCICULARIS │
   └─────────────┘                                    └──────────────────────┘
```
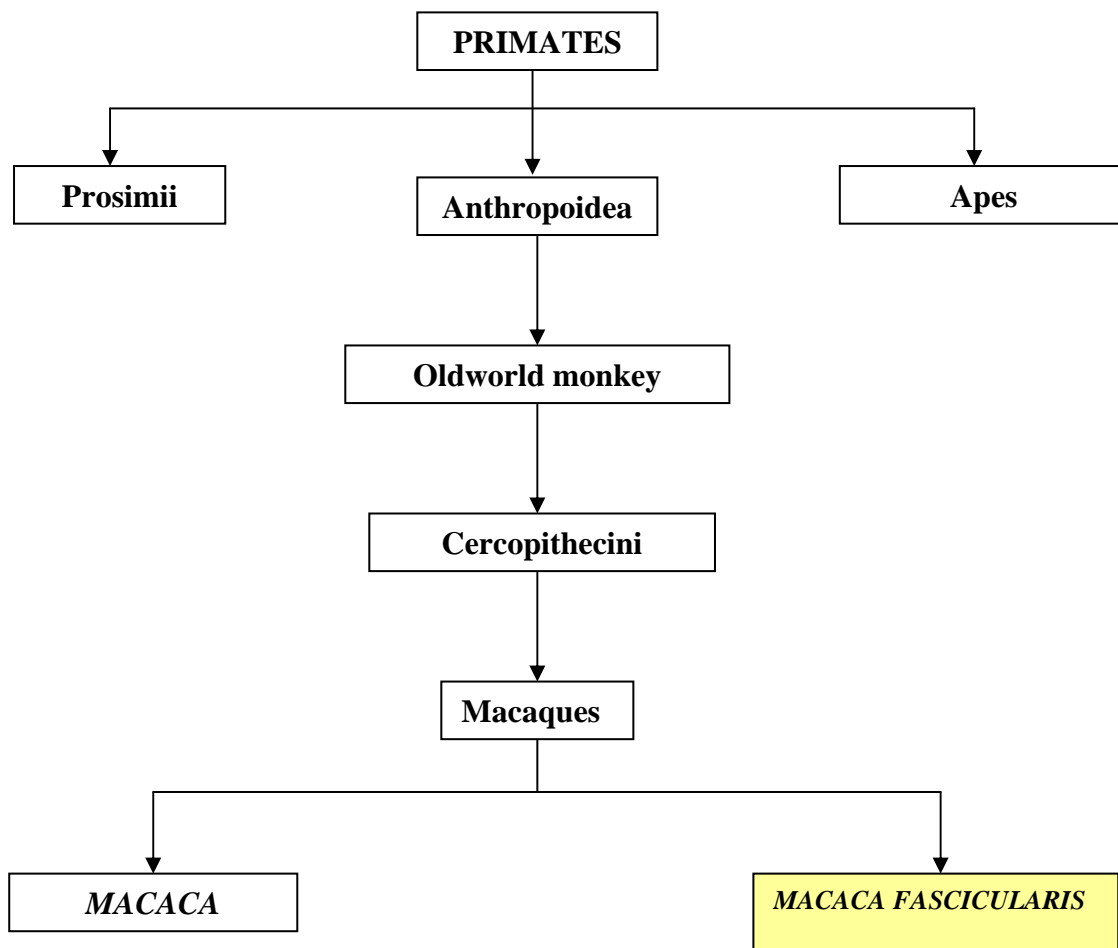
Figure 5.1: Systematic classification of adult macaca fascicularis

5.1.2 Important physiological parameters of macaque monkeys

- Bodyweight: Male 6,5-12 kg, Female 5-9 kg

- Head-trunk-length: Male 48-64 cm, Female 45-55 cm

- Tail length: 19-32 cm

- Body temperature: 36-40°C (mean value 39°C)

- Breath frequency: 30-50 Respirations/min (average 35)

- Breath volume: 50 ml

- Total breath volume/min: 1,6 l

- Heart rate: - at rest 98-100 beats/min

    - under stress 150-333 beats/min

- Blood pressure: systolic 125 mmHg; diastolic 75 mmHg

- Blood volume: 50-90 ml/kg Body weight

- Puberty: Male 4,5 years, Female 3,5 years

- Breed maturity: 4-6 years

- Menstruations cycle: 28 days (23-33 days)

- Duration of pregnancy: 160 days (135-194 days)

- Litter size: 1 young; seldom siblings

- Birth weight: 500 g

- Ablactation age: 3-6 months

- Food intake: 50-210 g/24 h

- Number of chromosomes (2n): 42

- Lifespan: average in the wildness 4 years; up to 30 years in captivity

5.1.3 Important aspects of training procedures and animal care

Generally, basic monkey training means the very first steps in the formation of the relationship between a monkey and the researcher conducting the subsequent experiments. There are key elements that are of high importance to successfully train a monkey. First of all, the animal has to be comfortable with the investigator in every possible situation. The best is that the investigator becomes a kind of leader, playing the role of a male monkey protecting and governing a colony in the wilderness. The advantage of this situation is that it is much easier to teach a task to

a specific monkey, as it will follow your orders without opposition. The reason for that is very simple: You are the boss. This way, you avoid all problems related to hierarchy challenging that could negatively influence the quality and efficiency of the planed scientific work. Second, the animal should never feel pain during the experiment or be afraid of the environment or objects surrounding him. Giving a reward for every well done step is also very helpful. Once this level reached, we start habituating the monkey on how to enter the primate chair and how it feels being restrained in it. Normally monkeys get used to this new situation within a couple of weeks. Afterwards, the monkey is brought to the lab, where we start to train them for the quantitative tests.

5.2 Definition of a stroke

Embraced by the term stroke four different cerebrovascular diseases are summed up: The ischemic insult, the cerebral hemorrhage, the subarachnoidal hemorrhage and the thrombosis of brain veins. The feature all these diseases have in common in clinics is the prompt apoplectic onset.

According to the widely used WHO definition (Hatano, 1976), one can distinguish three types of stroke with respect to **duration** of the attacks. This classification is purely clinical and allows a first but rather uncertain estimation of the severity of an insult.

A: The transient ischemic attack: Commonly lasting from 2 to 15 minutes, but occasionally lasting as long as a day (24h) with complete recovery of the observed impairments.

B: The complete insult: Shows a clinically persistent deficit, sometimes with a late, and in most cases incomplete recovery of the initial observed neurological symptoms.

C: The progrediente insult: In this case, after the first appearance, neurological symptoms become more severe within 24 hours and / or additional ones join them.

By the use of diagnostic procedures, strokes can be classified by their **cause.** A stroke can either be *ischemic* or *hemorrhagic.* Ischemic strokes are more frequent, representing about 85-90% of the cases, whereas 10-15% of strokes are caused by hemorrhages.

With respect to the **size of the occluded vessel,** ischemic strokes on their part either belong to the *macro-angiopathic* or the *micro-angiopathic* type. Details about these two subtypes of stroke are indicated in Tables 5.1 and 5.2.

A: Macro-angiopathic insult or territorial infarct (seldom border region infarct between a. anterior and a. media or a. posterior):

It is the result of an occlusion of a large extracerebral running brain supplying artery. The most common cause is an emboli, either of cardiac or atherosclerotic origin.

B: Micro-angiopathic insult or lacunar infarct (diameter < 1.5 cm):

It is the result of an atherosclerosis or lipohyalinosis induced occlusion of either a small intraparenchymic artery or an intraparenchymic arteriole.
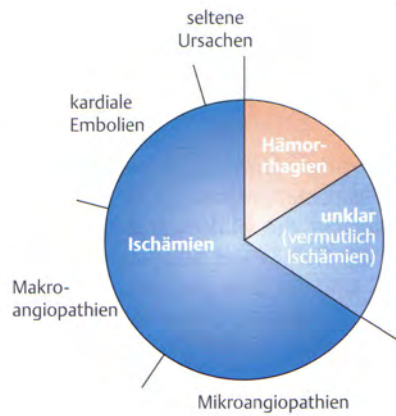
Figure 5.1: Proportions of stroke causes (from Schlaganfall, Taschenatlas spezial, ISBN 3-13-132751-0, Thieme 2002)

The biggest challenge for clinicians in the field is to interpret correctly the observed neurological symptoms as they are very variable. An additional difficulty is that, particularly during a brief episode of ischemia, the neurological symptoms can only reflect the activities in which the patient was engaged during the attack. So, there is a chance to oversee important symptoms. But basically it can be said that the functional modalities that are affected by transient ischemic attack and stroke reflect the areas of the brain which are involved in the ischemia or hemorrhage. Patients with cerebrovascular disease can be considered under the headings of disturbance of conscious level, higher cerebral function (speech and language, memory, attention and concentration), motor function, somatic sensory function, visual function and hearing, balance and coordination. As my thesis work deals with lesions of the motor cortex, in the following paragraphs I will mainly outline disturbances of the motor system. Furthermore, in most patients, motor deficits are the most characteristic manifestation of a stroke or a transient ischemic attack. Statistically, about 90% of stroke patients show motor deficits. Usually, these deficits appear as weakness affecting one side of the body: the face, arm, or leg in isolation (brachial or crural monoparesis or monoplegia); each limb as a whole or in part; or a combination of these (hemiparesis or hemiplegia). It is important to note that most fibers of the main motor pathways (corticospinal tract, corticobulbar tract) cross the midline at the level of the pons. Consequently, the observed motor signs have their origin in the hemisphere contralateral to the affected side of the body.

The best approach for a systematic survey over the multitude of motor impairments induced by stroke is to classify them with respect to blood supply of the different brain regions.

The Figure 5.2 below summarizes the most important brain arteries which can be occluded in stroke patients.
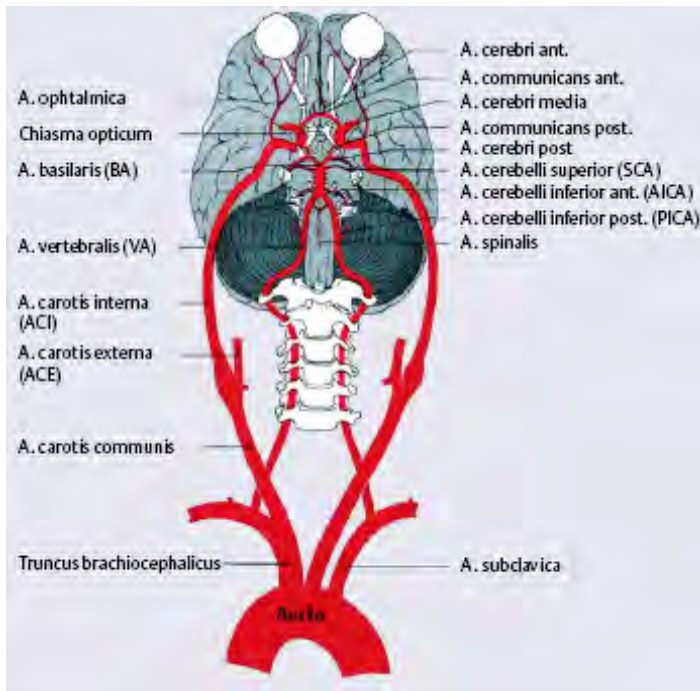
Figure 5.2: Arterial blood supply of the brain (taken from Psychoneuro 2005; 31 (5): 249–255)

Tables 5.1 and 5.2 below represent a selection of clinically frequent types of ischemia mainly affecting the motor system.

Micro-angiopathic insult			Lesion site / Occluded vessel	Clinical symptoms
	Lacunar syndrome			
		pure motor stroke	Occlusion of a perforating artery arising from the middle cerebral artery (anterior circulation) or the basilar artery (posterior circulation); Lesion sites most frequent in internal capsule or in basis pontis	Hemiparesis/hemiplegia equally severe (proportional) in the arm and leg and often not accompanied by other neurological symptoms and signs
		ataxic hemiparesis	Relevant lacunes, in most cases inside the basis pontis	Prominent vertical nystagmus, pyramidal weakness and cerebellar signs contralateral to the lesion site
		dysarthria-clumsy-hand-syndrome	Lesion, quiet always, situated in the anterior part of the capsula interna	Dysarthria and clumsiness of one hand, in most cases in combination with a light facial pareses; pyramidal dysfunction of the ipsilateral leg was also reported (Fisher,C.M. (1967) A lacunar stroke: the dysarthria-clumsy hand syndrome. Neurology 17, 614 – 617)

Table 5.1: The micro-angiopathic insult

Macro-angiopathic insult		
	Occluded vessel	**Clinical symptoms**
Territory of a. carotis interna	A. cerebri anterior (ACA)	Contralateral leg stressed sensorimotor hemipareses, pathological grip reflex of the foot (as if the foot is scotched on the floor) combined with urinary incontinence; in some cases variegated neuropsychological syndromes can be observed
	A. cerebri media (MCA)	Symptoms depend on the level at which the MCA is occluded. The deep or the superficial territory can be occluded alone or, as in most clinical cases, the occlusion occurs in the proximal mainstem. Consequently there is ischemia of both territories. Typically this presents as a contralateral continuous i.e. a face, arm and leg concerning hemimotor and sensory deficit. In addition to that, patients show a homonymous hemianopia (loss of visual field), initial gaze palsy to the contralateral side with tonic deviation of head and eyes to the healthy side. Disturbance of the relevant higher cortical functions (e.g. aphasia if in the dominant hemisphere)
Territory of a. vertebralis and a. basilaris		
	A. vertebralis and a. cerebelli inferior posterior (PICA)	Brain structures touched are the dorsal supply area of the medulla oblongata and the cerebellum, causing Wallenberg's syndrome. Note, that in clinical practice the complete form of Wallenberg's syndrome is relatively infrequent.
	A. cerebelli inferior anterior (AICA)	Touched area: dorsolateral pons and cerebellum

Symptoms: Wallenberg's syndrome, homolateral facial pareses and deafness |
| | A. cerebelli superior (SCA) | Ipsilateral Horner's syndrome, limb ataxia and intention tremor with contralateral spinothalamic sensory loss (temperature, pain), contralteral upper motor neuron type facial palsy and sometimes, a contralteral fourth nerve palsy. |
| | A. basilaris (BA) | The clinical symptoms were best described in 1980 by Caplan (Caplan, L.R. (1980) Top of the basilar syndrome. Neurology 30, 72 – 79): Variable papillary responses, supranuclear paresis |

		of vertical gaze, ptosis or lid retraction, somnolence, hallucinations, involuntary movements, such as hemiballismus (from involvement of rostral brainstem structures), visual abnormalities, such as cortical blindness (from involvement of the occipital lobes), and an amnesic state (from involvement of the temporal lobes or thalamus) Attention: in all cases of BA occlusion there is acute danger to life!
Posterior infarcts	A. cerebri posterior (PCA)	As there is a great inter-idividual and inter-hemispheric variability in the area supplied by the PCA (A van der Zwan, B Hillen, CA Tulleken and M Dujovny, **A quantitative investigation of the variability of the major cerebral arterial territories** *Stroke* 1993;24;1951-1959) the consequences of an ischemia in its territory are very variegated. For example, an occlusion of the deep perforating branches of the PCA induces an ischemia of the thalamus and upper brainstem. Then, major symptoms are hemiparesis and visual field defects which, on their hand, are the most commonly encountered syndrome from PCA infarction.There are also patients having disorders of language function ore even amnesic disorders.

Table 5.2: The macro angiopathic insult

5.2.1 Animal models of stroke

As outlined above, the "character" of a stroke is very diverse depending on size, location, duration, eliciting cause, age, sex, other diseases, daily behaviour, nutrition, genetic background, social class and ethnic group. To overcome the basic problem of such classical clinical studies, having to many uncontrolled variable parameters influencing the final outcome of stroke, the research community developed a huge number of animal models. The big advantage of these models is, to have only a limited number of controllable physiological parameters, influencing the evolution of the experimentally induced stroke. As a consequence, the resulting injury is reproducible and variability is reduced to a minimum. Nevertheless all these models often feature a new type of disadvantage. First, so far most animal stroke models used lissencephalic species, contrasting with humans who are gyrencephalic. Second, animal models generally do not take into account co-morbid disease states such as infections, hypertension and diabetes. Third, patients are mostly treated with a number of different drugs to combat co-morbid conditions that alter the

underlying milieu as compared to experimental conditions. Last but not least, animals used in stroke models are young and healthy, whereas stroke patients in clinics are typically aged and often suffer from other diseases. Therefore, today extrapolation from animal results in preclinical and clinical situations is limited. Nevertheless, all these models were of high importance to understand the concept of the ischemic penumbra and other basic pathophysiological mechanisms of stroke. In addition, the correct timing of therapeutic or pharmacologic interventions could be evaluated. Looking closer at the existing animal models of stroke reveals a lack of models reflecting real clinical conditions.

Models used so far can be classified according to different criteria (see Table 5.3, Figure 5.3 and paragraph c) below):

a) Size of animals

Animals	Size	Advantages	Disadvantages
• Mice • Rats • Gerbils • Rabbits	Small animals	• Not expensive • Low supply costs • Genetically homogeneous (particularly mice) • Relatively easy to create transgenic or knock out animals • Less concern over the use • Ability to utilize sophisticated neurosensory and motor behaviour measurements as outcome measure of injury from ischemia • Small brain size allows more histological fixation procedures and, as a consequence, more biochemical and neurochemical analysis	• **Lissencephalic** brains quite different in anatomy and functional aspects from human brains • Physiological monitoring is difficult • Measurements over time are limited or even not possible
• Dogs • Cats • Pigs • Sheep	Large animals	• Imaging techniques are easier to perform • Sophisticated physiological monitoring is easier • different measurements can be	• Use of invasive surgery for monitoring and for producing ischemia

• Monkeys		done simultaneously • Measurements can be coupled with neurological examination, neurobehavior, neurochemistry and neuropathology • Brains are **gyrencephalic** like in humans (except a few monkey species)	• Great injury or infarct size variability • Completeness of occlusion or ischemia may be unclear • Different anesthetic regimes may modify outcome from ischemia • Expensive • care intensive • Ethical problems

Table 5.3: Advantages and disadvantages of various animal species used as models of stroke

b) Focal (stroke) or global (cardiac arrest) cerebral ischemia
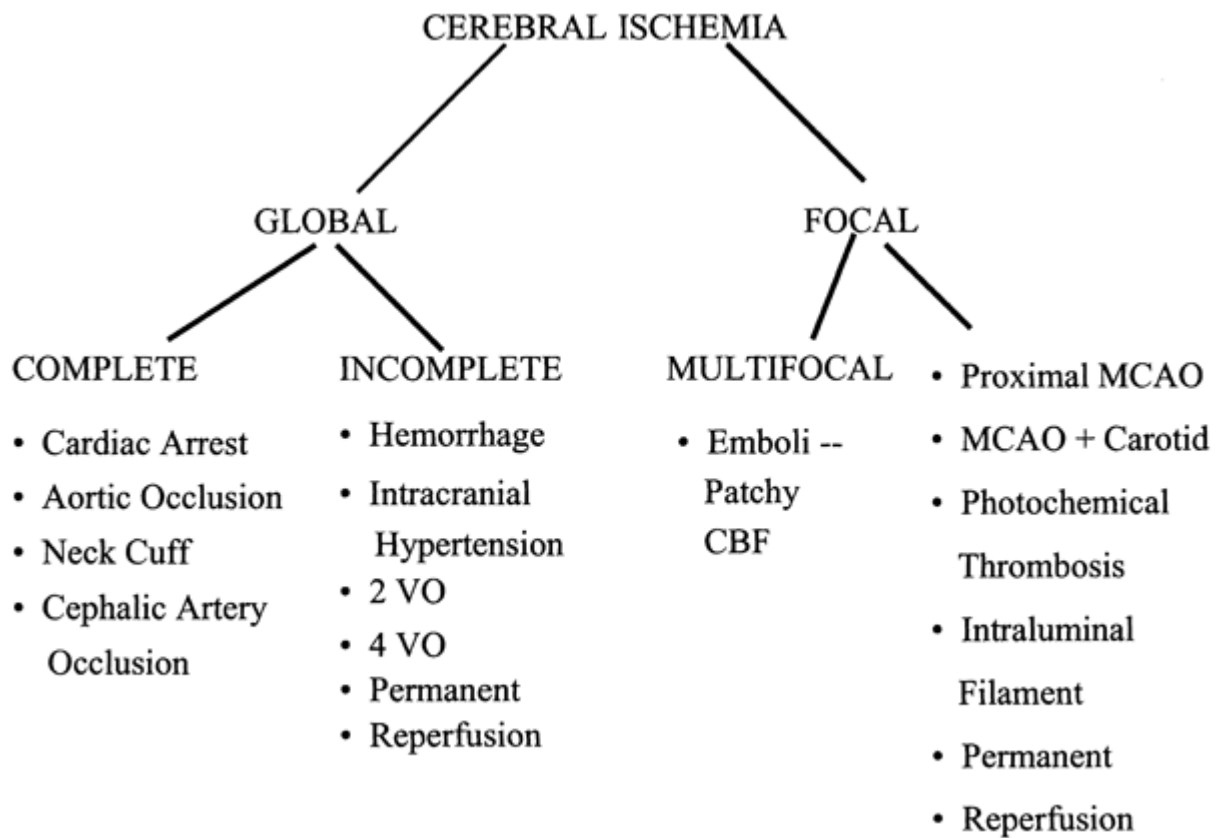
Figure 5.3:

Models of ischemia and corresponding technical approaches for induction (ILAR, 2003)

c) Models of focal cerebral ischemia in non-human primates

As already implied in Table 5.3 above, researchers tend to use small animals to explore the pathological pattern of ischemic stroke, mainly because of statistical, financial and handling considerations (Ginsberg, 1989). Unfortunately, translation to clinics is often limited (Zivin and Grotta, 1990). The basic problem seems to arise from the large phylogenetic distance from smaller animals to humans. Indeed, this leads to biological and genomic differences which, on their part, create insurmountable obstacles for translation of experimental work to clinical intervention. In contrast, non-human primates share a lot of biological attributes with humans. In particular, pharmacokinetics, pharmacodynamics, toxicology haemostatic and vascular mechanisms and haemostatic components are more similar to humans than those in rodents. Concerning haemostatic components, which are of high importance in the context of cerebral ischemia, the ultrastructure, antigenicity, function and concentration of platelets, plasma coagulation, fibrinolytic and inhibitory proteins and leukocytes are very similar in nonhuman primates and humans. In this context, it is evident that substances that can alter haemostatic/vascular dynamics, such as antithrombotic and fibrinolytic agents, have to be tested in nonhuman primates to be successfully translated to patients. In addition, cerebral vascular anatomy is analogous to humans. Primates have two vascular features in common with humans which are crucial for the outcome of an ischemic stroke. First, they have a complete Circle of Willis and, second, the distribution of the MCA and its branches is identical or similar to that in humans. In other words, there is a rich collateral circulation in the brain with the potential to alternatively supply an ischemic territory. In contrast to primates and humans, rodents lack such collateral vessels. Therefore, rodent models are not the appropriate model to mimic human stroke. Furthermore, the brain of non-human primates is generally gyrencephalic and has substantial white matter, as is the case in humans. So far squirrel monkeys, macaques and baboons have been used as stroke models. Technically speaking the clinical appearance of an ischemia can be induced by means of different approaches. The Table 5.4 below represents a selection of existing *cerebral arteries occlusion models* and indicates the purpose they were developed for.

Occlusion of cerebral arteries

Sources	Species	Location	Approach	T/P	Aw/An	Purpose
Clippings						
Hudgins and Garcia 1970	Squirrel	Proximal M1	TO	P	An	Neuropathology
Clipping						
Symon 1975	Baboon	Proximal/distal M1	TO	P	An	CBF
Liu et al. 1992	Baboon	Bilateral A1	TO	P	An	CBF
Young et al. 1997	Baboon	Proximal/distal M1	TO	T/P	An	Effect of reperfusion on infarct volume
Frazee et al. 1998	Baboon	Proximal M1	TO	T	An	Effect of RTN of t-PA on infarct volume
Huang et al. 2000	Baboon	Bilateral A1/distal ICA	TO	T	An	Larger infarction volume
Balloon occluder						
Spetzler and Selman 1979	Baboon	Proximal M1	TO	T	Aw	Repeatable stroke model in awake condition
del Zoppo et al. 1986a,b	Baboon	Proximal M1	TO	T	Aw	Multiple studies, microvascular degradation due to ischemia
Coagulation						
Yonas et al. 1990	Baboon	Lenticulostriate a.	RO	P	An	Basal ganglia infarction
Clipping						
Crorwell et al. 1970	Macaque	Proximal M1	IC	T	An	Neuropathology
Snare ligation						
Crowell et al. 1981	Macaque	Proximal M1	IC	T/P	Aw	Time course of ischemic injury
Embolization						
Molinari et al. 1974	Macaque	M1	IV	P	Aw	Stroke model without craniotomy
Watanabe et al. 1977	Macaque	ICA bifurcation	IV	P	An	Stroke model without craniotomy

An, anesthetized; Aw, awake; CBF, cerebral blood flow; IC, intracranial; ICA, internal carotid artery; IV, intravenous; M1, primary motor cortex; P, permanent; RO, retro-orbital; RTN, retrograde transvenous neuroperfusion; T, temporal; TO, transorbital; t-PA, tissue plasminogen activator.

Table 5.4: Cerebral arteries occlusion models (modified from ILAR Animal models of stroke and rehabilitation Volume 44, Number 2, p. 99 2003).

A second approach, which was used in this thesis work, is ***permanent chemical lesion of specific brain areas by ibotenic acid***. In the past, in monkeys, this method was mainly used to investigate the behavioural consequences of cortical lesions in different brain areas, rather than in the context of stroke (e.g. Rudolph and Pasternak, 1999; Liu and·Rouiller, 1999). Because, at a cellular level, this method induces a comparable pathophysiological milieu as it can be found in ischemic brain tissue just after the occlusion of a supplying vessel, it is potentially a suited new model to investigate future treatments of ischemic stroke. The more, as the present model is minimally invasive, rapid and a small target area can be selected more precisely than in an artery occlusion model. Details about the similarity of pathophysiological mechanisms and the cortical lesion procedure are lined out in paragraph 5.4.1.4 and in the method part of this thesis.

5.2.2 Present clinical situation for treatment of human stroke

For most of all agents used to treat patients suffering from acute stroke, there is no clear evidence to support the use in routine clinical practice. There is a persisting mistaken belief that these medications are safe and effective. In fact, there is a lack of reliable evidence from appropriately large randomized controlled trials. Existing studies are usually based on particular subgroups, too small samples or the monitoring over time was not systematic enough. So, the knowledge about the beneficial effects of a specific agent has to be handled with care and clinicians should inform themselves carefully about potential risks for the individual patient (e.g. website of the Cochrane Collaboration Stroke Review Group: http://www.dcn.ed.ac.uk/csrg). As a result of today's situation, there are enormous variations in the use of specific agents as well as in the general management of (and outcome after) acute stroke, both between and within different countries. In conclusion, can be said that we know a lot of potential multidisciplinary treatment strategies for stroke but the universal, best and most effective combination is not found yet. Meaning, today there is no complete treatment to heal stroke.

The lack of worldwide accepted therapies is also reflected by the fact that intravenous rt-PA remains the only Food and Drug Administration approved thrombolytic drug therapy for stroke in the United States (**TISSUE PLASMINOGEN ACTIVATOR FOR ACUTE ISCHEMIC STROKE. The New England Journal of Medecine,** Volume 333 DECEMBER 14, 1995 Number 24). But the progress in brain imaging techniques and vascular imaging techniques permits a topographical and etiological precise diagnosis. Furthermore, progresses in the treatment during the acute phase of a stroke, by means of thrombolytic, neuroprotective and aggregation inhibiting drugs offer new therapeutic approaches. So, to improve stroke treatment is still a big challenge for the research community and leaves a lot of space for new ideas. One of them may be in the future the use of ***anti-Nogo-A*** antibodies investigated in this thesis.

5.2.3 Multidisciplinary approaches to better treat human stroke

The first step is to inform the population that stroke has to be considered as an emergency condition with the same priority as acute myocardial infarction. In addition to that people at risk of stroke, doctors, families and friends should be alerted about the common symptoms of stroke. As irreversible focal injury takes place after only few minutes and in most patients is complete after 6 hours, in the context of stroke the statement "time is brain" is completely valid. Second, it is very important to have more hospitals with specialized stroke units in order to have specialists constantly

ready to help stroke patients. Third, and rather at long term, the actual knowledge about stroke treatment has to be analyzed carefully in order to develop "the" future treatment of stroke. Today, stroke treatment resembles an enormous confusing construction site with no finished building. As the existing therapies target different time points in the post-stroke period, they are best classified with respect to the time passed after the stroke event. Because stroke is a dynamic process evolving over time, future therapies must take this into account. Maybe, the best idea will be to develop a cocktail of therapies to cover the overlapping therapeutic windows. Such a combination therapy would have the advantage to reduce the dose-limiting toxicity of single agents because multiple agents can be administered at lower doses. This type of administration may also offer positive synergistic effects. Although this approach is very promising it is also very challenging as new unexpected perhaps negative side effects could be induced (for an excellent review about present and future treatments of stroke see Chapter 4 in Modern Neurosurgery, CRC PRESS 2005, ISBN 0-8493-1482-8).

5.3 The hemorrhagic stroke

5.3.1 Primary intracerebral hemorrhage

The hemorrhagic stroke is caused by a cerebral hemorrhage (bleeding) with disruption of the brain parenchyma, edema and consecutive formation of necrosis. Often secondary ischemic damage is caused by subsequent increase of pressure and volume because of edema (see 5.4.1.6) and obstruction of liquor outflow leading to impaired local cerebral blood flow, especially when the intracranial pressure reaches levels of the same order of magnitude as the arterial pressure, bringing the cerebral perfusion pressure close to zero. There is also a certain negative impact of direct mechanical compression of the brain tissue surrounding the haematoma. In addition to that, vasoconstrictor substances in extravasated blood impair local blood supply (Mendelow, 1993). If the hemorrhage is substantial, it can induce a secondary ischemic damage being much more important than the initial damage caused by the original bleeding. Normally, the hemorrhagic stroke comes from a rupture of a small penetrating arteriole. The most common causes are hypertonic mass bleeding, "spontaneous "cerebral bleeding, aneurysms, malformation of vessels and brain tumors. In the case of **primary intracerebral hemorrhages** propagation into the subarachnoidal space is frequent. A volume expansion towards the ventricular system (for details see Ropper, 1986) is quite rare. Unfortunately an additional intraventricular hemorrhage has a negative impact on the prognoses of an intraparenchymatose hemorrhage.

5.3.2 Secondary hemorrhagic infarct

A secondary hemorrhagic infarct is defined as a bleeding in a primary completely ischemic zone. This so called hemorrhagic transformation of ischemic areas can last as long as one month. Sequential computer tomography over this period of time revealed that one third of the initial ischemic territory underwent hemorrhagic transformation. So, occasionally, it can be very difficult to distinguish between a primary intracerebral hemorrhage and a cerebral infarct with secondary hemorrhage.

5.4 The ischemic stroke

The term cerebral ischemia is used for bloodlessness of the brain or for insufficient blood supply to the brain. If there is an ischemia, it is not said that an ischemic stroke is the consequence. In this context, two values are of major importance: First, the **ischemia threshold** and second, the **stroke threshold**.

The ischemia threshold is defined as the threshold value of the local brain blood flow at which a lower blood supply in the concerned brain area leads to neurological dysfunctions. In a healthy person, the cerebral blood flow is about 60-80 ml per 100g of brain tissue per minute. Only if cerebral blood flow sinks under approximate 1/3 to 1/4 of the background value (**20ml/100g/min**), neurological dysfunctions are induced. If this happens, the resulting ischemia can either be global (whole brain attained) or focal (only some parts of the brain are concerned). The dysfunctions are reversible if normal cerebral blood flow is re-established quickly. The situation completely changes if the low level of cerebral blood flow persists for a long time. Under such circumstances, moderate cerebral blood flow lowering can also lead to a subsequent stroke. On the other hand, cerebral blood flow, which attains values under the stroke threshold of **10ml/100g/min** for some minutes, always induces a stroke (Hossman et al 1994, Astrup et al 1981, Furlan et al 1996, Heiss et al 1997). The result is an irreversible loss of the function and structure in the affected brain tissue. To understand the complex mechanisms of stroke, it is important to know that different brain regions and different types of cells in the brain can be more or less susceptible to reduced cerebral blood flow. As a consequence the levels of ischemia threshold and stroke threshold are varying with respect to anatomical localization and the extension of a pathological blood supply. Besides the absolute level of residual blood flow and the oxygen-, respectively, glucose - amount in the blood, the exposure time of a given perfusion restriction has also to be taken into account, as well as the status of

collateral blood vessels which could potentially take over the function of the obstructed vessel. The interaction of all these parameters decides whether the clinician only diagnoses an ischemia or a real stroke.

If the clinical investigations reveal a stroke in the ischemic brain, commonly one can distinguish two tissue volumes, the **core of the infarction** and the surrounding zone, known as **ischemic penumbra** (Astrup et al., 1981). In view of cerebral blood flow, the penumbra has to lie in the range between the ischemic threshold and the stroke threshold at approximate **15ml/100g/min**. But, as the penumbra is also a dynamic concept, it also strongly depends on the parameters indicated above. So, the value of 15ml/100g/min rather has the meaning of an index value. The only way to determine precisely the extension of the penumbra in a specific patient is by complicated and time consuming PET and Diffusion-MRT investigations.

The cells in the core undergo necrosis within minutes and are permanently lost as a result of the severe perfusion deficit. The neurons in the penumbra undergo apoptosis because, in this part of the ischemia, some residual perfusion is maintained by collateral vessels. Such residual perfusion may be unable to maintain the full functional metabolism, but prevents immediate structural disintegration.

Initially, the penumbra tissue may constitute 50% of the volume which over time, without adequate treatment, will end up as infarction. So, the penumbra is brain tissue at risk during the maturation of the infarct, which as far as possible has to be rescued in order to minimize the persistent impairments in patients. These fundamental differences between the pathological statuses of the ischemic penumbra, as compared to the core of the infarction, make the penumbra very interesting as a target for specific neuroprotective therapies in brain regions challenged by ischemia. Today, all over the world, intense research is going on to find additional and better "tools" to stop the cascades of delayed neuronal death (Ginsberg, 2003; Dirnagl et al., 1999).

5.4.1 Ischemia: Causes and consequences

As already mentioned above, there are some key risk factors, which increase the chance for an individual person to suffer from a stroke during lifetime. Basically, the risk factors favoring ischemic stroke are the same as for cardiovascular diseases. Specific additional risk factors for an acute stroke are cardiological diseases with an augmented risk for embolism, more severe dysrhythmia, cardiac valve malformation or substitution, former myocardium infarct and cardio myopathy. All known potential risk factors can be divided up into **modifiable** and **non-modifiable**

ones. Age, sex and genetic disposition favoring cardio- and cerebrovascular diseases are considered as non-modifiable. Strokes occur more often in elderly people. Most concerned are persons at the age of 60 to 70, but also much younger individuals can be touched by severe strokes. Strokes are more frequent in men than in women. About 5-10% of the patients will suffer from a repeated stroke (Moroney et al., 1998). The Table 5.5 below summarizes the most important modifiable causes, their incidence in the population and the impact of each factor on the increase of the relative risk to suffer from stroke without treatment.

Risk factor	Relative risk (x-times)	Incidence in the population (%)
Arterial hypertension	4-5	25-40
Heart disease (not specified)	2-4	10-20
Idiopathic atrial fibrillation	6-10	5
Diabetes	2-3	4-8
alcohol	1-4	30-40
Hyperlipidemia	1-4	6-20
Smoke of cigarettes	2-4	20-40
Stenosis of the carotid artery • *asymptomatic* • *symptomatic*	 1-3 3-5	 3 2

Table 5.5: Risk factors of stroke

If one or several of the indicated risk factors are present over a long period of time, they can induce the typical etiology and pathogenesis of a mature stroke. There are people having all the features of such a risk profile, but they never suffer from a stroke, whereas other patients even with well controlled and reduced risk will fall ill because of their genetic disposition.

Today, clinicians classify ischemic strokes rather with respect to pathogenesis and the results of imaging diagnostics than by the traditional WHO definition. This new classification distinguishes two types of strokes. **Macro-angiopathies** refer to diseases of big vessels and **micro-angiopathies**

refer to diseases of small vessels. Macro-angiopathies develop from thrombembolic, autochthon thrombolic or hemodynamic origin. Angiopathies of this type can be divided in **territorial infarcts** and **hemodynamic infarcts**. The former are caused by embolic or local thrombolic occlusion of big arteries at the surface of the brain.

The embolus comes from the heart, the aorta ascendants and from atherosclerotic plaques. Local thromboses of brain vessels can be found in the case of vasculitis, atherosclerosis and coagulopathies (higher clotting readiness of the blood because of deficiency in AT –III, protein C and protein S). Hemodynamic infarcts consist of two subtypes: "Endstrominfarkte" (in the distal spreading area of the penetrating arteries) and "Grenzzonenifarkte" lying in between of two to three supply territories of big vessels. They are always based on extreme hemodynamic effective Stenosis of extra-cranial vessels (carotid bifurcation, origin of arteria vertebralis, distal arteria vertebralis) or big intra cranial arteries (arteria basilaris, proximal arteria media, carotid siphon). The etiology is most of atherosclerotic origin but, also dissections of arteries can induce hemodynamic infarcts. Dissections are bleedings in the wall of a vessel either in the intima, the media or in the adventitia. This is a very frequent cause for strokes in younger patients as it is for example induced by car accidents. Micro-angiopathies arise from single or multiple thrombosis of the small thin arteries penetrating deeply in the brain tissue and generate so called **lacunary infarcts**. Normally, a "systemic disease" of the small brain vessels is responsible for the subsequent clinical symptoms (risk factor: hypertension).

Of the ischemic strokes, 75% are caused by emboli, of either arterial or cardiac origin, while microvascular occlusion, i.e. hyalinosis or in-situ thrombosis, is responsible for 20% of the cases. Hemodynamic ischemia, caused by stenoses of brain-supplying arteries, account for less than 5% of ischemic strokes (Adams et al., 1993; Caplan, 2000).

5.4.1.1 Middle cerebral artery (MCA) occlusion

The media syndrome with arm stressed hemiparesis, hemihypaestesia, dysarthria, dysphasia, hemianopia or neglect is the most frequent clinical manifestation of stroke. About 60% of the territorial stroke syndromes are caused by diseases of the middle cerebral artery. These are good arguments for researchers to use MCA occlusion as a model to investigate the mechanisms of ischemic stroke. The more, by occluding this vessel a well described territory of the brain will undergo ischemia. That is why, the MCA occlusion model belongs to the focal cerebral ischemia models. (In contrast to that, some scientists use the global cerebral ischemia model as a model for circulatory arrest.) In such models, the extent of eventual infarct can be predicted quite accurately from the degree of reduction in regional cerebral blood flow (rCBF). If the rCBF is reduced by less

than 25% of normal, the chance of infarct in a given volume of brain tissue is greater than 95%. If rCBF does not fall below 50% of normal, then the likelihood of infarct is less than 5%. Hence the MCA occlusion model is very reliable and easy to control. Note that anticipated infarct and stroke are only induced on condition that no spontaneous or therapeutic reperfusion takes place. In addition to that, thresholds are valid for humans as well as for animals (Heiss et al., 2001; Ginsberg, 2003). As normally the concerned territory is mainly located in the motor cortex, there is an enormous diversity of experimental tasks, which can be used in order to compare the motor performance and dexterity of healthy control animals to those in which stroke was experimentally induced. Because most patients suffer from this subtype of stroke, new medication and more efficient treatments as well as the time course of partial recovery from stroke can be studied by means of the MCA occlusion model. Bearing in mind all mentioned advantages, it is not astonishing that a great deal of our knowledge about the pathophysiology of stroke comes from experimental research on MCA occlusions. The bulk of experimental studies have been carried out with rats and mice, although some primates have been used.

In the next paragraphs, I will line out in more detail the pathophysiolgical cascade of ischemic damage favoring the maturation of stroke, either when induced by MCA occlusions, or by experimental infusion of ibotenic acid in the cortex. Therefore, the next paragraphs will reveal the close relationship of the MCA occlusion and the ibotenic acid lesion model I used in the experiments of my thesis.

5.4.1.2 Pathophysiology of acute ischemic stroke

In most cases, acute cerebral ischemia begins with the occlusion of a cerebral blood vessel, usually by thrombus or embolus. Rarely, it is due to low flow alone, because the mechanisms of autoregulation can keep cerebral blood flow at a normal level, if the mean systemic arterial blood pressure lies within the physiological range of 60-160mmHg. As shown in the Figures 5.4, 5.5 and 5.6 below, autoregulation fails in the ischemic brain tissue, but even in this situation, first additional protective mechanisms will counteract progressive fall in cerebral perfusion pressure. Only if finally the cerebral perfusion reserve (Cerebral perfusion reserve = CBF : CBV; A ratio below about 6 indicates maximal vasodilatation and CBV, and exhausted reserve, even if the CBF is still normal) is also spent because of a severe vessel occlusion, ischemic symptoms appear. Without adequate treatment, an acute ischemic stroke will occur.

Figure 5.4

Legend:
- Normal brain tissue
- Normal brain tissue, chronic hypertension
- Mildly ischaemic brain tissue
- Moderately ischaemic brain tissue
- Severely ischaemic brain tissue
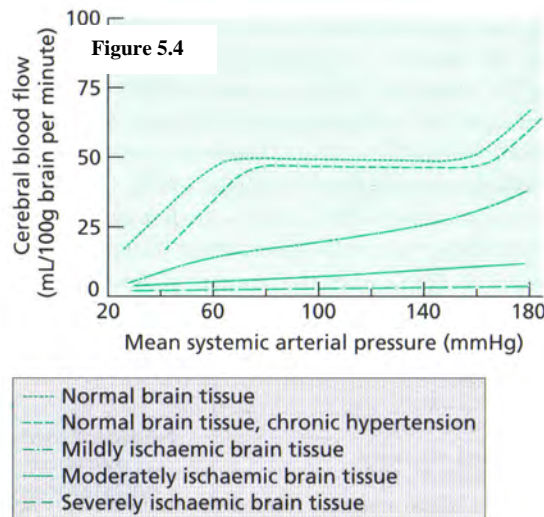
Autoregulation. Relationship between mean systemic arterial blood pressure and cerebral blood flow (CBF) in normal brain tissue and in brain ischaemia. Under normal conditions, CBF is maintained at a relatively constant level, independent of the systemic arterial blood pressure, as long as the mean pressure remains between about 60 and 160 mmHg. This capacity to maintain a constant CBF is due to the phenomenon of autoregulation. In chronic hypertension the curve is shifted to the right. When the brain tissue has been damaged by ischaemia, autoregulation is less effective and CBF follows more closely the changes in systemic arterial pressure. This is particularly important during mild ischaemia when reductions in systemic arterial blood pressure can produce reductions in CBF from above 20 mL/100 g/min, which is sufficient to sustain brain function, to lethal levels below 10 mL/100 g/min (from Strandgaard *et al.* 1973; Dirnagl & Pulsinelli 1990).

Figure 5.5

Schematic representation of the protective responses to a progressive fall in cerebral perfusion pressure (CPP). With falling CPP, intracranial arteries dilate to maintain cerebral blood flow (CBF)—autoregulation. This results in an increase in cerebral blood volume (CBV). When vasodilatation (and CBV) is maximal, further falls in CPP result in a fall in CBF and therefore a fall in the CBF:CBV ratio, and an increase in the oxygen extraction fraction (OEF) to maintain tissue oxygenation. This represents a state of impaired cerebral perfusion reserve. When the OEF is maximal, further falls in CPP lead to reduction in the cerebral metabolic rate of oxygen (CMRO$_2$) and the symptoms of cerebral ischaemia.

Relationship between the oxygen extraction fraction (OEF) and cerebral blood flow : cerebral blood volume (CBF : CBV) ratio in each of 82 middle cerebral artery regions from 32 patients with varying degrees of carotid artery stenosis and occlusion and nine normal subjects (with permission from Gibbs *et al.* 1984).
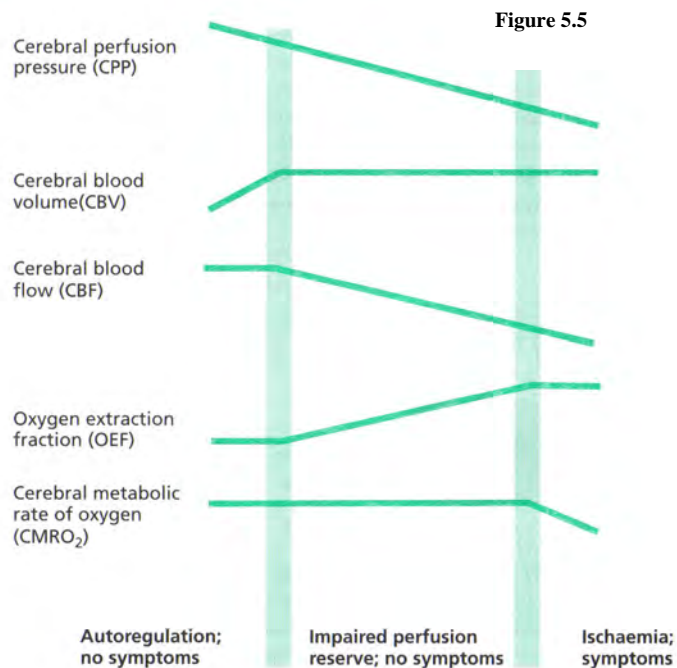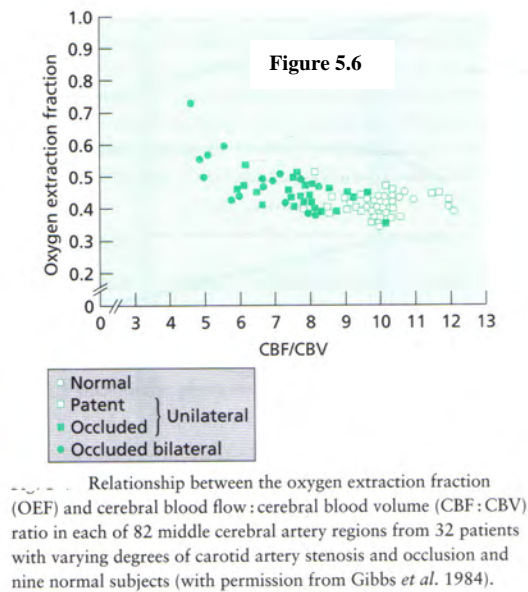
Figures 5.4-5.6: Adapted from: Stroke A pratical guide to management, Second Edition, ISBN 0-632-05418-2, Blackwell Publishing, 2003)

Hunter (1794) developed the concept of the famous triad that thrombosis is due to changes in the vessel wall, changes in the pattern of blood flow and changes in the constituents of the blood. Since then it turned out, that vascular endothelial injury is the most critical event in the formation of a thrombus. Commonly an abnormal endothelium is caused by atherosclerosis. There are several hypotheses about what could trigger dormant atherosclerotic plaques to become unstable and symptomatic. Most probable seem plaque inflammation processes elucidated by various causes, which finally lead to plaque rupture or endothelial erosion. Following that, blood is exposed to subendothelial structures, particularly fibrillar collagen, which induces platelet adhesion and activation, and blood coagulation. This happens although there are three major inhibitory systems which, under physiological conditions, would prevent coagulation in the blood vessels. It seems that at the point of vessel injury the activation of the coagulation mechanism is so powerful, that the inhibitory pathways of protein C, antithrombin and tissue factor pathway inhibitor (TFPI) are just overwhelmed. Once adherent platelets are localized at a particular place of an injured vessel, they recruit additional platelets and make the thrombus grow (Hirsh & Weitz, 1999). Because often the platelets and the fibrin are only loosely adherent, parts of such a thrombus can break off and embolize more distally, where they can induce an occlusive thrombus. As already mentioned in part 5.2, the metabolic and clinical consequences of such a thrombus induced cerebral ischemia also depend on the availability of collateral blood flow, site of cerebral ischemia, vulnerability of concerned brain cells (Heros, 1994), severity and duration of cerebral ischemia.

As the real pathophysiology of ischemia is very complex and itself would be the subject of an entire thesis (for review see Siesjö, 1992, a,b), in the next parts, I will only outline the aspects which are important in order to understand how and where in the ischemic brain the anti-Nogo-A antibody treatment could potentially have its beneficial effects. Nevertheless, the Figures 5.7 a-c below shortly summarize the potential mechanisms of injury from ischemia.
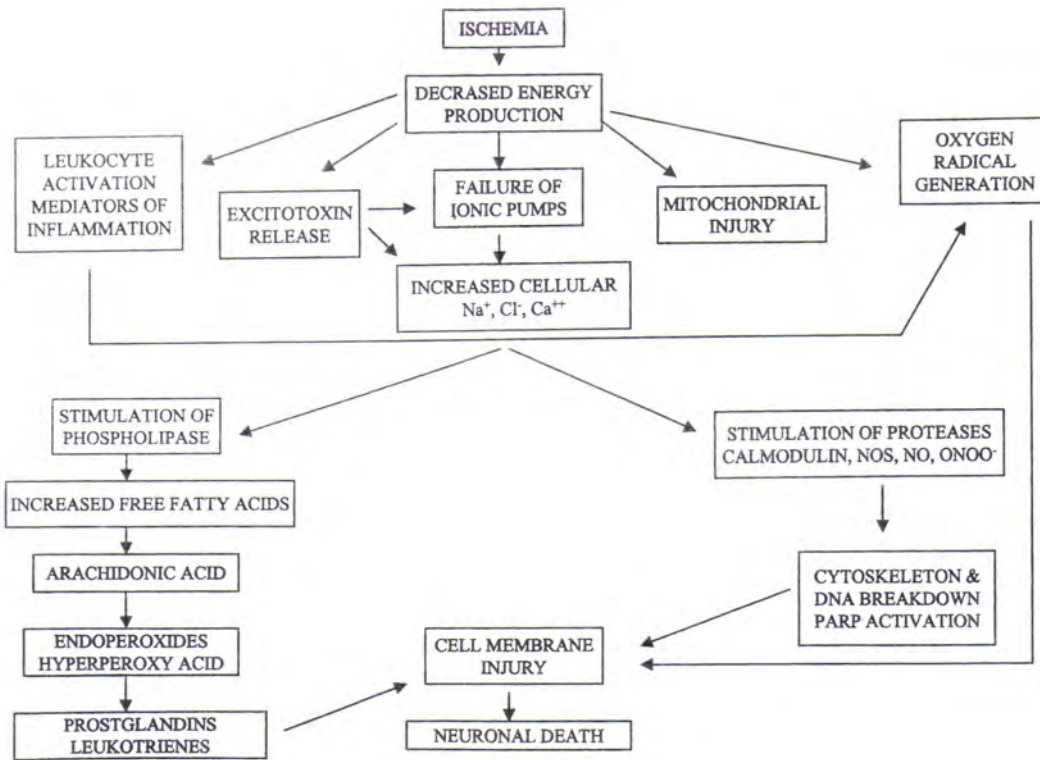
a) Potential mechanisms of injury from ischemia (from ILAR, Animal Models of Stroke and Rehabilitation, 2003, Vol. 44 Number 2: page 86).
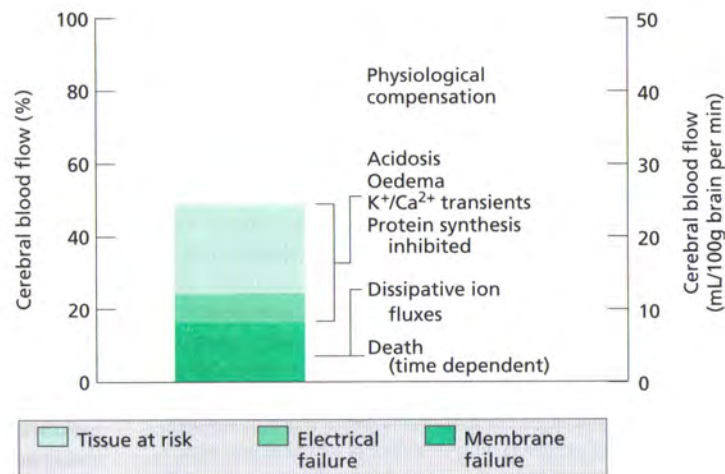
b) Cerebral blood flow (CBF) thresholds for cell dysfunction and death (from Siesjö, 1992)**.**
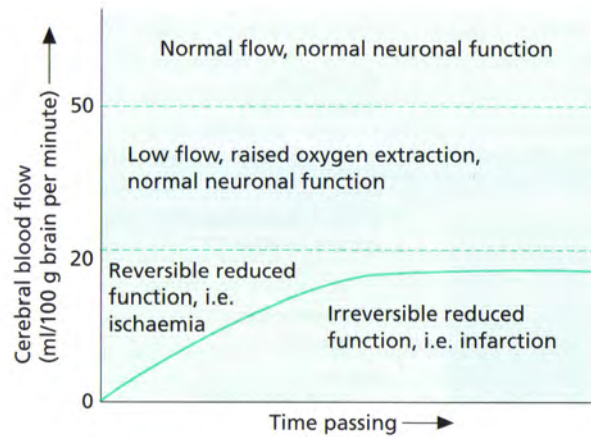
Combined effects of residual cerebral blood flow (CBF) and duration of ischaemia on reversibility of neuronal dysfunction during focal cerebral ischaemia. The solid line delineates the limits of severity and duration of ischaemia that allow survival of any neurones (from Jones *et al.* 1981; Heiss & Rosner 1983).

c) Impact of residual cerebral blood flow and duration of ischemia.

Figures 5.7 a-c: Mechanisms of injury in case of ischemia.

5.4.1.3 Concept of an ischemic penumbra

With respect to blood flow, the penumbra "area" lies in between 15ml/100g/brain/minute and 10ml/100g/brain/minute characterized by a loss of evoked potentials and a flattened EEG. In spite of cessation of electrical activity of brain cells in this intermediate zone, they preserve their membrane potential. Baron (1999), in his concept of "time is brain", defined the ischemic penumbra as an area of severely ischaemic, functionally impaired, but surviving brain tissue which is at risk of infarction but can be saved, and recover, if it is reperfused before it is irreversibly damaged. Of clinical importance is that substantial parts of the brain tissue within the penumbra can survive up to 16-17 hours after ischemic stroke in some patients. For clinical practice, this time window of effective therapeutic intervention has to be considered as not rigid as well as not universally applicable to all patients, because cerebral ischemia is a dynamic and fluctuating process over the first few hours varying from one patient to the other. It turned out that, compared to earlier animal studies, the therapeutic window is longer in humans. Jones et al. (1981) and Siesjö (1992) in their monkey models of middle cerebral artery occlusion, showed that short-term recovery of metabolic and electrical functions is possible with reperfusion after ischemic periods as long as 60 minutes,

and reperfusion within 4-8 hours in some animals can even reduce the size of lesion. Although in man benefits of reperfusion can be greater than hazards, the danger of additional reperfusion injury has to be taken into account.

The re-supply of water and osmotic equivalents may exacerbate vasogenic odema. Oxygen itself harbors the potential to trigger the production of injurious free radicals. Neutrophils may damage the ischemic brain tissue and active leucocytes migrating into the already injured region, and may for example occlude the remaining microvasculature inducing additional ischemic brain tissue (Ito, 1979; Martin, 1997; Mc Cord, 1985; Wardlaw et al., 1993; De Graba, 1998; De Graba et al., 1998; Prestigiacomo et al., 1999; Heiss and Graf, 1994; Baron et al., 1995). Not only the individuals themselves influence the therapeutic time window, but also the sites of arterial occlusion and brain ischemia have their impact. Depending on different interventions, the time window may also vary (Hakim, 1998). In summary, the penumbra has the potential to be a key element in actual and future strategies to treat ischemic stroke. But to come closer to the aim, namely healing stroke, further investigations and experiments have to be done. First, optimizing the characteristics of corresponding treatments and, second, to find out where the optimal time window of effective therapeutic intervention lies.

5.4.1.4 Excitotoxicity (why Ibotenic Acid?)

Excitotoxicity can be considered as the common trigger for apoptosis and necrosis. The consequences for individual brain cells depend on how intense they are in contact with the excitotoxic "milieu". Cells in the core of the infarct undergo ischemic necrosis (infarction). Cells situated in the penumbra, escaping this most dramatic form of disintegration excitotoxicity, may be an initiator of molecular events that lead to apoptosis and inflammation. Excitotoxicity on its part is only one step in the cascade of cerebral ischemia. Along this line, a decisive role is played by the excitatory transmitter Glutamate, which is released from ischemic cells by depolarisation. The released Glutamate stays in the intercellular space and in the synaptic cleft, as it can not be retaken up, resulting in a persistent depolarising influence on neurons.

Leão (1944, 1947) described this phenomenon as spreading depression. It is characterized by slowly moving, transient and reversible depression of cortical electrical activity that spreads like a wave from the site of onset with a speed of 2-5 mm/min. In normal healthy brain, this depolarization does not induce cell death, even if repeated over a 5 hour period. But it becomes especially dangerous in the penumbra if neurons 3-6 hours after energy failure are depolarized several times per hour. The core of the ischemic lesion increases with each depolarization until depolarization stops. The spreading depression can increase the ischemic volume by 23%

(Nedegrad, 1996; Koistinaho et al., 1999). Normally, Glutamate would be transported from the extracellular space into the intracellular space via the Na -K-ATPase, either by the neurons themselves or by astrocytes. But, as in the ischemic brain, there is a lack of ATP, making the transport of Glutamate no longer possible. Under physiological conditions, the extracellular Glutamate concentration is about 1-5 µmol/l whereas, intracellular, it is 5-10 µmol/l. In the early phase of ischemia, Glutamate release is responsible for the acute depolarization. Later on, when the ATP driven transport function is lost, one has to assume a non-synaptic concentration gradient driven transmembrane Glutamate release. Glutamate release starts if the decline in cerebral blood flow reaches a value of 20ml/100g/min. As a consequence of the uninhibited Glutamate release, the calcium metabolism is destabilized. The Glutamate dependent calcium channels let enter enormous amounts of free Ca^{++} ions into the intracellular space. Because of the permanent depolarization resulting from the Glutamate release, the voltage gated calcium channels are also permanently kept open. In addition to that, due to intracellular lost of energy, mitochondrias and the endoplasmatic reticulum release on their part calcium (see Figure 5.8 below).
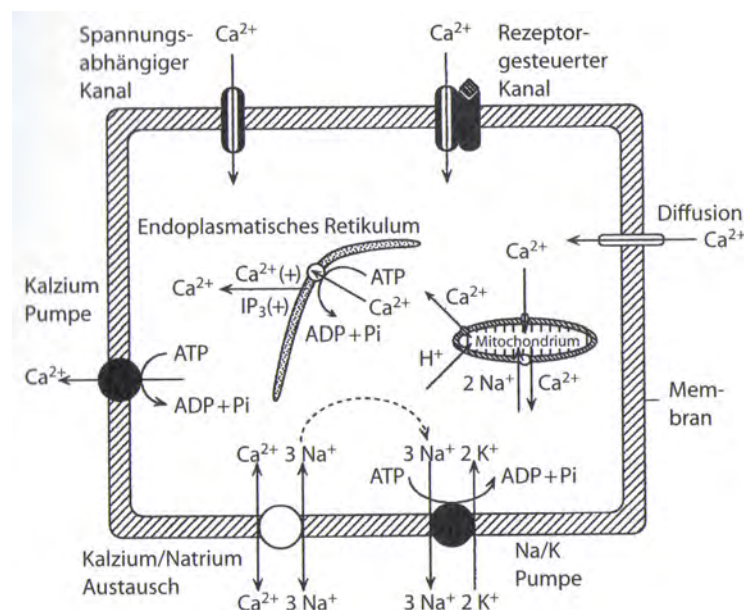

Figure 5.8: Cellular calcium metabolism during ischemia (taken from Neurologie-Kompendium, ISBN 3-456-83019-X, Verlag Hans Huber, 2002).

As a consequence of a lack of function of the energy dependent ATPase, calcium is no longer pumped out of the cell. The loss of the membrane potential leads to an additional calcium ion flow

in the cell and therefore again more calcium ions are liberated from the endoplasmatic reticulum. (ATP = Adenosine-tri-phosphate; ADP = Adenosine-di-phosphate)

The intracellular release of Ca^{++} causes an activation of calmodulin and the phospholipase A2. Calmodulin in turn activates the nitrogen oxide synthetase, the phosphokreatinkinase C, the cyclic adenosinmonophosphate (AMP), the gene expression of these enzymes and of several regulatory genes. Phospholipase A2 activates the formation of the platelet aggregation factors as well as the formation arachidonic acid. The cyclooxigenases 1 and 2 metabolize the arachidonic acid into prostaglandins and eicosanoids. Already half an hour after the initiation of the ischemia, leukocytes can be detected in the ischemic brain tissue. The leukocytes can impair the flow of erythrocytes through the microvasculature, cause vasoconstriction and platelet aggregation. Multiple surface receptor molecules become activated, such as the adhesion molecule 1 (ICAM-1) and CD11b/18. ICAM-1 is expressed on endothelium cells, induced by interleukin 1 and tumour necrosis factor alpha (TNFα) (Becker, 1998). As a consequence, the local endothelium is transformed into a prothrombotic/proinflammatory state and migration of leukocytes to the site of injury is induced (De Graba, 1998). Cellular ischemia also induces the production of highly reactive free radicals such as $O2^-$, peroxy radicals ($RO2^-$), NO or OH. As a consequence, unsaturated fatty acids can be turned into lipid peroxide, which again can act as radicals. The sulphur-containing amino acids and the polyunsaturated fatty acids found in high concentrations in the brain, are particularly vulnerable. The lipid peroxidation itself is catalyzed by free iron ($Fe2^+$, $Fe3^+$) or iron chelate released from haemoglobin and ferritin stores within ischemic brain cells. Again, in the brain, this release of catalytic iron species is more dangerous, because the cerebrospinal fluid has a low concentration of ferritin-binding proteins. So much of the iron released from damaged brain cells remains unbound. Therefore, it is available to catalyze the generation of OH the free radical species leading to iron-induced lipid peroxidation (Davalos et al., 1994). This high amount of OH radicals, besides the $O2^-$ radicals the most important radical species in cerebral ischemia, react particularly with the fatty acid component of membrane phospholipids producing changes in the fluidity and permeability of the cellular membrane (Halliwell, 1994). Finally, this leads to cell death by causing microvascular dysfunction and disruption of the blood-brain barrier. Together, all the above mentioned mechanisms finally culminate in an irreversible injury of the concerned brain region. The Figure 5.9 below briefly summarizes the most important steps leading to ischemic brain damage.
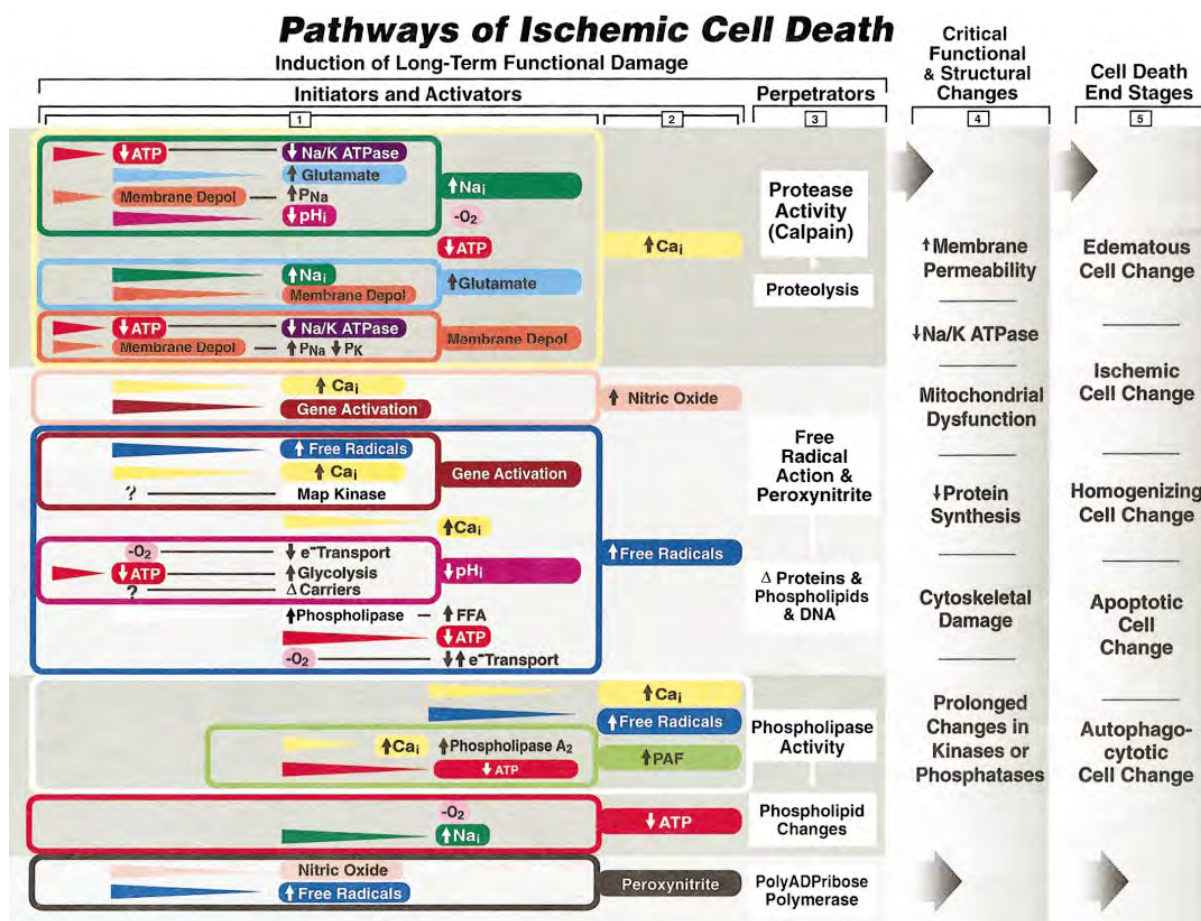
Figure 5.9: Pathways of ischemic cell death. This is an overview of processes involved in ischemic cell death that is consistent with organization of review. It illustrates major events that are hypothesized to contribute to cell death and also the extremely complex interactions between these events. This figure is not meant to be complete, but does include processes known or thought to be important at this stage. *Column 5* lists 5 principal morphological forms taken by dying or dead cells after an ischemic insult. Determining how these end stages are reached is the ultimate goal of research on ischemic cell death. *Column4* lists 6 long-term functional or structural changes, all of which, except changes in membrane permeability, are known to occur as a result of ischemia. It is hypothesized that one or more of these account for one or more forms of ischemic cell death. As indicated by lack of 1:1 connections in figure, no direct causal sequence has been established between any of functional changes in this column and particular end stages shown in *column 5*. Potential relationships are discussed extensively in text (see sect. III and IV). *Column 3* lists actions that are likely to cause long-term functional changes described in *column 4*. These are termed "perpetrators" because they are considered to be key damaging events in ischemic cell death. No direct effects of perpetrators on critical functional changes are insinuated in figure because none has been completely established. Many such effects are, however, reasonably well established and are discussed in text. *Columns 2* and *1* show changes in many variables, initiated by original inhibition of electron transport, whose most important end result is considered to be activation of perpetrators, but which may also have more direct effects on cell damage, that are not shown. Major outputs of these changes, lumped together as initiators and activators, are changes shown in *column 2*, which activate perpetrators. Direct causal interactions between specific changes are shown for these earlier events because far more is known than about interactions at later stages of the process. However, all these interactions are not established with same degree of assurance, as discussed in text. These causal interactions are indicated by including changes within same toned horizontal band, as shown for *columns 2* and *3*. For example, both increased nitric oxide and free radicals lead to damaging actions of free radicals and peroxynitrite. They are also indicated by including causal changes within a box whose outline color is same as that of variable they are changing. For example, both increased calcium and gene activation contribute to formation of increased nitric oxide. This way of describing events indicates the very high level of interaction between different changes caused by ischemia, involving many positive-feedback loops. Interpreting the figure: as indicated above, colored boxes encompass different changes that cause change in variable represented by that color. For example, increased nitric oxide (peach color) results from increased calcium and gene activation. Colored horizontal arrowheads represent all events within box of that color. For example, red arrowhead (for ATP) represents loss of oxygen and increase in sodium, which are enclosed within red box associated with ATP (near bottom of figure). Using this notation allows the very large connectivity of system to be represented in a manageable way. For example, changes putatively contributing to increase in sodium, enclosed within green box at top of figure, are extremely numerous when "contents" of each arrowhead are considered. In addition, changes contributing to increase in cytosolic calcium, and hence calpain activity, are all those included in boxes and arrowheads in top gray band. Large number of positive-feedback cycles is readily seen. Depol, depolarization; pHi, intracellular pH; Nai, intracellular Na1; Cai, intracellular Ca21; FFA, free fatty acids; PAF, platelet-activating factor; *e*2 Transport, electron transport.

(from: Ischemic Cell Death in Brain Neurons Peter Lipton Physiological Reviews Vol. 79, No. 4, October 1999)

5.4.1.5 Necrosis, apoptosis or neuronal survival after ischemia?
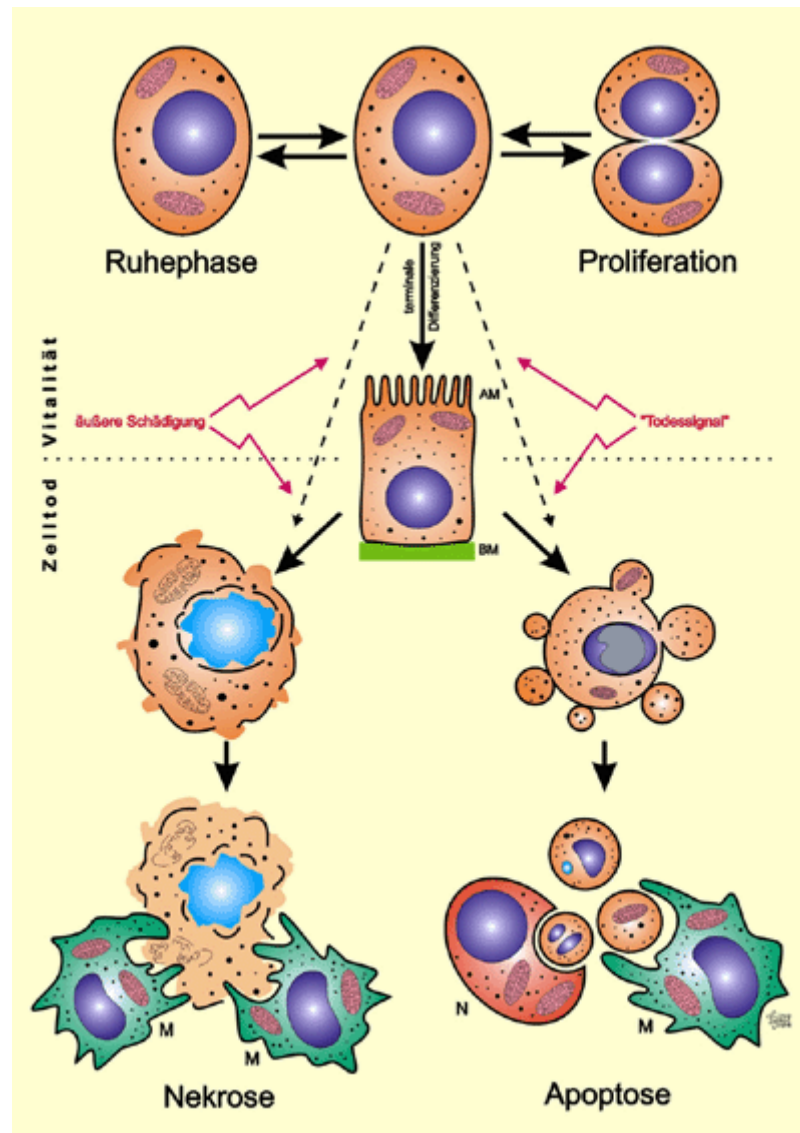
Figure 5.10:

(from: Stephan, H., Polzar, B., Mannherz, H.G.: Sein oder nicht sein? - Naturwissenschaftliche Rundschau 53 (6): 273-281, 2000).

Neurons and mature brain cells in general are highly differentiated and specialized cells. As all cells of the human body, they originate from undifferentiated precursor cells, which underwent a terminal differentiation. Under physiological conditions, they survive whereas, under pathological circumstances, they die either way if there is no immediate effective treatment to reestablish normal physiological environment. As already described, after ischemia there are two major ways how brain cells will die. Either by instant necrosis (core) or by delayed apoptosis (penumbra) (see Figure 5.10 above). Necrosis is a kind of "murder" as the concerned cells die because of external

353

impairments like burn, radiation, mechanical damage and, as in the case of cerebral ischemia (Glutamate) or experimental chemical lesions (Ibotenic acid), by poisoning. In considerable scopes of brain tissue one can observe condensation of the substances in the nucleus and a swelling of the cell organelles. As a consequence, the cells disintegrate because of the damaged cell membrane. In a next step, substances normally situated in the cytoplasm are released, which attract phagocytes. This induces an inflammation response. (for details see: Ischemic Cell Death in Brain Neurons Peter Lipton Physiological Reviews Vol. 79, No. 4, October 1999).

Apoptosis is a mode of genetic programmed cell death in which the cell synthesizes proteins and plays an active role in its own demise. Whereas necrosis is a purely pathological process, apoptosis occurs both pathologically and physiologically, for example, during normal human development. Normally, only a few cells are touched and they react to internal signals also in the case the elicitors of the signals are situated outside the cell. At the initial stage, there is shrinkage of the nucleus, cytoplasm and the mitochondria, but the cell membrane stays intact so that no inflammation reaction can be observed. As a result of the declining cell volume, the corresponding cell looses its contact to neighbouring cells and enters into a phase called "Zeiosis". During this phase, there is compaction of the chromatin (DNA and associated structural proteins) and finally the chromatin is fragmented. Eventually the cell disintegrates into membrane landlocked apoptotic particles, which are eliminated either by neighbouring cells or by phagocytes. The reabsorbed vesicles are biochemically digested by lysozymes. Thus, the rests of the dead cells are completely recycled (Kuschinsky and Gillardon, 2000). The activation of caspases is one of the key elements **late** in the cascade of apoptosis; strategies to inhibit caspase activity may block cell death in mild ischemia (Schulz et al., 1999; Ma et al., 1998). As the caspase only plays a role late in the apoptotic process, the time window for therapeutic interventions is substantially longer than for glutamate receptor antagonists in the case of necrosis. It seems that in the future, in order to decrease ischemic injury and expand the therapeutic window, we have to use treatment combinations with both classes of drugs.

Consistent with the idea above, Lee et al. (1999) came up with their speculative concept of the relationship between an apoptosis-necrosis continuum, the severity of ischemic injury and concentration of intracellular free Ca 2^+.
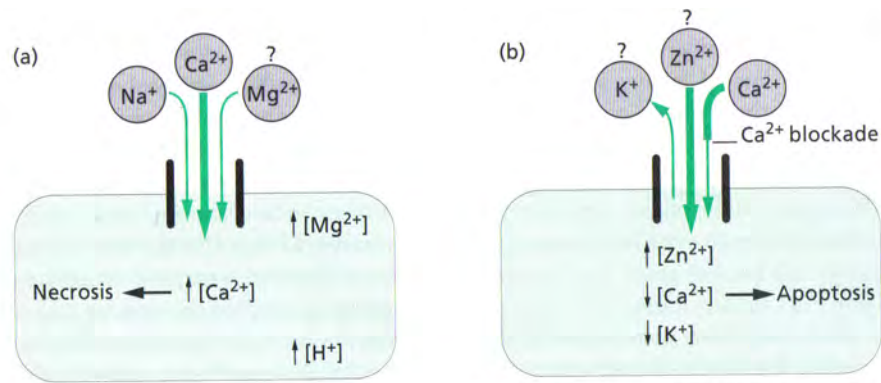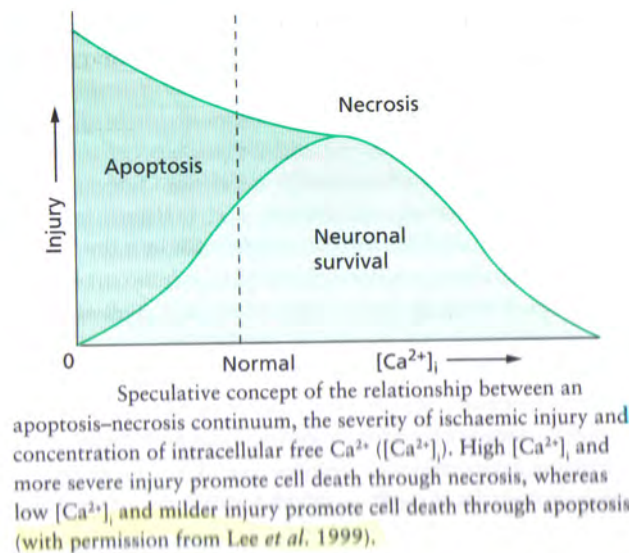
(a) Alterations in neuronal ionic homeostasis contributing to ischaemic neuronal death. (a) Attention has focused primarily on the possibility that excessive Ca^{2+} influx through several channel- and transporter-mediated routes, leading to intracellular Ca^{2+} overload, is a key factor underlying ischaemic neuronal necrosis. Na$^+$ entry contributes to acute neuronal swelling, and also facilitates Ca^{2+} entry through voltage-gated channels and the Na$^+$/Ca^{2+} exchanger. Mg^{2+} entry through the NMDA-receptor-gated channel may contribute to acute excitotoxic neuronal swelling and death. The drop in intracellular pH that follows NMDA-receptor-mediated Ca^{2+} influx may contribute to cell injury.

(b) Recent evidence indicates that other alterations in cellular ionic homeostasis may also contribute to neuronal death after ischaemic events, in particular under circumstances where programmed cell death is induced. Reduction of intracellular free Ca^{2+} ([Ca^{2+}]$_i$), whether due to diminished entry as depicted or due to alterations in intracellular homeostasis such as diminished release from intracellular stores, favours apoptosis, as does K$^+$ efflux. Excessive Zn^{2+} entry at lower levels can induce apoptosis, although high levels of toxic Zn^{2+} entry induce necrosis (with permission from Lee *et al.* 1999).

Figure 5.11:

Alterations in neuronal ionic homeostasis contributing to ischaemic neuronal death. (Adapted from: Stroke A practical guide to management, Second Edition, ISBN 0-632-05418-2, Blackwell Publishing, 2003).

Speculative concept of the relationship between an apoptosis–necrosis continuum, the severity of ischaemic injury and concentration of intracellular free Ca^{2+} ([Ca^{2+}]$_i$). High [Ca^{2+}]$_i$ and more severe injury promote cell death through necrosis, whereas low [Ca^{2+}]$_i$ and milder injury promote cell death through apoptosis (with permission from Lee *et al.* 1999).

Figure 5.12: Hypothetic concept of apoptosis – necrosis continuum. (Adapted from: Stroke A practical guide to management, Second Edition, ISBN 0-632-05418-2, Blackwell Publishing, 2003)

Already in 1996, Choi (1996) found that the features of apoptosis can be found in neurons and glia after ischemic injury but frequently with some additional morphological features of necrosis. So, his observations give additional indication that excitotoxicity and programmed cell death could be triggered in parallel in the ischemic brain. Under certain conditions, apoptosis could turn into pure necrosis inducing more severe damage to the ischemic brain with low chance to stop the negative course by means of classical therapeutic interventions.

5.4.1.6 Ischemic cerebral edema

A concomitant phenomenon of cerebral ischemia is the cerebral edema. As a major effect, cerebral edema compromises the already impaired blood flow even further and triggers pathological phenomenons. Clinicians observe a good correlation of cerebral edema with mass effect, midline shift, infarct size neurological status and outcome. The manifestation of an edema increases the pressure in the extravascular space, thus causing vascular congestion and sometimes haemorrhagic transformation. The **cytotoxic cerebral edema** occurs within minutes after the onset of ischemia as a consequence of cell membrane damage, allowing intracellular accumulation of water. In most cases, initially, the grey matter is more severely affected than the white matter (Symon et al., 1979). At first, the blood-brain barrier remains intact, but several days later it breaks down and induces **vasogenic cerebral edema**. This type of break down allows plasma constituents to enter the brain extracellular space. As a consequence, water passively follows and favors the increase of edema volume. In this particular situation, the white matter is more affected than the grey matter (Bounds et al., 1981; Bruce and Hurtig, 1979).

5.5 Bibliography for addendum

Adams HP Jr, Bendixen BH, Kapelle LJ, Biller J, Love BB, Gordon DL, Marsh EE, Stroke 1993, 24:35-41

Astrup J, Siesio BK, Symon L, Stroke 1981, 12: 723 – 725

Baron J.C. 1999 Mapping the ischemic penumbra with PET: implications for acute stroke treatment. Cerebrovascular Diseases 9, 193 – 201

Baron J.C., von Kummer, R. & del Zoppo, G. 1995 Treatment of acute ischemic stroke: challenging the concept of a rigid time window. Stroke 26, 2219 – 2221

Becker K.J. 1998 Inflammation and acute stroke.Current Opinion in Neurology 11, 45 – 49

Bounds JV, DO Wiebers, JP Whisnant and H Okazaki, Mechanisms and timing of deaths from cerebral infarction. Stroke 1981;12;474-477

Bruce D.A. & Hurtig, H.I. 1979 Incidence, course, and significance of cerebral edema associated with cerebral infarction. Cerebrovascular Diseases (eds T.R. Price & E. Nelson) pp. 191 – 198. Rave Press, New York

Caplan L.R, Caplan's Stroke: A clinical Approach. Butterworth-Heinemann, Boston, 2000

Choi D. W. (1996) Ischemia induced neuronal apoptosis. Current opinion in Neurobiology 6, 667-672

Davalos A. et al 1994 Iron-related damage in acute ischemic stroke. Stroke 24, 1543 - 1546

De Graba, T.J. 1998 The role of inflammation after acute stroke. Utility of pursuing anti-adhesion molecule therapy. Neurology 51 (Suppl. 3), S62 – S68

De Graba, T.J., Siren, A.-L., Penix, L. et al. 1998 Increased endothelial expression of intercellular adhesion molecul-1 in symptomatic versus asymptomatic human carodid atherosclerotic plaque. Stroke 29, 1405-410

Dirnagl U, Iadecola C, Moskowitz MA, Trends Neurosci. 1999, 22: 391 - 397

Fisher C.M. (1967) A lacunar stroke: the dysarthria-clumsy hand syndrome. Neurology 17, 614-617

Ginsberg MD, Busto R. 1989. Rodent models of cerebral ischemia. Stroke 20: 1627 – 1642

Ginsberg MD, Stroke 2003, 34: 214 – 223

Ginsberg MD, Stroke 2003, 34:214 - 223

Hakim A.M., Ischemic penumbra.; The therapeutic time window; Neurology 51 (Suppl. 3), S44 – S46, 1998

Halliwell B. 1994 Free radicals, antioxidants, and human disease: curiosity, cause or consequence? Lancet 344, 721 - 724

Hantano S (1976) Experience from a multicentre stroke register a preliminary report Bulletin of the World Health Organization-Google.url

Heiss W.D. & Graf, R. 1994 The ischemic penumbra. Current Opinion in Neurology 7, 11-19

Heiss WD, Kracht LW, Thiel A, Grond M, Pawlik G, Brain 2001, 124: 20-29

Heros R.C. (1994) Stroke: early pathophysiology and treatment, Stroke 25, 1877 – 1881)

Hirsh J. & Weitz J.I. (1999) New antithrombotic agents. Lancet 353, 1431 – 1436

Hunter, J. (1794) A treatise on the blood, inflammation and gunshot wounds. In: The work of John Hunter (1937) (ed J.F.Palmer), Longman, London

ILAR; Animal models of stroke and rehabilitation; Volume 44 Number 2 p., 87, 2003

Ito U., Ohno, K & Nakamura, R. 1979 Brain oedema during ischemia and after restoration of blood flow. Measurement of water, sodium, potassium content and plasma protein permeability. Stroke 10, 542 – 547

Jones et al., (1981)

Koistinaho J. et al. 1999 Spreading depression induced gene expression is regulated by plasma glucose. Stroke 30, 114 - 119

Kuschinsky W. & Gillardon, F. 2000 Apoptosis and cerebral ischemia. Cerebrovascular Diseases 10, 165-169

Leão, A.A.P., Further observations on the spreading depression of activity in the cerebral cortex). Journal of Neurophysiology 10 409 – 414, 1947

Leão, A.A.P., Spreading depression of activity in the cerebral cortex. Journal of Neurophysiology 7, 359 – 390, 1944

Lee et al. 1999, The changing landscape of ischemic brain injury mechanisms. Nature 399 (Suppl. 6738), A7-A14

Liu Yu and Eric M. Rouiller. Mechanisms of recovery of dexterity following unilateral lesion of the sensorimotor cortex in adult monkeys. Exp Brain Res (1999) 128:149–159

Ma J, Endres, M. & Moskowitz, M.A. (1998) Synergistic effects of caspase inhibitors and MK-801 in brain injury after transient focal cerebral ischemia in mice. British journal of pharmacology 124, 756-762

Martin R.L. 1997 Experimental neuronal protection in cerebral ischemia. Part 1: Experimental models and pathophysiological responses. Journal of Clinical Neuroscience 4 (2), 96-113

Mc Cord, J.M. 1985 Oxygen-derived free radicals in post-ischemic tissue injury. New England Journal of Medicine 312, 159 – 163

Mendelow A.D. 1993 Mechanisms of ischemic brain damage with intracerebral hemorrhage. Stroke 24 (Suppl.I), 115 – 117

Moroney et al., (1998)

Nedegrad, M. 1996 Spreading depression as a contributor to ischemic brain damage. Advances in Neurology 71, 75 - 83

Prestigiacomo, C.J., Kim, S.C., Connolly, S. Jr, Liao, H., Yan, S.-F. & Pinsky, D.J., 1999 CD 18 mediated neutrophil recruitment contributes to the pathogenesis of reperfused but not nonreperfused stroke. Stroke 30, 1110 – 1117

Ropper A.H.; Lateral displacement of the brain and level of consciousness in patients with an acute hemispheral mass; New England Journal of Medicine 314, 953 – 958, 1986

Rudolph K and Pasternak T. Transient and permanent deficits in motion perception after lesions of cortical areas MT and MST in the macaque monkey. Cerebral cortex 1999;9: 90-100

Schulz J.B., Weller, M. & Moskowitz, M.A. (1999) Caspase as a treatment targets in stroke and neurodegenerative diseases. Annals of Neurology 45, 421-429

Siesjö BK. Pathophysiology and treatment of focal cerebral ischemia. Part II: Mechanisms of damage and treatment. J Neurosurg. 1992 Sep;77(3):337-54. Review.

Siesjö BK. Pathophysiology and treatment of focal cerebral ischemia. Part I Pathophysiology. J Neurosurg. 1992 Aug;77(2):169-84

Symon L, NM Branston and O Chikovani Ischemic brain edema following middle cerebral artery occlusion in baboons: relationship between regional cerebral water content and blood flow at 1 to 2 hours. Stroke 1979;10;184-191

Wardlaw J.M., Dennis, M., Lindley, R.I., Warlow, C., Sandercock, P. & Sellar, R. 1993 Does early reperfusion of a cerebral infarct influence cerebral infarct swelling in the acute stage or the final clinical outcome? Cerebrovascular Diseases 3, 86 – 93

Zivin JA. Grotta JC. 1990 Animal stroke models: They are relevant to human disease. Stroke 21: 981 - 983)

Curriculum vitae:

Name:	Alexander Felix Wyss
Address:	Weidli, 3086 Zimmerwald, Switzerland
Birthday:	30. 12. 74
Nationality:	Swiss
Phone :	0041 31 819 58 73
Mobile:	0041 78 913 98 60
E-Mail:	AlexanderFelix.Wyss@unifr.ch
Siblings:	two younger brothers
Home town:	Landiswil / BE; grew up in Zimmerwald
Civil status:	single
Languages:	mother tongue: German foreign languages: English, French, Italian

Education:

1982 - 86	Primary school Zimmerwald, Switzerland
1986 - 90	Secondary school Kehrsatz, Switzerland
1990 - 95	Grammar school Kirchenfeld, Bern, Switzerland
Summer 95	General qualification for university entrance
Autumn 95 - Summer 99	Studies in Veterinary medicine in Bern, Switzerland
Autumn 99	Transition to studies in Biology at the University of Fribourg,Switzerland
Autumn 99 - Autumn 02	Studies in Biology at the University of Fribourg, Switzerland
Autumn 02	Diploma in Biologie
Since December 02	Thesis in Neurophysiology in the laboratory of Prof. E. M.Rouiller at the Department of medicine of the University of Fribourg, Switzerland

Summary:

In adult primates the plasticity in the central nervous system is very limited. Damage to the motor cortex often induces permanent loss of motor functions leading to drastic impairments of the hand dexterity for example. Unfortunately, so far there are only limited possibilities to effectively help patients. The usual treatment is limited to adapted rehabilitative physical therapy and few drugs limiting secondary damages in the central nervous system due to lesion extension. Nevertheless, the results from studies in untreated neonatal monkeys subjected to motor cortical lesions did not show such drastic permanent loss of the hand dexterity. This finding led to the conclusion, that plasticity in the central nervous system is one of the key elements to achieve nearly complete compensation of the lost motor functions. More recently, several studies in the rat showed that the intrathecal application of anti-Nogo-A antibodies enhances the plasticity in the adult central nervous system by stimulation of axonal growth, sprouting and formation of new synaptic buttons. These observations were paralleled by better functional motor recovery. Similar studies from our laboratory in anti-Nogo-A antibody treated non-human primates subjected to unilateral spinal cord lesion, also showed a significant recovery of the hand use.

The aim of the present study was to assess: 1) the recovery of the precision grip after unilateral cortical lesion of the finger representation in M1, 2) the motor cortex reorganization using intracortical microstimulation (ICMS), and 3) the role of the speared hand representation and premotor areas in the recovery of manual dexterity.

For the purpose of this study, 5 monkeys were trained in 2 modified Brinkman tests to perform a reach and prehension task. To increase statistical power, results of two other monkeys from a previous study were added. Once the monkeys reached a stable performance (plateau), we used ICMS to map the left and the right M1. A lesion in the digit representation of the left M1 was induced by injecting the neurotoxin ibotenic acid. The total volume of ibotenic acid injected in a particular monkey varied depending on the size of the hand area in M1. Four monkeys were used as untreated controls and three monkeys received the anti-Nogo-A antibody treatment for at least two weeks.

The results indicate that:

1) Without treatment such a lesion immediately leads to a permanent loss of the precise control of the fingers of the hand contralateral to the lesion site. Very typical is the loss of precision grip. In contrast, anti-Nogo-A antibody treated monkeys recover a manual dexterity allowing an individual control of the fingers close to normal. A clear indication of positive influences of anti-Nogo-A antibody treatment on the post-lesion recovery. This was reflected in better motor performances in the modified classical Brinkman tests of the lesion concerned hand in anti-Nogo-A antibody treated monkeys as compared to untreated control monkeys.

2) Data from the post-lesion intracortical microstimulation mapping show that stimulation thresholds in M1 and premotor area, needed to elicit movement or muscle twitches were lower in anti-Nogo-A antibody treated monkeys as compared to untreated controls.

3) Transient inactivation of specific motor cortical areas using muscimol infusions showed that in anti-Nogo-A antibody treated monkeys functional recovery of manual dexterity was due to reorganization occurring mainly in cortical areas of M1 close to the lesion site (penumbra) and partially also in premotor areas, whereas in untreated control monkeys the minimal post-lesion recovery was rather due to reorganization of more remote areas such as the premotor cortex.

In conclusion, the results show a preliminary tendency that the post-lesion recovery of manual dexterity in anti-Nogo-A antibody treated monkeys is better as compared to untreated control monkeys. This tendency appeared even, when the lesion was bigger in an anti-Nogo-A antibody treated monkey than in an untreated control monkey. However, this very promising tendency needs to be confirmed on a larger number of animals.

Zusammenfassung:

Beim erwachsenen Primaten ist die Plastizität des Zentralnervensystems sehr stark eingeschränkt. Daher führen Verletzungen des motorischen Kortex sehr oft zu einem permanenten Verlust an bestimmten motorischen Fähigkeiten, welcher sehr häufig die Hand betrifft. Leider gibt es bis heute nur sehr wenige Möglichkeiten, den betroffenen Patienten effektiv zu helfen. Die gängigen Behandlungen beschränken sich auf speziell angepasste rehabilitative Physiotherapien und eine geringe Anzahl an Medikamenten zur Linderung von expansiven sekundären Schäden in Zentralnervensystem. Trotz dieser ernüchternden Erkenntnis, haben Resultate von Studien mit unbehandelten neonatalen Affen, welchen eine Läsion im motorischen Kortex zugefügt wurde gezeigt, dass solche Tiere nach einiger Zeit nahezu die kompletten motorischen Fähigkeiten wiedererlangen. Dies führte zum Schluss, dass der Plastizität im zentralen Nervensystem eine entscheidende Rolle in der kompletten Kompensation von läsionsbedingten Verlusten an motorischen Fähigkeiten zukommt. In letzter Zeit haben zahlreiche Studien mit Ratten gezeigt, dass intrathecal applizierte Anti-Nogo-A Antikörper die Plastizität im adulten Zentralnervesystem mittels Stimulation von Axonwachstum und Neubildung von Synapsen erhöhen, und dass sich dies positiv auf die Wiedererlangung von verlorenen motorischen Fähigkeiten auswirkt. Studien unseres Labors haben kürzlich gezeigt, dass nach halbseitiger Durchtrennung des Corticospinaltrakts, Anti-Nogo-A Antikörper behandelte Affen sich klar besser erholen und ihre motorische Handfertigkeit derer unbehandelter Kontrolltiere deutlich überlegen ist.

Die Ziele der vorliegenden Studie waren die folgenden:1) Zu untersuchen, wie sich eine Kortexläsion in der Fingerregion des primären motorischen Kortex (M1) auf die Widererlangung des Präzisionsgriffs auswirkt, 2) mittels ICMS die Reorganisation im motorischen Kortex zu dokumentieren und 3) die Rolle der erhalten Repräsentation der Hand in M1 und die der prämotorischen Kortexareale, im Bezug auf die Widererlangung der Handfertigekeit, zu untersuchen.

Um diese Aspekte zu untersuchen, wurden 5 Affen darauf trainiert 2 modifizierte Brinkman Tests durchzuführen, die gezielte Greif- und Armbewegungen verlangen. Um die statistische Aussagekraft zu erhöhen, wurden zusätzlich Resultate zweier Affen einer vorherigen Studie beigezogen. Sobald die Affen konstante Leistungen erzielten (Plateau), wurden mittels ICMS eine Karte des rechten und eine des linken M1 erstellt. Danach wurde in der Fingerregion des linken M1, mittels Injektion des Neurotoxins Ibotensäure, eine Läsion induziert. Das Gesamtvolumen an injizierter Ibotensäure für jeden Affen war jeweils abhängig von der

Grösse der Handregion in M1. Vier Affen waren unbehandelte Kontrolltiere und drei Affen wurden mit dem Anti-Nogo-A Antikörper behandelt. Die Mindestdauer der Behandlung betrug zwei Wochen.

Die Resultate zeigen Folgendes:

1) Unbehandelt führt eine solche Läsion zum permanenten Verlust der präzisen Kontrolle über die Finger der kontralateral zur Läsion gelegenen Hand. Typisch ist der Verlust an Unabhängigkeit der Bewegung der einzelnen Finger. Insbesondere die Ausführung eines klassischen Präzisionsgriffs ist nicht mehr möglich. Im Gegensatz dazu, zeigen Anti-Nogo-A Antikörper behandelte Affen eine individuelle Fingerkontrolle, welche derer vor der Läsion sehr nahe kommt. Ein klares Zeichen dafür, dass die Anti-Nogo-A Antikörperbehandlung den Regenerationsverlauf nach Läsionen im motorischen Kortex positiv beeinflusst. Dies zeigte sich auch deutlich in besseren Leistungen der Anti-Nogo-A Antikörper behandelten Affen in den modifizierten klassischen Brinkmantests, für die von der Läsion beeinträchtigte Hand.

2) Die post-läsionellen ICMS Daten zeigen zudem, dass die Schwellenstimulationsintensitäten zur Auslösung einer Bewegung oder einer Muskelzuckung in M1 oder im prämotorischen Kortex, bei Anti-Nogo-A Antikörper behandelten Affen tiefer liegen, als bei unbehandelten Kontrolltieren.

3) Zeitlich begrenzte Inhibition bestimmter motorischer Cortexareale durch Muscimol haben gezeigt, dass in Anti-Nogo-A Antikörper behandelten Affen vorwiegend eine Reorganisation in Kortexarealen in M1 (Penumbra) und teilweise auch im prämotorischen Kortex für die Wiedererlangung motorischer Fähigkeiten zuständig waren, wogegen in Kontrolltieren die minimale Erholung der motorischen Fähigkeiten eher von weiter entfernten motorischen Cortexarealen, wie etwa dem prämotorischen Kortex ausging.

Zusammenfassend zeigen die vorliegenden ersten Resultate eine Tendenz, dass die post-läsionelle Wiedererlangung der Handfertigkeit bei Anti-Nogo-A Antikörper behandelten Tieren besser ist, als in entsprechenden unbehandelten Kontrolltieren. Diese Tendenz war auch dann sichtbar, wenn die Läsion des Anti-Nogo-A Antikörper behandelten Affen grösser war, als diejenige des unbehandelten Kontrolltiers. Trotzdem muss diese erste viel versprechende Tendenz mit zusätzlichen Versuchen erst noch bestätigt werden.

Eidesstattliche Versicherung

Ich versichere ausdrücklich, dass ich die Arbeit selbständig und ohne unerlaubte fremde Hilfe verfasst, andere als die von mir angegebenen Quellen und Hilfsmittel nicht benutzt und die aus den benutzten Werken wörtlich oder inhaltlich entnommenen Stellen kenntlich gemacht habe.

Fribourg, 21. September 2007

Alexander Felix Wyss: